ASEAN Journal of Scientific and Technological Reports (AJSTR)

Vol. 28 No. 4, July - August 2025

Development of Biodegradable Cat Litter from Water Hyacinth

Tanagon Junhamakasit and Puntaree Taeprayoon

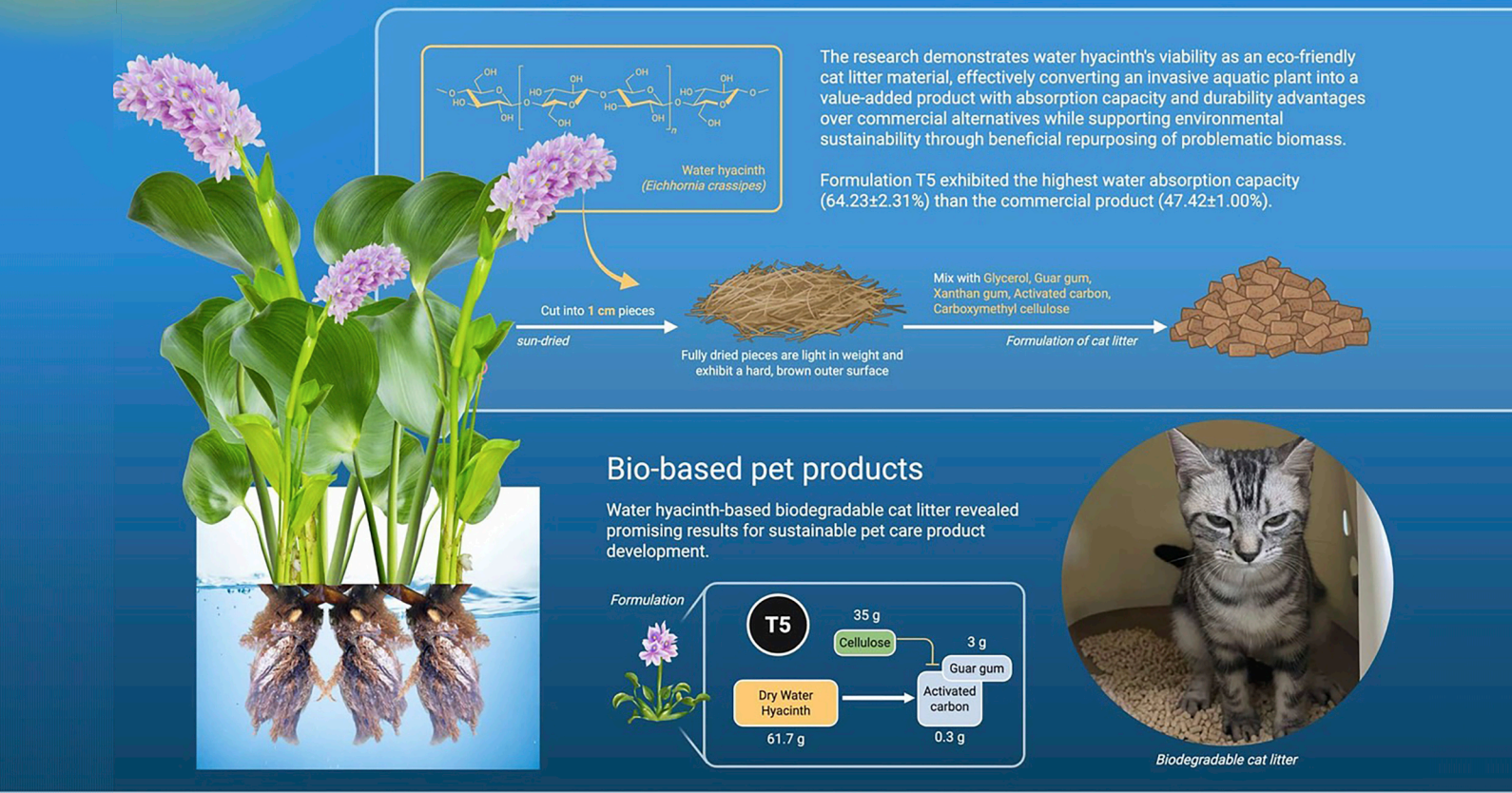

ISSN 2773-8752 (online)

https://ph02.tci-thaijo.org/index.php/tsujournal/issue/view/17310

ASEAN
Journal of Scientific and Technological Reports
Online ISSN:2773-8752

ASEAN Journal of Scientific and Technological Reports (AJSTR)

Contact Us Institute of Research and Innovation, Thaksin University
222 M. 2 Ban-Prao sub-district, Pa-Pra-Yom district, Phatthalung province, Thailand
Tel. 0 7460 9600 # 7242 , E-mail: aseanjstr@tsu.ac.th

List of Contents

List of Contents

ASEAN
Journal of Scientific and Technological Reports
Online ISSN:2773-8752

ASEAN
Journal of Scientific and Technological Reports
Online ISSN:2773-8752

Research article

Development of Khlu (*Pluchea indica* (L.) Less.) Leaves Drying Technology for Khlu Leaf Tea Production in Palian River Basin Community, Trang Province.

Warawood Duangsiri[1], Noppadon Podkumnerd[2*], Supranee Wunsri[3], Kosin Teeparuksapun[4], and Palachai Khaonuan[5]

[1] Faculty of Liberal Arts, Rajamangala University of Technology Srivijaya, Songkhla, 90000, Thailand
[2] Faculty of Liberal Arts, Rajamangala University of Technology Srivijaya, Songkhla, 90000, Thailand
[3] Faculty of Liberal Arts, Rajamangala University of Technology Srivijaya, Songkhla, 90000, Thailand
[4] Faculty of Liberal Arts, Rajamangala University of Technology Srivijaya, Songkhla, 90000, Thailand
[5] Faculty of Liberal Arts, Rajamangala University of Technology Srivijaya, Songkhla, 90000, Thailand
* Correspondence: Noppadon.p@rmutsv.ac.th

Citation:
Duangsiri, W.; Podkumnerd, N.; Wunsri, S.; Teeparuksapun, K.; Khaonuan, P. Development of Khlu (*Pluchea indica* (L.) leaf drying technology for Khlu leaves tea production in palina river basin community, Tran province. *ASEAN J. Sci. Tech. Report.* **2025**, *28*(4), e257672. https://doi.org/10.55164/ajstr.v28i4.257672.

Article history:
Received: January 27, 2025
Revised: May 20, 2025
Accepted: June 11, 2025
Available online: June 30, 2025

Abstract: This research aims to investigate the optimal temperature conditions for drying Khlu (*Pluchea indica* (L.) Less.) leaves (KLs) in a laboratory, develop KLs drying technology, and transfer the technology to the Palian River Basin Community in Trang Province. The results showed that after drying KLs at different temperatures for 7 hours, the optimal was 45°C, which resulted in a moisture content of 10.95 ± 0.54%, a lightness (L) value of 48.87 ± 1.58, and the lowest effective concentration (EC_{50}) of 0.200 ± 0.024 mg/mL. Drying at 55°C produced results similar to drying at 45°C, with a moisture content of 10.16 ± 1.27%, a lightness (L) value of 35.33 ± 1.75, and an EC_{50} of 0.370 ± 0.003 mg/mL. Drying at 65°C wasn't as effective. At the same time, the KLs had a low moisture content of 9.40 ± 1.24%, they turned out very dark (L value = 34.33 ± 0.38), and they also had the highest EC_{50} of 0.730 ± 0.007 mg/mL, indicating the weakest antioxidant ability. The KLs drying technology can utilize sunlight and heat from biomass to reduce the moisture content to just 5.80 ± 0.61% and 7.02 ± 1.97%, respectively, and has an EC_{50} of 0.240 ± 0.011 mg/mL and 0.290 ± 0.010 mg/mL, respectively. Finally, the researchers transferred the KLs drying technology to the community for drying KLs to produce Khlu leaf tea. This technology can dry about 10 kg of fresh KLs per period. Upon drying, the technology is expected to yield approximately 2 kg of dried KLs for the production of Khlu leaf tea.

Keywords: Khlu leaf (KLs); Drying technology; Khlu leaf tea; Palian river basin community

1. Introduction

The use of herbal plants is becoming increasingly popular, with applications in medicine, food, cosmetics, and beverages. In particular, herbal plants are being processed into herbal teas, which are widely consumed. These teas are made from herbs known for their health benefits, which undergo a drying process to preserve their properties. The tea is consumed by rehydrating the herbs in hot or cold water. Nowadays, the consumption of Thai herbal teas has increased, particularly among older individuals, who

drink them for their health benefits. Many types of plants have been processed into herbal teas, such as Mulberry leaf, Shallots, Crossandra, Safflower, Pandan leaf, and Gymnema [1- 6]. Khlu (*Pluchea indica* (L.) Less.) (Fig. 1) is a variety of plant that belongs to the Asteraceae family. This shrub grows to a height of 1-2 meters and is commonly found in tropical regions, including Africa, Asia, the America, Australia, and southern China. It has various local names, including Khlu (Thai), Kuo bao ju (Chinese), Kukrakonda (Bengali), and Beluntas (Bahasa) [7]. Khlu is a semi-mangrove plant that can thrive both in water and on land. Khlu leaves (KLs) are used to make healthy drinks and as a traditional herbal medicine, especially in Southeast Asia, including Thailand. KLs have medicinal properties used to treat inflammation, diabetes, cholera, arthritis, vaginal discharge, bad breath, body odor, pus, abscesses, and diarrhea, among other conditions [8-10]. Additionally, in Thailand, KLs are commonly used as a key ingredient in various local dishes. [11]. In the Palian River Basin, Trang Province, it is considered an area where KLs are found growing widely. In the past, villagers in the Palian River Basin community would eat KLs with chili paste or use them as an ingredient in cooking or even as medicine. The Palian River Basin community in Trang Province, specifically in Ban Hin Khok Khwai, Ban Na Subdistrict, Palian District, Trang Province, recognizes the value and importance of KLs by producing Khlu leaf tea products to generate income for the community. However, the community faces limitations in production due to quality issues with the raw materials, as the process of drying KLs must be performed before the production of Khlu leaf tea products can begin. However, there are problems during certain periods, such as when there is no sun or during the rainy season. If the raw materials cannot be dried in the sun, this results in the inability to produce products continuously. Therefore, this research aims to investigate the optimal conditions for preparing usable raw materials to produce high-quality Khlu leaf tea at the laboratory level. After that, a Khlu leaf drying system will be designed and constructed to obtain quality dried KLs and transfer the technology for use in producing Khlu leaf tea in the Palian River Basin community, Trang Province.

Figure 1. Khlu (*Pluchea indica* (L.) Less.) (Photo by the author)

2. Materials and Methods

2.1 Preliminary study of KLs

Samples of KLs were collected from the Ban Hin Khok Khwai community, Ban Na sub-district, Palian district, Trang province. Only the leaf parts of the Khlu were collected, washed with clean water, and drained. After that, they were packed in plastic bags and refrigerated at 5 ± 2°C for analysis of the basic characteristics of KLs. The moisture content of the KLs was determined by weighing an aluminum cup that had been dried to a constant weight and recording the weight. Weigh the sample into an aluminum cup with 2 grams and record the weight. The sample was placed in a hot air oven (Binder ED56, Germany) with the lid of the aluminum cup partially open. The hot air oven was heated at 105°C until the sample weight was constant. The moisture content was calculated using the AOAC method [12], and color values were obtained using a colorimeter (Konica Minolta CR-10, Japan).

2.2 Study of the optimum drying conditions for KLs in the laboratory

The research on the best drying conditions for KLs was based on the method used by Polyium and Sakulyunyongsuk [13], who dried KLs at various temperatures for 7 hours. The procedure will result in the production of KLs with a moisture content of not more than 10%. The study by Podkumnerd et al. [14] found that the drying of products in the solar dryer cabinet in the Palian River Basin area had temperatures ranging from 40.8°C to 57.2°C. Before developing the KLs drying technology, the researchers tested the optimal drying conditions in the lab using a hot air oven (Binder ED56, Germany) by varying the temperature to 45°C, 55°C, and 65°C for 7 hours. Samples were collected every hour for analysis of physical components, including moisture content, using the AOAC method [12], and color value using a colorimeter (Konica Minolta CR-10, Japan). Chemical composition analysis involved examining antioxidant activity using DPPH assays, starting from sample extraction, which was modified from the method of Sawaengkhot et al. [12]. This method involved extracting 5 g of KLs with boiling water (temperature 100°C) for 30 minutes. Next, we centrifuged the extract (Nuve CN 180, Turkiye) at 5,000 rpm for 10 minutes and filtered it using filter paper No. 1 (Whatman, Germany). The sample was stored in a tightly closed bottle at -20°C. Then, the antioxidant activity was assessed using DPPH assays, adapted from the method of Sawaengkhot et al. [15]. An extracted sample (1 mL) from KLs was aspirated into a test tube by mixing with 200 μL of DPPH (2,2-diphenyl-1-picrylhydrazyl) solution and leaving it in the dark for 30 minutes. The absorbance was measured using a spectrophotometer (BMG LABTECH SPECTROstar Nano, Germany) at a wavelength of 515 nm. The data were examined for differences using one-way ANOVA, and the differences between group averages were checked with Duncan's Multiple Range Test (DMRT) at a significance level of 0.05.

2.3 Design and development of KLs drying technology

The researchers used the data on the appropriate temperature conditions for drying KLs from section 2.2 to design KLs drying technology that works in all weather conditions, both with and without sunlight. After designing the KLs drying technology, the researchers created its prototype. They tested the efficiency of the system by studying the temperature changes in the drying system using a thermometer (PHYWE Cobra SMARTsense Temperature, Germany), the moisture content of the KLs using the AOAC method [12], the color value of the KLs using a colorimeter (Konica Minolta CR-10, Japan), and studying the antioxidant activity using the DPPH assays. We analyzed the data for differences between the means of the two conditions using the independent t-test, maintaining a significance level of 0.01. Finally, an analysis of microbe yeast and mold was done according to the AOAC method [12].

2.4 Technology transfer to the community

When the development of KLs drying technology was completed, the researchers transferred to the Palian River Basin Community in Trang Province, specifically to the area of Ban Hin Khok Khwai, Ban Na Subdistrict, Palian District, Trang Province, so that the community could utilize it for Khlu leaf tea production.

3. Results and Discussion

3.1 Results of the preliminary study of KLs

Based on the study of the basic features of KLs shown in Table 1, it was found that KLs had an average moisture content of 83.21 ± 0.27% and a brightness (L) of 52.95 ± 0.54, with a* and b* values of -3.50 ± 0.40 and 34.29 ± 1.06, respectively. KLs were dark green (Figure 2A), which indicates that a* values were negative. It can be seen that the KLs have a relatively high moisture content because they are plants that grow in wetlands, which is consistent with the research of Polyium and Sakulyunyongsuk [13], who found that the KLs used to produce Khlu tea from the Phraek Nam Daeng community, Amphawa District, Samut Songkhram Province, have a moisture content of 60.78±0.24%.

Table 1. Results of the study on the characteristics of KLs.

Basic characteristics of KLs	Amount
Moisture content (%)	83.21 ± 0.27
L (Brightness)	52.95 ± 0.54
a*	-3.50 ± 0.40
b*	34.29 ± 1.06

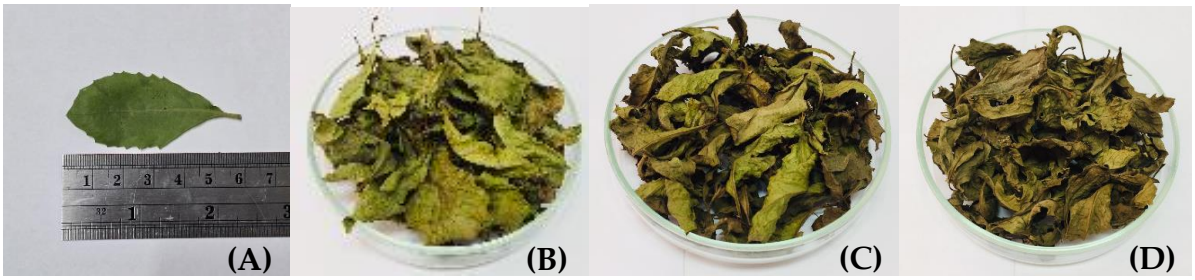

Figure 2. Characteristics of KLs in various conditions: A) Fresh KLs, B) dried at 45 °C, C) dried at 55 °C, and D) dried at 65 °C

3.2 Results of the study on the optimum drying conditions for KLs

Drying is widely used in various thermal energy applications, ranging from food drying to the drying of wood. To improve moisture migration from within the product, the dryer's goal is to provide the product with more heat than is possible in ambient settings. This process will increase the vapor pressure of the moisture contained within the product [16]. Based on the results of the moisture content of dried KLs in a hot air oven with varied temperatures at three different levels (45°C, 55°C, and 65°C), as shown in Table 2, it was found that the initial moisture content ranged from 82.12 ± 0.69% to 83.21 ± 0.27%. The moisture content gradually decreased over time. Then, the moisture content gradually remained constant after 7 hours. At 45°C, KLs had a moisture content of 10.95 ± 0.54%; at 55°C, the moisture content was 10.16 ± 1.27%; and at 65°C, the moisture content was 9.40 ± 1.24%.

Table 2. The moisture content of KLs at different temperatures

Time (Hour)	The moisture content (%)		
	45°C (Mean ± S.D.)	55°C (Mean ± S.D.)	65°C (Mean ± S.D.)
0	82.86 ± 1.04	82.14 ± 1.12	82.85 ± 1.07
1	82.14 ± 3.13	80.70 ± 1.05	76.63 ± 3.07
2	74.64 ± 1.01	70.71 ± 0.94	72.14 ± 0.93
3	58.21 ± 3.42	68.57 ± 1.03	69.29 ± 1.01
4	42.50 ± 1.54	34.29 ± 2.53	29.29 ± 1.00
5	35.00 ± 0.85	24.29 ± 4.14	20.36 ± 3.05
6	12.50 ± 0.82	11.43 ± 1.05	10.71 ± 0.93
7	10.95 ± 0.54	10.16 ± 1.27	9.40 ± 1.24

The characteristics of KLs at different temperatures and times varied in terms of L (brightness), a* (redness), and b* (yellowness) values. As shown in Table 3, the L value at 45°C, which was 52.95 ± 0.54, decreased to 48.87 ± 1.58 after 7 hours. The a* value, initially -3.33 ± 0.49, increased to -1.50 ± 0.30, while the b* value, initially 34.29 ± 1.06, decreased to 28.04 ± 6.49. KLs at 55°C showed the L value of 52.95 ± 0.54 decreased to 35.33 ± 1.75, the a* value of -3.33 ± 0.49 increased to 5.37 ± 0.40, and the b* value of 34.29 ± 1.06 decreased to 16.23 ± 0.93 after 7 hours. KLs at 55°C showed the L value of 52.95 ± 0.54 decreased to 35.33 ± 1.75, the

a* value of -3.33 ± 0.49 increased to 5.37 ± 0.40, and the b* value of 34.29 ± 1.06 decreased to 16.23 ± 0.93 after 7 hours. KLs at 65°C, the characteristics of the L value were 52.95 ± 0.54, which decreased to 34.33 ± 0.38; the a* value was -3.33 ± 0.49, which increased to 8.23 ± 0.35; and the b* value was 34.29 ± 1.06, which decreased to 15.44 ± 0.26 after 7 hours. From the experiment, we can see that raising the drying temperature of KLs resulted in their color becoming darker (Fig. 2), as indicated by the lower L and b* values and the higher a* values. This conclusion is consistent with the research of Punchuklang *et al*. [17], who found that when the drying time of young shoots of *Crotalaria juncea* was increased, the tea powder dried at a higher temperature had decreased L and b* values and increased a* as well.

Table 3. Color characteristics of KLs in the laboratory

Temperature (°C)	Time (Hour)	Color		
		L	a*	b*
45	0	52.95 ± 0.54	-3.33 ± 0.49	34.29 ± 1.06
	1	52.28 ± 0.65	-3.06 ± 0.10	33.77 ± 2.36
	2	51.50 ± 1.35	-2.67± 0.65	32.67± 1.46
	3	51.40 ± 1.35	-2.53 ± 0.58	31.29 ± 1.17
	4	50.16 ± 1.44	-2.41 ±0.12	30.80 ± 1.31
	5	49.67 ± 0.47	-1.87 ± 0.21	30.23 ± 0.87
	6	49.03 ± 1.34	-1.72 ± 0.11	28.23 ± 0.21
	7	48.87 ± 1.58	-1.50 ± 0.30	28.04 ± 6.49
55	0	52.95 ± 0.54	-3.33 ± 0.49	34.29 ± 1.06
	1	41.70 ± 1.41	-2.90 ± 0.26	23.33 ± 1.95
	2	40.53 ± 0.91	-2.04 ± 0.09	19.58 ± 0.67
	3	37.57 ± 0.97	3.00 ± 1.00	18.23 ± 2.71
	4	37.20± 0.88	4.69 ± 0.19	17.47 ± 0.61
	5	37.00 ± 1.61	5.23 ± 0.42	17.03 ± 0.68
	6	36.77 ± 1.03	5.27 ± 0.25	16.47 ± 0.76
	7	35.33 ± 1.75	5.37 ± 0.40	16.23 ± 0.93
65	0	52.95 ± 0.54	-3.33 ± 0.49	34.29 ± 1.06
	1	41.73 ± 1.16	6.97 ± 0.15	19.60 ± 0.75
	2	40.43 ± 0.69	7.24 ± 0.24	19.09 ± 0.38
	3	37.53 ± 0.75	7.43 ± 0.32	18.80 ± 0.56
	4	37.07 ± 0.40	7.57 ± 0.31	17.86 ± 0.16
	5	36.4 ± 2.65	8.07 ± 0.40	16.80 ± 0.26
	6	35.23 ± 0.70	8.14 ± 0.38	16.10 ± 0.36
	7	34.33 ± 0.38	8.23 ± 0.35	15.44 ± 0.26

One of the most significant variables influencing antioxidant activity is temperature. Generally, it is thought that heating causes an acceleration of the initiation reactions and hence a decrease in the activity of the present or added antioxidants. However, temperature variations may alter the modes of action of some antioxidants or have differing effects on them. [18-19]. The effective concentration (EC_{50}) is the concentration that reduces the concentration of DPPH free radicals by 50%. Therefore, the EC_{50} indicates good antioxidation performance [20, 21]. From drying the KLs at 45°C, 55°C, and 65°C for 7 hours, which gave the moisture content of dried KLs of 10.95%, 10.16%, and 9.40%, respectively, this amount of moisture meets the criteria for tea products from plants according to the Thai community product standard (1466/2556) [22], which must not contain more than 10% moisture. Therefore, the researchers analyzed the antioxidant activity of dried KLs at three different temperatures. The analysis of how drying temperatures of dried KLs affect DPPH radical scavenging activity (Table 4) revealed that these temperatures significantly influence the EC_{50} of the dried KLs. The dried KLs dried at 65°C gave the highest EC_{50} of 0.730 ± 0.007 mg/mL, which was

different from the other sample at a significance level of 0.05, followed by the dried KLs dried at 55°C with an EC_{50} of 0.370 ± 0.003 mg/mL, and followed by the dried KLs dried at 45°C with an EC_{50} of 0.200 ± 0.024 mg/mL. From the data, it can be seen that dried leaves dried at 45°C have the lowest EC_{50}, indicating the highest efficiency in antioxidation. The dried KLs at 55°C had the second-best efficiency. In contrast, those dried at 65°C had the least efficiency in antioxidation, which matches the findings of Noitubtim et al. [1], who discovered that drying mulberry tea leaves at higher temperatures resulted in higher EC_{50} values, indicating a decrease in antioxidant activity. This indicates that temperature has a significant impact on the degradation of antioxidant compounds.

Table 4. Effect of drying temperatures of dried KLs on DPPH radical scavenging activity

Temperature (°C)	EC_{50}* (mg/mL)
45	0.200 ± 0.024[a]
55	0.370 ± 0.003[b]
65	0.730 ± 0.007[c]

* Different characters in each column illustrated the average comparison by DMRT at a significantly different level of 0.05

3.3 Design and development of KLs drying technology

As regards the study of the appropriate conditions for producing dried KLs, it was found that temperature has a significant effect on the composition of important substances in KLs. The temperature must not be too high to destroy antioxidants, which are beneficial substances. The study indicated that the optimal temperature for drying KLs is between 45°C and 55°C for 7 hours, which maintains the moisture content at 10%, complies with the Thai community product standard 1466/2566 [22], and ensures that the dried KLs remain light in color. Additionally, these KLs exhibit better antioxidation properties compared to those dried at 65°C. The researchers developed a drying method for KLs that is effective regardless of the weather conditions. Additionally, they exhibited higher antioxidant efficiency than those dried at 65°C. The researchers designed the KLs drying technology, which can dry KLs efficiently regardless of weather conditions. Figure 3 displays the researchers' draft of the KLs drying technology.

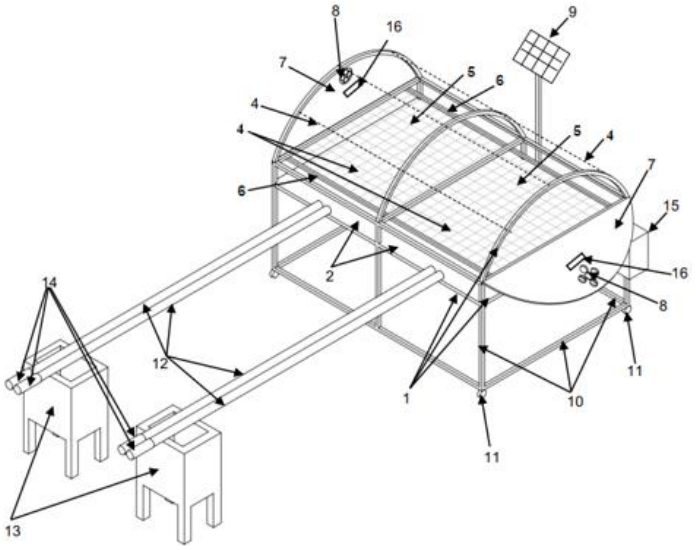

Figure 3. The schematic of KLs drying technology consists of: 1) Oven structure 2) Side walls 4) Roof 5) Oven chamber 6) Drying panel rails 7) Door 8) Dehumidification fan 9) Solar panels 10) Cabinet structure support 11) Casters 12) Heat transfer steel pipe 13) Biomass stove 14) Heat transfer fan 15) Oven temperature control system and 16) Door handle

This KL's drying technology is a drying system that utilizes solar energy in combination with biomass energy. The working principle is divided into two parts: the first part is the body structure, which consists of a square metal frame that is assembled and connected to a base with wheels. The front wall, side walls, and bottom wall are covered with metal sheets. The top wall of the body structure features a curved roof covered with clear polycarbonate sheets, allowing for good natural light. The inside of the body structure is divided into two drying chambers. Each room is equipped with one drying panel for drying KLs, and a steel rail is installed along the front wall to the back of the house structure, allowing the drying panel to be placed in the drying room and slid in and out conveniently. There is a second part that increases the heat. The installation of the heating system utilizes hot air generated by burning steel pipes sourced from biomass, such as wood chips, in a biomass stove. The heat accumulated in the steel pipes is transferred to the drying room using a heat fan installed at the end of the steel pipe, which blows hot air into the drying room. There is a temperature sensor that orders the heat fan to stop working when the temperature in the drying room exceeds the specified temperature. After the design was completed, the researchers proceeded to create KLs drying technology, as shown in Figure 4.

Figure 4. Prototype of KLs drying technology: A) Using solar energy, B) Temperature control system, and C) Using heat from biomass

After designing and prototyping the KL drying technology, the researchers tested the system's performance under both sunlight and non-sunlight conditions by setting the temperature control inside the dryer to a maximum of 55°C. After examining the temperature inside KLs's drying technology for drying KLs within a drying time of 7 hours, it was found that the temperature inside the dryer under the condition of using solar energy (with sunlight) was close to that of using heat from biomass (without sunlight), which gave temperatures of 54.70 ± 0.28°C and 53.85 ± 0.92°C, respectively (data shown in Table 5).

Table 5. Study of temperature inside KLs drying technology under different conditions

Time (Hour)	Temperature (°C)	
	Solar energy (With sunlight)	**Heat from biomass (Without sunlight)**
0	44.00 ± 2.40	32.95 ± 0.64
1	49.25 ± 2.76	40.25 ± 0.64
2	49.70 ± 1.41	45.95 ± 0.92
3	51.30 ± 1.13	46.70 ± 0.42
4	52.10 ± 1.84	47.90 ± 0.35
5	52.15 ± 2.33	52.35 ± 0.07
6	54.80 ± 1.13	54.20 ± 1.13
7	54.70 ± 0.28	53.85 ± 0.92

The study of the moisture content of dried KLs using KLs drying technology (data shown in Table 6) revealed that dried KLs, utilizing solar energy and heat from biomass, can effectively reduce the moisture

content in KLs. Dried KLs using solar energy had a moisture content of 8.35 ± 1.00%, and dried KLs using heat from biomass had a moisture content of 10.10 ± 0.92% after drying for only 5 hours. When dried for 7 hours, it was found that dried KLs using solar energy and heat from biomass had a moisture content of only 5.80 ± 0.61% and 7.02 ± 1.97%, respectively. From the experimental results, it can be seen that the use of this KLs drying technology can reduce the moisture content of KLs quickly, which is consistent with Podkumnerd *et al*. [14] who found that the use of the Nipa leaf drying system for use during sunlight and without sunlight can reduce the moisture content of Nipa leaf faster than natural sunlight drying. The reduction of moisture content to up to 10% in 4 hours.

Table 6. Moisture content of dried KLs using KLs drying technology in different conditions

Time (Hour)	Moisture content (%)	
	Solar energy (With sunlight)	Heat from biomass (Without sunlight)
0	80.14 ± 1.32	81.20 ± 1.14
1	67.16 ± 1.01	77.37 ± 2.01
2	53.28 ± 1.59	65.79 ± 1.89
3	32.65 ± 2.37	46.92 ± 1.48
4	20.08 ± 2.61	26.48 ± 2.92
5	8.35 ± 1.00	10.10 ± 0.92
6	5.97 ± 0.62	8.94 ± 0.17
7	5.80 ± 0.61	7.02 ± 1.97

The study of the color characteristics of dried KLs by KLs drying technology for 7 hours (Table 7) showed that dried KLs using solar energy (with sunlight) had L values (brightness) of 40.43 ± 0.69, a* values of 12.40 ± 0.52, and b* values of 19.09 ± 0.38, which were similar to dried KLs using heat from biomass (without sunlight), L values of 41.37 ± 0.91, a* values of 12.60 ± 1.28, and b* values of 18.60 ± 0.26.

Table 7. Results of the color values of KLs in KLs drying technology in different conditions

Time (Hour)	Solar energy (With sunlight)			Heat from biomass (Without sunlight)		
	L	a*	b*	L	a*	b*
0	51.95 ± 0.74	-3.00 ± 0.10	31.29 ± 1.17	51.50 ± 1.35	-2.67 ± 0.65	32.67 ± 1.46
1	44.47 ± 1.29	-3.57 ± 0.55	23.33 ± 1.95	45.60 ± 1.93	-2.04 ± 0.09	23.33 ± 1.95
2	43.57 ± 0.76	6.97 ± 0.15	23.13 ± 0.67	43.77 ± 1.67	7.24 ± 0.24	22.83 ± 1.16
3	43.03 ± 0.57	10.23 ± 0.32	22.70 ± 1.54	42.23 ± 0.42	10.30 ± 1.41	22.40 ± 0.87
4	42.60 ± 2.91	10.60 ± 0.26	22.57 ± 2.31	42.20 ± 1.39	11.57 ± 1.46	21.80 ± 0.72
5	42.47 ± 1.08	11.43 ± 1.62	21.67 ± 0.90	41.93 ± 0.70	11.77 ± 1.39	61.63 ± 0.80
6	40.53 ± 0.91	11.57 ± 0.81	19.58 ± 0.67	41.73 ± 1.16	12.03 ± 0.68	19.60 ± 0.75
7	40.43 ± 0.69	12.40 ± 0.52	19.09 ± 0.38	41.37 ± 0.91	12.60 ± 1.28	18.60 ± 0.26

From the effect on drying of dried KLs on DPPH radical scavenging activity (Table 8), an EC_{50} of the dried KLs using solar energy was 0.240±0.011 mg/mL, which was different at a significance level of 0.01 from the dried KLs using heat from biomass with an EC_{50} of 0.290±0.010 mg/mL. Furthermore, this technology yielded similar results to the dried KLs obtained by drying with a hot air oven at 45°C and 55°C (data shown in Table 4), which resulted in EC_{50} values of 0.200 ± 0.024 and 0.370 ± 0.003 mg/mL, respectively. From the EC_{50} of dried KLs obtained by KLs drying technology using solar energy and heat from biomass, it can be seen that the dried KLs obtained by this technology still retain antioxidant content comparable to that obtained by laboratory drying.

Table 8. Effect of drying of dried KLs using KLs drying technology on DPPH radical scavenging activity

Conditions	EC_{50} (mg/mL)	t	p-value
Solar energy	0.240 ± 0.011	-5.826**	0.004
Heat from biomass	0.290 ± 0.010		

**The mean difference is significant at the 0.01 level

The results of the study on microbial contamination in dried KLs using KLs drying technology showed that the technology was effective in reducing microbial contamination (data were shown in Table 9). Dried KLs using solar energy (with sunlight) had a total microbial count of 423.33 ± 75.06 (cfu/g) and yeast and mold counts of 63.33 ± 15.28 (cfu/g). Dried KLs produced using heat from biomass (without sunlight) had a total microbial count of 540.00 ± 75.50 (cfu/g) and yeast and mold counts of 86.67 ± 11.55 (cfu/g). The amount of microbes detected in dried KLs using this technology was within the Thai community product standard 1466-2556 (dried Gymnema for infusion), which specifies a total amount of microbes not exceeding 1 x 10^4 (cfu/g) and yeast and molds less than 100 (cfu/g) [22].

Table 9. Microbial quality of dried KLs by using KLs drying technology

Microbial	Solar energy (With sunlight)	Heat from biomass (Without sunlight)
Total microbial (cfu/g)	423.33 ± 75.06	63.33 ± 15.28
Yeast and mold (cfu/g)	540.00 ± 75.50	86.67 ± 11.55

From the development of the KLs drying technology, which can produce dried KLs under conditions with sunlight using solar energy and in conditions without sunlight using heat from biomass, the researchers compared the efficiency of the two drying systems (Table 10). They found that both drying systems can dry fresh KLs at a rate of approximately 10 kg per hour, and after 7 hours, the amount of dried KLs will be approximately the same. The KLs' drying technology using solar energy will produce an average of 1.94 kg of dried KLs, and the drying using biomass heat energy will produce an average of 2.13 kg of dry KLs. However, drying using heat from biomass energy will cost slightly more than using biomass, such as dry wood, which, when calculated as the cost of procurement, will cost approximately 0.8 baht/kg. The drying process that uses rubberwood as fuel will require approximately 25 kg of rubberwood per production cycle. However, if the community can procure fuel from dry wood scraps, this will reduce the cost in this part. When considering the installation cost, it was found that the KLs drying technology using solar energy would cost approximately 18,000 baht. If a drying system using heat from biomass is installed, the cost would be approximately 30,000 baht. However, even though the installation of KLs drying technology using heat from biomass would increase the installation cost, the advantage is that the community can produce dried KLs all the time, resulting in increased income for the community.

Table 10. Comparative analysis of the efficiency of KLs drying technology in different conditions

	Solar energy (With sunlight)	Heat from biomass (Without sunlight)
Fresh KLs (kg)	10.00	10.00
Dried KLs (kg)	1.94	2.13
Fuel costs (baht)	-	20.50
Installation cost (baht)	18,000.00	30,000.00

3.4 Transfer of KLs drying technology to the community

The researchers had transferred KLs drying technology for producing Khlu leaf tea to the target group, which is the fishery group that collects and preserves Khlu shells, Ban Hin Khok Khwai, Ban Na Subdistrict,

Palian District, Trang Province (Figure 5), along with developing production process techniques to increase quality and consumer confidence, from collecting KLs, cleaning, and drying processes. The KLs drying technology can dry about 10 kg of fresh KLs per period. After drying, it will yield approximately 2 kg of dried KLs, which can be used to produce Khlu leaf tea. After transferring the technology to the community, locals can utilize it to increase production potential and distribute their products within Trang Province.

Figure 5. Transfer of KLs drying technology to the Palian River Basin Community, Trang Province

4. Conclusions

Upon examining the appropriate temperature conditions for drying KLs to obtain quality in the laboratory, it was found that the appropriate temperature for the KLs drying process was in the range of 45°C - 55°C for 7 hours, which was shown to produce dried KLs with only 10% moisture content and not too dark in color. From the data on the effect of drying temperatures on the DPPH radical scavenging activity of dried KLs, it can be seen that leaves dried at 45°C have the lowest EC_{50}, indicating the highest efficiency in antioxidation. The EC_{50} is the concentration that reduces the DPPH free radicals by 50%. The EC_{50} indicates good antioxidation performance. The dried KLs at 55°C had the second-best efficiency, while those dried at 65°C had the least efficiency in antioxidation. Through the results of KLs drying in the laboratory, the researchers were able to design and develop KLs drying technology that can function in both conditions, i.e., with sunlight and without sunlight. The researchers were able to control the temperature within the system to prevent it from exceeding 55°C, thereby achieving drying conditions similar to those in the laboratory. The test results were satisfactory. The drying method, which utilized sunlight and solar energy heat, and the other method, which employed additional heat from biomass, yielded results for temperature, moisture content of dried KLs, and EC_{50} that were comparable to those obtained in the laboratory. After that, the researchers transferred KLs drying technology to the Palian River Basin Community (the shellfishing and shellfish conservation group, Ban Hin Khok Khwai, Ban Na Sub-district, Palian District, Trang Province) for use in drying KLs to produce Khlu leaf tea. This technology can dry about 10 kg of fresh KLs per period. Upon drying, the technology is expected to yield approximately 2 kg of dried KLs for the production of Khlu leaf tea. During the period of sunlight, KLs drying technology can be used to dry Khlu leaves directly. When there is no sunlight or it is raining, the community can utilize this technology by employing free biomass as a heat source to dry KLs. This approach allows the community to continuously produce dried KLs for use in the production of Khlu leaf tea. As a result, the community can utilize local resources to generate a sustainable income.

5. Acknowledgements

The authors would like to thank the community members in Ban Hin Khok Khwai, Ban Na Sub-district, Palian District, Trang Province, Thailand, for their participation and valuable insights throughout

the study. Special thanks to the anonymous reviewers for their constructive comments and suggestions, which helped improve the quality of this manuscript.

Author Contributions: Conceptualization, N.P., W.D,, and S.W.; methodology, N.P., W.D., S.W., and P.K.; software, P.K.; validation, N.P., W.D,, and S.W.; formal analysis, P.K.; investigation, N.P., W.D,, and S.W.; resources, N.P. and W.D.; data curation, K.T., and P.K.; writing—original draft preparation, N.P., W.D., S.W. and K.T.; writing—review and editing, N.P. W.D. and K.T.; visualization, P.K.; supervision, N.P., and W.D.; project administration, N.P. and W.D; funding acquisition, N.P., S.W. and W.D.

Funding: This research was funded by Rajamangala University of Technology Srivijaya. Fiscal year 2020 (SRI 63).

Conflicts of Interest: The authors declare no conflict of interest. The funders had no role in the study's design, data collection, analysis, or interpretation, nor in the writing of the manuscript or the decision to publish the results.

References

[1] Noitubtim, M.; Wattanayon, W.; Chooprajong, S.; Somwong, T.; Srichuay, W. Effect of temperature on antioxidant activity in mulberry leaf tea and mulberry leat tea powder production. *Maejo Journal of Agricultural Production* **2023,** *5*(2), 1-9. (In Thai)

[2] Musika, J.: Musika, T. Development of Healthy shallot herbal tea (*Allium ascalonicum* L.) with antioxidant activities. *Journal of Food Technology Siam University* **2021,** *16*(2), 148-159. (In Thai)

[3] Junsi, M.; Dangkhaw, N.; Klamklomjit, S. Development of antioxidant herbal tea product from Sang-Ko-Ra-Nee and Tree-Sha-Waas functional drink. *Journal of Science & Technology, Ubon Ratchatani University* **2024,** *26*(1), 93-103. (In Thai)

[4] Wongyai, W. Safflower tea. *RMUTSB Academic Journal*, **2013,** *1*(1), 10-15. (In Thai)

[5] Novelina, N.; Wellyalina, W.; Faramida, *S.* Characteristics of Herbal Tea Bags From a Mixture of Pandan Leaf Powder (*Pandanus amaryfolius* Roxb.) and Red Ginger (*Zingiber officinale* var. Rubrum). *Asian Journal of Applied Research for Community Development and Empowerment* **2024,** *8*(2), 230-234. https://doi.org/10.29165/ajarcde.v8i2.431

[6] Chunwijitra, K.; Phunthupan, P.; Phesatcha, B.; Thiwato, S.; Phesatcha, K. Effects of the production process on quality of *Gymnema inodorum* (Lour.) Decne. powder and enhancing their quality of herbal tea mixtures of the Phu Phan development study center community enterprise, Pla Pak District, Nakhon Phanom Province. *YRU Journal of Science and Technology* **2024**, *9*(2), 23-33. (In Thai)

[7] Suriyaphan, O. Nutrition, Health Benefits and Applications of *Pluchea indica* (L.) Less Leaves. *Pharmaceutical Sciences Asia* **2014,** *41*(4), 1-10.

[8] Chiangnoon, R.; Samee, W.; Uttayarat, P.; Jittachai, W.; Ruksiriwanich, W.; Rose Sommano, S.; Athikomkulchai, S.; Chittasupho, C. Phytochemical analysis, antioxidant, and wound healing activity of *Pluchea indica* L. (Less) branch extract nanoparticles. *Molecule* **2022**, *27*(3), 635. https://doi.org/10.3390/molecules27030635

[9] Ruan, J.; Li, Z.; Yan, J.; Huang, P.; Yu, H.; Han, L.; Zhang, Y.; Wang, T. Bioactive constituents from the aerial parts of *Pluchea indica* Less. *Molecules*, **2018**, *23*(9), 2104. https://doi.org/10.3390/molecules23092104

[10] Ibrahim, S.R.M.; Bagalagel, A.A.; Diri, R.M.; Noor, A.O.; Bakhsh, H.T.; Mohamed, G.A. Phytoconstituents and pharmacological activities of indian camphorweed (*Pluchea indica*): a multi-potential medicinal plant of nutritional and ethnomedicinal importance. *Molecules* **2022**, *27*(8), 2383. https://doi.org/10.3390/molecules27082383

[11] Nopparat, J.;INualla-ong, A.; Phongdara, A. Ethanolic extracts of *Pluchea indica* (L.) leaf pretreatment attenuates cytokine-induced β-cell apoptosis in mulyiple low-dose streptozotocin-induced diabetic mice. *PLoS ONE* **2019**, *14*(2), e0212133. https://doi.org/10.1371/journal.pone.0212133

[12] AOAC. Official method of analysis. 18th Edition. **2005**, Assosiation of Officating Analytical Chemists, Washington D.C.

[13] Polyium, U.; Sakulyunyongsuk, N. Biologolgical activities and optimal conditions for making Klu tea.

Applied Mechanics and Materials **2020**, *901*, 11-15. https://doi.org/10.4028/www.scientific.net/AMM.901.11

[14] Podkumnerd, N.; Wunsri, S.; Khairin, S. Production process development of Nipa bowl from Nipa palm *(Nypa fruticans* Wurmb.*)* waste by using solar dryer cabinet for sustainability of Palian river basin community. *Malaysian Journal of Fundamental and Applied Sciences* **2019**, *15*(4), 593-596. https://doi.org/10.11113/mjfas.v15n4.1334

[15] Sawaengkhot, W.; Prommakool, A.; Savedboworn, W.; Pattayakorn, K. Determination of phenolic compound and antioxidant activity in leaves of 2 mulberry (*Morus alba* L.) cultivar. *Khon Kaen Agriculture Journal* **2018**, *46*(Suppl.1), 359-362. (In Thai)

[16] Dincer, I.; Sahin, A.Z. A new model for thermodynamic analysis of drying process. *International Journal of Heat and Mass Transfer* **2004**, 47, 645-652. https://doi.org/10.1016/j.ijheatmasstransfer.2003.08.013

[17] Punchuklang, K.; Bunkrongcheap, R.; Petlamul, W.; Punchuklang, A. Antioxidant activity, total phenolic and tannin contents in *Crotalatia juncea* Tea. *Thai Science and Technology Journal* **2021**, *29*(4), 653-665. (In Thai)

[18] Pokony, J. Addition of antioxidant for food stabilization to control oxidative rancidity. *Czech Journal of Food Science* **1986**, *4*, 299-307.

[19] Yanishlieva, N.V. Inhibiting oxidation. J. Pokorny´; N. V. Yanishlieva; M. H. Gordon (Eds)., *Antioxidants in Food – Practical Applications* (pp. 22–70), Woodhead Publishing, Cambridge (UK). **2001**.

[20] Suriyatem, R.; Auras, R.A.; Intipunya, P.; Rachtanapun, P. Predictive mathematical modeling for EC_{50} calculation of antioxidant activity and antibacterial ability of Thai bee products. *Journal of Applied Pharmaceutical Science* **2017**, *7*(9), 122-133. https://doi.org/10.7324/JAPS.2017.70917

[21] Widyawati, P.S. Determination of antioxidant capacity in *Pluchea indica* Less leaves extract and its fractions. *International Journal of Pharmacy and Pharmaceutical Sciences* **2016**, *8*(9), 32-36. http://dx.doi.org/10.22159/ijpps.2016v8i9.11410

[22] Thai Industrail Standards Institute (TISI). Thai community product standard 1466/2556; Dried gymnema for infusion. **2013**, Ministry of Industry.

ASEAN
Journal of Scientific and Technological Reports
Online ISSN:2773-8752

Research article

Anticandidal Activities of Selected Thai Plant Extracts and Essential Oils Against Oral Candidiasis *Candida* spp. Isolates

Premnapa Sisopa[1, 2], Waree Tiyaboonchai[3], Ruchadaporn Kaomongkolgit[3], and Supaporn Lamlertthon[5*]

[1] Faculty of Pharmaceutical Sciences, Naresuan University, Phitsanulok, 65000, Thailand
[2] Faculty of Food and Agricultural Technology, Pibulsongkram Rajabhat University, Phitsanulok, 65000, Thailand
[3] Faculty of Pharmaceutical Sciences, Naresuan University, Phitsanulok, 65000, Thailand
[4] Faculty of Dentistry, Naresuan University, Phitsanulok, 65000, Thailand
[5] Faculty of Medical Sciences, Naresuan University, Phitsanulok, 65000, Thailand
* Correspondence: supapornl@nu.ac.th

Citation:
Sisopa, P.; Tiyaboonchai, W.; Kaomongkolgit, R.; Lamletthon, S. Anticandidal activities of selected Thai plant extracts and essential oils against oral candidiasis *Candida* spp. isolates. *ASEAN J. Sci. Tech. Report.* **2025**, *28*(4), e257980. https://doi.org/10.55164/ajstr.v28i4.257980.

Article history:
Received: February 19, 2025
Revised: May 22, 2025
Accepted: June 11, 2025
Available online: June 30, 2025

Abstract: The antifungal properties of 13 ethanol plant extracts (PE) and 6 essential oils (EO) of Thai traditional herbs were screened for their anti-*Candida* activity against a standard strain of *Candida albicans* ATCC 10231 using agar disk diffusion and broth microdilution methods. Two PE, *Piper betle* and *Alpinia galanga* extracts, showed the lowest MIC and MFC values against *C. albicans* of 0.313 mg/mL and 0.625 mg/mL, and three EO; cinnamon bark oil exhibited the lowest MIC and MFC value of 0.039 mg/mL, followed by lemongrass oil and clove bud oil. The main compounds of these EOs and PEs were identified using gas chromatography-mass spectrometry (GC-MS). The major compounds were geranial (42.7%) and neral (22.2%) in lemongrass oil, eugenol (85.5%) in clove bud oil, cinnamaldehyde (80.6%) in cinnamon bark oil, 4-allyl-1,2-diacetoxybenzene (29.5%) and hydroxychavicol (24.8%) in *P. betle* extract, and 1'-acetoxychavical acetate (78.0%) in *A. galanga* extract. All EO and PE showed antifungal activity against three oral candidiasis isolates, including *C. albicans* R01, *C. krusei*, and *C. dubliniensis*, with MIC/MFC ranging from 0.156 – 5.000 mg/mL. The checkerboard dilution method revealed that the combination of EO and PE showed an additive effect on *C. albicans* R01. In conclusion, the combination of EO with PE lowered the MIC of each agent, which could lead to decreased side effects; hence, this combination could be a promising treatment alternative for oral candidiasis.

Keywords: Antifungal activities; Plant extracts; Essential oils; *Candida* spp.; Oral candidiasis

1. Introduction

Candida species are common colonizers of the oral cavity but can also act as opportunistic pathogens, leading to oral fungal infections, also known as oral candidiasis. This infection is prevalent in immunocompromised individuals, the elderly, and individuals who wear dentures. While *Candida albicans* is the primary cause, non-albicans *Candida* (NAC) species such as *C. glabrata*, *C. tropicalis*, *C. parapsilosis*, *C. dubliniensis*, and *C. krusei* are also frequently identified [1-3]. Some commercially available antifungal agents are used to treat oral candidiasis; however, their applications are limited by side effects such as oral irritation, burning, and discoloration, as well as drug interactions and the development of resistance over prolonged use. [4]. Thus, these limitations lead to a search for novel antifungal agents with low side effects.

Interest in herbal medicines is growing, particularly in countries with rich ethnomedical traditions, such as Thailand. Natural products, rich in bioactive compounds, offer a promising alternative to synthetic drugs due to their diverse therapeutic properties and generally low side effect profiles. Several studies documented antifungal activities of plant extracts and essential oils. For instance, extracts from various plant parts (rhizome, root, leaves, stem, and flower) of species including *Piper betle*, *Punica granatum*, *Curcuma longa*, and *Alpinia galanga*, have been used in traditional medicine for bacterial and fungal infections and have demonstrated anticandidal activity [5-8]. The antifungal activity is attributed to phytochemicals, including flavonoids, saponins, and alkaloids, found in ethanolic extracts. Among the natural products, essential oils, such as lemongrass, clove, cinnamon, peppermint, and eucalyptus, are commonly used in complementary medicine to treat oral infections [9, 10]. However, there is limited knowledge about the activity of these plant extracts against oral candidiasis isolates of *C. albicans* and NAC, which are resistant to the major classes of antifungal drugs (polyenes and azoles) [3, 11]. Additionally, few studies have explored the combination of plant extracts and essential oils against *Candida* isolates. Therefore, effective combinations of these natural products could provide new antifungal agents for treating oral candidiasis.

This study aimed to investigate the anti-*Candida* activity of 13 ethanol extracts and 6 essential oils from Thai herbs. The most effective extracts and oils were tested against three oral candidiasis isolates, with their major compounds identified to explore potential anticandidal mechanisms. The synergistic antifungal effects of combining these extracts and oils were evaluated.

2. Materials and Methods

2.1 Preparation of plant extracts

Thirteen Thai traditional plants were collected from local areas in Phitsanulok, Thailand (Table 1). The samples were washed, dried at 60 °C for 24 hours, and then ground into a fine powder. They were extracted by maceration with 95% ethanol at room temperature for 3 days, repeated three times. The extracts were filtered and concentrated using a rotary evaporator (Buchi, Switzerland). A stock solution of plant extracts in dimethyl sulfoxide (DMSO, RCI Labscan, Thailand) was prepared and diluted with a solution of 4% DMSO and 4% Tween 80 (Phitsanu Chemical, Thailand) to a concentration of 10 mg/mL for anticandidal activity tests.

2.2 Preparation of essential oils

Essential oils, including lemongrass (product code; 2562-40003), clove bud (product code; 2562-20216), cinnamon bark (product code; 2562-20104), cinnamon leaf (product code; 2562-20086), peppermint (product code; 2562-20103), and eucalyptus (product code; 2562-20014), were purchased from Thai China Flavours & Fragrances Industry Co., Thailand. To test their antifungal activity, the essential oils were diluted in a solution of 4% DMSO and 4% Tween 80 to a concentration of 20 mg/mL.

2.3 Anticandidal activity

2.3.1 Strains and Culture Conditions

C. albicans ATCC10231 is obtained from the Faculty of Medical Sciences, Naresuan University. At the same time, clinical isolates of C. albicans R01, C. krusei, and C. dubliniensis were collected from the Faculty of Dentistry at Naresuan University. All strains were preserved on Sabouraud Dextrose Agar (SDA, Himedia, India) slants and subcultured onto SDA plates at 37 °C for 24 hours before testing.

2.3.2 Agar disk diffusion method

The plant extracts (PE) and essential oils (EO) were evaluated for their ability to inhibit *C. albicans* ATCC 10231 growth using a modified agar disk diffusion assay (Clinical and Laboratory Standards Institute (CLSI) M44-A2 protocol). A yeast suspension (1-5 × 10^6 cells/mL) was spread onto Mueller-Hinton agar containing 2% glucose and 0.5 μg/mL methylene blue dye. Paper disks, 6 mm, impregnated with the extracts or oils, were placed on agar surfaces, and their antifungal activity was assessed by measuring the size of the clear zones around the disc after incubation at 37 °C for 24 hours [12].

2.3.3 Determination of minimum inhibitory concentrations (MIC) and minimum fungicidal concentration (MFC)

The MIC against was determined by the broth dilution method following the method by Rodríguez-Tudela *et al*. (2001) [13]. The samples were serially diluted two-fold with RPMI-1640 medium (GibcoTM, Austria) in microtiter plates to concentrations ranging from 0.020 to 5.00 mg/mL. *C. albicans* ATCC 10231 suspension (1 x 10^6 cells/mL) was added to each well. Various concentrations of nystatin, ranging from 1.0 to 250 µg/mL, and Candida in RPMI-1640 medium were designated as the positive control and control, respectively. The plates were incubated at 37 °C for 24 hours. *Candida* growth was measured by optical density at 600 nm. The MIC was the lowest concentration that provided 90% growth inhibition. The percentage of growth inhibition was calculated using the following equation: %Inhibition = [1- (A_{t24} – A_{t0})/Ac_{t24} – Ac_{t0})] x 100, where A_{t24} and A_{t0} are the OD of the test well at 24 hours and 0 hours. Ac_{t24}, $A_{t0,}$ and Ac_{t0} are the OD of the control healthy growth at 24 hours and 0 hours. The MFC was evaluated by incubating turbidity-free wells on SDA plates at 37 °C for 24 hours. The lowest concentration preventing visible growth was determined. All experiments were conducted in triplicate [14]. The plant samples with large, clear zones and low MIC and MFC values were selected for further testing of anticandidal activity against clinical isolates of *C. albicans* R01 and NAC species (*C. krusei* and *C. dubliniensis*) (Table 3).

2.4 Identification of major compounds using GC-MS analysis

The component identification of PE and EO was achieved by the GC-MS analysis using HP-5MS series (Agilent, USA), with a capillary column (30 m × 250 µm, film thickness 0.25 µm). The column temperature was maintained at 50°C for 2 minutes. The column temperature was initially set at 70 °C for 5 min, then increased to 120 °C at a rate of 3 °C/min, followed by an additional 5 °C/min to 270 °C, and maintained at this temperature for 3 min. A 1 µL manual injection was performed in a split mode (1:100), with helium as the carrier gas at a flow rate of 1 mL/min. The scan range is 35–550 m/z with a scan rate of 1000 amu/s. The components were identified by comparing their mass spectra with published data and performing computer matching with the National Institute of Standards and Technology (NIST17.L) library.

2.5 Determination of synergistic activity from a combination of essential oils and plant extracts

The synergistic activities of selected EO and PE combinations were determined using the checkerboard dilution assay [15]. The respective MIC values of EO and PE were used together to define a fractional inhibitory concentration (FIC) of 1. The dilutions of each agent's FIC were prepared in a series of 0xMIC, 1.25xMIC, 0.25xMIC, 0.50xMIC, 0.75xMIC, and 1xMIC in a 96 well-plate. *C. albicans* R01 was added to the combinations and incubated at 37 °C for 24 hours. The MIC values were determined as described above. The FIC index (FICI) was determined according to the following equation [16]:

FIC_{EO} = MIC of EO in combination / MIC of EO alone

FIC_{PE} = MIC of PE in combination / MIC of PE alone

FICI = FIC_{EO} + FIC_{PE}

The results are interpreted as follows: FICI ≤ 0.5, synergistic; > 0.5 – 1.0, additive; > 1.0 – 4.0, indifference; > 4.0, antagonistic.

2.6 Statistical analysis

The extraction of plants was repeated three times, and the mean % yield values were calculated. All microbiological tests were repeated on three different occasions, with triplicate determinations on each occasion.

3. Results and Discussion

C. albicans is a common cause of oral fungal infections, especially in people with weakened immune systems. The overuse of antifungal agents has led to drug-resistant strains [17]. This study aims to identify natural, plant-based alternatives that can combat C. albicans, potentially through a synergistic combination. The selection of plant extracts for this study was based on their established antifungal potential and traditional use in treating fungal infections. Numerous studies have demonstrated the anticandidal activity of plants against various *Candida* species [17-19]. Ethanol was chosen as the extraction solvent due to its efficacy in extracting bioactive compounds, coupled with its non-toxic and biodegradable nature [20]. Commercial

essential oils were employed in this study to assess their feasibility for the large-scale production of potential products. The company provided certificates of analysis for each essential oil, confirming that each essential oil meets its specified characteristics.

Table 1. Anticandidal activity of plant extracts against *C. albicans* ATCC10231

Family	Scientific name	Part used	% yield (dry weight)	Inhibition zone diameter (mm)*	MIC (mg/mL)	MFC (mg/mL)
Euphorbiaceae	*Euphorbia hirta* L.	Leaf	17.30 ± 2.13	15.33 ± 2.52	5.000	> 5.000
	Baliospermum solanifolium (Burm.) Suresh	Leaf	14.62 ± 0.66	nz	> 5.000	> 5.000
	Acalypha indica L.	Leaf	15.74 ± 1.32	nz	> 5.000	> 5.000
Piperaceae	*Piper betle* L.	Leaf	20.65 ± 2.06	24.67 ± 0.58	0.313	0.625
	Piper sarmentosum Roxb	Leaf	11.63 ± 0.91	8.67 ± 0.58	0.625	> 5.000
Fabaceae	*Leucaena leucocephala* (Lam.) de Wit	Leaf	16.23 ± 0.50	nz	> 5.000	> 5.000
	Tamarindus indica L.	Seed coat	32.57 ± 2.67	nz	> 5.000	> 5.000
Zingiberaceae	*Curcuma longa* L.	Rhizome	27.20 ± 3.99	8.67 ± 1.15	> 5.000	> 5.000
	Curcuma manga Val.& Zijp	Rhizome	10.68 ± 0.50	Nz	> 5.000	> 5.000
	Alpinia galanga (L.) Willd	Rhizome	18.81 ± 1.98	9.33 ± 1.15	1.250	1.250
	Boesenbergia rotunda (L.) Mansf.	Rhizome	8.24 ± 0.26	8.33 ± 0.58	> 5.000	> 5.000
	Curcuma zedoaria (Christm.) Roscoe	Rhizome	11.35 ± 1.19	8.33 ± 0.58	> 5.000	> 5.000
Bignoniaceae	*Dolichandrone serrulata* (Wall. ex DC.) Seem.	Leaf	26.25 ± 1.03	nz	> 5.000	> 5.000
	Nystatin			17.00 ± 2.65	0.003	0.003

Data are reported as Mean ± SD; nz = No inhibition zone; * = 6 mm paper disk; MIC = Minimum inhibitory concentration; MFC = Minimum fungicidal concentration

3.1 Anticandidal activity of plant extracts and essential oils

Table 1 shows that ethanolic extracts from seven of thirteen plants had significant anticandidal activity. *Piper betle* exhibited the largest inhibition zone (~25 mm), followed by *Euphorbia hirta*, *Alpinia galanga*, *Curcuma longa*, *Boesenbergia rotunda*, and *Curcuma zedoaria*. *P. betle* was most active against *C. albicans* ATCC10231, with MIC and MFC values of 0.313 mg/mL and 0.625 mg/mL, respectively.

Table 2 shows the inhibitory zone, MIC, and MFC of six EOs against *C. albicans* ATCC10231. All EOs demonstrated antifungal activity, with MIC and MFC values ranging from 0.078 to 2.50 mg/mL and 0.078 to 5.00 mg/mL, respectively. Cinnamon bark oil had the lowest MIC and MFC (0.039 mg/mL), followed by lemongrass, clove bud, cinnamon leaf, peppermint, and eucalyptus oils.

Table 2. Anticandidal activity of essential oils against *C. albicans* ATCC10231

Essential oils	Inhibition zone diameter (mm)*	MIC (mg/mL)	MFC (mg/mL)
Lemongrass oil	17.67 ± 1.53	0.156	0.313
Clove bud oil	20.33 ± 0.58	0.313	0.625
Cinnamon bark oil	> 50	0.078	0.078
Cinnamon leaf oil	24.00 ± 1.00	0.156	1.250
Peppermint oil	Nz	2.500	5.000
Eucalyptus oil	Nz	>10	>10
Nystatin	17.00 ± 2.65	0.003	0.003

Data are reported as Mean ± SD; nz = No inhibition zone; * = 6 mm paper disk; MIC = Minimum inhibitory concentration; MFC = Minimum fungicidal concentration

P. betle and *A. galanga* extracts showed potential anticandidal activity with the lowest MIC and MFC values against *C. albicans* ATCC10231. However, the MIC and MFC values of these PE against *C. albicans* are inconsistent with those of previous studies. In another study using the same fungus and extract solvent, *P. betle* showed antifungal activity against *C. albicans*, with a much higher MIC value of 3.13 mg/mL and an MFC value of 4.17 mg/mL. On the other hand, their studies showed a slight antifungal activity of *A. galanga* against *C. albicans* [18]. In the study by Khodavandi *et al.* [19], the methanolic extract of A. galanga exhibited no antifungal activity against *C. albicans* and *C. krusei*, but showed activity against *C. glabrata* and *C. tropicalis*, with the same MIC value of 0.064 mg/mL. The different antifungal effects observed in previous studies compared to the present study may be attributed to variations in the main ingredients of the tested substance, the types of fungi used, or the method of extraction. Furthermore, among the tested essential oils, 3 EOs —cinnamon bark oil, lemongrass oil, and clove bud oil — exhibited the most effective antifungal activity, with cinnamon bark oil possessing the strongest inhibitory effect against *C. albicans* ATCC 10231. Similarly, Satthanakul *et al*. (2019) demonstrated that cinnamon oil exhibited the lowest MIC, followed by lemongrass oil and clove oil against *C. albicans* [15].

3.2 Chemical composition of plant extracts and essential oils

Two PE (*P. betle* and *A. galanga* extract) and 3 EO (lemongrass oil, clove oil, and cinnamon bark oil) with low MIC and MFC values were chosen for further studies on their chemical composition and the activity against clinical isolates. The major compounds of PE and EO are shown in Table 3. Four major compounds of *P. betle* extract were 4-allyl-1,2-diacetoxybenzene (29.5%), hydroxychavicol (24.8%), eugenol (24.7%), and eugenol acetate (21.0%). The major compound of *A. galanga* extract was 1'-acetoxychavical acetate (78.0%). Furthermore, the major compounds of all EO were geranial (42.7%) and neral (22.2%) in lemongrass oil, eugenol (85.5%) in clove bud oil, and cinnamaldehyde (80.6%) in cinnamon bark oil. The major compounds of the most effective 2 PE and 3 EO were further elucidated using GC-MS. The compounds identified in the tested samples are similar to those previously reported for *P. betle* extract (hydroxychavicol 69.46%, 4-chromanol 24% and eugenol 4.86%) [20]; and *A. galanga* extract (1,8-cineol, α-fenchyl acetate, β-farnesene, β-bisabolene, α-bergamotene, β-pinene, and 1'acetoxychavicol acetate) [21]. In the study by Nordin *et al*. (2014), *P. betle* extract treatment led to physical damage and morphological alterations in *Candida* cells [22]. Hydroxychavicol, isolated from P. betle leaves, was also reported to be effective against various fungal species [23]. The antifungal activity of *A. galanga* extract against *Candida* species has been reported [19]. The *A. galanga* extract is reported to cause damage to the outer and inner membranes, as well as coagulation of the cytoplasm, in *Staphylococcus aureus* cells [24].

Citral, eugenol, and cinnamaldehyde, the major compounds in lemongrass, clove bud, and cinnamon bark oils, have been shown to have antifungal activity against *Candida* species [15, 21]. Citral disrupts cell membrane integrity [25], while eugenol and cinnamaldehyde deactivate hydrolytic enzymes, generate reactive oxygen species, induce apoptosis, and modulate ergosterol content [26].

Table 3. The major compounds of plant extracts and essential oils were determined by GC-MS

Plant extracts/ Essential oils	Main compounds	Retention time (min)	Relative area (%)
P. betle extract	Eugenol	22.9	24.7
	Hydroxychavicol	26.5	24.8
	Eugenol acetate	28.2	21.0
	4-allyl-1,2-diacetoxybenzene	31.3	29.5
A. galanga extract	1′-acetoxychavical acetate	31.2	78.0
Lemongrass oil	6-methyl-5-hepten-2-one	6.6	3.6
	Beta-myrcene	6.7	12.5
	Isoneral	14.8	5.3
	Beta-citral (Neral)	17.8	22.2
	Geraniol	17.9	6.1
	Alpha-citral (Geranial)	18.7	42.7
Clove bud oil	Eugenol	22.4	85.5
	Caryophyllene	24.7	10.4
	Eugenol acetate	28.2	4.2
Cinnamon bark oil	Cinnamaldehyde	18.6	80.6
	Eugenol	22.4	19.4

Relative area = compound percentages were obtained electronically from the GC-MS percent area data.

3.3 Anticandidal activity of plant extracts and essential oils against clinical isolates of *Candida* species

P. betle extract, *A. galanga* extract, lemongrass oil, clove oil, and cinnamon bark oil demonstrated anticandidal activity against clinical isolates of *C. albicans* R01, *C. krusei*, and *C. dubliniensis*. All extracts had MIC/MFC values ranging from 0.156 to 5.000 mg/mL. Cinnamon bark oil had the lowest MIC among all *Candida* species. *A. galanga* extract was particularly effective against *C. krusei* (Table 4). Some *in vitro* studies have reported low susceptibility of antifungal agents or mouthwashes in oral *C. albicans* isolates [27, 28]. Thus, utilizing clinical isolates to test the effectiveness of antifungal agents is necessary for research on anticandidal activity. To this end, all EO and PE were tested against 3 clinical isolates of *Candida* species. Although they showed antifungal activity against all 3 *Candida* species, it was worth noting that *C. krusei* was more susceptible to *A. galanga* extract than *C. dubliniensis* and *C. albicans*. These results were possibly related to its ability to alter the cell surface hydrophobicity (CSH) of several *Candida* species. Harun and Razak (2013) demonstrated that *C. krusei* showed the highest degree of CSH, followed by C. dubliniensis and C. albicans, at 30.23%, 26.19%, and less than 10%, respectively [29]. The major antimicrobial phytochemicals in *A. galanga* extract are hydrophobic compounds, particularly 1′- acetoxychavicol acetate (1′-ACA) [6], which may alter the CSH of *Candida* cells and could penetrate the CSH in the cell wall matrix of *C. krusei* more easily than *C. dubliniensis* and *C. albicans*. However, this postulate requires more studies to confirm the mode of action of 1′-ACA in *A. galanga* extract against different *Candida* species.

Table 4. Minimum inhibitory concentrations (MIC) and minimum fungicidal concentration (MFC) of plant extracts and essential oils against clinical isolates of *Candida* species*

Essential oils/ plant extracts	MIC/MFC (mg/mL)		
	***C. albicans* R01**	***C. krusei***	***C. dubliniensis***
P. betle extract	2.500/2.500	1.250/2.500	2.500/2.500
A. galanga extract	2.500/5.000	0.313/0.313	1.250/1.250
Lemongrass oil	0.313/0.625	0.313/0.313	0.313/0.313
Clove bud oil	0.625/1.250	0.625/2.500	0.625/1.250
Cinnamon bark oil	0.156/0.156	0.156/0.156	0.156/0.156
Chlorhexidine	0.031/0.031	0.004/0.008	0.008/0.016

* Representative data from three duplicate experiments

3.4 Synergistic activity from a combination of essential oils and plant extracts

Table 5 shows that combining EOs and PEs reduced MIC values against *C. albicans* R01. Interestingly, adding all EO decreased the MIC values of P. *betle* 8-fold *and A. galanga* 4-fold, while two PE reduced the MIC values of all EO by 2-fold. All combinations had FICI values between 0.625 and 0.875, indicating an additive effect. Plant-based products, like *P. betle* and *A. galanga* extracts, offer potential alternatives to antifungal drugs. Therefore, the synergistic interaction between PE and EO may be a novel strategy for treating infections. The present study found that combining EOs with *P. betle* or *A. galanga* extracts effectively reduced MIC values against *C. albicans*, a common drug-resistant oral pathogen [30]. Recent studies have shown synergism between essential oils and antifungal drugs. The combination of CHX with either clove oil, cinnamon oil, or lemongrass oil exhibited synergistic effects (FICI ≤ 0.5) against *C. albicans* ATCC10231 and additive effects against clinical isolates of *C. tropicalis* and *C. krusei* [15]. Combining three essential oils (*Thymus leptobotrys, Origanum compactum, and Artemisia herba alba*) with two common antifungal drugs (fluconazole or amphotericin B) was more effective against four *Candida* strains. The addition of all tested EO at sub-inhibitory concentrations reduced the fluconazole and amphotericin B MICs of the tested *Candida* strains by 16 to 512-fold and 1 to 4-fold [31]. Previous studies have demonstrated that the synergistic effect of plants, when combined with other antimicrobials with different modes of action, may inhibit multiple targets.

Three common EO constituents (citral, eugenol, and cinnamaldehyde) disrupt membrane integrity by inhibiting ergosterol biosynthesis [30, 32]. Therefore, combining EO with PE might enhance PE penetration and reduce EO toxicity, offering a promising strategy for treating *Candida* infections. Recent studies have shown that *Candida* species, particularly *C. albicans*, tend to form complex biofilms, which are frequently detected on denture surfaces and oral tissues [3]. Biofilm formation represents a major virulence factor contributing to the pathogenesis of oral candidiasis, also known as denture stomatitis [33]. These biofilms exhibit increased resistance to most antifungal drugs, leading to treatment failure. This resistance is likely due to a combination of factors: high cell density, extracellular matrix, persister cells, drug efflux pumps, and phenotypic alterations in sessile cells [27, 33]. Consequently, the potential use of these combinations to inhibit and control biofilm formation associated with *Candida* infection is under investigation. These extracts and essential oils show high potential as healthcare product ingredients due to their biological activities and favorable toxicity profiles. For example, *Piper betle* leaf extract exhibited moderate toxicity to *Artemia salina* (LC_{50}: 0.58–0.61 mg/mL), and it was deemed safe in rats concerning hematotoxicity, hepatotoxicity, genotoxicity, organ weights, gross morphology, and behavior [34, 35]. Similarly, *Alpinia galanga* extract is safe in a subchronic rat toxicity study [36]. Lemongrass oil and citral exhibit low toxicity (LD_{50} > 2000 mg/kg) in albino rats and are classified as category 5/unclassified under the Globally Harmonized System for chemical hazards [37]. Clove buds and their extracts are FDA-approved food additives. A phenolic-rich clove fraction demonstrated no adverse effects in Wistar rats at 1000 mg/kg body weight/day [38]. Furthermore, cinnamon oil and its constituents offer a promising natural alternative with diverse therapeutic potential. Studies indicate that doses of cinnamon extract below 0.5 g/kg are generally safe for rats [39, 40].

Table 5. MIC and FICI of essential oils combinations with plant extracts against clinically isolated strains of *C. albicans* R01*

Combinations PE/EO	MIC**in combination PE/EO	FIC_{PE} /FIC_{EO}	FICI	Outcome
P. betle extract / Lemongrass oil	0.313/0.156	0.125/0.500	0.625	Additive
P. betle extract / Clove bud oil	0.313/0.313	0.125/0.500	0.625	Additive
P. betle extract / Cinnamon bark oil	0.313/0.078	0.125/0.500	0.625	Additive
A. galanga extract/ Lemongrass oil	0.625/0.156	0.250/0.500	0.750	Additive
A. galanga extract/ Clove bud oil	0.313/0.469	0.125/0.750	0.875	Additive
A. galanga extract/ Cinnamon bark oil	0.313/0.078	0.125/0.500	0.625	Additive

* Representative data from three duplicate experiments

** MIC of essential oil and plant extract expressed in mg/mL.

4. Conclusions

This study demonstrates that lemongrass oil, clove oil, cinnamon bark oil, and the extracts of *P. betle* and *A. galanga* possessed potent antifungal effects on oral candidiasis isolates, including *C. albicans* R01, *C. krusei*, and *C. dubliniensis*. The combination of these EOs, either *P. betle* extract or *A. galanga* extract, was observed to decrease the individual MIC value of all tested agents, indicating an additive effect against clinical isolates of *C. albicans*. Moreover, the presence of bioactive compounds in these EO and PE indicates the potential of their future application as plant-based antifungal agents for the treatment of oral candidiasis.

5. Acknowledgements

The authors gratefully acknowledge the financial support provided by Naresuan University, Thailand Science Research and Innovation (TSRI), National Science Research and Innovation Fund (NSRF) (Fundamental Fund: Grant No. R2566B016, 2023), and Thailand's Ministry of Science and Technology (MOST) under the Thai Government Science and Technology Scholarship.

Author Contributions: Conceptualization, methodology and validation, P.S., W.T., R.K. and S.L.; formal analysis, P.S., and S.L.; investigation, P.S., and S.L.; data curation, P.S., W.T., R.K. and S.L.; writing—original draft preparation, P.S.; writing—review and editing, W.T., R.K. and S.L.; supervision, W.T., and S.L.; project administration, W.T., R.K. and S.L.; funding acquisition, W.T., R.K. and S.L. All authors have read and agreed to the published version of the manuscript.

Conflicts of Interest: The authors declare no conflict of interest.

References

[1] Karajacob, A. S.; Azizan, N. B.; Al-Maleki, A. R. M.; Goh, J. P. E.; Loke, M. F.; Khor, H. M.; Ho, G. F.; Ponnampalavanar, S.; Tay, S. T., *Candida* species and oral mycobiota of patients clinically diagnosed with oral thrush. *PLoS One* **2023,** *18*(4), e0284043. https://doi.org/10.1371/journal.pone.0284043

[2] Mousa, M. A.; Lynch, E.; Kielbassa, A. M., Denture-related stomatitis in new complete denture wearers and its association with *Candida* species colonization: a prospective case-series. *Quintessence International* **2020,** *51*(7), p554.

[3] Tata, W.; Thepbundit, V.; Kuansuwan, C.; Preechasuth, K., Distribution of *Candida* species in oral candidiasis patients: association between sites of isolation, ability to form biofilm, and susceptibility to antifungal drugs. *Journal of Associated Medical Sciences* **2019,** *52*(1), 1-7.

[4] Quindós, G.; Gil-Alonso, S.; Marcos-Arias, C.; Sevillano, E.; Mateo, E.; Jauregizar, N.; Eraso, E., Therapeutic tools for oral candidiasis: current and new antifungal drugs. *Medicina Oral Patologia Oral y Cirugia Bucal* **2019,** *24*(2), e172-e180. https://doi.org/10.4317/medoral.22978

[5] Adamczak, A.; Ożarowski, M.; Karpiński, T. M., Curcumin, a natural antimicrobial agent with strain-specific activity. *Pharmaceuticals (Basel)* **2020,** *13*(7). https://doi.org/10.3390/ph13070153

[6] Kojima-Yuasa, A.; Matsui-Yuasa, I., Pharmacological effects of 1'-acetoxychavicol acetate, a major constituent in the rhizomes of *Alpinia galanga* and *Alpinia conchigera*. *Journal of Medicinal Food* **2020,** *23*(5), 465-475. https://doi.org/10.1089/jmf.2019.4490

[7] Meccatti, V. M.; Santos, L. F.; de Carvalho, L. S.; Souza, C. B.; Carvalho, C. A. T.; Marcucci, M. C.; Abu Hasna, A.; de Oliveira, L. D., Antifungal action of herbal plants' glycolic extracts against *Candida* species. *Molecules* **2023,** *28*(6), 2857. https://doi.org/10.3390/molecules28062857

[8] Nayaka, N. M.; Sasadara, M. M.; Sanjaya, D. A.; Yuda, P. E.; Dewi, N. L.; Cahyaningsih, E.; Hartati, R., *Piper betle* (L): recent review of antibacterial and antifungal properties, safety profiles, and commercial applications. *Molecules* **2021,** *26*(8). https://doi.org/10.3390/molecules26082321

[9] Hou, T.; Sana, S. S.; Li, H.; Xing, Y.; Nanda, A.; Netala, V. R.; Zhang, Z., Essential oils and its antibacterial, antifungal and anti-oxidant activity applications: a review. *Food Bioscience* **2022,** *47*, 101716. https://doi.org/10.1016/j.fbio.2022.101716

[10] Serra, E.; Hidalgo-Bastida, L. A.; Verran, J.; Williams, D.; Malic, S., Antifungal activity of commercial essential oils and biocides against *Candida albicans*. *Pathogens* **2018,** *7*(1), 15. https://doi.org/10.3390/pathogens7010015

[11] Kermani, F.; Taghizadeh-Armaki, M.; Hosseini, S. A.; Amirrajab, N.; Javidnia, J.; Fami Zaghrami, M.; Shokohi, T., Antifungal resistance of clinical *Candida albicans* isolates in Iran: a systematic review and meta-analysis. *Iranian Journal of Public Health* **2023,** *52*(2), 290-305. https://doi.org/10.18502/ijph.v52i2.11874

[12] Wong, S. S. W.; Kao, R. Y. T.; Yuen, K. Y.; Wang, Y.; Yang, D.; Samaranayake, L. P.; Seneviratne, C. J., In vitro and in vivo activity of a novel antifungal small molecule against *Candida* infections. *PLoS one* **2014,** *9*(1), e85836. https://doi.org/10.1371/journal.pone.0085836

[13] Rodríguez-Tudela, J. L.; Cuenca-Estrella, M.; Díaz-Guerra, T. M.; Mellado, E., Standardization of antifungal susceptibility variables for a semiautomated methodology. *Journal of Clinical Microbiology* **2001,** *39*(7), 2513-2517. https://doi.org/10.1128/JCM.39.7.2513-2517.2001

[14] Taweechaisupapong, S.; Aieamsaard, J.; Chitropas, P.; Khunkitti, W., Inhibitory effect of lemongrass oil and its major constituents on *Candida* biofilm and germ tube formation. *South African Journal of Botany* **2012,** *81*, 95-102. https://doi.org/10.1016/j.sajb.2012.06.003

[15] Satthanakul, P.; Taweechaisupapong, S.; Luengpailin, S.; Khunkitti, W., The antifungal efficacy of essential oils in combination with chlorhexidine against *Candida* spp. *Songklanakarin Journal of Science and Technology* **2019,** *41*(1), 144-150.

[16] Lambert, R. J.; Lambert, R., A model for the efficacy of combined inhibitors. *Journal of Applied Microbiology* **2003,** *95*(4), 734-43. https://doi.org/10.1046/j.1365-2672.2003.02039.x

[17] Uddin, T. M.; Chakraborty, A. J.; Khusro, A.; Zidan, B. M. R. M.; Mitra, S.; Emran, T. B.; Dhama, K.; Ripon, M. K. H.; Gajdács, M.; Sahibzada, M. U. K.; Hossain, M. J.; Koirala, N., Antibiotic resistance in microbes: history, mechanisms, therapeutic strategies and future prospects. *Journal of Infection and Public Health* **2021,** *14*(12), 1750-1766. https://doi.org/10.1016/j.jiph.2021.10.020

[18] Azhari, M.; Sengaji, R. F., Antimicrobial activity of turmeric, ginger, and galangal rhizome ethanol extracts in combination using the checkerboard method. *Journal Borneo* **2023,** *3*(3), 139-148. https://doi.org/10.57174/j.born.v3i3.108

[19] Khodavandi, A.; Tahzir, N.; Cheng, P.; Yong, P.; Alizadeh, F.; Harmal, N.; Chong, P., Antifungal activity of *Rhizome coptidis* and *Alpinia galangal* against *Candida* species. *Journal of Pure and Applied Microbiology* **2013,** *7*, 1725-1730.

[20] Muruganandam, L.; Krishna, A.; Reddy, J.; Nirmala, G., Optimization studies on extraction of phytocomponents from betel leaves. *Resource-Efficient Technologies* **2017,** *3*(4), 385-393. https://doi.org/10.1016/j.reffit.2017.02.007

[21] Shahina, Z.; Ndlovu, E.; Persaud, O.; Sultana, T.; Dahms, T. E., *Candida albicans* reactive oxygen species (ROS)-dependent lethality and ROS-independent hyphal and biofilm inhibition by eugenol and citral. *Microbiology Spectrum* **2022,** *10*(6), e03183-22. https://doi.org/10.1128/spectrum.03183-22

[22] Nordin, M. A.; Wan Harun, W. H.; Abdul Razak, F.; Musa, M. Y., Growth inhibitory response and ultrastructural modification of oral-associated candidal reference strains (ATCC) by *Piper betle* L. extract. *International Journal of Oral Science* **2014,** *6*(1), 15-21. https://doi.org/10.1038/ijos.2013.97

[23] Singburaudom, N., Hydroxychavicol from *Piper betel* leave is an antifungal activity against plant pathogenic fungi. *Journal of Biopesticides* **2015,** *8*, 82-92. https://doi.org/10.57182/jbiopestic.8.2.82-92

[24] Oonmetta-aree, J.; Suzuki, T.; Gasaluck, P.; Eumkeb, G., Antimicrobial properties and action of galangal (*Alpinia galanga* Linn.) on *Staphylococcus aureus*. *LWT - Food Science and Technology* **2006,** *39*(10), 1214-1220. https://doi.org/10.1016/j.lwt.2005.06.015

[25] Miranda-Cadena, K.; Marcos-Arias, C.; Perez-Rodriguez, A.; Cabello-Beitia, I.; Mateo, E.; Sevillano, E.; Madariaga, L.; Quindós, G.; Eraso, E., In vitro and in vivo anti-*Candida* activity of citral in combination with fluconazole. *Journal of Oral Microbiology* **2022,** *14*(1), 2045813. https://doi.org/10.1080/20002297.2022.2045813

[26] Gupta, P.; Gupta, S.; Sharma, M.; Kumar, N.; Pruthi, V.; Poluri, K. M., Effectiveness of phytoactive molecules on transcriptional expression, biofilm matrix, and cell wall components of *Candida glabrata* and its clinical isolates. *ACS Omega* **2018,** *3*(9), 12201-12214. https://doi.org/10.1021/acsomega.8b01856

[27] Kaur, J.; Nobile, C. J., Antifungal drug-resistance mechanisms in *Candida* biofilms. *Current Opinion in Microbiology* **2023,** *71*, 102237. https://doi.org/10.1016/j.mib.2022.102237

[28] Olejnik, E.; Biernasiuk, A.; Malm, A.; Szymanska, J., Evaluation of antibacterial and antifungal properties of selected mouthwashes: studies. *Current Issues in Pharmacy and Medical Sciences* **2021,** *34*(3), 164-168. https://doi.org/10.2478/cipms-2021-0029

[29] Harun, W. H. A. W.; Razak, F. A., An in vitro study on the anti-adherence effect of *Brucea javanica* and *Piper betle* extracts towards oral *Candida*. *Archives of Oral Biology* **2013,** *58*(10), 1335-1342. https://doi.org/10.1016/j.archoralbio.2013.07.001

[30] Herman, A.; Herman, A. P., Herbal products and their active constituents used alone and in combination with antifungal drugs against drug-resistant *Candida* sp. *Antibiotics (Basel)* **2021,** *10*(6). https://doi.org/10.3390/antibiotics10060655

[31] Soulaimani, B.; Varoni, E.; Iriti, M.; Mezrioui, N.-E.; Hassani, L.; Abbad, A., Synergistic anticandidal effects of six essential oils in combination with fluconazole or amphotericin B against four clinically isolated *Candida* strains. *Antibiotics* **2021,** *10*(9), 1049. https://doi.org/10.3390/antibiotics10091049

[32] Wang, Y.; Yang, Q.; Zhao, F.; Li, M.; Ju, J., Synergistic antifungal mechanism of eugenol and citral against *Aspergillus niger*: molecular level. *Industrial Crops and Products* **2024,** *213*, 118435. https://doi.org/10.1016/j.indcrop.2024.118435

[33] Wall, G.; Montelongo-Jauregui, D.; Vidal Bonifacio, B.; Lopez-Ribot, J. L.; Uppuluri, P., *Candida albicans* biofilm growth and dispersal: contributions to pathogenesis. *Current Opinion in Microbiology* **2019,** *52*, 1-6. https://doi.org/10.1016/j.mib.2019.04.001

[34] Sonphakdi, T.; Tani, A.; Payaka, A.; Ungcharoenwiwat, P., Antibacterial and toxicity studies of phytochemicals from *Piper betle* leaf extract. *Journal of King Saud University-Science* **2024,** *36*(10), 103430. https://doi.org/10.1016/j.jksus.2024.103430

[35] Arambewela, L. S.; Arawwawala, L. D.; Kumaratunga, K. G.; Dissanayake, D. S.; Ratnasooriya, W. D.; Kumarasingha, S. P., Investigations on *Piper betle* grown in Sri Lanka. *Pharmacognosy Review* **2011,** *5*(10), 159-163. https://doi.org/10.4103/0973-7847.91111

[36] Shanmugasundaram, D., Subchronic toxicological evaluation of EnXtra™ (standardised extract of *Alpinia galanga* rhizome) in rats. *Journal of Complementary and Integrative Medicine* **2022,** *19*(3), 645-659. https://doi.org/10.1515/jcim-2021-0526

[37] Xavier, A.; Rani, S. S.; Shankar, R.; Nisha, A.; Sujith, S.; Uma, R., Evaluation of acute oral toxicity of lemon grass oil and citral in albino rats. *The Journal of Phytopharmacology* **2022**. https://doi.org/10.31254/phyto.2022.11410

[38] Nirmala, M. J.; Shiny, P. J.; Raj, U. S.; Saikrishna, N.; Nagarajan, R., Chapter 39 - Toxicity of clove (*Syzygium aromaticum*) extract. In *Clove (Syzygium aromaticum)*, Ramadan, M. F., Ed. Academic Press: **2022**, pp 663-674. https://doi.org/10.1016/B978-0-323-85177-0.00007-0

[39] Guo, J.; Jiang, X.; Tian, Y.; Yan, S.; Liu, J.; Xie, J.; Zhang, F.; Yao, C.; Hao, E., Therapeutic potential of cinnamon oil: chemical composition, pharmacological actions, and applications. *Pharmaceuticals* **2024,** *17*(12), 1700. https://doi.org/10.3390/ph17121700

[40] Adawiyah, R.; Serati-Nouri, H.; Abdul majid, F.; Sarmidi, M.; Aziz, R., Assessment of potential toxicological effects of cinnamon bark aqueous extract in rats. *International Journal of Bioscience, Biochemistry and Bioinformatics* **2015,** *5*, 36-44. https://doi.org/10.17706/ijbbb.2015.5.1.36-44

ASEAN
Journal of Scientific and Technological Reports
Online ISSN:2773-8752

Research article

Evaluating the Influence of Transition Metal Oxides on Anaerobic Digestion Performance

Nina Anggita Wardani[1*], Dwi Amalia[2], Muhammad Redo Ramadhan[3], Danang Jaya[4], Tunjung Wahyu Widayati[5], Eko Nursubiyantoro[6], Rizki Amanda Putra[7], Muhammad Athaya Khaliq[8], Qudrotunada Shofia Najla[9], and Naufal Raffa Syailendra[10]

[1] Chemical Engineering Department, Universitas Pembangunan Nasional Veteran Yogyakarta, Indonesia 55283
[2] Chemical Engineering Department, Universitas Pembangunan Nasional Veteran Yogyakarta, Indonesia 55283
[3] Chemical Engineering Department, Universitas Pembangunan Nasional Veteran Yogyakarta, Indonesia 55283
[4] Chemical Engineering Department, Universitas Pembangunan Nasional Veteran Yogyakarta, Indonesia 55283
[5] Chemical Engineering Department, Universitas Pembangunan Nasional Veteran Yogyakarta, Indonesia 55283
[6] Industrial Engineering Department, Universitas Pembangunan Nasional Veteran Yogyakarta, Indonesia 55283
[7] Chemical Engineering Department, Universitas Pembangunan Nasional Veteran Yogyakarta, Indonesia 55283
[8] Chemical Engineering Department, Universitas Pembangunan Nasional Veteran Yogyakarta, Indonesia 55283
[9] Chemical Engineering Department, Universitas Pembangunan Nasional Veteran Yogyakarta, Indonesia 55283
[10] Chemical Engineering Department, Universitas Pembangunan Nasional Veteran Yogyakarta, Indonesia 55283
* Correspondence: nina.anggita@upnyk.ac.id

Citation:
Wardani, A.N.; Amalia, D.; Ramadhan, R.M.; Jaya, D.; Widayati, W.T.; Nursubiyantoro, E.; Putra, A.R.; Khaliq, A.M.; Najla, S.Q.; Syailendra, R.N. Evaluating the influence of transition metal oxides on anaerobic digestion preformance. *ASEAN J. Sci. Tech. Report.* **2025**, *28*(4), e257685. https://doi.org/10.55164/ajstr.v28i4.257685.

Article history:
Received: January 28, 2025
Revised: May 25, 2025
Accepted: June 11, 2025
Available online: June 30, 2025

Abstract: Palm oil, the world's most widely consumed edible oil, produces palm oil mill effluent (POME) as a byproduct, which poses significant environmental risks if untreated due to its high organic content and pollutants. Anaerobic digestion (AD) is a process that converts organic waste into biogas, a promising renewable and sustainable energy source, especially for areas with abundant feedstock. Accelerators play a vital role in enhancing the performance of AD systems through various mechanisms. The high conductivity of TMOs facilitates efficient electron transfer, providing the fastest pathway for electron exchange between microorganisms. MnO_2 and Fe_2O_3 are abundantly available in Indonesia. This study compared MnO_2 and Fe_2O_3 to identify the most effective TMO for improving mesophilic batch AD performance in POME treatment. Results indicated that Fe_2O_3 was superior, increasing methane production volume by 21% and methane yield by 32% compared to AD without TMOs.

Keywords: Accelerator; Electron transport; Biogas; Renewable energy; Waste treatment

1. Introduction

Palm oil is the most widely demanded edible oil globally [1]. Indonesia ranks as the world's leading exporter of palm oil. The land area dedicated to oil palm plantations and the production of crude palm oil (CPO) experienced significant growth in 2018 compared to previous years. By 2022, the total area of oil palm plantations was estimated to have reached 15.34 million hectares, as illustrated in Figure 1 [2]. Each hectare of oil palm yields 10–35 tons of fresh fruit bunches (FFB) annually, indicating that in 2022, Indonesia produced approximately 153.4–536.9 million tons of FFB [3]. The production of palm oil generates a byproduct known as palm oil mill effluent (POME) during its extraction process. For every ton of FFB processed in palm oil mills, the resulting waste comprises 23% empty fruit bunch fibers, 12% mesocarp fibers, 5% shells, and 60% POME [4]. These proportions indicate that POME constitutes the most significant fraction of waste in the palm oil industry, amounting to

approximately 92.04–322.14 million tons in Indonesia in 2022. The wet extraction process of palm oil requires a substantial volume of water, with about 1.5 m^3 of water used per ton of FFB processed [5]. Of the estimated 5.0–7.5 tons of water needed to produce one ton of crude palm oil, more than 2.5–3.75 tons are converted into POME [6], [7]. According to A. A. Z. Lorestani [8], the processes contributing the most to POME generation are FFB sterilization (36%), crude palm oil extraction and clarification (60%), and the separation of kernels and shells in hydrocyclones (4%).

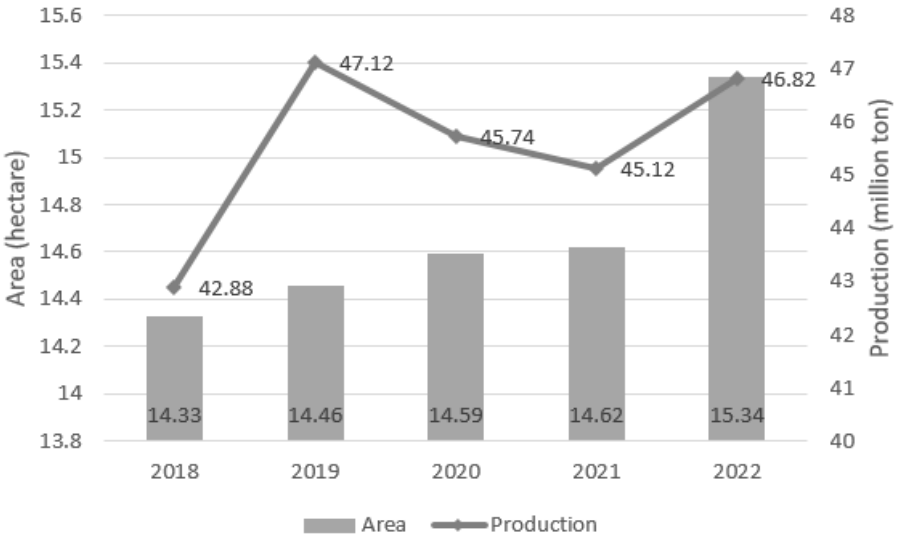

Figure 1. Palm oil plantation area in Indonesia [2]

If left untreated, industrial waste from POME poses a significant environmental risk due to its high concentration of organic matter and other pollutants, which can harm both fauna and flora, as well as compromise water quality. Exposure to POME has been linked to reduced plankton diversity and physiological and reproductive issues in fish [9]. Additionally, it can severely impact aquatic ecosystems by creating highly acidic conditions or triggering eutrophication, characterized by excessive algal growth on water surfaces. Traditional POME treatment methods typically employ anaerobic-aerobic lagoon systems, comprising at least two sequentially connected ponds, to reduce the organic content before discharge into surface waters. However, these systems face limitations, including solid accumulation, methane emissions, sludge and foam formation (which decrease treatment efficiency), and the requirement for large land areas. When POME is stored in open-air holding ponds for remediation, it releases methane, carbon dioxide, and hydrogen sulfide, contributing to global climate change [3].

The anaerobic digestion (AD) process converts organic waste into biogas, a promising renewable and sustainable energy source, particularly in regions with abundant feedstock. AD can be utilized for various organic materials, including agricultural waste, the organic fraction of municipal solid waste, sewage sludge, and industrial waste. POME has also been investigated as a potential substrate for AD systems due to its high organic content. Figure 2 shows the AD process scheme. The AD process involves several sequential microbial stages: hydrolysis, acidogenesis, acetogenesis, and methanogenesis. During methanogenesis, the collaborative interaction among diverse microorganisms is essential for efficient digestion, relying on effective interspecies electron transfer [10]. The process begins with fermentation, establishing a complex network of interspecies electron transfer to sustain cooperative microbial activity. Within this network, electron exchange between syntrophic bacteria (secondary fermenting bacteria) and methanogens is a critical step, addressing the intermediate bottleneck and ensuring the successful completion of final methanogenesis.

Accelerators play a vital role in enhancing the performance of AD systems through various mechanisms. These accelerators can be categorized into several types, including biological accelerators (such as enzymes, microbial consortia, and fungi), chemical reagents, macronutrients, minerals, trace elements, transition metal oxides (TMOs), and carbon-based materials [11], [12]. Under natural conditions, Direct Interspecies Electron Transport (DIET) occurs only through direct physical contact between bacteria and

methanogens. However, the addition of TMOs to AD systems eliminates the requirement for direct contact due to their conductive properties [13]. The high conductivity of TMOs facilitates efficient electron transfer, providing the fastest pathway for electron exchange between microorganisms [12], [14]. MnO_2 and Fe_2O_3 are abundantly available in Indonesia. This study aims to compare Fe_2O_3 and MnO_2 to determine the most effective TMO for enhancing the AD process in POME treatment.

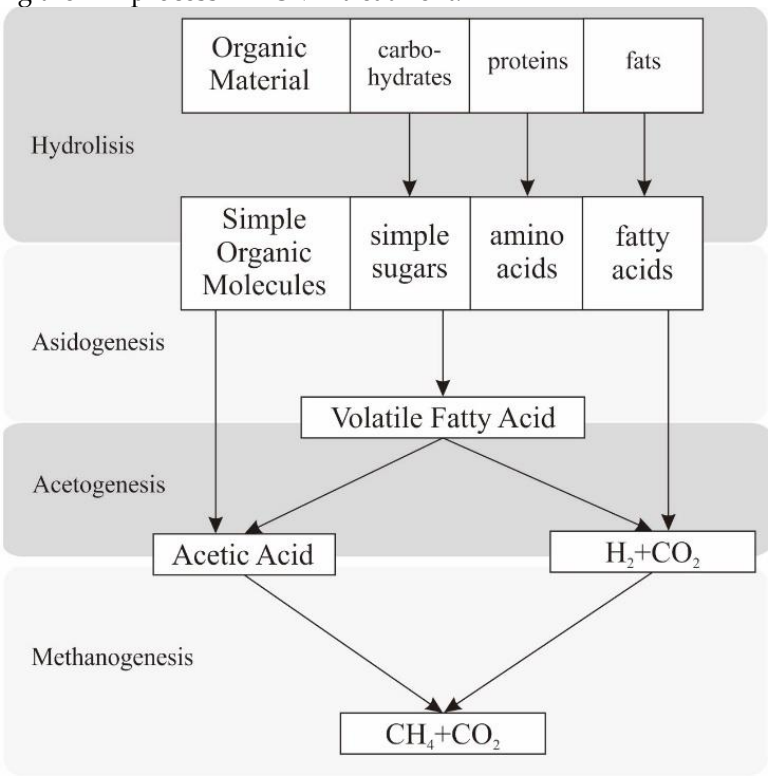

Figure 2. Anaerobic Digestion Scheme

2. Materials and Methods

2.1 Inoculum

The inoculum used in this research was digested cow manure (DCM) obtained from a biodigester at a cattle farm in Hargobinangun, Kaliurang, Yogyakarta, Indonesia. The inoculum was filtered to remove impurities and prevent clogging. The COD concentration of the inoculum was analyzed (with a measured value of 62,000 mg COD/L), and the inoculum was used on the same day the reactor was started.

2.2 Substrate

POME was used as the substrate for anaerobic digestion in this study. It was collected from a palm oil mill in Riau, Indonesia. To remove impurities, the POME was filtered using a 2 mm pore filter. The COD concentration of the POME was analyzed to determine the precise mixing ratio between the inoculum and the substrate. Table 1 presents the physical and chemical properties of the POME. The pH of the POME in this research was 4.5, indicating an acidic nature, which is typical for raw POME and aligns with the values reported by Saelor [15] (4.68 ± 0.27) and Suksong [16] (5.6). The COD concentration observed in this study was significantly higher (81,000 mg/L) compared to the values reported by Saelor [15] and Suksong [16]. The carbohydrate content in this research was 0.91%, equivalent to 73.71 g/L, which was also significantly higher than the values reported by Saelor [15] and Suksong [16]. The variation of both COD and carbohydrate may be attributed to differences in the palm oil milling process or feedstock composition [17].

Table 1. Physical and Chemical Properties of POME

Properties	This Research	[15]	[16]
pH	4.5	4.68 ± 0.27	5.6
COD (mg/L)	81000	42550 ± 6140	44000
C/N ratio	n/a	27.59	22.85
Carbohydrate	0.91%	9.00 ± 0.01 g/L	14.11 g/L

2.3 Reactor

Batch reactors with a working volume of 4 liters were used in this study. The reactors were operated at room temperature (27 °C). Each reactor was connected to a gasometer, based on the principle of water displacement. The gasometer was filled with a 75% salt-saturated solution at pH 2 to prevent gas absorption into the water [18]. Figure 3 illustrates the reactor setup used in this study.

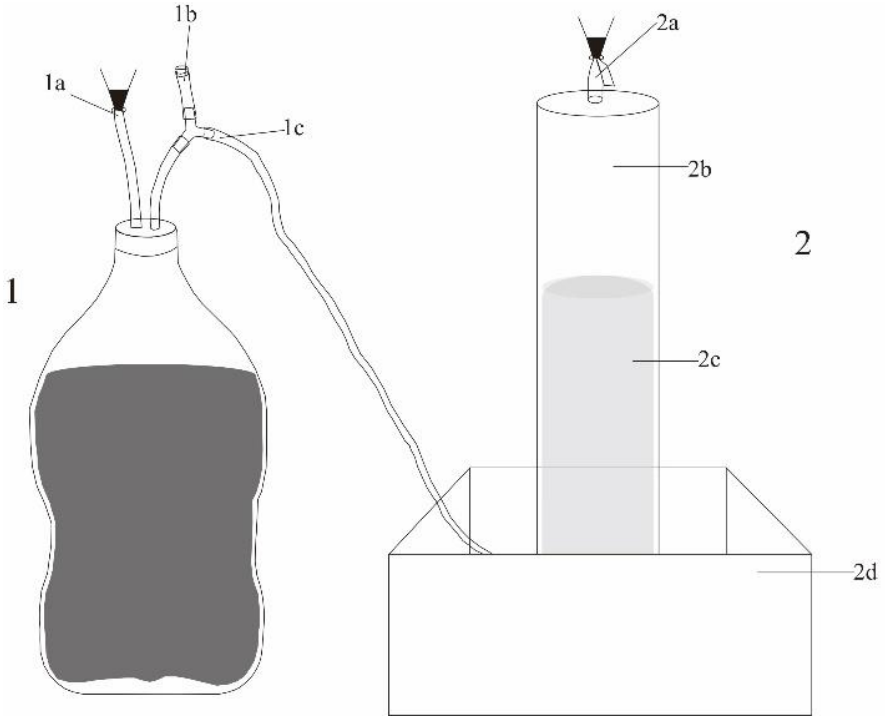

1	: reactor (4L)	2	: gasometer
1a	: liquid input and output port	2a	: gas output port
1b	: gas sampling port	2b	: column
1c	: gas output to gasometer	2c	: 75% saturated salt acidified
		2d	: water basin

Figure 3. Reactor Scheme in This Research

2.4 Experimental Part

2.4.1 Anaerobic Reactor Start Up

All reactors underwent a leakage test before use. The inoculum and substrate were mixed at an inoculum-to-substrate ratio of 4:1 (%COD). After mixing, the mixture was divided into 4-liter batches. The first two batches were loaded into two identical reactors without the addition of any TMO, serving as the control (RC). The second two batches were mixed with Fe_2O_3 (60 mg/L) until homogeneous and then loaded into two identical reactors (RFe). Similarly, the last two batches were mixed with MnO_2 (60 mg/L) and loaded

into two identical reactors (RMn). Each reactor was flushed with nitrogen to eliminate oxygen from the sludge and headspace. Following nitrogen flushing, each reactor was connected to a gasometer.

2.4.2 Anaerobic Reactor Operation

The batch reactors were operated under mesophilic conditions at 27 °C. Gas production volume was measured daily using the gasometer tube scale and basin scale [18]. The pH was maintained within the range of 7.0–7.5. If the pH dropped to 7.0 or below, 1 M NaOH was added to the reactor to adjust the pH.

2.4.3 Gas Analysis

Gas samples were collected weekly to analyze their CH_4 and CO_2 content. The analysis was performed using a Shimadzu GC-8A gas chromatograph equipped with a thermal conductivity detector (GC-TCD), manufactured in Japan.

2.4.4 Liquid Analysis

Liquid samples were collected twice a week. COD and sCOD analyses were conducted using the titrimetric method [19], while VFA analysis was performed using the distillation method [20].

3. Results and Discussion

3.1. Proximate Analysis

Proximate analysis was performed to characterize the substrate and inoculum. Table 2 presents the proximate analysis results for POME and DCM.

Table 2. Proximate Analysis Result of POME and DCM

Compound	POME	DCM
Protein	0.66% ± 0.01%	0.58% ± 0.03%
Lipid	0.85% ± 0.01%	0.08% ± 0.00%
Carbohydrate	0.91% ± 0.06%	0.84% ± 0.01%
Water	97.09% ± 0.06%	97.97% ± 0.01%
Ash	0.45% ± 0.42%	0.54% ± 0.03%

3.2 Biogas Analysis

Three reactors were used in this study: RC (control reactor), RFe (AD reactor with Fe_2O_3 addition), and RMn (AD reactor with MnO_2 addition). Figure 4 illustrates the biogas production of all three reactors. Two distinct peaks were observed, occurring around day 1 and day 9, which are associated with the degradation of carbohydrates and subsequently of complex macromolecules such as crude proteins, lignocelluloses, and aromatics. As reported by Yun [12], these complex compounds generally decompose more slowly compared to carbohydrates. Additionally, POME contains 32,505–36,894 ppm of long-chain fatty acids (LCFA), and the hydrolysis of lipids has been identified as the rate-limiting step in the anaerobic digestion of POME, which may explain why the second peak was more pronounced than the first [21]. Biogas production decreased significantly after Day 21. In line with this, cumulative methane production began to level off as shown in Figure 5. The lag phase lasted less than one day, and approximately 90% of the methane was produced by Day 12, indicating that the substrate was readily biodegradable [22]. RFe achieved the highest methane production, reaching 793.4 mL CH_4, which was 21% higher than that of the control reactor (RC). In contrast, RMn produced 7,6% less methane than the RC. Methane production volume was measured under controlled conditions at 25 ^{o}C and 1 atm.

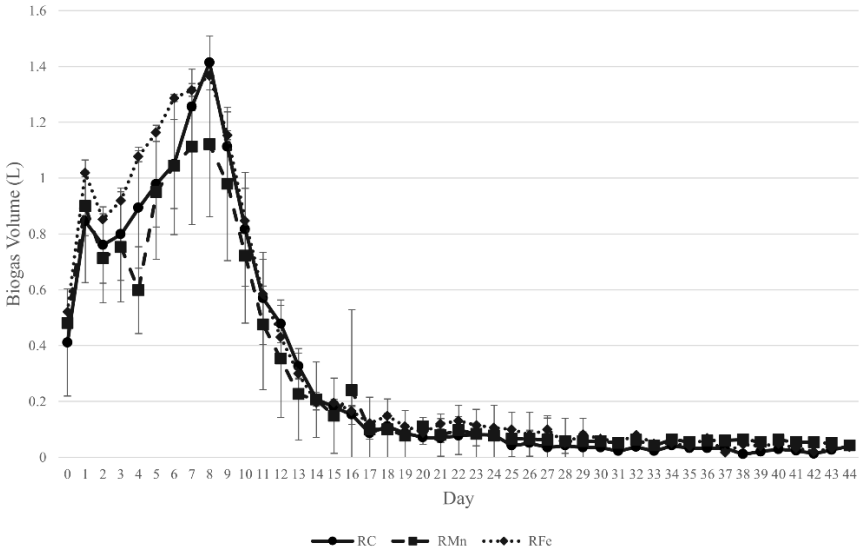

Figure 4. Biogas Production

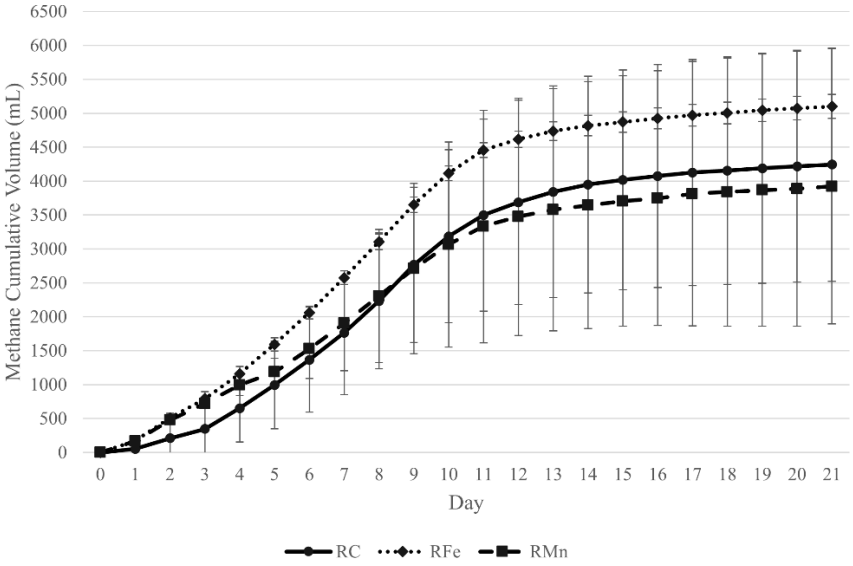

Figure 5. Cumulative Methane Production

3.3 Liquid Analysis

Figure 6 shows the volatile fatty acid (VFA) concentrations of all reactors, which remained stable and predominantly below 1,000 mg/L. VFAs are intermediate compounds in the AD process generated from acidogenesis and acetogenesis. However, VFAs accumulation can lower pH, becoming toxic to methanogens [23]. The optimal concentration of organic acids is less than 1,000 mg/L, with propionic acid levels below 200 mg/L [24]. All reactors experienced a sharp decline in VFA concentrations on Day 10, corresponding to the peak methane production on Day 9. This indicates high methanogen activity, as large amounts of VFAs were consumed and converted into methane.

Among the reactors, RMn had the lowest VFA concentration, yet its methane production was the lowest. Conversely, RFe exhibited the highest VFA concentration on Day 10 and also achieved the highest methane production, suggesting efficient acidogenic and acetogenic activity. After the peak methane production, VFA levels returned to their regular concentrations. On Day 21, when methane production was significantly reduced, RFe had the lowest VFA concentration.

At the beginning of the process, the VFA concentration in all reactors was 1,079 mg/L. By Day 21, VFA levels remained consistent across all reactors, indicating stable systems. The pH profile, shown in Figure 7, reflects this stability. Due to steady VFA levels, the pH remained stable in all reactors throughout the process. Figure 8 presents the profiles of COD and sCOD. Both COD and sCOD concentrations declined over time, with no accumulation of sCOD, indicating that the rates of acidogenesis and acetogenesis were higher than hydrolysis. On Day 10, when methane production peaked and VFA concentrations dropped, sCOD levels remained stable. This stability suggests that the reduction in VFA was due to enhanced methanogenic activity, with no inhibition of acidogenesis or acetogenesis. Similar trends of declining VFA during peak methane production have been observed in other studies [25], [26]. The type of substrate influences the rate-limiting step in anaerobic digestion. The observed trends in VFA and sCOD concentrations indicate that acidogenesis, acetogenesis, and methanogenesis proceeded rapidly. However, due to the high content of long-chain fatty acids (LCFA) in POME, lipid hydrolysis was identified as the rate-limiting step, as supported by these patterns [11], [21]. Figure 9 illustrates the percentage of COD removal for all reactors. The reactor without TMO (control reactor) exhibited the highest COD removal efficiency at 55.4%, compared to 50.6% for RFe and 43.7% for RMn.

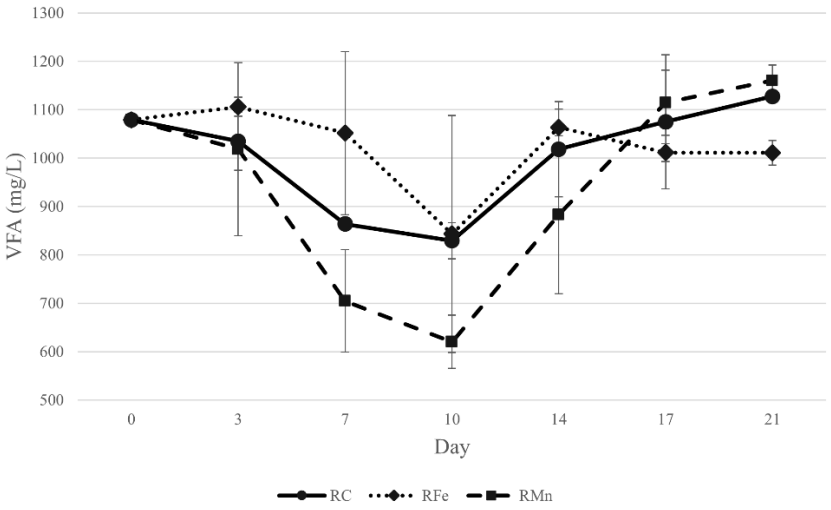

Figure 6. VFA Concentration Profile

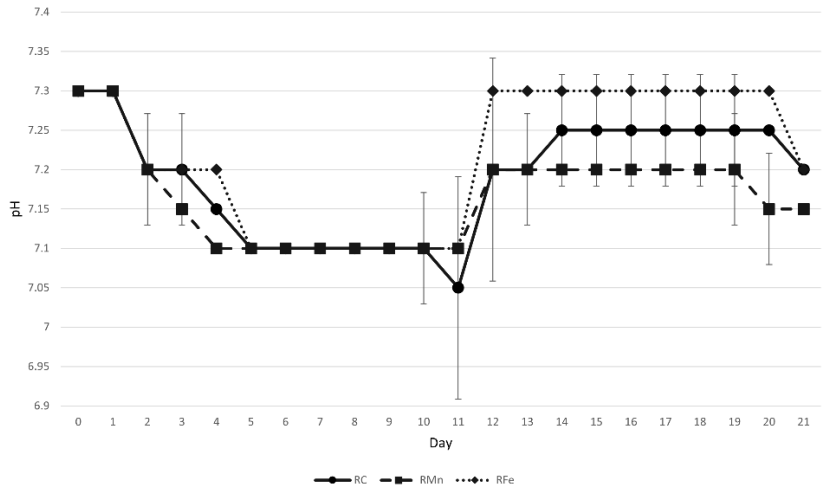

Figure 7. pH Profile

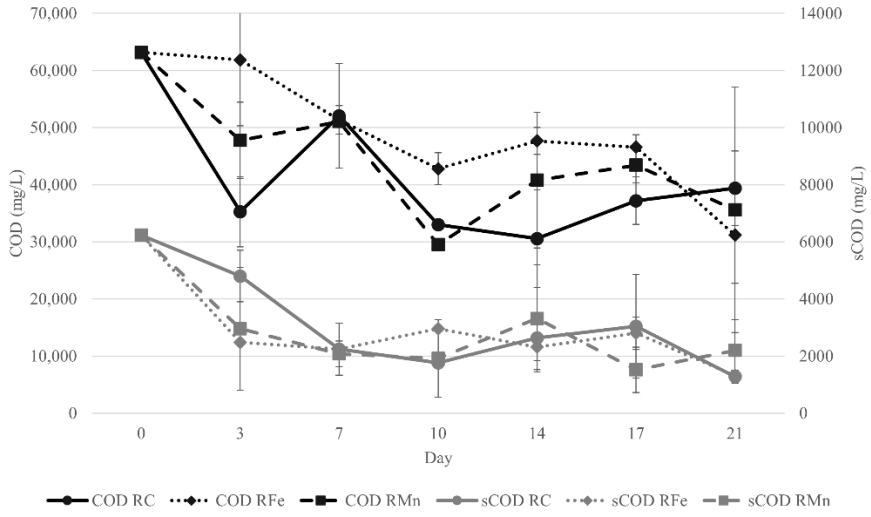

Figure 8. COD and sCOD Profile

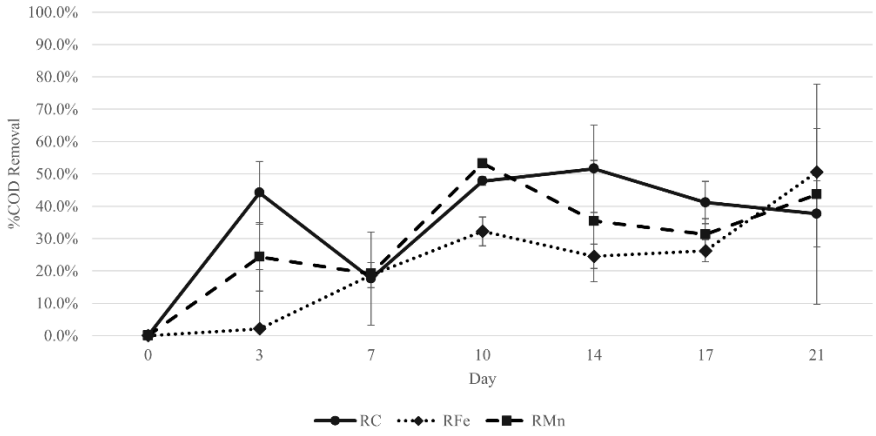

Figure 9. COD Removal Profile

3.4 TMO Effect Analysis

All reactors exhibited similar trends, but the effectiveness of the TMOs can be evaluated based on several parameters, as summarized in Table 3. While RC showed the highest COD removal, its methane production was relatively unsatisfactory. The methane yield of RFe, at 0.0391 mL CH_4/mg COD, was 32% higher than that of RC. Although RMn had lower methane production and %COD removal, its methane yield was 17.2% higher than RC. Based on these parameters, Fe_2O_3 was identified as the most effective TMO for anaerobic digestion. A study conducted by Tian (2019) [27] reported a 21.7% increase in methane production volume using MnO_2 as a TMO in AD. In another study, Kokdemir Ünsar and Perendeci (2018) [28], observed a 28.9% increase in methane production volume in AD with Fe_2O_3 addition. These findings align with the results of this study, confirming that Fe_2O_3 is more effective than MnO_2.

Table 3. Anaerobic Digestion Performance of All Reactors

No	Reactor	Methane Production (mL)	%COD removal	Methane Yield (mL/g COD)
1	RC	4153.5	55.4%	0.0297
2	RFe	5003.2	50.6%	0.0391
3	RMn	3839.2	43.7%	0.0348

As shown in Table 3, RC exhibited higher methane production than RMn, although the methane yield was lower. A similar phenomenon was reported by Chaiprapat [29], where, at a cycle time of 24 hours, the biogas production volume, methane concentration, and methane yield were 3.87 L gas/L wastewater, 44.9%, and 0.02 L CH_4/g TCOD removed, respectively. In contrast, at a 12-hour cycle time, the respective values were 2.55 L gas/L wastewater, 35.8%, and 0.12 L CH_4/g TCOD removed. Chaiprapat found that although methane production was higher at a 24-hour cycle time, the percentage of total chemical oxygen demand (TCOD) removed was 14.1%. In contrast, a higher percentage of TCOD removal, 16.4%, was achieved at the shorter cycle time of 12 hours, despite lower methane production. A similar trend is observed in Table 3, where RC showed the highest %COD removal, yet lower methane production than RFe. This could be attributed to the formation of other gases such as hydrogen. A study by Abdurahman [30], [31] also reported lower methane yield associated with higher %COD removal, supporting this observation.

4. Conclusions

The addition of TMOs to the AD process can enhance its performance. Fe_2O_3 has the potential to improve both methane production volume and methane yield in the AD process when POME is used as the feedstock. Fe_2O_3 could serve as an effective accelerant for the AD process, supporting the palm oil industry.

5. Acknowledgements

The author would like to thank Lembaga Penelitian dan Pengabdian Kepada Masyarakat, Universitas Pembangunan Nasional Veteran Yogyakarta (contract number 121/UN62.21/DT.07.00/2024) for funding this research. This work was also supported by a grant from the Directorate of Research, Technology and Community Service - Directorate General of Higher Education, Research and Technology – Ministry of Education, Culture, Research and Technology, following Research Contract Number: 080/E5/PG.02.00.PL/2024.

Author Contributions: Conceptualization, N.A.W., M.R.R.; methodology, N.A.W., M.R.R, D.J., T.W.W., and E.N.; validation, N.A.W., and M.R.R..; formal analysis, N.A.W., M.R.R., and D.A., and.; investigation, N.A.W., and D.A.; resources, N.A.W., and D.A.; data curation, N.A.W., M.A.K., R.A.P., Q.S.N., and N.R.S.; writing-original manuscript preparation, N.A.W., M.R.R, D.A.; visualization, N.A.W., M.A.K., R.A.P., Q.S.N., and N.R.S.; supervision, N.A.W., D.A., M.R.R., D.J., T.W.W., and E.N.; funding acquisition, N.A.W., M.R.R. All authors have read and agreed the manuscript.

Conflicts of Interest: The authors declare no conflict of interest.

References

[1] Choong, Y. Y.; Chou, K. W.; Norli, I. Strategies for improving biogas production of palm oil mill effluent (POME) anaerobic digestion: A critical review. *Renewable and Sustainable Energy Reviews* **2018**, *82*, 2993-3006. http://doi.org/10.1016/j.rser.2017.10.036.

[2] Badan Pusat Statistik, "Statistik Kelapa Sawit Indonesia 2022. **2023**.

[3] Mosunmola, A. G.; Olatunde, S. K. Palm Oil Mill Effluents (POME) and its Pollution Potentials: A biodegradable Prevalence. *J Pollut Eff Cont*, **2020**, *8*(5), 258. http://doi.org/10.35248/2375-4397.20.8.258.

[4] David Bala, J.; Lalung, J.; Ismail, N. Biodegradation of palm oil mill effluent (POME) by bacterial. *International Journal of Scientific and Research Publications* **2014**, *4*(3). [Online]. Available: www.ijsrp.org

[5] Azmi, N. A.; Yunos, K. F. M.; Zakaria, R. Application ofsandwich membrane for the treatment of palm oil mill effluent (POME) for water reuse. *Procedia Engineering* **2012**, *44*, 1980-1981. http://doi.org/10.1016/j.proeng.2012.09.014.

[6] Gamaralalage, D.; Sawai, O.; Nunoura, T. Degradation behavior of palm oil mill effluent in Fenton oxidation. *J Hazard Mater.* **2019**, *364*, 791-799. http://doi.org/10.1016/j.jhazmat.2018.07.023.

[7] Parthasarathy, S.; Gomes, R. L.; Manickam, S. Process intensification of anaerobically digested palm oil mill effluent (AAD-POME) treatment using combined chitosan coagulation, hydrogen peroxide (H2O2) and Fenton's oxidation. *Clean Technol Environ Policy* **2016,** *18*(1), 219-230. http://doi.org/10.1007/s10098-015-1009-7.

[8] Lorestani, A. A. Z. BIOLOGICAL TREATMENT OF PALM OIL MILL EFFLUENT (POME) USING AN UP-FLOW ANAEROBIC SLUDGE FIXED FILM (UASFF) BIOREACTOR. **2006**.

[9] Zulfahmi, I.Kandi, N.R.; Huslina, F.; Rahmawati, L.; Muliari, M.; Sumon, A.K.; Rahman, M.M. Phytoremediation of palm oil mill effluent (POME) using water spinach (Ipomoea aquatica Forsk). *Environ Technol Innov*. **2021**, *21*, 101260. http://doi.org/10.1016/j.eti.2020.101260.

[10] Baek, G.; Kim, J.; Kim, J.; Lee, C. Role and potential of direct interspecies electron transfer in anaerobic digestion. *Energies* **2018**, *11*(1), 107. http://doi.org/10.3390/en11010107.

[11] Baniamerian, H.; Isfahani, G.P.; Tsapekos, P.; Alvarado-Norales, M.; Shanhrokhi, M.; Vossoughi, M.; Angelidaki, I. Application of nano-structured materials in anaerobic digestion: Current status and perspectives. *Chemospher* **2019**, *229*, 188-199. http://doi.org/10.1016/j.chemosphere.2019.04.193.

[12] Yun, S.; Xing, T.; Han, F.; Shi, J.; Wang, Z.; Fan, Q.; Xu, H. Enhanced direct interspecies electron transfer with transition metal oxide accelerants in anaerobic digestion. *Bioresour Technol*. **2021**, *320*. http://doi.org/10.1016/j.biortech.2020.124294.

[13] Huang, Y.; Cai, B.; Dong, H.; Li, H.; Yuan, J.; Xu, H.; Wu, H.; Xu, Z.; Sun, D.; Dang, Y.; Holmes, E.D. Enhancing anaerobic digestion of food waste with granular activated carbon immobilized with riboflavin. *Science of the Total Environment*, **2022**, *851*. http://doi.org/10.1016/j.scitotenv.2022.158172.

[14] Lee, J. Y.; Lee, S. H.; Park, H. D. Enrichment of specific electro-active microorganisms and enhancement of methane production by adding granular activated carbon in anaerobic reactors. *Bioresour Technol*. **2016**, *205*, 205-212. http://doi.org/10.1016/j.biortech.2016.01.054.

[15] Saelor, S.; Kongjan, P.; O-Thong, S. Biogas Production from Anaerobic Co-digestion of Palm Oil Mill Effluent and Empty Fruit Bunches," in Energy Procedia, Elsevier Ltd, **2017**, pp. 717-722. http://doi.org/10.1016/j.egypro.2017.10.206.

[16] Suksong, W.; Promnuan, K.; Seengenyoung, J.; O-Thong, S. Anaerobic Co-Digestion of Palm Oil Mill Waste Residues with Sewage Sludge for Biogas Production in Energy Procedia, Elsevier Ltd, **2017**, pp. 789-794. http://doi.org/10.1016/j.egypro.2017.10.068.

[17] Bin Mohd Yusof, M. A.; Chan, Y. J.; Chong, C. H.; Chew, L. Effects of operational processes and equipment in palm oil mills on characteristics of raw Palm Oil Mill Effluent (POME): A comparative study of four mills. *Cleaner Waste Systems* **2023**, *5*. http://doi.org/10.1016/j.clwas.2023.100101.

[18] Walker, M.; Zhang, Y.; Heaven, S.; Banks, C. Potential errors in the quantitative evaluation of biogas production in anaerobic digestion processes. *Bioresour Technol*. **2009**, *100*(24), 6339-6346, http://doi.org/10.1016/j.biortech.2009.07.018.

[19] American Public Health Association, "5220 C Chemical Oxygen Demand (COD) - Closed Reflux, Titrimetric Method," in Standard Methods for The Examination of Water and Wastewater, 24th ed., **2023**, pp. 546–547.

[20] American Public Health Association, "5560 C Organic and Volatile Acids - Distillation Method," in Standard Methods for The Examination of Water and Wastewater, 24th ed., **2023**, pp. 593-594.

[21] Cheng, Y. W.; Chong, C.C.; Lam, K.M.; Leong, H.W.; Chuah, F.L.; Yusup, S.; Setiabudi, D. H.; Tang, Y.; Lim W.J. Identification of microbial inhibitions and mitigation strategies towards cleaner bioconversions of palm oil mill effluent (POME): A review. *Journal of Cleaner Production* **2021**, *280*, 124346. http://doi.org/10.1016/j.jclepro.2020.124346.

[22] Fang, C.; O-Thong, S.; Boe, K.; Angelidaki, I. Comparison of UASB and EGSB reactors performance, for treatment of raw and deoiled palm oil mill effluent (POME). *J Hazard Mater.* **2011**, *189*(1-2), 229-234, http://doi.org/10.1016/j.jhazmat.2011.02.025.

[23] Paul, S.; Parvez, S. S.; Goswami, A.; Banik, A. Exopolysaccharides from agriculturally important microorganisms: Conferring soil nutrient status and plant health. *Int J Biol Macromol*, **2024**, *262*, 129954, Mar. 2024, http://doi.org/10.1016/j.ijbiomac.2024.129954.

[24] D. and A. S. Deublein, Biogas from Waste and Renewable Resources, Second. Deggendorf: Wiley-VCH, 2011.

[25] Wardani, N. A.; Budhijanto, W. Mendukung Pengembangan Biofuel Generasi Kedua: Peruraian Anaerob Termofilik Vinasse untuk Berselaras dengan Kapasitas Pabrik Bioetanol Berbahan Dasar

Molasse Supporting Second Generation Biofuel Development: Thermophilic Anaerobic Digestion of Vinasse for Harmonizing with Molasses-Based Bioethanol Plant Capacity. **2023**.

[26] Wardani, W.; Afiqah, N. A.; Azis, N.; Budhijanto, M. M. Comparison of Biogas Productivity in Thermophilic and Mesophilic Anaerobic Digestion of Bioethanol Liquid Waste Comparison of Biogas Productivity in Thermophilic and Mesophilic Anaerobic Digestion of Bioethanol Liquid Waste. *Earth and Environmental Science*, **2020**, http://doi.org/10.1088/1755-1315/448/1/012002.

[27] Tian, T.; Qiao, S.; Yu, C.; Zhou, J. Effects of nano-sized MnO_2 on methanogenic propionate and butyrate degradation in anaerobic digestion. *J Hazard Mater*. **2019**, *364*, 11-18. http://doi.org/10.1016/j.jhazmat.2018.09.081.

[28] Ünşar, E. K.; Perendeci, N. A. What kind of effects do Fe_2O_3 and Al_2O_3 nanoparticles have on anaerobic digestion, inhibition or enhancement?. *Chemosphere.* **2018**, *211*, 726-735. http://doi.org/10.1016/j.chemosphere.2018.08.014.

[29] Chaiprapat, S.; Laklam, T. Enhancing digestion efficiency of POME in anaerobic sequencing batch reactor with ozonation pretreatment and cycle time reduction. *Bioresour Technol* **2011**, *102*(5), 4061-4068. http://doi.org/10.1016/j.biortech.2010.12.033.

[30] Ahmed, Y.; Yaakob, Z.; Akhtar, P.; Sopian, K. Production of biogas and performance evaluation of existing treatment processes in palm oil mill effluent (POME), **2015**, Elsevier Ltd. http://doi.org/10.1016/j.rser.2014.10.073.

[31] Abdurahman, N. H.; Rosli, Y. M.; Azhari, N. H. Development of a membrane anaerobic system (MAS) for palm oil mill effluent (POME) treatment. *Desalination* **2011**, *266*(1-3), 208-212. http://doi.org/10.1016/j.desal.2010.08.028.

ASEAN
Journal of Scientific and Technological Reports
Online ISSN:2773-8752

Research article

Effect of Different Luteinizing Hormone Releasing Hormone Analogs (LHRHa) on Spawning in Mahseer Barb (*Neolissochilus stracheyi*)

Ekachai Duangjai[1], Natthawoot Punroob[2], and Jittra Punroob[3*]

[1] Faculty of Science and Agriculture Technology, Rajamangala University of Technology Lanna Nan, 55000, Thailand
[2] Faculty of Business Administration and Liberal Arts, Rajamangala University of Technology Lanna Tak, 63000, Thailand
[3] Faculty of Business Administration and Liberal Arts, Rajamangala University of Technology Lanna Tak, 63000, Thailand
* Correspondence: nayty2521@rmutl.ac.th; ekachai@rmutl.ac.th

Citation:
Duangjai, E.; Punroob, N.; Punroob, J. Effect of different luteinizing hormone releasing hormone analogs (LHRHa) on spawning in mahseer barb *(Neolissochilus stracheyi). ASEAN J. Sci. Tech. Report.* **2025**, 28(4), e256823. https://doi.org/10.55164/ajstr.v28i4.256823.

Article history:
Received: November 26, 2024
Revised: May 22, 2025
Accepted: June 11, 2025
Available online: June 30, 2025

Abstract: The study assessed the impact of varying doses of luteinizing hormone-releasing hormone analogs (LHRHa) on key reproductive parameters in Mahseer barb fish (*N. stracheyi*). Four treatment groups were established. Trt1 (control) received 0.9% sodium chloride of 0.3 mL/kg BW with 10 mg domperidone (Dom)/kg BW; Trt2 was administered 20 µg/kg BW of LHRHa with 10 mg Dom/kg BW; Trt3 received 25 µg/kg BW of LHRHa with 10 mg Dom/kg BW; and Trt4 was given 30 µg/kg BW of LHRHa with 10 mg Dom/kg BW. Each treatment was replicated three times with three fish per replicate. The outcomes revealed a 100% success rate in ovulation induction across all groups using LHRHa with Dom. Trt4, with the highest dosage, achieved the most notable results, showing an ovulation index of 95.12 ± 2.54%. In contrast, the control group (Trt1) recorded the lowest ovulation index at 6.10 ± 0.73%. The application of 30 µg/kg BW of LHRHa with 10 mg Dom/kg BW in Trt4 resulted in the quickest latency period of 30.35 ± 0.60 hours. It significantly improved the fertilization rate compared to the lower dosages used in Trt2 and Trt3. However, Trt4 not only demonstrated the highest efficacy in terms of latency, number of ovulated eggs, fertilization rate, hatching rate, and survival rate but also confirmed the superior potential of the highest LHRHa dosage of 30 µg/kg BW combined with Dom for successful spawning induction in Mahseer barb fish.

Keywords: LHRHa; Mahseer barb; Fertilization rate; Dopamine antagonist

1. Introduction

The mahseer barb (*N. stracheyi,* 1871)[1] is a prominent freshwater fish found across Asia. They inhabit diverse habitats ranging from fast-flowing rivers to ponds and are known for their significance in local cultures as ornamental native fish. Despite their importance, many Mahseer species are now threatened due to habitat degradation and overfishing. Efforts are underway to conserve these species and their habitats to ensure their survival for future generations [2-4]. The mahseer barb is a significant fish species in Thailand. It is valued both as a source of food and as an ornamental fish. This has become problematic with the growth of the aquaculture industry, which has led to an increased demand for Mahseer fingerlings, especially in commercial aquaculture operations [5-7]. In the pond cultivation environment, Mahseer fish exhibit a discontinuous annual reproductive cycle characterized by alternate periods of resting, pre-spawning, and breeding, which are regulated by cyclically active gonadotrophs. Unlike

some other fish species, Mahseer do not spawn year-round; instead, they typically spawn once a year. In the countries north of the equator, such as Thailand, the spawning season for Mahseer fish typically occurs from June to September. During this period, the fish engage in reproductive behaviors and produce offspring [8-11]. Duangjai et al. [12] reported that omega-3 fatty acids from krill oil significantly improved sperm quality in *N. stracheyi* brooders. The study focused on captive-reared Mahseer barb and demonstrated enhanced reproductive performance.

Successful reproduction of Mahseer fish under captive conditions remains a significant challenge due to stress-induced ovarian atresia. Various stressors, such as poor water quality, handling confinement, social interaction, and inadequate nutrition, can disrupt the HPG axis, leading to hormonal imbalances and impaired ovarian development [13]. To address this challenge, aquaculturists have turned to hormonal manipulation to stimulate egg release in captive Mahseer fish. By using hormones, such as LHRHa, aquaculturists can induce spawning and overcome the limitations of captive egg production [13-17]. Nithirojpakdee et al. [18] reported that LHRHa combined with domperidone (DOM) effectively induced ovulation and spawning in *S. kohchangensis*. The study achieved 100% ovulation success across all treatment levels, with the shortest latency period and highest relative fecundity observed at a dose of 20 μg LHRHa/kg with 10 mg DOM/kg. Additionally, Washim et al. [19] reported that synthetic SGnRHa effectively facilitated artificial propagation in Spotted scat (*S. argus*), improving spawning outcomes and reproductive performance. However, the mechanism of action of LHRHa involves its crucial role in regulating reproductive processes. LHRHa acts by binding to specific receptors in the fish's hypothalamus, triggering the release of LH from the pituitary gland. This release of LH stimulates final ovarian follicle maturation and ovulation in females and testosterone production in males for sperm production [12-14]. Although LHRHa has been widely utilized for fish spawning, its optimal dosage varies among species [16–18]. For instance, Fermin [20] demonstrated that intraperitoneal injections of LHRHa combined with DOM induced ovulation in 75% of Bighead carp (*A. nobilis*), compared to 60% using HCG + LHRHa. Significant increases in oocyte diameter were observed in both groups, while fish treated with LHRHa, DOM, or saline alone did not ovulate. Egg production, fertilization, and hatching rates were comparable across the two protocols. Similarly, Harmin and Crim [21] reported that GnRHa induced ovulation and spawning in female Winter flounder (*P. americanus*), particularly when held at 5°C. GnRHa accelerated spawning responses, enabling ovulation approximately three months earlier than the natural spawning season, with high fertilization, hatching, and larval survival rates observed, especially when females were briefly exposed to cold winter seawater temperatures. Tan-Fermin et al. [22] demonstrated that a combination of LHRHa and pimozide effectively induced spawning in Asian catfish (C. macrocephalus) during different phases of the annual reproductive cycle, with treatments in May and August yielding the highest reproductive performance.

For the Indonesian Mahseer species, Cahyanti et al. [23] reported that artificial spawning and larvae performance were evaluated for three Indonesian Mahseer species (*T. douronensis*, *T. soro*, and *T. tambroides*). The study found that *T. tambroides* exhibited the largest egg diameter (3.00 ± 0.06 mm) and lowest fecundity (1061.19 ± 35.18 eggs/kg). In comparison, *T. douronensis* had the smallest egg diameter (2.3 ± 0.07 mm) and highest fecundity (4987.80 ± 17.25 eggs/kg). Fertilization and hatching rates ranged from 76.00 ± 7.21% to 93.33 ± 1.15% and 80.36 ± 6.00% to 93.32 ± 4.57%, respectively. Survival rates of 15-day-old larvae showed no significant differences between *T. soro* and *T. tambroides*, but both differed significantly from *T. douronensis.* However, studies on the optimal LHRHa dosage for the Mahseer barb in Thailand are currently lacking. To address this gap, the current study aimed to evaluate the effects of varying doses of LHRHa on the reproductive performance of Mahseer barb broodstock. Key parameters measured included latency period, number of ovulated eggs, fertilization rate, hatching rate, and survival rate, to determine the most effective LHRHa dosage for this species. This gap highlights the need for further investigation to understand how LHRHa hormones may affect induced spawning in Mahseer fish. This knowledge gap is crucial, as filling it could provide valuable insights to farmers in the upstream forests in Nan province, Thailand, offering them additional options to enhance the success of induced spawning in Mahseer fish. Therefore, the primary objective of our current study is to assess the effectiveness of different LHRHa dosages combined with a dopamine antagonist as potential agents for inducing spawning in Mahseer barb fish.

2. Materials and Methods

2.1 Broodfish selection

A total of 36 gravid female Mahseer barb fish (9 females/Trt), each weighing 490.08 ± 4.91 g and approximately 3.5 years old, were collected from an earth pond cultivated under a polyculture system. Additionally, 36 gravid male Mahseer barb fish, also in excellent health and condition, weighing 391.08 ± 3.67 g and approximately 3 years old, with an average total length of 23.15 ± 0.71 cm, were collected. The fish were in optimal health and condition, with an average total length of 18.99 ± 0.60 cm. These fish were fed twice daily (8:00 am and 5:00 pm) with commercial fish pellets containing 32% protein, equivalent to 3% of their body weight, from July to November 2024, before being selected for parameter observation. The earth pond located in amphoe Bo Kluea, Nan province had an average water depth of 1.20 meters (10x20x1.2 meters) and an average water temperature of 24.0 °C, maintained by a flow-through water system sourced from streams in upstream forests, flowed into the pond at a rate of 10 liters per minute, ensuring a clean and oxygen-rich environment for the fish. During the breeding season from July to November 2024, females were notably larger than males for broodfish selection (Figure 1). Gravid status was easily determined for both male and female broodfish based on their maturity characteristics. The females exhibited swollen and slightly pink genital papillae (Figure 1; A), while males displayed pointed and narrow genital papillae, with free-flowing milt observed upon slight abdominal pressure (Figure 1; B). Subsequently, they were transported to the fish breeding laboratory at the Faculty of Sciences and Agriculture Technology, Rajamangala University of Technology Lanna, Nan Province, Thailand. Male and female broodstocks were individually stocked into 500 L conditioning tanks to prevent unnecessary breeding. Each tank was equipped with artificial aeration and a flow-through water system at a rate of 5 L/min.

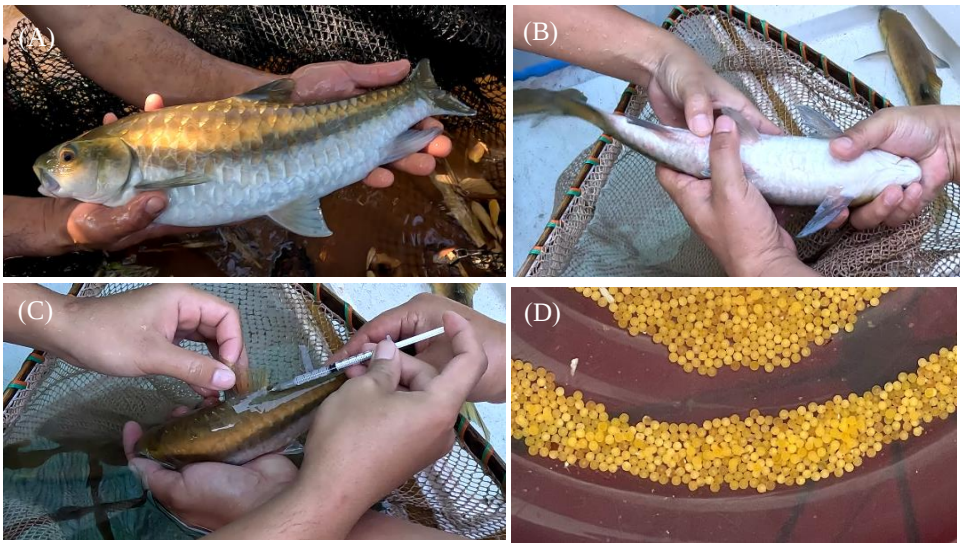

Figure 1. The selection process for gravid broodfish of the Mahseer barb (*N. stracheyi*) includes the comparison of the size of female (A) and male (B) broodstock. The injection site for stimulating spawning and milt release was located on the anterior dorsal fin (C). Mahseer barb eggs were characterized by being round, light yellow, and ranging in size from 1 to 1.2 millimeters (D).

2.2 Experimental design

The research was conducted at the Faculty of Sciences and Agriculture Technology, Rajamangala University of Technology Lanna, located in Nan province, Thailand. The study spanned four months. The gravid broodstocks of Mahseer barb (*N. stracheyi*) used in the experiment had an average total body weight of 489.30 ± 3.40, 489.70 ± 4.85, 490.40 ± 6.31, and 490.90 ± 5.25 g for Trt1, Trt2, Trt3, and Trt4, respectively. Meanwhile, the total lengths for Trt1, Trt2, Trt3, and Trt4 were 23.00 ± 0.82, 23.20 ± 0.79, 23.10 ± 0.74, and 23.40 ± 0.54 cm, respectively. A completely randomized design (CRD) was employed to compare different parameters between the various LHRHa dosage treatment groups to gain comprehensive insights into how

these dosages influence the development and viability of Mahseer fish populations. The experiment involved four treatments (Trt): Trt 1, fish were injected with sodium chloride at a dose of 0.9%/kg BW with 10 mg Dom/kg BW as the control group; Trt 2, receiving 20 μg/kg BW of LHRHa with 10 mg Dom/kg BW; Trt 3, administered with 25 μg/kg BW of LHRHa with 10 mg Dom/kg BW; and Trt 4, provided with 30 μg/kg BW of LHRHa with 10 mg Dom/kg BW. Each treatment was replicated three times, with three fish per replicate, ensuring that each fish served as a replication.

2.3 Hormone administration

Experimental fish were acclimatized to an average water temperature of 24°C using a flow-through water system for 24 hours before being exposed to induction with LHRHa, sourced from Aldamex Limited, Thailand, for artificial breeding induction. The fish underwent weighing to determine the appropriate hormonal dosage. Each male and female broodfish was injected once with the designated dosage per treatment, with each fish serving as a replication. This resulted in 9 fish per treatment, with three dosages of LHRHa administered. Trt 2 received 20 μg/kg BW of LHRHa, Trt 3 received 25 μg/kg BW of LHRHa, and Trt 4 received 30 μg/kg BW of LHRHa. Each treatment involved the injection of a solution combined with DOM at a dose of 10 mg/kg BW. Fish in the control group (Trt1) were injected with a solution of 0.9% NaCl at a dosage of 0.30 ml/kg BW. Fish received injections of the hormonal preparation at the allocated dose, administered below the base of the dorsal fin, between 5 pm and 5:30 pm. Fish were kept in aerated 2000L concrete tanks with a flow-through water system for ovulation monitoring.

2.4 Monitoring of ovulation

Ovulation monitoring in each treatment group commenced when fish oocytes began to release, typically with 1-2 eggs in each experimental set. Fish were euthanized using MS-222 (Merck) according to the method described by Pirhonen et al. [24], in which the solution was prepared by dissolving 1.0 g of MS-222 in 1 liter of tap water. The fish were placed in the solution, where they were observed to lose equilibrium and become sedated within a few minutes. Fertilization was conducted with a male per female sex ratio of 1:1. Females underwent ovulation assessment through hand-stripping of the abdomen, gently squeezing it toward the genital opening. Ovulation confirmation in each female occurred when a substantial number of eggs, round, light yellow, and ranging in size from 1 to 1.2 millimeters, were obtained. The artificial propagation technique for ovulation monitoring in each treatment group was implemented according to methods described by Mylonas and Zohar [25]. This approach involves controlled breeding environments and interventions that mimic natural conditions, supplemented by necessary supports to facilitate effective ovulation monitoring. The process involved the following steps: Firstly, males and females were euthanized, then stripped into an aluminum tray, followed by the application of sperm suspension from a male over the egg masses. Secondly, one gram of eggs from each female was collected and gently mixed with 1.0 ml of sperm suspension (milt). Subsequently, 0.5 liters of clean water were carefully added. The mixture was allowed to stand for a few minutes before the eggs were rinsed in clean water. Finally, the eggs were rinsed with water five minutes after fertilization and then rinsed twice more.

2.5 Monitoring of egg fertilization

The method for monitoring egg fertilization was adapted from several studies [23-25]. In summary, 1) One gram of eggs from an individual female was randomly selected and incubated in an aerated aluminum tray filled with clean water to a depth of 15 cm. Monitoring for egg fertilization occurred 24 hours after incubation, using an Olympus CKX41 fluorescence phase contrast inverted microscope 5mp camera to identify unfertilized eggs. 2) One hundred eggs were collected from each female's aluminum tray (measuring 30x20 cm) and subsequently examined under a binocular microscope with 10x magnification, provided by Microscopic. 3) Opaque, unfertilized eggs were segregated from the transparent, living ones, and the number of fertilized eggs was tallied. Unfertilized (white eggs) were counted and then removed to prevent fungal infection in each female's aluminum tray. 4) At the hatching stages, the embryos were observed to gather in specific areas of the aluminum trays. In contrast, any non-viable eggs, eggshells, and deformed embryos that floated to the surface were systematically removed. For the 60-day monitoring of larval survival rate (%), key water quality indicators were regularly assessed to maintain optimal rearing conditions. These indicators included pH, alkalinity, and hardness. All parameters were monitored once daily at 09:00 a.m. throughout the

experimental period. Measurements were conducted using advanced water quality instruments, including the Horiba U-50 series multi-parameter water quality meter and a standard test kit for alkalinity and hardness.

2.6 Data collection

One gram of eggs from each female Mahseer barb (*N. stracheyi*) was weighed and collected to determine spawning performance parameters, including latency period, fecundity, relative fecundity, fertilization rate, and hatching rate for each treatment. The calculations for these parameters were based on formulas from previous research [12, 18, 23, 24, 25], as outlined below: (1) The latency period was determined by calculating the time from the initial injection to ovulation, when the eggs were ready to be stripped. (2) Fecundity (total number of eggs) and relative fecundity (number of eggs/g BW of brooder) were determined using the following formula.

Fecundity = Total weight of eggs × number of eggs/g BW

$$(3)\ \text{Relative fecundity} = \frac{\text{Total number of eggs}}{\text{Body weight of the brooder}} \text{X}100$$

The fertilization rate was determined by counting the fertilized and unfertilized eggs under a microscope after 30 hours of incubation. Unfertilized eggs were identified by their opaque appearance, while fertilized eggs were characterized by transparency with a visible embryo. The fertilization rate was calculated as follows:

$$(4)\ \text{The fertilization rate} = \frac{\text{Total number of fertilized eggs}}{\text{Total number of unfertilized eggs}} \text{X}100$$

The monitoring of hatching time began with the distribution of the spermatozoan solution to the eggs and continued until complete hatching was achieved (100% hatching rate). A sample of eggs weighing one gram was placed in one liter of clean water with a continuous inflow to determine the hatching rate. The total number of hatched larvae was counted using the following formula:

$$(5)\ \text{Hatching rate} = \frac{\text{Total number of Hatched larvae}}{\text{Total number of sampled eggs}} \text{X}100$$

$$(6)\ \text{Survival Rate (\%)} = \frac{\text{Number of fry survived at day 60}}{\text{Total number of hatched fry}} \text{X}100$$

2.7 Statistical analysis

The study employed a statistical analysis to assess differences between treatment groups. Data were presented as the mean ± SD. One-way analysis of variance (ANOVA) was employed to examine differences among treatment groups. Post-hoc analysis was conducted using Duncan's multiple range test to identify specific differences between groups. A significance level of $p < 0.05$ was chosen.

3. Results and Discussion

3.1 Results

The spawning performance parameters for female Mahseer barb (*N. stracheyi*) broodfish, which received varying dosages of LHRHa, each supplemented with 10 mg Dom/kg BW, are presented in Table 1. The average initial weights of the female Mahseer barb were recorded as follows: 489.30 ± 3.40 g for Trt 1, 489.70 ± 4.85 g for Trt 2, 490.40 ± 6.31 g for Trt 3, and 490.90 ± 5.25 g for Trt 4 (Figure 2). No significant differences ($p > 0.05$) were observed in the mean weights among all experimental female fish. However, the highest average was presented in Trt 4, administered 30 μg/kg BW of LHRHa with 10 mg Dom/kg BW. For the male Mahseer barb, average weights were reported as 389.60 ± 4.81 g for Trt 1, 392.00 ± 3.09 g for Trt 2, 389.90 ± 5.30 g for Trt 3, and 390.40 ± 2.67 g for Trt 4 (Figure 2). Fifteen hours after the females had been injected, a combination of DOM at the same dose of 15 μg LHRHa and 10 mg Dom/kg BW was administered to each male in the treatment group. The mean weights of the male broodfish across all treatment groups were also found to have no significant differences ($p > 0.05$), though the highest mean weight was observed in Trt 2. Significant effects on the reproductive performance of female Mahseer barb broodfish, including latency period, relative number of ovulated eggs, fertilization rate, hatching rate, and survival rate, were revealed by

the ANOVA test due to different LHRHa dosages with 10 mg Dom/kg BW ($p < 0.05$). At a dosage of 30 μg/kg BW of LHRHa with 10 mg Dom/kg BW of Trt4, a shorter latency period was observed of 29.14 ± 0.52 hours, significantly differing from the other dosages. Additionally, higher relative numbers of ovulated eggs, as well as increased rates of fertilization, hatching, and survival, were recorded with the LHRHa dosage of 30 μg/kg BW and 10 mg Dom/kg BW, showing significant differences from other dosages. According to Table 1, a trend was observed where increasing LHRHa dosage led to higher relative numbers of ovulated eggs, as well as increased rates of fertilization, hatching, and survival. However, no significant differences were observed between the dosages of 20 μg/kg BW of LHRHa with 10 mg Dom/kg BW in Trt 2 and 25 μg/kg BW of LHRHa with 10 mg Dom/kg BW in Trt 3.

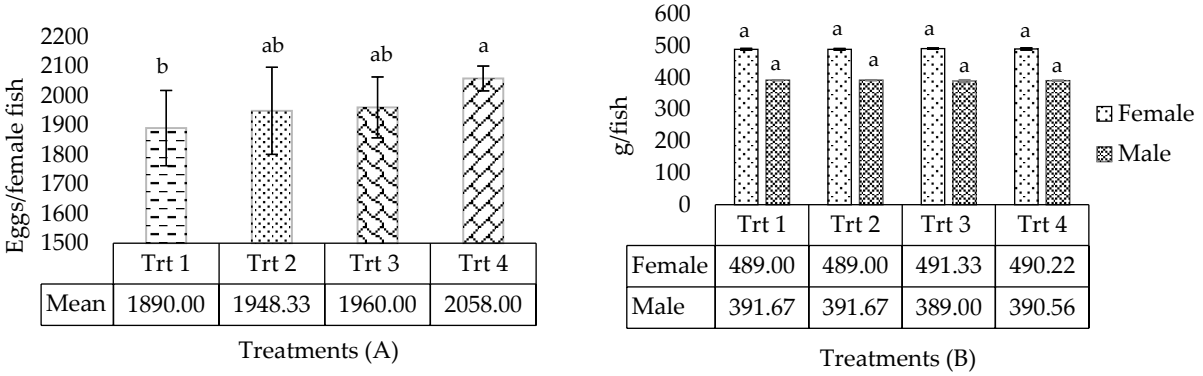

Figure 2. The comparison was conducted among treatment groups that received varying dosages of LHRHa, each supplemented with 10 mg Dom/kg BW, focusing on two primary metrics in Mahseer barb (*N. stracheyi*) broodfish: the total number of eggs (A) and the weight of both female and male fish(g/fish)(B). Data are presented as the mean ± SD, derived from four independent experiments. Different lowercase letters above the bars signify that the treatment groups across various concentrations exhibit significant differences ($p < 0.05$).

Successful ovulation induction was observed in all 36 female Mahseer barbs that were administered sodium chloride at a dosage of 0.9%/kg BW with 10 mg Dom/kg BW for Trt 1; 20 μg/kg BW of LHRHa with 10 mg Dom/kg BW for Trt 2; 25 μg/kg BW of LHRHa with 10 mg Dom/kg BW for Trt 3; and 30 μg/kg BW of LHRHa with 10 mg Dom/kg BW for Trt 4. Within 29-45 hours post-injection, ovulation occurred. No significant differences in relative fecundity were found among the treatment groups, indicating comparable results with all different LHRHa dosages used (Table 1). While the dosages of 20 μg/kg BW of LHRHa with 10 mg Dom/kg BW for Trt 2 and 25 μg/kg BW of LHRHa with 10 mg Dom/kg BW for Trt 3 did not significantly impact the results, higher values were observed with the dosage of 30 μg/kg BW of LHRHa with 10 mg Dom/kg BW. It is suggested that the recommended dosage is 30 μg/kg BW of LHRHa with 10 mg Dom/kg BW. A similar pattern of results was observed in terms of the relative number of ovulated eggs, with a total of 4.17 ± 0.21 eggs/g BW being spawned. A fertilization rate of 98.20 ± 0.78% was recorded. No significant difference was observed between fish supplied with a dosage of 20 μg/kg BW of LHRHa and 10 mg Dom/kg BW, and those administered with 25 μg/kg BW of LHRHa and 10 mg Dom/kg BW. A higher percentage of fertilized eggs might be resulted in by increasing the dosage of LHRHa/kg BW with 10 mg Dom/kg BW, as a significantly lower ($p < 0.05$) fertilization rate was observed with the higher dosage of 30 μg/kg BW of LHRHa with 10 mg Dom/kg BW compared to the lower dosage of 20 μg/kg BW of LHRHa with 10 mg Dom/kg BW. On day 60 of incubation, yolk absorption was observed in the hatched eggs. The hatching rate, which ranged from 38.40 ± 5.75% to 90.60 ± 1.22%, was significantly increased at the highest value (90.60 ± 1.22%) with 30 μg/kg BW of LHRHa and 10 mg Dom/kg BW ($p < 0.05$). The total number of eggs per female Mahseer barb was presented in Figure 2 (A). Mean total egg production for female Mahseer barb was recorded as 1890.00 ± 127.35 eggs/fish for Trt1, 1948.33 ± 147.55 eggs/fish for Trt2, 1960.00 ± 103.12 eggs/fish for Trt3, and 2058.00 ± 42.00 eggs/fish for Trt4, respectively. No significant effects on total egg production values were observed in the control groups 1 and 2 ($p > 0.05$). Significant differences ($p < 0.05$) were found between Trt1, which involved 0.9%/kg BW with 10 mg Dom/kg BW, and Trt4, which involved 30 μg/kg BW of LHRHa with 10 mg Dom/kg BW. During the

60-day monitoring of larval survival rate (%), water quality measurements revealed that dissolved oxygen averaged 5.50 ± 0.01 mg/L, pH was 5.50 ± 0.01, alkalinity was 101 ± 0.45 mg/L as $CaCO_3$, hardness was 32.60 ± 0.35 mg/L as $CaCO_3$, and water temperature remained constant at 26.00 ± 0.00°C.

Table 1. The spawning performance parameters of female Mahseer barb (*N. stracheyi*) broodfish

Parameters	LHRHa dosage (with 10 mg Dom/kg BW of broodfish)				F/Pr > F
	Trt1 (0.9% NaCl)	Trt2 (20 μg)	Trt3 (25 μg)	Trt4 (30 μg)	
Male weight (g)	389.60 ± 4.81^{a}	392.00 ± 3.09^{a}	389.90 ± 5.30^{a}	390.40 ± 2.67^{a}	0.67/0.574
Male length (cm)	18.95 ± 0.64^{a}	19.10 ± 0.57^{a}	18.95 ± 0.64^{a}	18.95 ± 0.64^{a}	0.14/0.932
Female weight (g)	489.30 ± 3.40^{a}	489.70 ± 4.85^{a}	490.40 ± 6.31^{a}	490.90 ± 5.25^{a}	0.20/0.896
Female length (cm)	23.00 ± 0.82^{a}	23.20 ± 0.79^{a}	23.10 ± 0.74^{a}	23.40 ± 0.54^{a}	0.56/0.647
Latency period (hour)	45.60 ± 1.51^{a}	40.02 ± 0.73^{b}	35.61 ± 0.46^{c}	29.14 ± 0.52^{d}	577.31/0.001
Relative fecundity (eggs/g BW)	3.86 ± 0.28^{b}	3.99 ± 0.32^{ab}	3.95 ± 0.36^{ab}	4.17 ± 0.21^{a}	1.93/0.041
Fertilization rate (%)	56.50 ± 6.66^{d}	75.90 ± 4.44^{c}	89.60 ± 1.79^{b}	98.20 ± 0.78^{a}	192.90/0.001
Hatching rate (%)	38.40 ± 5.75^{d}	62.80 ± 2.82^{c}	76.60 ± 2.64^{b}	90.60 ± 1.22^{a}	393.47/0.001
Survival rate (%)*	16.60 ± 4.65^{d}	36.50 ± 3.43^{c}	55.90 ± 3.60^{b}	73.00 ± 2.12^{a}	458.73/0.001

Data are presented as the mean ± SD, derived from four independent experiments. Means in a row superscripted with different lowercase letters are significantly ($p < 0.05$) different. *The survival rate on day 60 after hatching (%) serves as an indicator that the experimental conditions were optimal, allowing the fish larvae to thrive during early development.

3.2 Discussion

Recent studies have shown that the dosage of LHRHa significantly influences its pivotal role in manipulating reproductive outcomes in fish. It has been emphasized that a strong correlation exists between LHRHa dosage and crucial reproductive parameters. As the dosage of LHRHa was escalated, a concurrent reduction in the latency period was observed, indicating a hastened onset of reproductive activity. Furthermore, higher dosage levels have been linked to an increase in the number of ovulated eggs, alongside increased rates of fertilization, hatching, and survival [17,18,26]. Similarly, Mylonas and Zohar [25] also revealed that reproductive dysfunctions in cultured fish, such as unpredictable oocyte maturation and low sperm quality, are common challenges. Sustained-release GnRHa delivery systems, like implants and biodegradable microspheres, effectively induce final oocyte maturation and spermiation in over 40 cultured fish species. The identification of an optimal dosage regimen has been recognized as a pivotal milestone in achieving the most favorable reproductive outcomes. Specifically, the administration of 30 μg/kg BW of LHRHa with 10 mg Dom/kg BW of Trt4 has been identified as the most effective dosage, surpassing lower dosage levels (20 μg/kg BW of LHRHa with 10 mg Dom/kg BW of Trt2 and 25 μg/kg BW of LHRHa with 10 mg Dom/kg BW of Trt3) in inducing spawning among female Mahseer barb broodfish. Similarly, Nwokoye et al. [27] reported that the induced spawning of African giant catfish (H. bidorsalis) was successfully achieved using both synthetic and natural hormones. Ovaprim significantly outperformed pituitary extract in parameters such as hatchability (11,162.27 ± 362.00 larvae vs. 9,180.13 ± 343.37 larvae) and larval survival (99.88% vs. 99.61%), with fewer deformed larvae.

Enhanced gonad maturation and ovulation have been stimulated by this optimal dosage regimen, leading to the production of higher quantities and superior quality of ovulated eggs, as corroborated by increased fertilization rates. Consequently, it was inferred that the recommended dosage for eliciting optimal reproductive responses was 30 μg/kg BW of LHRHa with 10 mg Dom/kg BW of Trt4. A similar pattern in the relative number of ovulated eggs has consistently been observed, with a spawning rate of 4.17 ± 0.21 eggs/g BW. An impressive fertilization rate of 98.20 ± 0.78% has also been documented. However, fish that were

administered a dosage of 20 μg LHRHa/kg BW with 10 mg Dom/kg BW of Trt2 did not exhibit a significant difference compared to those receiving 25 μg LHRHa/kg BW with 10 mg Dom/kg BW of Trt3. This observation suggests that increasing the dosage of LHRHa/kg BW by 10 mg Dom/kg BW may lead to a higher percentage of fertilized eggs. This inference aligns with findings indicating that higher dosages of hormonal treatments may sometimes harm fertilization outcomes. A significantly lower fertilization rate ($p < 0.05$) was observed with the higher dosage of 30 μg/kg BW of LHRHa combined with 10 mg Dom/kg BW in Trt4 compared to the 20 μg/kg BW dosage in Trt2. Supporting this, Fermin [20] reported that intraperitoneal injections of LHRHa combined with DOM significantly induced oocyte maturation and ovulation in Bighead carp (*A. nobilis*), achieving ovulation rates of 75%, compared to 60% with HCG + LHRHa. Both protocols yielded comparable increases in oocyte diameter (7.0% and 7.5%, respectively) and fertilization and hatching rates. However, no ovulation was observed in fish treated with LHRHa, DOM, or saline alone. Notably, LHRHa + DOM proved to be more cost-efficient than HCG + LHRHa. The superior efficacy of the higher dosage regimen can be attributed to the synergistic interaction between LHRHa and DOM, which has led to an increased secretion of gonadotropins (GTH II or LH) from the pituitary gland [28].

This enhanced gonadotropin secretion has triggered a cascade of reproductive events, including the maturation of ovarian follicles and the release of mature oocytes. Furthermore, the study has shed light on the intricate hormonal mechanisms underlying the reproductive response to LHRHa treatment. In preliminary studies conducted by Sreenivasulu et al. [29], it was observed that a higher dosage regimen of LHRHa not only stimulated gonadotropin secretion but also modulated key enzymes involved in steroidogenesis, including 20-beta-hydroxysteroid dehydrogenase (20β-HSD). This outcome is attributed to the more effective stimulation of gonadal maturation and ovulation processes, which are often dose-dependent. Elevated levels of LHRHa can enhance the release of luteinizing hormone (LH) and follicle-stimulating hormone (FSH), thereby promoting synchronized and complete oocyte maturation. Consequently, eggs produced under these conditions are typically of higher quality, with enhanced fertilization potential[29].

Furthermore, Maradun et al. [30] concluded that successful spawning induction of African catfish breeders with body weights ranging from 600 g was achieved, and a high percentage of egg hatchability was attained using LHRHa. Additionally, it has been reported by Aruho et al. [31] that better egg hatchability in Ripon barbel (*L. altianalis*) was observed when pituitary extract from African catfish was used compared to a GnRH synthetic analogue with an antidopamine drug GnRH of 10 μg/kg BW with metoclopramide 20 mg/kg BW in artificial spawning. However, previous studies have shown that elevated hormone levels can either enhance or impair reproductive performance in fish; the present findings in Mahseer fish demonstrate a positive outcome with higher hormone dosage. The use of 30 μg LHRHa/kg body weight combined with 10 mg/kg DOM significantly improved fertilization efficiency and hatching success. Unlike other species where hormonal overstimulation may lead to endocrine disruption and reduced reproductive outcomes, Mahseer broodfish appear to respond more favorably to higher hormonal stimulation, likely due to their species-specific endocrine sensitivity and reproductive biology. The success observed in this study may also be attributed to favorable experimental conditions and effective broodstock management. These findings underscore the need to tailor hormone protocols and hatchery practices to the biological characteristics of each species to achieve optimal reproductive performance in aquaculture.

4. Conclusions

A satisfactory outcome in terms of fecundity, fertility, and hatchability of eggs was achieved with a single intramuscular injection of LHRHa (30 μg LHRHa/kg BW + 10 mg Dom/kg BW). Hence, it is suggested that LHRHa can effectively induce spawning in female Mahseer barb broodfish. The study concluded that the latency period, relative number of ovulated eggs, fertilization rate, hatching rate, and survival rates of female fish were significantly influenced by different doses of LHRHa. Among the tested dosages, it was determined that LHRHa was the most effective. Notably, there have been no previous reports of inducing spawning in female Mahseer barb using LHRHa dosages. Therefore, the results of this study offer preliminary insights into its spawning success.

5. Acknowledgements

The first author expresses gratitude for the financial support provided by the National Research Council of Thailand (NRCT) for the year 2024. This support has been allocated to the research project titled 'Management of Biodiversity and Fish Populations in the Wa River for Climate Change Mitigation in Nan Province,' a strategic fund (N24A670775) under the subject group focused on reducing the risks and impacts of natural disasters and climate change on economic animals. This funding was made possible through the strategic fund (SF) 2024 of the Research and Development Institute of Rajamangala University of Technology, Lanna.

6. Ethical approval

Approval for all experimental procedures, animal care practices, and biosafety measures was granted by the Animal Experiment Committee and the Biosafety Committee of Rajamangala University of Technology Lanna, as documented under approval number RMUTL-IACUC 007/2024, dated June 24, 2024, and valid until June 23, 2026. This approval ensured that the research adhered to established ethical standards and regulatory requirements concerning animal welfare and safety protocols.

7. Conflict of Interest

The authors declare that there are no conflicts of interest.

References

[1] Day, F. Monograph of Indian Cyprinidae. Parts 1–3. *J. Proc. Asiatic Soc. Bengal.* **1871**, *40*(2), 95-142. https://zoobank.org/References/3F4C7611-9627-4632-A5E8-CAA7C9D874E1.

[2] Pinder, A. C.; Raghavan, R. Conserving the Endangered Mahseers (*Tor* spp.) of India: The Positive Role of Recreational Fisheries. *Curr. Sci.* **2013,** *104*(11), 1472-1475. https://www.researchgate.net/publication/237067345.

[3] Pinder, A. C.; Britton, R.; Harrison, A. J.; Raghavan, R.; et al. Mahseer (*Tor* spp.) Fishes of the World: Status, Challenges and Opportunities for Conservation. *Rev. Fish Biol. Fish.* **2019,** *29*(2-3), 417-452. https://doi.org/10.1007/s11160-019-09566-y.

[4] Abass, Z.; Shah, T. H.; Bhat, F. A.; Ramteke, K.; Magloo, A. H.; Hamid, I.; Wanjari, R. N.; Somasundharam, I. The Mahseer: The Tiger of Water—An Angler's Delight in the Himalayas and the Undisputed King of Sport Fishing. *Fish. Res.* **2024,** *279,* 107147. https://doi.org/10.1016/j.fishres.2024.107147.

[5] Surachat, K.; Deachamag, P.; Wonglapsuwan, M. The First De Novo Genome Assembly and Sex Marker Identification of Pluang Chomphu Fish (*Tor tambra*) from Southern Thailand. *Comput. Struct. Biotechnol. J.* **2022,** *20,* 1470-1480. https://doi.org/10.1016/j.csbj.2022.03.021.

[6] Jaapar, M. Z.; Norhana, W. N. M. H.; Yusof, H. M.; Hamzah, A.; et al. Research and Innovation in Malaysian Mahseer (*Tor* sp.) Broodstock Development Programme. *Asian Fish. Sci.* **2023,** *36*(4), 219-232. https://doi.org/10.33997/j.afs.2023.36.4.004.

[7] Triyanti, R.; Suryawati, S. H.; Wijaya, R. A.; Hafsaridewi, R.; et al. Assessment of the Success Factors Influencing Rice-Fish Farming Innovation Village to Support Food Security. *IOP Conf. Ser. Earth Environ. Sci.* **2021,** *892*(1), 012052. https://doi.org/10.1088/1755-1315/892/1/012052.

[8] Das, S. C. S.; Pathak, R. K.; Khan, A. U.; Sarkar, U.; et al. Pattern of Reproductive Biology of the Endangered Golden Mahseer (*Tor putitora*, Hamilton 1822) with Special Reference to Regional Climate Change Implications on Breeding Phenology. *J. Appl. Anim. Res.* **2018,** *46*(1), 864-872. https://doi.org/10.1080/09712119.2018.1497493.

[9] Shahi, N.; Pandey, J.; Mallik, S.; Das, P.; et al. Gonadal Development Stages of Wild Male Golden Mahseer (*Tor putitora*) from Nainital Region of Uttarakhand, India. *J. Ecophysiol. Occup. Health* **2015,** *14*(3-4), 133. https://doi.org/10.15512/joeoh/2014/v14i3-4/59998.

[10] Sharma, A.; Sarma, D.; Joshi, R.; Das, P.; Akhtar, M. S.; Pande, V.; Sharma, P. Gonad Indices, Morphology, and Muscle Fatty Acid Compositions of Male and Female Golden Mahseer (*Tor putitora*)

Sampled from Lake Bhimtal (Himalaya) at Different Seasons of the Year. *Aquac. Fish.* **2024,** *9*(4), 603-616. https://doi.org/10.1016/j.aaf.2022.08.002.

[11] Dash, P.; Tandel, R. S.; Bhat, R. A. H.; Sarma, D.; Pandey, N.; Sawant, P. B.; Chadha, N. K. Spawning Substrate Preference and Spawning Behavior of Chocolate Mahseer (*Neolissochilus hexagonolepis*). *Anim. Reprod. Sci.* **2021,** *233,* 106847. https://doi.org/10.1016/j.anireprosci.2021.106847.

[12] Duangjai, E.; Punya-in, S.; A-ta, A.; Arin, S.; Sangkamruang, A.; Sresutham, P.; Punroob, J. Effects of Omega-3 Fatty Acids (from Krill Oil) on Sperm Quality of Mahseer Barb, *Neolissochilus stracheyi*, Brooders Reared in Captivity. *SNRU J. Sci. Technol.* **2017,** *9*(2), 474-482. https://thaiscience.info/Journals/Article/SNRU/10997775.pdf

[13] Ismail, M. F. S.; Siraj, S. S.; Daud, S. K.; Harmin, S. A. Association of Annual Hormonal Profile with Gonad Maturity of Mahseer (*Tor tambroides*) in Captivity. *Gen. Comp. Endocrinol.* **2011,** *170*(1), 125-130. https://doi.org/10.1016/j.ygcen.2010.09.021.

[14] El-Hawarry, W. N.; Abd El-Rahman, S. H.; Shourbela, R. M. Breeding Response and Larval Quality of African Catfish (*Clarias gariepinus*, Burchell 1822) Using Different Hormones/Hormonal Analogues with Dopamine Antagonist. *Egypt. J. Aquat. Res.* **2016,** *42*(2), 231-239. https://doi.org/10.1016/j.ejar.2016.06.003.

[15] Islam, P.; Hossain, M. I.; Khatun, P.; Masud, R. I.; Tasnim, S.; Anjum, M.; Islam, M. Z.; Nibir, S. S.; Rafiq, K.; Islam, M. A. Steroid Hormones in Fish, Caution for Present and Future: A Review. *Toxicol. Rep.* **2024,** *13,* 101733. https://doi.org/10.1016/j.toxrep.2024.101733.

[16] Mylonas, C. C.; Fostier, A.; Zanuy, S. Broodstock Management and Hormonal Manipulations of Fish Reproduction. *Gen. Comp. Endocrinol.* **2010,** *165*(3), 516-534. https://doi.org/10.1016/j.ygcen.2009.03.007.

[17] Roy, K. Rapid Review on the Use of New Age Induced Breeding Agent LHRHa in Indian Finfish Seed Production Sector. *J. Fish.* **2016,** *4 (2),* 401–407.https://doi.org/10.17017/jfish.v4i2.2016.145.

[18] Nithirojpakdee, P.; Jaisuk, C.; Keereelang, J.; Kongsuk, M. Effects of Luteinizing Hormone-Releasing Hormone Analogue (LHRHa) on Ovulation and Spawning of *Schistura kohchangensis*. *Int. J. Agric. Technol.* **2024,** *20*(2), 619-630. http://www.ijat-aatsea.com.

[19] Washim, M. R.; Ahmmed, S.; Rube, A. K. M. The Effects of Synthetic Gonadotropin Releasing Hormone Analogue (SGnRHa) on Artificial Propagation of Spotted Scat (*Scatophagus argus*). *Asian J. Anim. Sci.* **2022,** *16*(2), 123-132. https://file-khulna.portal.gov.bd.

[20] Fermin, A. C. LHRH-a and Domperidone-Induced Oocyte Maturation and Ovulation in Bighead Carp, *Aristichthys nobilis* (Richardson). *Aquaculture* **1991,** *93*(1), 87-94. https://doi.org/10.1016/0044-8486(91)90207-N.

[21] Harmin, S. A.; Crim, L. W. Gonadotropic Hormone-Releasing Hormone Analog (GnRH-A) Induced Ovulation and Spawning in Female Winter Flounder, *Pseudopleuronectes americanus* (Walbaum). *Aquaculture* **1992,** *104* (3–4), 375–390. https://doi.org/10.1016/0044-8486(92)90218-A.

[22] Tan-Fermin, J. D.; Pagador, R. R.; Chavez, R. C. LHRHa and Pimozide-Induced Spawning of Asian Catfish *Clarias macrocephalus* (Gunther) at Different Times During an Annual Reproductive Cycle. *Aquaculture* **1997,** *148*(4), 323–331. https://doi.org/10.1016/S0044-8486(96)01423-8.

[23] Cahyanti, W.; Soelistyowati, D. T.; Carman, O.; Kristanto, A. H. Artificial Spawning and Larvae Performance of Three Indonesian Mahseer Species. *AACL Bioflux* **2019,** *12*(1), 1-7. http://www.bioflux.com.ro/aacl.

[24] Pirhonen, J.; Schreck, C. B. Effects of Anaesthesia with MS-222, Clove Oil, and CO_2 on Feed Intake and Plasma Cortisol in Steelhead Trout (*Oncorhynchus mykiss*). *Aquaculture* **2003,** *220*(1-4), 507-514. https://doi.org/10.1016/S0044-8486(02)00624-5.

[25] Mylonas, C. C.; Zohar, Y. Use of GnRHa-Delivery Systems for the Control of Reproduction in Fish. *Rev. Fish Biol. Fish.* **2000,** *10*(4), 463–491. https://doi.org/10.1023/A:1012266030077.

[26] Mylonas, C. C.; Fostier, A.; Zanuy, S. Broodstock Management and Hormonal Manipulation of Fish Reproduction. *Gen. Comp. Endocrinol.* **2009,** *165*(3), 516-34. https://doi.org/10.1016/j.ygcen.2009.03.007.

[27] Nwokoye, C. O.; Nwuba, L. A.; Eyo, J. Induced Propagation of African Clariid Catfish, *Heterobranchus bidorsalis* (Geoffrey Saint Hillarie, 1809) Using Synthetic and Homoplastic Hormones. *Afr. J. Biotechnol.* **2007,** *6*(23). https://doi.org/10.5897/AJB2007.000-2430.

[28] Trachtenberg, J. The Effect of the Chronic Administration of a Potent Luteinizing Hormone Releasing Hormone Analog on the Rat Prostate. *J. Urol.* **1982,** *128*(5), 1097-1100. https://doi.org/10.1016/s0022-5347(17)53352-2.

[29] Sreenivasulu, G.; Senthilkumaran, B.; Sridevi, P.; Rajakumar, A.; Rasheeda, M. K. Expression and Immunolocalization of 20β-Hydroxysteroid Dehydrogenase during Testicular Cycle and after hCG Induction, in vivo in the Catfish, *Clarias gariepinus*. *Gen. Comp. Endocrinol.* **2012,** *175*(1), 48-54. https://doi.org/10.1016/j.ygcen.2011.09.002.

[30] Maradun, H. F.; Ahmad, M.; Sahabi, A. M.; Umar, F.; Ibrahim, J. Z.; Adamu, I. Effect of Different Male-Female Broodstock Ratios on the Induced Breeding Performance of *Clarias gariepinus*. *Int. J. Adv. Res.* **2018,** *6*(1), 388-393. https://doi.org/10.21474/IJAR01/6278.

[31] Aruho, C.; Nattabi, J. K.; Masembe, C.; Nyeko, J.; Rutaisire, J. Assessment of Artificial Breeding and Hatchery Management Practices of *Labeobarbus altianalis* in Uganda. *Aquacult. Res.* **2020,** *51*(6), 2384-2394. https://doi.org/10.1111/are.14602.

ASEAN
Journal of Scientific and Technological Reports
Online ISSN:2773-8752

Research article

Isolation, Characterization, and Identification of *Bacillus* spp. Strains from the Digestive Tract of Mad Carp (*Leptobarbus hoevenii*) and Their Potential Probiotic Properties

Suchanun Eamsakul[1], Ratchakrit Konrian[2], and Naraid Suanyuk[3*]

[1] Faculty of Natural Resources, Prince of Songkla University, Songkhla, 90110, Thailand
[2] Faculty of Natural Resources, Prince of Songkla University, Songkhla, 90110, Thailand
[3] Faculty of Natural Resources, Prince of Songkla University, Songkhla, 90110, Thailand
* Correspondence: naraid.s@psu.ac.th

Citation:
Eamsakul, S.; Konrian, R.; Suanyuk, N. Isolation, characterization, and identification of *Bacillus* spp. strains from the digestive tract of mad carp (*Leptobarbus hoevenii*) and their potential probiotic properties. *ASEAN J. Sci. Tech. Report.* **2025**, *28*(3), e258486. https://doi.org/10.55164/ajstr.v28i4.258486.

Article history:
Received: March 27, 2025
Revised: May 30, 2025
Accepted: June 11, 2025
Available online: June 30, 2025

Abstract: The present study aimed to collect isolates of *Bacillus* spp. from the digestive tracts of mad carps (*Leptobarbus hoevenii*) and to screen these for probiotic properties. In this study, 85 bacterial isolates were obtained from the digestive tracts of mad carps. Of these, 73 isolates were Gram-positive, rod-shaped, and catalase-positive, while only 48 bacterial isolates were endospore-forming. Evaluation of antagonistic effects of *Bacillus* spp. against pathogenic bacteria causing motile *Aeromonas* septicemia (MAS) in fish indicated that a total of 18 out of the 73 isolates exhibited antimicrobial activity, and especially the isolate MCSU14 expressed a significantly enlarged zone of inhibition ($p<0.05$). A study on the hemolytic activity of these 18 antimicrobial isolates revealed that 6 isolates were γ-hemolytic. Furthermore, the 6 γ-hemolytic isolates survived exposure to acidic and bile salt conditions and produced extracellular digestive enzymes. Among these six *Bacillus* spp., the isolate MCSU14 exhibited the most potent probiotic properties. Based on its biochemical characteristics and molecular analyses, the *Bacillus* sp. isolate MCSU14 is closely related to *Bacillus velezensis*. Our findings indicate that *Bacillus* spp. isolates from the digestive tracts of mad carp can be screened to find potent probiotics against MAS in aquaculture.

Keywords: *Bacillus* spp.; Probiotics; *Aeromonas* spp.; Mad carp

1. Introduction

Currently, aquaculture serves a crucial role in food security and nutrition, as it contributes to the production of aquatic animals to meet the growing global demand [1]. Freshwater aquaculture, in particular, is the main production source of aquatic animals, accounting for up to 77% of the world's total aquatic edible animal production [2]. However, infectious diseases remain a significant challenge in freshwater aquaculture, affecting both the cultured aquatic animals and the surrounding environment. In particular, motile *Aeromonas* septicemia (MAS) is a severe disease in fish and aquatic invertebrates, as well as amphibians, reptiles, mammals, and humans [3]. *Aeromonas* species known to cause severe MAS include *A. hydrophila* [4, 5], *A. veronii* [6-9], *A. jandaei* [10, 11] and *A. dhakensis* (formerly known as *A. aquariorum* or *A. hydrophila* subsp. *dhakensis*) [12]. Previously, *A. dhakensis* was often misidentified as *A. hydrophila* due to its close genetic relationship with this species, and was classified as a subspecies before a revision of taxonomy [13]. The use of antibiotics is one

alternative for treating diseases caused by *Aeromonas* spp. However, prolonged and incorrect use of antibiotics leads to bacterial resistance by the selection and development of strains that cause more severe diseases, and the antibiotics leave potential residues in aquatic animals, affecting consumers [14]. However, aquaculture must prioritize sustainability, environmental friendliness, and consumer safety. To achieve this, the use of probiotics is an alternative for supporting aquaculture, helping to replace chemicals and antibiotics [15]. Probiotics are microbial supplements that enhance nutrient digestion, inhibit pathogens, stimulate the immune system in the gut, and improve water quality [16]. These often include strains such as lactic acid bacteria (*Lactobacillus* sp., *Carnobacterium* sp., and *Enterococcus* sp.), yeast (*Saccharomyces cerevisiae*), and *Bacillus* spp. [17]. In particular, *Bacillus* spp. is widely used as a probiotic in aquaculture [18, 19] because this type of species can produce endospores that withstand harsh conditions, enabling survival in the acidic digestive tract [20]. These strains can produce antimicrobial substances against various microorganisms [21, 22], and most strains are not pathogenic to aquatic animals. The sources of potential probiotics in aquaculture, particularly of *Bacillus* spp., are commonly found in various environments, including fermented foods, natural aquatic environments such as sediments and water, as well as in the gastrointestinal tracts of healthy fish [17, 23]. Host-associated probiotics have garnered the most attention and offer a distinct advantage for the specific host, including improved growth performance, enhanced nutritional value, increased digestive enzyme activity, inhibition of pathogenic microorganism colonization, and improved hematological parameters and immune response [24]. Several studies have demonstrated the isolation of potential probiotics from the gastrointestinal tracts of freshwater fishes, such as Nile tilapia (*Oreochromis niloticus*) [25], common carp (*Cyprinus carpio* L.) [26], and snakehead fish (*Channa* sp.) [27]. To date, reports on the isolation of probiotics from the digestive tract of mad carp (*Leptobarbus hoevenii*), an economically important freshwater species native to Malaysia, Cambodia, Indonesia, Laos, Vietnam, and Thailand [28] remain limited. Sunarto *et al.* [29] reported the isolation of the probiotic bacterium *Proteus mirabilis* from the intestinal tract and culture environment of mad carp. Nevertheless, studies on the isolation of probiotics from the digestive tract of mad carp, particularly regarding *Bacillus* spp., are still lacking. Therefore, this study aimed to isolate and characterize *Bacillus* spp. possessing probiotic properties from the intestines of mad carp, which could be used as natural supplements in aquaculture.

2. Materials and Methods

2.1 Ethics statement

The experimental procedures in this study followed the guidelines of the Institute of Animals for Scientific Purposes Development, National Research Council, Thailand. The procedures were approved by the Institutional Animal Care and Use Committee, Prince of Songkla University, under permission number Ref. AQ037/2024.

2.2 Isolation of *Bacillus* spp.

Bacillus spp. were isolated from the digestive tracts of farmed and wild mad carp in southern Thailand using the heat-shock treatment method [30]. The digestive tract was aseptically dissected and washed with 0.85% (w/v) sterile saline. One gram of each sample was finely homogenized, then diluted with 9 ml of 0.85% sterile saline. The homogenates were further diluted to decrease their concentration by a factor of 10^{-3}. Subsequently, the sample was boiled at 80°C for 10 minutes and then immediately soaked in room-temperature water for 3 minutes. A sample volume of 100 µl was spread onto nutrient agar (NA) and incubated at 30°C for 24 to 48 hours. Afterward, morphologically different colonies were selected for re-streaking on NA to obtain pure cultures. The pure cultures were Gram-stained and examined microscopically for their Gram-staining reaction, shape, and endospore formation.

2.3 Screening of probiotic properties

2.3.1 Antimicrobial activity

2.3.1.1 Cross-streak method

Seventy-three candidate *Bacillus* spp. isolates were tested for antimicrobial activity using the cross-streak method [31]. *Bacillus* spp. strains were streaked on the center of a Muller-Hinton agar (MHA) plate (Himedia, India) and incubated at 30°C for 48 hours. After incubation, the pathogenic bacteria *A. veronii*,

A. dhakensis, and *A. jandaei* were streaked perpendiculary on the plate. The procedure was performed in triplicate for each bacterial isolate to validate the results. The plates were then incubated at 30°C for 24 hours to observe inhibitory activity. The ability of *Bacillus* spp. to inhibit the pathogenic bacteria was determined by measuring the inhibition zone, and the results are reported in millimeters.

2.3.1.2 Agar well diffusion method

Eighteen *Bacillus* spp. isolates exhibiting the ability to inhibit pathogens, as observed by the cross-streak method, were selected to assess their inhibitory effects against *A. veronii*, *A. dhakensis*, and *A. jandaei* using the agar well diffusion method modified from Baharudin *et al*. [32]. *Bacillus* spp. suspension, cell-free supernatant (CFS), and cell pellet were tested in this study. The suspension of *Bacillus* spp. cultured in nutrient broth (NB) was shaken at 30°C and 160 rpm for 72 hours. Half of the *Bacillus* spp. suspension was then centrifuged at 9,184 ×*g* for 10 min at 4°C. The CFS was collected and filtered using a sterile syringe filter with a 0.22 μm pore size. The pellets were washed twice with 0.85% sterile saline and then resuspended in 0.85% sterile saline. The resuspended cell pellet was adjusted to an optical density of 0.1 at a 600 nm wavelength. The pathogenic bacteria were prepared by adjusting the suspension of each *Aeromonas* spp. isolate with 0.85% sterile saline to achieve a final concentration equivalent to the 0.5 McFarland standard (10^8 CFU/ml). This bacterial suspension was then spread onto MHA and allowed to dry at room temperature. Subsequently, holes were drilled, each with a diameter of approximately 8 mm, at eight positions per plate. Subsequently, 50 μl of each suspension, CFS, or resuspended cell pellet of *Bacillus* spp. was loaded into its well and incubated at 30°C for 24 hours. Oxytetracycline at a concentration of 1.5 mg/ml and NB were used as positive and negative controls, respectively. The assay was conducted in triplicate for each bacterial isolate. The ability to inhibit the pathogenic bacteria was examined by measuring the inhibition zone. Results are reported in millimeters.

2.3.2 Hemolytic activity

Eighteen candidate *Bacillus* spp. isolates with the potential to inhibit pathogenic *Aeromonas* spp. were assessed for hemolytic activity. Each *Bacillus* sp. isolate was streaked on blood agar base containing 5% defibrinated sheep blood and then incubated at 30°C for 24-48 hours to observe the decomposition of red blood cells. The procedure was performed in triplicate for each bacterial isolate. *Bacillus* spp. strains that do not lyse red blood cells (γ-hemolytic *Bacillus* spp.) were selected for further study.

2.3.3 Acid tolerance

Six γ-hemolytic *Bacillus* spp. isolates were tested for pH tolerance using the method modified from Ritter *et al.* [33] and Dabiré *et al.* [34]. Briefly, *Bacillus* spp. strains were inoculated into NB with shaking at 160 rpm and 30°C for 24 hours. Subsequently, 1 mL of suspension was transferred into 10 mL of NB and adjusted to a final pH level of 1, 2, 3, 4, or 5 with 1 N hydrochloric acid and sodium hydroxide. The assay was carried out in triplicate for each bacterial isolate. After incubation at 30°C for 3 hours, the survival rate of bacteria was determined using the drop plating technique at 0 and 3 hours. The suspension of each sample was 10-fold serially diluted, and then 20 μl of the suspension from each dilution was dropped onto NA and incubated at 30°C for 24 hours. The colonies were then counted. The results were calculated in units of CFU/ml, and the survival rate was calculated using the following formula.

$$\text{Survival rate (\%)} = \frac{N_3}{N_0} \times 100$$

Note: N_3 = Number of colonies after incubation for 3 hours (log CFU/ml)

N_0 = Number of colonies at 0 hours (log CFU/ml)

2.3.4 Bile salt tolerance

Six γ-hemolytic *Bacillus* spp. isolates were tested for bile tolerance using the method modified from Dabiré *et al.* [34]. Briefly, *Bacillus* spp. strains were inoculated into NB and incubated at 30°C with shaking at 160 rpm for 24 hours. Subsequently, 1 mL of suspension was transferred into 10 mL of NB supplemented with 0.3% (w/v) bile salt (Oxoid) and incubated at 30°C for 3 hours. The procedure was conducted in triplicate and the survival rate was assessed using the drop plating technique at 0 and 3 hours.

2.3.5 Digestive enzyme production

Six *Bacillus* spp. isolates were tested for the production of digestive enzymes, including amylase, protease, and lipase, using the method modified from Santong *et al.* [35] and Proca *et al.* [36]. Briefly, *Bacillus* spp. strains were point inoculated onto NA supplemented with 1% starch, 2% skim milk, and 1% Tween 80 with 0.1 g of $CaCl_2$ for testing starch, protein, and fatty hydrolyses, respectively. The assay was done in triplicate for each bacterial isolate. The plates were then incubated at 30°C for 24 hours. Subsequently, for starch hydrolysis, Lugol's solution was dropped onto the surface of the starch agar medium and left for 10-15 minutes. The appearance of a clear zone around the *Bacillus* spp. colonies indicated digestive enzyme production. The results are reported as hydrolytic capacity, which was calculated as follows [37].

$$\text{Hydrolytic capacity} = \frac{\text{Diameter of the clear zone around the bacterial colonies (mm)}}{\text{Diameter of the bacterial colonies (mm)}}$$

2.4 Bacterial identification

The candidate *Bacillus* sp. with potential probiotic properties was selected for bacterial identification based on their biochemical characteristics using API 50CHB strips and API 20E strips (BioMérieux, France) according to the manufacturer's instructions. Candidate *Bacillus* sp. was further confirmed by molecular analysis. Bacterial DNA extraction was conducted using a DNA extraction kit (Qiagen). The DNA was then amplified using primers targeting the DNA gyrase subunit A (*gyrA*) and RNA polymerase subunit B (*rpoB*) genes [38]. Polymerase chain reaction (PCR) was performed in a total volume of 50 µL for each sample, consisting of 25 µL of 2x PCR master mix (RBC Bioscience, Taiwan), 1 µL of each primer (0.2 µM), 20.5 µL of distilled water, and 2.5 µL of DNA template. Amplification was done using a thermal cycler (Bio-Rad, USA). The conditions included an initial denaturation step at 95°C for 3 minutes, followed by 35 cycles of denaturation at 94°C for 30 seconds, annealing at 55°C (for *gyrA*) or 50°C (for *rpoB*) for 30 seconds, and extension at 72°C for 2 minutes. At the end of the cycle, a final extension at 72°C for 5 minutes was performed. The PCR products were analyzed by gel electrophoresis on a 1.8% agarose gel, and the DNA was visualized using gel documentation (Bio-Rad, USA). The amplified DNA was then purified using a gel extraction kit (Qiagen) and subsequently sent to Macrogen (Korea) for sequencing. The resulting sequence was compared to sequences in the GenBank/EMBL/DDBJ database using the Basic Local Alignment Search Tool (BLAST) for comparison. Additionally, phylogenetic analysis was performed using the Molecular Evolutionary Genetics Analysis (MEGA 11) software [39].

2.5 Statistical analysis

The results are expressed as an average with standard deviation (SD) from the mean. Percentage data were transformed to arcsine before the variance analysis. The data were analyzed using one-way ANOVA, and comparisons of mean values were analyzed using Duncan's Multiple Range Test (DMRT) at a 95% confidence interval ($p < 0.05$).

3. Results and Discussion

3.1. Isolation of *Bacillus* spp.

Nineteen digestive tract samples of mad carp were subjected to bacterial isolation by heat-shock treatment. A total of 85 isolates were obtained in the present study. Colony morphology was observed after growing colonies on NA and incubating them at 30°C for 48 hours. The colony colors, such as white, cream, pink, and yellow, were observed. The colony shapes varied, including circular, rhizoid, irregular, and filamentous forms. The margins of colonies were noted to be entire, irregular, lobate, or filamentous. It was found that 73 out of the 85 isolates were Gram-positive, rod-shaped, and catalase-positive. Of these, only 48 isolates were capable of forming endospores. *Bacillus* spp. is a group of bacterial strains that has long received attention for its probiotic properties in aquaculture. In particular, the ability of probiotics to control or prevent fish pathogens has been studied. *Bacillus* spp. strains isolated from the digestive tracts of freshwater fish have been effective in inhibiting pathogens in these fish [25, 27, 40].

3.2 Screening of probiotic properties

3.2.1 Antimicrobial activity

3.2.1.1 Cross-streak method

In this study, 73 *Bacillus* spp. isolates from the digestive tract of mad carp were evaluated for their potential to inhibit *A. veronii*, *A. dhakensis*, and *A. jandaei*, the causative agents responsible for MAS in freshwater fishes, using the cross-streak method. The results revealed that a total of 18 out of the 73 isolates exhibited antimicrobial activity against all *Aeromonas* spp. tested in this study. These *Bacillus* spp. isolates showed inhibition zones ranging from 2.17 ± 0.29 mm to 9.00 ± 1.00 mm (Figure 1). Among these, the *Bacillus* sp. isolate MCSU14 exhibited the largest zones of inhibition against *A. veronii* (9.00 ± 1.00 mm), *A. dhakensis* (8.33 ± 0.58 mm), and *A. jandaei* (8.33 ± 0.58 mm).

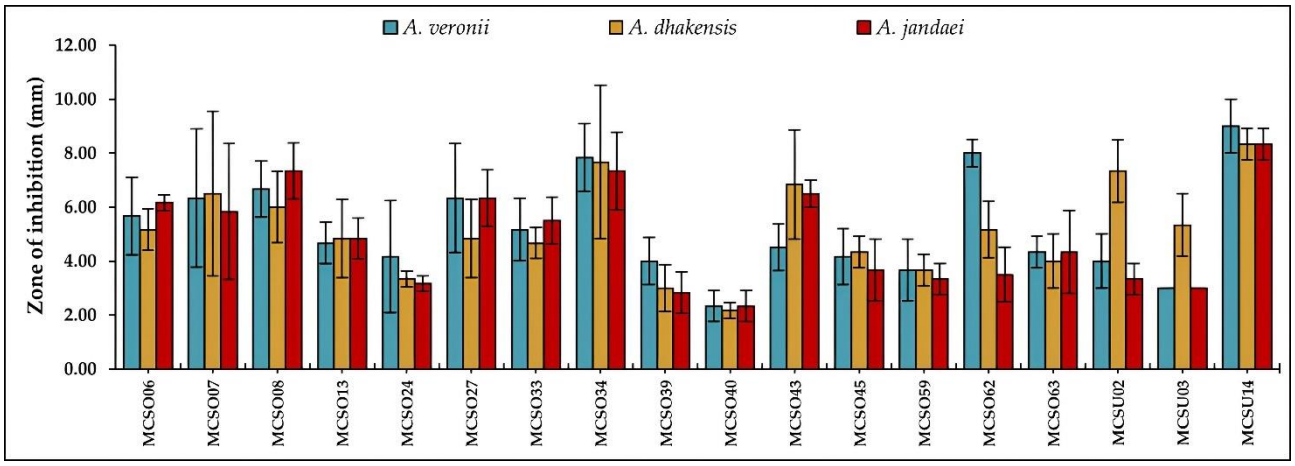

Figure 1. Antagonistic effect of *Bacillus* spp. against *A. veronii*, *A. dhakensis* and *A. jandaei* as determined in a cross-streak assay.

3.2.1.2 Agar well diffusion method

The eighteen *Bacillus* spp. isolates that exhibited antimicrobial activity by the cross-streak method were further assessed for antimicrobial activity against *A. veronii*, *A. dhakensis*, and *A. jandaei* using the agar well diffusion method. Using overnight culture suspensions, all *Bacillus* spp. isolates exhibited inhibition zones (Figure 2A), particularly those of *Bacillus* spp. isolates MCSO07, MCSU14, and MCSO34 showed the largest inhibition zones against *A. veronii* (14.67 ± 0.58 mm), *A. dhakensis* (17.33 ± 0.58 mm), and *A. jandaei* (16.00±1.00 mm), respectively. On using the CFS, only 9 *Bacillus* spp. isolates were capable of inhibiting *Aeromonas* spp. (Figure 2B). Notably, CFS from *Bacillus* sp. isolate MCSO34 showed the largest inhibition zones against *A. veronii* (11.00 ± 2.00 mm), *A. dhakensis* (9.33 ± 2.08 mm), and *A. jandaei* (9.67 ± 1.53 mm). Moreover, only three *Bacillus* spp. strains, namely MCSO13, MCSO34, and MCSU14, were capable of inhibiting all three *Aeromonas* spp. Additionally, using only cells at a concentration of 10^8 CFU/ml, *Bacillus* spp. isolates MCSO06, MCSU14 and MCSO34 exhibited the largest inhibition zones against *A. veronii* (12.33 ± 0.58 mm), *A. dhakensis* (14.33 ± 0.58 mm) and *A. jandaei* (13.67 ± 4.04 mm), respectively (Figure 2C). In this study, 18 out of the 73 *Bacillus* spp. isolates showed inhibitory effect against *Aeromonas* spp., as evidenced by the zone of inhibition, preventing the pathogen from growing on the culture medium. Notably, several *Bacillus* spp. isolates from the present study were found to inhibit *A. dhakensis*, a recently recognized species associated with MAS. Previous studies have indicated the activity of *Bacillus* spp. strains against *Aeromonas* spp., such as those of *B. velezensis* [41-42], *B. amyloliquefaciens* [43], *B. subtilis* [44-45], and *B. methylotrophicus* [46]. This is achieved through the function of *Bacillus* spp. in directly inhibiting pathogens, especially by producing pathogen inhibitors. The substances produced, such as bacteriocins, exert their antimicrobial effects by disrupting cell wall synthesis or creating pores in the cell membrane [47]; lipopeptides, including surfactin, iturin, and fengycin, are secondary metabolites known to disrupt bacterial membranes [48]; polyketides exhibit antibacterial activity by inhibiting protein synthesis [49]. In addition, *Bacillus* spp. are capable of producing the enzyme N-acyl homoserine lactones (AHL) lactonase, which plays a critical role in the quorum quenching process. This enzyme degrades

signaling molecules known as AHL, which are essential for quorum sensing, a mechanism used by pathogenic bacteria to coordinate gene expression related to virulence, toxin production, and biofilm formation [50]. Generally, these bioactive substances produced by bacteria are secreted outside the cell as extracellular bacteriostatic substances [51, 52].

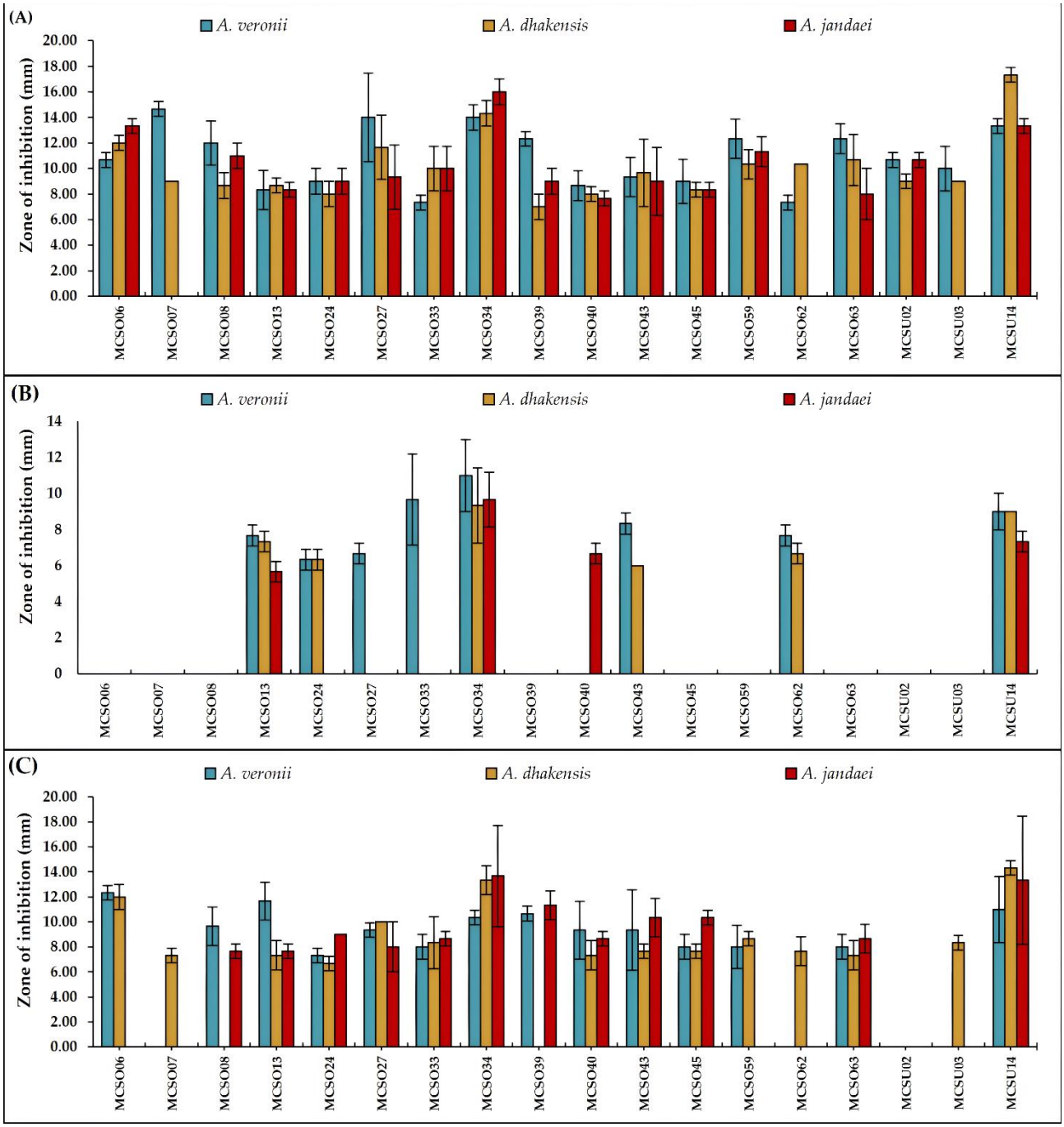

Figure 2. Antagonistic effects of (A) overnight culture suspension, (B) CFS, and (C) cells of *Bacillus* spp. against *A. veronii*, *A. dhakensis*, and *A. jandaei* as determined by agar well diffusion assay.

3.2.2 Hemolytic activity

In this study, eighteen *Bacillus* spp. isolates that exhibited antimicrobial activities were evaluated for hemolytic activity. The results showed that 6 out of these 18 isolates, namely MCSO07, MCSO13, MCSO33, MCSO45, MCSO62, and MCSU14, displayed γ-hemolysis, defined by the inability to lyse red blood cells. On the other

hand, twelve isolates exhibited α-hemolytic activity, with a slight ability to lyse red blood cells. A good probiotic bacterium should possess qualities beneficial to the host organism. Additionally, it must not cause disease or be toxic to the host [53]. The hemolytic activity test is a crucial examination in this regard. If the chosen probiotic exhibits hemolytic activity, it is considered a pathogen [54], as it may cause anemia and edema in the host [55].

3.2.3 Acid tolerance

The six γ-hemolytic *Bacillus* spp. isolates were evaluated for their survival under acidic conditions at pH levels ranging from 1 to 5 for 3 hours, indicating their potential as effective probiotics. It was found that all the isolates exhibited viability under acidic conditions (Figure 3). At pH 1 and 5, no significant difference ($p > 0.05$) was observed in the survival rate for any of the isolates tested in this study. Moreover, *Bacillus* spp. isolates MCSO45 and MCSU14 showed the highest survival rates at pH 2 and pH 3, respectively. Additionally, *Bacillus* sp. isolate MCSO45 demonstrated the highest survival rate at pH 4. The ability of probiotics to tolerate a wide range of environmental conditions is a crucial property that enables them to be well tolerated in the digestive tract [56]. Further investigation into their survival under a wide range of temperatures and salinities may provide more insight into understanding the adaptability and probiotic efficacy of the isolates within the complex gastrointestinal environments of aquatic animals.

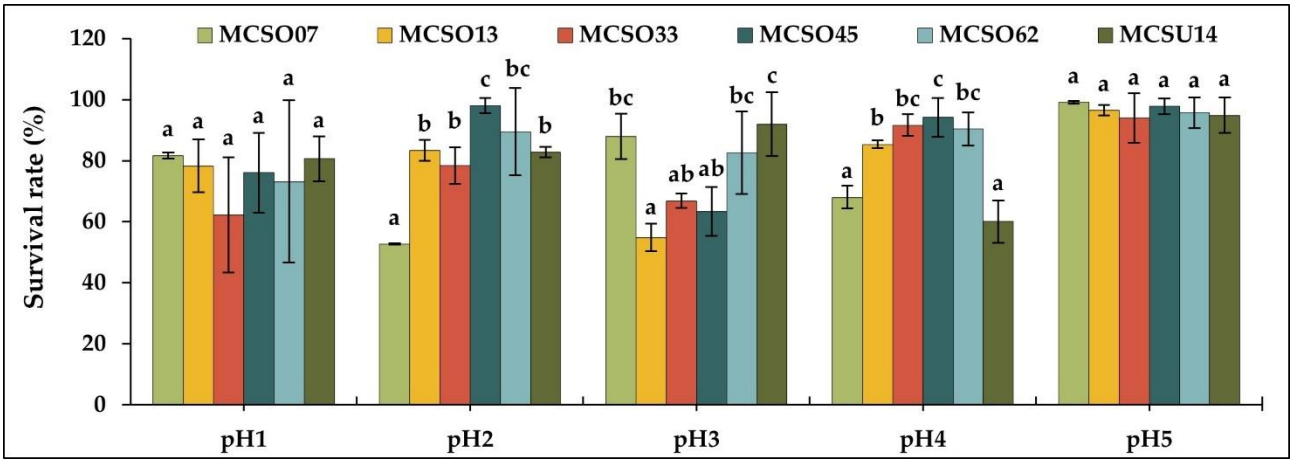

Figure 3. Survival rates of *Bacillus* spp. cultured under various acidity levels for 3 hours. Different letters indicate significant differences between the *Bacillus* sp. strains when compared at the same pH level ($p < 0.05$).

3.2.4 Bile salts tolerance

Evaluation of survival under exposure to bile for the six γ-hemolytic *Bacillus* spp. strains indicated that all these isolates exhibited viability, with a survival rate of over 90% after 3 hours (Figure 4). *Bacillus* sp. isolate MCSO33 showed the significantly lowest survival rate ($p < 0.05$). In this study, six isolates of *Bacillus* spp. were capable of enduring bile exposure for three hours, with a survival rate exceeding 90% suggesting that they have the potential for stability and survivability within the gastrointestinal tract. The resistance to stressful conditions by *Bacillus* spp. strains are attributed to their endospores, which can endure harsh environmental conditions [54]. Yousuf *et al.* [27] reported that *B. paramycoides* demonstrated tolerance to both acidic and alkaline pH levels, bile salts, and exhibited strong adhesion capacity. Therefore, further evaluations of persistence within the gastrointestinal tract, such as adhesion capacity, cell surface hydrophobicity,

autoaggregation, and coaggregation of *Bacillus* spp. from the present study, are necessary to understand better their functional properties and ability to colonize the host's gastrointestinal environment.

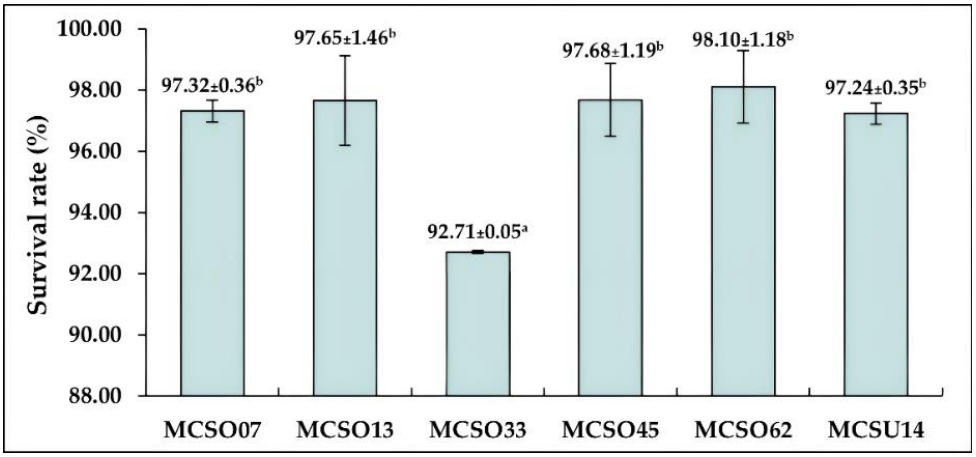

Figure 4. Tolerance of *Bacillus* spp. cultured in NB supplemented with 0.3% bile for 3 hours. Different superscripts indicate significant differences ($p < 0.05$).

3.2.5 Digestive enzyme production

The results revealed that six *Bacillus* spp. isolates produced extracellular digestive enzymes (Figure 5). All isolates showed hydrolysis capacity to digest starch in the range from 1.37 ± 0.38 to 3.53 ± 0.42, protein in the range from 1.17 ± 0.07 to 2.17 ± 0.48, and fat in the range from 1.12 ± 0.07 to 1.56 ± 0.38 (Figure 6). Additionally, it was found that *Bacillus* spp. isolates MCSO07, MCSO13, and MCSO33 exhibit the highest hydrolysis capacities for digesting starch, protein, and fat, respectively ($p < 0.05$). Important properties of probiotics for the host include helping to balance the intestinal microbiome and aiding in the digestion of food. Some probiotic bacteria can produce digestive enzymes that assist digestion, such as amylase for carbohydrate digestion, protease for protein digestion, and lipase for fat digestion [37]. In this study, six isolates of *Bacillus* spp. were found to be capable of producing digestive enzymes, specifically extracellular enzymes. Liu *et al.* [57] reported that *B. subtilis* HAINUP40 increased the protease and amylase activities in the digestive tract of Nile tilapia.

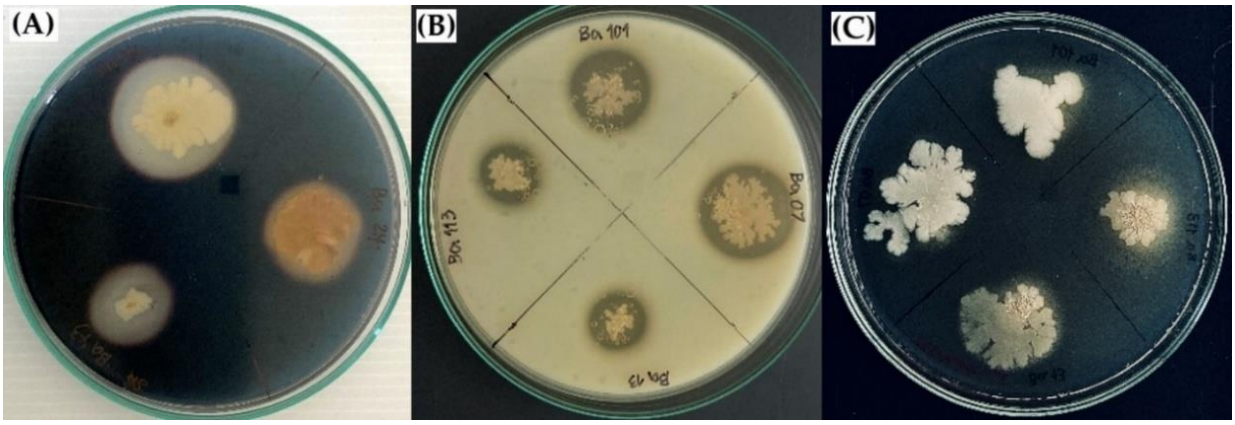

Figure 5. Zones of hydrolysis for (A) starch, (B) protein, and (C) fat, by *Bacillus* spp. isolates tested in the present study.

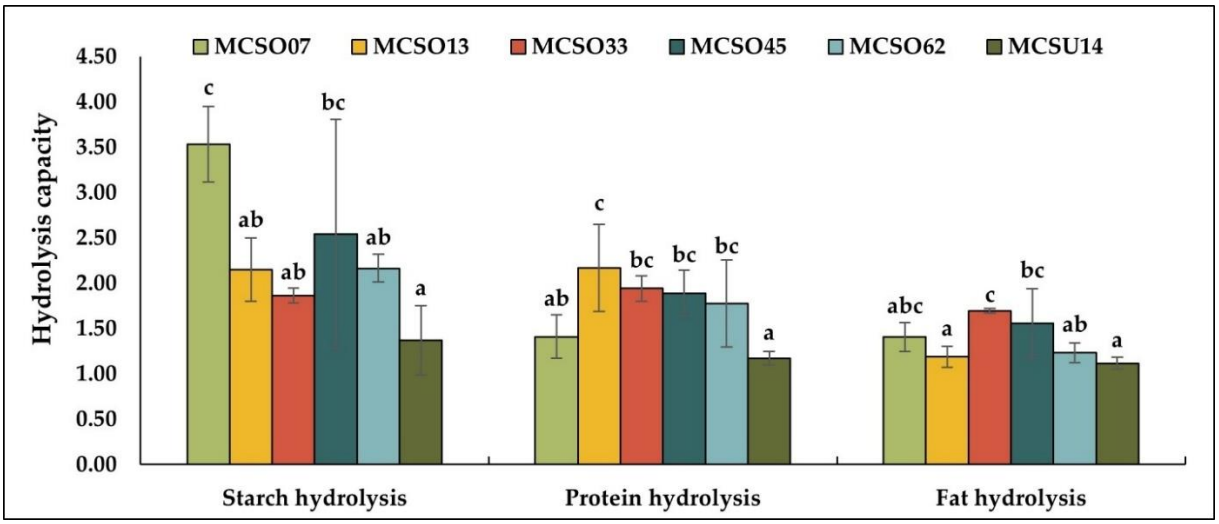

Figure 6. The capacity to hydrolyze starch, protein, and fat by six *Bacillus* spp. isolates tested in the present study. Different letters indicate significant differences between the *Bacillus* sp. strains with the same substrate ($p < 0.05$).

3.3 Bacterial identification

Among the six *Bacillus* spp. isolates, namely MCSO07, MCSO13, MCSO33, MCSO45, MCSO62, and MCSU14, which had exhibited probiotic properties, *Bacillus* sp. isolate MCSU14 demonstrated outstanding probiotic characteristics, including the highest inhibitory activity against *Aeromonas* spp. Furthermore, *Bacillus* sp. isolate MCSU14 did not hydrolyze red blood cells, exhibited survival in acidic and bile salt conditions, and produced extracellular digestive enzymes. As a result, *Bacillus* sp. isolate MCSU14 was chosen as the superior candidate for serving as a probiotic. *Bacillus* sp. isolate MCSU14 was identified based on its biochemical characteristics using API 50 CHB and API 20E strips. The results showed that *Bacillus* sp. isolate MCSU14 was capable of fermenting 27 carbohydrates, including glycerol, L-arabinose, D-ribose, D-xylose, D-glucose, D-fructose, D-mannose, inositol, D-mannitol, D-sorbitol, methyl α-D-glucopyranoside, amygdalin, arbutin, esculin, salicin, D-cellobiose, D-maltose, D-lactose, D-melibiose, D-sucrose, D-trehalose, inulin, D-raffinose, starch, glycogen, gentiobiose, and D-turanose (Table 1) Additionally, the isolate was capable of producing acetoin through glucose fermentation and exhibited gelatinase enzyme activity (Table 2) Based on the APIweb™ software, *Bacillus* sp. isolate MCSU14 was identified as *Bacillus subtilis/amyloliquefaciens* with a 99.6% similarity. The results do not clearly distinguish between the two species using the API 50CHB. This could be due to having only insufficient data for these species, or to difficulties in classification within the API 50CHB system. Moreover, the APIweb™ database does not contain data for other members of the *Bacillus subtilis* species complex, such as *B. velezensis, B. siamensis, B. tequilensis, B. valismortis*, and *B. mojavensis* [58]. Therefore, the classification of *Bacillus* sp. based only on the biochemical characteristics appears insufficient for accurate identification. As a result, additional molecular identification methods were necessary for proper classification. Moreover, the carbohydrate fermentation profile of *Bacillus* sp. isolate MCSU14 was compared with closely related strains, including *B. velezensis* CR-502 [59], *B. amyloliquefaciens* PMC-80 [60], and *B. siamensis* PD-A10 [61] (Table 1). The results indicate that *Bacillus* sp. isolate MCSU14 is closely related to these three species, suggesting that it may belong to the operational group of *B. amyloliquefaciens*.

The operational group of *B. amyloliquefaciens* (OGBa) consists of *B. amyloliquefaciens*, *B. velezensis*, *B. siamensis*, and *B. nakamurai* [62], all of which are part of the *Bacillus subtilis* species complex group [63]. Identification of *Bacillus* species using 16S rRNA gene sequencing may not provide clear differentiation for closely related species [64]. Therefore, *gyrA* and *rpoB* gene sequences were used to assess the identity of the chosen *Bacillus* sp. within the closely related *Bacillus* group. The *gyrA* gene sequence from *Bacillus* sp. isolate MCSU14 showed 99.89% similarity to *B. velezensis* PFX12 (accession number: MZ027153), *B. velezensis* gjfn4 (accession number: MW316630), and *B. velezensis* 26.3 (accession number: CP115185). The *rpoB* gene sequence

from *Bacillus* sp. isolate MCSU14 showed 100% similarity to *B. velezensis* AP45 (accession number: CP160218), *B. velezensis* R-71003 (accession number: CP092446), and *B. velezensis* SRCM102741 (accession number: CP028205). The phylogenetic trees based on the *gyrA* gene (Figure 7A) and *rpoB* gene (Figure 7B) sequences for the *Bacillus* sp. isolate MCSU14 revealed that it is closely related to *B. velezensis* in both genes. Therefore, it can be concluded that *Bacillus* sp. isolate MCSU14 is closely related to *B. velezensis*. However, it should be noted that additional techniques, such as whole-genome sequencing, fatty acid methyl ester profiling, or DNA G+C content analysis, could support a more precise identification. Previously, Kang *et al.* [26] reported the isolation of *B. velezensis* R-71003 from the intestine of common carp, while Wu *et al.* [40] reported the isolation of *B. velezensis* B8 from the gut of grass carp (*Ctenopharyngodon idella*). Our findings highlight the significance of *Bacillus* sp. isolate MCSU14, which is closely related to *B. velezensis* isolated from the intestine of mad carp, a novel source of *Bacillus* spp.

Table 1. Characterization of *Bacillus* sp. isolate MCSU14 by using API 50CHB strip. Comparison of the phenotypic characteristics of the present isolate with the reference strains.

No.	Biochemical test	1	2	3	4	No.	Biochemical test	1	2	3	4
0	Control	-	-	-	-	25	Esculin	+	+	+	+
1	Glycerol	+	+	+	+	26	Salicin	+	+	+	+
2	Erythritol	-	-	-	-	27	D-Cellobiose	+	+	+	+
3	D-Arabinose	-	-	-	-	28	D-Maltose	+	+	+	+
4	L-Arabinose	+	+	+	+	29	D-Lactose	+	+	-	+
5	D-Ribose	+	+	+	+	30	D-Melibiose	+	-	+	-
6	D-Xylose	+	+	-	+	31	D-Saccharose	+	+	+	+
7	L-Xylose	-	-	-	-	32	D-Trehalose	+	+	+	-
8	D-Adonitol	-	-	-	-	33	Inulin	+	-	+	-
9	Methyl-ß-D-xylopyranoside	-	-	-	-	34	D-Melezitose	-	-	-	-
10	D-Galactose	-	-	+	-	35	D-Raffinose	+	+	+	+
11	D-Glucose	+	+	-	+	36	Starch	+	ND	+	+
12	D-Fructose	+	+	+	+	37	Glycogen	+	+	+	+
13	D-Mannose	+	+	-	-	38	Xylitol	-	-	-	-
14	L-Sorbose	-	-	+	-	39	Gentiobiose	+	-	-	+
15	L-Rhamnose	-	-	-	-	40	D-Turanose	+	-	-	-
16	Dulcitol	-	-	-	-	41	D-Lyxose	-	-	-	-
17	Inositol	+	+	-	+	42	D-Tagatose	-	-	+	-
18	D-Mannitol	+	+	+	+	43	D-Fucose	-	-	-	-
19	D-Sorbitol	+	+	+	+	44	L-Fucose	-	-	-	-
20	Methyl α-D-mannopyranoside	-	-	-	-	45	D-Arabitol	-	-	-	-
21	Methyl α-D-glucopyranoside	+	+	+	+	46	L-Arabitol	-	-	-	-
22	N-Acetylglucosamine	-	-	-	-	47	Potassium gluconate	-	-	-	-
23	Amygdalin	+	+	+	+	48	Potassium 2-ketogluconate	-	-	-	-
24	Arbutin	+	+	+	+	49	Potassium 5-ketogluconate	-	-	-	-

Remark: 1; *Bacillus* sp. isolate MCSU14 (this study), 2; *B. velezensis* CR-502 [59], 3; *B. amyloliquefaciens* PMC-80 [60], 4; *B. siamensis* PD-A10 [61], +; Positive result, -; Negative result, and ND; Not determined.

Table 2. Characterization of *Bacillus* sp. isolate MCSU14 by using API 20E strip.

No.	Biochemical test	Result	No.	Biochemical test	Result
1	O-nitrophenyl-ß-D-galactopyranoside	-	7	Urease	-
2	Arginine dihydrolase	-	8	Tryptophan deaminase	-
3	Lysine decarboxylase	-	9	Indole	-
4	Ornithine decarboxylase	-	10	Voges-Proskauer	+
5	Citrate	-	11	Gelatinase	+
6	Hydrogen sulfide	-	12	Nitrate	-

Remark: +; Positive result and -; Negative result

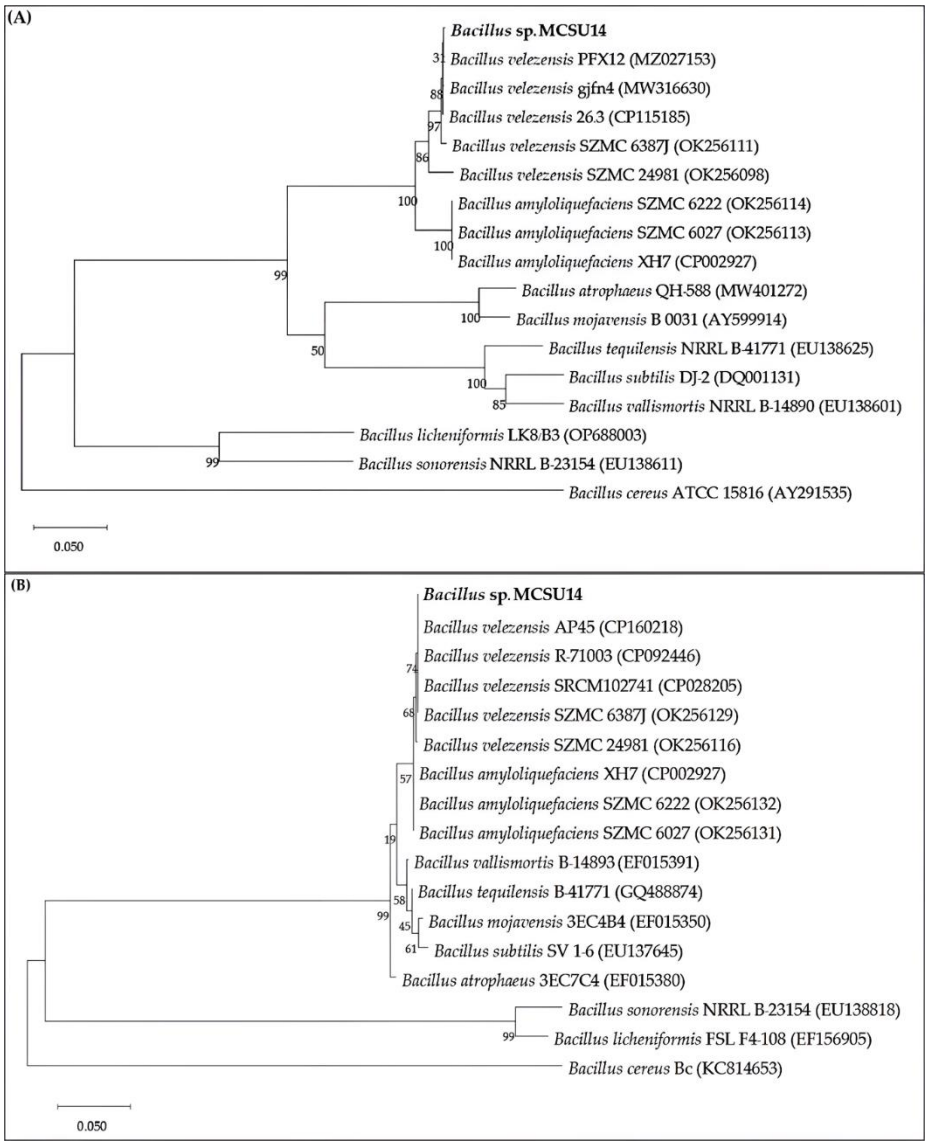

Figure 7. Neighbor-joining phylogenetic tree based on *gyrA* gene (A), and on *rpoB* gene (B) sequences of *Bacillus* species, showing positions of *Bacillus* sp. isolate MCSU14 and closely related members of the genus *Bacillus* sp. Bootstrap values (in percent) calculated from 1000 replications are shown at branch nodes. The evolutionary distances were computed using the Maximum Composite Likelihood method. The scale bar represents 0.05 nucleotide substitutions per nucleotide position. *B. cereus* ATCC 15816 and *B. cereus* Bc were used as the outgroups.

4. Conclusions

In the present study, 73 *Bacillus* spp. isolates from the gastrointestinal tracts of mad carps were examined for potential probiotic properties. Only 18 isolates of *Bacillus* spp. demonstrated antagonistic activity against *A. veronii*, *A. dhakensis*, and *A. jandaei*. Additionally, *Bacillus* spp. isolates MCSO07, MCSO13, MCSO33, MCSO45, MCSO62, and MCSU14 exhibited non-hemolytic activity, tolerance to acids and bile salts, and the production of digestive enzymes. Identification of the *Bacillus* isolate MCSU14, based on biochemical characteristics and molecular analysis, indicated that this bacterial isolate is closely related to *B. velezensis*. This study highlights that *Bacillus* spp. isolates from the gastrointestinal tracts of mad carps have significant potential to be screened for potent probiotics.

5. Acknowledgements

Thanks to Akkarawit Issaro, Suppanat Thaneerat, and Paweena Wanwang for their assistance throughout this research.

Author Contributions: Conceptualization, S.E. and N.S.; methodology, S.E, R.K. and N.S.; software, S.E.; validation, N.S.; formal analysis, S.E. and N.S.; investigation, S.E., R.K. and N.S.; resources, S.E., R.K. and N.S.; data curation, S.E.; writing—original draft preparation, S.E. and N.S.; writing—review and editing, S.E. and N.S.; supervision, N.S. All authors have read and agreed to the published version of the manuscript.

Funding: This research received no external funding.

Conflicts of Interest: The authors declare no conflict of interest.

References

[1] Beveridge, M. C. M.; Thilsted, S. H.; Phillips, M. J.; Metian, M.; Troell, M.; Hall, S. J. Meeting the food and nutrition needs of the poor: The role of fish and the opportunities and challenges emerging from the rise of aquaculture. *J. Fish Biol.* **2013**, *83*(4), 1067-1084. https://doi.org/10.1111/jfb.12187

[2] Zhang, W.; Belton, B.; Edwards, P.; Henriksson, P. J. G.; Little, D. C.; Newton, R.; Troell, M. Aquaculture will continue to depend more on land than sea. *Nature* **2022**, *603*, E2-E4. https://doi.org/10.1038/s41586-021-04331-3

[3] Hanson, L. A.; Hemsteet, W. G.; Hawke, J. P. *Motile Aeromonas Septicemia (MAS) in Fish*; Southern Regional Aquaculture Center: USA, **2019**; SRAC Publication No. 0478.

[4] Nhinh, D. T.; Le, D. V.; Van, K. V.; Huong Giang, N. T.; Dang, L. T.; Hoai, T. D. Prevalence, virulence gene distribution, and alarming multidrug resistance of *Aeromonas hydrophila* associated with disease outbreaks in freshwater aquaculture. *Antibiotics* **2021**, *10*(5), 532. https://doi.org/10.3390/antibiotics10050532

[5] Zhao, X. L.; Jin, Z. H.; Di, G. L.; Li, L.; Kong, X. H. Molecular characteristics, pathogenicity, and medication regimen of *Aeromonas hydrophila* isolated from common carp (*Cyprinus carpio* L.). *J. Vet. Med. Sci.* **2019**, *81*(12), 1769-1775. https://doi.org/10.1292/jvms.19-0025

[6] Ran, C.; Qin, C.; Xie, M.; Zhang, J.; Li, J.; Xie, Y.; Wang, Y.; Li, S.; Liu, L.; Fu, X.; Lin, Q.; Li, N.; Liles, M. R.; Zhou, Z. *Aeromonas veronii* and aerolysin are important for the pathogenesis of motile aeromonad septicemia in cyprinid fish. *Environ. Microbiol.* **2018**, *20*(9), 3442-3456. https://doi.org/10.1111/1462-2920.14390

[7] Chen, F.; Sun, J.; Han, Z.; Yang, X.; Xian, J. A.; Lv, A.; Hu, X.; Shi, H. Isolation, identification, and characteristics of *Aeromonas veronii* from diseased crucian carp (*Carassius auratus gibelio*). *Front. Microbiol.* **2019**, *10*, 2742. https://doi.org/10.3389/fmicb.2019.02742

[8] Hoai, T. D.; Trang, T. T.; Van Tuyen, N.; Giang, N. T. H.; Van Van, K. *Aeromonas veronii* caused disease and mortality in channel catfish in Vietnam. *Aquaculture* **2019**, *513*, 734425. https://doi.org/10.1016/j.aquaculture.2019.734425

[9] Dos Santos, S. B.; Alarcon, M. F.; Ballaben, A. S.; Harakava, R.; Galetti, R.; Guimarães, M. C.; Natori, M. M.; Takahashi, L. S.; Ildefonso, R.; Rozas-Serri, M. First report of *Aeromonas veronii* as an emerging bacterial pathogen of farmed Nile tilapia (*Oreochromis niloticus*) in Brazil. *Pathogens* **2023**, *12*(8), 1020. https://doi.org/10.3390/pathogens12081020

[10] Kumar, K.; Prasad, K.; Tripathi, G.; Raman, R.; Kumar, S.; Tembhurne, M.; Purushothaman, C. Isolation, identification, and pathogenicity of a virulent *Aeromonas jandaei* associated with mortality of farmed *Pangasianodon hypophthalmus*, in India. *Isr. J. Aquacult. Bamidgeh* **2014**, *67*. https://doi.org/10.46989/001c.20727

[11] Assane, I. M.; de Sousa, E. L.; Valladão, G. M. R.; Tamashiro, G. D.; Criscoulo-Urbinati, E.; Hashimoto, D. T.; Pilarski, F. Phenotypic and genotypic characterization of *Aeromonas jandaei* involved in mass mortalities of cultured Nile tilapia, *Oreochromis niloticus* (L.) in Brazil. *Aquaculture* **2021**, *541*, 736848. https://doi.org/10.1016/j.aquaculture.2021.736848

[12] Carriero, M. M.; Mendes Maia, A. A.; Moro Sousa, R. L.; Henrique-Silva, F. Characterization of a new strain of *Aeromonas dhakensis* isolated from diseased pacu fish (*Piaractus mesopotamicus*) in Brazil. *J. Fish Dis.* **2016**, *39*(11), 1285-1295. https://doi.org/10.1111/jfd.12457

[13] Bartie, K. L.; Desbois, A. P. *Aeromonas dhakensis*: A zoonotic bacterium of increasing importance in aquaculture. *Pathogens* **2024**, *13*(6), 465. https://doi.org/10.3390/pathogens13060465

[14] Bondad-Reantaso, M. G.; MacKinnon, B.; Karunasagar, I.; Fridman, S.; Alday-Sanz, V.; Brun, E.; Le Groumellec, M.; Li, A.; Surachetpong, W.; Karunasagar, I.; Hao, B.; Dall'Occo, A.; Urbani, R.; Caputo, A. Review of alternatives to antibiotic use in aquaculture. *Rev. Aquacult.* **2023**, *15*(4), 1421-1451. https://doi.org/10.1111/raq.12786

[15] Hoseinifar, S. H.; Sun, Y. Z.; Wang, A.; Zhou, Z. Probiotics as means of disease control in aquaculture, a review of current knowledge and future perspectives. *Front. Microbiol.* **2018**, *9*, 2429. https://doi.org/10.3389/fmicb.2018.02429

[16] Martínez Cruz, P.; Ibáñez, A. L.; Monroy Hermosillo, O. A.; Ramírez Saad, H. C. Use of probiotics in aquaculture. *ISRN Microbiol.* **2012**, *2012*, 916845. https://doi.org/10.5402/2012/916845

[17] Talukder Shefat, S. H. Probiotic strains used in aquaculture. *Int. Res. J. Microbiol.* **2018**, *7*(2), 43-55. https://doi.org/10.14303/irjm.2018.023

[18] Lin, S.; Mao, S.; Guan, Y.; Luo, L.; Luo, L.; Pan, Y. Effects of dietary chitosan oligosaccharides and *Bacillus coagulans* on the growth, innate immunity, and resistance of koi (*Cyprinus carpio koi*). *Aquaculture* **2012**, *342-343*, 36-41. https://doi.org/10.1016/j.aquaculture.2012.02.009

[19] Liu, C. H.; Chiu, C. H.; Wang, S. W.; Cheng, W. Dietary administration of the probiotic, *Bacillus subtilis* E20, enhances the growth, innate immune responses, and disease resistance of the grouper, *Epinephelus coioides*. *Fish Shellfish Immunol.* **2012**, *33*(4), 699-706. https://doi.org/10.1016/j.fsi.2012.06.012

[20] Bernardeau, M.; Lehtinen, M. J.; Forssten, S. D.; Nurminen, P. Importance of the gastrointestinal life cycle of *Bacillus* for probiotic functionality. *J. Food Sci. Technol.* **2017**, *54*(8), 2570-2584. https://doi.org/10.1007/s13197-017-2688-3

[21] Cheng, A. C.; Lin, H. L.; Shiu, Y. L.; Tyan, Y. C.; Liu, C. H. Isolation and characterization of antimicrobial peptides derived from *Bacillus subtilis* E20-fermented soybean meal and its use for preventing *Vibrio* infection in shrimp aquaculture. *Fish Shellfish Immunol.* **2017**, *67*, 270-279. https://doi.org/10.1016/j.fsi.2017.06.006

[22] Soto-Marfileño, K. A.; Molina Garza, Z. J.; Flores, R. G.; Molina-Garza, V. M.; Ibarra-Gámez, J. C.; Gil, B. G.; Galaviz-Silva, L. Genomic characterization of *Bacillus pumilus* Sonora, a strain with inhibitory activity against *Vibrio parahaemolyticus*-AHPND and probiotic candidate for shrimp aquaculture. *Microorganisms* **2024**, *12*(8), 1623. https://doi.org/10.3390/microorganisms12081623

[23] Rahayu, S.; Amoah, K.; Huang, Y.; Cai, J.; Wang, B.; Shija, V. M.; Jin, X.; Anokyewaa, M. A.; Jiang, M. Probiotics application in aquaculture: Its potential effects, current status in China, and future prospects. *Front. Mar. Sci.* **2024**, *11*, 1455905. https://doi.org/10.3389/fmars.2024.1455905

[24] Van Doan, H.; Hoseinifar, S. H.; Ringø, E.; Ángeles Esteban, M.; Dadar, M.; Dawood, M. A. O.; Faggio, C. Host-associated probiotics: A key factor in sustainable aquaculture. *Rev. Fish. Sci. Aquacult.* **2020**, *28*(1), 16-42. https://doi.org/10.1080/23308249.2019.1643288

[25] Nakharuthai, C.; Boonanuntanasarn, S.; Kaewda, J.; Manassila, P. Isolation of potential probiotic *Bacillus* spp. from the intestine of Nile tilapia to construct recombinant probiotic expressing CC chemokine and its effectiveness on innate immune responses in Nile tilapia. *Animals* **2023**, *13*(6), 986. https://doi.org/10.3390/ani13060986

[26] Kang, M.; Su, X.; Yun, L.; Shen, Y.; Feng, J.; Yang, G.; Meng, X.; Zhang, J.; Chang, X. Evaluation of probiotic characteristics and whole genome analysis of *Bacillus velezensis* R-71003 isolated from the intestine of common carp (*Cyprinus carpio* L.) for its use as a probiotic in aquaculture. *Aquac. Rep.* **2022**, *25*, 101254. https://doi.org/10.1016/j.aqrep.2022.101254

[27] Yousuf, S.; Jamal, M. T.; Al-Farawati, R. K.; Al-Mur, B. A.; Singh, R. Evaluation of *Bacillus paramycoides* strains isolated from *Channa* fish sp. on growth performance of *Labeo rohita* fingerlings challenged by fish pathogen *Aeromonas hydrophila* MTCC 12301. *Microorganisms* **2023**, *11*(4), 842. https://doi.org/10.3390/microorganisms11040842

[28] Srithongthum, S.; Au, H.-L.; Amornsakun, T.; Musikarun, P.; Mok, W. J.; Halid, N. F. A.; Kawamura, G.; Lim, L. S. Reproductive characteristics of the pond-farmed sultan fish (*Leptobarbus hoevenii*). *J. Ilmiah Perikanan Kelautan* **2021**, *13*(2), 171-180. https://doi.org/10.20473/jipk.v13i2.27264

[29] Sunarto; Sukenda; Widanarni. Screening of probiotic bacteria from intestine and culture environment of Hoeven's slender carp *Leptobarbus hoeveni* Blkr to control pathogenic bacteria. J. *Akuakult. Indones*. **2010**, *9*(2), 127-135. https://doi.org/10.19027/jai.9.127-135

[30] Hellany, H.; Assaf, J. C.; Barada, S.; el-Badan, D.; Hajj, R. E.; Abou Najem, S.; Abou Fayad, A. G.; Khalil, M. I. Isolation and characterization of *Bacillus subtilis* BSP1 from soil: Antimicrobial activity and optimization of fermentation conditions. *Processes* **2024**, *12*(8), 1621. https://doi.org/10.3390/pr12081621

[31] Lertcanawanichakul, M.; Sawangnop, S. A comparison of two methods used for measuring the antagonistic activity of *Bacillus* species. *Walailak J. Sci. Technol.* (WJST) **2008**, *5*(2), 161-171.

[32] Baharudin, M. M. A.; Ngalimat, M. S.; Mohd Shariff, F.; Balia Yusof, Z. N.; Karim, M.; Baharum, S. N.; Sabri, S. Antimicrobial activities of *Bacillus velezensis* strains isolated from stingless bee products against methicillin-resistant *Staphylococcus aureus*. *PLOS One* **2021**, *16*(5), e0251514. https://doi.org/10.1371/journal.pone.0251514

[33] Ritter, A. C.; Paula, A.; Correa, F.; Veras, F. F.; Brandelli, A. Characterization of *Bacillus subtilis* available as probiotics. *J. Microbiol. Res.* **2018**, *8*(2), 23-32.

[34] Dabiré, Y.; Somda, N. S.; Somda, M. K.; Compaoré, C. B.; Mogmenga, I.; Ezeogu, L. I.; Traoré, A. S.; Ugwuanyi, J. O.; Dicko, M. H. Assessment of probiotic and technological properties of *Bacillus* spp. isolated from Burkinabe Soumbala. *BMC Microbiol.* **2022**, *22*(1), 228. https://doi.org/10.1186/s12866-022-02642-7

[35] Santong, K.; Chunglok, W.; Lertcanwanichakul, M.; Bangrak, P. Screening and isolation of *Bacillus* sp. producing thermotolerant protease from raw milk. *Walailak J. Sci. Technol.* **2008**, *5*(2), 151-160.

[36] Proca, I. G.; Diguta, C. F.; Jurcoane, S.; Matei, F. Screening of halotolerant bacteria producing hydrolytic enzymes with biotechnology applications. *Sci. Bull. Ser. F Biotechnol.* **2020**, *XXIV*, 197-202.

[37] Latorre, J. D.; Hernandez-Velasco, X.; Wolfenden, R. E.; Vicente, J. L.; Wolfenden, A. D.; Menconi, A.; Bielke, L. R.; Hargis, B. M.; Tellez, G. Evaluation and selection of *Bacillus* species based on enzyme

production, antimicrobial activity, and biofilm synthesis as direct-fed microbial candidates for poultry. *Front. Vet. Sci.* **2016**, *3*, 95. https://doi.org/10.3389/fvets.2016.00095

[38] Zalma, S. A.; El-Sharoud, W. M. Diverse thermophilic *Bacillus* species with multiple biotechnological activities are associated within the Egyptian soil and compost samples. *Sci. Prog.* **2021**, *104*(4), 368504211055277. https://doi.org/10.1177/00368504211055277

[39] Tamura, K.; Stecher, G.; Kumar, S. MEGA11: Molecular evolutionary genetics analysis version 11. *Mol. Biol. Evol.* **2021**, *38* (7), 3022-3027. https://doi.org/10.1093/molbev/msab120

[40] Wu, Z.; Qi, X.; Qu, S.; Ling, F.; Wang, G. Dietary supplementation of *Bacillus velezensis* B8 enhances immune response and resistance against *Aeromonas veronii* in grass carp. *Fish Shellfish Immunol.* **2021**, *115*, 14-21. https://doi.org/10.1016/j.fsi.2021.05.012

[41] Zhang, D. X.; Kang, Y. H.; Zhan, S.; Zhao, Z. L.; Jin, S. N.; Chen, C.; Zhang, L.; Shen, J.-Y.; Wang, C. F.; Wang, G. Q.; Shan, X. F.; Qian, A. D. Effect of *Bacillus velezensis* on *Aeromonas veronii*-induced intestinal mucosal barrier function damage and inflammation in crucian carp (*Carassius auratus*). *Front. Microbiol.* **2019**, *10*, 2663. https://doi.org/10.3389/fmicb.2019.02663

[42] Li, X.; Gao, X.; Zhang, S.; Jiang, Z.; Yang, H.; Liu, X.; Jiang, Q.; Zhang, X. Characterization of a *Bacillus velezensis* with antibacterial activity and inhibitory effect on common aquatic pathogens. *Aquaculture* **2020**, *523*, 735165. https://doi.org/10.1016/j.aquaculture.2020.735165

[43] Zhou, P.; Chen, W.; Zhu, Z.; Zhou, K.; Luo, S.; Hu, S.; Xia, L.; Ding, X. Comparative study of *Bacillus amyloliquefaciens* X030 on the intestinal flora and antibacterial activity against *Aeromonas* of grass carp. *Front. Cell. Infect. Microbiol.* **2022**, *12*, 815436. https://doi.org/10.3389/fcimb.2022.815436

[44] Yao, Y. Y.; Xia, R.; Yang, Y. L.; Hao, Q.; Ran, C.; Zhang, Z.; Zhou, Z. G. Study about the combination strategy of *Bacillus subtilis* wt55 with AiiO-AIO6 to improve the resistance of zebrafish to *Aeromonas veronii* infection. *Fish Shellfish Immunol.* **2022**, *128*, 447-454. https://doi.org/10.1016/j.fsi.2022.08.019

[45] Nayak, A.; Harshitha, M.; Dubey, S.; Munang'andu, H. M.; Chakraborty, A.; Karunasagar, I.; Maiti, B. Evaluation of probiotic efficacy of *Bacillus subtilis* RODK28110C3 against pathogenic *Aeromonas hydrophila* and *Edwardsiella tarda* using in vitro studies and in vivo gnotobiotic zebrafish gut model system. *Probiotics Antimicrob. Proteins* **2024**, *16*(5), 1623-1637. https://doi.org/10.1007/s12602-023-10127-w

[46] Agustina, P.; Sarjito, A. H.; Haditomo, C. Study of *Bacillus methylotrophicus* as a probiotic candidate bacteria with different concentrations against *Aeromonas hydrophila* on water as a cultivation media of tilapia (*Oreochromis niloticus*). *IOP Conf. Ser. Earth Environ. Sci.* **2019**, *246*(1), 012030. https://doi.org/10.1088/1755-1315/246/1/012030

[47] Kumariya, R.; Garsa, A. K.; Rajput, Y. S.; Sood, S. K.; Akhtar, N.; Patel, S. Bacteriocins: Classification, synthesis, mechanism of action and resistance development in food spoilage causing bacteria. *Microb. Pathog*. **2019**, *128*, 171-177. https://doi.org/10.1016/j.micpath.2019.01.002

[48] Markelova, N.; Chumak, A. Antimicrobial activity of *Bacillus* cyclic lipopeptides and their role in the host adaptive response to changes in environmental conditions. *Int. J. Mol. Sci.* **2025**, *26*(1), 336. https://doi.org/10.3390/ijms26010336

[49] Olishevska, S.; Nickzad, A.; Déziel, E. *Bacillus* and *Paenibacillus* secreted polyketides and peptides involved in controlling human and plant pathogens. *Appl. Microbiol. Biotechnol*. **2019**, *103*(3), 1189-1215. https://doi.org/10.1007/s00253-018-9541-0

[50] Chen, R.; Zhou, Z.; Cao, Y.; Bai, Y.; Yao, B. High yield expression of an AHL-Lactonase from *Bacillus* sp. B546 in *Pichia pastoris* and its application to reduce *Aeromonas hydrophila* mortality in aquaculture. *Microb. Cell Fact.* **2010**, *9*, 39. https://doi.org/10.1186/1475-2859-9-39

[51] Li, L.; Hu, K.; Hong, B.; Lu, X.; Liu, Y.; Xie, J.; Jin, S.; Zhou, S.; Zhao, Q.; Lu, H.; Liu, Q.; Gao, M.; Li, X.; Fu, C.; Xu, H.; Guo, M.; Ma, R.; Zhang, H.; Qian, D. The inhibitory effect of *Bacillus amyloliquefaciens* L1 on *Aeromonas hydrophila* and its mechanism. *Aquaculture* **2021**, *539*, 736590. https://doi.org/10.1016/j.aquaculture.2021.736590

[52] Simón, R.; Docando, F.; Nuñez-Ortiz, N.; Tafalla, C.; Díaz-Rosales, P. Mechanisms used by probiotics to confer pathogen resistance to teleost fish. *Front. Immunol.* **2021**, *12*, 653025. https://doi.org/10.3389/fimmu.2021.653025

[53] Fuller, R. Probiotics in man and animals. *J. Appl. Bacteriol.* **1989**, *66*(5), 365-378. https://doi.org/10.1111/j.1365-2672.1989.tb05105.x

[54] Golnari, M.; Bahrami, N.; Milanian, Z.; Rabbani Khorasgani, M.; Asadollahi, M. A.; Shafiei, R.; Fatemi, S. S.-A. Isolation and characterization of novel *Bacillus* strains with superior probiotic potential: Comparative analysis and safety evaluation. *Sci. Rep.* **2024**, *14*(1), 1457. https://doi.org/10.1038/s41598-024-51823-z

[55] Altavas, P. J. dR.; Amoranto, M. B. C.; Kim, S. H.; Kang, D.-K.; Balolong, M. P.; Dalmacio, L. M. M. Safety assessment of five candidate probiotic *Lactobacilli* using comparative genome analysis. *Access Microbiol.* **2024**, *6*(1), 000715.v4. https://doi.org/10.1099/acmi.0.000715.v4

[56] Hancz, C. Application of probiotics for environmentally friendly and sustainable aquaculture: A review. *Sustainability* **2022**, *14* (22), 15479. https://doi.org/10.3390/su142215479

[57] Liu, H.; Wang, S.; Cai, Y.; Guo, X.; Cao, Z.; Zhang, Y.; Liu, S.; Yuan, W.; Zhu, W.; Zheng, Y.; Xie, Z.; Guo, W.; Zhou, Y. Dietary administration of *Bacillus subtilis* HAINUP40 enhances growth, digestive enzyme activities, innate immune responses and disease resistance of tilapia, *Oreochromis niloticus*. *Fish Shellfish Immunol.* **2017**, *60*, 326-333. https://doi.org/10.1016/j.fsi.2016.12.003

[58] Lee, G.; Heo, S.; Kim, T.; Na, H.-E.; Park, J.; Lee, E.; Lee, J.-H.; Jeong, D.-W. Discrimination of *Bacillus subtilis* from other *Bacillus* species using specific oligonucleotide primers for the pyruvate carboxylase and shikimate dehydrogenase genes. *J. Microbiol. Biotechnol.* **2022**, *32*(8), 1011-1016. https://doi.org/10.4014/jmb.2205.05014

[59] Ruiz-García, C.; Béjar, V.; Martínez-Checa, F.; Llamas, I.; Quesada, E. *Bacillus velezensis* sp. nov., a surfactant-producing bacterium isolated from the river Vélez in Málaga, southern Spain. *Int. J. Syst. Evol. Microbiol.* **2005**, *55*(Pt 1), 191-195. https://doi.org/10.1099/ijs.0.63310-0

[60] Islam, M. I.; Seo, H.; Redwan, A.; Kim, S.; Lee, S.; Siddiquee, M.; Song, H.-Y. In vitro and in vivo anti-*Clostridioides difficile* effect of a probiotic *Bacillus amyloliquefaciens* strain. *Polish J. Microbiol.* **2022**, *32*(1), 46-55. https://doi.org/10.4014/jmb.2107.07057

[61] Sumpavapol, P.; Tongyonk, L.; Tanasupawat, S.; Chokesajjawatee, N.; Luxananil, P.; Visessanguan, W. *Bacillus siamensis* sp. nov., isolated from salted crab (Poo-Khem) in Thailand. *Int. J. Syst. Evol. Microbiol.* **2010**, *60*(10), 2364-2370. https://doi.org/10.1099/ijs.0.018879-0

[62] Huynh, T.; Vörös, M.; Kedves, O.; Turbat, A.; Sipos, G.; Leitgeb, B.; Kredics, L.; Vágvölgyi, C.; Szekeres, A. Discrimination between the two closely related species of the operational group *B. amyloliquefaciens* based on whole-cell fatty acid profiling. *Microorganisms* **2022**, *10*(2), 418. https://doi.org/10.3390/microorganisms10020418

[63] Ngalimat, M. S.; Yahaya, R. S. R.; Baharudin, M. M. A.-A.; Yaminudin, S. M.; Karim, M.; Ahmad, S. A.; Sabri, S. A Review on the biotechnological applications of the operational group *Bacillus amyloliquefaciens*. *Microorganisms* **2021**, *9*(3), 614. https://doi.org/10.3390/microorganisms9030614

[64] Fan, B.; Blom, J.; Klenk, H.-P.; Borriss, R. *Bacillus amyloliquefaciens*, *Bacillus velezensis*, and *Bacillus siamensis* form an "Operational group *B. amyloliquefaciens*" within the *B. subtilis* species complex. *Front. Microbiol.* **2017**, *8*, 22. https://doi.org/10.3389/fmicb.2017.00022

ASEAN
Journal of Scientific and Technological Reports
Online ISSN:2773-8752

Research article

Influence of MS Medium Strengths and Types on *In Vitro* Shoot Multiplication and Development of *Nymphaea colorata* Peter

Nattawut Rodboot[1], Sompong Te-chato[1], and Sureerat Yenchon[1]*

[1] Faculty of Natural Resources, Prince of Songkla University, Songkhla, 90110, Thailand
[1] Faculty of Natural Resources, Prince of Songkla University, Songkhla, 90110, Thailand
[1] Faculty of Natural Resources, Prince of Songkla University, Songkhla, 90110, Thailand
* Corresponding author: sureerat.y@psu.ac.th; ORCID; 0000-0002-0089-7650

Citation:
Rodboot, N.; Te-chato, S.; Yenchon, S. Influence of MS medium strengths and types on *in vitro* shoot multiplication and development of *Nymphaea colorata*. *ASEAN J. Sci. Tech. Report*. **2025**, 28(4), e258176. https://doi.org/10.55164/ajstr.v28i4.258176.

Article history:
Received: March 5, 2025
Revised: May 25, 2025
Accepted: June 11, 2025
Available online: June 30, 2025

Abstract: Efficient *in vitro* propagation systems are essential for the large-scale commercial production and conservation of the important tropical waterlilies (*Nymphaea* spp.), particularly elite ornamental varieties and species. This study aimed to optimize culture medium conditions by evaluating the effects of Murashige and Skoog (MS) medium strengths and types on the *in vitro* growth of *Nymphaea colorata*, using it as a plant model. The derived shoots obtained from sterilized turions were cultured on different MS medium concentrations and types. The results demonstrated that full-strength MS medium significantly enhanced the survival percentage (100%), the number of shoots/explant (1.53 shoots), the number of leaves/explant (18.86 leaves), leaf width (2.66 cm), and petiole length (11.50 cm) compared to diluted formulations. Among different medium types, semi-solid MS medium effectively supported shoot growth while reducing hyperhydration, a common issue observed in liquid cultures. Shoots cultured on semi-solid MS medium exhibited well-developed leaves and elongated petioles, making them more suitable for subsequent acclimatization. These findings underscore the importance of optimizing both the nutrient composition and physical state of the culture medium to enhance micropropagation efficiency in *Nymphaea colorata*. The use of full-strength MS medium in combination with semi-solid culture conditions offers a promising approach for high-quality plantlet production, subsequent large-scale propagation, and conservation of elite waterlily genotypes.

Keywords: Waterlily micropropagation; Semi-solid medium; *Nymphaea colorata*

1. Introduction

Waterlilies (Nymphaeaceae) are emergent aquatic herbs comprising over 100 species distributed worldwide across tropical and subtropical regions [1, 2, 3]. Among these, ornamental waterlilies are widely cultivated due to their aesthetic appeal, playing a significant role in aquatic landscaping and the global horticultural market [4, 5]. Their striking floral colors, pleasant fragrance, and diverse foliage characteristics contribute to their increasing commercial demand. Among wild waterlily species, *Nymphaea colorata* (subgenus Brachyceras), native to East Africa, is particularly notable [6, 7]. This species is distinguished by its vibrant violet flowers, a rare trait among waterlilies, and is extensively utilized in breeding programs due to its ability to transmit unique floral colors and patterns to its progeny [8, 9, 10]. Beyond its ornamental significance, *N. colorata* serves as a valuable model species for studies on floral development, pigmentation, and waterlily genetics [1, 6, 11]. Notably, it is one of the few waterlily species with a sequenced genome, offering key insights into angiosperm evolution and the genetic mechanisms underlying aquatic adaptation [12-14].

Despite the growing demand for ornamental waterlilies in landscaping and horticulture, conventional propagation methods are limited by low multiplication rates and restrict large-scale commercial production [15]. Micropropagation presents an efficient alternative, enabling the rapid clonal propagation of elite genotypes, particularly for rare or hybrid varieties that are challenging to propagate through traditional means [16-17]. This technique ensures the production of genetically uniform plants while preserving desirable horticultural traits such as flower color, size, and disease resistance [18]. Additionally, *in vitro* propagation can overcome limitations associated with slow growth rates and seasonal constraints in natural propagation [19- 21]. By integrating micropropagation techniques, the ornamental waterlily industry can enhance production efficiency, support commercial expansion, and contribute to the conservation of genetically valuable or endangered species [15].

Murashige and Skoog (MS) medium is one of the most widely used plant culture media for micropropagation due to its well-balanced nutrient composition, effectively supporting shoot and root development in various plant species, such as *Dioscorea* sp., grapes, and *Aponogeton ulvaceus* [22-26]. The concentration, composition, and type of culture media play a critical role in regulating in vitro growth and development across different water lily species. Variations in nutrient levels and types of medium can significantly influence shoot regeneration, root induction, nutrient uptake, and overall plant health [27]. Several studies have demonstrated that optimizing these parameters can lead to substantial differences in developmental outcomes, emphasizing the necessity of precise media formulation to achieve optimal *in vitro* propagation efficiency [28-30]. Explant hyperhydration is a physiological disorder typically found in plant tissue culture, particularly in liquid medium systems. It is characterized by excessive water accumulation in tissues, leading to translucent, swollen, and brittle plantlets [31]. This condition can negatively affect growth, morphogenesis, and survival during acclimatization. For waterlily micropropagation, hyperhydration is a significant concern as it severely impacts plantlet establishment during ex vitro transition [14]. This phenomenon is strongly influenced by the composition of the culture medium, including the type and concentration of gelling agents, plant growth regulators (PGRs), and osmotic agents [31]. Given the importance of culture media optimization, this study aims to evaluate the key factors —medium concentration and type —that influence the production of healthy waterlily plantlets. The findings will contribute to the establishment of an efficient waterlily micropropagation protocol, ensuring high-quality and high-yield plant production for future commercial applications.

2. Materials and Methods

2.1 Plant material collection and preparation

The mature, bare-root rhizomes of *N. colorata* Peter, measuring 3.0–5.0 cm in diameter and 10.0–15.0 cm in length, along with their leaves, flowers, and turions, were collected (Figure 1a). The healthy attached turions, free from scars and diseases, were selected and used as the initial explant. The mother plants were cultivated in floating paddy fields under full sun and fertile loamy clay conditions. All plant materials were sourced from Baufah Garden (401 Watcharapol Road, Tha Raeng, Bang Khen District, Bangkok) between March and June. These turions served as the initial explants for *in vitro* propagation experiments. Turions of *N. colorata* with robust shoots were collected (**Figure** 1b). To remove residual dirt and dust, the explants were submerged in running tap water for 3 hours and gently brushed. The attached leaves, roots, and scale leaves were carefully removed. The outer layer of the turion was cleaned using pointed tweezers (Figure 1c). Finally, trichomes on the shoot crown were carefully removed under running tap water using forceps. The cleaned explants were sterilized according to a protocol by Rodboot et al. [14]. The procedure involved immersion in a 0.1% (w/v) Carbendazim solution (a systemic fungicide; Anhui Guangxin Agrochemical Co., Ltd., PRC) for 2 hours, followed by two rinses with sterilized distilled water. The explants were then shaken in 50% ethyl alcohol for 1 minute, treated with 20% (v/v) Clorox® containing five drops of Tween 20 for 20 minutes, and shaken in 0.1% (w/v) $HgCl_2$ for 15 minutes. Finally, any residual disinfectants were removed by five successive washes with sterilized distilled water. The disinfected explants were blotted dry on autoclaved tissue paper

and then cultured in liquid MS medium, free from plant growth regulators, for 8 weeks. The cultures were maintained on an orbital shaker optimized at 90 rpm.

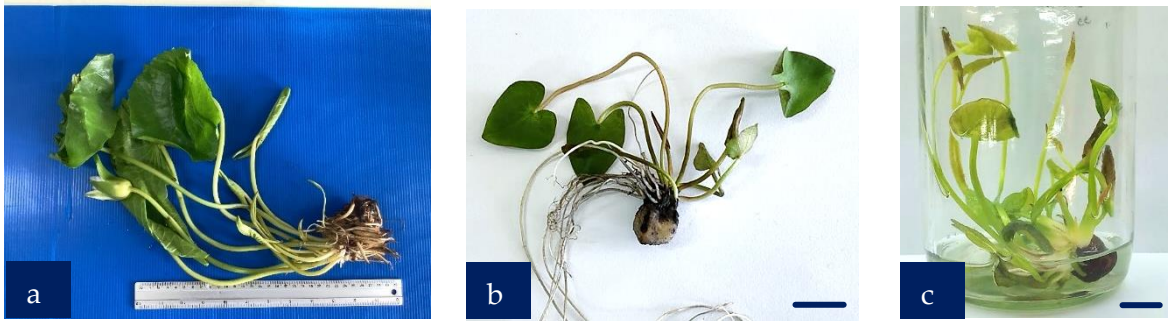

Figure 1. Initial explant establishment (bar = 1 cm)
(a) Mother plant
(b) Raw turion separated from the mother tuber, remaining leaves, and roots
(c) Sterilized turion in plant growth regulator-free liquid MS medium after culture for 8 weeks, exhibiting slightly hyperhydrated shoots

2.2 Effect of different strengths of MS basal medium on in vitro growth

Individual shoots removed from the turions at 8 weeks old in PGR-free liquid MS media, which had 2-3 mature, expanded leaves and measured 3-5 centimeters in length, were used to encourage healthy shoot growth. (Figure 1c). Different strengths of liquid MS medium (full, 1/2, 1/4, and 1/8 MS) were dispensed into 20 ml in 6.3 x 10.8 cm glass bottles. Each culture bottle contained a single explant. The experiment was repeated twice, with twenty replicates for each treatment. After culturing for 4 weeks, the survival rate, number of shoots, leaf length, petiole length, and visible characteristics were assessed.

2.3 Effect of different types of MS basal medium on in vitro growth

To evaluate the optimal type of culture medium for shoot growth, various types of MS basal medium (liquid, semi-solid, and bilayer) were tested. Individual shoots excised from the turions at 8 weeks old, grown in PGRs-free liquid MS medium consisting of 2-3 leaves and 3-5 cm in length, were used. Different types of MS medium were dispensed into 20 mL in 6.3 x 10.8 cm glass bottles. Each culture bottle contained a single explant. The experiment was repeated twice, with twenty replicates for each treatment. After culturing for 4 weeks, the survival rate, number of shoots, leaf length, petiole length, and visible characteristics were recorded.

2.4 Culture conditions

All experiments used the MS basal medium containing 30 g L^{-1} sucrose. The pH of the culture medium was adjusted to 5.7 with 1 N NaOH or HCl before being autoclaved at 121°C for 15 min. The cultures were incubated at 26 ± 2 °C with a 10/14 day-night cycle photoperiod under 12 μmol m^{-2} s^{-1} provided by fluorescent lamps.

2.5 Statistical analysis

All experiments above were arranged in a completely randomized design (CRD). Each treatment consisted of 20 replicates. Data from all parameters were expressed as mean values ± standard error (S.E.) and statistically analyzed using analysis of variance (ANOVA). The means among treatments are separated by Duncan's multiple range test (DMRT) using the SPSS 17.0 program for Windows (SPSS Inc., Chicago, IL, USA).

3. Results and Discussion

3.1 Effect of different strengths of MS basal medium on in vitro growth

The excised shoots were cultivated in liquid MS media of several strengths (full, 1/2, 1/4, and 1/8 MS), supplemented with 30 g/L sucrose, until the optimal medium strength for shoot growth was established. After four weeks of culture, all treatments exhibited a 100% survival rate; however, the explants displayed differential growth responses depending on the medium strength (Table 1, Figure 2). A gradual reduction in MS medium

concentration was associated with a decreased growth rate and a lower number of shoots. Full-strength MS medium proved to be the most effective in promoting shoot growth in *N. colorata*, yielding the highest average values across all measured parameters ($p \leq 0.05$) (Table 1). Specifically, the full-strength MS medium resulted in an average of 1.53 shoots/explant, which was not significantly different from the 1/2-strength MS medium (1.40 shoots/explant).

The number of leaves was also highest in full-strength MS medium, with an average of 18.86 leaves per explant. These leaves exhibited the greatest width (2.66 cm) and the longest petioles (11.50 cm). Explants cultured in full-strength MS medium demonstrated the most vigorous growth, characterized by dark green, fully expanded leaves and elongated petioles. In contrast, explants grown in diluted media exhibited slow growth, smaller leaves, and shorter petioles (Table 1, Figures 2b-d). In addition to superior growth, explants cultured in full-strength MS medium exhibited rapid shoot development. Within three weeks, the petioles extended beyond the bottleneck of the culture vessel, and the leaves were fully expanded with dark green coloration, indicative of healthy growth. However, hyperhydration, brittle leaf, and petiole structures were occasionally observed. These findings align with previous studies on some varieties of *Nymphaea* micropropagation, which reported that full-strength MS medium supports optimal shoot and leaf development from various explant sources, including tubers, turions, and rhizomes [32-35]. Full-strength MS medium is widely recognized as an optimal formulation for micropropagation due to its well-balanced composition of macro- and micronutrients [36-37]. The balanced presence of nitrate (NO_3^-) and ammonium (NH_4^+) ensures efficient nitrogen uptake, promoting protein synthesis and enzymatic activity essential for organogenesis [26, 38]. Furthermore, the inclusion of sucrose provides an external energy source, which is crucial for the development of non-photosynthetic explants [39-41]. When supplemented with appropriate PGRs, full-strength MS medium enhances direct shoot formation, shoot multiplication, and root formation. Its comprehensive nutrient profile makes it suitable for a wide range of aquatic plant species; however, adjustments may be necessary to prevent salt accumulation and pH stress in more sensitive species [42].

Reducing MS medium strength significantly enhanced root formation and overall plant quality under *in vitro* conditions. In the current experiment, we found that roots developed at the basal portion of shoots within 3–4 weeks in both 1/2- and 1/4-strength MS media, with approximately 35% of explants forming roots. This finding is consistent with previous studies, where 1/2-strength MS medium improved root formation in *Ceratonia siliqu* [43] and, when supplemented with 0.2 mg/L IBA, promoted maximum root and shoot production in *Tylophora indica* [44]. Additionally, nitrogen deficiency has been shown to increase salicylic acid levels, thereby modulating root growth [45]. Lowering macronutrient concentrations, particularly nitrogen, alleviates the inhibitory effects of high salt concentrations, thereby enhancing root induction [46-47]. An optimal nutrient balance in diluted MS medium not only minimizes osmotic stress but also enhances root elongation, nutrient uptake, and subsequent ex vitro acclimatization. However, excessive dilution may lead to nutrient deficiencies, resulting in weaker plantlets with reduced shoot vigor and lower survival rates.

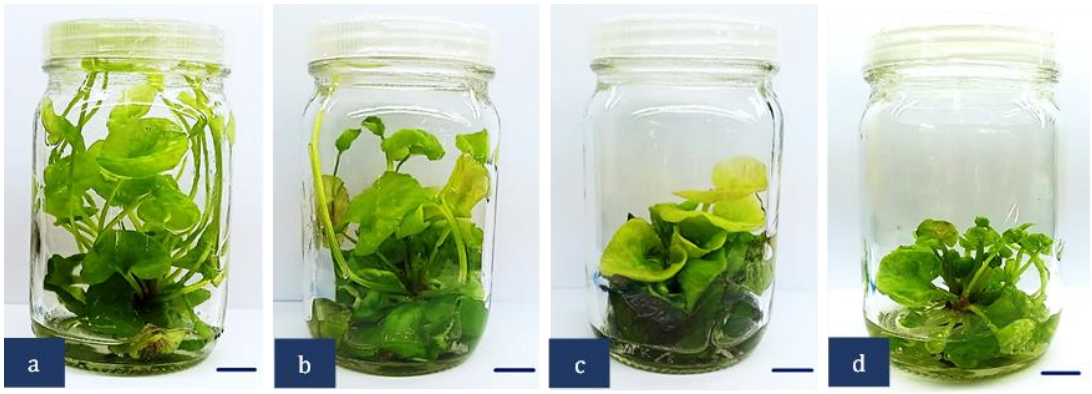

Figure 2. The different characteristics of shoot growth in various strengths of liquid MS medium without PGRs after culture for 4 weeks (bar = 1 cm)

(a) Full (b) 1/2 (c) 1/4 (d) 1/8

Table 1. Effects of different strengths of PGRs-free liquid MS medium on *in vitro* growth after culture for 4 weeks

Strengths of the medium	Survival rate (%)	No. of shoots (shoot)	No. of leaves (leaf)	Petiole length (cm)	Leaf width (cm)
Full	100	1.53[a]	18.86[a]	11.50[a]	2.66[a]
1/2	100	1.40[ab]	15.40[b]	6.72[b]	2.40[b]
1/4	100	1.33[b]	10.60[c]	4.67[b]	2.06[c]
1/8	100	1.33[b]	8.80[d]	3.95[d]	1.05[d]
F-test		*	**	**	**
C.V. (%)		26.77	38.39	30.3	34.66

* significantly different ($p \leq 0.05$), ** significantly different ($p \leq 0.01$)
Means ±SD having different letters in the same column are statistically significant differences by DMRT

3.2 Effect of different types of MS basal medium on in vitro growth

To determine the optimal culture medium for shoot growth, three types of MS basal medium were evaluated: liquid, semi-solid, and bilayer media. The bilayer medium consisted of two variants: a thin layer of sterile distilled water (SDW) or liquid MS medium overlaid on a semi-solid medium. After four weeks of culture, all explants exhibited a 100% survival rate, with varying growth responses depending on the type of medium. Among the treatments, the bilayer medium consisting of semi-solid MS overlaid with liquid MS medium produced the highest number of shoots (1.77 shoots/explant) and leaves (12.45 leaves/explant), with minimal occurrence of hyperhydration (Table 2). However, these differences were not statistically significant ($p \leq 0.05$). Liquid MS medium was identified as the most effective in promoting waterlily shoot growth, as explants cultured in this medium exhibited the highest number of leaves (13.66 leaves/explant), longest petioles (4.45 cm), and widest leaves (2.55 cm) (Table 2, Figure 3a). However, the number of shoots per explant (1.55 shoots) was not significantly different from that observed in other treatments ($p \leq 0.05$). The explants cultured in liquid MS medium exhibited rapid growth, characterized by dark green, fully expanded leaves and elongated petioles. Despite these positive growth attributes, plump, hyperhydrated, and brittle shoots were frequently observed, consistent with findings from Experiment 1.

The choice of culture medium has a significant influence on the growth and development of *N. colorata* during *in vitro* propagation. Each medium type has distinct advantages and limitations that affect shoot proliferation and overall plantlet quality. Several studies have reported that a liquid medium enhances shoot growth and development in water lilies [32, 34, 48]. Moreover, liquid MS medium plays a crucial role in plant tissue culture by improving nutrient uptake, accelerating shoot proliferation, and facilitating large-scale propagation, particularly in suspension cultures [49-50]. The absence of gelling agents in the liquid medium reduces production costs. However, challenges such as hyperhydration, inadequate mechanical support, and increased risk of contamination remain significant drawbacks. Excessive water uptake may lead to physiological abnormalities, while limited aeration can inhibit root development [31].

In contrast, semi-solid MS medium exhibited lower growth performance across all measured parameters (Table 2, Figure 3b). Explants cultured in this medium developed significantly shorter petioles (2.59 cm), leaf width (2.13 cm), and produced narrower leaves compared to those in liquid culture (Figure 3). Nevertheless, semi-solid MS medium offers distinct advantages, including structural support, reduced hyperhydration, and lower contamination risks, making it a suitable option for stable *in vitro* plant growth and structurally robust shoot formation [51]. Additionally, semi-solid medium regulates nutrient absorption, preventing excessive water uptake and thereby supporting balanced shoot and root development [36, 49-50]. These findings align with previous reports. For instance, a single-node explant of *Stevia rebaudiana* exhibited superior shoot elongation and a higher number of nodes when cultured in semi-solid medium, with minimal hyperhydration. Similarly, in *Phoenix dactylifera*, a semi-solid medium type was found to be more conducive

to normal shoot development, whereas a liquid medium resulted in hyperhydration and morphological abnormalities [52]. Despite the higher cost associated with gelling agents, semi-solid MS medium remains a practical choice for maintaining plant structure and reducing handling difficulties in micropropagation systems.

In the present study, explants cultured on semi-solid MS medium exhibited the lowest incidence of hyperhydration compared to those in liquid or bilayer media, underscoring their potential for *in vitro* micropropagation protocols where hyperhydration is a concern. Therefore, we propose that the semi-solid medium type is the most suitable solution for facilitating the stable growth and development of *N. colorata* under *in vitro* conditions.

Figure 3. The characteristics of shoots cultured in different types of medium after culture for 4 weeks (bar = 1 cm)
(a) Liquid MS medium
(b) Semi-solid MS medium
(c) Solid MS medium overlaid with sterilized distilled water
(d) Solid MS medium overlaid with liquid MS medium

Table 2. Effects of different MS medium types on in vitro growth after culture for 4 weeks

Types of medium	Survival rate (%)	No. of shoots (shoot)	No. of leaves (leaf)	Petiole length (cm)	Leaf width (cm)
Liquid (control)	100	1.55 ± 0.41	13.66 ± 2.44^{a}	4.45 ± 1.46^{a}	2.55 ± 0.49^{a}
Semi-solid	100	1.00 ± 0.0	10.04 ± 0.37^{b}	2.59 ± 0.43^{ab}	2.13 ± 0.3^{a}
Semi-solid/ SDW	100	1.11 ± 0.15	12.92 ± 1.42^{ab}	2.42 ± 0.71^{ab}	1.75 ± 0.58^{b}
Semi-solid/ liquid MS medium	100	1.77 ± 0.56	12.45 ± 0.62^{ab}	2.22 ± 0.22^{b}	2.49 ± 0.38^{c}
F-test		ns	*	*	*
C.V. (%)		32.35	46.09	35.55	22.94

ns; not significantly different, * significantly different ($p \leq 0.05$)
Means ±SD having different letters in the same column are statistically significant differences by DMRT

4. Conclusions

This study highlights the significant influence of MS medium strength and type on the *in vitro* growth and development of *Nymphaea colorata*. Full-strength MS medium was identified as the most effective for promoting explant survival percentage and overall plant growth, supporting optimal growth performance compared to diluted formulations. In addition to medium strength, the physical state of the culture medium played a crucial role in shoot development. Based on these findings, semi-solid medium is recommended for long-term subculture and subsequent plantlet acclimatization, as it effectively reduces hyperhydration while maintaining normal growth performance. Therefore, for the commercial production of waterlilies, the use of full-strength semi-solid MS medium is recommended to ensure robust and healthy plant development.

5. Acknowledgements

This research was supported by the Center of Excellence in Agricultural and Natural Resources Biotechnology Phase 3, Prince of Songkla University

Author Contributions: N.R. carried out the experiments and writing - original draft; S.Y. writing - review and editing: S.T. visualization. All authors read and approved the final manuscript.

Funding: This research was funded by the Center of Excellence in Agricultural and Natural Resources Biotechnology Phase 3**,** Prince of Songkla University

Conflicts of Interest: The authors declare that there are no conflicts of interest related to this article.

References

[1] Zhang, L.; Chen, F.; Zhang, X.; Li, Z.; Zhao, Y.; Lohaus, R.; Chang, X.; Dong, W.; Ho, S. Y. W.; Liu, X.; Song, A.; Chen, J.; Guo, W.; Wang, Z.; Zhuang, Y.; Wang, H.; Chen, X.; Hu, J.; Liu, Y.; Tang, H. The water lily genome and the early evolution of flowering plants. *Nature* **2019**, *577*(7788), 79-84. https://doi.org/10.1038/s41586-019-1852-5

[2] Xiong, X.; Zhang, J.; Yang, Y.; Chen, Y.; Su, Q.; Zhao, Y.; Wang, J.; Xia, Z.; Wang, L.; Zhang, L.; Chen, F. Water lily research: past, present, and future. *Trop. Plants* **2023**, *2*(1), 1-8. https://doi.org/10.48130/tp-2023-0001

[3] Masters, C. O. Encyclopedia of the Water-Lily; TFH Publications: Neptune City, NJ, 1974.

[4] Dumitras, A.; Sabo, G. M.; Singureanu, V.; Csok, E.; Moldovan, G. Flower species used in aquatic landscape design. *Bull. Univ. Agric. Sci. Vet. Med. Cluj-Napoca Hortic*. **2008**, *65*(1), 486. https://doi.org/10.15835/buasvmcn-hort:827.

[5] Sunian, E. Development of Sterilisation Procedures and In vitro studies of *Nymphaea lotus*; Doctoral Dissertation, Universiti Putra Malaysia, 2004. Universiti Putra Malaysia Institutional Repository.

[6] Liu, Q.; Li, S.; Li, T.; Wei, Q.; Zhang, Y. The characterization of R2R3-MYB genes in water lily *Nymphaea colorata* reveals the involvement of NcMYB25 in regulating anthocyanin synthesis. *Plants* **2024**, *13(*21), 2990. https://doi.org/10.3390/plants13212990.

[7] Borsch, T.; Loehne, C.; Mbaye, M.; Wiersema, J. Towards a complete species tree of *Nymphaea*: shedding further light on subg. *Brachyceras* and its relationships to the Australian water-lilies. *Telopea* **2011**, *13*(1-2), 193-217. https://doi.org/10.7751/telopea20116014.

[8] Li, H.; Shen, Z.; Niu, J.; Yang, S.; Zhu, T. *Nymphaea* 'Guifei', a new intersubgeneric cultivar with flower color transition. *HortScience* **2024**, *59*(9), 1391-1392. https://doi.org/10.21273/hortsci18046-24.

[9] Cheng, L.; Han, Q.; Chen, F.; Li, M.; Balbuena, T. S.; Zhao, Y. Phylogenomics as an effective approach to untangle cross-species hybridization event: A case study in the family *Nymphaeaceae*. *Front. Genet.* **2022**, *13*, 1031705. https://doi.org/10.3389/fgene.2022.1031705.

[10] Les, D. H.; Moody, M. L.; Doran, A. S.; Phillips, W. E. A genetically confirmed intersubgeneric hybrid in *Nymphaea* L. (*Nymphaeaceae salisb.*). *HortScience* **2004**, *39*(2), 219-222. https://doi.org/10.21273/hortsci.39.2.219.

[11] Khan, W. U.; Khan, L. U.; Khan, N. M.; Zhang, J.; Wenquan, W.; Chen, F. Comprehensive kuntze. *Bangladesh J. Bot.* **2025**, *51*(4), 697-704. https://doi.org/10.3329/bjb.v51i4.63488.

[12] Huang, X.; Yang, M.; Guo, J.; Liu, J.; Chu, G.; Xu, Y. Genome-wide survey and analysis of microsatellites in waterlily, and potential for polymorphic marker development. *Genes* **2022**, *13*(10), 1782. https://doi.org/10.3390/genes13101782.

[13] Chen, F.; Liu, X.; Yu, C.; Chen, Y.; Tang, H.; Zhang, L. Water lilies as emerging models for Darwin's abominable mystery. *Horticulture Res.* **2017**, *4*(1). https://doi.org/10.1038/hortres.2017.51.

[14] Rodboot, N.; Yenchon, S.; Te-Chato, S. Optimization of explant sterilization and plant growth regulators for enhancing the in vitro propagation of *Nymphaea colorata* Peter. *Plant Cell Tissue Organ Cult.* (PCTOC) **2024**, *159*(3). https://doi.org/10.1007/s11240-024-02911-5.

[15] Sivakumar, P.; Chitra, M.; Sasikala, K.; Selvamurugan, M.; Karunakaran, V. An overview of pharmaceutical applications and in vitro micropropagation techniques for rare and endangered plant species. *J. Adv. Biol. Biotechnol.* **2024**, *27*(9), 573-585. https://doi.org/10.9734/jabb/2024/v27i91330.

[16] Shukla, S.; Shukla, S. K. Micropropagation for crop improvement and its commercialization potential. In *Elsevier eBooks*; Elsevier, 2024; pp 271-287. https://doi.org/10.1016/b978-0-443-15924-4.00006-0.

[17] Gupta, S.; Singh, A.; Yadav, K.; Pandey, N.; Kumar, S. Micropropagation for multiplication of disease-free and genetically uniform sugarcane plantlets. In *Elsevier eBooks*; Elsevier, **2022**; pp 31–49. https://doi.org/10.1016/b978-0-323-90795-8.00015-1.

[18] Hasnain, A.; Naqvi, S. A. H.; Ayesha, S. I.; Khalid, F.; Ellahi, M.; Iqbal, S.; Hassan, M. Z.; Abbas, A.; Adamski, R.; Markowska, D.; Baazeem, A.; Mustafa, G.; Moustafa, M.; Hasan, M. E.; Abdelhamid, M. M. A. Plants in vitro propagation with its applications in food, pharmaceuticals, and cosmetic industries; current scenario and future approaches. *Front. Plant Sci.* **2022**, *13*, 1009395. https://doi.org/10.3389/fpls.2022.1009395.

[19] Abdalla, N.; El-Ramady, H.; Seliem, M. K.; El-Mahrouk, M. E.; Taha, N.; Bayoumi, Y.; Shalaby, T. A.; Dobránszki, J. An academic and technical overview on plant micropropagation challenges. *Horticulturae* **2022**, *8*(8), 677. https://doi.org/10.3390/horticulturae8080677.

[20] Mahanta, M.; Gantait, S. Trends in plant tissue culture and genetic improvement of gerbera. *Hortic. Plant J.* https://doi.org/10.1016/j.hpj.2024.03.003.

[21] Baby, G.; Rafeekher, M.; Soni, K.; Kumari, P. I.; CR, R.; SheenaA, N.; M, A. R. Advances in micropropagation techniques for aquascaping plants: A comprehensive review. *Arch. Curr. Res. Int.* **2024**, *24*(11), 14-22. https://doi.org/10.9734/acri/2024/v24i11944.

[22] Kam, M. Y. Y.; Chin, C. F. Micropropagation of the ornamental aquatic plant, *Aponogeton ulvaceus*, from immature buber explants. *Methods Mol. Biol.* **2024**, *189-196*. https://doi.org/10.1007/978-1-0716-3954-2_13.

[23] Verde, D. D. S. V.; De Souza Mendes, M. I.; Da Silva Souza, A.; Pinto, C. R.; Nobre, L. V. C.; Santos, K. C. F. D.; Da Silva Ledo, C. A. Culture media in the *in vitro* cultivation of *Dioscorea* spp. *Concilium* **2023**, *23*(9), 459–482. https://doi.org/10.53660/clm-1383-23k63.

[24] Batukaev, A.; Sobralieva, E.; Palaeva, D. Optimization studies of culture media for *in vitro* clonal micropropagation of new grape varieties. *KnE Life Sci.* **2021**. https://doi.org/10.18502/kls.v0i0.9013.

[25] Murashige, T.; Skoog, F. A Revised Medium for rapid growth and bio assays with tobacco tissue cultures. *Physiol. Plant.* **1962**, *15*(3), 473-497. https://doi.org/10.1111/j.1399-3054.1962.tb08052.x.

[26] Pasternak, T. P.; Steinmacher, D. Plant growth regulation in cell and tissue culture *in vitro*. *Plants* **2024**, *13*(2), 327. https://doi.org/10.3390/plants13020327.

[27] Dogan, M. High efficiency plant regeneration from shoot tip explants of *Staurogyne repens* (Nees) Kuntze. *Bangladesh J. Bot.* **2022**, *51*(4), 697-704. https://doi.org/10.3329/bjb.v51i4.63488.

[28] Sheelamary, S.; Nandhini, L. V. Effect of media concentration and growth hormones on shoot regeneration and *in vitro* rooting of sugarcane varieties (*Saccharum* spp.). *Int. J. Agric. Sci.* **2021**, *17*(1), 89-94. https://doi.org/10.15740/has/ijas/17.1/89-94.

[29] Romanova, M. S.; Khaksar, E. V.; Novikov, O. O.; Leonova, N. I.; Semenov, A. G. The effect of different compositions of growth media on the development of microplants of the *Antonina Potato* variety. *Sib. Her. Agric. Sci.* **2020**, *50*(6), 26-36. https://doi.org/10.26898/0370-8799-2020-6-3.

[30] Donjanthong, R.; Nopchai, N.; Sunlarp, S.; Nattawut, R. Micropropagation of Australian giant waterlily (*Nymphaea gigantea*). *RMUTTO R. J.* **2017**, *10*, 1-7.

[31] Polivanova, O. B.; Bedarev, V. A. Hyperhydricity in plant tissue culture. *Plants* **2022**, *11*(23), 3313. https://doi.org/10.3390/plants11233313.

[32] Noimai, Y. *Micropropagation of Nymphaea hybrid 'Chalong-Kwan'*. Master's Thesis, Rajamangala University of Technology Thanyaburi, **2012**.

[33] Ubonprasirt, B.; Nopchai, C.; Rungaroon, D. Micropropagation of night blooming waterlily (*Nymphaea pubescens*). *RMUTTO R. J.* **2011**, *4*(2).

[34] Lakshmanan, P. In vitro establishment and multiplication of *Nymphaea* hybrid 'James Brydon'. *Plant Cell Tissue Organ Cult.* **1994**, *36*, 145-148.

[35] Garg, G.; Bharadwaj, A.; Chaudhary, S.; Kataria, S. Nutrient medium and its fortification for in vitro cultivation of medicinal plants. In *CRC Press eBooks*; CRC Press, **2024**; pp 123-133. https://doi.org/10.1201/b23374-6.

[36] Matsneva, O. V.; Tashmatova, L. V.; Khromova, T. M. The influence of the nutrient composition medium on the intensity micropropagation in vitro *Fragaria* × *Ananassa* Duch. *Vestnik of the Russian Agricultural Science* **2024**, *1*, 26-29. https://doi.org/10.31857/s2500208224010065.

[37] Chen, J.; Li, J.; Li, W.; Li, P.; Zhu, R.; Zhong, Y.; Zhang, W.; Li, T. The optimal ammonium-nitrate ratio for various crops: A meta-analysis. *Field Crops Research* **2024**, *307*, 109240. https://doi.org/10.1016/j.fcr.2023.109240.

[38] Sudheer, W.; Praveen, N.; Al-Khayri, J.; Jain, S. Role of plant tissue culture medium components. In *Elsevier eBooks*; Elsevier, **2022**; pp 51-83. https://doi.org/10.1016/b978-0-323-90795-8.00012-6.

[39] De Alcantara, G. B.; Machado, M. P.; De Oliveira, R. A.; Filho, J. C. B. In vitro multiplication of sugar cane with different nitrogen and sucrose concentrations. *Científica* **2019**, *47*(1), 70-76. https://doi.org/10.15361/1984-5529.2019v47n1p70-76.

[40] Miranda, N. A.; Titon, M.; Pereira, I. M.; Fernandes, J. S. C.; Santos, M. M.; De Oliveira, R. N. Antioxidants, sucrose, and agar in the in vitro multiplication of *Eremanthus incanus*. *Floresta* **2018**, *48*(3), 311.

[41] Dönmez, D.; Erol, M. H.; Biçen, B.; Şimşek, Ö.; Kaçar, Y. A. The effects of different strength of MS media on in vitro propagation and rooting of *Spathiphyllum*. *Anadolu J. Agric. Sci.* **2022**, *37*(3), 583-592. https://doi.org/10.7161/omuanajas.1082219.

[42] Gonçalves, S.; Correia, P. J.; Martins-Loução, M. A.; Romano, A. A new medium formulation for in vitro rooting of carob tree based on leaf macronutrients concentrations. *Biol. Plantarum* **2005**, *49*(2), 277–280. https://doi.org/10.1007/s10535-005-7280-4.

[43] Haque, S. M.; Ghosh, B. Field evaluation and genetic stability assessment of regenerated plants produced via direct shoot organogenesis from leaf explant of an endangered 'Asthma Plant' (*Tylophora indica*) along with their in vitro conservation. *Nat. Acad. Sci. Lett.* **2013**, *36*(5), 551-562. https://doi.org/10.1007/s40009-013-0161-z.

[44] Conesa, C. M.; Saez, A.; Navarro-Neila, S.; De Lorenzo, L.; Hunt, A. G.; Sepúlveda, E. B.; Baigorri, R.; Garcia-Mina, J. M.; Zamarreño, A. M.; Sacristán, S.; Del Pozo, J. C. Alternative polyadenylation and salicylic acid modulate root responses to low nitrogen availability. *Plants* **2020**, *9*(2), 251. https://doi.org/10.3390/plants9020251.

[45] Munthali, C.; Kinoshita, R.; Onishi, K.; Rakotondrafara, A.; Mikami, K.; Koike, M.; Tani, M.; Palta, J.; Aiuchi, D. A model nutrition control system in potato tissue culture and its influence on plant elemental composition. *Plants* **2022**, *11*(20), 2718. https://doi.org/10.3390/plants11202718.

[46] De David, C. H. O.; De Paiva Neto, V. B.; Campos, C. N. S.; Da Silva Liber Lopes, P. M.; Teodoro, P. E.; De Mello Prado, R. Nutritional disorders of macronutrients in *Bletia catenulata*. *HortScience* **2019**, *54*(10), 1836-1839. https://doi.org/10.21273/hortsci14284-19.

[47] Jenks, M.; Kane, M.; Marousky, F.; McConnell, D.; Sheehan, T. In vitro establishment and epiphyllous regeneration of *Nymphaea* 'Daubeniana'. *HortScience* **1990**, *25*, 1664.

[48] De Klerk, G.; Van Den Dries, N.; Krens, F. Hyperhydricity: underlying mechanisms. *Acta Horticulturae* **2017**, *1155*, 269-276. https://doi.org/10.17660/actahortic.2017.1155.39.

[49] Dewir, Y. H.; Indoliya, Y.; Chakrabarty, D.; Paek, K. Biochemical and physiological aspects of hyperhydricity in liquid culture system. In *Springer eBooks*, **2014**, 693-709. https://doi.org/10.1007/978-94-017-9223-3_26.

[50] Marfori, E. D. C. Improving micropropagation of *Moringa oleifera*: the use of semi-Solid medium for rooting and sucrose-free liquid medium combined with temporary ventilation for hardening. *J. Appl. Biol. Biotechnol.* **2024**, *12*, https://doi.org/10.7324/jabb.2024.166818.

[51] Biswas, P.; Kumari, A.; Kumar, N. Impact of salt strength on in vitro propagation and rebaudioside a content in *Stevia rebaudiana* under semi-solid and liquid MS media. *Sci. Rep.* **2024**, *14*(1), https://doi.org/10.1038/s41598-024-70899-1.

[52] Mazri, M. A. Role of cytokinins and physical state of the culture medium to improve in vitro shoot multiplication, rooting and acclimatization of Date Palm (*Phoenix dactylifera* L.). Boufeggous. *J. Plant Biochem. Biotechnol.* **2014**, *24*(3), 268-275. https://doi.org/10.1007/s13562-014-0267-5.

ASEAN
Journal of Scientific and Technological Reports
Online ISSN:2773-8752

Research article

Carbon Footprint Assessment Using Synthetic Fertilizer and Liquid Organic Biofertilizer in Cassava Cultivation to Promote Good Cultivation Practices and Prevent Greenhouse Gas Emissions

Surasak Janchai[1], Nat Nakkorn[2*], Suparatchai Vorarat[3], and Sakol Thongprapa[4]

[1] College of Innovative Technology and Engineering, Dhurakij Pundit University, Bangkok, 10210, Thailand
[2] College of Innovative Technology and Engineering, Dhurakij Pundit University, Bangkok, 10210, Thailand
[3] College of Innovative Technology and Engineering, Dhurakij Pundit University, Bangkok, 10210, Thailand
[4] A-West Property Co., Ltd, Chonburi, 20130, Thailand
* Correspondence: natnakkorn@gmail.com

Citation:
Janchai, S.; Nakkorn, N.; Vararat, S.; Thongprapa, S. Carbon footprint assessment using synthetic fertilizer and liquid organic biofertilizer in cassava cultivation to promote good cultivation practices and prevent greenhouse gas fmissions. *ASEAN J. Sci. Tech. Report.* **2025**, *28*(4), e257702. https://doi.org/10.55164/ajstr.v28i4.257702.

Article history:
Received: January 29, 2025
Revised: June 10, 2025
Accepted: June 23, 2025
Available online: July 2, 2025

Abstract: Typically, agricultural crop production contributes to greenhouse gas (GHG) emissions, especially the use of synthetic fertilizers and, less frequently, the application of organic fertilizers. Synthetic fertilizers have both positive and deleterious effects on the natural ecosystem. The primary purpose of this study was to evaluate cassava root yields harvested using two different cultivation methods: synthetic fertilizers and liquid organic biofertilizers. We investigated the amount of raw material fertilizers required for each cultivation method to evaluate the effects of global warming potential (GWP) on cassava cultivation methods in northeastern Thailand. The system boundary was defined from cradle to farm gate, encompassing cultivation and progressing through to harvest, using life cycle assessment (LCA). The input and output data were analyzed to assess the potential impacts of global warming over 100 years. The experiments found that 1000 kg of cassava root product harvested with synthetic fertilizer released the most GHGs, 51.83 kg CO_2eq/1000 kg. This was 10 times that of the experimental plot using a liquid organic biofertilizer at 2.74 kg CO_2eq/1000 kg. Therefore, as farmers face challenges ranging from drought to low yields, and as agriculture becomes less predictable in the face of a changing climate, it is essential to help farmers transition to practices that increase resilience and dramatically decrease their reliance on fossil-fuel-based chemicals. To develop guidelines for reducing GHG emissions in cultivation, the focus should be on farmers' cultivation activities, especially fertilizer application.

Keywords: Carbon footprint; Greenhouse gas emissions; Synthetic fertilizer; Liquid organic biofertilizer; Cassava cultivation

1. Introduction

Fertilizers are a crucial component of global food production, essential for sustaining our growing population [1]. However, fertilizers can also generate greenhouse gas (GHG) emissions, with potential nutrient losses to the environment [2]. Agriculture, as a sector, is responsible for non-CO_2 emissions generated by crop cultivation and livestock activities. CO_2 emissions do not primarily come from changing forests, but rather from burning fossil fuels and volcanic eruptions. Another factor that affects global warming is the cultivation

of agricultural products [3]. The agricultural sector's use of synthetic nitrogen (N) to accelerate growth and increase crop yields is considered unsustainable. In 2018, the production of synthetic nitrogen fertilizer released approximately 1.13 billion tons of greenhouse gases, accounting for 10.6% of all greenhouse gas emissions. This figure comprised around 2.1% from farming and 38.8% from fertilizer production [4]. In 2019, Thailand emitted 373 million tons of carbon dioxide equivalents. Most are produced by the energy and transportation sector (261 million tons, 70%), followed by the agricultural sector (57 million tons, 15%), the industrial process and product use sector (38 million tons, 10%), and the waste sector (17 million tons, 5%). The most common source of GHG emissions in the agricultural sector (13 million tons, 22%) is the use of fertilizer and lime in plantation plots [5]. Chemical fertilizers are essential for agricultural development when soils lack the nutritional balance required for plants [6]. However, the continuous use of chemical fertilizers has negatively impacted the physicochemical and biological properties of soils. Using biofertilizer products is considered an alternative for reducing the environmental impact of chemical fertilizers [7]. Organic fertilizers are fertilizers that come from living things, both plants and animals, that have undergone processing or have been piled up until they have completely decayed. These fertilizers are in a form that plants can use, such as decayed leaves, compost, various animal manures, bone meal, bean meal, green manure, and municipal waste [8]. Liquid biofertilizers contain live microorganisms that improve soil properties and increase plant growth and yield. Liquid biofertilizers can be applied to various crops and are often more effective than chemical fertilizers; they help reduce the need for chemicals and enhance their effectiveness by promoting improved plant growth [9]. The use of biofertilizers is a crucial component of integrated nutrient management, as they are cost-effective and serve as a supplement to chemical fertilizers for sustainable agriculture [10]. Finally, further research is necessary to overcome the limitations of improved climate adaptation and develop effective liquid organic biofertilizers. We may utilize a superior liquid biofertilizer with a longer shelf life and lower cost, or utilize existing machinery for large-scale applications. In a study that looks at costs and benefits, it's important to assess how safe and effective liquid biofertilizers are over time and to work with different groups to see if they can be used successfully, taking into account the specific location, type of crop, soil type, and weather conditions [11]. Fertilizing with solid organic fertilizers before planting can accumulate and significantly increase N_2O emissions [12]. However, multiple applications of liquid organic biofertilizers do not affect N_2O emissions. Applying solid organic fertilizer before planting can lead to excessive emissions compared to using liquid organic fertilizer due to its higher C/N ratio, which results in increased CO_2 emissions.

Therefore, farmers should consider using liquid organic fertilizers in multiple applications to reduce GHG emissions from their soil plots and achieve high yields. Using liquid organic fertilizer multiple times can reduce GHG emissions. The type of fertilizer and application method can affect N_2O emissions, while soil temperature and water content also influence these emissions. [13]. Cassava is a field crop that produces tubers and is one of the most important economic crops in Thailand, which is the world's top exporter [14]. The cassava production in 2024 is expected to utilize 9.049 million rai (1 rai = 1,600 m²) and realize production of 27.941 million tons at an average yield of 3.088 tons per rai compared to 2023 with a harvest area of 9.350 million rai, a yield of 30.732 million tons, and an average yield of 3.287 tons per rai. The cultivated area, production, and yield per unit area decreased by 3.22%, 9.08%, and 6.05%, respectively. The drop is due to the drought crisis and the deterioration of soil quality resulting from cultivation. Thailand imported 4,103,668 tons of chemical fertilizers in 2023 as raw materials, primarily for agricultural cultivation. Chemical fertilizers used in cassava cultivation account for 5% of the total quantity of imported synthetic fertilizers [15]. For cassava cultivation in areas with sandy loam or sandy soil, farmers typically use a fertilizer formula of 15-15-15 at a rate of 100 kg per 1,600 m², applying it once after planting when the cassava is 1–3 months old [16]. In general, the carbon footprint for 15-15-15 chemical fertilizers is 1.5083 kg CO_2eq/kg [17]. Inorganic fertilizer is defined as a type of fertilizer composed of inorganic substances. Derived from natural and synthetic inorganic fertilizers, natural inorganic fertilizers are those that contain inorganic substances that occur naturally, such as ground phosphate rock and mineral sylvite (potassium chloride, KCl, a type of potassium fertilizer). Chemical methods produce synthetic inorganic fertilizers, including ammonium sulfate, triple superphosphate, and phosphates. Inorganic fertilizers can be synthetic chemical fertilizers or natural fertilizers [18]. The fertilizers imported into Thailand include ammonium sulfate (formula 21-0-0), urea (formula 46-0-0), potassium chloride (0-0-60), and diammonium phosphate (formula 18-46-0) [19]. Table 1 displays the quantity of synthetic fertilizers Thailand imported between 2018 and 2022. Thailand's cassava cultivation from 2018 to 2022 utilized a substantial amount of synthetic fertilizer, as indicated in Table 2.

Table 1. Quantity of chemical fertilizer imports in Thailand in 2018–2022.

Mono fertilizers/ compound fertilizers	Volume (%)	Mixed fertilizers/ various fertilizer	Volume (%)
Urea 46-0-0	42	16-20-0	7
21-0-0	4	15-15-15	7
0-0-60	14	13-13-21	16
18-46-0	19	16-16-8	1
Total	79		31

Source: Office of Agricultural Economics, Thailand (OAE) [15]

Thailand aims to achieve carbon neutrality by 2050 and net-zero GHG emissions by 2065. Chemical fertilizer production is a heavy industry with a high impact on carbon emissions. This industry may need to adapt quickly because it is at risk of being subjected to a carbon tax in many countries; in particular, the European Union began collecting carbon taxes in 2023 [20]. Urea fertilizer is a synthetic organic substance that contains nitrogen (N) as a component in a very high ratio, 46% by weight. Urea fertilizer is a standard chemical fertilizer. Most importantly, the fertilizer formula for urea is 46-0-0 because it has the highest proportion of nitrogen. Therefore, it serves as a primary source of nitrogen fertilization. Plants use urea fertilizer 46-0-0 as their primary nutrient. Early planting stages necessitate a rapid acceleration of plant growth. This results in the plant developing long stems, bushy leaves, and large, dark green leaves, as well as good weight. Additionally, the production of urea as a nitrogen (N) fertilizer has a greenhouse gas impact of 3.3036 kg CO_2eq per 1 kg of urea fertilizer (TGO) [17]. Ammonium sulfate is a type of nitrogen fertilizer commonly used in Thailand. The chemical formula is $(NH_4)_2SO_4$, and the fertilizer formula is 21-0-0, consisting of approximately 21% nitrogen (N) and approximately 23% sulfur (S). Ammonium sulfate is a simple nitrogen fertilizer that increases nitrogen levels in the soil and serves as an important nutrient for nourishing plant leaves. Making ammonium sulfate as a P_2O_5 fertilizer creates a greenhouse effect that is equal to 1.5716 kg of CO_2 for every 1 kg of AMS fertilizer produced (TGO) [17].

Potassium chloride fertilizer formula 0-0-60 contains 0% nitrogen, 0% beneficial phosphate, and 60% water-soluble potassium. Its duties and importance to plants are as follows: 1) promote root growth, enabling better water absorption in the roots, and 2) create good-quality fruit pulp. Making potassium chloride as a K_2O fertilizer produces greenhouse gases equivalent to 0.4974 kg of CO_2 for every 1 kg of K_2O fertilizer (TGO) [17]. Fertilizer 15-15-15 is a chemical fertilizer formula containing the same nutrients as nitrogen (N), phosphorus (P), and potassium (K) at 15% or in an NPK ratio of 1:1:1, which is suitable for general plant maintenance. It is commonly used on mature fruit trees and perennials. During the period after the harvest, its distinctive feature is that it contains all three main nutrients that plants need in equal amounts. Therefore, it nourishes every part of the plant simultaneously. It did not, however, highlight any one area. The production of GHG from 1 kg of fertilizer 15-15-15 has an impact equal to 1.5083 kg CO_2eq (TGO) [17].

Table 2. Quantity of chemical fertilizer imports in Thailand in 2018–2022.

Planting Harvest Year	Chemical fertilizer (kg/1600 m²)	Planting area (m²)	Average yield (kg/1600 m²)
2018	41	12,400,667,200	3,499
2019	41	12,005,803,200	3,527
2020	43	12,754,060,800	3,586
2021	42	13,019,736,000	3,252
2022	43	15,140,667,200	3,372

Source: Office of Agricultural Economics, Thailand (OAE) [15]

People also view the agricultural sector as contributing to global warming, as harvesting rice and livestock releases methane gas. Moreover, nitrous oxide released from fertilizer and livestock urine contributes more to the GHG climate than carbon dioxide, although in smaller amounts. However, the agricultural system

that creates GHGs is not small-scale farming. However, industrial agriculture, which relies on monocultural crops such as rice, corn, sugarcane, cassava, and rubber, as well as livestock, requires nitrogen fertilizers, pesticides, and fossil fuel-powered machinery. This type of industrial agriculture creates enormous ecological impacts, destroying soil, water, and forests that have the potential to absorb carbon dioxide. Additionally, the long-distance food transportation system relies on freezing and transport methods. When the food reaches urban consumers, a significant amount of food waste contributes to greenhouse gas emissions [21].

Agricultural cultivation practices for cassava provide accurate information about effective cultivation methods, covering all stages from planting to maintenance and harvesting, as well as the appropriate planting locations. If the area where cassava is planted or the water source is close to places that may be polluted with heavy metals and pesticides, such as near factories or areas that use many chemicals, then soil and water tests should be conducted to detect harmful substances. A record of the land's history should be kept for each plot, including details such as the farmers' names, addresses, the plot keeper's name (if applicable), their address, the size of the area, the location of the plot, the types and varieties of cassava, and any other relevant information. Soil preparation. Suppose cassava is grown in the same place for many consecutive years. In that case, the soil should be improved to maintain long-term production levels by adding manure compost from cassava peels or various legumes that can be planted in rotation to nourish the soil. Weeds should be eliminated before planting. The weeds should be plowed under in the plot to be planted, and they should be left for 20–30 days to allow the weeds to ferment and decompose into fertilizer in the soil. Using reduced tillage in combination with crop residue retention can increase soil organic carbon and reduce carbon footprints [22]. The plot should be plowed another 1–2 times as appropriate, and cassava can be planted while the soil is still moist.

Prepare the cuttings. You can cut fresh cassava cuttings that are 10–12 months old, but don't leave them for more than 15 days. They should be cut to a length of about 20 cm and have at least five buds. To protect against fungi and insects, dip the cuttings in a chemical solution. Cassava is planted in straight rows for ease of maintenance and weed control, with a row distance of 1.20 meters, a plant distance of 80 cm or 1 meter, and a plant distance of 100 cm. Plant the cuttings upright, about 10 cm deep in the soil. Spraying chemicals to control weed seed germination. When planting in the rainy season, the soil is typically moist, and chemicals should be applied within 3 days after planting cassava to control weed germination immediately or before the cassava plants emerge. If sprayed after the cassava plants sprout, the plant may be damaged. These interactions can range from climatic extremes that influence spray coverage and field access to direct effects of CO_2 or temperature on plant biochemistry and morphology [23]. The use of chemical fertilizers (e.g., urea, calcium nitrate, ammonium sulfate, diammonium phosphate, etc.) has great importance for the world's food production, as it works as fast food for plants, causing them to grow more rapidly and efficiently. However, adverse effects are being observed due to the excessive and imbalanced use of these synthetic inputs [24].

The first step involves weeding and fertilizing the plants. The first weed control should occur approximately 30–45 days after planting, using a small walk-behind tractor or a disc cultivator to eliminate weeds. We attached chemical fertilizers to the tractor's back, placing them 20 cm away from the cassava plants. We used a hoe to remove the remaining weeds. Along with covering it with fertilizer, it can be added by digging a hole 20 cm away from the base of the tree and then filling it with soil. Fertilizers should be applied while the soil is still moist. Apply weed control a second time, approximately 60–70 days after planting, using the same method as the initial application. If necessary, remove weeds a third time using a hoe or herbicide spraying. Use a cover on the spray nozzle to prevent chemicals from entering the cassava's buds and stems. However, one of the most significant carbon footprint “hotspots” for intensive agriculture is the use of fertilizers [25]. Cassava can be harvested at an appropriate age, which is approximately 10–12 months, after planning and preparing the cassava cuttings. For the next planting, chop and leave unused cassava plant parts (leaves, branches, and stems) in the plot to use as green manure [26]. Cassava stores the organic carbon it absorbs for photosynthesis in its roots, rhizomes, stems, and leaves. Plowing and covering the rhizomes, stems, leaves, and tubers left after harvest is therefore beneficial for reducing GHG emissions from cassava harvesting [27]. Cassava takes in carbon dioxide; plants open tiny pores in their leaves (called stomata) that allow water to exit through transpiration. They found that when carbon dioxide levels increase from 400 to 600 ppm, cassava leaves can conserve 58 percent more water on average by optimizing stomatal conductance, which is the rate at which carbon dioxide enters compared to water exiting the leaf [28].

One of the problems of agricultural cultivation is its adverse effects on global warming. Therefore, we studied GHG emissions from different methods of fertilizing cassava to help reduce GHG emissions. By

assessing the carbon footprint of different fertilization strategies in cassava cultivation, we aim to recommend strategies that help reduce GHG emissions on an international level. This study begins with the acquisition of raw materials and continues until they are processed into a cassava product. The volume of GHGs released in terms of carbon dioxide equivalents (CO_2 equivalent) using the global warming potential value in 100 years (GWP100) is as follows: CO_2 = 1, CH_4= 28, and N_2O = 265 [29].

2. Materials and Methods

Life cycle assessment (LCA) is a method for analyzing and quantifying the environmental impacts of producing a product or undertaking various activities [30]. This assessment considers the entire life cycle, including the extraction or acquisition of raw materials, the production process, transportation, and the use, maintenance, and distribution of the product. When considering the impact of the production process on the environment, the ecosystem, and hygiene, as well as environmental problems, the quantities of energy and raw materials used must be specified. The calculation must also include the amount of waste released into the environment. The ultimate aim is to improve the product and production processes that have the least environmental impact [31]. Carbon footprint analysis is a key indicator for mitigating environmental impacts. The carbon footprint is based on LCA methodology, which focuses only on the effects of global warming potential. The carbon footprint is defined as the total quantity of inputs within the system boundary used in the process that affects the overall quantity of global warming (output). Currently, to meet ISO 14040 standard requirements, the focus of this relies mainly on four requirements: 1) Definition of goals and scope, 2) Life cycle inventory analysis, 3) Assessment of life cycle impacts, and 4) Life cycle interpretation.

2.1 The study's goal and scope are defined.

In assessing the carbon footprint from cultivating cassava, one must account for the potential GHG emissions, which include estimated amounts of carbon dioxide (CO_2), methane (CH_4), and nitrous oxide (N_2O). We evaluated these according to the model "Cradle to Farm Gate," from the acquisition of raw materials through production practices until the product was sold [32]. Therefore, this study aimed to evaluate the reduction rate of GHG emissions by comparing global warming potential values over 100 years [33] from cassava cultivation using either chemical fertilizers or liquid organic biofertilizers. This study was conducted using 9 experimental plots with 3 replicates and various fertilizer applications (including a control), each plot measuring 1600 m^2 in the northeastern region of Thailand. We followed the guidelines of ISO 14040:2006 and calculated the carbon footprint of the material input, followed by Thailand's IPCC methodology, to assess the impacts (ISO 14040:2006, 2020). Finally, the results of the evaluation served as guidelines for cassava plantation farmers to promote good cultivation practices that minimize environmental impact while maintaining product quality. Data was collected from experimental plots during the 2023 planting season. Also, the harvesting data from the cassava experimental plots were analyzed for variance to find the average value using Tukey's method and family error range, by using the yield data to analyze and compare how effective and different the use of bio-fermented liquid from the fermentation process is compared to the use of chemical fertilizers and no fertilizers (control), with a confidence level of 95%.

2.2 Functional unit.

The study units were the biomass yields of cassava roots from each experimental plot and the quantity of fertilizer applied. These measures were used to calculate the annual quantity of carbon released by the quantity of fertilizer. These measures, which calculated carbon emissions from planting cassava, served as a unit of measure for evaluating the system's performance and were used to compare the relationship between inputs and outputs, making it possible to assess the three different planting methods and estimate GHG emissions [34]. The working units being compared are the same. Therefore, the functional unit used in this study was 1000 kg of harvested cassava, excluding transport and biomass removal after harvesting.

2.3 System boundary.

The system boundary includes cassava cultivation activities and root crop harvesting, excluding transportation to the sub-purchasing yard and removal of cassava residues. However, the system boundary encompassed various approaches to obtaining the product [35], as illustrated in Figure 1.

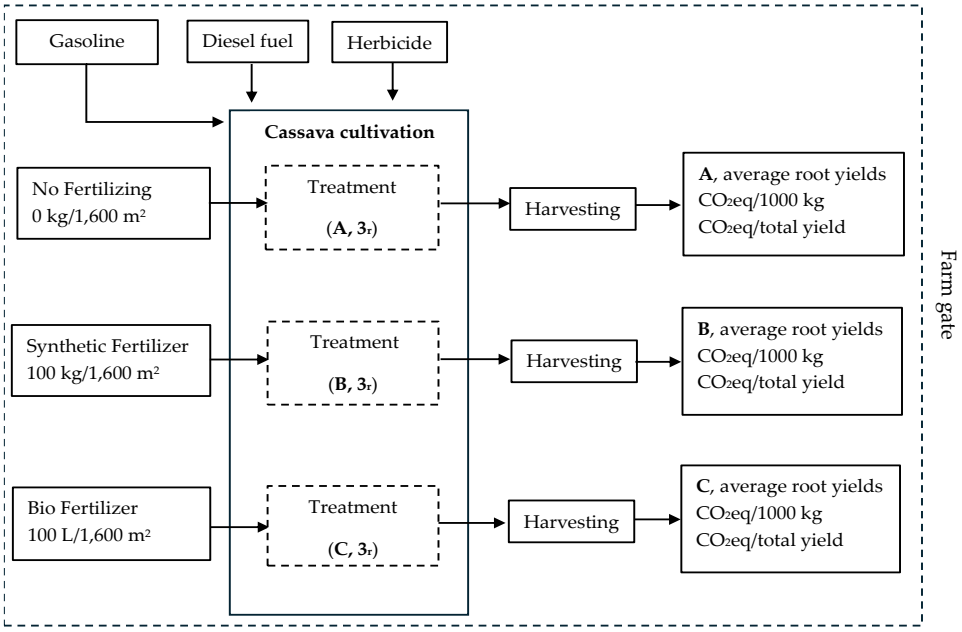

Figure 1. System boundary of cassava cultivation.

The carbon footprint is generally estimated by multiplying activity data by standard emissions factors [35]. Data collection for carbon footprint analysis included primary data obtained from experimental plots. Data collected from the three Cassava experimental plots were used to prepare an environmental life cycle inventory. Secondary data were obtained from database sources in Thailand, including the Life Cycle Database and carbon footprint databases, as well as related research that considered information similar to the situation in Thailand. This information was supplemented by data from international organizations and general publications, such as those by the IPCC. Normally, cassava cultivation relies on the addition of both synthetic and organic fertilizers. The recommendations for using different fertilizer formulas depend on the type of soil. In areas with sandy loam soil, a synthetic fertilizer with a formula of 15-15-15, applied at a rate of 100 kilograms per 1,600 m², is recommended. Such an outcome is generally achieved by adding fertilizer as a foundation, plowing for planting, and fertilizing the plants when they are about 2 months old or more. Non-chemically synthesized biofertilizers are biodegradable and can serve as fertilizers [36]. Biofertilizers are preparations that contain live or latent microorganisms. They are easy to handle, can be stored for a long time, and are also effective as biological fertilizers. Biofertilizer formulas act as carriers for microorganisms, transporting them from the production source to the soil in the plantation. [37] Liquid organic biofertilizer is a sustainable and environmentally friendly agricultural technique. Using organic biofertilizer helps increase crop yields, improve soil fertility, and enhance the nutrient content in the soil. Various organisms can be utilized as organic biofertilizers to increase soil fertility without causing pollution from biodegradation. [38]. Therefore, the production of bioorganic fertilizer for cassava cultivation in experiments was conducted using different amounts of cassava roots and molasses, supplemented with certified organic material and added microorganisms (Actinomyces). Namely Bio-1: 1 kg of fresh crushed cassava root, 1 kg of molasses. Bio-2: 1 kg of fresh crushed cassava, 2 kg of molasses. And-Bio-3: 1 kg of fresh crushed cassava, 3 kg of molasses, as materials for anaerobic bio-fermentation. All bio-fermented water is analyzed using a technique that examines plant nutrients in bio-fermented water to determine primary and secondary nutrients, such as nitrogen, which is digested and distilled, and then titrated with acid to measure the amount of nitrogen (Kjeldahl method). We digest phosphorus with acid, color it, and measure it using a UV-visible spectrophotometer. Calcium, magnesium, and potassium, as well as other cationic elements, can be digested with acid and then measured with an atomic absorption spectrophotometer. A pH and conductivity meter directly measures the pH and conductivity tests [39]. Liquid organic bio-fertilizer from fermentation process results and the values of the Macronutrients obtained from the laboratory analysis, the bio-organic liquid fertilizer contains the macronutrients in the amount that will be used for cultivation: Bio-3, contains 2.23 % of total macronutrients, Bio-2 contains 0.89 % of macronutrients, and Bio-1 contains 0.72 % of macronutrients [40]. Spraying liquid

organic biofertilizer both through the roots and through the leaves will begin when the plants have been in place for 2 months or more, similar to the application of chemical fertilizers. In this trial, the cassava cultivation in both experimental plots had sandy loam soil. The soil analysis revealed the following characteristics from 9 experiment plots before planting cassava: most of the soil in all plots was highly acidic, with an average pH of 4.98, and the average potassium content across all plots was 18.83%. As for organic matter (OM) in the soil from the analysis results, all soils are at low levels with an average of 1.2% and the suitable soil for cassava cultivation should be 1.5 - 2.5% (Land Development Department, referring to OM, Walkley and Black). Only phosphorus (P_2O_5) is available in high quantities, especially in the soil of the cassava experiment plot 1, which is as high as 31%. Therefore, an appropriate median phosphorus value for cassava cultivation plots is 11-15% (Land Development Department, referring to Available P, Bray II). pH 4.98, organic matter 1.12%, phosphorus 18.83%, and potassium 29.33% [41].

The synthetic fertilizer usage for the synthetic fertilizer plot (Treatment B) was 46-0-0, 15-15-15, and 0-0-60 at a total quantity of 100 kg per 1600 m² [42]. The liquid organic biofertilizer plot (experimental plot C) received 100 liters of liquid organic fertilizer per 1600 m², while Treatment A applied no fertilizers (Control plot). We applied chemical fertilizer and liquid organic biofertilizer to the soil when cassava had been planted for 2, 3, and 4 months, and harvested the product 12 months later. The cultivation activities of cassava remain consistent, except for the types and amounts of fertilizer applied. (1) Fuel and other petrol use. We used a tractor to plow the soil in the planting plots. We plowed furrows to plant cassava stems and remove fresh cassava roots. Diesel was mainly used. At 1 rai per hour, it has a fuel consumption rate of approximately 1.5–5 liters per rai (T1, T2, T3). Tillage the cassava experimental plots. Cassava cultivation does not involve tillage to reduce soil compaction, as cassava is sensitive to growth in compacted soil with poor water drainage. The procedure restores the physical and chemical properties of the soil to their original state while also enhancing the soil's potential to improve the stability of the soil structure in the plot. Then, cassava can be grown without tillage, allowing the plant to grow optimally and produce the desired yield while maintaining the physical properties of the soil [43].

- Raise the ridges to plant cassava stalks in every experiment plot. Raise the ridges to plant cassava, as the rainy season floods the area. Plow the planting furrows with a height of 30-40 centimeters and a distance between furrows of 100-120 centimeters to drain water and facilitate weeding and harvesting [44]. The planting area is raised to form a ridge, allowing for efficient drainage and preventing water retention. This prevents the cassava roots from absorbing oxygen, which can cause fungal diseases and limit nutrient absorption [45].

(2) And, no fertilization activities were performed in the control plots (TA)

(3) Chemical fertilizer application (TB). Cassava plants were fertilized 2 months after planting, and the soil in the cassava plantation was fertilized three times:

- 1st apply fertilizer formula 46-0-0, 25 kg,
- 2nd apply fertilizer formula 15-15-15, 50 kg,
- 3rd apply fertilizer formula 0-0-60, 25 kg,

(4) The experimental plot (TC) serves as the testing ground. An aerobic fermentation process produces liquid organic fertilizer. The process employs a solid fermentation technique that utilizes cassava roots left in the field after previous harvests as the raw material for fermentation. It is ground and dipped into a stirred fermentation tank, and actinomycete microorganisms are added. Molasses is used as a carbon source, and specific organic materials are utilized as culture media to produce liquid bio-fermented water, which is used in cassava cultivation. The electricity in the fermentation process, both stirring and electrolysis, comes from solar panels. The selected microbial strains are bacteria that are efficient in decomposing agricultural products or waste, and there is also a beneficial Aspergillus fungus. Liquid organic biofertilizer from the three reactor tanks process was collected and sprayed on the soil 3 times after planting cassava in the 2nd, 3rd, and 4th months:

- 1st soil spray with Bio formula .25-.02-.45, 20 L *[06].*
- 2nd soil spray with Bio formula .25-.04-.60, 30 L *[06].*
- 3rd soil spray with Bio formula .20-.83-1.2, 50 L *[06].*

(5) Herbicide is used to control weeds with chemicals. We can classify the chemicals for weed control into two categories based on the duration of their use: 1) use of pre-emergence herb control chemicals, sometimes called control agents or contraceptives, using chemical sprays (500 cc) as soon as cassava planting

is finished or no more than 3 days before weeds and plants germinate, and 2) chemicals to control weeds after emergence (weed killer), using herbicides when the cassava is more than 4 months old (T1, T2, T3) and the stem is more than 70 centimeters tall [46].

(6) Harvesting cassava products. When it's time to harvest fresh tubers for sale to the sub-purchasing yard, the harvesters gather cassava. Agricultural machinery is used to dig up cassava roots, and labor is used to collect cassava production [47].

2.4 Impact of the emission factor.

Emission factor values are associated with emissions. Precise information on EF is crucial for estimating emissions from a given system, as outlined in the guidelines provided by the IPCC report. We express EF by dividing the weight of a specific gas by the unit weight, volume, distance, or duration of the polluting activity. This study is based on a methodology for evaluating emissions and emission factor values, as outlined in guidelines for the carbon footprint of products. The evaluation of life cycle results in this experiment suggests the possibility of global warming over the next 100 years, focusing solely on the quantities of carbon dioxide (CO2), methane (CH4), and nitrous oxide (N2O) that will be emitted. We adjusted the global warming potential (GWP) over 100 years in 2021 to align with the country's GHG emissions assessment. The GWPs of CO_2, CH_4, and N_2O are 1, 28, and 265. GHG emissions to the atmosphere as kg CO_2e were calculated according to the following formula: Equation 1

$$CF = \sum(Activity\ data_i\ x\ EF_i) \quad (1)$$

Where:

CF = Carbon footprint (kg CO_2eq)
Activity data = Quantity of input or activity (e.g., kg of fertilizer, liters of fuel)
Emission factor = Emission factor for each input/activity (kg CO_2eq per unit), as shown in Table 3.

Table 3. Thailand National Database emission factor (IPCC).

Items	Unit	EF* (kg CO_2eq/unit)
Urea fertilizer as N (46-0-0)	kg	3.3036
Fertilizer as K2O (0-0-60)	kg	0.4974
Fertilizer as N, P, K (15-15-15)	kg	1.5083
Cassava	kg	0.0489
Molasses	kg	0.1381
Diesel	kg	0.3522
Gasoline	kg	0.4024
Glyphosate	kg	16.0000

Source: (TGO.; Thailand Greenhouse Gas Management Organization) [17]

3. Results and Discussion

3.1 Life cycle inventory of cassava cultivation.

The carbon footprint of cassava cultivation was evaluated across 9 treatment plots (1600 m²/plot), where the 1st treatment plot served as the control (T1), the 2nd treatment applied synthetic fertilizer (T2), and the 3rd treatment applied liquid organic biofertilizer (T3), with three replicates (n = 3). The evaluation of carbon emissions included soil preparation, planting, fertilizing, weed control, and harvesting. The data were gathered from the experiments, and to assess GHG emissions, only the average inputs from planting and harvesting cassava were considered for the results in each experiment. The collection of environmental inventory data used to evaluate the carbon footprint from cassava cultivation in Chaiyaphum Province, Thailand, was conducted during planting activities using the KU-50 cassava variety in 1,600 m² experimental plots. We studied the data obtained from the experimental plots. The control plots yielded an average of 1658 kg/1600 m², using chemical fertilizers produced a yield of an average of 3552 kg/1600 m², and using biofertilizers produced a yield of an average of 7605 kg/1600 m². The list of acquisitions of 1000 kg of cassava

was analyzed, and the weight of fresh cassava roots per area was taken from the average weight of each experimental cassava planting plot. In summary, the results showed that the plot using liquid organic biofertilizer (Bio-1, 2, 3) had the best effect on total yield and was significantly different from the other planting methods ($P < 0.05$), as indicated in Table 4.

Table 4. Average cassava root yields per experiment plot.

Treatment	Applied (kg, L/rai)	Root yield R_1, (kg /rai)	Root yield R_2, (kg /rai)	Root yield R_3, (kg /rai)	Average root yield (kg /rai)
Control (T1)	0-0-0	1520	1488	1968	1658.67^{c}
Che-Fertilizer (T2)	100 kg	4496	3008	3152	3552.00^{b}
Biofertilizer-1,2,3 (T3)	100 L	8336	6864	7626	7605.33^{a}
Mean =					4272
P = 0.000					***

Note*** = statistically highly significant difference *(P < 0.000)*; Different letters labeled in the same column showed statistically highly significant differences *(P < 0.000)* using Tukey's family error range test.

Cassava will be planted using three methods: a control plot, chemical fertilizers, and organic liquid fertilizers, with each method applied three times. Apply chemical fertilizers and liquid organic biofertilizers to cassava plants 45 days after planting, using chemical fertilizers at a rate of 100 kg per rai and biofertilizers at a rate of 100 Liters per Rai. This approach will evaluate the planting activities until the cassava harvest, including the yield rate, which affects greenhouse gas emissions. Preliminary results: The plot using biofertilizers (T3) produced root yield at a rate of 7.6 tons/rai and increased by 114% compared with the plot using chemical fertilizers (T2) and 358% compared to the control plot (T1).

Carbon Footprint (CF) from cassava cultivation, control, nitrogen fertilizer, and biofertilizer plots.

Calculation of carbon footprints from cultivation to estimate greenhouse gas emissions associated with various activities from cassava cultivation to harvest, considering emissions from land preparation, fertilizer use, herbicides, and energy (machinery) use, to use data for life cycle assessment (LCA) framework, considering emissions from all steps from cultivation to final harvest. The amount of pollutant emissions from plowing the ridges and harvesting in cassava plantation areas is expected to be affected by the use of pollutant factors, including the type of fuel used for land preparation machinery and fuel consumption of 4.5 liters. Emissions related to the production of glyphosate, a weed control chemical, and the burning of weeds that have already sprouted in cassava fields, with an average of 1 liter used. In control plots, gasoline is used in sprayers, with no electricity used, and the average consumption is 5 liters. The calculations indicate that 1000 kg of cassava can produce 11.80 kg CO_2eq, and CF/ton is calculated from (4.5 x 0.3522) + (5 x 0.4024) + (16 x 1) / 1.658 = 11.80, and the carbon footprint of the total yield was 19.60 kg CO_2eq, and CF/yield is calculated from (4.5 x 0.3522) + (5 x 0.4024) + (16 x 1) = 19.60, as shown in Table 5.

Table 5. Life Cycle Inventory (LCI) data of cassava root production with Control plot (T1), (1658 kg/1600 m^2).

Control plot	Quantity (kg/1600 m^2)	Carbon footprint		
		Source (kg CO_2eq)	Use (kg CO_2eq)	Total (kg CO_2eq)
2nd month, no fertilizing	0	0	0	0
3rd month, no fertilizing	0	0	0	0
4th month, no fertilizing	0	0	0	0
Fuel – Diesel (Land prepare & harvest)	4.50	1.58	-	1.58
Gasoline (Spray herbicide)	5.00	2.01	-	2.01
Glyphosate (Weed killer)	1.00	16.00	-	16.00
Total		19.60		19.60
Total (kg CO_2eq/1000 kg)		11.80	-	11.80

In the control plot, the use of glyphosate herbicide in cassava cultivation was evaluated against the yield per ton and total yield, and the results indicated that it affected greenhouse gas (GHG) emissions by 49.24% and 81.63%, respectively, of the average yield and total yield from the plot, as shown in Figure 2.

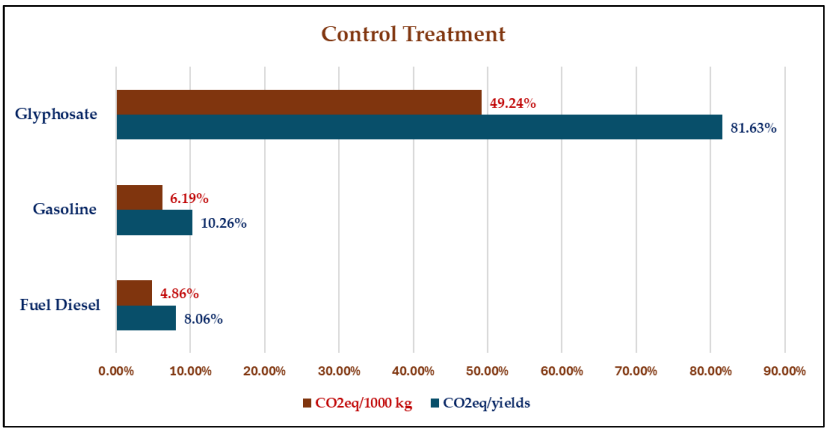

Figure 2. The contribution to the carbon footprint from the weight of 1000 kg and total yields of the unfertilized plot.

The degradation and absorption of chemicals into soil and water can generate nitrous oxide (N_2O), a greenhouse gas that affects the ecosystem and biodiversity.

Chemical fertilizers (TB).

Preparing the land: It is estimated that plowing and harvesting in cassava fields release 4.5 liters of pollutants for every 1,600 m², based on the type of fuel used by the machinery and the amount of fuel consumed. Fertilizing: A total of 100 kg of nitrogen fertilizer is used for cultivation, including the formulas 46-0-0, 15-15-15, and 0-0-60. Herbicides: We use glyphosate, a weed control chemical, to burn weeds that have already sprouted in the cassava fields. We use an average of 1 liter per 1600 meters. Sprayers and weed sprays consume an average of 5 liters of gasoline.

A total of 51.83 kg CO_2eq / 1000 kg of cassava weight, and CF/ton is calculated from: (0.46x3.3036) + (55x0) = 1.5196 x 25 = 37.9914 + (0.15x3.3036) + (0.15x1.5716) + (0.15x0.4974) + 0.55x0 = 0.8059 x 50 = 40.29 + (0.60x0.4974) + (40x0) = 0.29844 x 25 = 7.461 + (0.46x25/100) x 44/28 = 0.1807142857 x 265 = 47.8892857105 + (0.15x50/100) x 44/28 = 0.1178571429 x 265 = 31.2321 + (0.3522x4.5 = 1.5849) + (0.4024x5 = 2.012) + (16x1=16) /7.605 = 52.07).

And carbon footprint of total yield was 184.44 kg CO_2eq, which CF/yield is calculated from: (0.46x3.3036) + (55x0) = 1.5196 x 25 = 37.9914 + (0.15x3.3036) + (0.15x1.5716) + (0.15x0.4974) + 0.55x0 = 0.8059 x 50 = 40.29 + (0.60x0.4974) + (40x0) = 0.29844 x 25 = 7.461 + (0.46x25/100) x 44/28 = 0.1807142857 x 265 = 47.8892857105 + (0.15x50/100) x 44/28 = 0.1178571429 x 265 = 31.2321 + (0.3522x4.5 = 1.5849) + (0.4024x5 = 2.012) + (16x1=16) = 184.44), as shown in Table 6.

Table 6. Life Cycle Inventory (LCI) data of cassava root production using synthetic N, P, and K fertilizer (T2), (3552 kg/1600 m²).

Chemical fertilizer (N, P, K)	**Quantity (Kg, L/1600 m², $T2_{r1,2,3}$)**	**Carbon footprint**		
		Source (kg CO_2eq)	**Use (kg CO_2eq)**	**Total (kg CO_2eq)**
2nd month, apply 46-0-0	25	37.99	47.88	85.87
3rd month, apply 15-15-15	50	40.29	31.23	71.52
4th month, apply 0-0-60	25	7.461	-	7.46
Fuel – Diesel & 35 hp, tractor usage (hr.)	4.5	1.58	-	1.58
Gasoline	5.0	2.01	-	2.01
Glyphosate	1.0	16.0	-	16.00
Total		105	79	184.4
Total (kg CO_2 eq/1000 kg)		29.60	22.23	51.83

Note: All three chemical fertilizer formulas are used in different quantities.

The carbon footprint of 1000 kg of cassava roots produced using chemical fertilizers is approximately 51.83 kg CO_2eq/1000 kg of cassava yield, which relates to chemical fertilizer application and was as high as 25.17 percent, on average, as shown in Figure 3.

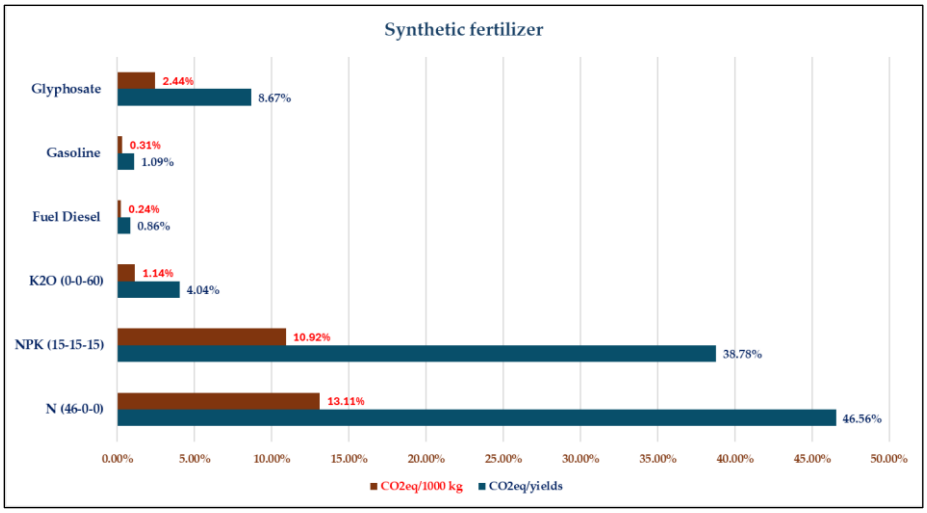

Figure 3. The contribution to the carbon footprint from the weight of 1000 kg and the total yields of cassava roots when using chemical fertilizers.

The use of chemical fertilizers in cassava production is a significant contributor to the overall carbon footprint of cassava cultivation, particularly in the production and application of synthetic fertilizers. Nitrogen fertilizers are a significant source of greenhouse gas emissions, accounting for 85.34% of the total emissions from cassava yield, which was 184.44 kg CO_2eq.

Liquid organic biofertilizer was applied to the plots.

Land preparation: The 35 HP tractor is used to plow the ridges and harvest in cassava plantation areas to estimate the effect of using pollutant factors of fuel used for land preparation machinery and fuel consumption of 4.5 liters per 1600 m². Biofertilizer application: Using liquid organic biofertilizers with low plant nutrient content will result in a lower carbon footprint compared to synthetic fertilizers, potentially significantly reducing greenhouse gas emissions. The production of organic biofertilizers can help reduce greenhouse gas emissions. The biofertilizers used in cassava cultivation are produced using a developed fermentation process that lowers the cost of compost material and reduces energy consumption during biofertilizer production. Apply 100 liters per 1600 m² experiment plot. Moreover, the raw materials used to make biofertilizers are as follows:

Bio-1 uses 1kg of cassava + 1kg of molasses.

Bio-2 uses 1kg of cassava + 2kg of molasses.

Bio-3 uses 1kg of cassava + 3kg of molasses.

Herbicides, such as glyphosate, a weed control chemical, are used, and weeds that have already sprouted in cassava fields are burned, typically using an average of 1 liter.Energy use: Gasoline emissions for use in sprayers in the control plot and no electricity use, averaging 5 liters. A total of 2.74 kg CO_2eq / 1000 kg of cassava weight, and CF/ton is calculated from: (0.0489x9) + (0.1381x6) + (0.3522x5) + (0.4024x4.5) + (16x1)/7.605 = 2.80. The carbon footprint of the total yield was calculated to be kg CO2eq, as well as CF/yield, which is calculated from: (0.0489 × 9) + (0.1381 × 6) + (0.3522 × 6.5) + (2.02 × 5) + (16 × 1) = 20.85, as shown in Table 7.

Table 7. Life Cycle Inventory (LCI) data of cassava root production in liquid organic biofertilizer applications (T3) (7605 kg/1600 m²).

Biofertilizer (N, P, K)	Quantity (L/1600 m²)	Carbon footprint		
		Source (kg CO_2eq)	Use (kg CO_2eq)	Total (kg CO_2eq)
2nd month, spray bio-1, 0.25-0.02-0.45	20	0.28	-	0.28
3rd month, spray bio-2, 0.25-0.04-0.60	30	0.42	-	0.42
4th month, spray bio-3, 0.20-0.83-1.20	50	0.56	-	0.56
Fuel Diesel (soil preparation & harvest)	4.5	1.58	-	1.58
Gasoline (spraying herbicide)	5.0	2.01	-	2.01
Glyphosate (weed control)	1.0	16.0	-	16.0
Total		20.85	-	20.85
Total (kg CO_2eq/1000 kg)		2.74	-	2.74

Note: All three formulas of liquid organic biofertilizer are made from cassava roots and molasses fermented in different quantities.

The carbon footprint of cassava grown in a sandy loam soil plantation, using liquid organic biofertilizer and sprays, yielded approximately 2.74 kg CO_2eq (0.79%/ton) for every 1000 kg produced per 1600 m², which is lower than that of other planting materials used in the plot, as shown in Figure 4.

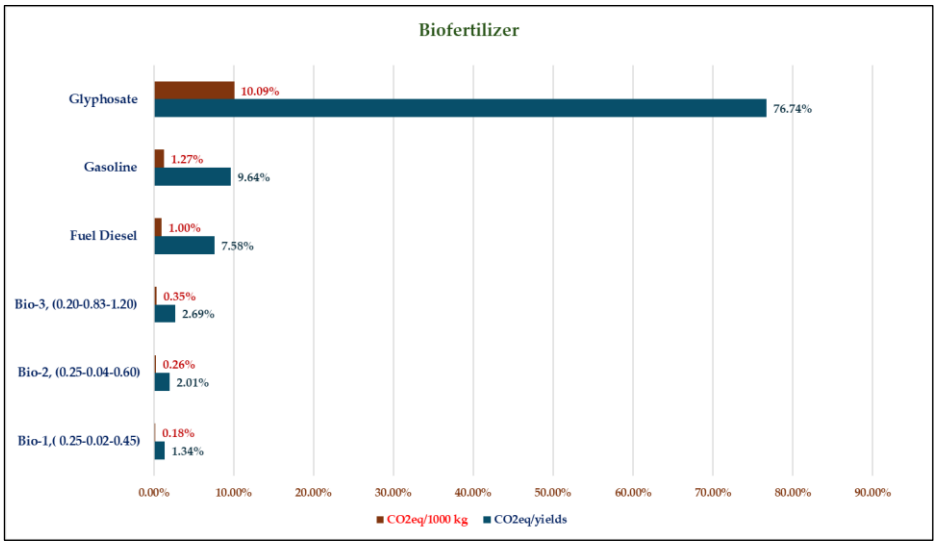

Figure 4. The contribution to the carbon footprint from the weight of 1000 kg of cassava roots when using liquid biofertilizers.

Using liquid organic biofertilizers in cassava cultivation can help reduce carbon emissions when compared to the total weight of cassava roots per area. The greenhouse gas emissions from liquid organic biofertilizers per 1,600 m² of cassava production are 20.85 kg CO_2eq (6.04%). The emissions are related to production, which is the main factor affecting the overall carbon stock of cassava cultivation.

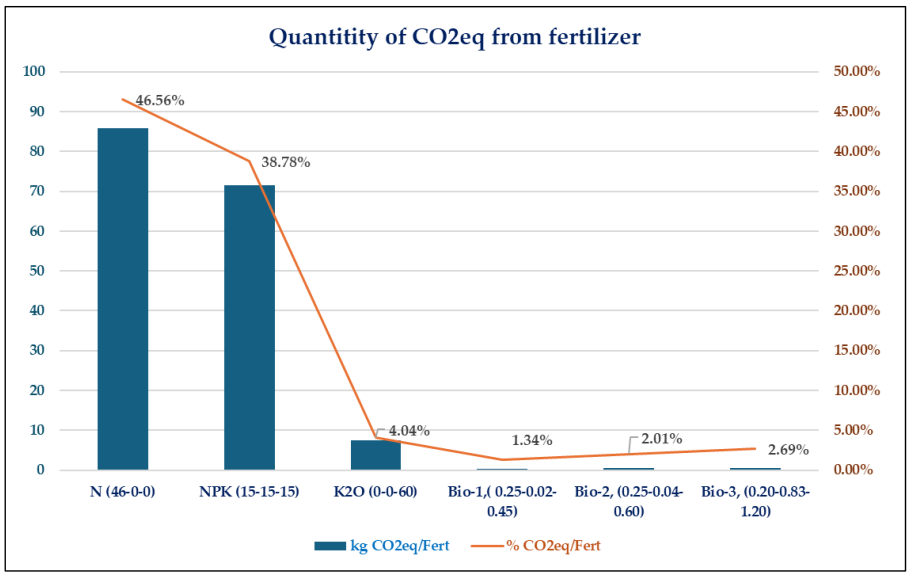

Figure 5. Total contribution of carbon footprint fertilizers.

3.2 Life cycle inventory results and discussion.

The carbon footprint of cassava cultivation from "cradle to farm-gate" for the TA, TB, and TC methods, as well as the carbon footprint associated with cassava root yield, was 11.80 kg CO_2eq/1000 kg, 51.83 kg CO_2eq /1000 kg, and 2.80 kg CO_2eq/1000 kg, respectively; this was observed in an experimental design that varied fertilizer types and amounts. The carbon footprint in cassava cultivation is primarily attributed to the use of chemical fertilizers, which release N_2O gas during their production and application. Cassava cultivation using chemical fertilizers (TB) still significantly impacts approximately 89% of the carbon footprint on cassava yield. On the other hand, the yield of TB cassava was only 50% higher than that of TA and 50% lower than that of TC. At the same time, the cultivation cost was higher than that of all other cultivation methods, and the impact of greenhouse gas emissions was greater than that of other plantations. The carbon footprint of cassava cultivation treatment A (control) with no fertilizing and harvesting of yields, evaluated in kg CO_2eq per 1000 kg, was 11.80. B, including cultivation and harvesting of yields, was evaluated in kg CO_2eq per 1000 kg and was 51.83. The carbon footprint of cassava cultivation treatment C, including cultivation and yield harvesting, was 2.80 kg CO_2eq/1000 kg of root product. The impact of global warming potential varied depending on the type of fertilizer used, and a significant increase in yield was observed. This means that using chemical fertilizers in cassava cultivation will increase the quantity of GHG emissions every year. The use of liquid organic biofertilizers is considered to have minimal GHG emissions. A more carbon-neutral strategy would be to switch from synthetic to liquid organic biofertilization of cassava crops. Furthermore, yields were increased when using liquid organic fertilizers, demonstrating the advantages of this type of fertilizer, which has a significantly reduced environmental impact. This study was conducted over a single growing season in a specific region of northeastern Thailand, which may limit the generalizability of the findings to other regions or agricultural conditions. We did not thoroughly analyze the economic feasibility and supply chain constraints of liquid organic biofertilizers, particularly in terms of production costs, scalability, and farmer accessibility. These limitations suggest that, while promising in terms of environmental benefits, broader adoption would require further study across multiple seasons, agro-climatic zones, and economic contexts. However, we must adopt a sustainable approach to reduce production costs without compromising the environment.

Liquid organic bio-fertilizers can vary significantly in nutrient concentrations and are pricier than chemical fertilizers. Large-scale and prolonged use can accumulate salts, nutrients, and heavy metals, which can have adverse effects on plant growth, soil organism development, water quality, and human health. Large-scale use of organic bio-fertilizers is necessary for the soil because they contain fewer nutrients than chemical fertilizers. Primary nutrients may not be sufficient for plant growth and development, and nutrient deficiencies may occur, which are caused by low transfer of primary and secondary nutrients. To overcome

the limitations of liquid organic biofertilizer production, low-cost techniques should be employed. For instance, liquid organic biofertilizer can be made from inexpensive cassava roots and supplemented with organic nutrients, such as those obtained through aerobic fermentation processes, which can help reduce CH_4 emissions. Collecting the remaining cassava roots in the field after harvest, instead of letting them decompose naturally (anaerobically), crushing them, and fermenting them in an aerobic reactor tank to produce an organic liquid biofertilizer, can reduce CH_4 emission during decomposition. Clean energy sources, such as solar panels, operating at low DC voltage, should be considered to create a redox balance reaction by producing reduced carbon compounds (fermentation) and reducing electricity use in biofertilizers.

4. Conclusions

From a study of the carbon footprint of cassava, calculated per 1000 kg of cassava yield, the scope of the study encompasses the entire process, from acquiring raw materials through cultivation and harvesting to the production of the final product. This study was conducted in nine planting plots, each of 1600 m², in the Khon Sawan District, Chaiyaphum Province. This study found that planting cassava using chemical fertilizers resulted in an average cassava yield of approximately 3,552 kg per 1,600 m². The carbon footprint analysis results for fresh cassava were estimated to be approximately equal to 51.83 kg CO_2eq/1,000 kg and 184.4 kg CO_2eq/1,600 m² of planting area. Meanwhile, the treatment using organic liquid biofertilizers yielded an average cassava yield of approximately 7,605 kg/1,600 m². The carbon footprint analysis results for fresh cassava were estimated to be approximately equal to 2.74 kg CO_2eq/1,000 kg. The total per area was 20.85 kg CO_2eq/1600 m². Considering the carbon footprint from Thailand's average cassava planting area of 13,064,186,880 m² in 2018–2022, chemical fertilizer applications would result in GHG emissions equivalent to 1,505,647,537 kg CO_2eq/year. Using liquid organic biofertilizer would result in a much lower GHG emissions rate of 170,242,685 kg CO_2eq/year. Therefore, experimental plots with cultivation methods using chemical fertilizers have the highest GHG emissions over the entire life cycle. Meanwhile, liquid organic biofertilizers and fertilizers have the lowest GHG emissions. Therefore, liquid organic biofertilizers that use agricultural waste materials would significantly reduce cassava's carbon footprint. In addition, the yield of cassava using liquid organic biofertilizers alone has been shown to increase by over 2 times that when using chemical fertilizers alone. Hence, liquid organic biofertilizers from agricultural products have high economic and environmental value, reduce the cost of agricultural crop production, are less harmful to people than inorganic fertilizers, reduce pollution, and improve soil fertility without the accumulation of heavy metals and long-term residues from biodegradation, resulting in higher yields while having less impact on the environment. However, nationwide implementation would face challenges related to scalability, cost-effectiveness, farmer acceptance, and the development of the supply chain. These factors must be addressed to realize the full potential of GHG reduction at the national level.

5. Acknowledgements

The authors express their gratitude to the College of Innovative Technology and Engineering at Dhurakij Pundit University for facilitating this research. Special thanks to the support of the Agricultural Research and Development Station, Department of Agriculture, and the Department of Land Development, as well as the Rayong Field Crops Research Center.

Author Contributions: Conceptualization, experimental design, S.J., N.N., S.V., S.T., carrying out the experiment and data acquisition, S.J., N.N., S.V., S.T., writing and editing, N.N., S.V., S.T.

Funding: None

Conflicts of Interest: The authors declare no conflict of interest.

References

[1] Penuelas, J.; Coello, F.; Sardans, J. A better use of fertilizers is needed for global food security and environmental sustainability. *Agriculture & Food Security* **2023**. *12*(1), 5. https://doi.org/10.1186/s40066-023-00409-5

[2] Walling, E.; Vaneeckhaute, C. Greenhouse gas emissions from inorganic and organic fertilizer production and use: A review of emission factors and their variability. *Journal of Environmental Management,* **2020**. *276*, 111211. https://doi.org/10.1016/j.jenvman.2020.111211.

[3] Blonk, H.; van Paassen, M.; Draijer, N.; Tyszler, M.; Braconi, N.; van Rijn, J. Agri-Footprint 6 Methodology Report. Blonk Sustainability. **2022.** https://www.blonksustainability.nl

[4] Menegat, S.; Ledo, A.; Tirado, R. Greenhouse gas emissions from global production and use of nitrogen synthetic fertilisers in agriculture. *Scientific Reports* **2022**. *12*(1), 14490. https://doi.org/10.1038/s41598-022-18773-w

[5] Office of Agricultural Economics. The agricultural sector plans to reduce greenhouse gas emissions by 1 million tons. Office of Agricultural Economics, Ministry of Agriculture and Cooperatives. **2024**. https://www.oae.go.th/view/1/43062/TH-TH

[6] Pahalvi, H. N.; Rafiya, L.; Rashid, S.; Nisar, B.; Kamili, A. N. Chemical fertilizers and their impact on soil health. In *Microbiota and Biofertilizers*, **2021**; pp. 1-20. Springer International Publishing. https://doi.org/10.1007/978-3-030-61010-4_1

[7] Burbano-Cuasapud, J. M.; Solarte-Toro, J. C.; Restrepo-Serna, D. L.; Cardona Alzate, C. A. Process sustainability analysis of biorefineries to produce biofertilizers and bioenergy from biodegradable residues. *Fermentation,* **2023**. *9*(9), 788. https://doi.org/10.3390/fermentation9090788

[8] Shaji, H.; Chandran, V.; Mathew, L. Organic fertilizers as a route to controlled release of nutrients. In *Controlled Release Fertilizers for Sustainable Agriculture* **2021**; pp. 231-245. Elsevier. https://doi.org/10.1016/B978-0-12-819555-0.00013-3

[9] Dasgupta, D.; Kumar, K.; Miglani, R.; Mishra, R.; Panda, A. K.; Bisht, S. S. Microbial biofertilizers: Recent trends and future outlook. In *Recent Advancement in Microbial Biotechnology* **2021**; pp. 1-26. Elsevier. https://doi.org/10.1016/B978-0-12-822098-6.00001-X

[10] Anubrata, P.; Rajendra, D. Isolation, characterization, production of biofertilizer & its effect on vegetable plants with and without carrier materials. *International Journal of Current Research* **2014**, *6*(08), 7986-7995

[11] Allouzi, M. M. A.; Allouzi, S. M. A.; Keng, Z. X.; Supramaniam, C. V.; Singh, A.; Chong, S. Liquid biofertilizers as a sustainable solution for agriculture. *Heliyon* **2022,** *8*(12), e12609. https://doi.org/10.1016/j.heliyon.2022.e12609

[12] Häfner, F.; Ruser, R.; Claß-Mahler, I.; Möller, K. Field application of organic fertilizers triggers N_2O emissions from the soil N pool as indicated by ^{15}N-labeled digestates. *Frontiers in Sustainable Food Systems* **2021**, 4. https://doi.org/10.3389/fsufs.2020.614349

[13] Toonsiri, P.; Del Grosso, S. J.; Sukor, A.; Davis, J. G. Greenhouse gas emissions from solid and liquid organic fertilizers applied to lettuce. *Journal of Environmental Quality* **2016**, *45*(6), 1812-1821. https://doi.org/10.2134/jeq2015.12.0623

[14] Piyachomkwan, K.; Tanticharoen, M. Cassava industry in Thailand: Prospects. *Journal of the Royal Institute of Thailand* **2011,** 3.

[15] Chalermsaenyakorn, L. Thai chemical fertilizer business outlook (KResearch Industry Analysis and Outlook No. 30). Kasikorn Research Center. **2025**. https://kasikornresearch.com/

[16] Rojanaridpiched, C. Good agricultural practices for cassava under the agricultural standards. Agricultural Commodity and Food Standards (ACFS). **2010**. Retrieved from https://www.acfs.go.th/standard/download/eng/GAP_cassava.pdf

[17] TGO. Emission factor values divided by industry group. Thailand Greenhouse Gas Management Organization. **2023**. Retrieved December 23, 2023, from https://www.tgo.or.th/2023/index.php/th/

[18] Vittayakorn, N. Soil fertility and plant nutrition. Khon Kaen University, Faculty of Agriculture. **2016**. Retrieved from https://ag2.kku.ac.th/eLearning/132351/Doc%5C122351 Lec14-15 Fertilizer-59-1.pdf

[19] Krungsri ResearchBusiness trend / Industrial outlook for the chemical fertilizer industry in 2023–2025. Bank of Ayudhya Public Company Limited. **2023**. https://www.krungsri.com/th/research/industry/industry-outlook/chemicals/chemical-fertilizers/io/io-chemical-fertilizers-2023-2025

[20] Konradt, M.; Weder di Mauro, B. Carbon taxation and greenflation: Evidence from Europe and Canada. *Journal of the European Economic Association* 2023, *21*(6), 2518-2546. https://doi.org/10.1093/jeea/jvad020

[21] Boonchai, K. What will agriculture and world food security look like in the climate of global warming. ThaiPublica. **2021**, Retrieved October 20, 2023, from https://thaipublica.org/2021/07/thai-climate-justice-for-all05/

[22] Liu, C.; Cutforth, H.; Chai, Q.; Gan, Y. Farming tactics to reduce the carbon footprint of crop cultivation in semiarid areas: A review. *Agronomy for Sustainable Development* **2016**, *36*(4), 69. https://doi.org/10.1007/s13593-016-0404-8

[23] Ziska, L. H. The role of climate change and increasing atmospheric carbon dioxide on weed management: Herbicide efficacy. *Agriculture, Ecosystems & Environment* **2016**, *231*, 304-309. https://doi.org/10.1016/j.agee.2016.07.014

[24] Suhag, M. Potential of biofertilizers to replace chemical fertilizers. *International Advanced Research Journal in Science, Engineering and Technology* **2016**, *3*(5). https://doi.org/10.17148/IARJSET.2016.3534

[25] Litskas, V. D.; Platis, D. P.; Anagnostopoulos, C. D.; Tsaboula, A. C.; Menexes, G. C.; Kalburtji, K. L.; Stavrinides, M. C.; Mamolos, A. P. Climate change and agriculture. In *Sustainability of the Food System* **2020**; pp. 33-49. Elsevier. https://doi.org/10.1016/B978-0-12-818293-2.00003-3

[26] Luanmanee, S. Building up of carbon bank under field and renewable energy crops production areas. Department of Agriculture, Thailand. **2023.** Retrieved December 23, 2023, from https://www.doa.go.th/research/archive/index.php?thread-2383.html

[27] Prakobboon, N.; Vahdati, M.; Shahrestani, M. An environmental impact assessment of the management of cassava waste: A case study in Thailand. *International Journal of Biomass and Renewables* **2018**, *7*(2), 18-29. https://doi.org/10.61762/ijbrvol7iss2art4868

[28] Benjamin, C. Cassava may benefit from atmospheric change more than other crops. Carl R. Woese Institute for Genomic Biology, University of Illinois. **2023**. Retrieved December 20, 2023, from https://www.igb.illinois.edu/article/cassava-may-benefit-atmospheric-change-more-other-crops

[29] IPCC. Climate change 2014: Synthesis report. Contribution of Working Groups I, II and III to the Fifth Assessment Report of the Intergovernmental Panel on Climate Change. Geneva, Switzerland. **2014**. Retrieved from https://www.ipcc.ch/report/ar5/syr/

[30] Muralikrishna, I. V.; Manickam, V. Life cycle assessment. In *Environmental Management* **2017**; pp. 57-75. Elsevier. https://doi.org/10.1016/B978-0-12-811989-1.00005-1

[31] Bunprom, P.; Thirawanutpong, P. Life cycle assessment tools for environmental management. *Journal of KMUTNB* **2013**, *23*(1).

[32] Bakker, C. A.; Wever, R.; Teoh, C.; De Clercq, S. Designing cradle-to-cradle products: A reality check. *International Journal of Sustainable Engineering* **2010**, *3*(1), 2-8. https://doi.org/10.1080/19397030903395166

[33] IPCC. Climate change 2014: Synthesis report. Contribution of Working Groups I, II and III to the Fifth Assessment Report of the Intergovernmental Panel on Climate Change. Geneva, Switzerland. **2014**. Retrieved from https://www.ipcc.ch/report/ar5/syr/

[34] Widheden, J.; Ringström, E. Life cycle assessment. In *Handbook for Cleaning/Decontamination of Surfaces* **2007**; pp. 695-720. Elsevier. https://doi.org/10.1016/B978-044451664-0/50021-8

[35] Alengebawy, A.; Ghimire, N.; Abdelkhalek, S. T.; Samer, M. Conversion of bioenergy materials to secondary fuels. In *Encyclopedia of Renewable Energy, Sustainability and the Environment* **2024**; pp. 825-838. Elsevier. https://doi.org/10.1016/B978-0-323-93940-9.00030-X

[36] Yashavantha Rao, H. C.; Mohana, N. C.; Satish, S. Biocommercial aspects of microbial endophytes for sustainable agriculture. In *Microbial Endophytes: Functional Biology and Applications* **2020**; pp. 323-347. Elsevier. https://www.sciencedirect.com/science/article/abs/pii/B9780128196540000132

[37] Ammar, E. E.; Rady, H. A.; Khattab, A. M.; Amer, M. H.; Mohamed, S. A.; Elodamy, N. I.; AL-Farga, A.; Aioub, A. A. A. A comprehensive overview of eco-friendly bio-fertilizers extracted from living organisms. *Environmental Science and Pollution Research International* **2023**, *30*(53), 113119-113137. https://doi.org/10.1007/s11356-023-30260-x

[38] Kumar, S.; Diksha, Sindhu, S. S.; Kumar, R. Biofertilizers: An ecofriendly technology for nutrient recycling and environmental sustainability. *Current Research in Microbial Sciences* **2022**, *3*, 100094. https://doi.org/10.1016/j.crmicr.2021.100094

[39] Department of Agriculture. Organic fertilizer analysis method guide. Department of Agriculture Archives (ISBN 978-974-436-679-5). **2022**. Retrieved from http://lib.doa.go.th/multim/e-book/EB00061.pdf

[40] Department of Agriculture. Raksapram, U.; Chanthapiriyapun, K. Bio fertilizer plant nutrient analysis report. Referring to Organic Fertilizer Analysis Method Guide, 2008. Department of Agriculture. **2023**. Retrieved from http://lib.doa.go.th/multim/e-book/EB00061.pdf

[41] Department of Land Development. Wiriyakitjanateekul, N.; Kerdchana, C. Soil condition analysis report. Referring to Methods of Soil Analysis and Interpretation for Soil Survey and Classification: Physical Properties, 2016. Office of Science for Land Development, Ministry of Agriculture and Cooperatives. 2021. Retrieved from http://www1.ldd.go.th/WEB_PSD/pdf/expert%20work/ex22/3-3.pdf

[42] Land Development Office Area 1. Fertilizer usage advice. Land Development Office Area 1. **2023**. Retrieved from http://r01.ldd.go.th/spb/download/DinThai53/MAIN/SP/Fer/FSP_36cas.html

[43] Fasinmirin, J. T.; Reichert, J. M. Conservation tillage for cassava (Manihot esculenta Crantz) production in the tropics. *Soil & Tillage Research* **2011**, *113*(1), 1-10. https://doi.org/10.1016/j.still.2011.01.008

[44] Ekanayake, I. J.; Osiru, D. S. O.; Porto, M. C. M. Agronomy of cassava. *IITA Research Guide* **1997**, *60*.

[45] Emeh, C. What are the soil requirements for cassava for optimum yield?. Cassava Value Chain. **2025**. Retrieved from https://cassavavaluechain.com/soil-requirements-for-cassava/

[46] Bongkang, A. N. N. Weeds control in cassava plants development. ResearchGate. **2021**. Retrieved from https://www.researchgate.net/publication/357467936_Weeds_Control_in_Cassava_Plants_Development. https://doi.org/10.37899/journallalifesci.v2i5.522

[47] Manthamkan, V.; Rattanasrimetha, S.; Suriwong, M. Development of cassava root lifted up by pulling stump harvester type. Postharvest Technology Innovation Center (PHTIC). **2009**. Retrieved from https://www.phtnet.org/download/phtic-research/137.pdf

ASEAN
Journal of Scientific and Technological Reports
Online ISSN:2773-8752

Research article

Enhancing Napier Grass Degradation Efficiency through Microwave Pretreatment and Cellulase Enzyme Application

Adulsman Sukkaew[1*], Jutamas Kaewmanee[2], and Wasantanawin Harinppanwich[3]

[1] Faculty of Sciences, Technology and Agriculture, Yala Rajabhat University, Yala, 95000, Thailand
[2] Faculty of Public Health and Allied Health Sciences, Yala Rajabhat University, Yala, 95000, Thailand
[3] Faculty of Management Science, Yala Rajabhat University, Yala, 95000, Thailand
* Correspondence: adulsman.s@yru.ac.th

Citation:
Sukkaew, A.; Kaewmanee, J.; Harinppanwich, W. Enhancing napier grass degradation efficiency through microwave pretreatment and cellulase enzyme application. *ASEAN J. Sci. Tech. Report.* **2025**, *28*(4), e257505. https://doi.org/10.55164/ajstr.v28i4.257505.

Article history:
Received: January 15, 2025
Revised: May 12, 2025
Accepted: July 1, 2025
Available online: July 5, 2025

Abstract: Napier grass is a promising energy crop for renewable sugar-based carbon production, where effective pretreatment is essential to enhance its biomaterial value. The objective of this research is to determine the optimal conditions for Napier grass pretreatment and achieve the highest level of efficiency in analyzing the initial lignocellulose content, total dissolved solids, and reducing sugars. The research applies Napier grass from the Pak Chong variation in the province of Phra Nakhon Si Ayutthaya, Thailand. Napier grass was pretreated with 0.5% sulfuric acid (v/v) at 140°C for 60 minutes, yielding a maximum cellulose content of 89.62%. This treatment effectively removed hemicellulose and lignin, with only 5.22% and 0.58% remaining, respectively. When the pretreated Napier grass is subjected to thermal and cellulase enzyme degradation and then treated with a microwave at 700 watts for 15 minutes, the initial total dissolved solids amount is 8.13 g/L, with total sugars and reducing sugars at 7.03 g/L and 91.34 mg/g dry weight, respectively. Adding 20 U of cellulase enzyme for 48 hours significantly enhances the degradation rate, resulting in a total sugar content of 13.95 g/L and reducing sugar content of 165.61 mg/g dry weight of Napier grass. The findings of this research are crucial for advancing biomass energy as a sustainable and environmentally friendly renewable energy source. Methane emissions commonly produced during fermentation can be minimized, thereby lowering the carbon footprint of biofuel production. Enhancing the degradation efficiency of Napier grass increases sugar yield, thereby improving its suitability for bioethanol and biofuel production.

Keywords: Biomass energy; Napier grass pretreatment; Ethanol production; Cellulase enzyme; Microwave pretreatment

1. Introduction

Napier grass, scientifically known as *Pennisetum purpureum*, originates from the African region and belongs to the Gramineae family[1-3]. It is also commonly referred to as Napier Grass or Elephant Grass. Napier grass is widely cultivated due to its large stems and leaves, which provide high nutritional value for animal feed. It grows rapidly, has a high yield per acre, and can be harvested year-round for 5-7 years per planting cycle. It thrives well in tropical climates, is a perennial plant with clump-forming and erect stems, and propagates through cuttings similar to sugarcane. There are several varieties of Napier grass, including the common Napier and hybrid varieties. When fully grown, the grass

can reach a height of up to 4 meters and can form dense clumps. Commonly studied and cultivated varieties include Giant Napier (*Pennisetum purpureum* x *P. glaucum* Hybrid cv. King grass), Pakchong 1 (Pennisetum purpureum x P. glaucum Pakchong1), and Alfalfa Napier (Pennisetum purpureum x P. glaucum Hybrid), which, at 45 days of growth, have volatile solid contents of 21.4%, 18.2%, and 23.0%, respectively [2, 4, 12] Additionally, another variety, the Dwarf Napier *(P. purpureum*), has been studied and found to have a total solid content of 23.1% per fresh weight, volatile solid content of 21.5% per fresh weight, and a carbon-to-nitrogen ratio of 59.1:1 [1, 3, 8]. Based on these characteristics, Napier grass is suitable for microbial degradation processes, serving as a substrate for ethanol production. Research indicates that the ethanol yield from Napier grass after microbial degradation, following pretreatment, ranges between 6 and 45 g/L, depending on various production system factors [3, 7, 14]. Napier grass, also known as Elephant Grass, originates from the African region and belongs to the Poaceae (formerly Gramineae) family. This grass is widely cultivated due to its high nutritional value, making it an excellent source of animal feed, thanks to its large stems and leaves. Additionally, Napier grass thrives well in tropical climates, grows in clumps, and propagates through cuttings similar to sugarcane. Napier grass is primarily composed of cellulose, hemicellulose, and lignin, which are resistant to degradation. Cellulose is a polysaccharide chain consisting of D-glucose units linked by β-1,4 glycosidic bonds, containing over 10,000 glucose units. Hemicellulose is a branched polysaccharide composed of various sugars, including hexoses (glucose, galactose, and mannose) and pentoses (xylose and arabinose). Lignin, an organic polymer consisting of phenylpropane units, exceeds 10,000 units and acts as a binding agent for cellulose and hemicellulose fibers, contributing to the structural rigidity and resistance to degradation of the grass [2]. Pretreating Napier grass before converting it to biogas is crucial to breaking down its rigid lignocellulosic structure, allowing enzymes or microorganisms to access and digest it more easily. Pretreatment methods include chemical (acid-alkaline), biological, thermal, and combined treatments. Chemical pretreatment (acid-alkaline) is particularly effective for rapid structural breakdown. This research aims to determine the optimal conditions for decomposing Napier grass and maximizing the efficiency of preliminary lignocellulose analysis, as well as the total dissolved solids, reducing sugar content, and total sugar content [3, 6]. This knowledge will enhance the process of ethanol production from Napier grass [4-5]. Therefore, the objective of this research is to investigate suitable conditions for the decomposition of Napier grass to achieve maximum efficiency in analyzing the preliminary lignocellulose content, total dissolved solids, reducing sugar content, and total sugar content. This study aims to advance the potential of ethanol production processes from Napier grass.

2. Materials and Methods

2.1 The preparation of Napier grass

The Napier grass should be cut into pieces of 4-5 cm. Then, it should be dried in an oven at 70 ˚C for 48 hours. After drying, the grass should be finely ground using a sample grinder. The ground material should be sieved using an automatic sample sieving machine to ensure the particle size is less than or equal to 125 microns. Finally, the sieved grass powder should be packed in plastic bags and stored in a desiccator at room temperature to maintain its dryness [3, 5-6].

2.2 The determination of the Moisture Content of Napier Grass

Fresh Napier grass, aged 5 years, is chopped into small pieces, approximately 1-2 cm long, using a knife. A portion of the sample is used to study the moisture content by drying the container in an electric oven at 105°C for 2–3 hours for moisture determination. Then, remove the container from the hot air oven and place it in a desiccator. After that, weigh the sample and dry it again in the same manner as in step 1, until the weight difference between the two consecutive weighings is no more than 1-3 milligrams. Weigh the treated sample accurately to a known weight and place it in a moisture determination container of known weight. Then, dry it in an electric oven at 105°C for 5–6 hours. Please remove it from the oven and place it in a desiccator. After that, weigh the sample, dry it again for approximately 30 minutes, and repeat the process until the weight difference between the two consecutive weighings is no more than 1–3 milligrams. Calculate the moisture content using the formula according to equation 1 [7-9]. A portion of the Napier grass sample is used to determine the yield, standard wet basis moisture content (as per equation 2), and standard dry basis moisture content (equation 3) [10-11]. This is done by weighing the sample with a four-decimal-place balance to record

the initial weight. Then, the sample is dried in a hot air oven at 105°C for 24 hours. The experiment was performed in triplicate [6,12].

$$Moisture\ content\ (\%) = \frac{100 \times (Initial\ sample\ weight - Final\ sample\ weight)}{Initial\ sample\ weight} \quad (1)$$

$$Wet\ basis\ moisture\ content\ (\%) = \frac{100 \times (Weight\ of\ water\ in\ sample)}{Total\ weight\ of\ sample} \quad (2)$$

$$Dry\ basis\ moisture\ content\ (\%) = \frac{100 \times (Weight\ of\ water\ in\ sample)}{Weight\ of\ dry\ matter\ sample} \quad (3)$$

2.3 Study on Optimal Conditions for Napier Grass Pretreatment

The sample was analyzed for initial lignocellulosic content, then pretreated using a 0.5% sulfuric acid solution and a 0.5% sodium hydroxide solution at temperatures of 80, 100, 120, and 140°C for durations of 30 and 60 minutes. The pretreated samples were analyzed for initial lignocellulosic content, total dissolved solids, reducing sugars, and total sugars. The best pretreatment conditions were selected based on these analyses. The selected pretreated sample was then subjected to microwave treatment at 700 watts for durations of 5 and 15 minutes. Cellulase enzyme was added at concentrations of 10 and 20 U for 48 hours. Samples were collected every 2 hours to measure total dissolved solids, total sugars, and reducing sugars [5,19]. The experimental data were then statistically analyzed to determine the optimal conditions. The experiments were conducted in triplicate to ensure accuracy and reliability.

2.4 Analysis of Reducing Sugars and Total Sugars

2.4.1 Analysis of Reducing Sugars

The sample solution was pipetted into a test tube at 1 milliliter. DNS reagent was added 1 ml to the test tube. The mixture samples were heated in a boiling water bath at 100°C for 10 minutes. The test tube was immediately cooled by placing it in an ice bath. Add 10 milliliters of distilled water to the cooled mixture. The absorbance of the resulting solution was measured at 540 nanometers using a spectrophotometer. The experimental results were compared to a standard curve prepared using glucose solutions with concentrations ranging from 0 to 2.0 mg/mL [5, 10, 16].

2.4.2 The analysis of total sugar content

The total sugar content is measured by preparing a sample with varying concentrations of glucose solution (1 mL each), adding a 5% phenol solution (1 mL), and mixing thoroughly using a Vortex mixer. Then, 5 ml of concentrated sulfuric acid is added and left to stand for 10 minutes. After that, the sample is incubated in a water bath at 30 °C for 20 minutes. The absorbance at 490 nanometers is then measured. The standard graph of sugar concentration versus absorbance values is then created on these measurements [5, 15, 17-18].

3. Results and Discussion

3.1 Yield results obtained from Napier grass

The experiment investigated the yield (%) of Napier grass by cutting it into 4-5 cm pieces and then drying it at 70°C for 48 hours. Subsequently, the grass was finely ground and sieved to a particle size of ≤125 microns using automated grinding and sieving equipment. The experiment yielded an average production of 6.81 ± 2.98% of fresh Napier grass, indicating the maximum production achievable through chemical processing. The study demonstrated the potential to enhance the yield efficiency of Napier grass through controlled temperature and precise timing, coupled with automated grinding and sieving, ensuring reliable and accurate data. Therefore, this study is crucial for developing more efficient production processes for Napier grass in the future.

3.2 Moisture content of Napier grass

The study on the moisture content of Napier grass includes both the standard dry basis moisture (%db) and wet basis moisture (%wb). Fresh Napier grass was partially cut into pieces approximately 1-2 cm in size and oven-dried in containers at 105°C for 2-3 hours. Subsequently, the samples were removed from the oven and placed in desiccators to cool, after which they were weighed to determine their moisture content.

This process was repeated until the weight difference between consecutive weighings did not exceed 1-3 milligrams. Samples adjusted to a precise weight were then oven-dried in an electric oven at 105°C for 5-6 hours. After removal from the oven, they were placed in desiccators to cool and be weighed. This oven-drying process was repeated in 30-minute intervals until the weight difference between consecutive weighings did not exceed 1-3 milligrams. The moisture content was calculated according to the standard formula. The results indicate that the standard dry basis moisture content of Napier grass is 93.19 ± 3.45%, and the wet basis moisture content is 1.21 ± 0.36%.

3.3 Results of the optimal conditions for Napier grass pretreatment and saccharification

This study investigated the optimal conditions for decomposing Napier grass using 0.5% sulfuric acid and 0.5% sodium hydroxide solutions. The experiments were conducted at four different temperatures—80, 100, 120, and 140°C—for durations of 30 and 60 minutes. The results showed that, as both temperature and treatment time increased, the lignocellulosic content, total reducing sugars, and total sugars in the solubilized solids also increased. These results effectively stimulate the decomposition process of Napier grass, enhancing its efficiency. The analysis results of cellulose, hemicellulose, and lignin content from Napier grass treated with 0.5% sulfuric acid solution at temperatures of 80, 100, 120, and 140°C for 30 minutes showed that untreated Napier grass had cellulose, hemicellulose, and lignin contents of 33.19 ± 5.65%, 43.24 ± 7.29%, and 12.32 ± 2.33%, respectively. Treated at 80°C, the contents were 40.65 ± 2.62%, 20.65 ± 3.65%, and 6.98 ± 1.69%, respectively. At 100 °C, the contents were 51.18 ± 5.36%, 19.65 ± 1.98%, and 5.32 ± 1.52%, respectively. At 120 °C, the contents were 64.22 ± 5.32%, 12.63 ± 2.06%, and 2.1 ± 0.98%, respectively. At 140°C, the contents were 75.39 ± 5.95%, 9.65 ± 2.25%, and 1.95 ± 1.29%, respectively, as shown in Figure 2. All conditions showed statistically significant differences at a 95% confidence level ($P \leq 0.05$), as shown in Table 1. The treatment temperature with 0.5% sulfuric acid had a statistically significant effect on the cellulose content in Napier grass at the 95% confidence level ($P = 0.000252$). The F value (17.88) was higher than F crit (3.89), confirming that the difference between each temperature group was significant. Therefore, it can be concluded that increasing the treatment temperature had a clear effect on the change in cellulose content in Napier grass. The findings underscore the effectiveness of 0.5% sulfuric acid treatment in enhancing cellulose enrichment and reducing hemicellulose and lignin content in Napier grass. These results are pivotal for advancing biomass conversion technologies, particularly in biofuel production and biorefinery processes. Future studies could further explore optimal treatment conditions and scale-up strategies to maximize the efficiency and sustainability of biomass utilization in industrial applications.

Table 1. Analysis of Variance in Cellulose Content (%) of Napier Grass Treated with 0.5% Sulfuric Acid for 30 Minutes at Various Temperatures.

ANOVA						
Source of Variation	**SS**	**df**	**MS**	**F**	**P-value**	**F crit**
Between Groups	5789.99	2	2894.99	17.88	0.000252*	3.89
Within Groups	1943.38	12	161.95			
Total	7733.37	14				

Note*: Cellulose content (%) of Napier grass treated with 0.5% sulfuric acid by volume at temperatures of 80, 100, 120, and 140 °C for 30 minutes differs significantly statistically at a confidence level of 95% ($P \leq 0.05$).

The analysis of cellulose, hemicellulose, and lignin content from Napier grass treated with 0.5% sulfuric acid at temperatures of 80°C, 100°C, 120°C, and 140°C for 60 minutes yielded the following results: At 80°C: Cellulose content was 45.33% ± 5.35, hemicellulose was 17.32 ± 5.22%, and lignin was 4.33±1.95%. At 100°C: Cellulose content increased to 58.65 ± 4.66%, hemicellulose decreased to 12.32±2.65%, and lignin decreased further to 2.11± 0.39%. At 120°C, Cellulose content continued to increase to 72.98% ± 6.32, hemicellulose decreased to 7.65± 2.63%, and lignin decreased significantly to 1.03 ± 0.59%. At 140°C, cellulose content reached its highest at 89.62 ± 8.33%, hemicellulose decreased to 5.22 ± 1.11%, and lignin was lowest at 0.58 ± 0.21%, as shown in Figure 2. Statistical analysis confirmed significant differences ($P \leq 0.05$) in cellulose,

hemicellulose, and lignin content across all treatment temperatures, indicating that temperature variation has a significant impact on the chemical composition of Napier grass treated with sulfuric acid. This study found that treating Napier grass with 0.5% sulfuric acid at different temperatures (80°C, 100°C, 120°C, and 140°C) for 60 minutes significantly impacted the cellulose content, which consistently increased from 45.33% at 80°C to 89.62% at 140°C. Meanwhile, hemicellulose decreased from 17.32% at 80°C to 5.22% at 140°C, and lignin decreased from 4.33% at 80°C to 0.58% at 140°C, as shown in Table 2. These results demonstrate the ability to modify the chemical composition of Napier grass, which is crucial for producing biofuels and refining biomass materials industrially [11-14]. The study provides scientifically robust insights and is beneficial for advancing more efficient technologies in the future.

Table 2. Analysis of Variance (ANOVA) of Lignocellulose Content in Napier Grass Treated with 0.5% Sulfuric Acid for 60 Minutes under Various Treatments

ANOVA						
Source of Variation	**SS**	**df**	**MS**	**F**	**P-value**	**F crit**
Between Groups	9852.72	2	4926.36	37.57	4.2852E-05	4.26
Within Groups	1180.39	9	131.16			
Total	11033.11	11				

Note: *The lignocellulose content of Napier grass treated with 0.5% sulfuric acid (volume by volume) at temperatures of 80, 100, 120, and 140 °C for 60 minutes shows statistically significant differences at the 95% confidence level ($P \leq 0.05$).

The analysis of cellulose, hemicellulose, and lignin content in Napier grass treated with 0.5% sodium hydroxide solution at temperatures of 80, 100, 120, and 140 °C for 30 minutes revealed the following results: Napier grass treated at 80 °C contained 35.26 ± 3.35%, 37.32 ± 4.65%, and 8.36 ± 1.65% of cellulose, hemicellulose, and lignin, respectively. At 100 °C, the content was 40.25 ± 6.33%, 28.32 ± 4.09%, and 7.65 ± 3.54%, respectively. At 120 °C, the content was 49.63 ± 4.19%, 17.32 ± 4.11%, and 5.32 ± 1.52%, respectively. At 140 °C, the content was 56.65 ± 8.19%, 12.48 ± 2.29%, and 2.29 ± 1.05%, respectively. All conditions showed statistically significant differences at a 95% confidence level ($P \leq 0.05$), as shown in Table 3. The results indicate that the cellulose content increases significantly as the temperature rises, while the hemicellulose and lignin contents decrease. This demonstrates that higher temperatures in sodium hydroxide treatment can significantly increase the cellulose content in Napier grass.

Table 3. Analysis of Variance (ANOVA) of Lignocellulose Content in Napier Grass Treated with 0.5% Sodium Hydroxide for 30 Minutes under Various Treatments

ANOVA						
Source of Variation	**SS**	**df**	**MS**	**F**	**P-value**	**F crit**
Between Groups	3136.02	2	1568.01	21.08	0.000402*	4.26
Within Groups	669.61	9	74.40			
Total	3805.63	11				

Note: *The lignocellulose content of Napier grass treated with 0.5% sodium hydroxide (weight by volume) at temperatures of 80, 100, 120, and 140 °C for 30 minutes shows statistically significant differences at the 95% confidence level ($P \leq 0.05$)

The analysis of cellulose, hemicellulose, and lignin content in Napier grass treated with 0.5% sodium hydroxide solution at temperatures of 80, 100, 120, and 140 °C for 60 minutes revealed the following results: Napier grass treated at 80 °C contained 48.32 ± 4.29%, 18.62 ± 2.96%, and 6.12 ± 1.29% of cellulose, hemicellulose, and lignin, respectively. At 120 °C, the content was 57.62 ± 5.65%, 15.32 ± 2.29%, and 1.78 ± 0.65%, respectively. At 140 °C, the content was 72.66 ± 7.09%, 11.32 ± 2.48%, and 1.28 ± 0.19%, respectively. All conditions showed statistically significant differences at a 95% confidence level ($P \leq 0.05$), as shown in Table 4.

Table 4. Analysis of Variance (ANOVA) of Lignocellulose Content in Napier Grass Treated with 0.5% Sodium Hydroxide for 60 Minutes under Various Treatments

ANOVA						
Source of Variation	**SS**	**df**	**MS**	**F**	**P-value**	**F crit**
Between Groups	5492.39	2	2746.19	35.41	5.43E-05	4.26
Within Groups	697.9291	9	77.55			
Total	6190.319	11				

Note: *The lignocellulose content of Napier grass treated with 0.5% sodium hydroxide (weight by volume) at temperatures of 80, 100, 120, and 140 °C for 60 minutes shows statistically significant differences at the 95% confidence level ($P \leq 0.05$).

The result shows that using sulfuric acid to pretreat Napier grass is more effective than using sodium hydroxide. Increasing the treatment time also enhances the effectiveness of the pretreatment. Statistically significant results were obtained for removing hemicellulose and lignin at a 95% confidence level ($P \leq 0.05$). Napier grass treated with 0.5% sulfuric acid (by volume) at 140°C for 60 minutes yielded the highest cellulose content of 89.62 ± 8.33%, and the maximum removal of hemicellulose and lignin was 5.22 ± 1.11% and 0.58 ± 0.21%, respectively, as shown in Figure 1.

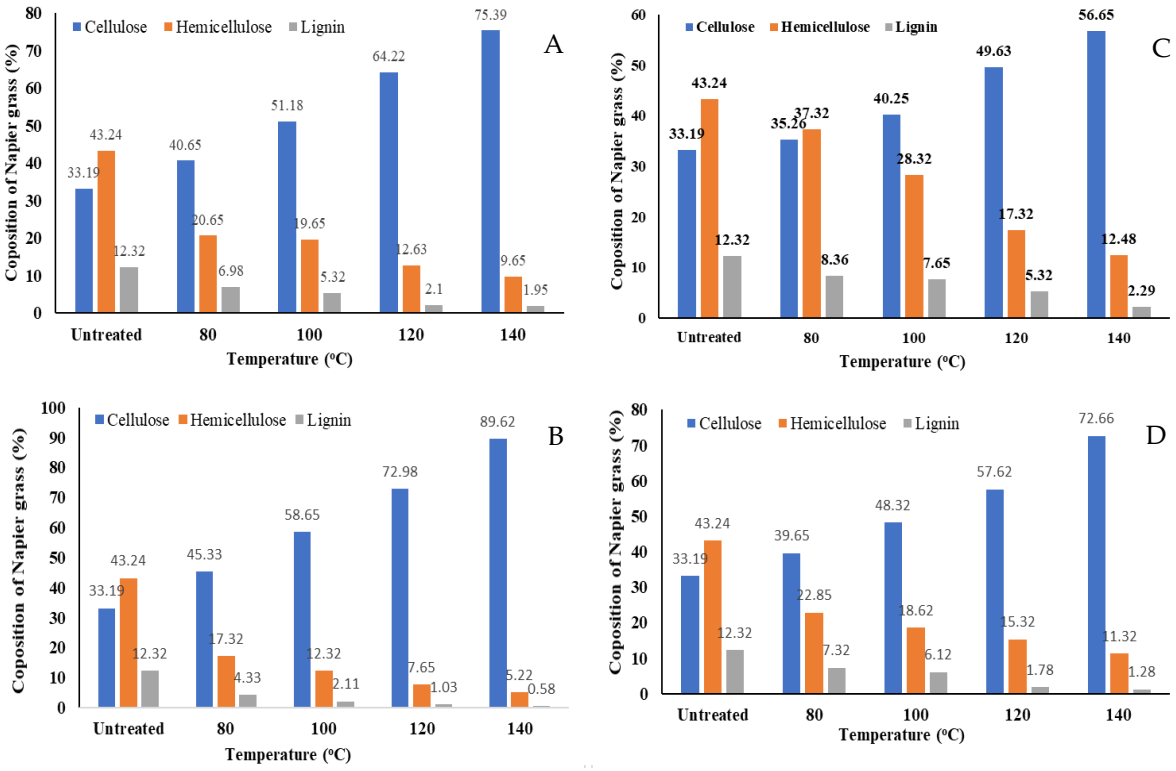

Figure 1. Napier grass treated under different conditions. A) Treated with 0.5% sulfuric acid for 30 minutes. B) Treated with 0.5% sulfuric acid for 60 minutes. C) Treated with 0.5% sodium hydroxide for 30 minutes. D) Treated with 0.5% sodium hydroxide for 60 minutes.

The solution of Napier grass, treated with 0.5% sulfuric acid and 0.5% sodium hydroxide, was tested at temperatures of 80, 100, 120, and 140 °C for 30 and 60 minutes and then analyzed for total dissolved solids, total sugar content, and reducing sugar content, the following results were observed: For 0.5% sulfuric acid at temperatures of 80, 100, 120, and 140 °C for 30 minutes, the total dissolved solids were 2.5, 3.7, 5.62, and 6.81 °Brix, the total sugar content was 2.12, 3.11, 3.75, and 5.22 g/L, and the reducing sugar content was 1.98, 2.85,

3.02, and 4.25 g/L, respectively. For 60 minutes, the total dissolved solids were 3.29, 4.45, 6.27, and 7.32 °Brix, the total sugar content was 2.57, 3.75, 4.01, and 6.38 g/L, and the reducing sugar content was 2.19, 3.04, 3.65, and 4.91 g/L, respectively. For 0.5% sodium hydroxide at temperatures of 80, 100, 120, and 140 °C for 30 minutes, the total dissolved solids were 1.92, 2.45, 3.63, and 5.33 °Brix, the total sugar content was 1.48, 2.11, 3.09, and 4.56 g/L, and the reducing sugar content was 0.85, 1.57, 2.44, and 3.29 g/L, respectively. For 60 minutes, the total dissolved solids were 2.32, 2.97, 4.12, and 6.05 °Brix, the total sugar content was 1.91, 2.45, 3.44, and 5.26 g/L, and the reducing sugar content was 1.12, 1.99, 3.01, and 4.23 g/L, respectively. As shown in Figure 2, the results indicate that higher temperatures and longer treatment times increase the total dissolved solids, total sugar content, and reducing sugar content. Furthermore, sulfuric acid treatment proved to be more effective than sodium hydroxide treatment. This research aims to minimize the use of chemicals, as high concentrations of chemicals can impact the conversion of biomass to furfural [9, 20]. The pretreatment of biomass was noted to be effective at breaking bonds, but high concentrations of chemicals do not lead to the desired main products.

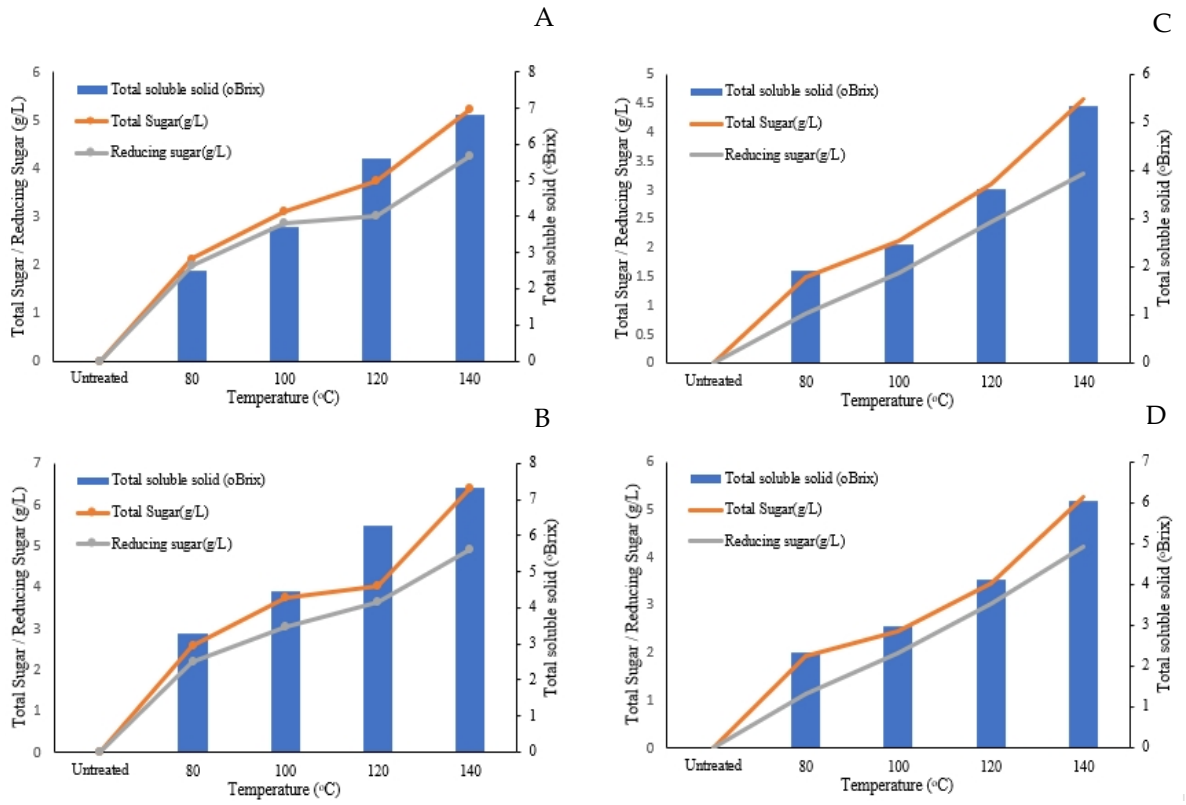

Figure 2. Total Dissolved Solids, Total Sugar Content, and Reducing Sugar Content of Napier Grass Solutions Treated Under Various Conditions A) Treated with 0.5% Sulfuric Acid for 30 Minutes B) Treated with 0.5% Sulfuric Acid for 60 Minutes C) Treated with 0.5% Sodium Hydroxide for 30 Minutes D) Treated with 0.5% Sodium Hydroxide for 60 Minutes.

Napier grass was selected from the above conditions (pretreated with 0.5% sulfuric acid by volume at 140°C for 60 minutes) and subjected to hydrolysis by heat and cellulase enzyme addition. The samples were then pretreated using a microwave at 700 watts for 5 and 15 minutes. Then, cellulase enzyme was added at 10 and 20 U for 48 hours, with samples collected every 2 hours. In these conditions, heat was applied using a microwave at 700 watts. Increasing the duration resulted in higher dissolution and an increase in total sugar and reducing sugar content. The initial total dissolved solids were 7.15 ± 0.39 (5 minutes) and 8.13 ± 1.52 (15 minutes), as shown in Table 5 and Figure 3. The total sugar and reducing sugar were 6.71 ± 0.95 (5 minutes) and 7.03 ± 1.12 (15 minutes) grams per liter, respectively. The initial reducing sugar content was 81.06 ± 5.29 (5 minutes) and 91.34 ± 3.66 (15 minutes) milligrams per gram of dry weight of Napier grass, as shown in Table 6 and Figure 4.

Table 5. Comparison of Total Soluble Solids between Treatments of Treated Napier Grass under Different Incubation Conditions

	Test Value = 0.05					
	T	df	Sig. (2-tailed)	Mean Difference	95% Confidence Interval of the Difference	
					Lower	Upper
A	232.76	24	.000	7.98	7.91	8.05
B	119.82	24	.000	8.27	8.13	8.41
C	250.63	24	.000	8.35	8.28	8.41
D	125.33	24	.000	8.65	8.51	8.79

Note: Incubation with cellulase enzyme from 0 to 48 hours with statistically significant differences at a 95% confidence level ($P \leq 0.05$). A) Using microwave for heating at 700 Watt, 5 minutes with 20 U of cellulase B) Using microwave for heating at 700 Watt, 5 minutes with 20 U of cellulase C) Using microwave for heating at 700 Watt, 15 minutes with 10 U of cellulase D) Using microwave for heating at 700 Watt, 15 minutes with 20 U of cellulase

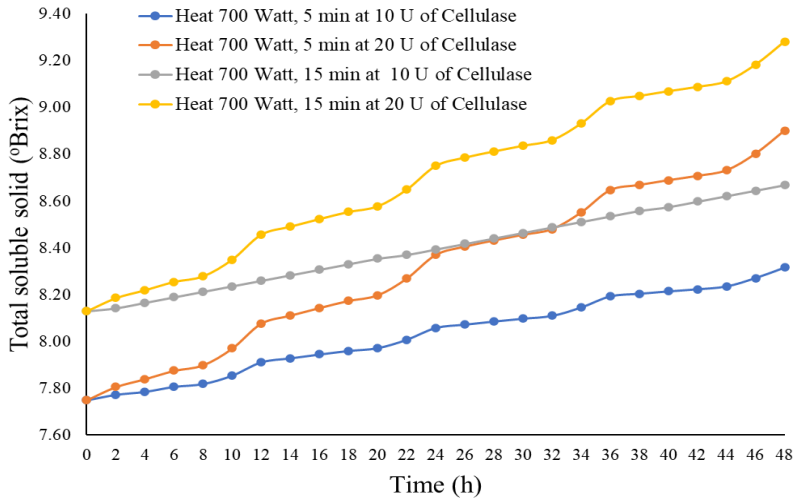

Figure 3. Total Soluble Solids Content of Treated Napier Grass

Table 6. Comparison of Total Sugar Content between Treatments of Treated Napier Grass under Different Incubation Conditions

	Test Value = 0.05					
	t	df	Sig. (2-tailed)	Mean Difference	95% Confidence Interval of the Difference	
					Lower	Upper
A	30.08	24	.000	8.28	7.71	8.85
B	21.90	24	.000	8.86	8.029	9.69
C	31.24	24	.000	8.59	8.029	9.17
D	21.67	24	.000	9.44	8.54	10.34

Note: Incubation with cellulase enzyme from 0 to 48 hours with statistically significant differences at a 95% confidence level ($P \leq 0.05$). A) Using microwave for heating at 700 Watt, 5 minutes with 20 U of cellulase B) Using microwave for heating at 700 Watt, 5 minutes with 20 U of cellulase C) Using microwave for heating at 700 Watt, 15 minutes with 10 U of cellulase D) Using microwave for heating at 700 Watt, 15 minutes with 20 U of cellulase

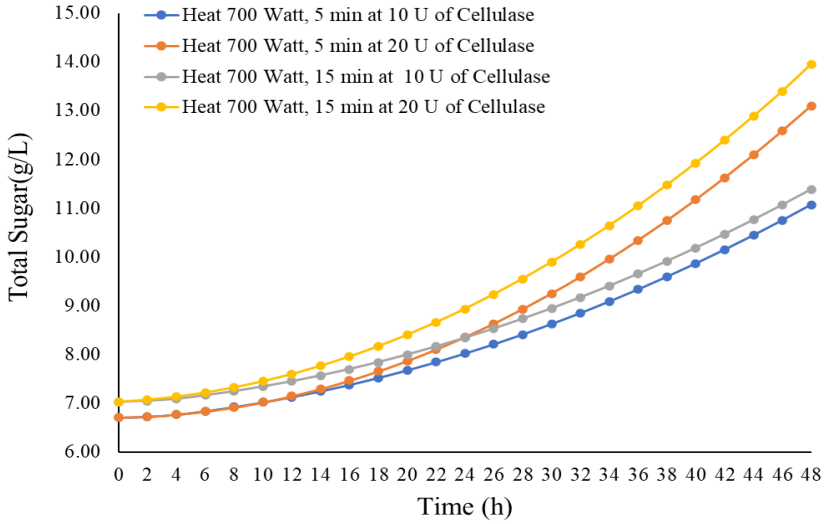

Figure 4. Total Sugar Content of Treated Napier Grass

When Napier grass preheated at 700 watts was treated with 5 U and 10 U of cellulase enzyme, it was found that the hydrolysis rate was reasonable in all conditions. However, there were significant differences at a 95% confidence level ($P \leq 0.05$). The best hydrolysis condition was when 20 U of cellulase enzyme was added and incubated for 48 hours after pretreatment by heating at 700 watts for 15 minutes, resulting in 9.28 degrees Brix, with a total sugar content of 13.95 ± 1.62 grams per liter and a reducing sugar content of 165.61 ± 9.22 milligrams per gram of dry weight of Napier grass. As shown in Table 7 and Figure 5. These findings highlight the effectiveness of microwave pretreatment and enzymatic hydrolysis in enhancing sugar yields from Napier grass, crucial for improving the efficiency of biofuel production processes [14, 20]. Acid pretreatment at high temperatures can produce inhibitory compounds that affect fermentation, including furans (HMF, furfural) derived from six-carbon and five-carbon sugars, phenolic compounds from lignin, and organic acids (acetic acid, formic acid) from hemicellulose. These compounds can inhibit the growth of microorganisms and the production of ethanol, butanol, or biogas. [4, 15, 19]

Table 7. Comparison of Reducing Sugar Content between Treatments of Treated Napier Grass under Different Incubation Conditions with Cellulase Enzyme

	Test Value = 0.05					
	t	**df**	**Sig. (2-tailed)**	**Mean Difference**	**95% Confidence Interval of the Difference**	
					Lower	**Upper**
A	83.23	24	.000	87.27	85.16	89.44
B	27.82	24	.000	101.33	93.82	108.85
C	93.01	24	.000	97.55	95.39	99.71
D	24.97	24	.000	117.28	107.58	126.97

Note: Incubation with cellulase enzyme from 0 to 48 hours with statistically significant differences at a 95% confidence level ($P \leq 0.05$) A) Using microwave for heating at 700 Watt, 5 minutes with 20 U of cellulase B) Using microwave for heating at 700 Watt, 5 minutes with 20 U of cellulase C) Using microwave for heating at 700 Watt, 15 minutes with 10 U of cellulase D) Using microwave for heating at 700 Watt, 15 minutes with 20 U of cellulase.

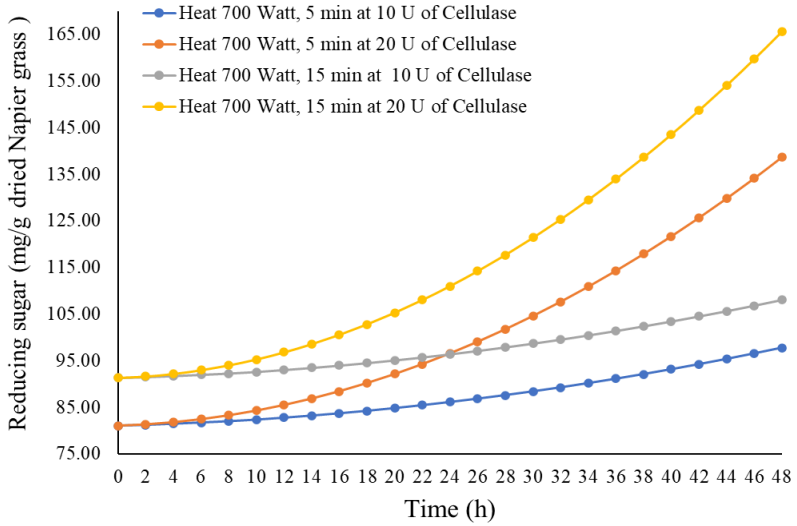

Figure 5. Reducing Sugar Content of Treated Napier Grass

When the best-treated Napier grass was examined under a scanning electron microscope at a magnification of 3,000× and an accelerating voltage of 20 kV, the microstructural images revealed significant surface degradation. The cell walls of the Napier grass appeared to be severely damaged—scattered, torn, and peeled off into thin sheets. The surface morphology was rough and uneven, with numerous holes and gaps visible. The application of microwave pretreatment effectively disrupted the hydrogen bonds within the cellulose fibers, causing the rapid evaporation of intracellular water and resulting in internal pressure buildup and cell rupture, thereby forming porous structures. In addition, the action of cellulase enzymes facilitated further biodegradation by accelerating the hydrolysis of glycosidic bonds in cellulose, resulting in the release of fermentable sugars, including high-purity glucose. The SEM images demonstrated extensive structural breakdown, indicating that the enzymes could efficiently penetrate and access the internal matrix of the biomass. Consequently, such a high degree of pretreatment effectiveness is expected to significantly enhance the production of biofuels, such as bioethanol, biobutanol, or biogas, by improving the digestibility of the biomass and yielding more efficient substrates for microbial fermentation, as shown in Figure 6.

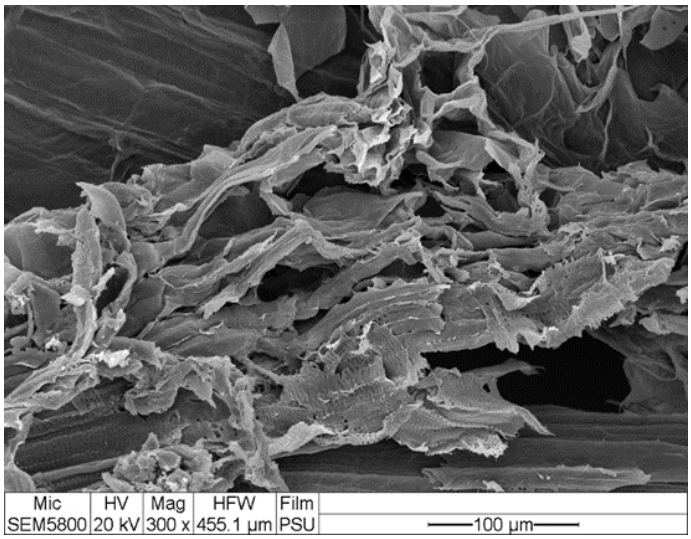

Figure 6. SEM micrograph of napier grass after microwave pretreatment and cellulase hydrolysis showing extensive cell wall bio-degradation

4. Conclusions

Developing an efficient decomposition process for Napier grass revealed that sulfuric acid is more effective than sodium hydroxide in pretreating the grass. Increased processing time significantly improved the pretreatment results, effectively removing hemicellulose and lignin with a 95% confidence level ($P \leq 0.05$). Napier grass treated with 0.5% (v/v) sulfuric acid at 140°C for 60 minutes yielded the highest cellulose content at 89.62 ± 8.33% and achieved the most substantial removal of hemicellulose and lignin, at 5.22 ± 1.11% and 0.58 ± 0.21%, respectively. When the pretreated Napier grass was further decomposed under optimal conditions by heating and the addition of cellulase enzyme, microwave treatment at 700 watts for 15 minutes resulted in an initial total dissolved solids concentration of 8.13 ± 1.52 g/L. The total sugar and reducing sugar concentrations were 7.03 ± 1.12 g/L, with an initial reducing sugar concentration of 91.34 ± 3.66 mg/g of dry Napier grass. After the addition of 20 U of cellulase enzyme for 48 hours, with sampling every 2 hours, the total sugar concentration increased to 13.95 ± 1.62 g/L, and the reducing sugar concentration rose to 165.61 ± 9.22 mg/g of dry Napier grass. Microwave pretreatment of Napier grass, combined with cellulase enzymes, effectively enhanced the degradation of cellulose structures. SEM images revealed cell wall degradation and porosity formation, facilitating better access and enzymatic degradation, which led to the release of fermentable sugars.

5. Acknowledgements

The authors would like to acknowledge the financial support provided by the Fundamental Fund (FF) for the fiscal year 2022. The researchers would like to express their gratitude to the Southern Border Researchers Association for supporting the research facility and to the staff of the Faculty of Science, Technology, and Agriculture at Yala Rajabhat University for their continuous encouragement, support, and assistance.

References

[1] Malik, K.; Sharma, P.; Yang, Y.; Zhang, P.; Zhang, L.; Xing, X.; Yue, J.; Song, Z.; Nan, L.; Yujun, S. Lignocellulosic biomass for bioethanol: Insight into the advanced pretreatment and fermentation approaches. *Ind. Crops Prod*. **2022**, *188*, 115569. http://doi.org/10.1016/j.indcrop.2022.115569

[2] Azhar, M.; Hajar, S.; Rahmath, A.J.; Azmah, S.M.; Hartinie, G.; Azlan, J.; Faik, M.; Azifa, A.; Rodrigues, K.F. Yeasts in sustainable bioethanol production: A review. Biochem. *Biophys. Rep*. **2017**, *10*, 52-61. http://doi.org/10.1016/j.bbrep.2017.03.002

[3] Chakraborty, P.; Kumar, R.; Chakrabortty, S.; Saha, S.; Chattaraj, S.; Roy, S.; Banerjee, A.; Tripathy, S.K.; Ghosh, A.K.; Jeon, B.H. Technological advancements in the pretreatment of lignocellulosic biomass for effective valorization: A review of challenges and prospects. *J. Ind. Eng. Chem,* **2024**, *36*, 145-152. http://doi.org/10.1016/j.jiec.2023.09.001

[4] Miller, G.L. Use of Dinitrosalicylic Acid Reagent for Determination of Reducing Sugar. *Anal. Chem*. **1959**, *31*(3), 426-428. http://doi.org/10.1021/ac60147a030

[5] Smith, J.D.; Johnson, A.B. Analysis of total sugar content using spectrophotometry. *J. Anal. Chem*. **2020**, *15*(3), 210-225.

[6] Sukkaew, A. The Optimal Conditions of Saccharification and Fermentation Processes for Ethanol Production from Bagasse and Economic Feasibility Analysis. *J. Phys. Conf. Ser*. **2021**, *1835*(1), b012113. http://doi.org/10.1088/1742-6596/1835/1/012113

[7] Subden, R.E.; Krizus, A.; Osothsilp, C.; Viljoen, H.J.J.; van Vuuren, C. Mutational analysis of malate pathways in *Schizosaccharomyces pombe*. *Food Res. Int.* **1998**, *31*(1), 37-42. http://doi.org/10.1016/S0963-9969(98)00056-8

[8] Zhang, H.; Zhang, R.; Song, Y.; Miu, X.; Zhang, Q.; Qu, J.; Sun, Y. Enhanced enzymatic saccharification and ethanol production of corn stover via pretreatment with urea and steam explosion. *Bioresour. Technol*. **2023**, *376*, 128856. http://doi.org/10.1016/j.biortech.2023.128856

[9] Baruah, J.; Nath, B.; Sharma, R.; Kumar, S.; Ramesh, D.; Debendra, B.; Eeshan, K. Recent Trends in the Pretreatment of Lignocellulosic Biomass for Value-Added Products. *Energy Res*. **2018**, *25*, 141. http://doi.org/10.3389/fenrg.2018.00141

[10] David, A.N.; Sewsynker-Sukai, Y.; Kana, E.B.G. Development of Kraft waste-based pretreatment strategies for enhanced sugar recovery from lignocellulosic waste. *Ind. Crops Prod*. **2021**, *174*, 114222. http://doi.org/10.1016/j.indcrop.2021.114222

[11] Dharmaraja, J.; Shobana, S.; Arvindnarayan, S.; Francis, R.R.; Jeyakumar, R.B.; Saratale, R.G.; Ashokkumar, V.; Bhatia, S.K.; Kumar, V.; Kumar, G. Lignocellulosic biomass conversion via greener pretreatment methods towards biorefinery applications. *Bioresour. Technol.* **2023**, *369*, 128328. http://doi.org/10.1016/j.biortech.2023.128328

[12] Mohapatra, S.; Mishra, C.; Behera, S.S.; Thatoi, H. Application of pretreatment, fermentation and molecular techniques for enhancing bioethanol production from grass biomass – A review. Renew. Sustain. *Energy Rev*. **2017**, *78*, 1007-1032. http://doi.org/10.1016/j.rser.2017.05.026

[13] Poolakkalody, N.J.; Ramesh, K.; Palliprath, S.; Nittoor, S.N.; Santiago, R.; Kabekkodu, S.P.; Manisseri, C. Understanding triethylammonium hydrogen sulfate ([TEA][HSO_4]) pretreatment induced changes in Pennisetum polystachion cell wall matrix and its implications on biofuel yield. *Renew. Energy*. **2023**, *209*, 420-430. http://doi.org/10.1016/j.renene.2023.04.008

[14] Raina, N.; Boonmee, R.; Kirdponpattara, S.; Narasingha, M.; Sriariyanun, M.; Phitsuwan, P.; Chuetor, S. Process performance evaluation of different chemical pretreatments of lignocellulosic biomass for bioethanol production. *Ind. Crops Prod*. **2024**, *211*, 118207. http://doi.org/10.1016/j.indcrop.2024.118207

[15] Srivastava, N.; Singh, P.; Srivastava, M.; Lal, B.; Singh, R.; Ahmad, I.; Gupta, V.K. A review on the scope and challenges of *Saccharum spontaneum* waste in the context of lignocellulosic biomass for sustainable bioenergy applications. *Renew. Sustain. Energy Rev.* **2024**, *199*, 114477. http://doi.org/10.1016/j.rser.2024.114477

[16] Antunes, F. A. F., Machado, P. E. M., Rocha, T. M., Melo, Y. C. S., Santos, J. C., & da Silva, S. S. (2021). Column reactors in fluidized bed configuration as intensification system for xylitol and ethanol production from napier grass (*Pennisetum Purpureum*). *Chemical Engineering and Processing - Process Intensification, 164*, 108399. https://doi.org/10.1016/j.cep.2021.108399

[17] Ismail, K. S. K.; Matano, Y.; Sakihama, Y.; Inokuma, K.; Nambu, Y.; Hasunuma, T.; Kondo, A. Pretreatment of extruded Napier grass byhydrothermal process with dilute sulfuric acid and fermentation using a cellulose-hydrolyzing and xylose-assimilating yeast for ethanol production. *Bioresource Technology* **2022**, *343*, 126071. https://doi.org/10.1016/j.biortech.2021.126071

[18] Jomnonkhaow, U.; Imai, T.; Reungsang, A. Microwave-assisted acid and alkali pretreatment of Napier grass for enhanced biohydrogen production and integrated biorefinery potential. *Chemical Engineering Journal Advances* **2024**, *20*, 100672. https://doi.org/10.1016/j.ceja.2024.100672

[19] Liu, H.; Kong, Y.; Song, W.; Zhang, R.; Zhang, J.; Sun, Y.; Peng, L. Pretreatment greatly facilitates ethyl levulinate production from catalytic alcoholysis of Napier grass stem. *Chemical Engineering Journal* **2024**, *481*, 148559. https://doi.org/10.1016/j.cej.2024.148559

[20] Panakkal, E. J.; Cheenkachorn, K.; Chuetor, S.; Tantayotai, P.; Raina, N.; Cheng, Y.-S.; Sriariyanun, M. Optimization of deep eutectic solvent pretreatment for bioethanol production from Napier grass. *Sustainable Energy Technologies and Assessments* **2022**, *54*, 102856. https://doi.org/10.1016/j.seta.2022.102856

ASEAN
Journal of Scientific and Technological Reports
Online ISSN:2773-8752

Research article

Development of Biodegradable Cat Litter from Water Hyacinth

Tanagon Junhamakasit[1], and Puntaree Taeprayoon[2*]

[1] Research and Academic Service Center, Mahidol University, Nakhonsawan, 60130, Thailand
[2] Agricultural and Environmental Utilization Research Unit, Mahidol University, Nakhonsawan, 60130, Thailand
* Correspondence: puntaree.tae@mahidol.ac.th

Citation:
Junhamakasit, T.; Taeprayoon, P. Development of biodegradable cat litter from water hyacinth. *ASEAN J. Sci. Tech. Report.* **2025**, *28*(4), e258185. https://doi.org/10.55164/ajstr.v28i4.258185.

Article history:
Received: March 3, 2025
Revised: June 21, 2025
Accepted: July 3, 2025
Available online: July 5, 2025

Abstract: This study focused on the technical feasibility and optimization of formulation performance characteristics to explore the potential of water hyacinth (*Eichhornia crassipes*) for biodegradable cat litter development. Five water hyacinth-based formulations (T1-T5) were developed and compared with commercial tofu-based cat litter (T6). Formulation T5 exhibited the highest water absorption capacity (64.23 ± 2.31%) compared to T6, the commercial product (47.42 ± 1.00%). T5 contained water hyacinth (61.7 g) and carboxymethyl cellulose (35 g), creating an optimal synergy for moisture retention. Water hyacinth formulations demonstrated superior structural integrity under impact testing, with T2-T5 showing zero breakage when dropped from heights up to 3 m, compared to T6's 2.10% fragmentation rate. Commercial litter dried faster (0.21 g/m²/s) than water hyacinth formulations (0.11-0.17 g/m²/s), presenting an area for optimization. The research demonstrates the viability of water hyacinth as an eco-friendly cat litter material, effectively converting an invasive aquatic plant into a value-added product with absorption capacity and durability advantages over commercial alternatives, while supporting environmental sustainability through the beneficial repurposing of problematic biomass.

Keywords: Water hyacinth; Biodegradable cat litter; Eco-friendly products; Sustainability; Circular economy

1. Introduction

Thailand's population has steadily declined from 66.56 million in 2019 to 66.05 million in 2023, continuing a decade-long trend of falling birth rates [1]. Concurrently, pet humanization has surged, with pets increasingly treated as family members. BrandAge Team [2] reports Thailand's pet-related market is now valued at 35-40 billion THB, with owners spending 10,000-20,000 THB annually per pet. Previously, it was reported that cat-related product sales now exceed other pet categories, with cat litter representing the second-highest expense for owners after dry food [3]. The cat litter market is divided into two primary segments: synthetic and natural options. Synthetic products include magnesium oxide-based litter (good absorbency, non-clumping), bentonite-based litter (forms clumps upon moisture contact), and silica gel-based litter (lightweight with effective odor control but expensive). Natural-based alternatives derive from plant materials such as sawdust, pine wood, barley, and soybean residue, offering biodegradability but typically at higher costs [4].

Increasing environmental awareness has led to a prioritization of eco-friendly cat litter options. Radanova [5] documented a growing consumer preference for biodegradable pet products, prompting researchers to explore alternative plant-derived materials as a solution. Various natural sources have

shown potential, including wood bark, grains, coffee, coconut, bamboo, citrus fruits, and byproducts from ethanol production [6]. Ideal cat litter should comprise natural materials, contain harmless chemicals, cause no irritation, biodegrade readily, absorb effectively, produce minimal dust, control odors efficiently, remain lightweight, and avoid artificial fragrances [6]. The development of bio-based pet products aligns with broader trends in sustainable materials science and the implementation of a circular economy. The utilization of natural fibers in consumer products builds upon established cellulosic material theory [7], while addressing the growing environmental consciousness in pet product markets [8]. Invasive species valorization represents an emerging paradigm combining ecosystem management with sustainable manufacturing principles [9]

Water hyacinth (*Eichhornia crassipes*), known locally by various names including pak top and pak bua loi, presents an intriguing raw material option. Its chemical composition has been analyzed, reporting approximately 52.2% neutral detergent fiber (NDF) and 90% acid detergent fiber (ADF) [10]. These components contain hydroxyl (-OH) groups that efficiently bind with water molecules. Documented water hyacinth's water absorption capacity at 38.8%, suggesting potential utility for moisture-absorbent applications [11]. This abundant aquatic plant has become problematically invasive in natural water sources, negatively affecting ecosystems through excessive growth and resource competition. This research investigates water hyacinth's feasibility as a biodegradable cat litter material, specifically evaluating water hyacinth-based formulations (T1-T5) for essential cat litter properties (water absorption, drying rate, structural integrity), comparing performance against commercial cat litter products (T6), and identifying optimal formulation for potential commercialization.

Umor et al. [12] demonstrated successful cat litter production from other plant materials, including pinewood, tofu waste, and palm oil byproducts. Saikeaw et al. [13] found that cassava trunks could be effectively processed into biodegradable cat litter with the use of appropriate binders. These studies support the potential application of water hyacinth. Saxena [14] demonstrated that natural fibers can achieve performance comparable to synthetic alternatives in various applications when adequately processed and combined with appropriate binding agents. This study aligns with Thailand's environmental management priorities while addressing market demands for affordable, biodegradable pet products. The findings may inform the commercial development of water hyacinth-based cat litter as an environmentally responsible alternative to conventional products, potentially creating economic opportunities in regions where this invasive plant proliferates. High-quality cat litter should produce minimal dust to minimize respiratory irritation, exhibit strong clumping ability for easy removal of waste and urine, provide effective odor control both before and after use, and offer high moisture absorption to keep the litter box dry. It should also be made from materials that are safe for pets and environmentally friendly. These characteristics serve as key criteria for evaluating and developing new cat litter formulas that meet market demands.

This research scope aims to establish technical feasibility and optimize formulation performance as the foundational phase of product development. Introducing the water hyacinth as a problematic plant in eco-friendly cat litter products. The approach addresses two key challenges: mitigating the impact of invasive species while meeting the growing demand for sustainable pet products. The methodology follows the approach of Nidarath [4] in evaluating cat litter, examining water absorption capacity, drying properties, and structural integrity. Modifications include formulations incorporating varying ratios of water hyacinth with additives such as glycerol, guar gum, xanthan gum, and carboxymethyl cellulose to enhance performance characteristics. This research contributes to the development of circular economy principles by transforming environmental liabilities into valuable resources.

2. Materials and Methods

2.1 Preparation of cat litter from water hyacinth

2.1.1 Processing of water hyacinth

Freshwater hyacinth 6-month mature water hyacinth plants (pre-flowering stage plants with fully developed petioles) were collected from a clean water source. Only petioles with cylindrical structures and sponge-like interiors were selected. These parts were thoroughly washed, cut into approximately 1 cm pieces, and sun-dried until completely dry (fully dried pieces are light in weight and exhibit a hard, brown outer surface). The dried material was ground using a Powder Grinder model HR20B and sieved through a 1 mm mesh to obtain a fine powder.

2.1.2 Formulation of cat litter

The water hyacinth powder was mixed with various raw materials to develop six different formulations (T1-T5, plus commercial tofu-based litter T6), as shown in Table 1.

Table 1. Proportion of raw materials in each experimental formulation

Ingredients	Formula (g)					
	T1	**T2**	**T3**	**T4**	**T5**	**T6**
Dry Water Hyacinth	79.7	59.7	39.7	62	61.7	-
Glycerol	10	20	30	-	-	-
Guar gum	5	10	15	3	3	-
Xanthan gum	5	10	15	-		-
Activated carbon	0.3	0.3	0.3	-	0.3	-
Carboxymethyl cellulose	-	-	-	35	35	-
Commercial Cat Litter (Made from Soybean Residue)	-	-	-	-	-	100

2.2 Molding process

Sterilized water (50 mL) was poured into a 250 mL beaker. Thickening agents were gradually added, starting with CMC, followed by Guar Gum, Xanthan Gum, and Activated Carbon while continuously stirring. Glycerol was incorporated slowly, with water hyacinth powder gradually added until the moisture was evenly distributed. The mixture was transferred to a smooth surface and kneaded by hand until thoroughly combined to achieve a clay-like consistency. If too crumbly, small amounts of water were added. The material was divided into approximately 0.5 g portions, hand-molded into cylindrical shapes (2-3 mm diameter), and rested for 20 minutes. It was then cut into 1-2 cm sections and dried in a hot air oven at 70 ± 2 °C with a fan and ventilation at 50% for 24 hours. The oven was preheated to the target temperature and allowed to stabilize for 30 minutes before the sample was inserted. After drying, all samples were immediately transferred to sealed desiccator chambers containing silica gel to maintain a moisture content below 5% and prevent reabsorption of atmospheric moisture.

2.3 Water absorption test

Approximately 5 g of each formulation was placed on a petri dish and equilibrated at room temperature for 30 minutes. Using a calibrated dropper (0.08 ± 0.01 mL per drop, verified by 100-drop calibration), distilled water was applied from a consistent height of 2.5 cm at a controlled rate of 1 drop every 3 seconds. Water was added in increments of 10 drops (≈approximately 0.8 mL) with 30-second equilibration intervals between each addition. The saturation endpoint was defined as visible surface water persisting across more than 50% of the sample area for 60 seconds without absorption. Excess water was removed using the same dropper. The test was repeated 5 times per formulation. Water absorption was calculated using Equation 1: Nidarath [4]

$$\text{Absorption (\%)} = \frac{(Ms-Md)}{Ms} \text{ x } 100 \quad (1)$$

Where:

Ms is the weight of the material after absorbing water (in kilograms),

Md is the weight of the dry material (in kilograms).

2.4 Testing of drying properties

Samples from water absorption testing were immediately transferred to a pre-heated hot air oven maintained at 70±2°C with fan and ventilation at 50%. The initial wet weight was recorded before the sample was inserted into the oven. Samples were weighed at 10 and 20 minutes using an analytical balance (±0.001g precision) with minimal exposure time (< 30 seconds per measurement). All samples were handled identically with immediate return to the oven after weighing. Moisture content and drying rate were calculated using Equations 2 and 3: Nidarath (2019) [4]

$$\text{MC (\%)} = \frac{(Mw - Md)}{Mw} \times 100 \quad (2)$$

$$\text{Drying rate} = \frac{-Md}{A}\left(\frac{dMC}{dt}\right) \quad (3)$$

Where MC = Moisture content
Mw = weight of wet material (grams)
Md = weight of dry material (grams)
A = Area used for evaporation (square meters)
t = Time taken (seconds)

2.5 Shape retention ability

The pellets of water hyacinth from different formulations, which have undergone the drying process, along with commercially available cat litter products, were tested for shape retention using the Drop Test method [4]. A total of 30 g of each cat litter formulation was dropped from heights of 1, 2, and 3 m, respectively. After the samples were dropped, they were sieved through mesh screens with 4.00 mm and 2.80 mm sizes. The remaining pellets were then weighed, and the percentage of breakage was calculated using the following formula (4).

$$\text{breakage percentage} = \frac{weight\ of\ the\ broken\ sample}{weight\ of\ the\ sample\ used\ for\ testing} \times 100 \quad (4)$$

2.6 Statistical analysis

All statistical analyses were performed using R Statistical Software (version 4.3.3) [15]. Data normality was assessed using Shapiro-Wilk tests. One-way ANOVA followed by LSD (Least Significant Difference) evaluated differences between formulations. Results were expressed as mean ± standard deviation (SD), with the coefficient of variation (CV%) used to assess data precision; values <10% indicated good precision. Pearson correlation examined relationships between variables, while linear regression models determined relationships between formulation and performance outcomes. Multivariate analysis included cluster analysis using Euclidean distance and Ward's linkage, validated by silhouette analysis. Principal component analysis (PCA) identified patterns. MANOVA was used to test overall cluster differences, with results considered significant at $p \leq 0.05$.

3. Results and Discussion

3.1 Water absorption capacity analysis of different formulations

The water absorption capacity test revealed significant differences among formulations. Formulation T5 demonstrated the highest capacity (64.23±2.31%), followed by T4 (61.01±3.47%), T1 (57.47±3.60%), commercial cat litter T6 (47.42±1.00%), T2 (43.87±2.54%), and T3 (32.59±6.62%) (Table 2). The superior absorption performance of optimized formulations compared to literature values for untreated water hyacinth (38.8% vs 64.23% for T5) demonstrates the effectiveness of composite formulation approaches [11]. This improvement aligns with the natural fiber composite theory, where the selection of an appropriate binder can significantly enhance the properties of the base material. Somchai and Thanongsak (2023) [11] reported that 100% dry water hyacinth has a water absorption capacity of 38.8%, indicating that blending water hyacinth with complementary materials can enhance its absorption properties. The superior performance of formulation T5 (64.23%) aligns with findings from Nidarath (2019), who showed similar capacities for cassava residue (67%) and pine wood (60%) cat litter [4]. The absorption capacity of the bentonite-based litter (49%) reported in that study approximates our T6 and T2 formulations. Umor et al. (2023) [12] found that cat litter from palm oil waste mixed with pine wood and tofu absorbed 100-131 mL of water. Comparatively, our formulations T1, T4, and T5 (50 g each) absorbed 118 mL, 129 mL, and 141 mL, respectively, while commercial tofu-based litter T6 absorbed 95 mL.

Table 2. Water absorption properties of water hyacinth cat litter formulations (T1-T5) compared with commercial tofu-based cat litter (T6)

Formula	Water Absorption Capacity (%) ± SD	Absorption Volume (mL/50 g) ± SD
T1	57.47 ± 3.60 b	118 ± 10.69 b
T2	43.87 ± 2.54 c	95 ± 4.17 c
T3	32.59 ± 6.62 d	75 ± 7.34 d
T4	61.01 ± 3.47 ab	129 ± 11.6 ab
T5	64.23 ± 2.31 a	141 ± 8.44 a
T6	47.42 ± 1.00 c	95 ± 1.81 c

Note: LSD (Least Significant Difference) analysis with letter groupings, different letters indicate statistically significant differences ($P \leq 0.05$)

The exceptional absorption capacity of formulations T4 and T5 primarily stems from the fibrous structure of water hyacinth, rich in cellulose and hemicellulose, which naturally binds water molecules. The drying process preserves the porous, cellular structure that facilitates water retention. Water hyacinth has a lignocellulosic structure, with cellulose and hemicellulose components playing a key role in water absorption. Water hyacinth contains an average of approximately 25–30% cellulose and 20–25% hemicellulose by dry weight [16-17]. These components are rich in – OH functional groups, which readily form hydrogen bonds with water molecules, enabling the fibers of water hyacinth to serve as an effective water-absorbing material.

Additionally, incorporating carboxymethyl cellulose (CMC) significantly enhances water absorption while maintaining structural integrity. Maryam et al. [18] confirmed that CMC increases moisture retention in food products, while Harsono et al. [19] demonstrated that CMC at 0.5-2% alters moisture content in rice bran-enriched bread. T5's superior performance reflects its optimized ingredient ratio, which is based on material science theory: the combination of water hyacinth's natural porosity and CMC's hydrophilic enhancement creates synergistic absorption mechanisms. The slower drying reflects stronger water-polymer interactions, consistent with hydrocolloid theory, where carboxymethyl groups increase water binding energy. Despite T1 containing a greater amount of water hyacinth compared to T4 and T5, its absorption capacity is lower due to the absence of carboxymethyl cellulose (CMC). Conversely, T3's lower performance stems from reduced water hyacinth content and high concentrations of Guar Gum and Xanthan Gum, which primarily increase viscosity rather than absorption. Saikeaw et al. [13] found that 5% of Guar Gum did not enhance hydration in cassava-based cat litter, while Xanthan Gum did improve hydration compared to cassava alone. While water hyacinth-based formulations demonstrated absorption capacities comparable to or exceeding commercial products, they lacked the clumping property exhibited by the tofu-based T6 formulation. This difference stems from the protein structure of tofu residue, which forms gel-like networks through hydrogen bonding, and its manufacturing process, which creates micropores that facilitate capillary action and osmosis [20-22], as shown in Figure 1.

Absorption	T1	T2	T3	T4	T5	T6
Before						
After						

Figure 1. Shows the characteristics of each cat litter formula before and after the water absorption test

3.2 Comparison with commercial cat litter (T6)

Several significant variations in performance attributes were noted when comparing the commercial tofu-based cat litter (T6) with the water hyacinth-based formulations. The optimal water hyacinth formulation (T5) demonstrated superior water absorption capacity (64.23%) compared to the commercial product (47.42%). This result aligns with Nidarath [4] findings about similar absorption capacities in other plant-based materials. The enhanced absorption of T5 can be attributed to the synergistic effect of water hyacinth's fibrous structure and the addition of carboxymethyl cellulose (CMC), which Saxena [14] identified as an effective hydrophilic binding agent. Regarding drying properties, T6 exhibited the fastest drying rate (0.21 g/m²/s) compared to all water hyacinth formulations, with T5 being the slowest (0.11 g/m²/s). Cliff and Heymann [23] emphasized that drying rates significantly impact the reusability of cat litter and odor control. The slower drying rate of water hyacinth formulations represents a limitation that could affect practical application. The drop test revealed superior structural integrity in water hyacinth formulations compared to T6. When dropped from heights of 1-3 m, T6 showed progressive breakage (0.90-2.10%), while most water hyacinth formulations remained intact. Saikeaw et al. [13] similarly found that natural fiber reinforcement enhances structural stability in biodegradable cat litter. The most significant functional difference was the ability to clump.

The comparison of clumping ability revealed a significant functional difference between the water hyacinth formulations (T1-T5) and commercial tofu-based cat litter (T6). All water hyacinth formulations demonstrated poor clumping ability, failing to form cohesive masses upon moisture absorption and retaining their pellet shapes, despite incorporating various binding agents, including CMC (35 g in T4, T5), glycerol, guar gum, and xanthan gum. T6 demonstrated excellent clumping, forming cohesive masses after absorbing moisture, whereas the water hyacinth formulations retained their shapes. Wu and Wang [22] explained this phenomenon through the formation of protein-based gel networks in soy-derived products, such as tofu. This clumping limitation represents a critical area for improvement in future water hyacinth formulations. Despite these differences, the overall performance of T5 suggests that water hyacinth-based cat litter represents a viable, eco-friendly alternative to commercial products, particularly in markets where biodegradability outweighs the need for clumping functionality. As Radanova [5] noted, the increasing consumer preference for sustainable pet products creates market opportunities for innovative biomass applications.

The comparative analysis reveals that while the water hyacinth-based formulation T5 demonstrates a superior absorption capacity (35.4% higher than T6) and exceptional structural integrity (zero breakage vs. 2.10% for T6), the commercial product maintains advantages in drying efficiency (90.9% faster) and clumping functionality. These findings suggest that water hyacinth-based cat litter could serve specific market segments prioritizing absorption capacity and durability over rapid drying, particularly among environmentally conscious consumers willing to trade some convenience for sustainability benefits. Our analysis revealed that the commercial tofu-based litter's clumping ability comes from its protein-based gel formation through hydrogen bonding, combined with its manufacturing process that creates micropores facilitating capillary action and osmosis. In contrast, water hyacinth formulations based on cellulosic fiber structure and CMC binding enhance absorption but lack the protein matrix necessary for a gel-like clumping behavior.

3.3 Drying rate analysis

The drying properties of cat litter formulations revealed significant performance differences, as shown in Table 3. Commercial cat litter (T6) demonstrated the highest drying rate (0.21 g/m²/s), substantially outperforming all water hyacinth formulations. Cliff and Heymann [23] identified drying rate as a critical factor for cat litter reusability, noting that optimal products could dry within 14.5 hours, while suboptimal formulations required 30-65 hours. Among water hyacinth formulations, T3 exhibited the fastest drying (0.17 g/m²/s), followed by T1 and T2 (both 0.15 g/m²/s), T4 (0.12 g/m²/s), and T5 (0.11 g/m²/s). The slower drying of water hyacinth-based products compared to tofu-based litter suggests inherent differences in material structure and moisture retention. Formulation T3, with the lowest water hyacinth content (39.7 g), dried more rapidly than other experimental formulations. Khantiwatanakul [24] explained that additives like glycerol, xanthan gum, and guar gum contribute to moisture retention. Clarke and Franklin [25] noted that glycerol reduces water surface tension at higher T3 concentrations, potentially facilitating faster evaporation. Gravelle

[26] further suggested that glycerol reduces the viscosity of the mixture, thereby affecting water evaporation rates. Formulations T4 and T5, containing carboxymethyl cellulose (CMC), exhibited the slowest drying rates. Choi [27] identified CMC as a hydrophilic substance that absorbs water and increases viscosity, impeding moisture evaporation. Saxena [14] confirmed that CMC binds and retains water within structures, explaining the reduced drying efficiency of T4 and T5. The optimization challenge centers on the competing requirements created by CMC's dual role as both the primary absorption enhancer and the main factor limiting drying rate. Simple CMC reduction would improve drying but potentially compromise the absorption advantage that differentiates water hyacinth formulations from commercial alternatives. Nidarath [4] reported that cat litter made from cassava pulp had a drying rate of 1.09 g/m²/s, which significantly exceeded that of all other formulations in this study. This comparison highlights the relatively poor drying performance of water hyacinth-based formulations, a limitation that requires further optimization. The inverse relationship between absorption capacity and drying rate presents a design challenge. Formulation T5, with the highest absorption (64.23%), exhibited the slowest drying (0.11 g/m²/s). Future research should explore additives or processing techniques that balance these competing properties.

Table 3. Mean comparison of drying rate (g/m²/s) and % moisture content after 10 and 20 minutes in each formulation with 100% of initial moisture

Formula	Main Components	Drying Rate (g/m²/s) ± SD	% Moisture Content after ± SD	
			10 min	20 min
T1	WH (79.7 g), Guar/Xanthan (5 g each)	0.15±0.02 bc	51.00±1.56 c	41.73±1.93 c
T2	WH (59.7 g), Guar/Xanthan (10 g each)	0.15±0.02 bc	47.19±2.01 cd	37.63±2.74 cd
T3	WH (39.7 g), Guar/Xanthan (15 g each)	0.17±0.02 b	44.64±3.33 d	34.10±4.10 d
T4	WH (62 g), CMC (35 g)	0.12±0.02 cd	59.83±2.99 ab	52.53±4.19 ab
T5	WH (61.7 g), CMC (35 g)	0.11±0.02 d	62.72±2.43 a	55.84±3.65 a
T6	Commercial (Tofu-based)	0.21±0.03 a	57.43±1.55 ab	44.24±2.80 ab

Note: LSD (Least Significant Difference) analysis with letter groupings, different letters indicate statistically significant differences ($p \leq 0.05$), WH = Water Hyacinth, CMC = Carboxymethyl cellulose.

3.4 Shape retention and durability assessment

Impact testing revealed substantial differences in durability between water hyacinth formulations and commercial cat litter (Table 4). Commercial tofu-based litter (T6) exhibited significant fragmentation when dropped from various heights, with breakage percentages of 0.90%, 1.27%, and 2.10% at heights of 1 m, 2 m, and 3 m, respectively. In contrast, formulations T2-T5 maintained complete structural integrity at all tested heights, while T1 showed minimal breakage (0.03% at 2 m and 0.07% at 3 m). Formulation T1's limited structural integrity compared to other water hyacinth formulations can be attributed to its high water hyacinth content (79.7 g) combined with a minimal amount of glycerol (10 g). BeMiller and Whistler [28] noted that insufficient binding agents in fiber-rich materials can lead to brittle structures that are prone to fracture under impact. The excellent durability of T2 and T3 aligns with Gravelle [26] findings that increased glycerol content enhances material flexibility and cohesiveness. Saikeaw et al. [13] similarly observed that xanthan gum significantly increases material agglomeration compared to guar gum alone, explaining the superior performance of these formulations.

Formulations T4 and T5, containing 35 g CMC, demonstrated exceptional structural integrity at all drop heights. Silalai et al. [29] reported that incorporating 0.4% CMC in noodle formulations significantly enhanced tensile strength. This reinforcing effect is evident in our cat litter formulations, where CMC functions as an effective binder while maintaining flexibility. Nidarath [4] observed that cassava-based cat litter exhibited fractures at 2 m drops with more pronounced breakage at 3 m, indicating that water hyacinth formulations offer superior impact resistance compared to other biodegradable alternatives. The experimental data suggest that glycerol, gums, and CMC create synergistic effects with water hyacinth fibers, producing cat litter pellets with exceptional durability. This structural integrity advantage over commercial products

represents a significant selling point for water hyacinth-based cat litter, particularly in terms of transportation and handling considerations.

Table 4. Shape retention properties of cat litter formulations under impact testing

Formula	Composition Highlights	Breakage at 1 m (%)	Breakage at 2 m (%)	Breakage at 3 m (%)	Integrity Rating
T1	High WH (79.7 g), Low glycerol (10 g)	0.00	0.03	0.07	Good
T2	Medium WH (59.7 g), Medium glycerol (20 g)	0.00	0.00	0.00	Excellent
T3	Low WH (39.7 g), High glycerol (30 g)	0.00	0.00	0.00	Excellent
T4	High WH (62 g), High CMC (35 g)	0.00	0.00	0.00	Excellent
T5	High WH (61.7 g), High CMC (35 g)	0.00	0.00	0.00	Excellent
T6	Commercial (Tofu-based)	0.90	1.27	2.10	Poor

*WH = Water Hyacinth, CMC = Carboxymethyl Cellulose

3.5 Discussion of the role of key ingredients (CMC, glycerol, guar gum, xanthan gum)

According to Table 5, the type and quantity of additives had a significant impact on the functional and physical characteristics of the water hyacinth cat litter.

Table 5. Role of key ingredients in water hyacinth cat litter formulations

Ingredient	Primary Function	Effect on Water Absorption	Effect on Drying Rate	Effect on Structural Integrity	Optimal Content-Range per 100 g
Water Hyacinth	Base material	Moderate absorption (38.8%)	Slow drying due to the fibrous structure	It provides bulk but is brittle alone	60-65 g
Carboxymethyl Cellulose (CMC)	Binding agent	Significantly increases absorption	Decreases drying rate	Enhances cohesion and strength	30-35 g
Glycerol	Plasticizer	Moderate reduction in absorption	Increases drying rate by reducing surface tension	Improves flexibility, reduces brittleness	20-30 g
Guar Gum	Thickening agent	Minimal impact on absorption	Slows drying through moisture retention	Improves cohesion at moderate levels	3-10 g
Xanthan Gum	Viscosity enhancer	Moderate increase in absorption	Significantly slows drying	Strengthens internal bonding	5-15 g
Activated Carbon	Odor control	Negligible impact	Negligible impact	Negligible impact	0.3 g

Carboxymethyl cellulose (CMC) emerged as the most influential additive in formulations T4 and T5, substantially enhancing water absorption and structural integrity. Saxena [14] described CMC as a hydrophilic derivative of cellulose that creates strong hydrogen bonds with water molecules. Maryam et al. [18] confirmed its efficacy in enhancing moisture retention in food products, while Silalai et al. [29] demonstrated its ability to increase tensile strength when added at a concentration of 0.4%. The superior performance of formulation T5 (64.23% absorption) can be attributed primarily to the synergistic interaction between water hyacinth fibers and CMC. Glycerol, incorporated in formulations T1-T3, demonstrated complex effects on performance properties. Clarke and Franklin [25] noted that glycerol reduces the surface tension of water, facilitating faster evaporation during drying. This explains T3's higher drying rate (0.17 g/m²/s) than CMC-containing

formulations. Gravelle [26] described glycerol's function as a plasticizer that enhances flexibility while reducing brittleness, accounting for the excellent impact resistance observed in T2 and T3. However, Saikeaw et al. [13] cautioned that glycerol absorbs atmospheric moisture over time, potentially causing dimensional changes in the final product.

Guar gum and xanthan gum, present in formulations T1-T3, primarily functioned as viscosity modifiers with secondary effects on water retention. Khantiwatanakul [24] found that these gums increase the cohesiveness of the mixture during processing. BeMiller and Whistler [28] differentiated their functions, noting that xanthan gum forms stronger gel networks than guar gum, which explains the observation by Saikeaw et al. [13] that xanthan gum increased hydration capacities more effectively than guar gum in cassava-based cat litter. The optimal water hyacinth formulation (T5) achieved its superior performance through balanced ingredient proportions: moderate water hyacinth content (61.7 g) providing fiber structure, high CMC content (35 g) enhancing absorption and cohesion, minimal guar gum (3 g) improving processability, and carbon (0.3 g) for odor control. This combination maximized absorption capacity (64.23%) while maintaining excellent structural integrity, though at the cost of reduced drying rate (0.11 g/m²/s).

3.6 Environmental and economic benefits

The development of water hyacinth-based cat litter offers significant environmental and economic advantages over conventional products (Table 6).

Table 6. Environmental and economic benefits of water hyacinth cat litter

Benefit Category	Water Hyacinth Cat Litter	Commercial Synthetic Litter
Raw Material Cost	Low (invasive species removal can be subsidized) [30]	High (bentonite mining, silica gel production) [4]
Biodegradability	2-3 months under composting conditions [31]	Non-biodegradable or very slow (years to decades)
Carbon Footprint	Low (minimal processing, local sourcing) [30]	High (mining, intensive processing, transportation)
Ecosystem Impact	Positive (removes harmful invasive species) [32]	Negative (resource extraction, waste generation) [30]
Waste Management	Compostable, reduced landfill burden [4]	Contributes to landfill accumulation
Production Energy	Low-moderate (drying, grinding, molding)	High (mining, heating, chemical processing)
Scalability	High (abundant raw material in tropical regions)	Medium (dependent on mineral deposits)

Water hyacinth (*Eichhornia crassipes*) is recognized as one of the world's most invasive aquatic plants. Prapaiphan [10] documented its rapid growth rate and negative impacts on water quality, biodiversity, and infrastructure. Repurposing this problematic species creates a dual benefit: ecosystem restoration and sustainable product development. From an economic perspective, the harvesting and utilization of water hyacinths creates value from waste. Hejlik [6] noted that natural-based cat litter typically retails at higher prices than synthetic alternatives despite potentially lower raw material costs. The present study suggests potential cost advantages, as environmental management programs could subsidize the harvesting of water hyacinth. Radanova [5] highlighted the growing consumer demand for biodegradable pet products, presenting market opportunities for alternatives such as water hyacinth cat litter. The biodegradability of these formulations addresses waste management concerns raised by Umor et al. [12], who estimated that conventional cat litter contributes significantly to landfill volumes with minimal degradation. The manufacturing process for water hyacinth cat litter requires less energy than bentonite or silica-based products. While commercial products involve mining, high-temperature processing, and long-distance transportation, water hyacinth processing primarily entails harvesting, drying, grinding, and molding at

moderate temperatures (70 °C). Furthermore, the localized nature of water hyacinth harvesting and processing creates economic opportunities in rural communities where the plant is abundant. This aligns with circular economy principles, transforming an environmental liability into a valuable resource while supporting the Sustainable Development Goals (SDGs) 6, 12, 13, 14, and 15. A preliminary environmental assessment indicates significant benefits; however, future research should quantify these impacts through a systematic life cycle assessment methodology, including carbon footprint calculation, energy consumption analysis, and a comprehensive evaluation of ecosystem impacts.

3.7 Drying rate limitations and optimization pathways

The slower drying rate of the optimal formulation T5 (0.11 g/m²/s) compared to commercial alternatives (0.21 g/m²/s) presents the primary limitation that requires mitigation. Several approaches can address this constraint while preserving superior absorption capacity. Immediate optimization strategies include reducing CMC concentration from 35 g to 25-30 g, which preliminary calculations suggest could improve drying rates by 25-35% while maintaining absorption above 55%. Alternative approaches involve incorporating hybrid binding systems combining reduced CMC with glycerol or developing pellet geometries with enhanced surface area for accelerated evaporation. Future research should systematically evaluate these modifications through factorial experimental design, targeting drying rates of 0.15-0.17 g/m²/s while preserving the absorption advantages that position water hyacinth formulations as superior alternatives to commercial products.

3.8 Statistical analysis

3.8.1 One-way ANOVA, Coefficient of Variation, and LSD Analysis

All six formulas (T1-T6) demonstrated acceptable normal distribution patterns based on standard deviation ratios (2.29-2.56) and skewness values (-0.20 to 0.62). One-way ANOVA confirmed highly significant differences between formulations for all measured parameters ($p < 0.001$): water absorption capacity ($F_{5,24} = 52.84$, $R^2 = 0.917$), drying rate ($F_{5,24} = 15.18$, $R^2 = 0.760$), and absorption volume ($F_{5,24} = 49.25$, $R^2 = 0.911$). CV values ranging from 2.1% to 20.3% across treatments, with 5 out of 6 formulations showing CV < 15% for water absorption, indicating reliable and consistent measurements. LSD analysis ($LSD_{0.05} = 4.817\%$ for water absorption, 0.028 g/m²/s for drying rate, and 10.587 mL/50g for absorption volume) confirmed that formulation T5 exhibited significantly higher water absorption capacity (64.23 ± 2.31%) compared to all other treatments except T4 (61.01 ± 3.47%), with both CMC containing formulations significantly outperforming the commercial benchmark T6 (47.42 ± 1.00%). Commercial litter T6 demonstrated a significantly faster drying rate (0.21 ± 0.03 g/m²/s) compared to all water hyacinth formulations (0.11-0.17 g/m²/s), while formulations T2, T3, T4, and T5 showed no significant differences among themselves for drying rate.

3.8.2 Pearson correlation and linear regression

Pearson correlation analysis revealed significant relationships between key performance variables and formulation parameters. Strong positive correlations were observed between water absorption capacity and absorption volume ($r = 0.98$, $p < 0.001$), as well as between water absorption and moisture retention at 20 minutes ($r = 0.87$, $p < 0.001$), indicating that higher absorption capacity directly translates to greater functional volume and enhanced moisture retention. The strong positive correlation ($r = 0.71$, $p < 0.001$) between CMC content and water absorption capacity is attributed to the inherent hydrophilic properties of CMC. A moderate negative correlation existed between water absorption and drying rate ($r = -0.59$, $p < 0.01$).

Linear regression analysis established predictive models for key performance relationships: absorption volume demonstrated a strong linear relationship with water absorption capacity ($y = 1.99 + 2.075x$, $R^2 = 0.95$). At the same time, moisture retention at 20 minutes showed good predictability ($y = 12.28 + 0.628x$, $R^2 = 0.75$). The correlation validates the formulation where treatments T4 and T5 (both containing 35g CMC) achieved superior absorption performance compared to CMC-free formulations. The linear regression equation (Water Absorption (%) = 45.34 + 0.494 × CMC content (g)) provides a reliable tool for predicting absorption capacity based on CMC content.

3.8.3 Cluster analysis

Multivariate statistical analysis was performed to classify the T1-T6 based on their performance characteristics systematically. Hierarchical cluster analysis using Euclidean distance and Ward's linkage method identified three distinct formulation groups with statistically significant differences (MANOVA: Wilks' $\lambda = 0.023$, $F = 156.7$, $p < 0.001$). The optimal 3-cluster solution demonstrated good clustering quality (silhouette width = 0.68). Cluster 1 comprised formulations T4 and T5, characterized by superior water absorption (61.01-64.23%), excellent structural integrity, and CMC-based binding systems. Cluster 2 included T1 and T2, showing moderate absorption performance (43.87-57.47%) with glycerol-gum binding systems. Cluster 3 contained T3 (low absorption, fast drying) and T6 (commercial benchmark with unique clumping properties).

3.8.4 Principal component analysis (PCA)

PCA revealed that 2 components explained 81.0% of the variance in performance. PC1 (52.3% variance) represented an absorption drying axis, while PC2 (28.7% variance) captured structural integrity and moisture retention characteristics. The PCA biplot separated T4 and T5 in the high performance quadrant, confirming their superior absorption and structural properties.

4. Conclusions

Investigating water hyacinth-based biodegradable cat litter yielded promising results for sustainable product development in pet care. Formulation T5, comprising water hyacinth (61.7 g) and carboxymethyl cellulose (35 g), exhibited superior performance with the highest water absorption capacity (64.23%), surpassing commercial tofu-based litter (47.42%). Water hyacinth formulations demonstrated exceptional structural integrity in impact testing, with minimal to no breakage when dropped from heights of up to 3 m, significantly outperforming commercial litter, which exhibited progressive fragmentation (up to 2.10% at 3 m). This durability advantage represents a key selling point for transportation and handling. The primary limitation identified was the drying rate, with water hyacinth formulations drying more slowly (0.11-0.17 $g/m^2/s$) than commercial alternatives (0.21 $g/m^2/s$). Additionally, water hyacinth formulations lacked the clumping property of tofu-based litter, which could potentially affect ease of use. Particularly regarding the removal of feces and urine, this limitation may stem from the primary materials in the formulation, such as water hyacinth fibers and the binding agents used, being unable to form a sufficient network structure or achieve the necessary bonding strength to enable clumping upon exposure to moisture. Therefore, future development should consider improving the formulation by adding clumping agents, such as Guar Gum or Xanthan Gum, at appropriate ratios to enhance the clumping properties. Clumping ability should be tested after incorporating these additives, along with evaluations of clump strength, ease of removal, and the impact on water absorption and drying properties. This research demonstrates the feasibility of converting an invasive aquatic plant into a value-added biodegradable product, addressing environmental challenges and consumer demand for eco-friendly pet care products. Future development should focus on improving drying rates and developing clumping properties while maintaining the excellent absorption and structural integrity of the current formulations. Future studies should include (1) comprehensive production cost analysis, (2) market price comparison with existing biodegradable products, (3) economic feasibility assessment for commercial scale-up, (4) break-even analysis for different market segments, (5) biodegradability testing methods in natural conditions such as ASTM D5338 (Aerobic Biodegradation Test), and (6) practical durability assessment such as simulated cat behavior testing, moisture cycling and long-term stability evaluation to ensure commercial viability.

5. Acknowledgements

The authors would like to express sincere gratitude to all the research units that contributed to the successful completion of this research. We gratefully acknowledge the Water and Soil Environmental Research Unit and the Biofuel and Biocatalysis Innovation Research Unit, Nakhonsawan Campus, Mahidol University, Nakhon Sawan 60130, Thailand, for providing the laboratory facilities, equipment, and resources necessary for conducting this research.

Author Contributions: Conceptualization, T.J. and P.T.; methodology, T.J. and P.T.; software, P.T.; validation, T.J. and P.T.; formal analysis, T.J.; investigation, T.J.; resources, P.T.; data curation, T.J.; writing—original draft preparation, T.J.; writing—review and editing, P.T.; visualization, T.J.; supervision, P.T.; project administration, P.T. Both authors have read and agreed to the published version of the manuscript.

Conflicts of Interest: The authors declare no conflict of interest. This research received no external funding and was conducted using the authors' personal resources. The authors had complete autonomy in the design of the study; in the collection, analyses, or interpretation of data; in the writing of the manuscript, and in the decision to publish the results.

References

[1] National Statistical Office. July 11... World Population Day 2024. https://www.nso.go.th/public/e-book/NSOLetsRead/population.html (accessed 2024-10-28). (In Thai)

[2] BrandAge Team. Pet Humanization the Era When Pets Are Equivalent to Family Members. https://www.brandage.com/article/29294/Pet-Humanization (accessed 2024-08-20).

[3] Marketingoops. Trends in Pet Parenting Thai People Treating Pets Like Children and Spending Big for Their Beloved Pets, Boosting Pet Product and Service Industries.https://www.marketingoops.com/reports/behaviors/pet-parent/ (accessed 2023-07-08). (In Thai)

[4] Nidarath, C. J. Development of cat waste absorbent materials from cassava residues; Master's thesis, Thammasat University. **2019**. http://digital.library.tu.ac.th/tu_dc/frontend/Info/item/dc:168836 (accessed 2023-05-16) (In Thai)

[5] Radanova, S. Biodegradable Plant-Based Cat Litter Fillers: Relevance of the Topic in Bulgaria. *Eastern Academic Journal*. **2021**, *4*, 78-86.

[6] Hejlik, A. How to choose the best natural cat litter A comprehensive guide. https://soykitty.com/blogs/news/how-to-choose-the-best-natural-cat-litter (accessed 2024-09-02).

[7] Fazal, H.; Mehwish, K.; Iffat, A. K.; Sahid, M.; Tariq, A.; Muhammad, H. Exploring the pathways to sustainability: A comprehensive review of biodegradable plastics in the circular economy. *Materials Today Sustainability*. **2025**, *29*, 1-26. https://doi.org/10.1016/j.mtsust.2024.101067.

[8] Jiahao, K.; Dongxu, L.; Qingzhuo, W. Data-Driven Insights into the Pet Industry: Market Dynamics, Trade Policies, and Sustainable Growth Strategies. Accounting, *Marketing and Organization*. **2025**, *1*(1), 1000037, 1-29. https://doi.org/10.71204/cwfbwq11 (accessed 2023-04-07)

[9] Metogbe B.D.; Mark O.; Louis C.C.; Fohla M.; Martin P.A. Paradigm shifts for sustainable management of water hyacinth in tropical ecosystems: A review and overview of current challenges, *Environmental Challenges*. **2023**, *11*, 100705, https://doi.org/10.1016/j.envc.2023.100705

[10] Prapaiphan, J. Composting Water Hyacinth with Excess Sludge from Wastewater Treatment in Latex Factories and STR 20 Rubber Factories. Master's Thesis, Prince of Songkla University, **2016**. https://kb.psu.ac.th/psukb/handle/2016/12097 (accessed 2023-02-25) (In Thai)

[11] Somchai, J.; Thanongsak, N. *Heat Insulation Production Project from Water Hyacinth Fiber and Natural Rubber (Research Report) Naresuan University*, July 20, **2023**; https://nuir.lib.nu.ac.th/dspace/bitstream/123456789/905/1/Fulltext.pdf. (accessed 2023-12-25) (In Thai)

[12] Umor, N.; Adenan, N. H.; Hajar, N.; Akil, N.; Malik, N.; Ismail, S.; Meskam, Z. Comparing Properties and Potential of Pinewood, Dried Tofu, and Oil Palm Empty Fruit Bunch (EFB) Pellet as Cat Litter; In *Proceedings of the International Conference on Cellulose-Based Materials*, **2023**; 300-308. https://doi.org/10.1201/9781003358084-21

[13] Saikeaw, N.; Rungsardthong, V.; Pornwongthong, P.; Vatanyoopaisarn, S.; Thumthanaruk, B.; Pattharaprachayakul, N.; Wongsa, J.; Mussatto, S. I.; Uttapap, D. Preparation and properties of biodegradable cat litter produced from cassava (Manihot esculenta L. Crantz) trunk; E3S Web of Conferences, **2021**, 302. https://doi.org/10.1051/e3sconf/202130202017 (accessed 2023-03-01)

[14] Saxena, S. Rheological properties and applications of carboxymethyl cellulose. *Carbohydrate Polymers*. **2011**, *83*(3), 1447–1456. https://doi.org/10.1016/j.carbpol.2010.09.019

[15] R Core Team. (2024). *R: A language and environment for statistical computing (Version 4.3.3)*. R Foundation for Statistical Computing. https://www.R-project.org/ (accessed 2025-06-15)

[16] Jaruwan, N.; Panya, S.; Suchart, S. Study on chemical properties of water hyacinth for development as water-absorbing material. *Kasetsart J Res Dev*. **2014**, *31*(3), 405-412.

[17] Somsri, S. Chemical characteristics of water hyacinth fiber grown in the central region of Thailand. *J Agric Sci*. **2017**, *48*(2), 112-120.

[18] Maryam, M.; Ali, H.; Mehdi, T.; Aryou, E.; Fatemeh, E. The influence of carboxymethyl cellulose and hydroxypropyl methylcellulose on physicochemical, texture, and sensory characteristics of gluten-free pancake. *Food Science & Nutrition*. **2023**, *12*(3), 1-14. https://doi.org/10.1002/fsn3.375819159

[19] Harsono, C.; Trisnawati, C. Y.; Srianta, I.; Nugerahani, I.; Marsono, Y. Effect of carboxymethyl cellulose on the physicochemical and sensory properties of bread enriched with rice bran. *Food Research*. **2021**, *5*(4), 322-328.

[20] Damodaran, S.; Parkin, K. L.; Fennema, O. R. *Fennema's food chemistry (5th ed.).* CRC Press: **2017**. https://doi.org/10.1201/9781315372914 (accessed 2024-05-11)

[21] Tang, C. H. Functional and nutritional properties of soy protein products. *Food Chemistry*. **2017**, *231*, 577-584. https://doi.org/10.1016/j.foodchem.2017.03.123

[22] Wu, H.; Wang, X. Water absorption characteristics of soy protein gel matrices. *Journal of Food Science and Technology*. **2020**, *57*(5), 1202–1210. https://doi.org/10.1007/s13197-019-04147-8

[23] Cliff, M.; Heymann, H. Physical and Sensory Characteristics of Cat Litter. *Journal of Sensory Studies*. **2007**, *6*, 255-266. https://doi.org/10.1111/j.1745-459X.1991.tb00518.x

[24] Khantiwatanakul, Y. Effect of xanthan gum and guar gum on physical properties of rice starch https://kukr.lib.ku.ac.th/db/index.php?%2FBKN%2Fsearch_detail%2Fresult%2F155349= (accessed 2024-11-6). (In Thai)

[25] Clarke, D.; Franklin, A. Surface tension and interfacial properties of glycerol-based liquids.*The Journal of Chemical Thermodynamics*. **2002**, *135*, 241-251. https://doi.org/10.1006/jcis.2002.8473

[26] Gravelle, M. E. Rheological and functional properties of glycerol as a food additive. *Food Hydrocolloids*. **2015**, *50*, 49–58. https://doi.org/10.1016/j.foodhyd.2015.04.001

[27] Choi, S. J. Effect of CMC and other hydrocolloids on the stability and rheology of water-in-oil emulsions. *Journal of Food Science and Technology*. **2008**, *45*(5), 413-418. https://doi.org/10.1007/s11483-008-0048-0

[28] BeMiller, J. N.; Whistler, R. L. Guar gum and xanthan gum properties and applications in food systems. *Food Hydrocolloids*. **1996**, *10*(1), 79-83. https://doi.org/10.1016/S0268-005X(96)80033-2

[29] Silalai, N.; Sirilert, T.; Tocharoensap, S.; Sarawong, C. Effect of carboxymethyl cellulose on physicochemical properties of composite flour and noodle characteristics. *Burapha Science Journal*. **2019**, *24*(3), 1029-1042. https://ojs.lib.buu.ac.th/index.php/science/article/view/6541 (In Thai)

[30] Balart, R.; Montanes, N.; Dominici, F.; Torres-Giner, S.; Boronat, T. *Environmentally Friendly Polymers and Polymer Composites*; MDPI: Basel, Switzerland, 2021; ISBN 978-3-0365-0036-2.

[31] Potivara, K.; Phisalaphong, M. Development and characterization of bacterial cellulose reinforced with natural rubber. *Polymers.* **2019**, *11*, 1142. https://doi.org/10.3390/polym11071142

[32] Chaiwarit, T.; Chanabodeechalermrung, B.; Kantrong, N.; Chittasupho, C.; Jantrawut, P. Fabrication and evaluation of water hyacinth cellulose-composited hydrogel containing quercetin for topical antibacterial applications. *Gels*. **2022**, *8*(12), 767. https://doi.org/10.3390/gels8120767.

ASEAN
Journal of Scientific and Technological Reports
Online ISSN:2773-8752

Research article

Melted Polyethylene Terephthalate Plastic Waste as a Binder in the Manufacture of Sand Bricks

Arusmalem Ginting[1*], Muhammad Suryo Wibowo[2], Prasetya Adi[3], and Bing Santosa[4]

[1] Department of Civil Engineering, Janabadra University, Yogyakarta, 55231, Indonesia; aginting@janabadra.ac.id
[2] Department of Civil Engineering, Janabadra University, Yogyakarta, 55231, Indonesia; suryawibaw@gmail.com
[3] Department of Civil Engineering, Janabadra University, Yogyakarta, 55231, Indonesia; prasetya@janabadra.ac.id
[4] Department of Civil Engineering, Janabadra University, Yogyakarta, 55231, Indonesia; bing@janabadra.ac.id
* Correspondence: aginting@janabadra.ac.id

Citation:
Ginting, A.; Wibowo, M.S., Adi, P.; Santosa, B. Melted polyethylene terephthalate plastic waste as a binder in the manufacture of sand bricks. *ASEAN J. Sci. Tech. Report.* **2025**, *28*(4), e256661. https://doi.org/10.55164/ajstr.v28i4.256661.

Article history:
Received: November 12, 2024
Revised: June 22, 2025
Accepted: July 14, 2025
Available online: July 21, 2025

Abstract: In the province of D.I. Yogyakarta, Indonesia, plastic waste reaches 26.37% of the province's total waste. Plastic waste ranks second after food waste. Given this, managing plastic waste for essential building materials, such as sand bricks, is necessary. This study aims to determine the effect of using melted PET waste as a binding material in sand bricks on compressive strength and water absorption. The weight ratios of PET waste to sand used are: 1:2, 1:2.2, 1:2.5, 1:2.9, 1:3.3, 1:4, and 1:5. The test specimen is a 6cm x 6cm x 6cm cube. Each variation consists of 5 test specimens. The tests carried out were absorption testing and compressive strength testing. From the research obtained, the weight ratio of 1:2 to 1:4 is deemed to satisfy the criteria for quality level 3, with a minimum average compressive strength of 4 MPa. The weight ratio of 1:5 meets the requirements of quality level 4 with a minimum average compressive strength of 2.5 MPa. The weight ratio of 1:2 to 1:5 is deemed to satisfy the requisite quality level 1 bricks for walls standards, with a maximum average absorption of 25%. The density of sand bricks with various weight ratios of PET plastic waste to sand is less than that of clay brick masonry, which has a density of 1700 kg/m^3.

Keywords: PET plastic waste; Sand bricks; Compressive strength; Absorption; Density

1. Introduction

Most of the plastic produced is not reprocessed and tends to end up in landfills or become marine waste. Only about 25% of plastic produced globally is reprocessed [1]. Plastic waste can be classified into several types. PET (Polyethylene terephthalate) is used for beverage bottles, LDPE (Low-density polyethylene) is used for trash bags, HDPE (High-density polyethylene) is used for buckets and detergent bottles, PVC (Polyvinyl chloride) is used for plumbing, PP (Polypropylene) is used for food boxes, PS (Polystyrene) is used for toys and disposable tableware, and PE (Polyester) is used for seat belts and conveyor belts [2]. The use of plastic waste in the construction sector aims to overcome environmental issues and to save non-renewable natural resources [3, 4]. Plastic waste can be used as material for making plastic bricks. High-Density Polyethylene (HDPE) and Polypropylene (PP) plastics, which are melted at a temperature of 230 °C, are used as materials for making plastic bricks. The compressive strength of HDPE bricks is higher than that of conventional bricks, and the compressive strength of PP bricks is lower than that of conventional bricks [5].

It is possible to utilise PET waste as both an aggregate and a fibre in the production of concrete. The incorporation of PET waste as an aggregate in concrete does not affect the compressive or flexural strength of the resulting concrete. However, excessive use may impact the quality of the construction [6]. Polyethylene terephthalate (PET) plastic is employed as a coarse aggregate in the production of concrete. The plastic waste derived from PET is melted at a temperature of approximately 300°C to create artificial aggregates. It was observed that as the percentage of coarse aggregate substituted with artificial PET aggregate increased, the compressive strength, flexural strength, and density of the concrete exhibited a corresponding decline. PET aggregate can be employed in the production of lightweight concrete, which is utilized in non-structural or semi-structural applications [7].

Polyethylene terephthalate (PET) waste is employed as a fibre, while low-density polyethylene (LDPE) waste is utilised as a fine aggregate in the production of mortar [8]. The use of shredded PET (polyethylene terephthalate) waste as a substitute for conventional coarse aggregate in the production of concrete is investigated at proportions of 0%, 5%, 10% and 20% by volume [9]. The melted plastic waste, which is a combination of HDPE and LDPE, is employed as a binder in the production of mortar. The use of liquid plastic waste as a binder in mortar has been found to result in superior performance compared to paving with Portland cement [10]. The utilisation of melted plastic waste as a binder represents a contribution to waste reduction. Recycled plastic waste (RPW), including polyethylene bags, sachet water bags, wrappers, and other materials, can be employed as an alternative binder in the production of paving blocks. RPW exhibits thermoplastic properties that permit reforming when melted [11]. The manufacture of sand-plastic composite bricks involves the use of LDPE and HDPE plastic waste in conjunction with sand. LDPE and HDPE plastic waste are melted and combined with sand. The maximum compressive strength achieved was 4.95 MPa, with a plastic waste content of 60% (40% LDPE and 20% HDPE) and a sand content of 40% (25% size 1.18 mm and 15% size 0.5 mm) [12].

Polyethylene terephthalate (PET) is one of the most widely produced polymers globally, with applications in the manufacture of synthetic fibres and bottles. The incorporation of PET fibres into concrete can enhance flexural strength while reducing density, thereby creating a structure that is both lightweight and earthquake-resistant [13]. The utilisation of PET plastic waste and river sand in the production of roof tiles has been demonstrated. Polyethylene terephthalate (PET) waste is employed as a cement substitute in the production of roof tiles. The weight ratio of PET waste to sand employed is 10%:90%, 20%:80%, 30%:70%, 40%:60%, 50%:50%, 60%:40%, and 100%:0%. The PET waste is melted at 230°C and subsequently combined with sand to create roof tiles. The highest compressive strength was observed at a weight ratio of 40%:60%, with a value of 1.5868 MPa. The utilisation of PET waste as a cement substitute has been observed to result in enhanced compressive strength and absorption properties [14]. Polyethylene plastic waste is used as a binder in making sand bricks. The ratio of plastic waste and sand used is 1:3, 1:4, and 1:5 based on weight ratio. Plastic waste is melted at a temperature of 105°C to 115°C, then sand is added and mixed until homogeneous. The highest compressive strength occurred in a ratio of plastic waste and sand of 1:4. Absorption for ratios 1:3, 1:4, and 1:5 is zero [15]. The utilisation of PET plastic waste and sand in the production of plastic sand bricks represents a novel approach to the utilisation of these materials. The weight ratio of PET plastic waste to sand is 1:2, 1:3, and 1:4. The PET plastic waste is melted at a temperature range of 180°C to 200°C and mixed with sand to create plastic sand bricks. The resulting plastic sand bricks exhibit low porosity, a lightweight composition, and a higher compressive strength than conventional clay bricks [16].

The utilisation of PET plastic waste and sand as materials for the production of tiles has been demonstrated. The melted PET plastic waste is combined with sand, agitated, and subsequently shaped into tiles. The proportion of PET plastic waste utilised is 20%, 30% and 40%. The compressive strength of tiles manufactured using PET plastic waste is superior to that of conventional bricks and concrete blocks [17]. Bricks are manufactured from melted PET plastic waste and crushed glass. The mass ratio of PET plastic waste to crushed glass employed is 20%:80%, 30%:70%, and 40%:60%. The findings of the research indicated that the tensile strength of bricks produced from a mixture of melted PET plastic waste and crushed glass was 70.15% higher than that of conventional clay bricks, while the compressive strength was 54.85% higher [18]. Mixed plastic waste from polyethylene terephthalate (PET) and high-density polyethylene (HDPE), melted at a temperature of 257-315°C, is combined with sand in varying weight ratios, specifically 1:2, 1:3, 1:4, and 1:5, to create hollow blocks. The mean compressive strength of the ratios 1:2, 1:3, 1:4, and 1:5 is 3.87 MPa, 3.41 MPa, 3.29 MPa, and 3.09 MPa, respectively. The absorption ratios for the 1:2, 1:3, 1:4, and 1:5 mixtures were found

to be 1.67%, 2.51%, 2.62%, and 2.81%, respectively [19]. Three types of waste are employed as substitutes for cement in mortar production: sawdust, shredded polyethylene terephthalate (PET) plastic bottles, and shredded used diapers. The proportion of cement substituted with waste material is 0%, 5%, 10%, 15%, and 20% by weight. The compressive strength of mortar with cement substitution using shredded PET plastic bottles is observed to be higher than that of the other materials [20]. In the manufacture of sand bricks, plastic waste, glass bottle waste, and paper waste are employed as alternative materials. The plastic waste employed is a combination of polyethylene terephthalate (PET), high-density polyethylene (HDPE), and low-density polyethylene (LDPE). The compressive strength obtained exceeds the requisite compressive strength for masonry. The absorption values are below the maximum absorption requirements for sand bricks [21].

In the province of D.I. Yogyakarta, Indonesia, plastic waste represents 26.37% of the province's total waste. This is the second most significant component of the waste stream after food waste [22]. Given this context, it is necessary to manage plastic waste for use in the production of sand bricks, a material with a clear and pressing need for such materials. This study aims to determine the effect of using melted PET waste as a binding material in sand bricks on compressive strength and water absorption.

2. Materials and Methods

The PET waste utilised in this process is derived from mineral water bottles sourced from the province of D.I. Yogyakarta in Indonesia with a specific gravity of 1.3. The sand utilized in this process is sourced from the riverbeds of the Indonesian province of D.I. Yogyakarta with a specific gravity of 2.6 and a size of 0.15 mm - 5 mm. The weight ratios of PET waste to sand employed are as follows: 1:2, 1:2.2, 1:2.5, 1:2.9, 1:3.3, 1:4, and 1:5. These ratios are based on trial results. The weight ratio of PET waste to sand exceeds 5; consequently, the melted PET plastic is insufficient to bind the sand. The test specimen is a cube with dimensions of 6 cm on each side, as shown in Figure 2. Each variant comprises five test specimens. The methodology employed for this research project is as follows:

a. Cleaning: The collected PET Plastic bottles were cleaned to remove adhering dirt.
b. Shredding: The collected PET Plastic bottles were shredded into small pieces to speed up the melting process.
c. Weighing: Weighing PET plastic bottles and sand according to the needs of each variation.
d. Melting: The shredded PET plastic bottle waste was melted.
e. Mixing: The sand and melted PET plastic bottle waste were mixed and stirred until a homogeneous mixture was achieved.
f. Molding: The mixtures were moulded on a wooden mould.
g. Curing: The test specimens were removed from the mould after 24 hours.

The methodology employed in the production of sand bricks is illustrated in Figure 1. The tests carried out were absorption testing and compressive strength testing. Compressive strength testing based on ASTM C109 using a digital compression test machine with a capacity of 2000 kN. The hardened sand bricks are weighed, then soaked in water for 24 hours. The sand bricks are removed from the soaking, the surface is dried, and then weighed. Absorption is calculated by subtracting the weight of the sand bricks after soaking from the weight of the sand bricks before soaking, then dividing by the weight of the sand bricks before soaking.

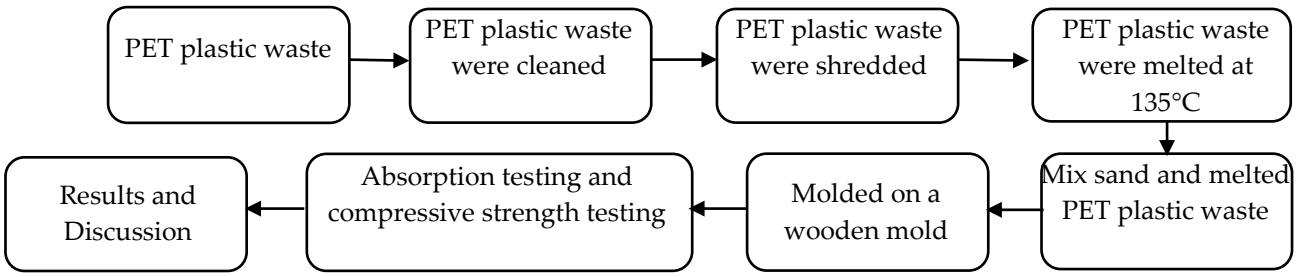

Figure 1. Process of making sand bricks

Figure 2. Sand bricks

3. Results and Discussion

3.1 Compressive strength of sand bricks

The average compressive strength of sand bricks with various weight ratios of PET plastic waste to sand is shown in Table 1 and Figure 3.

Table 1. Compressive strength of sand bricks

Weight ratio of PET plastic waste to sand	Average compressive strength (MPa)	P-Value
1:2	4.79	
1:2,2	4.05	
1:2,5	4.77	
1:2,9	4.29	0.0517
1:3,3	4.64	
1:4	4.00	
1:5	2.56	

Table 1 and Figure 3 illustrate that the highest compressive strength is observed at a weight ratio of PET plastic to sand of 1:2. In contrast, the lowest is observed at a weight ratio of 1:5. The compressive strength of the weight ratio of 1:2 to 1:4 exhibits fluctuations between 4.79 MPa and 4 MPa. This result is not much different from the report of Maunahan and Adeba [19]. This phenomenon can be attributed to the continued utilisation of a relatively rudimentary compaction technique, namely the use of a trowel. The compressive strength at a weight ratio of 1:5 is low due to the insufficient quantity of melted PET plastic to bind the sand.

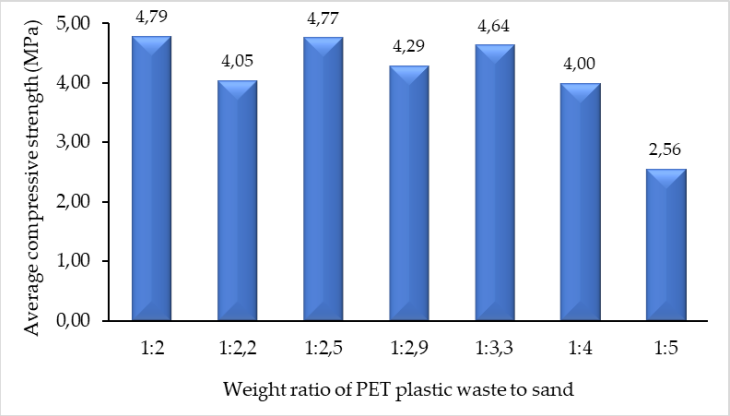

Figure 3. Compressive strength of sand bricks

Following the Indonesian National Standard SNI 03-0349-1989 [23] about concrete bricks for walls, the weight ratio of 1:2 to 1:4 is deemed to satisfy the criteria for quality level 3, with a minimum average compressive strength of 4 MPa. The weight ratio of 1:5 meets the requirements of quality level 4 with a minimum average compressive strength of 2.5 MPa. It can therefore be concluded that sand bricks with various weight ratios of PET plastic waste to sand meet the compressive strength requirements. From the ANOVA analysis, the P-value was obtained as 0.0517 > 0.05, which shows that the weight ratio of PET plastic waste to sand used does not have a significant effect on compressive strength.

3.2 Absorption of sand bricks

The average absorption of sand bricks with various weight ratios of PET plastic waste to sand is shown in Table 2 and Figure 4.

Table 2. Absorption of sand bricks

Weight ratio of PET plastic waste to sand	Average absorption (%)	P-Value
1:2	8,69	
1:2,2	8,57	
1:2,5	8,79	
1:2,9	8,55	0.84016
1:3,3	7,62	
1:4	7,93	
1:5	9,18	

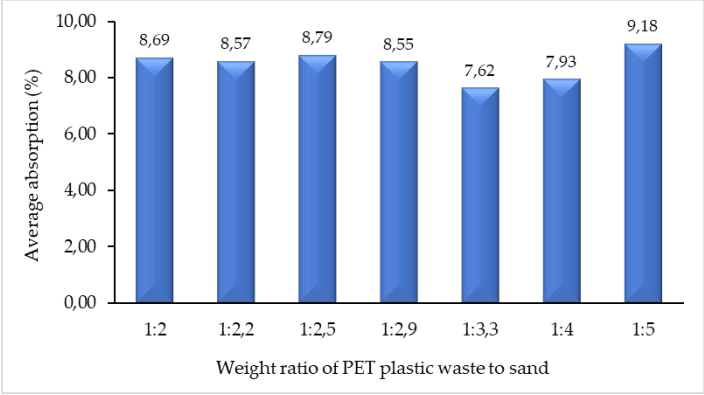

Figure 4. Absorption of sand bricks

Table 2 and Figure 4 indicate that the highest absorption is 9.18%, while the lowest is 7.62%. Following the Indonesian National Standard SNI 03-0349-1989 [23] about concrete bricks for walls, the weight ratio of 1:2 to 1:5 is deemed to satisfy the requisite quality level 1 standards, with a maximum average absorption of 25%. Following the Indonesian National Standard SNI 15-2094-2000 [24] about clay bricks, the maximum permissible absorption is 20%. In light of the findings above, it can be posited that sand bricks comprising varying proportions of PET plastic waste satisfy the requisite absorption standards. From the ANOVA analysis, the P-value was obtained as 0.84016 > 0.05, which shows that the weight ratio of PET plastic waste to sand used does not have a significant effect on absorption.

3.3 Density of sand bricks

The average density of sand bricks with various weight ratios of PET plastic waste to sand is shown in Table 3 and Figure 5.

Table 3. Density of sand bricks

Weight ratio of PET plastic waste to sand	Average density (kg/m³)	P-Value
1:2	1140	
1:2,2	1102	
1:2,5	1076	
1:2,9	958	0.00003
1:3,3	958	
1:4	885	
1:5	994	

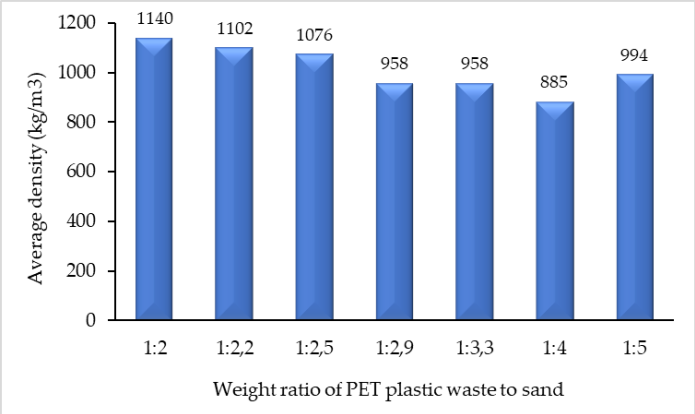

Figure 5. Density of sand bricks

As illustrated in Table 3 and Figure 5, the highest density is observed at weight ratios of PET plastic waste to sand of 1:2. In contrast, the lowest density is observed at weight ratios of 1:4. This phenomenon can be attributed to the fact that the melted PET plastic content at weight ratios of 1:2 is the highest, while at weight ratios of 1:4, it is the lowest. The density of the sand bricks produced in the course of the experiment ranged from 885 to 1140 kg/m³. The density of sand bricks with various weight ratios of PET plastic waste to sand is less than that of clay brick masonry, which has a density of 1700 kg/m³. From the ANOVA analysis, the P-value was obtained as 0.00003 < 0.05, which shows that the weight ratio of PET plastic waste to sand used has a significant effect on density.

4. Conclusions

The incorporation of melted PET plastic waste as a binder in the production of sand bricks effectively enhances the material's properties, ensuring it meets necessary construction standards, including compressive strength and water absorption requirements. The addition of PET plastic, which acts as a bonding agent, significantly contributes to achieving the required compressive strength, thereby making these bricks

structurally sound and suitable for various building applications. Moreover, the integration of this plastic waste results in sand bricks with improved absorption characteristics, aligning with established building material standards. Another advantageous property of utilizing PET plastic as a binder is the resultant decrease in the bricks' overall weight compared to traditional clay-based bricks, which can facilitate easier handling and reduce transportation costs. This approach not only provides an innovative solution to plastic waste management but also offers a sustainable and potentially cost-effective alternative to conventional building materials.

5. Acknowledgements

The authors would like to thank the Civil Engineering Study Program, Faculty of Engineering, Janabadra University, Yogyakarta, for all the facilities and assistance in completing this research.

Author Contributions: Conceptualization, experimental design, A.G., M.S.W., P.A., B.S., conducting experiments and data acquisition, M.S.W., A.G., P.A., B.S., writing and editing, A.G. and M.S.W. All authors have read and approved the published version of the manuscript.

Funding: None.

Conflicts of Interest: The authors declare no conflict of interest.

References

[1] Abdel Tawab OF; Amin MR; Ibrahim MM; Abdel Wahab M; Abd El Rahman EN; Hassanien RH; Hatem MH; Ghaly AE. Recycling Waste Plastic Bags as a Replacement for Cement in Production of Building Bricks and Concrete Blocks Advanced Applications of Solar Energy in Greenhouses for Energy and Food Production. ID:33456 View Project. *J. Waste Resour. Recycl.* **2020**, *1* (05300205020516009), 1-13.

[2] Al-Sinan, M. A.; Bubshait, A. A. Using Plastic Sand as a Construction Material toward a Circular Economy: A Review. *Sustainability* **2022**, *14*(11), 1-17. https://doi.org/10.3390/su14116446.

[3] Ikechukwu, A. F.; Naghizadeh, A. Utilization of Plastic Waste Material in Masonry Bricks Production Towards Strength, Durability and Environmental Sustainability. *J. Sustain. Archit. Civ. Eng.* **2022**, *30*(1), 121-141. https://doi.org/10.5755/j01.sace.30.1.29495.

[4] Suriyaa, M.; Hareharan, P.; Nageshwaran, J.; Nandhini, S.; Sathyamoorthy, R. Experimental Study on Strength Behaviour of Plastic Sand Bricks. *Int. J. Sci. Eng. Res.* **2020**, *9*(6), 1-9. https://doi.org/10.21275/SE21524114751.

[5] Kulkarni, P.; Ravekar, V.; Rao, P. R.; Waigokar, S.; Hingankar, S. Recycling of Waste HDPE and PP Plastic in Preparation of Plastic Brick and Its Mechanical Properties. *Clean. Mater.* **2022**, *5*(June), 1-7. https://doi.org/10.1016/j.clema.2022.100113.

[6] Chowdhury, T. U.; Mahi, M. A.; Haque, K. A.; Rahman, M. M. A Review on the Use of Polyethylene Terephthalate (PET) as Aggregates in Concrete. *Malaysian J. Sci.* **2018**, *37*(2), 118-136. https://doi.org/10.22452/mjs.vol37no2.4.

[7] Bachtiar, E.; Mustaan; Jumawan, F.; Artayani, M.; Tahang; Rahman, M. J.; Setiawan, A.; Ihsan, M. Examining Polyethylene Terephthalate (Pet) as Artificial Coarse Aggregates in Concrete. *Civ. Eng. J.* **2020**, *6*(12), 2416-2424. https://doi.org/10.28991/cej-2020-03091626.

[8] Guendouz, M.; Debieb, F.; Boukendakdji, O.; Kadri, E. H.; Bentchikou, M.; Soualhi, H. Use of Plastic Waste in Sand Concrete. *J. Mater. Environ. Sci.* **2016**, *7*(2), 382-389.

[9] Hossain, M.; Bhowmik, P.; Shaad, K. Use of Waste Plastic Aggregation in Concrete as a Constituent Material. *Progress. Agric.* **2016**, *27*(3), 383-391. https://doi.org/10.3329/pa.v27i3.30835.

[10] Thiam, M.; Fall, M.; Diarra, M. S. Mechanical Properties of a Mortar with Melted Plastic Waste as the Only Binder: Influence of Material Composition and Curing Regime, and Application in Bamako. *Case Stud. Constr. Mater.* **2021**, *15*(May), 1-12. https://doi.org/10.1016/j.cscm.2021.e00634.

[11] Agyeman, S.; Obeng-Ahenkora, N. K.; Assiamah, S.; Twumasi, G. Exploiting Recycled Plastic Waste as an Alternative Binder for Paving Blocks Production. *Case Stud. Constr. Mater.* **2019**, *11*(2019), 1-8. https://doi.org/10.1016/j.cscm.2019.e00246.

[12] Tufa, M.; Tafesse, D.; Tolosa, S.; Murgan, S. Study of Sand-Plastic Composite Using Optimal Mixture Design of Experiments for Best Compressive Strength. *Mater. Today Proc.* **2021**, *47*(Part 1), 480-487. https://doi.org/10.1016/j.matpr.2021.05.031.
[13] Sulyman, M.; Haponiuk, J.; Formela, K. Utilization of Recycled Polyethylene Terephthalate (PET) in Engineering Materials: A Review. *Int. J. Environ. Sci. Dev.* **2016**, *7*(2), 100-108. https://doi.org/10.7763/ijesd.2016.v7.749.
[14] Bamigboye, G. O.; Ngene, B. U.; Ademola, D.; Jolayemi, J. K. Experimental Study on the Use of Waste Polyethylene Terephthalate (PET) and River Sand in Roof Tile Production. *J. Phys. Conf. Ser.* **2019**, *1378*(4), 1-9. https://doi.org/10.1088/1742-6596/1378/4/042105.
[15] Sahani, K.; Joshi, B. R.; Khatri, K.; Magar, A. T.; Chapagain, S.; Karmacharya, N. Mechanical Properties of Plastic Sand Brick Containing Plastic Waste. *Adv. Civ. Eng.* **2022**, *2022*, 1-10. https://doi.org/10.1155/2022/8305670.
[16] Chauhan, S. S.; Kumar, B.; Singh, P. S.; Khan, A.; Goyal, H.; Goyal, S. Fabrication and Testing of Plastic Sand Bricks. *IOP Conf. Ser. Mater. Sci. Eng.* **2019**, *691*(1), 1-12. https://doi.org/10.1088/1757-899X/691/1/012083.
[17] Reta, Y.; Mahto, S. Manufacture of Tiles Using Waste Plastic and River Sand. *Int. J. Res.* **2019**, *06*(10), 335-341.
[18] Ikechukwu, A. F.; Shabangu, C. Strength and Durability Performance of Masonry Bricks Produced with Crushed Glass and Melted PET Plastics. *Case Stud. Constr. Mater.* **2021**, *14*, e00542. https://doi.org/10.1016/j.cscm.2021.e00542.
[19] Maunahan, B.; Adeba, K. Production of Hollow Block Using Waste Plastic and Sand. *Am. J. Sci. Eng. Technol.* **2021**, *6*(4), 127-143. https://doi.org/10.11648/j.ajset.20210604.15.
[20] Zuraida, S.; Harmaji, A.; Pratiwi, S.; Ruitan, X. D. E. A.; Anggraini, A. N.; Kurniadevi, Y. S.; Dewancker, B. J. Comparative Study on Mechanical Properties of Waste Composite Materials for Bricks Application. *J. Phys. Sci. Eng.* **2022**, *7*(2), 92-98. https://doi.org/10.17977/um024v7i22022p092.
[21] Ursua, J. R. S. Plastic Wastes, Glass Bottles, and Paper: Eco-Building Materials for Making Sand Bricks. *J. Nat. Allied Sci.* **2019**, *3*(1), 46-52.
[22] SIPSN. *Sistem Informasi Pengelolaan Sampah Nasional, Komposisi Sampah*. https://sipsn.menlhk.go.id/sipsn/public/data/komposisi.
[23] SNI 03-0349-1989. Bata Beton Untuk Pasangan Dinding. Badan Standarisasi Nasional: Jakarta, Indonesia **1989**, pp 1-6.
[24] SNI-15-2094-2000. Bata Merah Pejal Untuk Pasangan Dinding. *Badan Standar Nasional Indonesia*. Badan Standardisasi Nasional: Jakarta, Indonesia **2000**, pp 11-22. http://sispk.bsn.go.id/.

ASEAN
Journal of Scientific and Technological Reports
Online ISSN:2773-8752

Research article

Germination-Mediated Alterations in Physicochemical, Functional and Cooking Properties of Vigna aconitifolia Flour

Venipriyadharshini Loganathan[1*], and Kavitha Kandhasamy[2]

[1] Department of Nutrition and Dietetics, Periyar University, Salem, India; 636 011
[2] Department of Foods and Nutrition, Vellalar College for Women, Erode, India, 638 012
* Correspondence: venicnd@gmail.com

Citation:
Longanathan, V.; Kandhasamy, K. Germination-Mediated alterations in physicochemical, functional, and cooking properties of vigna conitifolia flour. *ASEAN J. Sci. Tech. Report.* **2025**, *28*(4), e258185. https://doi.org/10.55164/ajstr.v28i4.256897.

Article history:
Received: November 20, 2024
Revised: May 26, 2025
Accepted: June 11, 2025
Available online: July 25, 2025

Abstract: A *Vigna aconitifolia (V.aconitifolia),* also known as moth bean, is a nutrient-rich legume that is commonly consumed in many parts of the world. Germination is a process that can enhance the nutritional and functional properties of legumes. However, there is limited information on the effects of germination on the physicochemical, functional, and cooking attributes of *V. aconitifolia.* The objectives of this study were to evaluate the effects of germination on the physicochemical, functional, and cooking attributes of *V. aconitifolia* and to compare the properties of germinated and ungerminated *V. aconitifolia* seeds. Seeds were germinated for 24 hours and then dried and milled into flour. The physico-chemical properties of the flour, including moisture content, ash content, and pH, were evaluated. The functional properties, including water absorption, oil absorption, and emulsification capacities, were also evaluated. The cooking characteristics, including cooking time, water uptake ratio, and swelling power, were evaluated using standard methods. The results showed that germination significantly improved the physicochemical properties of *V.aconitifolia*, including moisture content, ash content, and pH. The functional properties, including water absorption, oil absorption, and emulsification capacities, were also significantly improved. The cooking characteristics, including cooking time, water uptake ratio and swelling power, were significantly reduced. The results suggest that germination can enhance the nutritional and functional properties of *V.aconitifolia*, but may also affect its cooking characteristics. The findings of this study have significant implications for the food industry, as they suggest that germination can be a simple and effective method to enhance the quality and functionality of legume flours.

Keywords: *V.aconitifolia*; germination; physico-chemical & functional properties; cooking characteristics; nutritional quality

1. Introduction

Vigna aconitifolia (V.aconitifolia), a nutrient-rich legume native to western and northern India, has been an underutilized crop in regular diets, despite its potential as a valuable source of protein, fiber, and antioxidants [1]. This legume plays a vital economic role, particularly in rural India, where it serves as a cash crop, providing income for farmers. Moreover, *V.aconitifolia* 's nutritional profile makes it an attractive alternative to cereals, which dominate Indian diets but often lack protein digestibility [2].However, *V.aconitifolia's utilization is hindered by limitations such as low protein digestibility,*

high phytic acid content, and a coarse texture. Germination, a cost-effective and straightforward processing technique, has been shown to enhance the nutritional and functional properties of legumes[3]. This process involves soaking, sprouting, and drying the seeds, which activates enzymes that break down phytic acid and other anti-nutrients. Germination has been demonstrated to improve protein digestibility, mineral bioavailability, and antioxidant activity in *V.aconitifolia* [4].The findings of this study have significant implications for the food industry, particularly in the development of novel, nutrient-dense food products. By enhancing the nutritional and functional properties of *V.aconitifolia*, germination can unlock new opportunities for food manufacturers, processors, and marketers. Moreover, the increased availability of nutrient-rich, germinated *V.aconitifolia* can contribute to addressing malnutrition, promoting sustainable agriculture, and supporting the growth of the food industry in India and beyond.

2. Methodology

2.1 Selection and Processing of *V.aconitifolia*

V.aconitifolia (moth bean) is a nutrient-rich legume that is widely cultivated in Tamil Nadu, India. Two genotypes of *V.aconitifolia*, TN 12 (wild type) and TN 27 (cultivation), were identified by Tomooka et al. [5] and Tomooka et al. [6]. Based on cultivation and availability throughout the year, TN 27 was selected for this study. The selected variety was procured from farmers in the Namakkal district of Tamil Nadu. The legume was manually winnowed to remove dust and other unwanted solid matter. The selected legume was authenticated by the Botanical Survey of India, Southern Regional Center, Coimbatore, Tamil Nadu. The *V.aconitifolia* seeds were cleaned, washed, and sun-dried at 38°C for 24 hours. The seeds were then roasted in an iron tawa and finely powdered using a high-speed food processor equipped with a stainless steel blade. The powder was processed to achieve a uniform particle size, passing through a 60-mesh sieve (particle size ≤ 250 μm). The powder was stored in an airtight container for later use.

2.2 Germination

The germination process of *V.aconitifolia* was initiated by selecting healthy, mature seeds. To prevent fungal growth, the seeds were washed with distilled water to remove any residual mercuric chloride, and then soaked in distilled water for 8 hours to facilitate germination. The soaked seeds were transferred to a germination tray lined with moist paper towels, covered with a thin layer of moist paper towels, and maintained at a temperature of 25°C and relative humidity of 80%. The seeds were allowed to germinate for different periods, namely 12, 24, 36, and 48 hours, and monitored for changes in color intensity, which was evaluated using a subjective scale (High, Medium, Low). The color intensity was recorded at each time point to assess the progression of germination. The germination process was terminated by drying the germinated seeds in a hot air oven at 50°C for 2 hours [7].

2.3 Physicochemical characteristics of Ungerminated and Germinated *V.aconitifolia* Flour

The physical characterization of *V.aconitifolia* was determined, as its characterization indicates the adaptability of the legume. Analyzing the physical characteristics of the legume is most important, as it helps to anticipate the performance of the legume. The most common parameters used for assessment were shape, size, weight, volume, sphericity, and Density [8]. The understanding of the physical characterization of legumes, such as surface area, true density, sphericity, volume, bulk Density, projected area, and dimensions, is crucial to counter the difficulties and enhance the capacity of the legume during post-harvesting, processing, and storage. The procedure followed is explained under the following headings. Physico–chemical properties influence the processing, storage period, preparation process, and consumption, and hence, palatability increases when the quality of physico-chemical reactions is within a proper range [9]. The following physicochemical characteristics of *V.aconitifolia* flour (ungerminated and germinated) were studied using standard procedures (triplicate):

2.3.1 Thousand Legume Weight

The thousand legumes were randomly selected and weighed using an electronic weighing balance. The weight of *V. aconitifolia* was taken as the mean of triplicate measurements and noted in grams [10].

2.3.2 Thousand Legume Volumes

The thousand selected legumes were taken in a measuring cylinder. A measured quantity of distilled water (250 ml) was added, and the difference obtained was recorded in milliliters [10].

2.3.3 Length, Breadth, and Thickness of the Legume

The three dimensions were calculated by taking an average of 100 legumes using a vernier caliper (least count = 0.01 cm). If the arrangements of starch matrix in the granules are high, then the thickness of the legume or granule strip is also high [11-12].

2.3.4 Equivalent Diameter

The equivalent diameter or geometric mean of the *V.aconitifolia* was determined by using the given formula by Mohesenin [13]. The measurements were expressed in mm.

$$Dm = (LBT)^{1/3}$$ Where L= length, B= Breadth, T=Thickness

2.3.5 Sphericity

The sphericity of the ungerminated and germinated *V.aconitifolia was* determined as the proportion of the volume of the seed with the same surface area as a sphere. It is calculated by the given formula [14].

$$S\phi\ (\%) = (l \cdot b \cdot t)1/3 \div l$$

2.3.6 Density

The Density of *V. aconitifolia* was determined using the formula Mass/Volume, where V = ((l) × (b) × (h)), and it is expressed in mm. Less moisture and crystallinity result in less Density [11].

2.3.7 Standardization of Germination

The *V.aconitifolia* was soaked for 12 hours and allowed to germinate over four different periods, as follows, and the growth of the sprout was noted [15]. The temperature was under control at 300 °C (Table I). The International Seed Testing Association (ISTA) has standardized testing procedures for several medicinal plants and seeds. It also exposed the procedures [16]. The calculated parameters included shoot length, seed germination, and weight [17]. The properties of germinated legumes with different germination hours were calculated and discussed in the results.

2.3.8 Bulk density

Bulk Density of ungerminated and germinated *V.aconitifolia* flour was calculated by the measurement of proportion of mass of the legumes to its volume in total (Ungerminated & germinated) was determined (g/ml) by the formula and method used in the article Shreelalitha [14]. When the physicochemical factors of a legume are said to be beneficial, the impact of anti–nutritional factors in the legume will be lower [10].

2.3.9 True Density

True Density of *V.aconitifolia* flour (Ungerminated & germinated) was estimated by the method of sand displacement [18]. When the moisture content is high, the true density will decrease. True density was determined by the following equation quoted by Matouk et al. [19].

$$Pt = \frac{Ms}{V1}, kg/m3.$$

Where, Pt True Density of *V.aconitifolia*, kg/
M^3; M_s; Weight of the *V.aconitifolia*, kg;

V_i: Displaced Volume of Toluene, M^3

2.3.10 Porosity

Porosity of *V.aconitifolia* flour (Germinated & ungerminated) was estimated by measuring the percentage of space of the inner volume of the legume into the volume of legume bulk [19].

Porosity = P1-P2/ P2
Where P= Porosity of *V.aconitifolia* flour (%);
P1 – Constant pressure inside the tank 1
P2 - Constant pressure inside the tanks 1 and 2

2.3.11 Scanning Electron Microscope (SEM)

SEM analysis was done in the laboratory of Periyar University a clear picture of starches present in ungerminated and germinated *V.aconitifolia* (The morphological study of starch)were recorded with the magnification of 300x, 1000x 2000x, 3000x and 5000x with the range of 100µm,20 µm, 10µm,10 µm and 5 µm(Make: Carl Zeiss Microscopy GmbH Germany). The SEM analysis helps in understanding the structure of films present in both ungerminated and germinated *V.aconitifolia* flour [11].

2.3.12 Fourier Transform Infrared (FT-IR) Spectra

V.aconitifolia germinated, and a PerkinElmer FT-IR spectrophotometer analyzed non-germinated flour to find the chemical composition of the flour qualitatively; a Vector 22 model made inGermany was used to record the FT–IR in solid state with the Frequency range – 4000 – 400 cm^{-1}[20].

2.4 Functional characteristics of Ungerminated and Germinated *V.aconitifolia* Flour

The good functional properties of legumes result in good output during processing, storage, development, and consumption of the food product. The functional characterization of *V.aconitifolia*, which includes Water absorption capacity, Oil absorption capacity, water solubility index, foaming capacity and index, emulsification, and antinutritional factors, was determined as it determines the quality of the legume. A functional characteristic purely depends on the activities of physicochemical properties, structure, and composition of the legume [14]. The functional properties of legumes depend on the structure and composition of proteins and amino acids, as well as the influence of other external components [21]. The procedure followed is explained under the following headings

2.4.1 Water Absorption Capacity

Water Absorption Capacity (WAC) is used to determine the legume's ability to absorb water. The assessment is more important because legumes that possess lower WAC have less water-holding capacity, resulting in a poor food product. Legumes that possess high WAC have a high water-holding capacity, which results in achieving brittle and dry conditions [9]. WAC was determined by adding 40 mL of water to the mixture of 2 g of *V. aconitifolia* flour and stirring well at a continuous speed for one hour using a Griffin flask shaker. The mixture was then centrifuged at 220 rpm for 10 minutes. The following formula was used for the calculation of the capacity of water absorption [22], and the results obtained were denoted in grams/grams

$$WAC = \frac{Final\ weight\ -\ initial\ weight}{initial\ weight}\ X\ 100$$

2.4.2 Oil Absorption Capacity

Oil Absorption Capacity (OAC) or Fat Absorption Capacity (FAC) was high when the legume contains a high amount of fibre, because of the fibre's capability of holding or trapping fat ata higher level [9]. OAC was determined by the reference of Shuang et al. [23]. 2.5 g of both the ungerminated and germinated *V.aconitifolia* flour in separate test tubes were mixed with peanut oil (30 mL). The mixture was stirred for one minute, left undisturbed for 30 minutes, and then centrifuged for 30 minutes at 3000 g. When the oil formed as a separate layer, it was filtered out using a pipette, and the remaining oil was removed by keeping the tube inverted for 30 minutes. The quantity of oil absorbed by the sample was measured and denoted in grams per gram.

2.4.3 Water Solubility Index

Water solubility index indicates the quantity of the polysaccharide present or released from the legume by adding excess water. The mixture was constantly stirred to control the higher speed during

centrifugation and also to prevent the putrefaction of the starch granules. Both samples were heated in a controlled temperature environment at 85 °C for half an hour with continuous stirring. After heating, the samples were kept outside to cool down to room temperature. The samples were centrifuged at 560g for 15 minutes. The capacity of solubility was determined by evaporating the supernatant solution. The remaining residues were weighed. Using the formula provided below, the water solubility index was calculated [22].

$$\text{WSI (\%)} = \frac{\textit{Weight of the dissolved solid in supernatant}}{\textit{weight of the dry solids}} \text{X100}$$

2.4.4 Foaming Capacity and Stability

Foaming capacity was determined by the reference of Salma, H. A., Nahid et al. [24]. 2g of the sample was mixed with 10 ml of buffer solution at pH ranges in a blender (Moulinex) for 2 minutes at "HI" speed. The blended mixture was transferred to a measuring cylinder (250 ml) After 30 seconds, the volume of foam was measured and noted in %.

$$\text{FC (\%)} = \frac{\text{Volume of flour after whipping} - \text{Volume of flour before whipping}}{\text{Volume of flour before whipping}} \text{X 100}$$

Where FC = Foaming Capacity

Foaming stability was determined using the same procedure, but the volume of foam was measured after a 15-minute time interval. The formula used was taken from the reference of Nahid etal. [24], and it was given below

$$\text{FS (\%)} = \frac{\textit{Foam volume of the flour after 15 minutes}}{\textit{Initial foam volume of the flour}} \text{X100}$$

Where FS = Foaming Stability

2.4.5 Emulsification Capacity

The capacity used to determine the emulsifying property of the legume flour was determined by the method followed by Shuang et al. ([23] and Adeleke and Odedeji[25]. 3.5 g of ungerminated and germinated *V.aconitifolia* flour was mixed with distilled water in a separate test tube and homogenized at 10,000 rpm for 30 seconds using a High-Speed Homogenizer. Then another 25 ml of oil (peanut) was mixed with the same sample and homogenized for another 90 seconds. The formed emulsion was equally divided and transferred into centrifuge tubes, which were then centrifuged for 5 minutes at 1100 g. The capacity of emulsification was calculated by dividing the volume of foam produced after centrifugation by the volume before centrifugation.

2.5 Cooking Characteristics of Ungerminated and Germinated *V.aconitifolia* Flour

When compared to the utilization of pulses, the use of food in the form of legumes is less due to multiple factors. The hardness present in the legumes makes difficult to cook and decreases the palatability; inhibiting enzymes etc but good quality cooking can help in counteract those factors [26]. cooking characteristics of the legume can be assessed to precise the value of a legume to develop a good food product and also for the process of incorporation of a food product.

2.5.1 Optimum Cooking Time (min)

The cooking time of *V.aconitifolia* was determined by cooking 2g of *V.aconitifolia* grains in 20 ml of distilled water. The distilled water was kept in a 100 ml beaker and heated using a boiling water bath. The *V.aconitifolia grains were taken after 25 minutes of cooking and pressed between two plates;* the time taken for optimum cooking was recorded [14].

2.5.2 Water Uptake Ratio (%)

The water uptake ratio of *V.aconitifolia* grains was calculated by cooking 2 grams of grains with 20 ml of distilled water. The grains were then placed in a 100 ml beaker with water and allowed to heat in an electric heater. After the grains were cooked, they were removed. It was calculated using the formula below [14].

$$\text{Water uptake ratio}(\%) = \frac{\text{Weight of cooked grains}}{\text{Weight of uncooked grains}} \times 100$$

2.5.3 Elongation Ratio (mm)

The average length of the uncooked *V.aconitifolia* grains was recorded. Then, 2g of V. aconitifolia grains were taken in a beaker with 20 ml of distilled water and cooked using an electric heater. When the grains reached their optimum cooking time, they were taken to measure the length of the grain. The elongation ratio was calculated using the formula below[14].

$$\text{Elongation ratio (mm)} = \frac{\textit{Legthofthe cooked grains}}{\textit{length of the uncooked grains}}$$

2.5.4 Alkali Spreading Value

V.aconitifolia (10 seeds) were taken and placed with individual spacing in a petri dish with 1.7% Potassium Hydroxide solution (10 ml). The petri dish was then placed in an incubator at a temperature of 27.8 °C for 24 hours. The value of the spreading of each grain was measured by a 7-point numerical scale [22].

2.5.5 Swelling Power (%)

Swelling power was determined by the Reference of Malomo et al. [22-27]. 40 ml of distilled water was added to a 50 ml centrifuge tube, along with 1 gram of ungerminated and germinated V. aconitifolia flour, and the volume was denoted in ml/grams. The divergence in positioning of starch and amylase within the granules influences the capacity for swelling and solubility [27].

2.6 Statistical Analysis

The data were analyzed using descriptive statistics to summarize the physical and functional properties of *V.aconitifolia.* The mean and standard deviation (SD) were calculated for each parameter. The experiment was conducted in triplicate (n = 3). The data were presented in tables to provide a clear overview of the results. All statistical analyses were conducted using SPSS version 20.

3. Results and Discussion

3. 1 Standardization of Germination

Table 1. Growth of the sprout with different colours based on hours

Variation	Germination Hours	Colour intensity
I	12	High
II	24	High
III	36	Medium
IV	48	Low

The changes in color intensity of the sprout over time (Table 1) can be attributed to physiological changes during germination. Initially, the high color intensity observed at 12 and 24 hours may be due to the breakdown of seed dormancy and the initiation of germination, characterized by enzyme activation and the mobilization of stored nutrients. As germination progresses, the seedling's reliance on stored nutrients decreases, transitioning to a photosynthesis-based food production system. This shift may be reflected in the decrease in color intensity from medium to low between 36 and 48 hours.

The decrease in color intensity over time may also be related to pigment degradation, such as anthocyanins responsible for initial sprout coloration [28]. As the seedling grows, new pigment production (e.g., chlorophyll) may contribute to changes in color intensity. This is consistent with studies showing that chlorophyll biosynthesis and photosynthesis increase during germination [29]. Additionally, physiological and biochemical changes during germination, such as the breakdown of stored nutrients and the activation of enzymes, can also influence seedling coloration.

3.2 Physicochemical Characterization of Ungerminated and Germinated *V.aconitifolia*

The physical properties like legume length, breadth, thousand kernel weight, equivalent diameter, and sphericity of *V.aconitifolia* are presented in Table .2.

Table 2. Physical characterization of *V.aconitifolia* legume

S. No.	Physical Properties	Ungerminated *V.aconitifolia* legume	Germinated *V.aconitifolia* legume
1.	Thousand Legume weight (g)	4.00±0.23	6±0.22
2.	Thousand kernel volume (ml)	3.6±0.16	5.4±0.27
3.	Legume length(cm)	0.46±0.02	0.57±0.03
4.	Legume breadth (cm)	0.3±0.01	0.6±0.01
5.	Thickness (cm)	0.47±0.02	0.52±0.03
6.	Equivalent diameter(cm)	0.0135±0.001	0.0148±0.001
7.	Sphericity (cm)	0.03±0.001	0.05±0.002
8.	Density (mm)	1.1±0.01	1.6±0.02

The physical properties of *V.aconitifolia* legume were significantly affected by germination. The thousand-legume weight and thousand kernel volume increased by 50% and 50%, respectively, after germination. This increase in weight and volume is consistent with previous studies, which reported that germination can improve the physical properties of legumes [3-4]. The legume length, breadth, and thickness also increased after germination, indicating an overall increase in size. The equivalent diameter and sphericity of the legume increased slightly from 0.03 to 0.05 after germination, indicating a minor change in shape.

These results are in agreement with a recent study, which reported that germination can improve the physical properties of legumes, including size, shape, and texture [14].

The density of the legume also increased after germination, indicating an improvement in compactness. This result is consistent with previous studies, which reported that germination can improve the density of legumes [3-4]. Overall, the results suggest that germination can significantly improve the physical properties of *V.aconitifolia* legume, making it a more desirable ingredient for food applications.

Table 3. Physical characterization - Bulk Density, True Density, and Porosity

S.No.	Physical Characterization	Ungerminated *V.aconitifolia*flour (g)	Germinated *V.aconitifolia*flour(g)
1.	Bulk density (ml)	0.783 ± 0.02	0.691 ± 0.02
2.	True Density (ml)	1.349 ± 0.01	1.234 ± 0.01
3.	Porosity (%)	41.76 ± 2.66	44.31 ± 2.04

The physical characterization (Table 3) of *V.aconitifolia* flour revealed interesting results. The bulk density and true density values were found to be similar, indicating minimal porosity or void space between the particles. This suggests that the germination process may not have significantly altered the physical structure of the *V.aconitifolia* flour. The similar density values could be attributed to the dense packing of particles, which may not have been affected by the germination process.

The porosity of ungerminated *V.aconitifolia* flour was 41.76%, which increased to 44.31% after germination. This increase in porosity can be attributed to the breakdown of complex cellular structures and the activation of enzymes during the germination process. Specifically, the enzymes α-amylase, β-amylase, and proteases are activated, breaking down starches and proteins into simpler molecules [4]. This breakdown creates more spaces within the flour, leading to increased porosity. Furthermore, the germination process also involves the degradation of phytic acid, a compound that can inhibit enzyme activity and bind minerals [3]. The reduction of phytic acid during germination can contribute to the increased porosity and improved

nutritional availability of the flour. Overall, the results suggest that germination can improve the physical properties of *V.aconitifolia* flour, making it a more desirable ingredient for food applications."

Table 4. Scanning Electron Microscopy (SEM) Analysis of Ungerminated and Germinated *V.aconitifolia* Flour

S. No	Particulars		*V.aconitifolia* Flour	Germinated *V.aconitifolia* Flour
	Magnitude (X)	Range (μm)		
1.	300	100	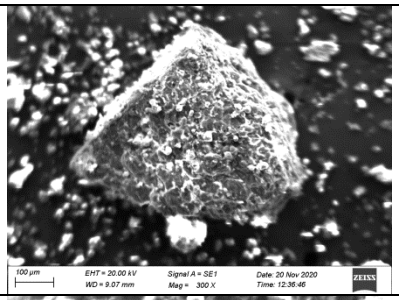	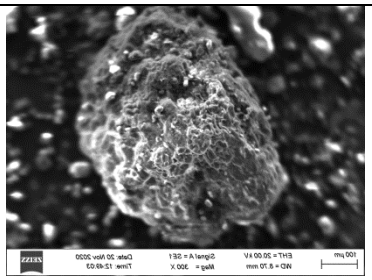
2.	1000	20	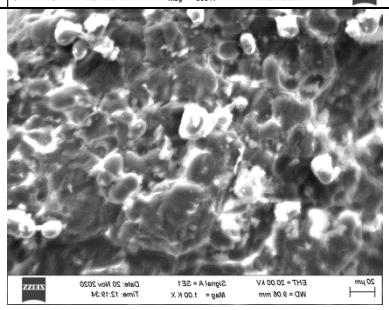	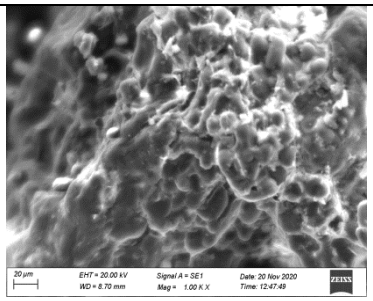
3.	2000	10	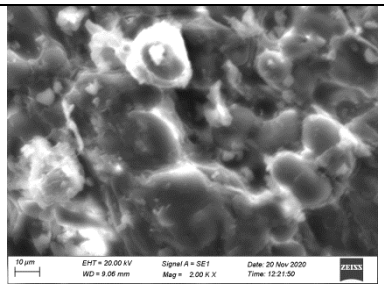	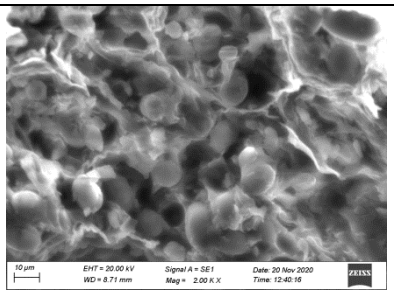
4.	3000	10	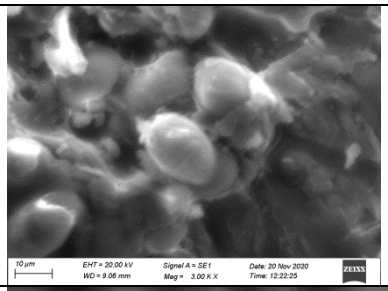	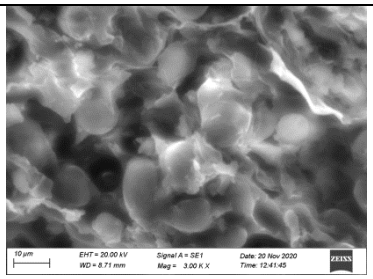
5.	5000	5	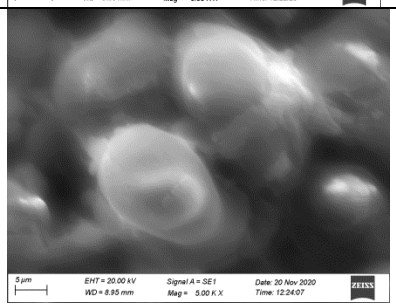	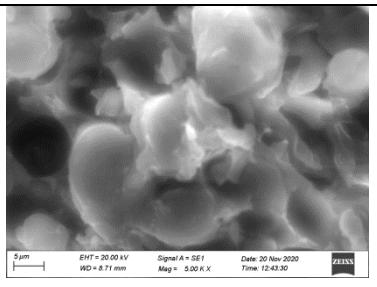

The SEM micrographs of *V.aconitifolia* flour and germinated *V.aconitifolia* flour (Table 4) revealed distinct topographical features, underscoring the impact of germination on the physical properties of the flour. The images, captured at various magnifications, showcased a range of surface morphologies, including triangular, elliptical, pipe arch, and oval shapes, which were more pronounced in the germinated sample.

The SEM analysis revealed a soft and smooth surface texture for both ungerminated and germinated *V.aconitifolia* flour, with no visible pores. This observation is consistent with previous studies, which reported similar surface characteristics in moth bean granules [30]. Furthermore, the SEM images revealed the presence of both small and large starch granules in both ungerminated and germinated *V.aconitifolia* flour, with shapes ranging from cylindrical to oval and elliptical. This finding is corroborated by the high starch content reported in *V.aconitifolia*[4].

The germinated sample exhibited a more heterogeneous surface morphology, with a greater presence of irregularly shaped starch granules. The SEM analysis revealed changes in the starch granule structure of *V.aconitifolia* flour after germination, suggesting potential alterations in its functional properties. During germination, the activity of enzymes such as amylase and protease can lead to the partial degradation of starch granule structures, resulting in changes to the molecular structure and breakdown of starch. These changes may impact the flour's texture, solubility, and digestibility. Further research is needed to fully understand the effects of germination on starch breakdown and molecular structural changes in *V. aconitifolia* flour.

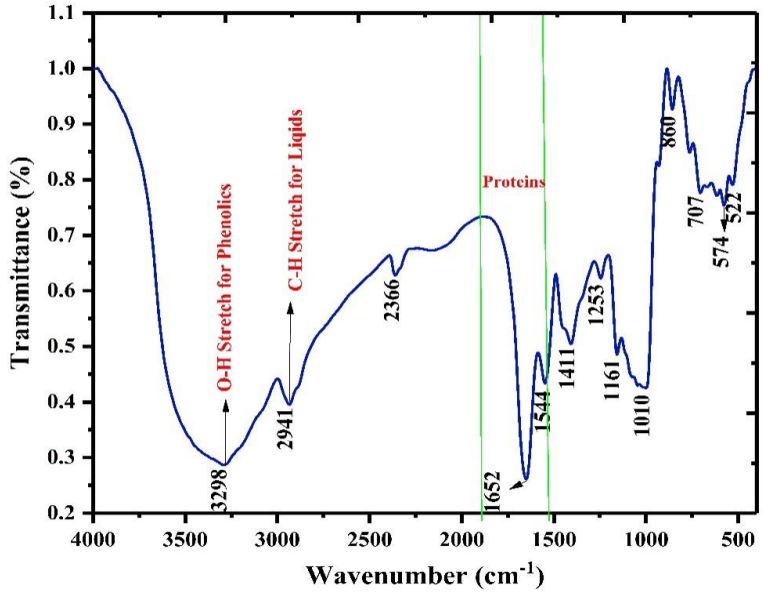

Figure 1. Graphical Representation of Fourier Transform Infrared (FT-IR) Spectra of ungerminated *V.aconitifolia*

The FTIR spectral imaging comparison between ungerminated and germinated *V.aconitifolia* flour reveals significant biochemical differences associated with germination. FTIR absorbance intensity at various wave numbers is indicative of the concentration of biomolecular functional groups such as proteins, lipids, and phenolic compounds.

Fourier Transform Infrared (FTIR) spectroscopy was employed to investigate germination-induced alterations in the molecular composition of *V.aconitifolia* flour. Comparison between ungerminated (S1) and germinated (S2) samples revealed significant changes in the infrared absorption patterns, particularly in regions corresponding to key biomolecules. The germinated sample exhibited higher mean absorbance intensity (3.47) compared to the ungerminated one (4), indicating an increased presence of functional groups associated with bioactive and nutritional compounds. This molecular enrichment is consistent with the activation of enzymatic and metabolic pathways during germination, leading to hydrolysis of macromolecules and synthesis of simpler, more bioavailable compounds [31].

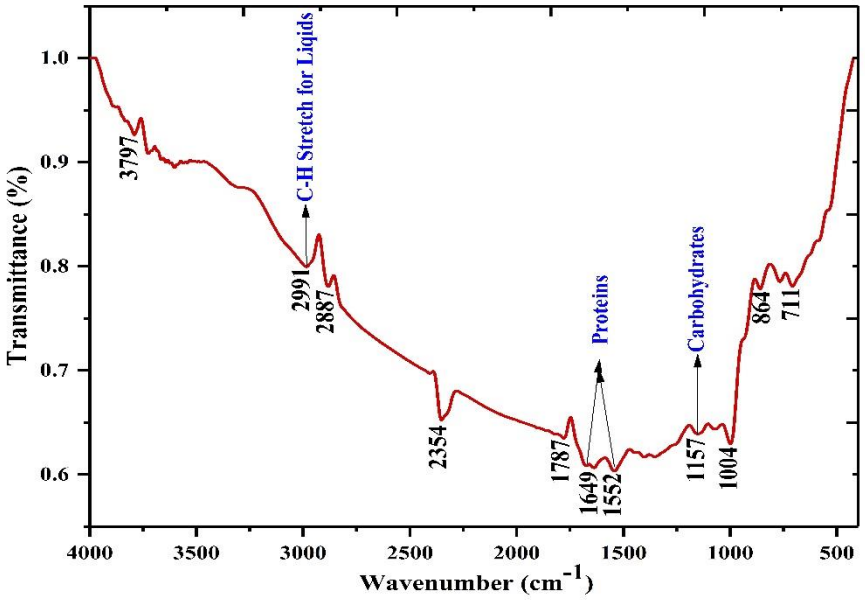

Figure 2 Graphical Representation of Fourier Transform Infrared (FT-IR) Spectra of germinated *V.aconitifolia*

Characteristic absorption bands observed near ~3300 cm^{-1} (O–H stretch) were more prominent in the germinated sample, signifying an increase in hydroxyl-containing compounds, such as phenolics and carbohydrates. These compounds contribute to enhanced antioxidant activity and improved physicochemical functionality. Likewise, the elevated peak intensity around ~2940 cm^{-1}, attributed to C–H stretching in lipids, suggests changes in lipid profiles, possibly through lipid mobilization or remodeling during germination. The bands observed at ~1650 cm^{-1} and ~1540 cm^{-1} correspond to amide I and II regions respectively, and their increased intensity in the germinated flour points to elevated protein levels or conformational changes in existing proteins—alterations that are closely linked with improved dough-forming ability, water absorption, and textural properties relevant to cooking performance.

These structural changes, highlighted by FTIR imaging, support the observed enhancements in the functional and cooking properties of the germinated flour. Improved solubility, emulsifying activity, and thermal behavior, as documented in similar studies, can be attributed to these biochemical transformations [32]. The molecular insights from FTIR spectroscopy thus reinforce the potential of germination as a natural and effective method to enhance the physicochemical and functional value of *V.aconitifolia* flour for use in nutritionally enriched food formulations.

3.3 Functional Properties of Ungerminated and Germinated *V.aconitifolia*

The functional properties (Table 5) of *V.aconitifolia* flour were significantly affected by germination. The water absorption capacity (WAC) of germinated *V.aconitifolia* flour was significantly higher (21 ± 1.65%) compared to ungerminated flour (18 ± 1.66%). This increase in WAC can be attributed to the structural changes in starch granules upon germination. Specifically, the activation of enzymes such as amylase during germination can lead to the disruption of starch granules, increasing the availability of hydrophilic groups, such as hydroxyl and amino groups, on the surface of the starch granules [4]. Additionally, the breakdown of starch molecules into simpler sugars can also contribute to the increased water absorption capacity. These changes in starch structure and composition can enhance the hydrophilic properties of the flour, leading to improved water absorption capacity

Table 5. Functional Properties

S.No.	Functional Properties	Ungerminated *V.aconitifolia*	Germinated *V.aconitifolia*
1.	Water Absorption Capacity (%)	18 ± 1.66	21 ± 1.65
2.	Oil Absorption Capacity (%)	23 ± 1.95	15.62 ± 1.20
3.	Foaming capacity (%)	25 ± 2.05	28 ± 1.85
4.	Emulsification capacity (%)	10.5 ± 0.95	13 ± 1.06
5.	Water solubility index (%)	71.17 ± 4.66	82 ± 4.44

In contrast, the oil absorption capacity (OAC) of germinated *V.aconitifolia* flour was lower (15.62 ± 1.20%) compared to ungerminated flour (23 ± 1.95%). This decrease in OAC can be attributed to the increased availability of hydrophilic groups on the surface of the starch granules after germination, which reduces the ability of the flour to absorb oil [14]. The foaming capacity (FC) of germinated *V.aconitifolia* flour was higher (28 ± 1.85%) compared to ungerminated flour (25 ± 2.05%).

This increase in FC can be attributed to the increased availability of proteins and other surface-active compounds after germination, which enhances the ability of the flour to form and stabilize foams [3]. The emulsification capacity (EC) of germinated *V.aconitifolia* flour was higher (13 ± 1.06%) compared to ungerminated flour (10.5 ± 0.95%). This increase in EC can be attributed to the increased availability of proteins and other surface-active compounds after germination, which enhances the ability of the flour to form and stabilize emulsions [4].

The water solubility index (WSI) of germinated *V.aconitifolia* flour was significantly higher (82 ± 4.44%) compared to ungerminated flour (71.17 ± 4.66%). This increase in WSI can be attributed to the enhanced enzyme activity during germination, which leads to partial starch degradation. The breakdown of starch molecules into simpler sugars and the increased availability of hydrophilic groups on the surface of the starch granules contribute to improved water solubility [14]. Specifically, the activation of enzymes such as amylase during germination facilitates the hydrolysis of starch molecules, resulting in increased solubility and enhanced ability of the flour to dissolve in water.

3.4 Cooking properties of Ungerminated and Germinated *V.aconitifolia*

The cooking properties (**Table 6.)** of *V.aconitifolia* flour were significantly affected by germination. The optimum cooking time (OCT) of germinated *V.aconitifolia* flour was shorter (18 ± 1.40 minutes) compared to ungerminated flour (25 ± 1.90 minutes). The decrease in Optimum Cooking Time (OCT) can be attributed to the structural modifications of starch and proteins caused by enzymatic activity during germination. Specifically, enzymes such as amylase may partially hydrolyze starch, leading to a softer structure and a shorter cooking time. Additionally, the increased availability of hydrophilic groups on the surface of the starch granules after germination may also contribute to enhanced water absorption, further reducing the cooking time [4].

Table 6. Cooking properties

S.No.	Cooking Properties	Ungerminated *V.aconitifolia* flour	Germinated *V.aconitifolia* flour
1.	Optimum cooking time (min)	25 ± 1.90	18 ± 1.40
2.	Water uptake ratio (%)	18.5 ± 1.22	20 ± 1.82
3.	Elongation ratio(mm)	2.25 ± 0.15	2.95 ± 1.67
4.	Swelling Power (%)	15 ± 0.95	21 ± 1.35

The water uptake ratio (WUR) of germinated *V.aconitifolia* flour was higher (20 ± 1.82%) compared to ungerminated flour (18.5 ± 1.22%). This increase in WUR can be attributed to the increased availability of

hydrophilic groups on the surface of the starch granules after germination, which enhances the ability of the flour to absorb water [14].

The elongation ratio (ER) of germinated *V.aconitifolia* flour was significantly higher (2.95 ± 1.67 mm) compared to ungerminated flour (2.25 ± 0.15 mm). This increase in ER can be attributed to the changes in protein structure and composition during germination, which in turn affect the starch structure. Specifically, the breakdown of protein-starch complexes and the increased availability of proteins and other surface-active compounds after germination can enhance the flexibility of the starch structure, leading to improved gel formation and stability [3]. A higher ER indicates better gel formation in starch, which can contribute to improved texture and structure in food products made from germinated *V.aconitifolia* flour.

The swelling power (SP) of germinated *V.aconitifolia* flour was higher (21 ± 1.35%) compared to ungerminated flour (15 ± 0.95%). This increase in SP can be attributed to the increased availability of hydrophilic groups on the surface of the starch granules after germination, which enhances the ability of the flour to absorb water and swell [4].

4. Conclusion

In conclusion, the present study investigated the effect of germination on the physical, functional, and cooking properties of *V.aconitifolia* flour. The results showed that germination significantly altered the physical properties of the flour, including bulk Density, true Density, and porosity. Specifically, germination led to a decrease in bulk density and true density, while increasing porosity. These changes can impact the functionality and cooking behavior of the flour.

The functional properties, such as water absorption capacity, foaming capacity, and emulsification capacity, were also enhanced after germination. Furthermore, the cooking properties, including optimum cooking time, water uptake ratio, elongation ratio, and swelling power, were improved after germination.

Overall, the study suggests that germination can be a useful technique to improve the physical, functional, and cooking properties of *V.aconitifolia* flour, making it a more desirable ingredient for food applications. The improved properties of germinated *V.aconitifolia* flour can be attributed to the increased availability of hydrophilic groups, proteins, and other surface-active compounds after germination.

The findings of this study have important implications for the food industry, as they suggest that germination can be a simple and effective way to improve the quality and functionality of legume flours. Further research is needed to explore the potential applications of germinated *V.aconitifolia* flour in specific food products, such as gluten-free baked goods, starch-based gel formulations, or functional snack foods, where its modified physical and functional properties can be leveraged to enhance nutritional value, texture, and overall product quality.

5. Acknowledgements

Author Contributions:

- Venipriyadharshini Loganathan - The sole author was responsible for the conceptualization, methodology, data collection, analysis and writing
- Kavitha – Supervision and final approval of the manuscript

Funding: This research received no external funding

Conflicts of Interest: The authors declare no conflict of interest

References

[1] Kumar, D.; Singh, M.; Kushwaha, M. Nutrient content, uptake and NUE of oats (2). *Indian Journal of Agronomy* **2021**, *66*, 466-473.

[2] National Nutrition Monitoring Board Report. *Government of India*. **2019**.

[3] Singh, R.; Kølvraa, S.; Bross, P.; Christensen, K.; Bathum, L.; Gregersen, N.; Tan, Q.; Rattan, S.I.S. Anti-inflammatory heat shock protein 70 genes are positively associated with human survival, *Current Pharmaceutical Design* **2010**, *16*(7), 796-801. https://doi.org/10.2174/138161210790883499

[4] Tomooka, N.; Senthil, N.; Pandiyan, M.; Ramamoorthi, N.; Kaga, A.; Vaughan, D.A. Collection and conservation of leguminous crops and their wild relatives in Tamil Nadu, India, *Annual Report on Exploration and Introduction of Plant Genetic Resources (NIAS, Tsukuba, Japan)* **2008**, *24*, 113-125.

[5] Tomooka, N.; Pandiyan, M.; Senthil, N.; Ramamoorthi, N.; Kaga, A.; Vaughan, D.A. Collection and conservation of leguminous crops and their wild relatives in Tamil Nadu, India, *Annual Report on Exploration and Introduction of Plant Genetic Resources (NIAS,Tsukuba, Japan)* **2009,** *25*, 83-109.

[6] Kumar, R.; Ghoshal, G.; Goyal, M. Biodegradable composite films/coatings of modified corn starch/gelatin for shelf life improvement of cucumber. *J Food Sci Technol*. **2021**, *58*(4), 1227-1237. https://doi.org/10.1007 /s13197-020-04685-y

[7] Venipriyadharshini, L.; Kavitha, K. Moth Bean (Vigna aconitifolia) as Potential Supplement to Evaluate the Weight Gain in Wistar Albino Rats (Rattus norvegicus). *International Journal of Experimental Research and Review* **2023**, *36*, 127-134. https://doi.org/10.52756/ijerr.2023.v36.012

[8] González-Fonteboa, F.; Martínez-Abella, R.; Rodríguez-Álvaro, E.; Rey-Bouzón, S.; Seara-Paz, M.F. Herrador,3 - Use of coal bottom ash and other waste as fine aggregates in lightweight cement-based materials, *Woodhead Publishing* **2021**, 53-87. https://doi.org/10.1016/B978-0-12-820549-5.00026-7

[9] Zare, F.; Orsat, V.; Boye, J. Functional, Physical and Sensory Properties of Pulse Ingredients Incorporated into Orange and Apple Juice Beverages, *Journal of Food Research* **2015**, *4*, 5. https://doi.org/10.5539/jfr.v4n5p143

[10] Olika, E.; Abera, S.; Fikre, A. Physicochemical Properties and Effect of Processing Methods on Mineral Composition and Antinutritional Factors of Improved Chickpea *(CicerarietinumL.)* Varieties Grown in Ethiopia**,** *International Journal of Food Science* **2019,** 1-7. https://doi.org/10.1155/2019/9614570

[11] Kumar, R.; Ghoshal, G.; Goyal, M. Moth bean starch (Vignaaconitifolia): isolation, characterization, and development of edible/biodegradable films, *Journal of Food Science and Technology* **2019**, *56*(11), 4891-4900. https://doi.org/10.1007/s13197-019-03959-4

[12] Azeredo, HMC.; Waldron, KW. Crosslinking in polysaccharide and protein films and coatings for food contact–a review, *Trends Food Science Technology* **2016**, *52*, 109-122. https://doi.org/10.1016/j.tifs.2016.04.008

[13] Mohsenin, N.N. Physical properties of plant and animal materials. Vol. 1. Structure, physical characterisitics and mechanical properties **1970**, *1*, 734.

[14] Shreelalitha, S.J.; Sridhar, K.R. Physical and Cooking Properties of Seeds of Two Wild Legume Landraces of Sesbania, *International Journal of Agricultural Technology* **2018**, 14(3), 363-376.

[15] Ghasemi-Varnamkhasti, M.; Mobli, H.; Jafari, A.; Keyhani, A.R.; Hedori Soltanabadi, M.; Rafiee, S.; Kheiralipour, K. Some physical properties of rough rice (Oryza Sativa L.) grain. *Journal of Cereal Science* **2008**, 47, 496-501. https://doi.org/10.1016/j.jcs.2007.05.014

[16] Mijivoievic, M.; Zita, R.; Tania, P. Izmene ISTA rules changes in seed germination testing at the beginning of the 21st century, *Journal on Processing and Energy in Agriculture* **2018,** *22*(2), 40-45 https://doi.org/10.5937/JPEA1801040M

[17] Surender, M.; Sagare, D.; Setti, P. Durga, Ch.V.; FarzanaJabeen, Rani.; Sudarshan, M.R.; Sokka Reddy, S. Mean Performance of Normal and QPM Maize Genotypes forYield and Tryptophan Content, *International Journal of Current Microbiology and Applied Sciences* **2017**, *6*(11), 830-844. https://doi.org/10.20546/ijcmas.2017.611.098

[18] American Society of Agricultural Engineers. ASAE S352.2: Moisture Measurement-Unground grain and seeds. *In ASAE Standards* **2001,** 549-555.

[19] Matouk. Physical properties of legumes. *Journal of Food Science and Technology* **2018,** *55*(2), 533-539.

[20] Tosh, S.M.; Yada, S. Dietary fibres in pulse seeds and fractions: characterization, functional attributes and applications. *Food Research International* **2010**, *43*, 450-460. https://doi.org/10.1016/j.foodres.2009.09.005

[21] Flores, F.; Singh, J.; Kerr, W.L.; Parrish, D.; Shi, Y. Physical and chemical properties of sweet potato purees during processing. *Journal of Food Science* **2012**, *77*(4), S1448-S1455. https://doi.org/10.1111/j.1750-3841.2012.02672.x

[22] Evelyn, S.; Buckman, Ibok Oduro,Wisdom A. Plahar,Charles Tortoe, Determination of the chemical and functional properties of yam bean (*Pachyrhizuserosus* (L.) Urban) flour for food systems, *Food Science & Nutrition* **2017**, *6*(2), 457-463. https://doi.org/10.1002/fsn3.574

[23] Shuang-kui, D.; Hongxin, J.; Xiuzhu,Y.; Jay-lin, J. Physicochemical and functional properties of whole legume flour, *LWT-Food Science and Technology* **2014**, *55*(1), 308-313. https://doi.org/10.1016/j.lwt.2013.06.001

[24] Salma, H. A.; Nahid, A. A.; ElShazali, A. M.; Isam, Elfadil E. B. Changes in the functional properties as a function of NaCl concentration of legumes protein isolate by Trans glutaminase cross linking *International Food Research Journal* **2010**, *17*, 817-824.

[25] Adeleke, R.O.; Odedeji, J.O. Functional Properties of Wheat and Sweet Potato Flour Blends. *Pakistan Journal of Nutrition* **2010**, *9*, 535-538. http://dx.doi.org/10.3923/pjn.2010.535.538

[26] Ghumman, A.; Kaur, A.; Singh, N. Functionality and digestibility of albumins and globulins from lentil and horse gram and their effect on starch rheology, *Food Hydrocoll* **2016,** *61*, 843-850. https://doi.org/10.1016/j.foodhyd.2016.07.013

[27] Wani, IA.; Sogi, DS. Hamdani. Isolation, composition, and physicochemical properties of starch from legumes: a review. *Starch/Starke* **2016,** *68*, 834-845. https://doi.org/10.1002/star.201600007

[28] Zhang, Y.; Li, M.; Wang, X. Anthocyanins regulate seedling growth and development by modulating auxin signaling. *Plant Physiology* **2019**, *181*(2), 641-653. https://doi.org/10.1104/pp.19.00851

[29] Wang, X.; Li, Z.; Chen, G. Chlorophyll biosynthesis and photosynthesis in germinating rice seeds. *Journal of Plant Physiology*, **2020**, *247*, 153141. https://doi.org/10.1016/j.jplph.2020.153141

[30] Balakrishnan, P.; Sreekala, MS., Thomas, S. Morphology, transport characteristics and viscoelastic polymer chain confinement in nano composites based on thermoplastic potato starch and cellulose nano fibers from pineapple leaf. *CarbohydrPolym* **2017,** *169,* 176-188. https://doi.org/10.1016/j.carbpol.2017.04.017

[31] Chandrasekara, A.; Shahidi, F. Determination of antioxidant activity in free and hydrolyzed fractions of millet grains and characterization of their phenolic profiles by HPLC-DAD-ESI-MS^n. *Journal of Functional Foods* **2011**, *3*(3), 144-158. https://doi.org/10.1016/j.jff.2011.03.006

[32] Nkhata, S. G.; Ayua, E.; Kamau, E. H.; Shingiro, J. B. Fermentation and germination improve nutritional value and functionality of foods: A review. *Food Science & Nutrition* **2018,** *6*(8), 2449-2458. https://doi.org/10.1002/fsn3.846

ASEAN
Journal of Scientific and Technological Reports
Online ISSN:2773-8752

Research article

Varietal Performance of Hybrid Corn Fertilized with Ammonium Fertilizers in an Alkaline Soil Under Drought Conditions

Sheryl Eden Gay Puyod[1], and Pet Roey Pascual[2]

[1] Graduate School, Cebu Technological University-Barili Campus, Barili, Cebu, Philippines
[2] Agribusiness and Development Communication, Cebu Technological University-Barili Campus, Barili, Cebu, Philippines
* Correspondence: sherylpuyod@gmail.com

Citation:
Puyod, S.E.G.; Pascual, P.R. Varietal performance of hybrid corn fertilized with ammonium fertilizers in an alkaline soil under drought conditions. *ASEAN J. Sci. Tech. Report.* **2025**, *28*(4), e257403. https://doi.org/10.55164/ajstr.v28i4.257403.

Article history:
Received: January 7, 2025
Revised: June 1, 2025
Accepted: July 1, 2025
Available online: July 25, 2025

Publisher's Note:
This article has been published and distributed under the terms of Thaksin University.

Abstract: Nitrogen is a vital nutrient that becomes a growth-limiting factor in alkaline soils. Opting for high-quality ammonia fertilizer ensures that crops receive optimal nutrition, tailored to their specific requirements, and facilitates the easier absorption and utilization of nutrients by the soil. A field experiment was conducted to determine the response of corn varieties in alkaline soil applied with different ammonium fertilizers in terms of growth, yield, and physicochemical characteristics. The study was laid out in Randomized Complete Block Design looking into four varieties; two high yielding and two low yielding, applied with two kinds of ammonia fertilizer: di-ammonium phosphate (18-46-0, 187.5 grams/linear meter) and ammonium sulfate (21-0-0, 225 grams/linear meter) based on the 90 N recommended rate. To supplement the P and K requirement, 10 t/ha of organic fertilizer was applied to all treatments. Regarding the high-yielding varieties, one favored ammonium sulfate fertilization in terms of plant height (185.10 ± 0.59 cm), days to silking (57.70 ± 6.05 days), and tasseling (51.83 ± 0.66 days), as well as total soluble solids (1.53 ± 0.08 Brix). The other favored di-ammonium phosphate fertilization in terms of ear weight (118.21 ± 13.91 g/ear), grain weight (98.42 ± 6.35 g/ear), and ear diameter (4.09 ± 0.16 cm). On the other hand, neither of the low-yielding varieties was affected by the type of ammonium fertilizer, except for titratable acidity (34.50 ± 0.49%). Showing, therefore, high-yielding varieties being more responsive to the type of ammonium fertilizer.

Keywords: Ammonium sulfate; di-ammonium phosphate; total soluble solids; hybrid corn; drought

1. Introduction

Corn (*Zea mays* L.) ranks as one of the world's most essential crops and is regarded as the leading cereal cultivated in tropical and subtropical regions [1]. This crop holds significant economic value as it provides a rich source of energy, minerals, vitamins, and essential amino acids [2]. Corn is primarily utilized as food for humans, animal feed, seed, and as an industry in its own right, with around 20% of the population consuming it. It serves as the main component in animal feed production, making up roughly 60-70% of feed ingredients, and is also used in various food and industrial products [3]. More importantly, corn provides a livelihood for 600,000 small farming families [4].

Alkaline soils, which have a high pH, can limit nutrient absorption, posing a challenge to achieving optimal crop yields. Using high-quality fertilizers based on ammonia ensures that crops receive the optimal nutrition for

their specific requirements and enables the soil to absorb and utilize these nutrients efficiently. Nitrogen is frequently a limiting factor for plant growth in both natural ecosystems and agricultural crop production. Ammonium plays a crucial role in the assimilation of nitrogen into organic compounds, regardless of whether the nitrogen comes from ammonium absorption, nitrate reduction, or nitrogen fixation [5]. Effective management of nitrogen fertilization is crucial for both productivity and profitability. However, the existing fertilization system results in the loss of about 60 to 70% of the nitrogen applied [6]. These losses are attributed to various factors, including the type of nitrogen fertilizer, application method, varietal differences, soil characteristics, and cropping systems [7].

This study was conducted to determine how varieties grown under alkaline soil respond to different ammonium fertilizers.

2. Materials and Methods

2.1 Site Description

The study was conducted in the experimental area of Cebu Technological University-Barili Campus, situated approximately 10° 7 57.96′ N latitude, 123° 32′41.2′ E longitude. The experimental area has alkaline soils with distinct physical and chemical characteristics that impact crop performance and nutrient status. The color of soils ranges from dark brown to yellowish brown, with significant differences in consistency between wet and dry states—hard and compact when dry but plastic and sticky when wet. The soils contain high clay content of 46–70% and retain a water-holding capacity of more than 40%. They are alkaline with pH values always above 7.5 [8]. The field experiment was conducted from March to June 2024. This period in Cebu, Philippines, was marked by progressively worsening drought conditions, which are typical for the dry season. During March, temperatures were between 25°C and 31°C, with moderate rains amounting to around 103mm spread over only8 days, suggesting unpredictable precipitation patterns. April showed the beginning of drought stress conditions with temperatures increasing to their peak at 32°C, accompanied by considerably low rainfall of about 81 mm within just 7 days. This was a 21% drop in precipitation from March and defined water-limiting conditions. May witnessed the increase in drought stress with temperatures going into their peak season at 33°C. Even as rainfall rose to 127–147 mm over 8–9 days, the high temperatures and high evapotranspiration levels formed high water deficit conditions. The patches of rainfall formed instances of intense water stress during the inter-catch intervals. June maintained the drought trend with a prolonged high of 30°C, which was very warm for the area. Though a 65% daily average probability of rain, rainfall during the growing season averaged just 11.6 mm per day, which caused cumulative drought stress during the season [9]. These conditions were natural drought conditions for assessing hybrid corn performance in alkaline soils.

2.2 Experimental Design and Treatment

The study was conducted using a Randomized Complete Block Design with three replications. Four varieties of corn were tested, two high-yielding and two low-yielding. The high-yielding and low-yielding designation of the varieties was performed based on past yield performance. These were:

High-yielding 1- A genetically engineered hybrid corn with high grain yield potential (Generally 8–10 t/ha), featuring drought tolerance and excellent stalk strength.

High-yielding 2- A top-performing hybrid type with a yield potential of over 9 t/ha, tolerance to key pests and diseases, and excellent dryland adaptation.

Low-yielding 1 – An open-pollinated variety (OPV) with comparatively low yields (3–5 t/ha) often used for local consumption, with average yield potential and long maturity duration.

Low-yielding 2 – A conventional type with average yield performance (2.5–4 t/ha), adapted to marginal conditions but with lower productivity when under stress.

The experiment was conducted to evaluate the varietal performance of corn under alkaline soil conditions through the application of two ammonium-based fertilizers: Di-ammonium phosphate (DAP, 18-46-0) and Ammonium sulfate (AS, 21-0-0).

To provide balanced nutrition and fulfill the phosphorus (P) and potassium (K) needs of the crop, 10 t/ha of fully decomposed poultry manure was basally and uniformly applied to all treatments before sowing.

2.3 Preparation and Application of Fertilizer

Poultry manure was selected because of its high nutrient concentration and availability in the study region. The fertilizer was obtained from a nearby poultry farm and dried in sunlight for seven days to lower the moisture level and reduce pathogen load. The dried material was crushed and sieved to present a uniform particle size before use. The nutrient content was constituted by: nitrogen (N): 4%; phosphorus (P_2O_5): 3.0%; and potassium (K_2O): 2.0%. Manure from poultry was broadcast uniformly by hand and mixed with the soil one week before planting to provide time for partial decomposition and mineralization of nutrients.

Fertilizers based on ammonium—diammonium phosphate (18-46-0) and ammonium sulfate (21-0-0-—were applied during the V8 corn growth stage based on the suggested rate of nitrogen application of 90 kg N/ha..

2.4 Plot Size and Planting Arrangement

Each experimental unit was 5 linear meters long with 20 corn plants. One treatment involved a single 5-meter row. Row planting was used to allow for even spacing and ease of data collection. Each of the 5 meters wide by 16 meters long blocks consisted of eight treatments. The experiment was based on the Randomized Complete Block Design (RCBD) with three replications. Therefore, each block had all eight treatments in a randomly arranged manner, and the whole experiment was repeated three times

2.5 Land Preparation

The field was cleared by cutting all grasses and other vegetation, and was plowed to a depth of 15 to 20 cm. Plowing was done twice, followed by harrowing, which was alternated weekly to pulverize the soil, promote weed seed germination, and allow for their eventual removal. After the final harrowing, furrows were made 50 cm apart.

2.6 Seed Preparation and Sowing

Seeds were obtained from trusted sources and soaked in coconut water for 24 hours before sowing. Following the soaking process, the seeds were sown directly into the field at a rate of 2 to 3 seeds per hill. One week after emergence, the plants were thinned to one seedling per hill to ensure optimal growth conditions.

2.7 Management and Pest Control

The corn was watered daily, and weeding was carried out throughout the study period. Cartap hydrochloride was applied as a last resort to control insect pests during the reproductive growth stage of the target pests. Harvesting was done at the physiologically mature stage, 120 days after planting (DAP).

2.8 Data Gathered

The data of the following parameters were collected in this study:

- Plant height (cm)- measured with a tape measure from the base of the plant to the base of the tassel at 30 DAP and 60 DAP
- Days to tasseling- recorded by counting the number of days from sowing until 85% of the plants had developed tassels
- Days to silking- recorded by counting the number of days from sowing until 85% of the plants had developed silks.
- Ear weight and weight of grains/ear- weighed using a digital balance to measure the ear and the grains.
- Ear diameter (cm)- measured with a caliper at the ear's broadest point, usually around the center.
- Total Soluble Solids (TSS, °Brix)- five grams of blended kernels homogenized with 50mL distilled water were measured by digital refractometer (Hanna brand, HI-96801, USA)
- Titrability acid (%)- five ml of juice from blended samples prepared from TSS diluted with 45ml distilled water was measured and put into an Erlenmeyer flask and added with 2 drops of 1% phenolphthalein indicator, this was titrated with 0.1% NaOH until paint pink color was achieved using a Cordial 1642TF Glass burette and the volume of NaOH was recorded. TA was calculated as described by [10].

3. Results and Discussion

3.1 Agronomic Characteristics

The agronomic characteristics of the combined effect of variety and fertilizer showed that at 30 and 60 DAP, high-yielding variety 1 (V1) fertilized with Ammonium sulfate (F2) produced the tallest plant height, with a height of 95.15 cm and 185.10 cm which is significantly taller compared to those fertilized with Di- ammonium Phosphate (F1) (Table 1). These findings concur with those reported in [11], which demonstrated that maize treated with ammonium sulfate exhibited increased plant height. Furthermore, applying ammonium sulfate increased the heights of maize plants compared to those applied with other ammonium fertilizers [12].

Table 1. Plant Height at 30 and 60 Days after Planting as Affected by Ammonium Fertilization and Corn Varieties.

Varieties	Ammonium Fertilizers			
	Di-ammonium Phosphate (F1)	Ammonium Sulfate (F2)	Di-ammonium Phosphate (F1)	Ammonium Sulfate (F2)
	30 DAP	30 DAP	60 DAP	60 DAP
High-yielding 1 (V1)	87.38^{c}	95.15^{a}	170.75^{c}	185.10^{a}
High-yielding 2 (V3)	83.15^{d}	89.50^{b}	169.80^{d}	179.25^{b}
Low-yielding 1 (V2)	72.63^{f}	74.73^{e}	146.67^{f}	154.44^{e}
Low-yielding 2 (V4)	74.50^{e}	76.01^{g}	150.40^{g}	150.51^{g}
CV (%)	1.30		0.95	

Moreover, high-yielding variety 1 (V1) fertilized with Ammonium Sulfate (F2) also exhibited a faster time to tassel (51.83 days) and silk (57.70 days), indicating earlier development (**Table 2**). Ammonium Sulfate (F2) fertilization resulted in superior agronomic performance across all varieties compared to Di-ammonium Phosphate (F1). The high-yielding varieties, particularly variety 1 (V1), showed the most significant positive response, demonstrating the highest plant height and the earliest time to silk and tassel. The results suggest that the choice of ammonium fertilizer plays a critical role in optimizing corn performance, especially in challenging soil conditions. Ammonium sulfate provides critical plant nitrogen and sulfur nutrients compared with other N fertilizers, such as urea, diammonium phosphate, and ammonium nitrate [13]. Sulfur (S) is an essential element for crops and is vital to ensuring food security [14]. It plays a vital role in many physiological processes.

Such as photosynthesis, enzyme regulation, protein and lipid synthesis, stress resistance, and other metabolic pathways [15-19].

Table 2. Days to Tasseling and Silking as Affected by Ammonium Fertilization and Corn Varieties.

Varieties	Ammonium Fertilizer			
	Di-ammonium Phosphate (F1)	Ammonium sulfate (F2)	Di-ammonium Phosphate (F1)	Ammonium sulfate (F2)
	Days to Tasseling		Days to Silking	
High-yielding 1 (V1)	53.43^{g}	51.83^{h}	64.97^{f}	57.70^{g}
High-yielding 2 (V3)	57.67^{e}	55.90^{f}	69.50^{e}	68.40^{e}
Low-yielding 1 (V2)	69.82^{a}	68.60^{ab}	78.30^{a}	70.67^{d}
Low-yielding 2 (V4)	62.53^{d}	65.60^{c}	72.53^{c}	76.27^{b}
CV (%)	1.07		0.89	

3.2 Yield Performance

The result showed that high yielding variety 2 (V3) fertilized with Di-ammonium Phosphate (F1) resulted to highest ear weight (118.21 g/ear), heaviest grain weight (98.42 g/ear) and largest ear diameter (4.09 cm), suggesting this combination exhibit the most excellent responsiveness to ammonium fertilization, leading to superior ear and grain weights as well as larger ear diameters (**Table 3**). This agrees with the findings of other studies that the increased yield of maize cultivar is due to the nitrogen and phosphorus

held by the doses of Di-Ammonium Phosphate (DAP) [20]. The cultivar receiving DAP fertilizer significantly produced heavier fresh and dry weights. Nitrogen is an integral component of many compounds, associated with photosynthetic activity and a major yield-determining factor required for maize production [21]. Its quantity availability during the growing season is crucial for the highest possible yield of maize. Phosphorus is another essential nutrient required to increase maize yield; the lack of phosphorus is as significant as the lack of nitrogen in limiting maize performance [22]. Phosphorus is essential for grain formation, ripening, and the reproductive parts of the maize plant [23].

Table 3. Yield Performance as Affected by Ammonium Fertilization and Corn Varieties.

	Ear Weight (g/ear)		**Grain Weight (g/ear)**		**Ear Diameter**	
	Di-ammonium Phosphate (F1)	Ammonium sulfate (F2)	Di-ammonium Phosphate (F1)	Ammonium sulfate (F2)	Di-ammonium Phosphate (F1)	Ammonium sulfate (F2)
High-yielding 1 (V1)	109.17^{b}	102.98^{d}	83.93^{b}	77.41^{d}	3.96^{ab}	3.89^{b}
High-yielding 2 (V3)	118.21^{a}	107.13^{bc}	98.42^{a}	80.07^{c}	4.09^{a}	3.71^{cd}
Low-yielding 1 (V2)	89.90^{e}	81.22^{f}	70.92^{f}	63.37^{g}	3.60^{d}	3.67^{d}
Low-yielding 2 (V4)	85.15^{fg}	77.08^{g}	76.18^{e}	54.43^{h}	3.83^{bc}	3.43^{e}
CV (%)	5.50		6.39		2.12	

3.3 Physico-chemical Properties

The results indicate that high-yielding variety 1 (V1) fertilized with Ammonium Sulfate (F2) promotes higher TSS but harms the low-yielding varieties (V2 and V4). This conforms to other studies that the highest TSS of fruit was obtained by using ammonium sulfate. Mineral nutrient, especially sulfur and nitrogen supplied by ammonium sulphate, promotes the photosynthetic rate of the chloroplast, phloem transport of photosynthates to sink tissues, and finally improve the quality and yield of the fruit, which is associated with high sugar content [24]. In contrast, fertilizing Di-ammonium Phosphate (F1) leads to higher TA levels, particularly in the low-yielding variety 2 (V4), which shows an exceptionally high TA content. This suggests that while Ammonium Sulfate may enhance sugar content, Di-ammonium Phosphate tends to promote greater acid accumulation, potentially affecting the flavor and storage characteristics of the corn varieties. Phosphorus from fertilizers like DAP can enhance the production of organic acids in plants. The increased production of organic acids can raise the acidity level in certain plant tissues, which may extend to fruits or kernels, such as corn [25].

Table 4. Physico-chemical Properties as Affected by Ammonium Fertilization and Corn Varieties.

	Ammonium Fertilizers			
	Di-ammonium Phosphate (F1)	**Ammonium sulfate (F2)**	**Di-ammonium Phosphate (F1)**	**Ammonium sulfate (F2)**
Varieties	TSS		TA	
High-yielding 1 (V1)	1.17^{b}	1.53^{a}	22.67^{a}	15.20^{b}
High-yielding 2 (V3)	0.47^{e}	0.67^{d}	27.67^{a}	13.63^{bc}
Low-yielding 1 (V2)	0.83^{c}	0.23^{fg}	16.90^{b}	11.17^{c}
Low-yielding 2 (V4)	0.30^{f}	0.10^{g}	34.50^{a}	24.50^{a}
CV (%)	13.3		14.9	

4. Conclusions

High-yielding varieties are more sensitive to the type of fertilizer, which affects either growth or yield characteristics. Ammonium sulfate fertilizer affects mainly plant growth and the soluble solid content. While di-ammonium phosphate fertilizer greatly influences yield and yield components. However, the type of nitrogen fertilizer employed has less of an impact on low-yielding maize cultivars.

5. Acknowledgements

The authors wish to acknowledge the support provided by Department of Science and Technology-Science Education Institute-STRAND-N Scholarship and Cebu Technological University-Barili Campus Graduate School.

Author Contributions: Conceptualization, P.R.P.; methodology, S.E.G.P.; software, S.E.G.P., and P.R.P.; validation, S.E.G.P.; formal analysis, S.E.G.P.; investigation, S.E.G.P.; resources, S.E.G.P.; data curation, S.E.G.P.; writing- original draft preparation, S.E.G.P.; writing- review and editing, S.E.G.P., and P.R.P.; visualization, S.E.G.P.; supervision, P.R.P.; project administration, S.E.G.P.; funding acquisition, S.E.G.P. All authors have read and agreed to the published version of the manuscript.

Funding: This research was made possible through the support of the Department of Science and Technology- Science Education Institute (DOST-SEI) under the STRAND-N Scholarship Program, and the Graduate School of Cebu Technological University- Barili Campus.

Conflicts of Interest: The author declares no conflict of interest , as the funding agency did not influence the study's design, methodology, data analysis, or conclusions.

References

[1] Mahmood, Y. A.; Ahmed, F. W.; Mohammed, I. Q.; Wheib, K. A. Effect of Organic, Mineral Fertilizers, and Foliar Application of Humic Acid on Growth and Yield of Corn (Zea mays L.). *Indian J. Ecol.* **2020**, *47*(10), 39-44.

[2] Hossain, M. S.; Majumder, A. K. Impact of Climate Change on Agricultural Production and Food Security: A Review on Coastal Regions of Bangladesh. *Int. J. Agric. Res. Innov. Technol.* **2018**, *8*(1), 62-69. http://dx.doi.org/10.22004/ag.econ.305449

[3] Loy, D. D.; Lundy, E. L. Nutritional Properties and Feeding Value of Corn and Its Coproducts. In *Corn*; AACC International Press, **2019**; pp 633-659. https://doi.org/10.1016/B978-0-12-811971-6.00023-1

[4] Department of Agriculture - Bureau of Agricultural Research through the UPLB Foundation, Inc. in Collaboration with the Philippine Council for Agriculture and Fisheries. **2022**.

[5] Ohyama, T. Nitrogen as a Major Essential Element of Plants. *Nitrogen Assim. Plants* **2010**, *37*, 1-17. ISBN: 978-81-308-0406-4

[6] Morales, H.; Perfecto, I.; Ferguson, B. Traditional Fertilization and Its Effect on Corn Insect Populations in the Guatemalan Highlands. *Agric. Ecosyst. Environ.* **2001**, *84*(2), 145-155. https://doi.org/10.1016/S0167-8809(00)00200-0

[7] Wang, Q.; Li, F.; Zhao, L.; Zhang, E.; Shi, S.; Zhao, W.; Song, W.; Vance, M. M. Effects of Irrigation and Nitrogen Application Rates on Nitrate Nitrogen Distribution and Fertilizer Nitrogen Loss, Wheat Yield, and Nitrogen Uptake on a Recently Reclaimed Sandy Farmland. *Plant Soil* **2010**, *337*, 325-339. https://doi.org/10.1007/s11104-010-0530-z

[8] Enojada, G. R.; Asio, V. B. Morphological, Physical, and Chemical Characteristics of Soils Derived from Limestone Rocks in Barili, Cebu. *J. Agric. Technol. Manag.* **2018**.

[9] Wanderlog Weather (https://wanderlog.com/weather/188/6/cebu-city-weather

[10] Acedo, A. L., Jr.; Data, E. S.; Quevedo, M. A. Genotypic Variations in Quality and Shelf-Life of Fresh Roots of Philippine Sweet Potato Grown in Two Planting Seasons. *J. Sci. Food Agric.* **1996**, *72*(2), 209-212. https://doi.org/10.1002/(SICI)1097-0010(199610)72:2<209::AID-JSFA640>3.0.CO;2-N

[11] Sadak, S. M.; Abdelhamid, M. T.; Schmidhalter, U. Effect of Foliar Application of Amino Acids on Plant Yield and Some Physiological Parameters in Bean Plants Irrigated with Seawater. *Acta Biol. Colomb.* **2015**, *20*(1), 141-152.

[12] Siam, H. S.; Abd-El-Kader, M. G.; El-Alia, H. I. Yield and Yield Components of Maize as Affected by Different Sources and Application Rates of Nitrogen Fertilizer. *Res. J. Agric. Biol. Sci.* **2008**, *4*(5), 399-412. INSInet Publication

[13] Chien, S. H.; Gearhart, M. M.; Villagarcía, S. Comparison of Ammonium Sulfate with Other Nitrogen and Sulfur Fertilizers in Increasing Crop Production and Minimizing Environmental Impact: A Review. *Soil Sci.* **2011**, *176*(7), 327-335. https://doi.org/10.1097/SS.0b013e31821f0816

[14] Feinberg, A.; Stenke, A.; Peter, T.; et al. Reductions in the Deposition of Sulfur and Selenium to Agricultural Soils Pose Risk of Future Nutrient Deficiencies. *Commun. Earth Environ.* **2021**, *2*, 101. https://doi.org/10.1038/s43247-021-00172-0

[15] Bouranis, D. L.; Malagoli, M.; Avice, J.-C.; Bloem, E. Advances in Plant Sulfur Research. *Plants* **2020**, *9*(2), 256. https://doi.org/10.3390/plants9020256

[16] Droux, M. Sulfur Assimilation and the Role of Sulfur in Plant Metabolism: A Survey. *Photosynth. Res.* **2004**, *79*(3), 331-348. https://doi.org/10.1023/B:PRES.0000017196.95499.11

[17] Li, Q.; Gao, Y.; Yang, A. Sulfur Homeostasis in Plants. *Int. J. Mol. Sci.* **2020**, *21*(23), 8926. https://doi.org/10.3390/ijms21238926

[18] Narayan, O. P.; Kumar, P.; Yadav, B.; Dua, M.; Johri, A. K. Sulfur Nutrition and Its Role in Plant Growth and Development. *Plant Signal. Behav.* **2023**, *18*(1), 2030082. https://doi.org/10.1080/15592324.2022.2030082

[19] Kopriva, S.; Malagoli, M.; Takahashi, H. Sulfur Nutrition: Impacts on Plant Development, Metabolism, and Stress Responses. *J. Exp. Bot.* **2019**, *70*(16), 4069-4073. https://doi.org/10.1093/jxb/erz319

[20] Hussein, O. A. K.; Gadallah, A. F. I.; Ibrahim, M. E. M. Enhancement of Production and Quality of Sugarcane Using Nitrogen and Vinasses. *Egypt. Sugar J.* **2023**, *20*(0), 63-76. https://doi.org/10.21608/esugj.2023.215818.1040

[21] Khan, F.; Khan, S.; Hussain, S.; Fahad, S.; Faisal, S. Different Strategies for Maintaining Carbon Sequestration in Crop Lands. *Sci. Agric.* **2014**, *2*, 62-76

[22] Onasanya, R. O.; Aiyelari, O. P.; Onasanya, A.; Oikeh, S.; Nwilene, F. E.; Oyelakin, O. O. Growth and Yield Response of Maize (Zea mays L.) to Different Rates of Nitrogen and Phosphorus Fertilizers in Southern Nigeria. *World J. Agric. Sci.* **2009**, *5*(4), 400-407.

[23] Ibrahim, S. A.; Kandil, H. Growth, Yield, and Chemical Constituents of Corn (Zea Mays L.) as Affected by Nitrogen and Phosphorus Fertilization under Different Irrigation Intervals. *J. Appl. Sci. Res.* **2007**, *3*(10), 1112-1120. INSInet Publication

[24] Aryakia, E.; Roosta, H. R.; Rahmizade, N. Effects of Cow Manure, Ammonium Sulfate and Potassium Sulfate on Physico-Chemical Indices of Fruit and Leaf of Mazafati Date (Phoenix dactylifera L.). *J. Hortic.Sci.* **2017**, *31*(3), 457-468. https://doi.org/10.22067/jhorts4.v31i3.36474

[25] Fageria, N. K.; Baligar, V. C.; Li, Y. C. The Role of Nutrient-Efficient Plants in Improving Crop Yields in the Twenty-First Century. *J. Plant Nutr.* **2008**, *31*(6), 1121-1157. https://doi.org/10.1080/01904160802116068

ASEAN
Journal of Scientific and Technological Reports
Online ISSN:2773-8752

Research article

Biochar from sewage sludge on soil and plant characteristics of Arugula *(Eruca sativa)*

Chem Lloyd P. Alburo[1*], and Engr. Alfredo C. Neri[2]

[1] Graduate School, Cebu Technological University -Barili, Barili 6036, Cebu, Philippines
[2] Institute of Agriculture and Biosystems Engineering, Cebu Technological University -Barili 6036, Barili, Cebu, Philippines
* Correspondence: chemlloyd.pascual@ctu.edu.ph

Citation:
Alburo, C.L.P.; Neri, A.C. Biochar from sewage sludge on soil and plant characteristics of Arugula (*Eruca sativa*). *ASEAN J. Sci. Tech. Report.* **2025**, *28*(4), e257297. https://doi.org/10.55164/ajstr.v28i4.257297.

Article history:
Received: December 30, 2024
Revised: May 21, 2025
Accepted: July 1, 2025
Available online: 16 August, 2025

Publisher's Note:
This article has been published and distributed under the terms of Thaksin University.

Abstract: Swine sewage sludge is challenging to manage due to the large volumes produced and its high pathogen content. Recently, thermal treatments such as pyrolysis have gained interest as a means to convert dried swine sewage sludge into biochar, which is increasingly applied to soils to enhance plant growth. This study evaluated the effects of biochar produced from dried swine sewage sludge on the growth of Arugula (*Eruca sativa*) in a greenhouse. Biochar was created through fast pyrolysis at 500°C. This was applied to the test plants with a Completely Randomized Design (CRD) involving six treatments (T0: Dried Swine Sewage Sludge 100g; T1: biochar 20g; T2: biochar 40g; T3: biochar 60g; T4: biochar 80g; T5: biochar 100g) in four replications. Results indicated that biochar is high in nitrogen (2.52%) and phosphorus (9.85%), while Dried Swine Sewage Sludge is rich in potassium (0.7057%). Increasing biochar to certain levels improved nutrient availability in the soil, leading to significant gains in chlorophyll content (0.1144 µg/mL), total soluble solids (4.50 °Brix), leaf count (7.6 number of leaves per plant at 4th week), and plant height (37.75mm during the 2nd week). Biochar application above 40g had a negative impact on horticultural characteristics, specifically the plant height, plant mass (fresh weight) and number of leaves, suggesting that excessive biochar may inhibit development. Despite this, higher biochar levels still enriched soil nutrients (N, 2.52%; Cu, 0.1448%; Fe, 5.44895%; Mn, 0.61375%; Ca, 0.69275%; P_2O_5, 7.964%; K_2O, 2.303%), highlighting the importance of balancing biochar rates for optimal plant performance.

Keywords: Waste treatment; Pyrolysis; Soil amendment; Horticultural characteristics; Soil nutrient properties

1. Introduction

The management of sewage has been a critical issue since the advent of human settlements, necessitated by the need to process large volumes of wastewater, primarily human excreta [1]. Urbanization and industrialization have intensified water pollution, driving the development of advanced wastewater treatment systems [2]. These advancements, while necessary for managing effluent, have inadvertently increased the production of sewage sludge, creating a growing waste management challenge. Similarly, managing swine waste represents a substantial challenge, characterized by the large quantities produced and its elevated pathogen concentrations, highlighting the urgent need for innovative treatment and resource recovery strategies to mitigate environmental and public health risks [3].

Lately, there has been increased interest regarding thermal processing of this waste. In addition to the conventional methods of sewage sludge disposal such as direct application in agriculture, incineration, and landfilling. The pyrolytic conversion of sewage sludge to biochar is a promising method to manage this waste and simultaneously take advantage of the aforementioned environmental benefits [4]. Thermal treatment offers a promising alternative to traditional approaches, with options like pyrolysis and gasification gaining traction for their ability to reduce waste volume and convert it into useful byproducts. Among the various alternative methods, microwave thermal treatment has also emerged as a potential technique, offering efficient energy use and rapid processing times for sludge management [5].

This study investigates the feasibility of producing biochar from swine waste in varying amounts. The study focuses on evaluating its potential for agricultural use, specifically improving soil and plant characteristics in Arugula cultivation. This approach aims to enhance agricultural soil functions and promote plant growth. The response of plants to biochar is influenced by its interaction with soil properties, nutrient availability, and environmental conditions. However, the effect of biochar application on plant growth can be different due to the variability in the quantity of biochar. In this study, the effect of different amounts of biochar application on the growth of Arugula (*Eruca sativa*) was assessed in a pot experiment.

2. Materials and Methods

2.1 Sewage Sludge

Sewage sludge was obtained from the pig pens of Cebu Technological University –Barili Campus in Cagay, Barili, Cebu, Philippines. The sewage sludge was filtered, sorted and impurities such as leaves and other materials were removed. Sludge was then laid out on a canvass and air dried. Air drying lasted for one month, until it attained a crumbling texture (Figure 1).

Figure 1. Proper texture of dried swine sewage sludge for ready for biochar.

2.2 Biochar Production and Application

Initially, samples were crumbled into pieces about 7–9 cm in diameter to allow for even heat distribution during pyrolysis. Once loaded into the pyrolyzer, the samples were heated to 500°C and regularly checked if the samples had reached the desired blackened state without turning into ash. One hundred grams of dried swine sewage sludge (DSSS) when pyrolyzed will yield approximately 50g of biochar. After complete pyrolysis, the biochar was pulverized with a mortar and pestle and passed through a 0.5mm sieve. The biochar was then weighed according to the study's treatment levels: T0 (DSSS, 100g), T1 (Biochar, 20g), T2 (Biochar, 40g), T3 (Biochar, 60g), T4 (Biochar, 80g), and T5 (Biochar, 100g). Each treatment was thoroughly mixed with soil to ensure even distribution.

2.3 Soil and Biochar Analysis

2.3.1 Laboratory Site

Soil and biochar analysis were conducted in the Department of Chemistry Laboratory at the University of San Carlos – Talamban Campus, Cebu City, Philippines.

2.3.2 Sample Preparation

Upon arrival in the laboratory, the raw soil and biochar samples were air dried for one week, sieved using 180 μm mesh, and homogenized using a ball mill. The samples were then placed in a resealable plastic container for storage and moisture analysis.

2.3.3 Available Phosphorus

The available phosphorus was analyzed using the Chlorostannous Method (Senthilkumar et al. [6]). A 0.5-gram portion of < 2mm air-dried soil was placed in a 50 mL shaking bottle. Fifty milliliters of extracting solution were added, the bottle was stopped, and the contents were shaken for 30 minutes. The supernatant liquid was filtered using Whatman No. 42 filter paper. An aliquot of the sample was transferred to a 50 mL volumetric flask, and a standard P solution containing 2-40 μg P was also prepared using TraceCERT certified reference material (CRM), Pcode: 101743260, in 2% HNO_3 (Sigma Aldrich, Switzerland). Ten milliliters of ammonium molybdate solution and 1 mL of dilute $SnCl_2$ solution were added. The flask was brought to volume with deionized water and mixed well. The absorbance was measured using a UV-Visible Spectrometer at 660 nm after 5-6 minutes but before 10 minutes. A blank, containing all the reagents except the phosphate solutions, was also prepared. The samples were analyzed in triplicate and a recovery test was performed.

2.3.4 Available Potassium

Exactly 5 grams of < 2mm air-dried soil were placed in a 50 mL shaking bottle. Twenty-five milliliters of 1.0 M ammonium acetate extracting solution were added, the bottle was stopped, and the contents were shaken for 30 minutes. The supernatant was filtered using Whatman No. 42 filter paper. The sample was diluted by pipetting a 0.2 mL aliquot and bringing the volume to 10 mL with the extracting solution. The unknown concentration was determined by preparing a standard calibration curve of 10, 20, 30, and 40 ppm using potassium standard solution (TraceCERT certified reference material (CRM), Pcode: 101731961, in 2% HNO_3, Sigma Aldrich, Switzerland) and a wavelength of 766 nm in a microwave plasma atomic emission spectroscopy (MP-AES 4210) following EPA Method 3050B.

2.3.5. Available Nitrogen

Analysis was conducted following the Kjeldahl method. One gram of sample was weighed and placed in an 800 mL Kjeldahl flask that contained approximately 10 grams of sodium sulfate and 0.3-0.5 grams of copper sulfate. Thirty milliliters of concentrated sulfuric acid were added. If any portion stuck to the side of the flask, it was washed down with the acid. The flask was shaken to ensure all sample portions were wet. Digestion was started until all the organic matter was oxidized and a clear blue liquid remained. The mixture was cooled and diluted to 450 mL with deionized water. Exactly 50 mL of 4% boric acid were delivered into a 500 mL Erlenmeyer flask, and 5 drops of methyl red-methylene blue indicator were added. The flask was placed at the collection end of the distillation setup. Seventy milliliters of 50% NaOH were measured and carefully added to the Kjeldahl flask through the side to avoid mixing with the content. Two to three zinc granules were added to prevent bumping during boiling. The flask was stoppered and connected to the distillation apparatus, and the contents were mixed by gently swirling the flask. A low boil was maintained for 15 minutes, then boiling was increased until about 350 mL of distillate was collected in the Erlenmeyer flask. The distillate was titrated with 0.1N sulfuric acid standard solution until a light pink color was observed. A correction blank was run with every batch of determination. Each sample was analyzed in triplicate. The percentage of nitrogen was calculated using the equation provided below:

$$\%N = \frac{((Ts-Tb)\ x\ N\ H2SO4\ x\ N)\ /1000}{weight\ sample,\ g} \text{ x } 100$$

2.3.6 Analysis of Iron

The samples were oven-dried at 50 °C and 0.5 g of air-dried soil samples were accurately weighed and passed through 2 mm sieve. Wet digestion procedure using EPA Method 3050B using acid mixture of $HClO_4/HNO_3/H_2SO_4$ was used for total digestion of soil samples before elemental analysis at a wavelength of 373 nm in Microwave Plasma Atomic Emission Spectrometry (MP-AES 4210).

2.3.7 Analysis of Copper, Zinc, Manganese and Calcium

The samples were oven-dried at 50 °C and 1.000 g of air-dried samples were accurately weighed and passed through 2 mm sieve. Wet acid digestion procedure using EPA Method 3050B was used for total digestion of samples before elemental analysis using Flame Atomic Absorption Spectroscopy (FAAS). A recovery test was also performed.

2.4 Plant Management

Plants were monitored and watered twice daily, or three times on hot days. Each pot received 10 mL of water in the early stage, increasing to 30 mL in the later stage.

2.5 Measurement of Growth Parameters

2.5.1 Number of Leaves

The number of leaves (NL) per plant was obtained by counting the leaves of the Arugula plant.

2.5.2 Plant Height

The plant height (PH) was measured from the base of the plant at the soil level to the tip of the tallest leaf.

2.5.3 Plant Mass Above and Below Ground

The plant mass above ground was obtained by weighing all the parts of the plant that are above ground, while the plant mass below ground was obtained by weighing all the parts of the plant below ground.

2.6 Chlorophyll Content (Chlorophyll A and B, Total Chlorophyll)

The chlorophyll content was estimated spectrophotometrically by the method of Sadasivan and Manicham [7]. Mashed Arugula was macerated with the addition of 20 ml of 80 % acetone to a fine pulp in a mortar and pestle. The paste was centrifuged for 5 min at 5000 rpm. The supernatant was decanted, and the left residue was then ground with 20 ml of 80 % acetone, centrifuged for 5 min at 5000 rpm, and the supernatant was again decanted. The extraction was repeated 4–5 times until the residue was colorless. The extracts were collected in a beaker, filtered and made up to 100 ml with 80 % acetone in a volumetri c flask. The absorbances of the extracted solutions were recorded (Shimadzu UV-1800, Kyoto, Japan) at 645 nm and 663 nm against the solvent (80 % acetone) blank. The amount of chlorophyll present in extract i.e. mg of chlorophyll per gram of tissue on fresh weight basis, was calculated using the following equations:

$$\text{Chlorophyll 'a'(mg/g of tissue)} = [12.7 * X - 2.69 * Y] \times v(1000 \times W)$$

$$\text{Chlorophyll 'b'(mg/g of tissue)} = [22.9 * Y - 4.68 * X] \times v(1000 \times W)$$

$$\text{'Total chlorophyll'(mg/g of tissue)} = [20.2 * Y + 8.02 * X] \times v(1000 \times W)$$

Where:

X = absorbance at 663 nm

Y = absorbance at 645 nm

W = weight of fresh tissue extracted (1 g)

V = final volume of extract in 80 % acetone (100 ml)

2.7 Total Soluble Solids (TSS)

Five grams of freshly harvested Arugula was soaked with 200ml. distilled water for one (1) hour and was mashed with mortar and pestle and filtered. The filtrate was subjected to TSS measurement. TSS in °Brix was measured using a hand-held digital refractometer (Hanna HI 96801) calibrated with distilled water by placing 1-3 drops of juice on the instrument's prism and taking the reading.

2.8 Titratable Acidity (TA)

The TA was determined by titration. A volume of 49.0 mL of distilled water was added to 1.0 mL of pulp in an Erlenmeyer flask, and after stirring, it was titrated with a standardized solution of NaOH at 0.1 M using 1% phenolphthalein as an indicator. The results were expressed in grams of citric acid per 100 g of pulp [8] with the data expressed as a percent TA.

2.9 Experimental Design and Treatments

The study was laid out in a Completely Randomized Design (CRD) with six treatments in four replications. Each replication had five pots that served as a buffer for the unexpected death of the plant. The treatments are the following:

T_0= Dried Swine Sewage Sludge 100g
T_1= 20g biochar
T_2= 40g biochar
T_3= 60g biochar
T_4= 80g biochar
T_5= 100g biochar

Microsoft Excel was used to compute the average values and data variability. Analysis of variance (ANOVA) was performed in STAR Program to assess differences in the parameters across treatments.

3. Results and Discussion

3.1 Nutrient Profile

Values for river water samples ranged from 6.71 to 6.82 ppm for dissolved oxygen. The dissolved oxygen values indicate sufficient oxygen supply to support aquatic life in the river. pH values also ranged between 6.68 and 6.77 for water samples and sediments and 6.71 and 6.82 for sediments.

The nutrient analysis shows significant differences among dried swine sewage sludge, soil, and biochar (Figure 2). Dried sludge had the highest levels of copper (0.15145%), zinc (0.58425%), and manganese (0.5106%), making it a potent source of these trace metals, though high levels raise potential toxicity concerns. These trace metals could have come from the commercial feed additives Mu et al. [9]. On the other hand, soil contained the most iron (4.807%), about 3.5 times higher than in sludge and 43 times higher than in biochar, marking it as the best iron source.

For macronutrients, potassium was highest in sludge (0.7057%), followed by biochar (0.5583%), with soil being much lower (0.0807%). Soil had the highest calcium (0.8914%), while sludge led in magnesium (0.2324%). Biochar was nutrient-dense in nitrogen (2.52%) and phosphorus (9.85%), surpassing soil and sludge, which supports its role as a valuable soil amendment.

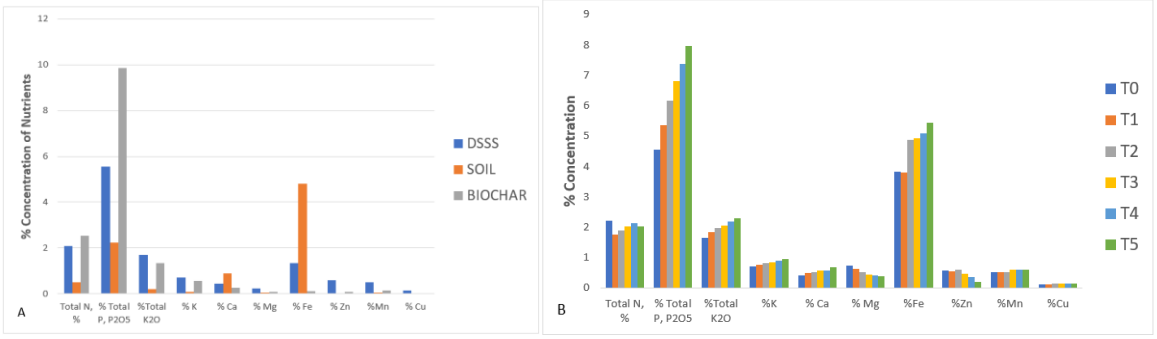

Figure 2. Nutrient Profile (%) of the Raw Materials for Potting Medium (A) and Nutrient Profile (%) of Different Experimental Treatments (B) after Harvest.

Overall, biochar provides essential nutrients like nitrogen, phosphorus, and potassium, while sludge is rich in trace metals and magnesium. Soil, though lower in several nutrients, remains an important calcium and iron source. These distinctions highlight the potential of combining biochar and sludge to enhance soil fertility, though monitoring of trace metals is advised to prevent harmful accumulation.

Trace metal analysis showed copper (Cu) levels increasing from 0.1296% in T_0 to 0.1448% in T_5, while iron (Fe) rose from 3.8141% in T_0 to 5.44895% in T_5, indicating Fe accumulation. Zinc (Zn) peaks at 0.6053% in T_2 but drops sharply to 0.1951% in T5, suggesting reduced Zn retention in higher treatments. Manganese (Mn) steadily increases from 0.51% in T_0 to 0.61375% in T_5, implying improved retention.

For macronutrients, potassium (K) content rises from 0.7217% in T_0 to 0.9561% in T_5, and calcium (Ca) also increases from 0.4173% to 0.69275%. However, magnesium (Mg) declines from 0.73645% in T_0 to 0.39935% in T_5, suggesting reduced availability over time. In overall nutrient content, total nitrogen (N) fluctuates slightly but is lower in T_5 than in T_0. Phosphorus (P_2O_5) increases significantly from 4.551% in T0 to 7.964% in T_5, while potassium oxide (K_2O) grows from 1.66% to 2.303%. Overall, T4 and T_5 are nutrient-rich, particularly in phosphorus and potassium, while nitrogen and magnesium show less consistent trends.

Biochar can influence soil nutrients by reducing leaching losses, a process where nutrients are washed away from the soil profile Laird et al. [10]. Its porous structure, extensive surface area, and negative surface charge enhance the soil's cation exchange capacity, enabling the retention of essential nutrients such as potassium (K) Bird et al. [11], Cheng et al. [12], Downie et al. [13], Novak et al. [14]. Additionally, biochar reduces cation loss by altering soil water movement, promoting a shift from bypass flow to matrix flow, which allows for more efficient nutrient transport and retention Laird et al. [10]. Phosphorus (P), in particular, can adhere to biochar's surface, effectively slowing its leaching and enhancing nutrient availability in the soil Laird et al. [10], Beck et al. [15].

3.2 Horticultural Characteristics

Variations in germination time across treatments were observed in Table 1. Germination times varied slightly among treatments but showed no significant differences. DSSS-alone treatment averaged 7.3 days, serving as a baseline. Treatment with 40g biochar was the fastest at 5.45 days, while with 100g biochar was the slowest at 8.35 days. Intermediate averages were recorded for treatments with 20g, 60g and 80g at 7.05, 7.2 days, and 6.1 days, respectively. This suggests that, while some treatments appeared to promote faster or slower germination, these differences were not substantial enough to indicate a meaningful impact on the germination process. Various studies have also yielded varying results on the effect of biochar on germination rates; high-dose biochar had significant negative effect on germination rate, shoot length and root length of rice and corn seeds Bai et al. [16]; corn-cub bio mixed with soil have positive effects on seed germination of maize seedlings Ali et al. [17], while the study of Carril et al. [18] resulted to no effect on the germination of lettuce.

In terms of number of leaves, varying mean values were observed. For DSSS alone, the number of leaves ranged between 6.25 and 6.75, with an average of 6.65 leaves, marking the lowest leaf count among the treatments. The average number of leaves per plant increased as the level of biochar was increased at 20g increment, peaking at 80g application with an average of 7.6. It decreased to 7.25 leaves when biochar was increased to 100g. Biochar enhances leaf production by improving soil fertility, water retention, and nutrient cycling, supporting vegetative growth. Optimal application boosts leaf development, while excessive amounts may hinder growth due to imbalances or soil alkalinity (Yu et al. [19]. Statistical analysis revealed significant differences in the number of leaves between treatments. This suggests that the treatments had an effect on leaf development, indicating that variations in the number of leaves could be attributed to the different treatments applied. In the study conducted by Jabborova et al. [20], on ginger (*Zingiber officinale*), showed that 2% and 3% addition of biochar significantly increased the number of leaves compared to the control.

Biomass, both above- and below-ground, was highest at 20g and 60g biochar but declined as biochar level was increased, suggesting inhibition. Excess biochar levels appeared inhibitory (Wang et al. [21], though differences were not statistically significant. According to Schulz et al. [22], biochar had no significant impact on plant biomass when applied to sandy substrates. However, on loamy substrates, biomass yield was significantly reduced at the highest application. No consistent trend was observed with increasing biochar application rates.

Table 1. Horticultural characteristics of Arugula as affected by levels of biochar application.

Treatment	Days to Germination	Number of Leaves	Plant Mass Above (gram/plant)	Plant Mass Below (gram/plant)
T_0 = 100g DSSS	7.30^{nsd}	6.65^{b}	2.26^{nsd}	0.33^{nsd}
T_1 = 20g Biochar	7.05^{nsd}	7.00^{ab}	2.55^{nsd}	0.31^{nsd}
T_2 = 40g Biochar	5.45^{nsd}	7.50^{a}	3.69^{nsd}	0.49^{nsd}
T_3 = 60g Biochar	7.20^{nsd}	7.30^{ab}	3.28^{nsd}	0.49^{nsd}
T_4 = 80g Biochar	6.10^{nsd}	7.60^{a}	1.98^{nsd}	0.29^{nsd}
T_5 = 100g Biochar	8.35^{nsd}	7.25^{ab}	1.43^{nsd}	0.14^{nsd}

Values with the same letter are not significantly different ($p>0.05$)
nsd = no significant difference

3.3 Plant Height

At 15 days, significant differences in plant height emerged among treatments, with 40g biochar exhibiting the highest average (37.75mm) implying significant effect at this critical stage. The 15th day provides a valuable snapshot of early plant vigor and the treatment's potential to enhance growth, offering both scientific and practical relevance in agricultural research Baker et al. [23]. The first 15 days, being crucial for seedling establishment, help to gauge how biochar modifies nutrient availability, root development, and overall plant vigor, which are essential for determining its potential in enhancing crop growth and productivity in the long term (Shamim et al. [24], Uslu et al. [25], Liu et al. [26]. Therefore, this early observation period is vital for identifying how biochar treatments might influence the early plant development stages, helping to optimize biochar application in agricultural practices.

These results underscore that biochar application at 40g and 60g positively impacted plant height, with the former showing significantly faster growth by the 15-day mark. The study of Murtaza et al. [27] *Medicago sativa*, *Amaranthus caudatus* and *Zea mays* in saline soils showed that biochar significantly improved by 30% of these crops.

Table 2. Plant Height (n) days from planting, measured in (mm) as affected by levels of biochar application.

Treatment	5 days	10 days	15 days	20 days	25 days
T0 = 100g DSSS	3.85^{nsd}	8.5^{nsd}	25.65^{ab}	56.1^{nsd}	86.4^{nsd}
T1 = 20g Biochar	6.4^{nsd}	12.25^{nsd}	29.7^{ab}	63.95^{nsd}	98.2^{nsd}
T2 = 40g Biochar	9.8^{nsd}	17.95^{nsd}	37.75^{a}	71.3^{nsd}	104.85^{nsd}
T3 = 60g Biochar	6.7^{nsd}	13.65^{nsd}	27.9^{ab}	61.3^{nsd}	94.7^{nsd}
T4 = 80g Biochar	7.75^{nsd}	14.3^{nsd}	33.45^{ab}	67.8^{nsd}	109.35^{nsd}
T5 = 100g Biochar	4.35^{nsd}	8.15^{nsd}	22.3^{b}	48.2^{nsd}	76.1^{nsd}

Values with the same letter are not significantly different ($p>0.05$)
nsd = no significant difference

3.4 Chlorophyll Content

Chlorophyll content increased from dried sewage sludge application to increasing levels of biochar. The control treatment with dried swine sewage sludge consistently recorded the lowest levels of chlorophyll in all measurements while the treatments with highest biochar had the highest chlorophyll concentrations, indicating they most effectively enhanced chlorophyll production in plants (Fig. 3). The results are consistent with other studies that showed biochar treatment significantly increasing the chlorophyll a, chlorophyll b, total chlorophyll and carotenoid relative water of leaf cover Hafeez et al. [28], Yousaf et al. [29] by enhancing soil nutrient availability, improving soil structure, and promoting water retention Zhang et al. [30]. These factors support better overall plant health, which in turn leads to increased chlorophyll levels. It was found that biochar application increased the photosynthesis, chlorophyll content, and transpiration rate in different plants Murtaza et al. [27].

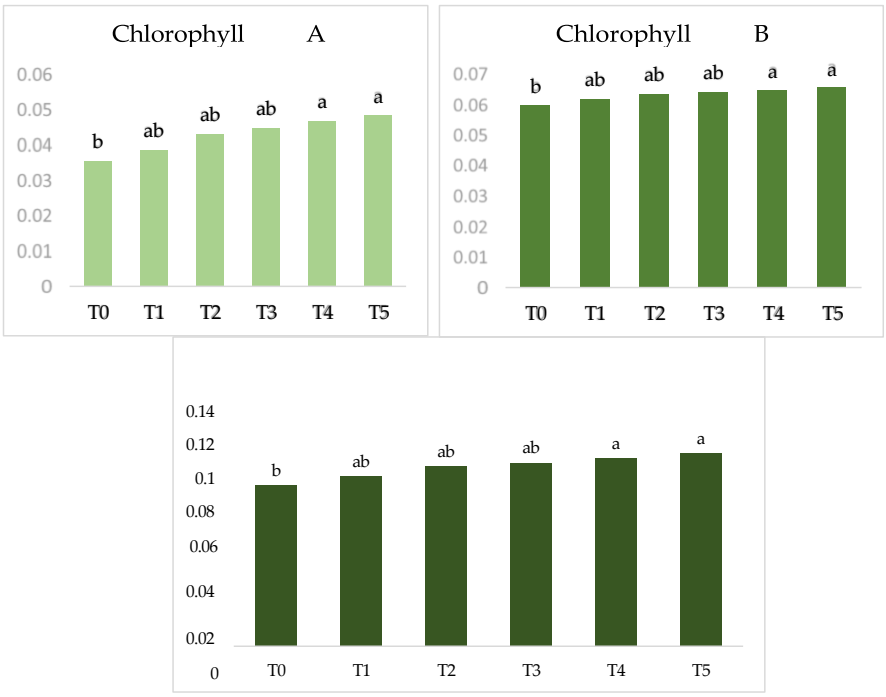

Figure 3. Chlorophyll a (A), b (B) and Total Chlorophyll (C)

3.5 Total Soluble Solids and Titratable Acidity

Figure 4 (A) highlights significant variation in Total Soluble Solids (TSS) across treatments. DSSS-treated plants exhibited the highest TSS mean at 9.63 °Brix indicating maximum soluble solids without biochar application. Conversely, increasing biochar levels reduced TSS, with the most substantial declines observed at 60–100 g biochar. This trend suggests that excessive biochar may suppress soluble solids, likely due to altered nutrient dynamics or stress responses, consistent with findings that high biochar levels can adversely affect plant growth parameters Wang et al. [21]. While biochar has generally been associated with improving plant growth and fruit quality in many cases, its effect on TSS seems to vary depending on factors like the type of biochar, soil conditions, and other treatments applied [31].

Figure 4 (B) shows that the DSSS-treated Arugula had the lowest titratable acidity (TA) at 22.42%, while 80g and 100g biochar showed the highest TA at 28.82% and 32.02%, respectively, suggesting a link between higher biochar levels and increased acidity. Despite these variations, statistical analysis revealed no significant differences in TA across treatments.

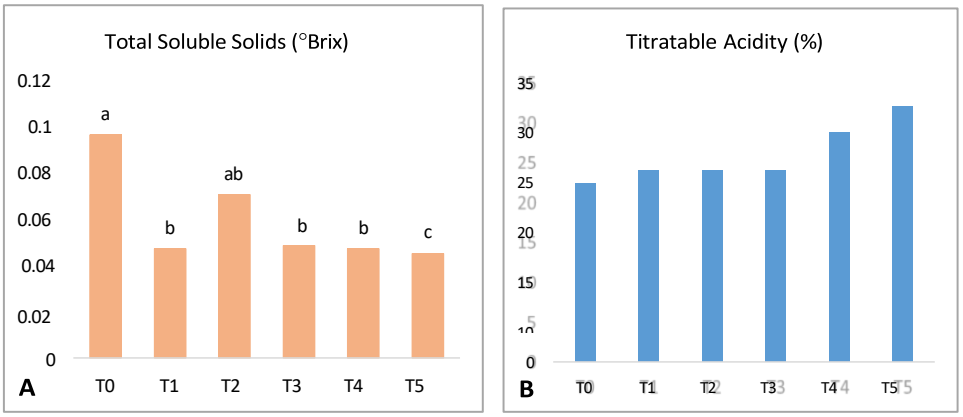

Figure 4. Total Soluble Solids (A) and Titratable Acidity (B).

4. Conclusion

The research indicates that biochar derived from the pyrolytic conversion of swine sewage sludge is a nutrient-rich soil amendment, containing high levels of nitrogen and phosphorus. In contrast, dried sludge is particularly high in potassium. Both materials can be valuable for enhancing soil fertility, with the choice depending on the nutrient needs of specific crops and soil conditions. For optimal results, a biochar application rate of 40 grams per treatment is recommended. This dosage significantly improves soil nutrient content, particularly iron, manganese, potassium, calcium, and phosphorus, while avoiding the inhibitory effects observed with higher application rates. Within just 15 days of application, biochar has been shown to enhance key plant growth parameters, including increased total soluble solids, higher chlorophyll content, a high number of leaves, and improved plant height. These improvements reflect biochar's dual benefit: enhancing crop productivity and soil quality while contributing to sustainable waste management. Careful application based on crop and soil requirements is essential to maximize the agronomic benefits of biochar without risking nutrient imbalance or growth suppression.

5. Acknowledgement

This research work was made possible through the support of the Department of Science and Technology - STRAND N program and Cebu Technological University – Barili Campus.

Author Contributions: The following are the contributions of each author in this research: Conceptualization: C.L.P. Alburo and A.C. Neri; Methodology: C.L.P. Alburo and A.C. Neri; Software: A.C. Neri; Validation: C.L.P. Alburo and A.C. Neri; Formal analysis: C.L.P. Alburo; Investigation: C.L.P. Alburo; Resources: C.L.P. Alburo and A.C. Neri; Data curation: C.L.P. Alburo; Writing – original draft preparation: C.L.P. Alburo; Writing – review and editing: C.L.P. Alburo; Visualization: C.L.P. Alburo; Supervision: A.C. Neri; Project administration: C.L.P. Alburo; Funding acquisition: C.L.P. Alburo. Additionally, all authors have read and agreed to the published version of the manuscript.

Funding: The research received no external funding.

Conflicts of Interest: The authors declare no conflict of interest

References

[1] Pillai, B. B. K.; Meghvansi, M. K.; Sudha, M. C.; Sreenivasulu, M. Recent Trends in Performance Assessment of Anaerobic Biodigestion for Sewage Waste Management: A Critical Review. *Environmental and Microbial Biotechnology* **2022**, 113-136.

[2] Cairone, S.; Hasan, S. W.; Choo, K. H.; Lekkas, D. F.; Fortunato, L.; Zorpas, A. A.; Korshin, G.; Zarra, T.; Belgiorno, V.; Naddeo, V. Revolutionizing wastewater treatment toward circular economy and carbon neutrality goals: Pioneering sustainable and efficient solutions for automation and advanced process control with smart and cutting-edge technologies. *J. Water Process Eng.* **2024**, *63*, 105486. https://doi.org/10.1016/j.jwpe.2024.105486.

[3] Masse, D. I.; Saady, N. M. C. Current state and future challenges of manure management technologies for livestock operations. *Agric. Biosyst. Eng.* **2015**.

[4] Pathak, A.; Dastidar, M. G.; Sreekrishnan, T. R. Bioleaching of heavy metals from sewage sludge: A review. *J. Environ. Manage.* **2009**, *90*, 2343-2353.

[5] Franca, A. S.; Oliveira, L. S.; Nunes, A. A.; Alves, C. C. O. Microwave-assisted thermal treatment of defective coffee beans press cake for the production of adsorbents. *Bioresour. Technol.* **2010**, *101*, 1068-1074.

[6] Senthilkumar, M., Amaresan, N., Sankaranarayanan, A. Estimation of Phosphate Solubilizing Capacity of Microorganisms. In: Plant-Microbe Interactions. Springer Protocols Handbooks. Humana, New York, NY. **2021**. https://doi.org/10.1007/978-1-0716-1080-0_10

[7] Sadasivan, S.; Manickam, A. Biochemical Methods, New Age International Publishers, New Delhi, **1997**, 256.

[8] Instituto A. L. Conservasvegetais, frutas e produtos de frutas. In: Instituto Adolfo Lutz, Ed., Cap. XV Métodosfísico-químicosparaanálise de alimentos, 4th Edition, Anvisa, Brasília, **2005**, 571-591.

[9] Mu, H. Y.; Zhuang, Z.; Li, Y. M.; et al. Heavy metal contents in animal manure in China and the related soil accumulation risks. *Huanjing Kexue.* **2020**, *41* (2), 986–996..

[10] Laird, D.; Fleming, P.; Wang, B.; Horton, R.; Karlen, D. Biochar impact on nutrient leaching from a Midwestern agricultural soil. *Geoderma.* **2010**, *158*(3-4), 436-442. https://doi.org/10.1016/j.geoderma.2010.05.012.

[11] Bird, M. I.; Ascough, P. L.; Young, I. M.; Wood, C. V.; Scott, A. C. X-ray microtomographic imaging of charcoal. *J. Archaeol. Sci.* **2008**, *35*(10), 2698-2706. https://doi.org/10.1016/j.jas.2008.04.017.

[12] Cheng, C.-H.; Lehmann, J.; Engelhard, M. H. Natural oxidation of black carbon in soils: Changes in molecular form and surface charge along a climosequence. *Geochim. Cosmochim. Acta.* **2008**, *72*(6), 1598-1610. https://doi.org/10.1016/j.gca.2008.01.010.

[13] Downie, A.; Crosky, A.; Munroe, P. Physical properties of biochar. In *Biochar for Environmental Management*; Lehman, J., Joseph, S., Eds.; Earthrscan: London, **2009,** pp 13-29

[14] Novak, J. M.; Lima, I.; Xing, B.; Gaskin, J. W.; Steiner, C.; Das, K. C.; Ahmedna, M.; Rehrah, D.; Watts, D. W.; Busscher, W. J.; Schomberg, H. Characterization of Designer Biochar Produced at Different Temperatures and Their Effects on a Loamy *Sand. Ann. Environ. Sci*. **2009**, *3*(1), 195-206.

[15] Beck, D. A.; Johnson, G. R.; Spolek, G. A. Amending green roof soil with biochar to affect runoff water quantity and quality. *Environ. Pollut.* **2011**, *159*(8-9), 2111-2118. https://doi.org/10.1016/j.envpol.2011.03.015

[16] Bai, X.; Zhang, S.; Shao, J.; Chen, A.; Jiang, J.; Chen, A.; Luo, S. Exploring the negative effects of biochars on the germination, growth, and antioxidant system of rice and corn. *J. Environ. Chem. Eng.* **2022**, *10*(3), 107398

[17] Ali, L.; Xiukang, W.; Naveed, M.; Ashraf, S.; Nadeem, S.M.; Haider, F.U.; Mustafa, A. Impact of Biochar Application on Germination Behavior and Early Growth of Maize Seedlings: Insights from a Growth Room Experiment. *Appl. Sci.* **2021**, *11*(24), 11666. https://doi.org/10.3390/app112411666

[18] Carril, P.; Ghorbani, M.; Loppi, S.; Celletti, S. Effect of Biochar Type, Concentration and Washing Conditions on the Germination Parameters of Three Model Crops. *Plants.* **2023**, https://doi.org/10.3390/plants12122235

[19] Yu, P.; Gu, M. (2024, January). Biochar Basics 2. Biochar's Effects on Plant Growth. UGA Cooperative Extension Circular 1292. extension.uga.edu/publications/detail.html?number=C1292-02.

[20] Jabborova, D.; Wirth, S.; Halwani, M.; Ibrahim, M.F.M.; El Azab, I.H.; El-Mogy, M.M.; Elkelish, A. Growth Response of Ginger (*Zingiber officinale*), Its Physiological Properties and Soil Enzyme Activities after Biochar Application under Greenhouse Conditions. *Horticulturae.* **2021**.

[21] Wang, J.; Shi, D.; Huang, C.; Zhai, B.; Feng, S. Effects of Common Biochar and Acid-Modified Biochar on Growth and Quality of Spinach in Coastal Saline Soils. *Plants.* **2023**, *12*, 3232. https://doi.org/10.3390/plants12183232

[22] Schulz, H.; Dunst, G.; Glaser, B. No effect level of co-composted biochar on plant growth and soil properties in a greenhouse experiment. *Agron.* **2014**, *4*(1), 34-51. https://doi.org/10.3390/agronomy4010034

[23] Baker, D. P., & Nunez, M. Early Growth Stages and Their Impact on the Performance of Plants. *Plant Growth Regul*. **2009**, *59*(2), 105-118

[24] Shamim, M.; Saha, N.; Hye, F.B. Effect of biochar on seed germination, early growth of Oryza sativa L. and soil nutrients. *Trop. Plant Res.* **2018**, *5*(3), 336-342. https://doi.org/10.22271/tpr.2018.v5.i3.042

[25] Uslu, O.S.; Babur, E.; Alma, M.H., Solaiman, Z.M. Walnut Shell Biochar Increases Seed Germination and Early Growth of Seedlings of Fodder Crops. *Agric.* **2020**, *10*(10), 427. https://doi.org/10.3390/agriculture10100427

[26] Liu, M.; Lin, Z.; Ke, X.; Fan, X.; Joseph, S.; Taherymoosavi, S.; Liu, X.; Bian, R.; Solaiman, Z.M.; Li, L.; Pan, G. Rice Seedling Growth Promotion by Biochar Varies With Genotypes and Application Dosages. *Front. Plant Sci*. **2021**, 12. https://doi.org/10.3389/fpls.2021.580462

[27] Murtaza, G.; Rizwan, M.; Usman, M. et al. Biochar enhances the growth and physiological characteristics of *Medicago sativa*, *Amaranthus caudatus* and *Zea mays* in saline soils. *BMC Plant Biol*. **2024**, *24*, 304. https://doi.org/10.1186/s12870-024-04957-1

[28] Hafeez, Y.; Iqbal, S.; Jabeen, K.; Shahzad, S. Effect of biochar application on seed germination and seedling growth of Glycine max (L.) Merr. under drought stress. *Pak. J. Bot*. **2017**.

[29] Yousaf, M. T. B.; Nawaz, M. F.; Zia ur Rehman, M.; Gul, S.; Yasin, G.; Rizwan, M.; Ali, S. Effect of three different types of biochars on eco-physiological response of important agroforestry tree species under salt stress. *Int. J. Phytoremediation* **2021**, *23*(13), 1412-1422. https://doi.org/10.1080/15226514.2021.1901849

[30] Zhang, C.; Lin, Y.; Tian, X.; Xu, Q.; Chen, Z.; Lin, W. Tobacco bacterial wilt suppression with biochar soil addition associates to improved soil physiochemical properties and increased rhizosphere bacteria abundance. *Appl. Soil Ecol.* **2017**, *112*, 90-96.

[31] Ikram, M.; Minhas, A.; Ghoneim, A.M.; Mahmoud, E.; Mehran, M.; Rauf, A.; Ali, W. Promoting Tomato Resilience: Effects of Ascorbic Acid and Sulphur-Treated Biochar in Saline and Non-Saline Cultivation Environments. *Res. Sq*. **2024**. https://doi.org/10.21203/rs.3.rs-4922115/v1.

ASEAN
Journal of Scientific and Technological Reports
Online ISSN:2773-8752

Research article

Decision-Making Factors for Installing a Solar Roof Top System of 10 kWp in Thailand

Asamaporn Photim[1], Pisit Maneechot[2*], and Prapita Thanarak[3]

[1] School of Renewable Energy and Smart Grid Technology, Naresuan University, Phitsanulok, 65000, Thailand
[2] School of Renewable Energy and Smart Grid Technology, Naresuan University, Phitsanulok, 65000, Thailand
[3] School of Renewable Energy and Smart Grid Technology, Naresuan University, Phitsanulok, 65000, Thailand
* Correspondence: pisitm@nu.ac.th

Citation:
Photim, A.; Maneechot, P.; Thanarak, P. Decision-making factors for installing a solar rooftop system of 10 kWp in Thailand. *ASEAN J. Sci. Tech. Report.* **2025**, *28*(4), e258541. https://doi.org/10.55164/ajstr.v28i4.258541.

Article history:
Received: March 9, 2025
Revised: July 1, 2025
Accepted: July 20, 2025
Available online: August 16, 2025

Abstract: This research aims to investigate the factors influencing the purchase of insurance for solar rooftop systems with a capacity of not more than 10 kilowatts. The sample consists of 513 households that install such systems nationwide. To use convenient sampling online and analyze the data using descriptive statistics. It is necessary. And the standard control sets the significance level at 0.05. The research report found that the sample group examined efficiency (62.4%), individuals aged 40–50 years old (44.5%), frequency (53.2%), system operation (38.4%), and an average monthly income of 50,000 baht (37.6%). The average rate is 4.63 (SD = 0.13). Consider reviewing the overall purchase by the respondent, who is reviewing the insurance for the first time, to ensure the organization supports the repair or replacement of products annually.

Keywords: Solar Roof Top; Insurance; Solar PV panel installation; Marketing mix; Service decision

1. Introduction

Electrical energy is a crucial factor in performing various daily activities. The current electricity demand tends to increase in both the industrial sector, the business and administrative sectors, and households. In addition, most people are aware of the importance of the global warming problem and have begun to pay more attention to alternative energy sources. Alternative energy sources, such as hydroelectric power, wind power, and solar power, can help mitigate the adverse effects and pollution that harm the environment. Therefore, current electricity producers and service providers are more interested in electricity production, product production, and various services related to alternative energy [1].

Solar energy is a renewable energy that can be naturally regenerated. It is clean and has high potential. The use of solar energy can be divided into 2 types: using solar energy to generate electricity and using solar energy to generate heat (drying technology and hot water production technology). The most popular technology for using solar energy to generate electricity today is solar PV or what is known as solar PV. Solar energy is one of the renewable energy sources that has received significant support, as it is well-suited for Thailand, which experiences strong sunlight almost year-round. The government has set a target for the solar cell power generation project at 3,286 MW. The government has established a clear strategic plan to promote the installation of

solar PV rooftop power generation systems, including a measure to buy back electricity from residential groups that can generate electricity from sunlight. The electricity buyback rate is 1.68 baht/unit for 10 years, and there is a connection cost to the electricity grid with PEA of 8,500 baht (this price does not include 7% VAT and does not cover the cost of installing the Solar PV Rooftop system). Additionally, special criteria are in place for reducing the cost of connecting to the grid and related equipment for those interested in joining the project. Electricity generation from renewable energy is considered a technology that can help the country reduce fuel imports from abroad. It is also the use of clean energy, which is environmentally friendly and helps create energy security for the country. Solar PV on the roof of the house to produce electricity for own use (Rooftop PV system) is an electricity generation technology suitable for both city and rural houses, reducing electricity costs for homeowners. It also helps reduce the electricity shortage during peak load periods. It serves as a good starting point for promoting and expanding the business of electricity generation from rooftop solar energy, which can be widely adopted in the household sector to create benefits for electricity users and support national policies [2].

Therefore, those interested in such business must give more importance to the solar cell system, as most people's behavior when deciding to install solar cell energy is a key factor. And what are the reasons that make people decide to install or not install solar cell energy? What factors affect consumers' decisions to invest in solar cell energy? Siripoj studied the factors affecting the decision to install A solar power generation system for residential houses of consumers in Chiang Mai Province and found that the overall marketing mix factors that affect the decision to install a solar power generation system for residential houses of consumers in Chiang Mai Province are at the highest level, with most respondents giving importance to price, distribution channels, products, physical characteristics, marketing promotion, personnel, and processes, respectively [3]. Factors of decision to install a solar power system for residential homes by using the Analytic Hierarchy Process from experts in the energy business, 20 samples, and also collecting information about the satisfaction of various factors, 400 samples from consumer groups, to provide complete information. The results of the study were as follows: The most important main factor of decision is the reliability factor, with an importance factor level of 38.94%, and the most important sub-factor is the service quality factor. The primary factor that follows is the marketing mix, with a 34.17% importance level, and the most significant sub-factor is the price factor. From processing, the Consistency Ratio is based on the principle of comparison in the Analytic Hierarchy Process, and it ensures the satisfaction of both the expert group and the consumer group [4]. From the study of demographic factors and marketing mix factors (7Ps) that affect the decision to purchase solar cells of retail electricity users in Nonthaburi Province, it was found that the demographic factors of gender, age and occupation that are different affect the decision to purchase solar cells of retail electricity users in Nonthaburi Province with statistical significance at the .05 level of significance. In addition, the marketing mix factors of product, price, promotion, and physical environment, which differ significantly, affect the decision to purchase solar cells for retail electricity users in Nonthaburi Province at the .05 level of significance [5].

Currently, the solar power generation system installed on the roof and various buildings has started to require additional solar rooftop installations. However, there are still concerns about the impact of the installation, particularly in terms of electrical fires in the house due to the installation, as well as the cleaning of the panels, which can affect the system's efficiency. These concerns, therefore, affect the decision not to install the Solar rooftop system. Therefore, insurance for the Solar Roof Top System is another option that can alleviate concerns and encourage homeowners to install the System. Currently, no company has taken action on this matter, so customers' concerns persist.

From the problems mentioned above, the researcher has studied the factors affecting the decision to purchase insurance for the insured Solar Rooftop System with a size not exceeding 10 kWp in Thailand. The objective is to survey the insurance purchasing behavior of individuals with solar rooftop systems to understand their needs and attitudes towards purchasing insurance for systems with a size not exceeding 10 kWp. This will be used to develop, improve, and enhance the solar cell system, including services, to better respond to the needs of consumers.

Research objectives

1. To survey the needs of users and those who have never used Solar Roof Top system services of no more than 10 kWp in Thailand.

2. To study the marketing mix factors (7Ps) that affect the decision to purchase insurance for installing a Solar Roof Top system with a size not exceeding 10 kWp.

Expected benefits

1. To enable entrepreneurs to understand the marketing mix factors (7Ps) that affect the decision to use a Solar Roof Top system service of no more than 10 kWp, and to be able to use this research as a database for planning, developing strategies, improving, and expanding services.

2. To enable operators to know the factors in deciding to use the Solar Roof Top system and the trends of users of the Solar Roof Top system, and to use the information to think and analyze in determining the strategies of the Solar Roof Top system to meet the needs of users.

3. To inform entrepreneurs about demographic factors, occupations, and average monthly income, which influence their decision to use the Solar Roof Top system or not, to use as a database for improving, developing, and planning future service strategies.

2. Materials and Methods

The statistical method is divided into four steps as follows:

1. Collection of data is the collection of news, information, or facts required from the population with characteristics that are consistent with the needs. The collection and compilation of this data is considered to be the most important step in statistical methodology Because collecting data that is less reliable will result in the results of analysis and interpretation being of low reliability Therefore, this step requires planning for data collection, control of the data collection process, and thorough inspection of the data to ensure it can be analyzed.

2. Data presentation is a presentation of collected statistical data for dissemination to the general public to understand and prepare data for further analysis. There are various ways to present data, depending on the type of data and its volume.

3. Analysis of data. It involves analyzing the collected data and processing it in accordance with the established objectives, hypotheses, and research questions. For example, this involves comparing the difference in means between two populations using the Z or t test, and comparing the difference between the means of more than two populations. By using the variance test, the test statistic is F, which is used to test the relationship between qualitative variables. Alternatively, X2 is used to test the relationship between two sets of quantitative data, such as using correlation analysis, testing influence, forecasting, or using regression analysis. Additionally, advanced multivariate statistics, including MANOVA, canonical analysis, factor analysis, and discriminant analysis, can be employed. Processing can be done by hand or with a computer. Currently, there are ready-made statistical programs that can help analyze data efficiently and quickly, and can be used at every step, such as SPSS for Windows, MINITAB, and SAS. The processing can be done manually or by computer. Currently, there are ready-made statistical programs that can help analyze data efficiently and quickly, and can be used at every step, such as SPSS for Windows, MINITAB, and SAS.

4. Interpretation or conclusion of data. It involves using the results from the analysis to draw a conclusion. Written as a report of results, such as t = 3.1, what does it mean? Is there a difference between the means of the two population groups? The value R = -0.85 indicates a significant relationship. How much or little? What direction is there? This requires further study to acquire the necessary knowledge.

Theories and concepts related to marketing mix factors (7PS)

The marketing mix refers to the variables or marketing tools that can be controlled and manipulated. Companies often use them together to meet the needs and wants of their target customers. Traditionally, the marketing mix consisted of only four variables. These include product, price, product distribution location or channel, and promotion. Later, three additional variables were developed. It consists of People, Physical Evidence, and Process to align with the important concepts of modern marketing, especially in service businesses. Therefore, together they can be called the 7Ps marketing mix.

2.1 Product aspect refers to things that the company offers for sale to generate interest through consumption or by using services that can make customers satisfied. This satisfaction may come from tangible or intangible aspects, such as design, packaging, smell, color, price, brand, product quality, and the reputation of the manufacturer or distributor.

2.2 Price refers to the amount of money that must be paid to receive the company's products, goods, or services, or it may be the total value that the customer perceives to receive benefits from using the products, goods, or services that are worth the amount paid. Which customers use to compare prices that have to be paid out with value. What customers will receive in return for the product. If the value is higher than the price, the customer will make a buying decision. However, the business should consider the following factors when determining its pricing strategy: the market situation, conditions, and forms of competition, as well as direct and indirect costs.

2.3 Distribution channels refer to the distribution channels of products or services, including methods for delivering those products or services to consumers to meet demand. Specific criteria must be considered to determine the target group and through which channels products or services should be distributed to consumers to be most effective.

2.4 Promotion refers to marketing communication tools to create motivation, thoughts, feelings, needs, and satisfaction in products or services. This will be used to motivate target customers to want the product or remind them of it. It is expected that marketing promotions will have an influence on feelings, beliefs, and behavior in buying products or services, or may involve communication to exchange information between sellers and buyers. However, a combination of various marketing communication tools must be used.

2.5 Personnel refers to employees who work to benefit various organizations, including business owners, top executives, middle executives, lower executives, general employees, housekeepers, etc. Personnel are considered an important part of the marketing mix, as they are the ones who think, plan, and operate to drive the organization in the strategic direction. Additionally, personnel play another important role in forming relationships with and interacting with customers, which is crucial in ensuring customer satisfaction.

2.6 Process aspect refers to activities related to procedures and practices in the service that are offered to service users to provide services correctly and quickly. In each process, there can be numerous activities, depending on the organization's structure and operational methods. If the various activities within the process are linked and coordinated, the overall process will be efficient, resulting in customer satisfaction.

2.7 Physical characteristics refer to things that customers can experience from choosing the organization's products or services. It is a creation of outstanding and high-quality differences, such as store decoration, the clothing of store employees, the way they interact with customers, and fast service. These things are necessary for business operations, especially service businesses that should create quality.

Related research

Kamontip Yubol [6] said: The objective of the research study was: 1) to study the marketing factors affecting the decision to install a solar roof among people in Bangkok, and 2) to study the relationship model of marketing factors affecting the decision to install a solar roof among people in Bangkok. The study population consisted of individuals in Bangkok who had installed solar roofs. A total of 400 people were surveyed using questionnaires and statistical processing, including Frequency Distribution, Percentage, Mean, and Standard Deviation. The results of hypothesis testing used the Pearson product-moment correlation coefficient and Multiple regression analysis. The research results show that:

Most respondents were female, 222 people amounts to 55.5%, 31 - 40 year of age, 150 people amounts to 37.5%, graduated with bachelor's degree, 302 people amounts to 75.5%, worked in Government officials/state enterprise employees, 145 people amounts to 36.2% and average incomes 20,001 – 30,000 Baht, 171 people amounts to 42.7%

The marketing factors affecting the decision to install a solar roof among people in Bangkok were found to be the highest. The most critical factors were product, physical evidence, place, process, promotion, price, and people, in that order. A study on the decision to install solar roofs among people in Bangkok found that the overall level was the highest. Customers provided the most opinions in terms of purchasing decisions, post-purchase behavior, evaluation of alternatives, and searching for information, respectively.

Hypothesis testing revealed that the marketing factors affecting the decision to install a solar roof among people in Bangkok were statistically significant at the 0.01 level. The main factor influencing the decision to install a solar roof for people in Bangkok was price. The following ranking was promotion, people, product, place, and physical evidence, in that order. The least factor was process. The marketing factors affecting the decision to install a solar roof for people in Bangkok can be predicted with about 85.3 percent accuracy, with the statistical significance at the level of 0.05.

Siriphon Sriwirat [7] stated that this study aimed to examine the factors affecting customers' decision-making in Chiang Mai Province regarding the installation of home solar power systems. Samples for this study were identified among 400 individuals who expressed interest in and had the decision-making authority to install solar power systems in their homes in Chiang Mai. Data were analyzed by descriptive statistics: frequency, percentage, mean, and standard deviation (S.D.), and the inferential statistics: T-test to compare differences between the means of two sample groups and One-Way Analysis of Variance: ANOVA to compare means of more than two groups of variables.

The findings showed that most respondents were female, under 30 years of age, and employed as employees or private individuals. Their educational background was a bachelor's degree or its equivalent. They held the status of owners of a single-attached three-story house, and 3-4 members resided in the house. They mostly used electricity between 6:00 p.m. and 12:00 a.m.

Results of the study showed that in an overview, service marketing mixed factors, which affected decision-making of customers in Chiang Mai province towards installing home solar power systems at the highest level and on which they paid the highest level of concern were price, place, product, physical evidence, promotion, people, and process, respectively.

Conceptual framework of the research

From the study of research data, theories, and various articles mentioned above, the researcher has used information from the literature review to determine the conceptual framework of the research to be used as a guideline for conducting research on the factors of decision making in purchasing insurance for installing a Solar Roof Top system of no more than 10 kWp., using information on marketing mix factors (7Ps) that influence the decision making in purchasing insurance for installing a Solar Roof Top system of no more than 10 kWp.

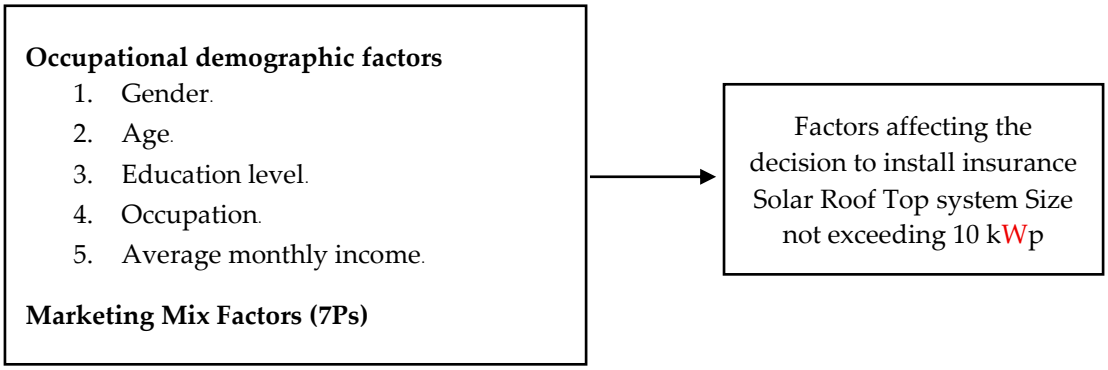

Figure 1. Research Framework

3. Research Methodology

This research is survey research, which has the following details:

The study of "Factors affecting the decision to purchase insurance for installing a Solar Roof Top system of no more than 10 kWp" is quantitative research. It is survey research. Use questionnaires to collect data, analyze statistical data using ready-made programs, and summarize research results to present them in the form of tables and lectures.

3.1 Population and sample group

The target population for this research study is the population residing in Thailand, specifically the consumer group that decides to purchase solar PV in Thailand, comprising 513 households across all regions of the country.

3.2 Creation of research instruments

The research instruments used in this study were questionnaires, which were used to collect data. The data collection instruments for this study were questionnaires on the marketing mix, focusing on the decision-making factors in purchasing insurance for installing a Solar Rooftop system of no more than 10 kWp. These

questionnaires were developed by the researcher based on a review of the relevant literature to address the research objectives. By dividing the details of the questionnaire into 3 parts, the details are as follows:

Part 1 is a question about the personal characteristics of the respondents, including gender, age, educational status, and monthly income.

Part 2 Information on marketing mix factors (7Ps) for solar cell systems for Solar Roof Top systems, size not exceeding 10 kWp.

Part 3 is a question about Part 3: Information, specifically creating an insurance business model and a solar cell system for small Solar Rooftops.

For data analysis in sections 2 and 3, the questionnaire employed a rating scale in the form of a Likert Scale, allowing respondents to select only one answer. There were 5 levels of scores, using an Interval Scale type of data measurement level. The scoring criteria were as follows:

A score of 5 means the most
A score of 4 means a lot
A score of 3 means moderate
A score of 2 means little
A score of 1 means the least

3.3 Checking the quality of research tools

Testing Tools from the questionnaire created for the study. The researcher has tested for reliability and confidence of the questionnaire as follows: 1) Take the designed questionnaire to ask for advice from an advisor, and consider and check the accuracy of the content. 2) Take the questionnaire that has been checked and has suggestions from the advisor, edit and improve the questionnaire to make it more accurate, complete, and cover more content. 3) The questionnaire was used to find the quality of the instrument, and the researcher tested its reliability by finding the Cronbach's Alpha Coefficient with a ready-made statistical program. If the reliability of the questionnaire is greater than or equal to 0.70, it is considered reliable. The researcher therefore used the questionnaire to calculate the reliability using the method above and obtained the Cronbach's Alpha Coefficient (0.83).

3.4 Data collection

The researcher developed and refined the questionnaire until it reached a high quality and then used Google Forms to distribute the questionnaire link through various online channels to a sample of 513 households that had decided to purchase solar PV in Thailand. The collected questionnaire was checked for accuracy and completeness. Then save the information and analyze the data.

3.5 Data Analysis

Once the data on factors influencing the decision to install a solar rooftop system with a capacity not exceeding 10 kilowatts has been collected completely and sufficiently, the researcher will analyze the data using Microsoft Excel. Descriptive statistics, including frequency distribution, percentage, mean, and standard deviation, will be used to summarize and describe the general characteristics of the data obtained from the sample group.

4. Results and Discussion

1. Demography group

From the analysis of the questionnaire data, it was found that the sample group had a higher proportion of males than females, with 62.4% males, 33.9% females, and 3.7% unspecified gender. Most of the sample group were 40-50 years old, accounting for 44.5 percent, and had a bachelor's degree, accounting for 53.2 percent of the sample group. Most of them worked as employees of private companies, accounting for 38.4 percent, and the majority had an average monthly income of less than 50,000 baht, which comprised 37.6 percent of the sample group.

Table 1. Data of the demographic respondents

Category	Respondents (%)
Gender	
Male	320 (62.4)
Female	174 (33.9)
Not specific	19 (3.7)
Age	
Lower than or equal to 40 years	147 (28.6)
41-50 Years	228 (44.5)
51-60 Years	127 (24.7)
More than 60 years	10 (1.9)
Marital status	
Married	308 (60)
Single	147 (28.7)
Widowed/divorced/separated	58 (11.3)
Highest level of education	
Undergraduate	48 (9.4)
Bachelor's degree	273 (53.2)
Master's degree or above	192 (37.4)
Occupation	
Business Owner	160 (31.2)
Civil servants/state enterprises	108 (21.1)
Private employees	197 (38.4)
Students	13 (2.5)
Other	35(6.8)
Average family monthly income	
Below 50,000 baht	193 (37.6)
50,001 – 100,000 baht	179 (34.9)
100,001 – 150,000 baht	69 (13.5)
150,001 baht or more	72 (14)
Resident location	
North	90 (17.5)
Northeast	66 (12.9)
Middle	237 (46.2)
East	47 (9.2)
South	73 (14.2)

Personal factors that affect the decision to purchase insurance for installing a Solar Roof Top system of no more than 10 kWp are as follows:

Categorized by gender, age, and education, it can be concluded that gender, age, and education have different effects on the decision to choose insurance for installing a Solar Rooftop system. And it affects choosing to get solar cell insurance. People with less than a master's degree are worried about deciding to install solar PV. People with lower education levels than a master's degree are more concerned about deciding to install solar PV than those with a master's degree, who think that installing solar PV will be worthwhile and that the benefits will be received from its use, including the service provider's reliability and truthful information.

Classified by monthly income, it can be concluded that there are groups of consumers with different monthly incomes. It affects the decision-making factors in selecting insurance for installing a Solar rooftop system. The products are different. It was found that consumers with a monthly income of less than 50,000 baht and those with an income of more than 50,001 baht exhibit different market factors when choosing solar cell products. Due to the high price of the product

2. Marketing mix factors

From the analysis of data on marketing mix factors (7Ps) that affect the decision to purchase Solar Sell for the installation of a Solar Roof Top system size not exceeding 10 kWp.

Table 2. Mean and Standard Deviation of Market Factors Affecting the Decision to Purchase Insurance for the Installation of Solar Rooftop Systems with a Capacity of Up to 10 kWp.

Marketing mix factors	$\bar{x}$	SD	level
1. Product factors			
Solar Cell panels and Inverters are brands that must have distributors in Thailand.	4.74	0.50	the most
Materials and equipment must comply with installation standards.	4.95	0.24	the most
Installation companies require their installers to receive installation training from a reliable institute or organization.	4.95	0.24	the most
2. Price factors			
The insurance price should be calculated based on the quality of the products selected for installation, including PV, Inverters, and equipment that meet electrical standards, as well as the business credit of the installer.	4.53	0.70	the most
The price of insurance should be calculated based on the reliability and experience of the installer.	4.63	0.55	the most
The price of the insurance should be calculated based on the warranty period provided by the installer.	4.54	0.73	the most
3. Factors related to distribution channels			
It is convenient and easy to contact, with immediate responses available through various channels, including Facebook, Line, telephone, and Email.	4.58	0.68	the most
The service location looks trustworthy.	4.56	0.70	the most
The service location provides knowledge and training for solar cell system installers. for homes to help make decisions, buy additional insurance	4.59	0.68	the most
4. Marketing promotion factors			
There are various advertising channels, such as Facebook, Line@, YouTube, and Email, among others.	4.47	0.78	a lot
There are discounts, promotional prices, free maintenance services, and free panel cleaning for 2 years, among other benefits.	4.60	0.71	the most
There is a request for a parallel electricity permit at a special price.	4.60	0.71	the most
5. People factors			
The staff can provide accurate, quick, and straightforward advice on insurance premium rates.	4.59	0.68	the most
The staff are polite and speak nicely.	4.67	0.59	the most
The staff are knowledgeable and experienced in providing solar power generation system services and guaranteeing solar cell systems for residential homes.	4.70	0.62	the most

Table 2. Mean and Standard Deviation of Market Factors Affecting the Decision to Purchase Insurance for the Installation of Solar Rooftop Systems with a Capacity of Up to 10 kWp. (Continue)

Marketing mix factors	$\bar{x}$	SD	level
6. Physical environmental factors			
Entrepreneurs must provide the public with helpful information.	4.55	0.67	the most
The entrepreneur guarantees a physical store where you can visit and view the product before making a purchase decision.	4.58	0.71	the most
Entrepreneurs have access to standard and reliable tools.	4.67	0.61	the most
7. Service process factors			
Insurance operators must be reliable and have a good image.	4.65	0.61	the most
Insurance operators must have experience in underwriting various types of insurance.	4.63	0.64	the most
The insurance operator must be able to meet your needs exactly as you want, with flexibility like the insurance.	4.60	0.62	the most
Total	**4.63**	**0.13**	**the most**

From Table 2, it is found that the factors affecting the decision to choose insurance for installing a Solar Rooftop system with a size not exceeding 10 kWp are overall at the level that most significantly affects the purchase decision ($\bar{x}$ = 4.63), at the highest level. When considering each aspect, it was found as follows:

Product factors at the highest level. Consumer groups who have purchased solar cell products believe that the brand must be reliable, the product must be of high quality, and it must meet a certified standard (TIS), which influences their decision to purchase Solar Sell and their choice of insurance for installing a Solar Rooftop system.

Price factors are at the highest level. Groups of consumers who have previously purchased solar cell products believe that the price of the product is commensurate with its quality. And it is worth it, as it affects the decision to buy solar and choose to get insurance for installing a solar rooftop system.

Distribution channels at the highest level. Groups of consumers who have previously purchased solar cell products believe that the place of sale is a reliable source of information. This affects the decision to choose to buy solar panels and opt for insurance for installing a Solar Rooftop system.

Marketing promotions at the highest level. A group of consumers who have previously purchased Solar sell products commented that providing information and product recommendations affects their decision to choose Solar sell and opt for insurance for installing a Solar Rooftop system.

The staff at the highest level. Service affects the decision to install a Solar rooftop system. The company's delivery process is fast and accurate. After-sales service is provided. The company's product installation process is correct. The technicians are experienced and have received thorough training.

Physical environment at the highest level. The solar power generation company provides a warranty after delivery. The solar power generation company provides a convenient service.

The service process is at the highest level. The personnel who influence the decision to choose the Solar Roof Top system, the employees of the solar power generation system company, provide excellent service and have polite manners, smiling and dressing well, which makes them look trustworthy. The company's employees possess good knowledge and ability regarding solar power generation systems.

5. Conclusions

The marketing factors that affect the decision to purchase solar energy and choose insurance for installing a Solar Rooftop system with a size not exceeding 10 kW. Include product, price, location, and marketing promotion. The researcher can discuss the results of each aspect as follows:

1. Seven marketing mix factors influence the decision to install Solar Sell. Overall, it is at the highest level. Consumers make purchase decisions based on product quality, user manual, and long service life. There are promotions for low-priced purchases, discounts, and installment plans. There are gifts and a website. This finding is consistent with the research of [8], which studied the marketing mix factors from the customer's perspective that influence the decision to purchase scientific equipment online. The research results found that factors affecting the purchase decision include product safety, a price appropriate for the product quality, cash on delivery, fast contact channels for ordering, timely information updates, quick contact, warranty for damaged products, receiving the correct product, and speedy delivery.

2. Different statuses and incomes affect the decision to buy solar cell products. Different occupations affect the decision. Because the price of the product is relatively high, it affects the decision to buy. While different occupations have other knowledge about the product, it is a factor that affects the decision to buy. This finding is consistent with the research of [9], which analyzed factors affecting the social acceptance of rooftop solar power generation projects. The study found that income and occupation are related to the acceptance of household solar power generation systems. The most important factor influencing the decision to accept is the reduction of global warming. The guidelines for creating acceptance found that the entrepreneur's sales promotion measures are the most important, such as insurance or compensation for damages caused by natural disasters and after-sales service, especially maintenance, including tax deduction measures.

Therefore, most people are still concerned about deciding to install a Solar Roof Top system due to the contractor's work standards and the quality of materials and equipment used to install solar panels on the roof, which can cause "fires". Most contractors lack sufficient knowledge and understanding of electrical safety. In addition, homeowners who install Solar Rooftop systems often lack the budget to hire consultants to oversee the installation. The installation of Solar Rooftop systems should be designed and installed by an electrical engineer who is an expert in solar cell system installation, directly from a relevant agency. Quality equipment should be used to install solar cell systems on the roof. Additionally, annual maintenance is necessary to ensure that the solar panels and other equipment continue to function safely and without damage during operation. Including being able to check various protection systems, to ensure it is still in a safe condition, and can be protected in the event of an emergency

6. Acknowledgements

The authors would like to express their gratitude to the executives from the private sector who played an important role in supporting the data used in this research, including facilitating various aspects throughout the study and conducting this research, as follows Major General Khosit Thiampetch for supporting the knowledge and providing advice; Mr. Thanachai Sae-iang, Executive of Siam Solar Cell Co., Ltd.; Mr. Pichai Chetsupa, Executive of PCOA Technology Co., Ltd.; Mr. Worawit Plookcharoen, Executive of Coco Capital Co., Ltd.; Mr. Phubes Butrungroj, Executive of Hatyai Solar Innotech Co., Ltd.; Mr. Sarachai Techotanon, Executive of Energy Green Plus Co., Ltd.; Mr. Phongsupa Wingwon, Executive of Sunflower Intersolution Co., Ltd.; and Mr. Sittichai Thongnet, Executive of Solar Supply Energy Co., Ltd.

Author Contributions: A.P. and P.T.; methodology, P.M. and P.T.; validation, A.P., and P.M.; formal analysis, A.P., and P.M.; writing—original draft preparation, A.P., and P.M.; writing—review and editing, A.P., and P.M.; visualization, P.M. and P.T.; supervision. All authors have read and agreed to the published version of the manuscript.

Funding: none

Conflicts of Interest: The authors declare no conflicts of interest. The funders had no role in the study's design; in the collection, analyses, or interpretation of data; in the writing of the manuscript; or in the decision to publish the results.

References

[1] Kanokphan, N. Factors affecting the decision to install solar PV and solar rooftops of small electricity users in the metropolitan area. Mahidol University, Thailand, **2018**.

[2] Sriwirat, S., Factors affecting consumers' decision to install solar power generation systems for residential homes in Chiang Mai Province. *Chiang Mai University Journal of Business Administration* **2021**, *7*(3).

[3] Sriwirat, S., Factors affecting the decision to install a solar power generation system for residential homes of consumers in Chiang Mai Province. *Chiang Mai University Business Journal* **2021**, *7* (3).

[4] Thisopha, C., Influencing the Decision to Install a Solar Power System for Residential Homes by Using Analytic Hierarchy Process. *Interdisciplinary Research Journal: Graduate Studies l* **2019**, *8*(2). https://doi.org/10.2139/ssrn.3552406

[5] Chimpae, S. FACTORS AFFECTING THE DECISION TO USE SOLAR CELL OF RETAIL ELECTRICITY CONSUMERS IN NONTHABURI. Ramkhamhaeng University, Thailand.

[6] Yubol, K. MARKETING FACTORS AFFECTING THE DECISION TO INSTALL SOLAR ROOF OF PEOPLE IN BANGKOK. Ramkhamhaeng University.

[7] Sriwirat, S., Factors Affecting Decision to Install a Solar Power System for Residential Homes of Consumers in Chiang Mai Province. *Chiang Mai University Journal of Business Administration* **2021**, *7*(3).

[8] Ariyadetch, M., The Marketing Mix in Customer Perspective Which Influence the Buying Decision of Science Equipment Products in Online Customers. *Journal of Modern Learning Development* **2020**, *5*(5), 100-111.

[9] Suppanich, P. Analysis of Factors for Social Acceptance of Solar Rooftop Project. Chulalongkorn University, **2014**.

ASEAN
Journal of Scientific and Technological Reports
Online ISSN:2773-8752

Research article

Solving Transshipment Problem in Glove Manufacturing Under the FSC Standard

Mareena Mihad[1], Sakesun Suthummanon[2], and Dollaya Buakum[3*]

[1] Faculty of Engineering, Prince of Songkla University, Songkhla, 90110, Thailand
[2] Faculty of Engineering, Prince of Songkla University, Songkhla, 90110, Thailand
[3] Faculty of Engineering, Prince of Songkla University, Songkhla, 90110, Thailand
* Correspondence: dollaya.b@psu.ac.th

Citation:
Mihad, M.; Suthummanon, S.; Buakum, D. Solving transshipment problem in glove manufacturing under the FSC standard. *ASEAN J. Sci. Tech. Report.* **2025**, *28*(4), e259187. https://doi.org/10.55164/ajstr.v28i4.259187.

Article history:
Received: May 6, 2025
Revised: July 14, 2025
Accepted: July 20, 2025
Available online: August 16, 2025

Abstract: This study proposes a mathematical transshipment model to optimize transportation in glove manufacturing by Forest Stewardship Council (FSC) standards. The objective is to minimize total transportation costs across a multi-tiered network comprising rubber farmers, small-scale intermediary traders, large-scale intermediary traders, a concentrated latex factory, and a rubber glove factory. Unlike conventional transshipment models, this approach explicitly distinguishes parallel product flows from FSC-certified and non-FSC-certified sources, reflecting segregation requirements mandated by FSC standards. This dual-flow structure introduces unique routing constraints and decision variables that are rarely addressed in the existing literature. The model incorporates real-world constraints related to supply availability, demand fulfillment, and transportation capacity, based on empirical data from a representative case study. The optimization problem was solved using LINGO software. The case study involved 250 farmers (125 non-FSC-certified and 125 FSC-certified), 125 small-scale intermediary traders, 6 large-scale intermediary traders, a concentrated latex factory, and a rubber glove factory producing approximately 50% FSC-certified and 50% non-FSC-certified gloves. This separation is critical for ensuring FSC compliance and achieving precise cost optimization. Before implementation, transportation costs totaled 82,228 baht per million gloves produced. Upon applying the model, costs decreased to 75,503.33 baht per million gloves, indicating a reduction of 6,724.67 baht or approximately 8.18%. These results affirm the effectiveness of mathematical modeling in reducing logistics costs within sustainable supply chains and offer a framework adaptable to other industries with similarly structured supply chains.

Keywords: Transshipment model; logistics cost reduction; transportation cost optimization; rubber glove manufacturing; mathematical model

1. Introduction

Thailand's rubber glove manufacturing industry is crucial in the global market, particularly during the COVID-19 pandemic, which significantly increased global demand for rubber gloves. As a result, Thailand became one of the leading producers and exporters of high-quality rubber gloves. However, despite Thailand's production capabilities, the process of transporting raw materials from production sources to factories is complex and faces several challenges, particularly high transportation costs. This is due to the multiple stages in the supply chain and the involvement of many stakeholders, ranging

from farmers who grow rubber to small and large intermediaries, then to latex concentration factories, and finally to rubber glove manufacturing plants. These factors contribute to the high transportation costs, which affect the industry's competitiveness in the global market [1]. Additionally, the rubber glove manufacturing industry faces pressure to adhere to sustainable management standards, as requested by customers, such as the Forest Stewardship Council (FSC) standards.

The Forest Stewardship Council (FSC) standard represents an internationally recognized certification for sustainable forest management. Products bearing this certification must be produced in a manner that is environmentally, economically, and socially responsible. For example, rubber trees harvested during production must be replanted or allowed to regenerate naturally. Forest management under FSC guidelines requires careful consideration of environmental impacts, biodiversity, and the well-being of surrounding communities [2]. While compliance with FSC standards promotes sustainability, it also adds complexity to the supply chain due to the need for strict oversight and comprehensive control throughout both production and transportation processes. These requirements can lead to increased operational and logistics costs. Nevertheless, FSC-certified products often gain a competitive edge, with studies showing potential sales growth of over 4%. 66% of consumers express a willingness to support brands that demonstrate environmental commitment [3]. In 2020, the European Union (EU), Japan, and several other countries announced that they would cease importing wood, rubber, and derivative products unless sourced from FSC-certified plantations. This shift has elevated the importance of FSC compliance in industries such as rubber glove manufacturing. Although FSC-certified gloves are generally more expensive to produce than their conventional counterparts, global demand has surged to approximately 280 billion pieces annually. To remain competitive while adhering to FSC standards, manufacturers must adopt advanced technologies and decision-support tools to enhance the efficiency of their logistics operations. Among these tools, the LINGO optimization program has proven particularly effective for solving complex supply chain problems. Additionally, building a sustainable supply chain by FSC principles requires systematic planning and strategic optimization. Mathematical models play a crucial role in simulating complex supply chain networks and identifying cost-saving opportunities [4–7]. For instance, Mula et al. developed models for coordinating production and transportation across multi-stage supply chains, addressing both cost and capacity constraints [8]. In the agri-food sector, Ahumada and Villalobos demonstrated how mathematical programming can facilitate efficient resource allocation and strategic planning [9].

Lingo is a powerful software tool developed by LINDO Systems Inc. that is used to solve mathematical models that have already been developed. This program is designed to assist analysts and researchers in solving complex optimization problems, particularly those that require finding the best solution under specified constraints [10]. Several studies have confirmed Lingo's effectiveness in solving logistics network problems, especially in uncertain or complex environments, such as stochastic supply chain network planning [11], fresh food supply chain simulation [12], and milk run transportation optimization [13]. Lingo has been widely applied in both agricultural and industrial logistics research [16], providing precise and cost-efficient solutions for complex decision problems [10, 15, 18]. For example, the case study by F. M. Puspita et al. [14] focused on optimizing waste collection routes in the Kalidoni district of Palembang. The objective was to minimize both transportation distance and time by considering critical factors such as “time windows” and “deadlines.” Waste was categorized into work zones, and the RC-OCVRPTWD model was solved using LINGO 13.0. Results showed that Work Area 1 had a distance of 28.6 km with a completion time of 2 hours and 51 minutes, Work Area 2 covered 23.6 km in 1 hour and 42 minutes, and Work Area 3 covered 38 km in 3 hours and 16 minutes. Dandi Nurdiansyah [15] also demonstrated Lingo’s usefulness in optimizing egg delivery costs at AyamSehat.com in Cimahi. Initially, the North West Corner (NWC) method was used, resulting in a cost reduction from Rp. 278,000 to Rp. 255,000. Further optimization with LINGO reduced the cost to Rp. 240,000. This study highlights how combining heuristic methods, such as NWC, with mathematical tools, like LINGO, can significantly improve distribution efficiency. In a related study, E. Yuliza et al. [16] addressed the Capacitated Vehicle Routing Problem (CVRP) in the context of LPG gas distribution. They first applied the Clarke and Wright heuristic and then refined the solution using Lingo. The heuristic approach resulted in a total distance of 151.94 km, while Lingo yielded 161.59 km, suggesting that the heuristic method was more efficient for this particular case. This reinforces the value of hybrid approaches in routing

optimization. Finally, D. Buakum and W. Wisittipanich [17] proposed a mixed-integer programming (MIP) model to solve internal task scheduling in a cross-docking terminal, inspired by operations at Thailand Post Distribution Co., Ltd. Their model, solved with LINGO 14.0, aimed to minimize makespan while managing limited resources such as working teams and transfer equipment. The results showed that while LINGO provided optimal solutions for small instances, larger problems posed computational challenges. The study's cost and sensitivity analysis confirmed the trade-off between resource usage and operational efficiency. Together, these studies confirm Lingo's reliability and flexibility in solving diverse logistics optimization problems from waste management and food distribution to cross-docking and industrial routing. These findings support the application of this approach in the current research to enhance cost efficiency within the FSC-certified rubber glove supply chain. While these studies collectively demonstrate the broad applicability and effectiveness of LINGO in solving various logistics optimization problems, they primarily address general transportation, routing, or scheduling challenges without explicitly incorporating sustainability certification requirements. Unlike prior models, the transshipment model proposed in this study directly integrates FSC Chain of Custody constraints by explicitly separating FSC-certified and non-certified latex flows through dedicated decision variables and independent supply-demand constraints. This structural distinction ensures compliance with rigorous FSC standards throughout all transportation stages, setting this work apart from conventional transshipment approaches that do not address certification-mandated segregation. As a result, the model contributes a novel framework for simultaneously optimizing logistics costs and sustainability compliance within certified supply chains.

In this study, the goal is to determine the most cost-effective transportation route from the rubber plantations to the rubber glove manufacturing factory, which involves multiple stakeholders, including 250 farmers, 125 small intermediaries, 6 large intermediaries, a latex production factory, and a rubber glove manufacturing plant. The supply chain includes both FSC-certified and non-FSC-certified raw materials, which adds complexity to the logistics process. Lingo software is used to solve the mathematical model that calculates transportation costs, addressing the Transshipment Problem, which involves intermediate distribution points in the supply chain. The objective is to reduce transportation costs under the FSC standard while optimizing the multi-stage supply chain. By applying the Lingo program, the study aims to identify the lowest-cost transportation methods while ensuring compliance with sustainability standards. Ultimately, this research seeks to enhance the competitiveness of Thailand's rubber glove manufacturing industry in the global market. Furthermore, to demonstrate the robustness and adaptability of the proposed model, this study also includes a sensitivity analysis on key parameters such as fuel prices and product demand levels. By simply modifying the input data used in the computations, the model can evaluate different economic scenarios and assess the impact of fluctuations in operational costs and market demand. This highlights the flexibility of the mathematical framework to accommodate diverse conditions, thereby reinforcing its practical value as a decision-support tool for sustainable and cost-efficient supply chain management under FSC standards.

2. Materials and Methods

To enhance the accuracy and effectiveness of transportation cost reduction in the rubber glove manufacturing industry, adhering to Forest Stewardship Council (FSC) standards, this study was designed using a mathematical modeling approach. The methodology involves collecting real-world supply chain data, constructing a transshipment model to simulate transportation flows, and applying the Lingo program to solve and optimize the model. The following sections describe the data collection process, model development, and solution approach.

2.1 Data Collection

This research aims to reduce transportation costs in the rubber glove manufacturing supply chain, adhering to Forest Stewardship Council (FSC) standards, by utilizing real-world data from a powder-free glove factory certified by FSC. The supply chain in this case study comprises 250 farmers, consisting of 125 non-FSC-certified farmers and 125 FSC-certified farmers, 125 small-scale intermediary traders, 6 large-scale intermediary traders, 1 concentrated latex factory, and 1 rubber glove factory. The key data used to develop the model includes

2.1.1 Transportation distances between supply chain points

2.1.2 Supply and demand quantities at each stage

2.1.3 Transportation capacity limits

2.1.4 Unit transportation costs

All data were collected through structured questionnaires and in-depth interviews with stakeholders across the supply chain, conducted between March and April 2023. An overview of the supply chain structure is illustrated in Figure 1.

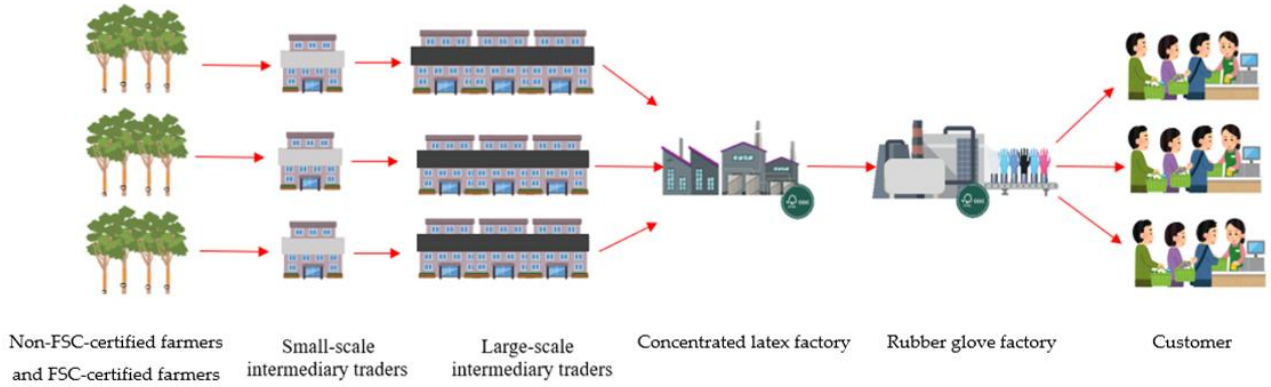

Figure 1. Rubber Glove Industry Supply Chain.

2.2 Transshipment Model Development

This research developed a transshipment model, a type of linear programming model, to identify the most cost-effective multi-stage transportation routes for latex in the supply chain. The model aims to minimize total transportation costs while adhering to the constraints of the FSC system, which includes environmental, social, and economic considerations.

2.2.1 Transportation Network Structure

The model is structured into five stages, reflecting the actual sequence of the supply chain

i : Non-FSC-certified farmers
i' : FSC-certified farmers
j : Small-scale intermediary traders
k : Large-scale intermediary traders
l : Concentrated latex factory
m : Rubber glove factory

2.2.2 Definition of constraints

The objective of the model is to minimize total transportation costs, subject to the following three key constraints

2.2.2.1 Supply constraints at the farmer level

2.2.2.2 Demand constraints at the rubber glove factory

2.2.2.3 Capacity constraints for each transportation route

To ensure compliance with FSC Chain of Custody (CoC) standards, the mathematical model explicitly separates the transportation flows of FSC-certified and non-FSC-certified latex. This segregation is enforced by using distinct decision variables and independent supply-demand constraints for each type of latex. As a result, the model prevents the mixing of FSC and non-FSC materials across all transportation and transshipment stages. This directly affects routing decisions by mandating dedicated transportation trips and transshipment handling for FSC latex, reflecting the operational requirements imposed by FSC certification.

Additionally, the model incorporates parameters such as the number of vehicles and their capacities, which are based on actual transportation data collected from the case study. Each vehicle type (n = 1, 2, 3, 4) corresponds to a specific transportation link in the supply chain, reflecting operational realities. For example, n=1 and n=2 represent trips from farmers to small-scale intermediary traders, n=3 covers transportation from small to large intermediaries, and n=4 handles movements from the latex factory to the glove factory. These

parameters ensure that vehicle assignment and capacity constraints are realistically applied, directly influencing transportation planning and cost optimization within the FSC-certified supply chain.

Furthermore, by ensuring the strict segregation and traceability of FSC-certified latex throughout the supply chain, the model inherently upholds the social and environmental objectives of the FSC standard. This includes supporting fair practices for certified smallholder farmers and protecting ecosystems by maintaining the integrity of certified sourcing. The mathematical constraints thus do not merely enforce logistical separation but also safeguard the environmental stewardship and community welfare principles embedded in FSC certification.

2.2.3 Mathematical Model Formulation

The transshipment model was formulated using a linear programming approach.

Indices

i : Non-FSC-certified farmers
i' : FSC-certified farmers
j : Small-scale intermediary traders
k : Large-scale intermediary traders
l : Concentrated latex factory
m : Rubber glove factory

Parameters

c_{ij} : Transportation cost from non-FSC-certified farmers to small-scale intermediary traders (Baht per trip)
$c_{i'j}$: Transportation cost from FSC-certified farmer to small-scale intermediary traders (Baht per trip)
c_{jk} : Transportation cost from small-scale intermediary traders to large-scale intermediary traders (Baht per trip)
c_{kl} : Transportation cost from large-scale intermediary traders to concentrated latex factory (Baht per trip)
c_{lm} : Transportation cost from concentrated latex factory to rubber glove factory (Baht per trip)
s_i : Latex production capacity of non-FSC-certified farmer (kilograms per lot)
$s_{i'}$: Latex production capacity of FSC-certified farmer (kilograms per lot)
s_j : Latex receiving capacity of small-scale intermediary traders (kilograms per lot)
s_k : Latex receiving capacity of large-scale intermediary traders (kilograms per lot)
s_l : Latex receiving capacity of concentrated latex factory (kilograms per lot)
D_j : Latex demand of small-scale intermediary traders (kilograms per lot)
D_k : Latex demand of large-scale intermediary traders (kilograms per lot)
D_l : Latex demand of concentrated latex factory (kilograms per lot)
D_m : Latex demand of rubber glove factory (kilograms per lot)
$capa_{i'n}$: Transportation capacity of latex from FSC-certified farmer (kilograms per trip)
$capa_{in}$: Transportation capacity of latex from non-FSC-certified farmer (kilograms per trip)
$capa_{jn}$: Transportation capacity of latex from small-scale intermediary traders (kilograms per trip)
$capa_{kn}$: Transportation capacity of latex from large-scale intermediary traders (kilograms per trip)
$capa_{ln}$: Transportation capacity of latex from concentrated latex factory (kilograms per trip)
$dist_{i'j}$: Transportation distance from FSC-certified farmer to small-scale intermediary traders (kilometers)
$dist_{ij}$: Transportation distance from non-FSC-certified farmer to small-scale intermediary traders (kilometers)
$dist_{jk}$: Transportation distance from small-scale intermediary traders to large-scale intermediary traders (kilometers)
$dist_{kl}$: Transportation distance from large-scale intermediary traders to concentrated latex factory (kilometers)
$dist_{lm}$: Transportation distance from concentrated latex factor to rubber glove factory (kilometers)
$tran_n$: Transportation cost per kilometer for vehicle type n (Baht per kilometer)
n : Type of vehicle (n = 1,2,3,4)

Decision Variable

x_{ij} : Number of trips from non-FSC-certified farmers to small-scale intermediary traders (trips)
$x_{i'j}$: Number of trips from FSC-certified farmers to small-scale intermediary traders (trips)
x_{jk} : Number of trips from small-scale intermediary traders to large-scale intermediary traders (trips)
x_{kl} : Number of trips from large-scale intermediary traders to concentrated latex factory (trips)
x_{lm} : Number of trips from concentrated latex factory to rubber glove factory (trips)
$y_{i'j}$: Quantity of latex transported from FSC-certified farmers to small-scale intermediary traders (kilograms per lot)
y_{ij} : Quantity of latex transported from non-FSC-certified farmers to small-scale intermediary traders (kilograms per lot)
y_{jk} : Quantity of latex transported from small-scale intermediary traders to large-scale intermediary traders (kilograms per lot)
y_{kl} : Quantity of latex transported from large-scale intermediary traders to concentrated latex factory (kilograms per lot)
y_{lm} : Quantity of latex transported from concentrated latex factory to rubber glove factory (kilograms per lot)

The mathematical model formulated to solve this transportation optimization problem is as follows.

Objective function

$$\text{Min Cost} = \sum_i \sum_j c_{ij}\, x_{ij} + \sum_{i'} \sum_j c_{i'j}\, x_{i'j} + \sum_j \sum_k c_{jk} x_{jk} + \sum_k \sum_l c_{kl}\, x_{kl} + \sum_l \sum_m c_{lm}\, x_{lm} \quad (1)$$

Constraints

Supply Constraints: Ensure that the amount of latex transported does not exceed the supply capacity at each stage.

$\sum_j y_{i'j} \le s_{i'}$; $\forall_{i'}$ (1)
$\sum_j y_{ij} \le s_i$; $\forall_i$ (2)
$\sum_k y_{jk} \le s_j$; $\forall_j$ (3)
$\sum_l y_{kl} \le s_k$; $\forall_k$ (4)
$\sum_m y_{lm} \le s_l$; $\forall_l$ (5)

Demand Satisfaction: Ensure that the demand at each downstream node is met.

$\sum_{i'} y_{i'j} \ge D_j$; $\forall_j$ (6)
$\sum_i y_{ij} \ge D_j$; $\forall_j$ (7)
$\sum_j y_{jk} \ge D_k$; $\forall_k$ (8)
$\sum_k y_{kl} \ge D_l$; $\forall_l$ (9)
$\sum_l y_{lm} \ge D_m$; $\forall_m$ (10)

Capacity Constraints: Ensure that the transported amount is consistent with the transportation capacity.

$\sum_{i'} y_{i'j} \le capa_{i'n} x_{i'j}$; $\forall_j, n = 1,2$ (11)
$\sum_i y_{ij} \le capa_{in} x_{ij}$; $\forall_j, n = 1,2$ (12)
$\sum_j y_{jk} \le capa_{jn} x_{jk}$; $\forall_k, n = 3$ (13)
$\sum_k y_{kl} \le capa_{kn} x_{kl}$; $\forall_l, n = 4$ (14)
$\sum_l y_{lm} \le capa_{ln} x_{lm}$; $\forall_m, n = 4$ (15)

Cost Calculation: Used to determine transportation costs based on distance and vehicle type.

$c_{i'j} = dist_{i'j}\, tran_n$; $\forall_{i'j}$, $n = 1,2$ (16)
$c_{ij} = dist_{ij}\, tran_n$; $\forall_{ij}$, $n = 1,2$ (17)
$c_{jk} = dist_{jk}\, tran_n$; $\forall_{jk}$, $n = 3$ (18)
$c_{kl} = dist_{kl}\, tran_n$; $\forall_{kl}$, $n = 4$ (19)
$c_{lm} = dist_{lm}\, tran_n$; $\forall_{lm}$, $n = 4$ (20)

Balancing Constraints: Ensure flow continuity where no storage is allowed: inflow equals outflow at each intermediate node.

$$\sum_i y_{ij} + \sum_{i'} y_{i'j} = \sum_k y_{jk} \quad ; \forall_j \qquad (21)$$

$$\sum_j y_{jk} = \sum_l y_{kl} \quad ; \forall_k \qquad (22)$$

$$\sum_k y_{kl} = \sum_m y_{lm} \quad ; \forall_l \qquad (23)$$

Negativity Constraints: Ensure that all decision variables are non-negative.

$$x_{i'j}, x_{ij}, x_{jk}, x_{kl}, x_{lm} \geq 0 \quad ; \forall_{i'j,ij,jk,kl,lm} \qquad (24)$$

$$c_{i'j}, c_{ij}, c_{jk}, c_{kl}, c_{lm} \geq 0 \quad ; \forall_{i'j,ij,jk,kl,lm} \qquad (25)$$

$$s_{i'}, s_i, s_j, s_k, s_l \geq 0 \quad ; \forall_{i',i,j,k,l} \qquad (26)$$

$$D_j, D_k, D_l, D_m \geq 0 \quad ; \forall_{j,k,l,m} \qquad (27)$$

$$y_{i'j}, y_{ij}, y_{jk}, y_{kl}, y_{lm} \geq 0 \quad ; \forall_{i'j,ij,jk,kl,lm} \qquad (28)$$

$$capa_{i'n}, capa_{in}, capa_{jn}, capa_{kn}' capa_{ln} \geq 0 \quad ; \forall_{i'n,in,jn,kn,ln} \qquad (29)$$

$$dist_{i'n}, dist_{in}, dist_{jn}, dist_{kn}, dist_{ln} \geq 0 \quad ; \forall_{i'n,in,jn,kn,ln} \qquad (30)$$

$$tran_n \geq 0 \quad ; \forall_n \qquad (31)$$

Assumption: All intermediary traders (both small-scale and large-scale), concentrated latex factories, and rubber glove factories are assumed to be able to accept latex from both non-FSC-certified and FSC-certified farmers.

2.3 Using the Lingo Program to Solve the Transshipment Model

After the transshipment model was developed, it was solved using the LINGO program, a mathematical optimization software suitable for solving linear and nonlinear programming problems. In this study, Lingo was applied to compute the most cost-effective transportation routes from farmers to the rubber glove factory by minimizing the total transportation cost. In this study, the model formulation was input into Lingo using a matrix representation of the transportation flow, with the variable denoting the quantity of latex transported from farmer Non FSC Standards i, through under FSC Standards i', small-scale intermediary traders j, large-scale intermediary traders k, concentrated latex factory l to the rubber glove factory m. The program computed the optimal routing that minimized transportation costs while satisfying all supply, demand, and capacity constraints. The optimization results obtained from Lingo were then compared to the actual transportation costs before model implementation. The comparison demonstrated the model's effectiveness in significantly reducing logistics costs while maintaining full FSC compliance across the entire supply chain. Finally, the assessment of Lingo's effectiveness in computing the most cost-efficient transportation routes highlighted its benefits in reducing logistics costs. Not only did it improve transportation efficiency, but it also supported sustainability goals within the FSC-certified rubber glove supply chain.

This study adapts the general multi-stage transshipment optimization frameworks previously applied in logistics and supply chain contexts, such as the cross-docking scheduling model formulated by Buakum and Wisittipanich [17]. While their work focused on optimizing internal task scheduling to minimize makespan under resource constraints, the current study extends such mathematical programming approaches by explicitly incorporating FSC Chain of Custody (CoC) requirements. The main contribution lies in enforcing the segregation of FSC-certified and non-certified latex flows through separate decision variables and constraints within the transshipment model, ensuring full compliance with sustainability certification standards—an aspect not addressed in the earlier models.

3. Results and Discussion

3.1 Supply Chain Characteristics from Collected Data

The supply chain for FSC-compliant rubber gloves consists of three main segments: upstream, midstream, and downstream. The upstream segment comprises smallholder latex farmers or farmer groups that grow rubber trees and tap latex by FSC principles. These farmers must be certified by an authorized organization and maintain traceability through an FSC license code. The midstream segment includes FSC-certified latex processing plants that purchase raw latex from upstream farmers. These facilities process raw latex into concentrated latex, strictly adhering to FSC Chain of Custody (CoC) standards. The entire process, from receiving and storage to transportation and processing, must meet the FSC criteria before the product is passed on to the downstream stage. In the downstream segment, FSC-certified rubber glove manufacturers receive the processed latex and produce gloves while maintaining full product traceability. These

manufacturers are also required to obtain FSC CoC certification. The finished products are then packaged and labeled with the FSC logo to signify that they meet social and environmental responsibility standards. The gloves are subsequently distributed to customers worldwide, including hospitals, retailers, and wholesalers.

In this study, the actual supply chain data were collected from an FSC-certified powder-free rubber glove manufacturer in southern Thailand. The structure analyzed includes 250 farmers (a mix of FSC-certified and non-certified), 125 small-scale intermediary traders, 6 large-scale intermediary traders, 1 concentrated latex factory, and 1 rubber glove factory. These stakeholders encompass the entire spectrum of supply chain roles, ranging from raw material production to final product distribution.

Quantitative data were collected on transportation distances between nodes, the quantity of latex supplied and demanded at each node, vehicle capacity limitations, and unit transportation costs. These data inputs reflect the real operational constraints, enabling the formulation of a transshipment model that captures the actual complexity of logistics operations within the FSC-certified supply chain. Incorporating both certified and non-certified nodes reflects real-world practices, particularly in terms of supply integration and logistical efficiency. This multi-tier data collection approach ensures the mathematical model can simulate various cost-minimization scenarios under both economic and sustainability constraints.

3.2 Cost Optimization Results Using Lingo

In this study, a transshipment model was developed to minimize transportation costs across the FSC-certified glove manufacturing supply chain. The model comprises 250 rubber farmers, including 125 non-FSC-certified farmers and 125 FSC-certified farmers, 125 small-scale intermediary traders, 6 large-scale intermediary traders, one concentrated latex factory, and one rubber glove factory. It incorporates practical operational constraints, including supply-demand balancing, transportation capacity limits, and route distances. The model was solved using an exact optimization method via the LINGO Solver (version 21.0.37), which was executed on a system equipped with an Intel Core i7 processor. Figure 2 presents the optimized transportation flows of latex across the supply chain tiers, along with the associated transportation costs. Before optimization, the total cost of transporting latex to produce 1 million gloves was THB 82,228. After solving the model, the optimized cost was reduced to THB 75,503.33, achieving a total reduction of THB 6,724.67, or 8.18%. These results demonstrate the model's effectiveness in achieving cost efficiency while maintaining feasibility across a multi-tiered supply network.

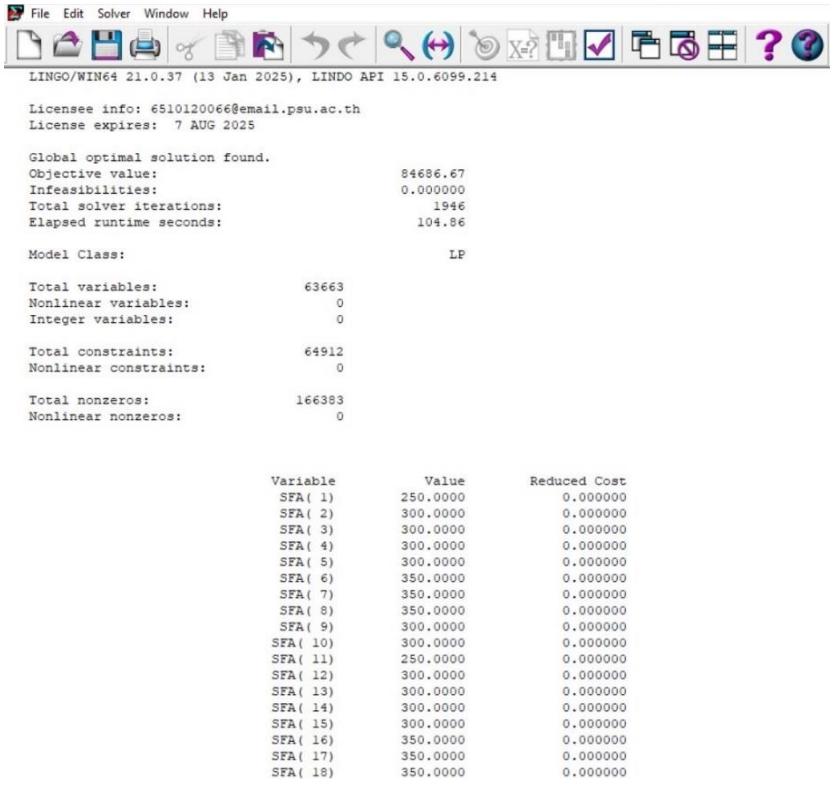

Figure 2. Transshipment Model Output via LINGO

To evaluate the accuracy and applicability of the model, the predicted transportation costs were compared with actual transportation costs from the case study, as shown in Table 1. The model's outputs closely aligned with real transportation expenditures, confirming the reliability of the proposed approach. Each dataset, structured according to the network size parameters (*i–i'–j–k–l–m*), successfully generated feasible solutions with accurate transportation quantities and minimized total costs.

Table 1. Preliminary Experimental Result by LINGO Optimization Solver.

No	Data set (*i–i'–j–k–l–m*)	Number of Transport Trips	Quantity of Transported Latex	Minimum Supply Chain Cost
1	2*2*2*2*1*1	✓	✓	✓
2	3*3*3*3*1*1	✓	✓	✓
3	4*4*4*4*1*1	✓	✓	✓
4	5*5*5*5*1*1	✓	✓	✓
5	6*6*6*6*1*1	✓	✓	✓
6	7*7*7*6*1*1	✓	✓	✓
7	8*8*8*6*1*1	✓	✓	✓
8	9*9*9*6*1*1	✓	✓	✓
9	10*10*10*6*1*1	✓	✓	✓
10	20*20*20*6*1*1	✓	✓	✓

Note: ✓ is correct solution by proposed model

Note: (*i–i'–j–k–l–m*)denotes the number of Non-FSC-certified farmers, FSC-certified farmers, Small-scale intermediary traders, Large-scale intermediary traders, Concentrated latex factory, and Rubber glove factory.

This table presents the results obtained from various network configurations, verifying the model's ability to handle different supply chain scales. As the complexity of the dataset increases, so too does the computational effort required to reach optimal solutions. Figure 3 illustrates the exponential growth in computation time as the number of supply chain nodes increases. While the model remains computationally feasible for small to medium-sized networks, the extended solution time for larger datasets may hinder its practical, real-time application in large-scale operations.

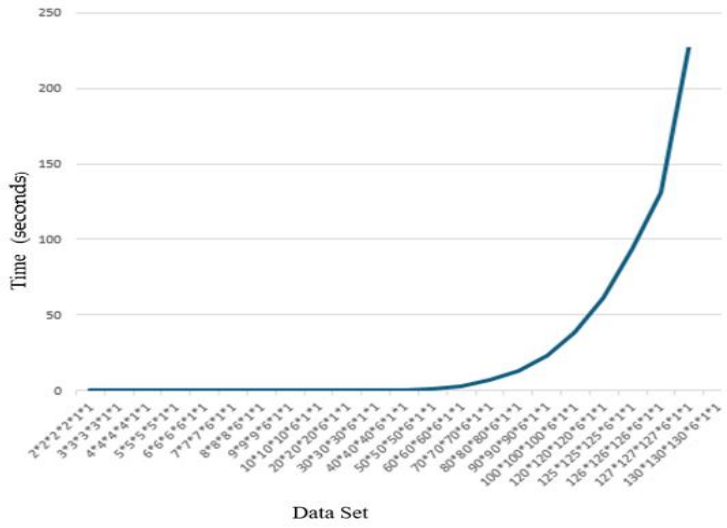

Figure 3. Relationship between dataset size and computation time

This performance trend highlights a fundamental trade-off between solution accuracy and computational efficiency. While exact methods, such as LINGO, are capable of delivering exact solutions, their scalability is inherently limited due to the exponential growth in processing time as the problem size increases.

3.3 Sensitivity Analysis on Fuel Prices and Demand Variations

A sensitivity analysis was conducted to assess the impact of changes in key economic parameters on total transportation costs. When fuel prices increased by 20%, the optimized transportation cost rose from THB 75,503.33 to THB 80,419. This represents a 6.5% increase, demonstrating that while costs are sensitive to fuel volatility, the model continues to provide cost-optimized routing compared to manual planning. Similarly, a 10% increase in demand (requiring additional latex volumes) resulted in a proportional rise in transportation cost to THB 83,053, reflecting the model's capacity to scale under varying operational scenarios. These findings reinforce the practical robustness of the model as a decision-support tool adaptable to different market and cost environments.

4. Conclusions

This study addressed the challenge of high transportation costs in the rubber glove manufacturing supply chain, adhering to Forest Stewardship Council (FSC) standards, by developing a mathematical transshipment model and solving it using the LINGO optimization program. The model was constructed based on real-world data from a certified powder-free glove factory, incorporating multiple stakeholders across five stages: from non-FSC and FSC-certified farmers to small-scale and large-scale intermediary traders, then to the concentrated latex factory, and finally to the rubber glove factory.

The model was solved using exact methods via the LINGO optimization software, which enabled the identification of the most cost-efficient transportation routes while satisfying various real-world constraints, including supply availability, factory demand, and vehicle capacity limits. LINGO's ability to process large-scale linear programming models with multiple variables and constraints proved essential to the successful resolution of the complex transshipment network. The results indicate a significant reduction in total transportation costs from THB 82,228 to THB 75,503.33 per one million gloves produced, representing an 8.18% improvement in logistics efficiency. Additionally, sensitivity analysis on key parameters such as fuel prices and demand levels demonstrated that while total logistics costs adjust under different scenarios, the model continues to deliver cost-optimized solutions, underscoring its robustness and practical applicability in real-world operations. This outcome demonstrates the effectiveness of the mathematical model and LINGO in identifying optimal transportation pathways in a constrained and sustainability-focused logistics environment. Beyond the numerical optimization, this study highlights the critical role of quantitative modeling in aligning supply chain efficiency with environmental certification standards. The inclusion of FSC-related parameters such as traceability, chain-of-custody compliance, and differentiated treatment of certified and non-certified farmers ensures that the model aligns not only with cost-saving goals but also with social and environmental imperatives. The proposed model thus reinforces the viability of integrating sustainability constraints within a formalized mathematical framework, making it especially relevant in today's global market, where eco-certification is both a regulatory requirement and a competitive differentiator. In practical terms, the findings provide a decision-support tool for logistics planners, supply chain analysts, and policymakers in the agro-industrial sector. The methodology developed in this research is replicable and can be adapted to other sectors that involve multi-stage production and distribution systems with sustainability requirements. For instance, agricultural cooperatives, bio-based chemical farmers, and eco-labeled consumer product manufacturers could all benefit from a similar optimization framework.

To address this limitation, future research should explore hybrid optimization strategies that integrate exact algorithms with heuristic or metaheuristic approaches. These methods offer a promising path forward, enabling improved scalability and faster response times without sacrificing the level of accuracy required in FSC-certified logistics systems where transparency, traceability, and cost control are critical. Moreover, the study's findings emphasize the strategic value of optimization-based tools in supporting sustainable logistics planning within certified supply chains. In the context of FSC-certified glove manufacturing, achieving transportation cost efficiency must be accompanied by adherence to environmental and ethical standards. The proposed transshipment model not only demonstrates substantial cost-saving potential but also respects the structural complexity and rigorous traceability requirements imposed by the FSC system. As supply chains

become increasingly dynamic and multi-tiered, the integration of advanced decision support systems, such as the LINGO-based transshipment model, will be essential. With further enhancement, particularly through hybrid algorithmic techniques, this modeling framework holds promise as a scalable and adaptable solution for a wide range of industries seeking to balance sustainability, operational efficiency, and compliance.

Moreover, the study offers a platform for future research that could include dynamic or stochastic modeling approaches to address demand variability, seasonal fluctuations in latex production, and changes in fuel prices or transportation availability. Multi-objective optimization could also be introduced to balance cost reduction with carbon footprint minimization. Additionally, integrating geospatial data with the LINGO model could enable real-time route adjustments and enhance the practical implementation. In conclusion, this research not only validates the use of LINGO as a robust optimization tool but also contributes a novel transshipment modeling approach tailored for FSC-certified supply chains. It provides empirical evidence and practical guidelines for improving cost efficiency while adhering to international sustainability standards. As such, it stands as a valuable contribution to both academic literature and the operational management of sustainable supply chains. Looking forward, the adoption of such optimization-driven frameworks could be instrumental in shaping policy decisions around green logistics and sustainable certification systems. Governments and international organizations could leverage similar models to establish guidelines that encourage eco-compliance while promoting economic viability. In a global landscape increasingly shaped by climate targets and responsible sourcing, the integration of mathematically rigorous, sustainability-aware tools represents not only an operational necessity but also a strategic advantage. Therefore, the continued advancement and application of transshipment models such as the one presented in this study will play a crucial role in supporting resilient, transparent, and cost-effective supply chains of the future.

5. Acknowledgements

The authors would like to express their sincere gratitude to the Faculty of Engineering at Prince of Songkla University for providing continuous academic support, research guidance, and access to the computational resources necessary for the successful completion of this study. The university's infrastructure, including computing laboratories and library facilities, played an essential role in enabling the data analysis and modeling processes. The authors would also like to extend special thanks to the management and staff of the participating FSC-certified rubber glove manufacturing facility, whose cooperation and willingness to share operational data significantly contributed to the realism and applicability of the proposed model. Additional appreciation is extended to the smallholder farmers, intermediary traders, and latex factory representatives who participated in stakeholder interviews and consultations, providing valuable insights that enhanced the model's structural accuracy and alignment with real-world logistics practices.

Author Contributions: Conceptualization, Mareena Mihad, Sakesun Suthummanon and Dollaya Buakum; methodology, Mareena Mihad, Sakesun Suthummanon and Dollaya Buakum; software, Mareena Mihad and Dollaya Buakum; validation, Mareena Mihad; formal analysis, Mareena Mihad; investigation, Mareena Mihad; resources, Mareena Mihad; data curation, Mareena Mihad; writing original draft preparation, Mareena Mihad; writing review and editing, Sakesun Suthummanon and Dollaya Buakum; visualization, Mareena Mihad; supervision, Sakesun Suthummanon and Dollaya Buakum; project administration, Sakesun Suthummanon and Dollaya Buakum; All authors have read and agreed to the published version of the manuscript.

Funding: This research did not receive any specific grant from funding agencies in the public, commercial, or not-for-profit sectors. The work was entirely supported by institutional resources provided by Prince of Songkla University.

Conflicts of Interest: The authors declare no conflict of interest. The funders had no role in the design of the study, in the collection, analysis, or interpretation of data, in the writing of the manuscript, or in the decision to publish the results.

References

[1] Kanitasart. *Situation of Thai Rubber Glove Production and Export during the COVID-19 Pandemic*; Thai Economic Research Institute: Bangkok, **2020**; pp 45-58.

[2] Cp Corporation. FSC CERTIFICATED: *What It Is and Why It Is Important*; https://www.epccorps.com /knowhow/what-is-fsc-certificated-and-why-important/ (accessed November 10, 2022).
[3] Tetrapak. *Unpacking Opportunities: What is FSC™*; https://www.tetrapak.com/en-th/insights/cases-articles/what-is-fsc (accessed November 15, 2022).
[4] Taha, H. A. *Operations Research: An Introduction*, 10th ed.; Pearson: Boston, **2017**.
[5] Chopra, S.; Meindl, P. *Supply Chain Management: Strategy, Planning, and Operation*, 7th ed.; Pearson: Boston, **2019**.
[6] Glover, F.; Kochenberger, G. A. *Handbook of Metaheuristics*, 2nd ed.; Springer: New York, 2010.
[7] Dantzig, G. B.; Thapa, M. N. *Linear Programming 1: Introduction*; Springer: New York, 2003.
[8] Mula, J.; Peidro, D.; Díaz-Madroñero, M.; Vicens, E. Math. Program. Models Supply Chain Prod. Transp. Plan. *Eur. J. Oper. Res.* **2010**, *204*, 377-390. https://doi.org/10.1016/j.ejor.2009.09.008
[9] Ahumada, O.; Villalobos, J. R. Application of planning models in the agri-food supply chain: A review. *Eur. J. Oper. Res.* **2009**, *196*, 1-20. https://doi.org/10.1016/j.ejor.2008.02.014
[10] Lingo Systems. *Lingo Optimization Software: Overview and Applications in Logistics*; https://www.lingosystems.com (accessed December 28, 2024).
[11] Santoso, T.; Ahmed, S.; Goetschalckx, M.; Shapiro, A. A stochastic programming approach for supply chain network design under uncertainty. *Eur. J. Oper. Res.* **2005**, *167*, 96-115. https://doi.org/10.1016 /j.ejor.2004.01.046
[12] Banasik, A.; Kanellopoulos, A.; Bloemhof, J. M.; van der Vorst, J. G. A multi-echelon stochastic programming approach for planning fresh food supply chains. *Int. J. Prod. Econ.* **2017**, *193*, 11-21.
[13] Nguyen Dat Minh; Duong Trung Kien; Pham Khac Hau. Applying Milk-run Method to Optimize Cost of Transport: An Empirical Evidence. *Int. J. Supply Oper. Manage.* **2020**, *7*(2), 178-188. https://doi.org/ 10.22034/IJSOM.2020.2.6.
[14] Puspita, F. M.; Melati, R.; Simanjuntak, A. S. Br; Yuliza, E.; Octarina, S. *Robust Counterpart Open-Capacitated Vehicle Routing Problem with Time Windows and Deadline (RCOCVRPTWD) Model in Optimization of Waste Transportation in Subdistrict Kalidoni, Palembang Using LINGO 13.0. J. Phys. Conf. Ser.* **2021**, *1940*, 012017. https://doi.org/10.1088/1742-6596/1940/1/012017 (accessed Nov 8, 2023).
[15] Nurdiansyah, D. *Optimasi Biaya Pengiriman Telur Ayam Menggunakan Pendekatan Model Transportasi NWC dan Software LINGO. J. Lebesgue J. Ilm. Pendidik. Mat., Mat. Stat.* **2021**. https://doi.org/10.46306/lb.v2i3.77
[16] Yuliza, E.; Puspita, F. M.; Yahdin, S.; Emiliya, R. *Solving Capacitated Vehicle Routing Problem Using of Clarke and Wright Algorithm and LINGO in LPG Distribution*. *J. Phys. Conf. Ser.* **2021**, *1663*, 012055. https://doi.org/10.1088/1742-6596/1663/1/012027
[17] Buakum, D.; Wisittipanich, W. A Mathematical Model for Internal Task Scheduling in Cross Docking. *Proc. IEEE Int. Conf. Ind. Eng. Eng. Manag.*, **2019**, 1-8. https://doi.org/10.1109/IEEM44572.2019.8978692.
[18] Van der Vorst, J. G. A.; Tromp, S. O.; Zee, D. J. Simulation modeling for food supply chain redesign. *Br. Food J.* **2009**, *111*, 762-775.

ASEAN
Journal of Scientific and Technological Reports
Online ISSN:2773-8752

Research article

Total Flavonoid Content, Antioxidant Properties, and COX Inhibition of a Dual-Extract Herbal Blend: Formulation of a Gel for Anti-Inflammatory and Wound-Healing Applications

Valarmathi S.[1], Komal Kriti[2], Tabrej Mujawar[3*], Maneesha Bhardwaj[4], Sweta Negi[5], Kavitha S[6], Touseef Begum[7], and Mohammad Muztaba[8]

[1] MGR Educational and Research institute, Velapanchavadi, Chennai-600077, India
[2] Department of Pharmaceutical Sciences, Dhanbad College of Pharmacy and Research Institute, Near BBMKU, Shakti Nagar, Nag Nagar, Dhanbad, Jharkhand – 826004, India
[3] Department of Pharmacology, Gangamai College of Pharmacy, Nagaon Dhule MS, 424005, India
4 Department of Pharmacognosy, Universal Institute of Pharmacy, Lalru-140501, India
[5] Department of Pharmacy, Galgotias University Plot No. 2, Yamuna Expy, opposite Buddha International Circuit, Sector 17A, Greater Noida, Uttar Pradesh-203201, India
[6] Department of Biochemistry, The Apollo University, Chittoor, Andhra Pradesh – 517127, India
[7] Department of Pharmaceutical Sciences, Ibn Sina National College for Medical Studies, Jeddah - 21418, Saudi Arabia
[8] Department of Pharmacology, Praduman Singh SPS Pharmacy College, Phutahiya Sansarpur Basti, Uttar Pradesh -272001, India
* Correspondence: tabrejpharma@rediffmail.com

Citation:
Valarmathi, S.; Kriti, K.; Mujawar, T.; Bhardwaj, M.; Negi, S.; Kavitha, S.; Begum, T.; Muztaba, M.. Total flavonoid content, antioxidant properties, and COX inhibition of a dual-extract herbal blend: formulation of a gel for anti-inflammatory and wound-healing applications. *ASEAN J. Sci. Tech. Report.* **2025**, *28*(4), e257666. https://doi.org/10.55164/ajstr.v28i4.257666.

Article history:
Received: February 2, 2025
Revised: June 6, 2025
Accepted: June 23, 2025
Available online: August 16, 2025

Abstract: The current work examined UDASP-HB, a novel herbal formulation comprising Urtica dioica methanol leaf extract and Angelica sinensis polysaccharide, for its pharmacological activity. It examined the total flavonoid content and its antioxidant and anti-inflammatory activity. UDASP-HB exhibited high concentrations of flavonoids, with considerable inhibition of lipid peroxidation in egg yolk and liver homogenate model compared with controls. UDASP-HB inhibited COX-1 and COX-2 enzymes and, therefore, can exhibit anti-inflammatory activity. Additionally, six new topical gel formulations and preparations were developed and examined for their physicochemical properties and in vitro drug delivery studies. All six preparations facilitated sustained delivery and effective dermal delivery.

Keywords: *Urtica dioica; Angelica sinensis*; Flavonoid content; *Angelica sinensis* polysaccharide; Lipid peroxide inhibition; Antioxidant activity

1. Introduction

Oxidative stress and inflammation represent two crucial biological processes with critical functions in cellular signaling and protection, but with the potential for chronic disease when not properly regulated. Oxidative stress occurs when a disproportion between ROS production and detoxification, and/or restoration of generated damage, takes place in a living organism [1, 2]. Inflammation, a physiologic reaction to noxious stimuli present in all tissues, can become persistent and disease-producing, as seen in conditions such as arthritis, diabetes, and cardiovascular disease. Regulation of such processes is not only critical for acute diseases, but also for long-term diseases, including degenerative diseases [1, 3, 4]. The modulating effects of oxidative stress and inflammation are well-established in traditional medical practice and are increasingly supported by scientific experiments. Application of such drugs is preferred for their lesser side effects, availability, and economy over conventional drugs [5-7].

Medicinal herbs contain a diverse range of bioactive compounds with high antioxidant and anti-inflammatory properties. Such compounds can trap free radicals, enhance antioxidant defense in the organism, and modulate inflammatory processes, thereby conveying protection against a variety of oxidative and inflammation-related ailments [1, 7-10].

Urtica dioica, or stinging nettle, has been used in traditional cultures, such as Ayurveda and Western herbalism, for centuries to control disease processes including arthritis, anaemia, and long-term dermatological conditions [11-13]. All its therapeutic efficacy can be attributed to its rich content of phytochemicals such as flavonoids, lignans, and polysaccharides. *Angelica sinensis*, popularly known as Dong Quai or female ginseng, is famous in traditional Chinese medicine for its use in treating gynaecologic diseases, weakness, mild anaemia, and high blood pressure. Polysaccharides of *Angelica sinensis* (ASP) have been shown to possess strong anti-inflammatory and immunomodulatory properties, making them a beneficial constituent in herbal drugs for wound healing and anti-inflammatory activity [2, 14].

The premise for developing a herbal mixture of *Urtica dioica* leaf methanol extract and polysaccharide of *Angelica sinensis* (ASP) for the development of herbal gels is the synergistic effect between their bioactivities, enhancing anti-inflammatory activity and wound healing. Complementarily, it leverages *Urtica dioica's* high anti-inflammatory activity and ASP's proven wound healing ability [15, 16]. Such a preparation not only aims to counteract the processes of inflammation but also to accelerate tissue regeneration and healing processes [15]. Gels, when locally applied, have the added advantage of localized delivery, which can maximize therapeutic activity at the site of trauma and inflammation while minimizing systemic toxicity. In harmony with a growing demand for effective and natural substitutes for traditional drugs in controlling trauma and inflammation and healing wounds, such an approach holds a lot of hope for future development in herbal therapy [17].

Therefore, the purpose of the current study is to investigate the pharmacological potential of a methanol extract derived from *Urtica dioica* leaves with a microwave-assisted extraction process. The pharmacological potential of *Angelica sinensis* polysaccharides is another goal of the investigation. Additionally, the study aims to develop a topical herbal gel formulation using an herbal blend of *Angelica sinensis* polysaccharide and *Urtica dioica* methanol leaf extract. Building on their traditional uses and earlier research, these historically prized medicinal plants will be evaluated in various models to determine their effects on inflammation and oxidative stress. The purpose of this study is to advance our understanding of its therapeutic applications and encourage its potential integration into contemporary medical procedures.

2. Materials and Methods

2.1 Drugs, Chemicals, Polymers, and Reagents

Zen Pharmaceuticals, Karnal, India, generously supplied free samples of Catechin and quercetin. Himedia Biosciences Company in India provided the following: Triethanolamine, disodium edetate, DTNB solution (Ellman's reagent), sodium nitroprusside, Griess Reagent, thiobarbituric acid, sodium dodecyl sulphate, and tris-KCl buffer. The trichloroacetic acid (TCA) was purchased from Sigma Aldrich in India. Additionally, Sigma-Aldrich in India provided propylene glycol, Carbopol 934, and Carbopol 940. All additional chemicals and reagents utilised in this investigation, bought from verified vendors such as SRL Mumbai and E. Merck India, were of reagent grade and ensured high-quality standards.

2.2 Plant material collection and authentication

Between November 2023 and February 2024, *Urtica dioica* leaves were carefully collected from their natural environment to ensure a steady supply of mature and healthy plant material. The polysaccharide of *Angelica sinensis* was sourced from Herbal Waves in Mandi, Himachal Pradesh, India. During leaf collection, special attention was paid to preserving the *Urtica dioica* habitat in its natural setting. A local herbalist named Mr. Ashok Gupta, who works with Herbal Waves in Himachal Pradesh, India, verified and identified the samples after they were harvested. During the authenticity stage, voucher samples stored in the Department of Pharmacognosy Herbarium (MSK/ACP/2023/3398-72) were carefully examined. This meticulous analysis ensured that the plant material under study was appropriately classified through taxonomy.

2.3 Preparation of extraction utilizing a microwave-assisted method

The collected *Urtica dioica* leaves were gently washed to remove contaminants, such as dust and grime. The cleansed leaves were then dried in a shaded area to preserve the integrity of the phytochemicals and prevent deterioration from direct sunlight. The leaves were dried and then ground into a fine powder using a motorised grinder to achieve consistency in particle size for efficient extraction. According to Mandal et al. (2007), the extraction method employed a microwave-assisted extraction approach [18]. Twenty-five grams of the powdered leaves were combined with 200 millilitres of methanol in a 1:8 powder-to-solvent ratio. Microwave irradiation was applied to the mixture with a power setting of 160 W. During the first six minutes of the extraction procedure, the mixture was heated to the optimal temperature for maximum extraction. To ensure the full extraction of bioactive components, the temperature was then allowed to drop to room temperature before initiating a second 2-minute microwave cycle. Particulate materials and plant debris were eliminated from the resultant extract using filtering. After the solvent was removed from the filtrate using a water bath, a dense and concentrated extract was produced. *Angelica sinensis* polysaccharide (ASP) was subsequently added to the finished extract in a 1:1 ratio. The final herbal blend was subsequently codenamed UDASP-HB and stored for future testing.

2.4 Determination of total flavonoid content

A spectrophotometric aluminum chloride technique, described earlier with minor modifications, was utilized for the determination of the total flavonoid content of UDASP-HB [19]. Aluminium chloride ($AlCl_3$), which exhibits a detectable absorption peak at a specific wavelength with flavonoids, was used in this protocol. Flavonoid contents were calculated in terms of milligrams of equivalent quercetin (mg QE/g) per gram of extract in a plant. In a 1-mL UDASP-HB solution (1 mg/mL), 1 mL and an equivalent (1 mL) 2% methanolic solution of $AlCl_3$ were mixed in a test tube to form a sample for analysis. After a brief vortex to achieve homogeneity, the mixture was kept at room temperature for 1 hour to allow the reaction between the flavonoids and $AlCl_3$ to proceed to completion. After incubation, the absorption at 415 nm was measured using a Shimadzu UV-1900 spectrophotometer in a solution. Since 415 nm is equivalent to the absorption at a maximum for the $AlCl_3$-flavonoid complex, it was used to enable proper determination. All samples were prepared and analyzed three times for repeatability and accuracy. Additional computations were performed using the mean values for absorption in these samples. In a similar manner, a series of solutions with a range of known concentrations of quercetin was used to obtain a standard curve. A calibration curve, used as a guideline for determining the extract level of flavonoids, was produced by plotting the values for absorption of these standards concerning their respective concentrations. Value for absorption of the sample was interpolated from the curve for the standards for quercetin in an attempt to calculate UDASP-HB level of flavonoids. The quantitation of the extract level of flavonoids was provided in the output, expressed in terms of equivalent milligrams of quercetin per unit extract per gram (mg QE/g). It is an efficient and effective method for determining flavonoids in plant samples.

2.5 Evaluation of the lipid peroxidation inhibition using egg yolk and liver homogenate model

Using egg yolk as a lipid-rich medium and a modified thiobarbituric acid reactive species (TBARS) assay, the amount of lipid peroxide product generated was quantified [20]. Using egg yolk/liver homogenate as a source of high fat, inhibition of lipid peroxidation was examined using a modified thiobarbituric acid reactive species (TBARS) assay, according to Badmus et al. (2011). By testing for malondialdehyde (MDA) production, a significant metabolite of lipid peroxides, through its reaction with thiobarbituric acid (TBA), analysis for inhibition in lipid peroxidation is performed. As a substrate for lipids, 0.7 mL of 14% (v/v) egg yolk/liver homogenate emulsion and 0.5 mL of extract (UDASP-HB) at variable concentrations (15–180 μg/mL) were mixed to make a reaction mixture. To create a uniform reaction mixture, 1.6 mL of distilled water was added. Lipid peroxidation was initiated by incubating the mixture with 0.06 mL of a freshly prepared ferrous sulfate ($FeSO_4$) solution. Incubation of the reaction mixture at 37°C for 35 minutes provided a sufficient duration for oxidative degradation of the lipids. Following incubation, 1.7 mL of acetic acid and 1.8 mL of TBA in sodium dodecyl sulphate (SDS) solution were added to it. TBA and MDA react readily in an acidic environment to form a pink-colored chromogen, the presence of which can be determined using a spectrophotometer. After shaking the mixture well to achieve homogeneity, it was placed in a water bath and incubated for 1 hour at 95°C. Heating helps in intensifying the reaction between TBA and MDA. For the extraction of the TBA-MDA complex into an organic layer, 6 mL of butanol was added when the mixture was

cooled to room temperature. For phase partitioning, the mixture was centrifuged for 15 minutes at 4000 rpm. TBA-MDA complex-containing organic upper layer was collected with extreme care, and a UV-visible spectrophotometer was used to determine its absorption at 532 nm.

$$\%\ \text{Lipid peroxidation inhibition } \left(\frac{100 - X_{SAMPLE}}{X_{CONTROL}}\right) \times 100$$

2.6 Appraising the Anti-inflammatory activity: Cyclooxygenase (COX) inhibition assay

The assay for Cyclooxygenase-1 (COX-1) and Cyclooxygenase-2 (COX-2) enzymes was conducted using the protocol described elsewhere [21, 22]. The UDASP-HB extract's cyclooxygenase (COX) inhibitory activity was measured through COX-1 and COX-2 enzyme tests following protocols designed by Redl et al. (1994) and Aguilar et al. (2002). Inhibition of COX-1, an enzyme responsible for prostaglandin synthesis for a normal physiologic function, was measured through the COX-1 test. 195 µL of 0.4 M Tris-HCl (pH 7.4), 20 µL of L-adrenaline-D-hydrogentartrate working as a reductant, 15 µL of haematin working as a cofactor, and 15 µL of a sample solution were added to the reaction mixture before starting the experiment. 0.4 U of COX-1, added later, initiated incubation for 7 minutes at 37°C to initiate the reaction in the enzyme. 7 µL of arachidonic acid, serving as a substrate, was added later, and the mixture was incubated at 37°C for 35 minutes to initiate the reaction. The addition of 15 µL of 14% formic acid later inhibited the enzyme's activity. The COX pathway produced prostaglandin E2 (PGE2), and its activity level was determined using a PGE2 enzyme immunoassay kit (R&D Systems). Likewise, in the COX-2 study, a similar sequence of operations was conducted to assess the inhibition of COX-2 by UDASP-HB, an enzyme with a predominantly causative role in producing inflammation. In its reaction mixture, 15 µL of sodium edetate (Na_2-EDTA) was added to chelate metal ions, 15 µL of haematin, 20 µL of L-adrenaline-D-hydrogentartrate, 195 µL of 0.4 M 7.4-pH Tris-HCl, and 15 µL of a sample solution were added. After the addition of 0.4 U of COX-2 enzyme, the mixture was incubated for 6 minutes at 37°C. After the addition of 7 µL arachidonic acid substrate, a 35-minute reaction at 37°C, and a 35-minute reaction duration, 14 µL of 14% formic acid was added, which inhibited its activity. In its determination, the generated PGE2 level in the COX-2 pathway was measured using a PGE2 enzyme immunoassay kit (Cayman Systems) [21, 22]. For accuracy and repeatability, both tests were conducted in triplicate. By comparing the results with and without the extract blend, the inhibition level of PGE2, the inhibition of COX activity, and the percentage inhibition of COX activity were calculated. By employing this technique, a comprehensive analysis of the inhibition of the extract on COX-1 and COX-2 enzymes could be conducted.

2.7 Formulation development: The fabrication of the herbal gel

2.7.1 Preparation of the gel base

The gel base preparation involved careful homogeneity and uniformity in any preparation form. In preparation, 1.5 g of Carbopol 934 was added first under slow and continuous stirring in such a form that no clumps and uniformity in form existed. It was a key stage in hydrating the polymer and creating a uniform dispersion, a crucial property for achieving uniformity in the finished form, as well as its stability and shape. A triethanolamine and disodium EDTA solution was prepared in a separate form after hydrating the Carbopol. To maintain chemical integrity in the gel, 0.005 g of disodium EDTA was utilized in a chelating and chemical integrity-maintaining role, and 1.5 g of triethanolamine was used in a pH-adjusting and neutralizing role. To allow proper solubilization, both chemicals were vigorously mixed in a combined form with deionized water. Following continuous stirring, the drop-by-drop addition of triethanolamine and disodium EDTA, and slow, drop-by-drop blending, a transparent and thick gel matrix is developed in its presence, with a pH level of about 7.4 before addition. This critical stage offers an opportunity for Carbopol neutralization. Similarly, 5.5 g of propylene glycol, a humectant and solvent, was added to moisturize and strengthen the gel, providing a transparent, uniform base for the developed gel. This was achieved by blending all ingredients under continuous stirring for proper integration [23].

2.7.2 Preparation of gel formulation

The drug formulation manual was followed in the preparation of a total of six topical gel formulations [24]. Following base gel preparation, six individual gel preparations, HGF1 to HGF6, were prepared with

variable UDASP-HB concentrations (a mixture of *Urtica dioica* methanol leaf extract and *Angelica sinensis* polysaccharide). UDASP-HB concentrations ranged in gradation, starting with 0.5 g in HGF1 and increasing by 0.5 g in each successive preparation, with a final concentration of 3.0 g in HGF6. One could evaluate the impact of a mixture of polysaccharides on the therapeutic activity of the gel with such a gradation. To ensure a uniform proportion of basis materials in each preparation, a portion of UDASP-HB was added to a base gel and brought to a 100 g weight with a mixture of demineralized water. In terms of anti-inflammatory activity and wound healing, each batch was properly prepared for future testing and therapeutic application by using a consistent preparation for both the base and subsequent formulations.

Table 1. The list of components used in the formulations of herbal gels.

	Gel Formulation code					
Ingredients	**HGF1**	**HGF2**	**HGF3**	**HGF4**	**HGF5**	**HGF6**
UDASP-HB (g)	0.5	1.0	1.5	2.0	2.5	3.0
Carbopol 934 (g)	1.5	1.5	1.5	1.5	1.5	1.5
Triethanolamine (g)	1.5	1.5	1.5	1.5	1.5	1.5
Disodium EDTA (g)	0.005	0.005	0.005	0.005	0.005	0.005
Propylene Glycol (g)	5.5	5.5	5.5	5.5	5.5	5.5
D.M. water (100 g)	q.s	q.s	q.s	q.s	q.s	q.s

2.8 Characterization of the gel formulation

2.8.1 Assessment of active constituents

To precisely identify the phenolic contents as an assay method for the active elements in the herbal gel preparation, effective techniques were used, including total phenolics analysis using the Folin-Ciocalteu method. A 1 g portion of the gel was taken in a 50 mL volumetric flask, and methanol was added to make a solution for the active contents. Methanol and the flask contents were mixed vigorously to form a homogeneous solution of the contents in methanol. Whatman filter paper was then used to remove any residues that did not dissolve in methanol. 0.1 mL of filtrate was measured with care and diluted to a final volume of 10 mL with methanol to form a testing solution for analysis. Concentrations of active contents in such a solution are calculated using two approaches with the use of UV spectrophotometry at a proper wavelength, a wavelength at λmax for active compounds [25]. After preparing the herb gel in a mixture with ethanol or methanol, a determined quantity of Folin-Ciocalteu reagent was added, and the mixture was incubated for around ten minutes. Blue colour development was carried out for ninety minutes after sodium carbonate was applied for neutralisation. The absorbance was measured at 765 nm. A gallic acid standard curve was used to quantify the phenolic chemicals.

2.8.2 Extrudability

An essential factor for user convenience, the gel formulation's extrudability was evaluated to determine how easily it could be extruded from the container. A common weight (such as 500 g) was placed on top of the slide after a collapsible aluminium or plastic tube carrying the gel was sandwiched between two glass slides. Weighing was performed to determine the amount of gel extruded in 10 seconds. The amount of gel extruded per unit weight applied was used to express the extrudability of the gel. This test confirmed that the gel had the ideal consistency for easy and smooth dispensing [26].

2.8.3 pH Measurement

To minimize irritation during use and ensure compliance with the skin's natural pH, the pH of the gel preparation was determined. For the preparation of a uniform solution, a small portion (1 g) of gel was blended with 10 milliliters of deionized water. A calibrated electronic pH meter with an inserted electrode was used to measure and scan the pH value of the gel dispersion. For use in derms, its value in the acceptable range (typically 6.8–7.5) was reached, and a value of 7.4 was maintained throughout the entire formulative exercise [27].

2.8.4 Evaluation of appearance, viscosity, and homogeneity

Appearance

A visual examination was performed to evaluate the transparency, color, and overall cosmetic properties of the gel preparation. Consistency in transparency and colour between the two sets of the gel was examined to ensure compliance with the desired specifications for use in a topically applicable preparation [28].

Viscosity

The viscosity of the gel preparation was measured using a Brookfield viscometer to assess its rheological properties. The spindle (which can be used for semi-solid preparations) was subjected to variable velocities (in rpm) at room temperature with the gel loaded onto the viscometer. To analyze the flow behavior of the gel, viscosity values were measured at a range of velocities. Shear-thinning or pseudo-plastic behavior is ideal for a gel, allowing for spreadability and ease of application while maintaining long-term stability. To maximize dermal application consistency of the gel, such viscosity determination was imperative [28].

Homogeneity

To assess the homogeneity of the gel, a small portion of the mixture was left on a sanitized glass slide and inspected under a light source. We searched for lumps, clumps, and particulate matter in the gel. The easy and unhindered dispersion of the ingredients suggested that the gel would be successfully prepared and properly mixed [28].

2.8.5 Spreadability

One important property that controls the ease with which the gel can penetrate and cover the skin is its Spreadability. Spreadability controls both happiness and comfort in use, as well as the therapeutic effectiveness of a preparation, directly. The spreadability of a gel was measured using a slide and drag technique. In it, two flawless plates of glass were placed between a definite amount of gel (e.g., 1 g). For allowing the spreading of a gel, a uniform weight (500 g, for example) was kept on a top plate for a definite duration, such as one minute. After removing the weight, the diameter or cover area was measured. Spreadability of a formula was calculated through:

$$S = M \times L / T$$

where:

- S is the spreadability,
- M is the weight applied (in grams),
- L is the length of gel spread (in cm),
- T is the time taken (in seconds).

Higher values for spreadability in the form of a gel mean easier and uniform application onto the skin's surface. In testing, care is taken to ensure the gel is effective and convenient for topical distribution due to its uniform dispersibility, requiring minimal effort [29].

2.8.6 In vitro Diffusion study evaluating the permeation through skin

Goat ear skin was then used in *in vitro* diffusion experiments to evaluate its capacity to penetrate through dermal tissue and simulate transdermal distribution. Goat ear skin for use in experiments was harvested at a nearby slaughterhouse, and peeling off of the dermal tissue was handled with care, with consideration for keeping the dermal tissue intact. After peeling off fat and subcutaneous tissue, saline was used to wash off the dermal tissue, and it was stored at -20°C for use as needed. Before use in experiments, the dermal tissue was incubated in phosphate buffer (pH 7.4) for one hour at room temperature. A Franz diffusion cell with a receptor compartment volume of 15 mL and an effective diffusion area of 2.5 cm^2 was used in the study. With the stratum corneum towards the donor side and the dermis in touch with the receptor medium, the hydrated skin was positioned between the donor and receptor compartments. The receptor medium was phosphate buffer (pH 7.4), which was maintained at 37 ± 1°C and stirred constantly to replicate physiological conditions. The donor compartment was uniformly coated with a predetermined quantity of the gel formulation (about 1 g). At specified intervals (e.g., 0, 1, 2, 4, 6, 8, and 12 hours), samples (1 mL) were removed from the receptor compartment and replaced with an equivalent volume of new phosphate buffer to preserve sink conditions. The active ingredients that penetrated the skin were measured by spectrophotometric analysis of the collected samples as described earlier in the assay method. The permeation profile was generated by plotting the cumulative amount of penetrated drug per unit area ($\mu g/cm^2$) against time. The linear portion of the permeation curve was used to determine the steady-state flux (Jss), and the flux

was correlated with the active ingredient in the donor compartment to determine the permeability coefficient (Kp). In the present work, it facilitated the optimization of the gel's form for effective transdermal delivery and therapeutic activity by providing useful information about its penetration and release behavior in well-regulated *in vitro* environments. A goat ear membrane was used as a model to evaluate the function of the gel in closely monitored *in vitro* environments [29].

2.8.7 Release Kinetics of Gel Formulation

To evaluate the kinetics of release of the active components from the gel preparation, an in vitro Franz diffusion cell setup was used with phosphate buffer (pH 7.4) at 37 ± 1°C. A specific quantity of gel in the donor chamber and samples extracted from the receiver medium at regular intervals are necessary to maintain sink conditions. The volume was withdrawn, and a fresh buffer was added. Samples were examined using UV-Vis spectrophotometry [30]. To ascertain the release mechanism, cumulative release data were plotted against time and examined using mathematical models, including zero-order, first-order, Higuchi, and Korsmeyer-Peppas models. The model with the highest correlation coefficient best represented the release kinetics. This procedure verified that the gel formulation offered sustained, controlled release, which is necessary for its therapeutic effectiveness and directs further optimisation for the required drug delivery profiles.

2.9 Statistical analysis

Statistical analysis was conducted to ensure the reliability and reproducibility of experimental results. All experiments were performed in triplicate, with data expressed as mean ± standard deviation (SD). For significance testing between groups, one-way ANOVA followed by Tukey's *post hoc* tests was used for multiple groups, and independent t-tests were used for two groups, considering p-values less than 0.05 as statistically significant. Regression analysis was used to fit the release data to various kinetic models, evaluating model adherence through the correlation coefficient (r^2), with higher r^2 values indicating a better fit. All statistical procedures were executed using GraphPad Prism (Version 8), ensuring precision and efficiency. The programs' R and Python were used for graphing. This robust statistical framework validated the findings and supported interpretations of the gel formulations' efficacy and performance.

3. Results and Discussion

3.1 Total flavonoid content estimation

UDASP-HB was found to have a total flavonoid content (TFC) of 357.75 mg/g of quercetin equivalent (QE). The calculated absorbance values were used to estimate the flavonoid concentration using the calibration curve equation, y = 0.0031x + 0.0693, with R^2 = 0.9691. The significant flavonoid content of the extract emphasises its potential for antioxidant and therapeutic applications.

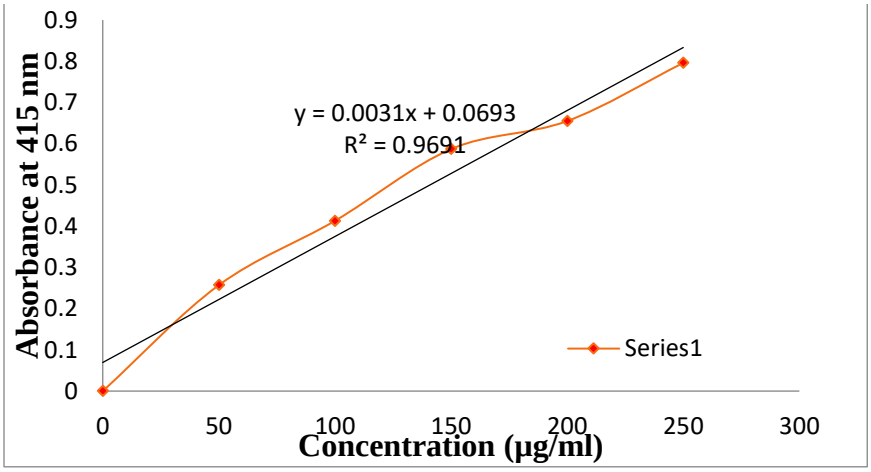

Figure 1. Quercetin standard curve to estimate total flavonoid concentration in UDASP-HB.

3.2 Inhibition of Lipid peroxidation in the egg yolk model

The inhibition activity of UDASP-HB on egg yolk model lipid peroxidation at varying concentrations, compared to ascorbic acid, a well-known antioxidant, is presented in Table 2. UDASP-HB, at its highest under investigation concentration (180 μg/ml), showed a high inhibition value of 84.87 ± 1.26%, closely following that of ascorbic acid, whose inhibition value at 95.39 ± 1.22% was marginally increased. With a decrease in UDASP-HB concentrations, its inhibition activity for egg yolk model lipid peroxidation consistently lowered: 75.68 ± 1.28% at 90 μg/ml, 67.91 ± 1.28% at 60 μg/ml, 56.82 ± 1.22% at 30 μg/ml, and 44.71 ± 1.14% at 15 μg/ml. Ascorbic acid, in its part, showed lowered inhibition with a decrease in concentrations, but at a level higher than UDASP-HB at all concentrations under investigation. That behaviour indicates UDASP-HB's dose-dependent effectiveness, which is noteworthy for its antioxidant activity, although it is even less potent than that of ascorbic acid. Notably, even at the minimum level (15 μg/ml), UDASP-HB exhibited a significant inhibition percentage, confirming its effectiveness as a powerful antioxidant.

Table 2. In the model of egg yolk homogenates, the percentage of lipid peroxidation inhibition of UDASP-HB

Media	Concentration (μg/ml)	UDASP-HB (%)	Ascorbic acid (%)
Egg yolk	180 μg/ml	84.87 ± 1.26*	95.39 ± 1.22*
	90 μg/ml	75.68 ± 1.28*	86.64 ± 1.90*
	60 μg/ml	67.91 ± 1.28*	80.49 ± 1.78*
	30 μg/ml	56.82 ± 1.22*	62.24 ± 1.67*
	15 μg/ml	44.71 ± 1.14*	56.54 ± 1.25

Values are expressed using the standard deviation (SD) plus the mean of three replicate measurements.
*$p < 0.05$ significant deviations from ascorbic acid.

3.3 Inhibition of Lipid peroxidation in liver homogenate model

Table 3 below shows the in vitro inhibition of LPO in liver homogenate at UDASP-HB doses of catechin, a potent antioxidant. At 180 μg/ml, UDASP-HB exhibited a high inhibition value of 91.54 ± 1.98%, indicating high antioxidant activity, albeit somewhat lower than the 98.88 ± 1.67% observed for catechin. The efficacy of UDASP-HB decreases as concentrations rise: 82.63 ± 1.93% at 90 μg/ml, 73.38 ± 1.41% at 60 μg/ml, plateaus at 72.91 ± 1.32% at 30 μg/ml, and then falls to its lowest value of 51.78 ± 1.22% at 15 μg/ml. Conversely, catechin exhibited a strong inhibitory effect at all concentrations, but a steep decline at lower concentrations, decreasing from 94.68 ± 1.69% at 90 μg/ml to 69.84 ± 1.37% at 30 μg/ml. While catechin exhibits slightly higher antioxidant activity at comparable concentrations, the trend in this instance reflects the dose-dependent efficacy of both UDASP-HB and catechin. In terms of *$p < 0.05$ and **$p < 0.01$, statistical analysis demonstrates that the inhibition rate differences between UDASP-HB and catechin are significant at any level, but particularly at high concentrations. It also demonstrates that UDASP-HB is a potent antioxidant in its own right, even when it does not exhibit the same level of efficacy as catechin.

Table 3. *In vitro* evaluation of lipid peroxidation (LPO) inhibition using liver homogenate

Media	Concentration (μg/ml)	UDASP-HB (%)	Catechin (%)
Liver homogenate	180 μg/ml	91.54 ± 1.98**	98.88 ± 1.67**
	90 μg/ml	82.63 ± 1.93**	94.68 ± 1.69*
	60 μg/ml	73.38 ± 1.41*	83.91 ± 1.43*
	30 μg/ml	72.91 ± 1.32*	69.84 ± 1.37*
	15 μg/ml	51.78 ± 1.22*	62.59 ± 1.27*

Values are expressed as the standard deviation (SD) plus the mean of three replicate measurements. Differences from the Catechin group are significant at *$p < 0.05$ and **$p < 0.01$.

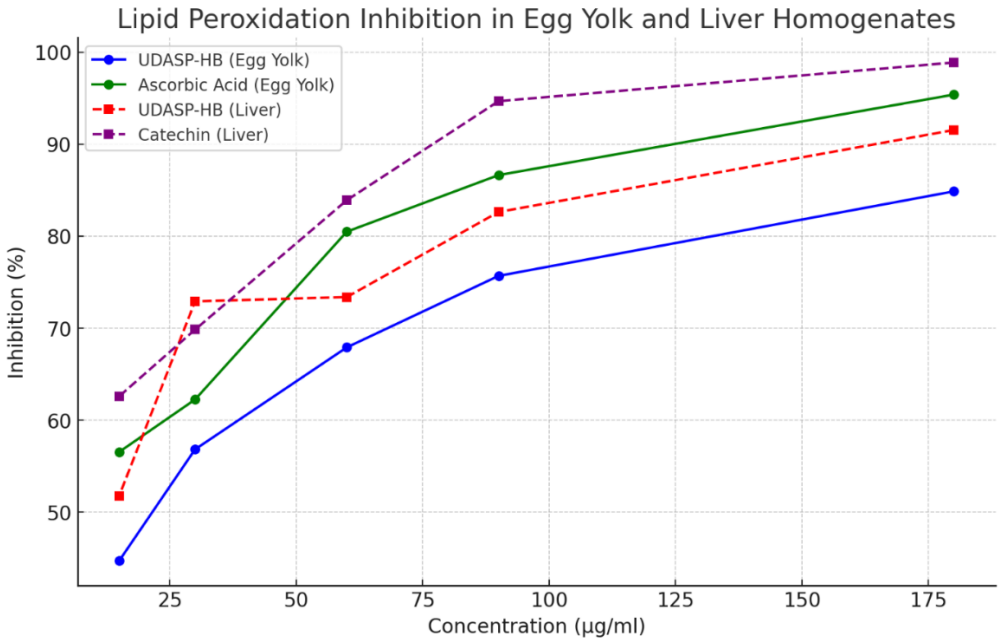

Figure 2. In vitro lipid peroxidation (LPO) Inhibition of UDASP-HB using egg yolk homogenates and liver homogenates

3.4 Evaluation of anti-inflammatory activity

3.4.1 Assessing the cyclooxygenase-1 (COX-1) and cyclooxygenase-2 (COX-2) enzyme inhibition

The inhibitory activity of UDASP-HB, the herbal blend, towards COX-1 and COX-2 enzymes at the indicated concentrations is shown in Table 4. There is an increased inhibition in a concentration-dependent manner for both enzymes. At a concentration of 60 µg/mL, inhibition was relatively low, with 3.791±0.89% inhibition for COX-1 and a relatively increased inhibition for COX-2 at 4.678±0.96%. With a heightened concentration to 120 µg/mL, inhibition for COX-1 reached almost double at 6.272±0.97%, and for COX-2, inhibition rose over double at 10.366±0.99%, with a reflection of a strong impact towards COX-2 at this level. The trend continued with increased concentrations. In 180 µg/mL, COX-1 inhibition increased to 22.231±1.01%, and COX-2 inhibition increased to 27.821±1.21%. It is a significant trend, suggesting a deeper inhibition of COX-2, a target for anti-inflammatory drugs in most instances, due to its direct role in inflammatory processes. In its most extreme inhibition, at 240 µg/mL, COX-1 inhibition increased to 45.306±1.21%, and COX-2 inhibition increased to 44.793±1.77%. These observations suggest that UDASP-HB has significant therapeutic value as an anti-inflammatory agent, primarily through the inhibition of COX-2. Concentration-dependent activity creates opportunities for individualized dosing tailored to specific therapeutic objectives. Observations validate the need for continued investigation regarding UDASP-HB therapeutic use, specifically in cases of disease where COX-2 is a significant participant.

Table 4. Percentage of COX system enzymes inhibited by the herbal blend (UDASP-HB).

	% Enzyme Inhibition	
Concentration (µg/mL)	**COX-1**	**COX-2**
60	3.791 ± 0.89	4.678 ± 0.96
120	6.272 ± 0.97	10.366 ± 0.99
180	22.231 ± 1.01	27.821 ± 1.21
240	45.306 ± 1.21	44.793 ± 1.77
300	94.698 ± 1.67	86.576 ± 1.82
IC_{50}	233.21 µg/mL	229.89 µg/mL

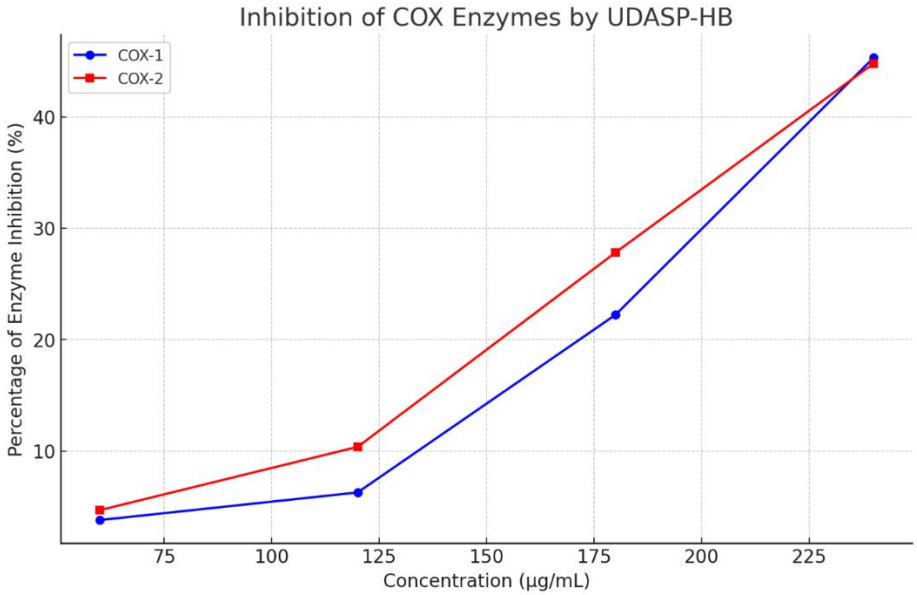

Figure 3. Percentage of COX system enzymes inhibited by the herbal blend (UDASP-HB).

3.5 Herbal Gel Formulation: development and evaluation of the topical herbal gel

Gel formulations are typically preferred over other topical semisolid treatments for several reasons. Their long-lasting effects on the skin, high viscosity, occlusive qualities that moisturise flaky skin, improved bioadhesiveness, decreased irritation, independence from the water solubility of active ingredients, ease of application, and improved release characteristics are just a few of their many benefits [31-33]. The anti-inflammatory, antioxidant, protective, and anti-aging properties of flavonoids and phenolic compounds found in herbs have been the subject of numerous studies. Furthermore, it has been shown that these polyphenolic flavonoids can permeate human skin [34-37]. These results led to the development of a topical herbal gel formulation that includes extracts high in flavonoids and phenolic components for the prevention and treatment of inflammation, wounds, and related disorders [38-40].

3.6 Fabrication and Characterisation for the Formulated Topical Herbal Gel

Table 5 presents the characteristics of various prepared topical gel formulations, each prepared with 1.5% Carbopol 934, highlighting differences in pH, viscosity, spreadability, and net content across six formulations coded HGF1 through HGF6.

3.6.1 pH Levels: The pH of all formulations is near neutrality (approximately 7.4), which is optimal for dermal use, as it closely corresponds to the in-situ skin pH and reduces irritation. A slight deviation in pH (ranging from 7.39 to 7.54) between the formulations is within a narrow range. It reflects a high level of uniformity in terms of the acid-base character of the formulation.

3.6.2 Viscosity: A definite rise in viscosity with HGF1 through HGF6, with a range of 4.5 poise through 9.4 poise, was seen. A rise in viscosity will likely result in a thicker gel structure, making it easier for the gel to maintain its placed position and not drip excessively. Viscosity can work beneficially when applied directly to the skin, particularly with a thicker level used for an extended duration of activity.

3.6.3 Spreadability: Correspondingly, with increased viscosity, spreadability also increases; for instance, 35.71 g/cm/s in HGF1 and 79.36 g/cm/s in HGF6. Spreadability is an important property for topical gels, describing how a gel spreads when it comes into contact with the skin. Greater spreadability will mean less force is required to spread the gel, providing increased comfort and efficiency in covering larger areas of skin.

3.6.4 Net Content: The net contents of all samples have remarkably similar 100% values, with little variation (98.96% to 101.00%). Such homogeneity in net contents ensures precise dosing, confidence in consumption, and superior manufacturing without overfilling or underfilling. In general, the improvement in viscosity and spreadability between HGF1 and HGF6 reflects that the formulations have been optimized for

application performance improvement, and thus can function even better for subjects with variable requirements for gel textures and spreading velocities. High accuracy in all formulations' net contents reflects a high level of care and accuracy in production.

Table 5. Characteristics of the topical gel formulations prepared with 1.5% Carbopol 934 Concentration.

Code	pH	Viscosity (poise)	Spreadability (g cm/sec)	Net Content (% w/w)
HGF1	7.41 ± 0.17	4.5 ± 0.11	35.71 ± 1.14	98.96 ± 1.45
HGF2	7.39 ± 0.18	5.5 ± 0.12	47.44 ± 1.34	99.95 ± 1.99
HGF3	7.54 ± 0.16	5.9 ± 0.13	58.81 ± 1.39	100.20 ± 1.94
HGF4	7.46 ± 0.19	7.2 ± 0.21	66.77 ± 1.45	101.00 ± 1.89
HGF5	7.51 ± 0.13	8.6 ± 0.18	73.62 ± 1.60	100.00 ± 1.85
HGF6	7.39 ± 0.11	9.4 ± 0.01	79.36 ± 1.72	99.91 ± 1.85

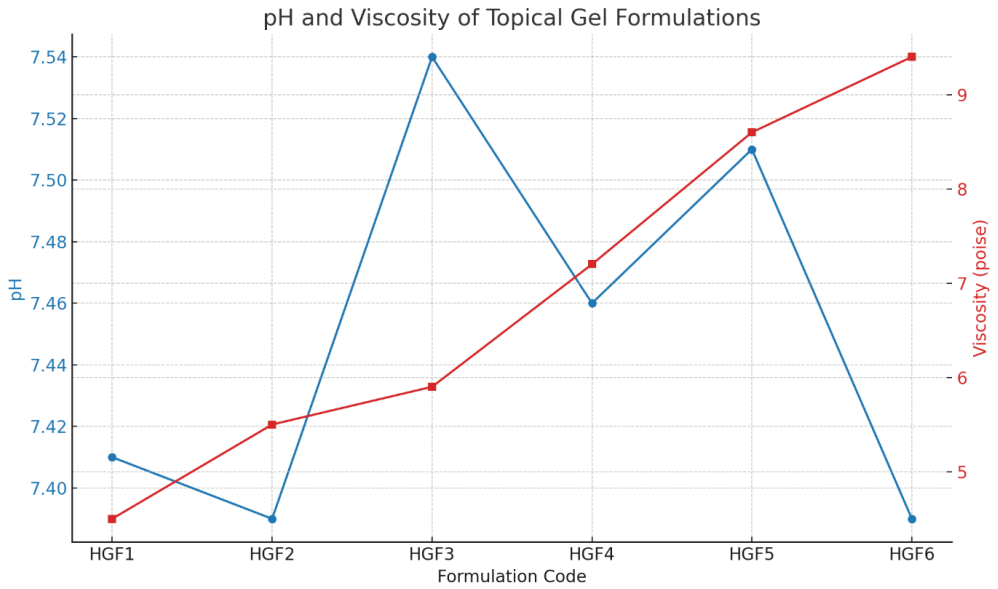

Figure 4. pH and Viscosity (poise) of Gel Formulations

3.6.5 Extrudability and Physical Appearance

The following is a general overview of the extrudability and physico-morphology of a range of topical gel forms, prepared at 1.5% w/w of Carbopol 934, coded HGF1 to HGF6, respectively.

Extrudability: One of its key functions is user-friendliness, which reflects how easily the gel can be extruded from its packaging. Since HGF1, HGF4, and HGF5 have "Excellent" extrudability, these gels should be quite easy to squeeze out, perhaps as a result of viscosity at the optimal level for unhindered free flow. Although they are effective, HGF2, HGF3, and HGF6 exhibit "Good" extrudability and less free flow than "Excellent."

Physical Appearance: All of these formulations have been uniformly described as dark greenish, transparent, and homogeneous in form. Homogeneity in form is an indicator of correct mixing during production, ensuring that no form separation or variation in colours occurs, which can be important for trust in consumption and product consistency. Transparency and homogeneity in form in the gels also mean that particulate impurities have been circumvented and successfully stabilized, which can be important for cosmetic appearances and uniformity in application over the skin. In inference, these observations in Table 6 validate the successful development of these topical gels, both functionally and cosmetically. Overall, good to excellent extrudability in all cases confirms ease of use and effectiveness during use, as well as a uniform, pleasing physical appearance that enhances marketability and acceptance, and promotes increased patient acceptance and use. All these, in addition to the physical characteristics mentioned in the preceding tables, contribute to the overall quality and therapeutic efficacy of these gel preparations.

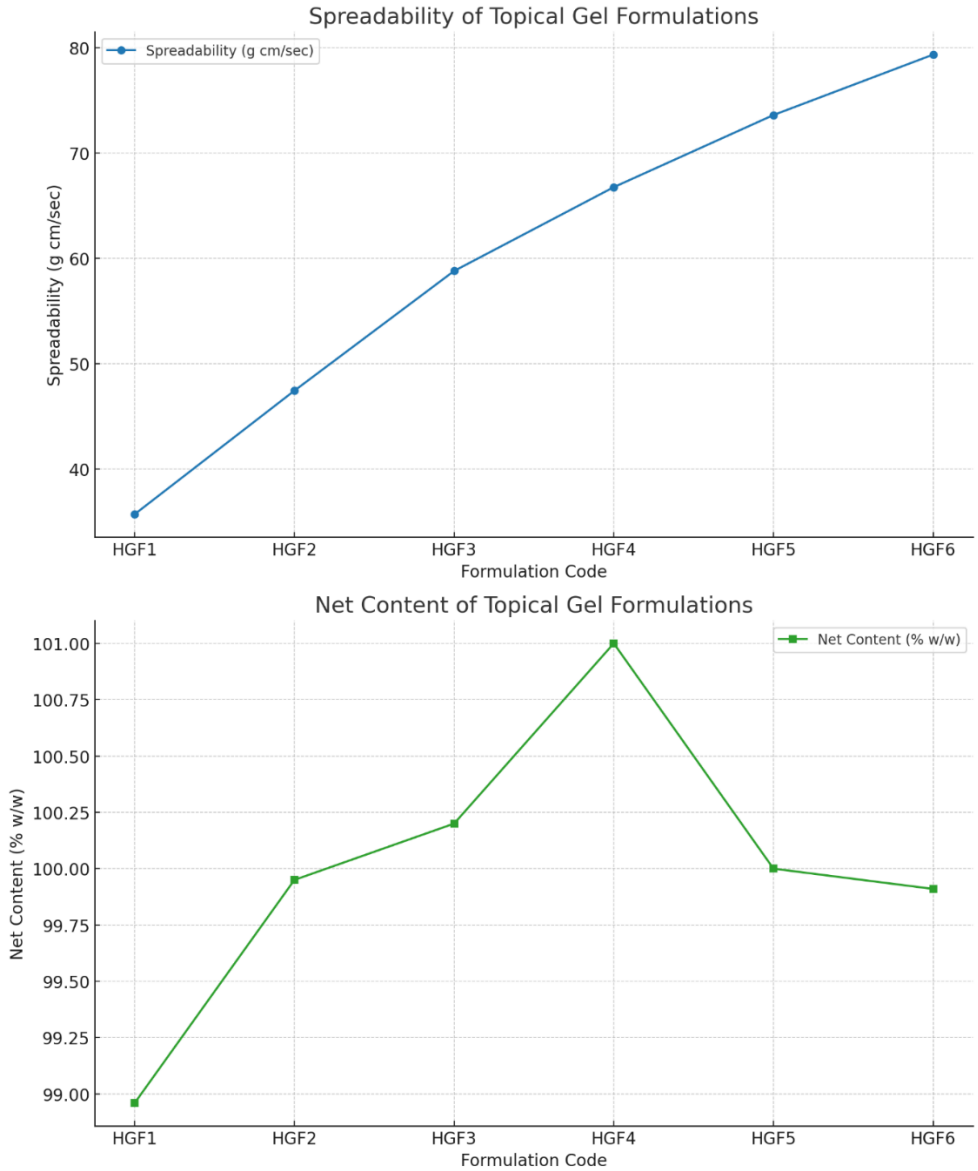

Figure 5. Spreadability and Net Content of Gel Formulations

Table 6. Extrudability and Physical Appearance for the topical gel formulations fabricated with Carbopol 934 at 1.5% concentration.

Code	Extrudability	Physical Appearance
HGF1	Excellent	Dark-greenish, homogeneous, and transparent
HGF2	Good	Dark-greenish, homogeneous, and transparent
HGF3	Good	Dark-greenish, homogeneous, and transparent
HGF4	Excellent	Dark-greenish, homogeneous, and transparent
HGF5	Excellent	Dark-greenish, homogeneous, and transparent
HGF6	Good	Dark-greenish, homogeneous, and transparent

3.6.6 Diffusion profile in vitro and kinetics of drug release

Table 7 presents the in vitro diffusion profile for six gels with variable compositions (HGF1 to HGF6), with a five-hour duration for cumulative drug release expressed as a percentage. Comparing each one, one can see how each releases its active compound over a period, which is relevant in terms of understanding its efficacy and potential application in a therapeutic scenario. HGF4 and HGF2 exhibit a significantly accelerated one-hour release of the drug, with values of 21.41 ± 1.20% and 21.28 ± 1.21%, respectively. That kind of accelerated

delivery could be beneficial in cases with a rapid onset of action demand. HGF1 and HGF5 have a slow and intermediate level of release, and that could be useful for use in cases in which an immediate increase in drug level is not desired. By three hours, HGF2 prevails with a high cumulative release of 73.38 ± 1.24%, followed closely by HGF4 and HGF6. Sustained diffusion could represent a less viscous preparation or one with high solubility of the active ingredient, facilitating quick absorption. By four hours, HGF2 reaches a high value of 93.37 ± 1.31%, then dips a little at five hours to 83.31 ± 1.29%. HGF4 reaches an unprecedented high reading of 102.42 ± 1.33% at five hours, which may be attributed to an experimental flaw, possibly over-saturation, resulting in an overshoot reading. HGF3, HGF5, and HGF6 build slowly and level off, eventually achieving a sustained release for long-term therapeutic activity. The overall diffusion profiles reveal that each gel possesses specific properties, making them applicable for a variety of therapeutic requirements. HGF2 and HGF4 are best suited for therapeutic requirements with a demand for rapid drug delivery, while HGF1, HGF3, HGF5, and HGF6 may be applicable for extended drug delivery, providing therapeutic efficacy over a prolonged period. Differences in the composition of the gel matrix probably cause these differences, with an impact on the kinetics of drug release and diffusion behaviour. This investigation is crucial for developing targeted topical drugs for specific medical conditions by manipulating these formational properties.

Table 7. Diffusion profile *in vitro*

TIME (Hr)	Gel Formulations					
	% Cumulative drug release					
	HGF1	**HGF2**	**HGF3**	**HGF4**	**HGF5**	**HGF6**
1	11.89 ± 1.20	21.41 ± 1.20	14.28 ± 1.19	21.28 ± 1.21	14.91 ± 1.20	17.39 ± 1.28
2	20.00 ± 1.19	38.01 ± 1.22	28.45 ± 1.20	37.17 ± 1.22	30.06 ± 1.20	31.00 ± 1.29
3	36.26 ± 1.22	73.38 ± 1.24	51.47 ± 1.26	56.34 ± 1.22	54.09 ± 1.27	58.99 ± 1.32
4	44.97 ± 1.23	93.37 ± 1.31	67.20 ± 1.29	73.27 ± 1.27	71.40 ± 1.28	69.08 ± 1.30
5	69.38 ± 1.30	83.31 ± 1.29	82.40 ± 1.30	102.42 ± 1.33	87.41 ± 1.29	86.90 ± 1.33

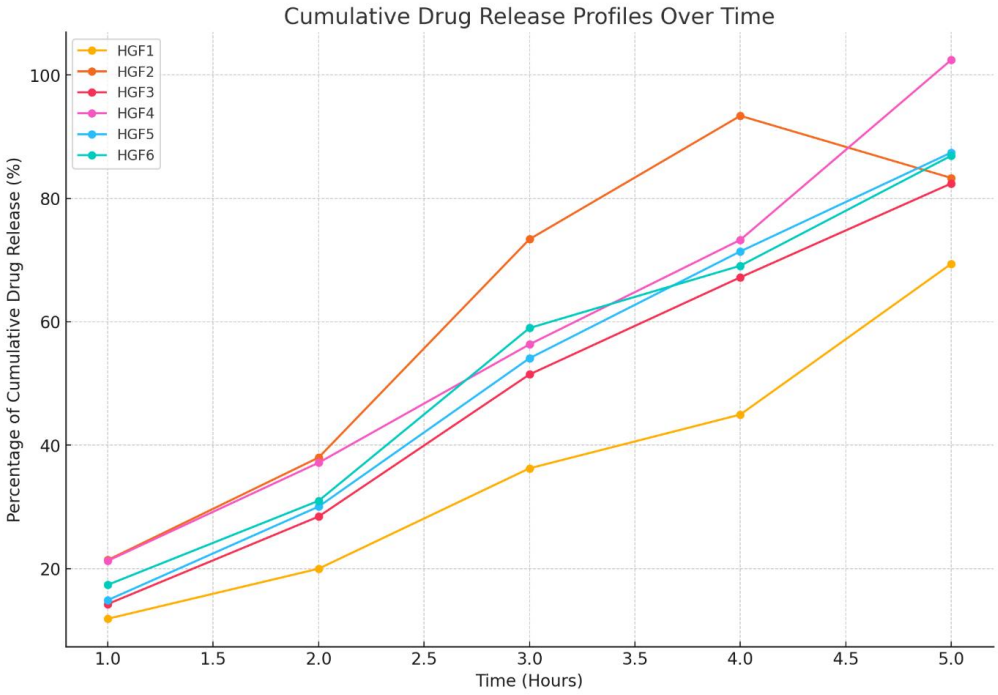

Figure 6. In vitro diffusion profile of topical herbal gels.

3.6.7 Kinetic modelling of data from in vitro releases

Table 8 presents a detailed examination of the kinetic modeling of six gel formulations (HGF1 through HGF6) under three kinetic models: Zero Order, First Order, and Higuchi Diffusion Model. For determining

the best-fitting model for each, a high value for R^2 is selected as the best-fit model for explaining the mechanism of drug delivery. The Zero Order model, which represents a constant release in terms of concentration, best fits HGF1, HGF3, HGF4, HGF5, and HGF6, with R^2 values of 0.9645, 0.9941, 0.9860, 0.9947, and 0.9816, respectively. That such a model holds for these drugs tells us that such drugs deliver at a constant level, a property beneficial in sustained level maintenance over a duration of time. High values for R^2 for such drugs confirm them to have a high probability of delivering drugs over a sustained duration, a property beneficial for long-term dosing needs. For HGF2, in contrast, the Higuchi model best describes it, with the delivery of the drug determined via diffusion in the gel matrix, yielding an R^2 value of 0.8876. That such a model best characterizes HGF2 informs us about its behavior, being most determined by the physico-mechanical properties of the gel, such as its porosity, compatibility with drugs, and its constituent materials. In general, kinetic modelling of such preparations not only helps describe their mechanism of delivery but also optimizes them for a desired therapeutic demand in terms of the desired profiles of delivery. All such information helps develop effective delivery systems capable of delivering a predictable and sustained therapeutic effect.

Table 8. Kinetic modelling of drug release data in vitro

Code for Formulations	Zero order	First Order	Higuchi diffusion model	Best-fitted model
	R^2	R^2	R^2	
HGF1	0.9645	0.8921	0.9214	Zero Order
HGF2	0.8468	0.7051	0.8876	Higuchi
HGF3	0.9941	0.9635	0.9843	Zero Order
HGF4	0.9860	0.9470	0.9524	Zero Order
HGF5	0.9947	0.9466	0.9843	Zero Order
HGF6	0.9816	0.9425	0.9764	Zero Order

3.7 The optimum formulation

HGF5 stands out with its exceedingly high R^2 value (0.9947) in Zero Order, indicating an exceedingly predictable and constant release profile. That will work ideally for therapies in which dosing accuracy is critical and in scenarios where variation in drug levels can threaten the efficacy of the therapy or patient safety. Thus, HGF5 can be considered an ideal delivery form for the long-term and sustained delivery of drugs, provided its physico-mechanical properties (viscosity, pH, etc.) and spreadability meet the requirements for therapeutic use. With such a form, one can hope for increased compliance, fewer side effects, and successful treatment for this disease.

4. Conclusions

The conclusion of this research work confirms the effectiveness of UDASP-HB in providing antioxidant and anti-inflammatory activity, supported by its high flavonoid level and its capacity to inhibit key anti-inflammatory enzymes. Optimal delivery performance was achieved for developed topical gel forms, characterized by sustained kinetics that support therapeutic activity. Most importantly, the herbal topical gel formulation, HGF5, exhibited the best release behavior, with implications for its application in long-term treatment. All observations validate UDASP-HB as a worthy therapeutic modality for the treatment of inflammatory diseases, providing a basis for future development in a clinical environment.

5. Acknowledgements

Zen Pharmaceuticals, Karnal, India, kindly provided free samples of quercetin and catechin, which were crucial for conducting this study, for which the authors are grateful. We appreciate their support.

Author Contributions: Dr. S. Valarmathi and Dr. Tabrej Mujawar were responsible for the conceptualization and methodology of the study. Miss Komal Kriti and Ms. Maneesha Bhardwaj conducted the investigation and data collection, while Ms. Sweta Negi and Dr. Kavitha S handled data curation and formal analysis. The original draft was prepared by Dr. Touseef Begum and Mr. Mohammad Muztaba, who also contributed to the review and editing of the manuscript. Funding acquisition was equally supported by all authors, ensuring the

successful completion of the research. Dr. Tabrej Mujawar provided overall supervision. All authors have read and approved the final manuscript.

Funding: This research was entirely self-funded by the authors. Dr. S. Valarmathi, Miss Komal Kriti, Dr. Tabrej Mujawar, Ms. Maneesha Bhardwaj, Ms. Sweta Negi, Dr. Kavitha S., Dr. Touseef Begum, and Mr. Mohammad Muztaba equally contributed to the financial support necessary for the project's successful completion. No external funding sources were involved.

Conflicts of Interest: The authors declare no conflict of interest.

References

[1] Hendrix, J.; Nijs, J.; Ickmans, K.; Godderis, L.; Ghosh, M.; Polli, A. The Interplay between Oxidative Stress, Exercise, and Pain in Health and Disease: Potential Role of Autonomic Regulation and Epigenetic Mechanisms. *Antioxidants (Basel).* **2020,** *9*(11), 1166. https://doi.org/10.3390/antiox9111166

[2]. Kakoti, B. B.; Hernandez-Ontiveros, D. G.; Kataki, M. S.; Shah, K.; Pathak, Y.; Panguluri, S. K. J. F. i. c. m. Resveratrol and omega-3 fatty acid: its implications in cardiovascular diseases. 2015**,** *2*, 38. https://doi.org/10.3389/fcvm.2015.00038

[3] Sreejayan, N.; Rao, M. N. A. Nitric oxide scavenging by curcuminoids. *J Pharm Pharmacol.* **1997,** *49*, 105-107. https://doi.org/10.1111/j.2042-7158.1997.tb06761.x

[4 Li, C.; Huang, Q.; Fu, X.; Yue, X. J.; Liu, R. H.; You, L. J. Characterization, antioxidant and immunomodulatory activities of polysaccharides from Prunella vulgaris Linn. *International journal of biological macromolecules.* **2015,** *75*, 298-305. https://doi.org/10.1016/j.ijbiomac.2015.01.010

[5] Li, H.-L.; Liu, D.-P.; Liang, C.-C. Paraoxonase gene polymorphisms, oxidative stress, and diseases. *Journal of Molecular Medicine.* **2003,** *81*(12), 766-779. https://doi.org/10.1007/s00109-003-0481-4

[6] Wu, Y.; Li, L.; Wen, T.; Li, Y.-Q. Protective effects of echinacoside on carbon tetrachloride-induced hepatotoxicity in rats. *Toxicology.* **2007,** *232*(1–2), 50-56. https://doi.org/10.1016/j.tox.2006.12.013

[7] Soga, M.; Matsuzawa, A.; Ichijo, H. Oxidative Stress-Induced Diseases via the ASK1 Signaling Pathway. *International Journal of Cell Biology.* **2012,** *2012*, 439587. https://doi.org/10.1155/2012/439587

[8] Re, R.; Pellegrini, N.; Proteggente, A.; Pannala, A.; Yang, M.; Rice-Evans, C. Antioxidant activity applying an improved ABTS radical cation decolorization assay. *Free Radical Biology and Medicine.* **1998,** *72*, 1231-1237. https://doi.org/10.1016/S0891-5849(98)00315-3

[9] Packer, L., *Handbook of Antioxidants*. Taylor & Francis: **2001**. https://doi.org/10.1201/9780203904046

[10] Kataki, M. S.; Murugamani, V.; Rajkumari, A.; Mehra, P.; Awasthi, D.; Yadav, R. S. Antioxidant, Hepatoprotective, and Anthelmintic Activities of Methanol Extract of Urtica dioica L. Leaves. *Pharmaceutical Crops.* **2012,** *3*(1), 38-46. https://doi.org/10.2174/2210290601203010038

[11] Ruch, R. J.; Cheng, S. J.; Klaunig, J. E. Prevention of cytotoxicity and inhibition of intracellular communication by antioxidant catechins isolated from Chinese green tea. *Carcinogenesis.* **1989,** *10*, 1003-1008. https://doi.org/10.1093/carcin/10.6.1003

[12] Ahmad, S.; Ullah, F.; Zeb, A.; Ayaz, M.; Ullah, F.; Sadiq, A. Evaluation of Rumex hastatus D. Don for cytotoxic potential against HeLa and NIH/3T3 cell lines: chemical characterization of chloroform fraction and identification of bioactive compounds. *BMC complementary and alternative medicine.* **2016,** *16*(1), 308. https://doi.org/10.1038/s41598-019-41372-1

[13] D'Abrosca, B.; Ciaramella, V.; Graziani, V.; Papaccio, F.; Della Corte, C. M.; Potenza, N.; Fiorentino, A.; Ciardiello, F.; Morgillo, F. Urtica dioica L. inhibits proliferation and enhances cisplatin cytotoxicity in NSCLC cells via Endoplasmic Reticulum-stress mediated apoptosis. *Scientific reports.* **2019,** *9*(1), 4986. https://doi.org/10.1201/9781315153711-18

[14] Kataki, M. S.; Rajkumari, A.; Mazumder, B. J. N.; Relevance, N. C.; Prevention, D. Nutrition and Healthy Aging. **2017**, 451.

[15] Khare, C. P., *Indian medicinal plants: an illustrated dictionary*. Springer Science & Business Media: **2008**. https://doi.org/10.1007/978-0-387-70638-2

[16] Kataki, M. S.; Murugamani, V.; Rajkumari, A.; Mehra, P. S.; Awasthi, D.; Yadav, R. S. Antioxidant, hepatoprotective, and anthelmintic activities of methanol extract of Urtica dioica L. leaves. *Pharmaceutical Crops.* **2012,** *3*(1), 38-46. https://doi.org/10.2174/2210290601203010038

[17] Huq, A.; Jamal, J. A.; Stanslas, J. J. E.-B. C.; Medicine, A. Ethnobotanical, phytochemical, pharmacological, and toxicological aspects of Persicaria hydropiper (L.) Delarbre. **2014,** *2014*. https://doi.org/10.1155/2014/782830

[18] Mandal, V.; Mohan, Y.; Hemalatha, S. Microwave assisted extraction—an innovative and promising extraction tool for medicinal plant research. *Pharmacognosy reviews.* **2007,** *1*(1), 7-18.

[19] Ghasemi, K.; Ghasemi, Y.; Ebrahimzadeh, M. A. Antioxidant activity, phenol and flavonoid contents of 13 citrus species peels and tissues. *Pakistan journal of pharmaceutical sciences.* **2009,** *22*(3), 277-81.

[20] Badmus, J. A.; Adedosu, T. O.; Fatoki, J. O.; Adegbite, V. A.; Adaramoye, O. A.; Odunola, O. A. Lipid Peroxidation Inhibition and Antiradical Activities of Some Leaf Fractions of *Mangifera Indica*. *Acta Poloniae Pharmaceutica - Drug Research.* **2011,** *68*(1), 23-29.

[21] Redl, K.; Breu, W.; Davis, B.; Bauer, R. Anti-inflammatory active polyacetylenes from *Bidens campylotheca* [J]. *Planta Medica.* **1994,** *60*(58-62). https://doi.org/10.1055/s-2006-959409

[22] Aguilar, J. L.; Rojas, P.; Marcelo, A.; Plaza, A.; Bauer, R.; Reininger, E.; Klaas, C. A.; Merfort, I. Anti-inflammatory activity of two different extracts of *Uncaria tomentosa* (Rubiaceae) [J]. *Journal of Ethnopharmacology.* **2002,** *81*, 271-276. https://doi.org/10.1016/S0378-8741(02)00093-4

[23] Aiyalu, R.; Govindarjan, A.; Ramasamy, A. Formulation and evaluation of topical herbal gel for the treatment of arthritis in animal model. *Brazilian Journal of Pharmaceutical Sciences.* **2016,** *52*. https://doi.org/10.1590/s1984-82502016000300015

[24] Kohli, D. P. S.; Shah, D. H., *Drug Formulations Manual*. Eastern Publishers: 1998.

[25] Nandgude, T.; Thube, R.; Jaiswal, N.; Deshmukh, P.; Chatap, V.; Hire, N. Formulation and evaluation of pH induced in-situ nasal gel of salbutamol sulphate. *International Journal of Pharmaceutical Sciences and Nanotechnology (IJPSN).* **2008,** *1*(2), 177-183. https://doi.org/10.37285/ijpsn.2008.1.2.9

[26] Aiyalu, R.; Govindarjan, A.; Ramasamy, A. Formulation and evaluation of topical herbal gel for the treatment of arthritis in animal model. *Brazilian Journal of Pharmaceutical Sciences.* **2016,** *52*, 493-507. https://doi.org/10.1590/s1984-82502016000300015

[27] Queiroz, M. B. R.; Marcelino, N. B.; Ribeiro, M. V.; Espindola, L. S.; Cunha, F. R.; Silva, M. V. d. Development of gel with Matricaria recutita L. extract for topic application and evaluation of physical-chemical stability and toxicity. *Lat. Am. J. Pharm.* **2009,** *28*(4), 574-579.

[28] Nayak, S. H.; Nakhat, P. D.; Yeole, P. G. Development and evaluation of cosmeceutical hair styling gels of ketoconazole. *Indian journal of pharmaceutical sciences.* **2005,** *67*(2), 231.

[29] Jain, B. D. Formulation Development And Evaluation Of Fluconazole Gel In Various Polymer Basesformulation Development And Evaluation Of Fluconazole Gel In Various Polymer BaseS. *Asian Journal of Pharmaceutics (AJP).* **2007,** *1*(1).

[30] Martin, A. N.; Sinko, P. J.; Singh, Y., *Martin's Physical Pharmacy and Pharmaceutical Sciences: Physical Chemical and Biopharmaceutical Principles in the Pharmaceutical Sciences*. Lippincott Williams & Wilkins: **2011**.

[31] Loganathan, V.; Manimaran, S.; Jaswanth, A.; Sulaiman, A.; Reddy, M. V. S.; Kumar, B. S.; Rajaseskaran, A. The effects of polymers and permeation enhancers on releases of flurbiprofen from gel formulations. *Indian Journal of Pharmaceutical Sciences.* **2001,** *63*(3), 200.

[32] Oktay, A. N.; Ilbasmis-Tamer, S.; Han, S.; Uludag, O.; Celebi, N. Preparation and in vitro/in vivo evaluation of flurbiprofen nanosuspension-based gel for dermal application. *European Journal of Pharmaceutical Sciences.* **2020,** *155*, 105548. https://doi.org/10.1016/j.ejps.2020.105548

[33] Panigrahi, L.; Ghosal, S. K.; Pattnaik, S.; Maharana, L.; Barik, B. B. Effect of permeation enhancers on the release and permeation kinetics of lincomycin hydrochloride gel formulations through mouse skin. *Indian journal of pharmaceutical sciences.* **2006,** *68*(2). https://doi.org/10.4103/0250-474X.25716

[34] Ghasemzadeh, A.; Ghasemzadeh, N. Flavonoids and phenolic acids: Role and biochemical activity in plants and human. *J. Med. Plants Res.* **2011,** *5*(31), 6697-6703. https://doi.org/10.5897/JMPR11.1404

[35] Ratz-Łyko, A.; Arct, J.; Majewski, S.; Pytkowska, K. Influence of polyphenols on the physiological processes in the skin. *Phytotherapy Research.* **2015,** *29*(4), 509-517. https://doi.org/10.1002/ptr.5289

[36] Stelmakienė, A.; Ramanauskienė, K.; Briedis, V. Release of rosmarinic acid from semisolid formulations, and its penetration through the human skin ex vivo. *Acta Pharmaceutica.* **2015,** *65*(2), 199-205. https://doi.org/10.1515/acph-2015-0012

[37] Seelinger, G.; Merfort, I.; Wölfle, U.; Schempp, C. M. Anti-carcinogenic effects of the flavonoid luteolin. *Molecules.* **2008,** *13*(10), 2628-2651. https://doi.org/10.3390/molecules13102628

[38] Blanco-Fuente, H.; Anguiano-Igea, S.; Otero-Espinar, F. J.; Blanco-Méndez, J. In-vitro bioadhesion of carbopol hydrogels. *International journal of pharmaceutics.* **1996,** *142*(2), 169-174. https://doi.org/10.1016/0378-5173(96)04665-0

[39] Walker, R. B.; Smith, E. W. The role of percutaneous penetration enhancers. *Advanced Drug Delivery Reviews.* **1996,** *18*(3), 295-301. https://doi.org/10.1016/0169-409X(95)00078-L

[40] Murthy, S. N.; Shivakumar, H. N., Topical and transdermal drug delivery. In *Handbook of non-invasive drug delivery systems*, Elsevier: **2010**; pp 1-36. https://doi.org/10.1016/B978-0-8155-2025-2.10001-0

ASEAN
Journal of Scientific and Technological Reports
Online ISSN:2773-8752

Research article

Potential of Tobacco Extracts in Controlling Stable Flies (*Stomoxys calcitrans* L.) in Beef Cattle

Janejira Namee[1], and Panut Sooksoi[2*]

[1] Faculty of Agricultural Technology, Valaya Alongkorn Rajabhat University under the Royal Patronage, Pathum Thani, 13180, Thailand
[2] Faculty of Agricultural Technology, Valaya Alongkorn Rajabhat University under the Royal Patronage, Pathum Thani, 13180, Thailand
* Correspondence: panut@vru.ac.th

Citation:
Namee , J.; Sooksoi, P. Potential of tobacco extracts in controlling stable flies (*Stomoxys calcitrans* L.) in beef cattle. *ASEAN J. Sci. Tech. Report.* **2025**, *28*(4), e258723. https://doi.org/10.55164/ajstr.v28i4.258723.

Article history:
Received: April 10, 2025
Revised: July 18, 2025
Accepted: August 5, 2025
Available online: August 17, 2025

Abstract: This research aimed to evaluate the potential of tobacco extract for controlling stable flies (*Stomoxys calcitrans* L.) in beef cattle. The study was divided into three experiments: 1) determination of nicotine concentration in tobacco extract using different fermentation times, 2) laboratory assessment of tobacco extract efficacy against stable flies, and 3) field evaluation of tobacco extract efficacy against stable flies. Results showed that fermenting tobacco with 95% ethanol for 48 hours yielded the highest nicotine content at 46.71 μg/mg, which was significantly different ($P<0.001$) compared to other fermentation periods. Laboratory studies revealed that the efficacy of tobacco extract in eliminating stable flies increased with concentration and exposure time. The 20% tobacco extract showed maximum efficacy with mortality rates of 98.33% at 24 hours and 100% at 48 hours, while 3% tobacco extract achieved 95% mortality of stable flies at 72 hours. In field trials, 3% tobacco extract demonstrated significantly better control of stable flies compared to the control treatment (distilled water) ($P<0.001$), but was less effective than 35% cypermethrin. The efficacy of tobacco extract decreased after 96 hours post-application, corresponding with increased fly-repelling behaviors in cattle, including tail flicking, skin twitching, foot stamping, and head swinging. Results from this study indicate that tobacco extract has potential as an alternative to synthetic chemicals for controlling stable flies in beef cattle, which helps reduce chemical use and is environmentally friendly.

Keywords: Tobacco extract; Nicotine; Stable fly; Beef cattle; Biological insecticide

1. Introduction

Stable flies (*Stomoxys calcitrans* (L.) [Diptera: Muscidae]) cause significant economic damage to the livestock industry by irritating and inflicting painful bites on animals as they feed on their blood [1]. Several species of stable flies exist, but *S. calcitrans* L. is the most prevalent in Thailand [2]. According to Arjkumpa et al. [3], blood-feeding by stable flies can reduce cattle weight by 0.22 kg per day and decrease milk production by 30-40 percent. Additionally, stable flies serve as vectors for lumpy skin disease, an emerging disease first detected in Thailand in 2021. This severe disease results in morbidity rates of 5-45% in infected animals, with mortality rates being particularly high in regions where the disease had not previously occurred [4].

Farmers typically control stable flies using synthetic chemicals, which may adversely affect the health of both animals and users [5]. Therefore, natural

insecticidal extracts, such as tobacco extract, represent an enjoyable alternative to chemical pesticides [6]. Natural extracts offer several advantages, including specificity in targeting insects [7], low toxicity, rapid degradation, and minimal environmental impact [8]. Tobacco extract contains nicotine as its primary active compound, which is a natural alkaloid that acts on insect nervous systems through both contact and ingestion, demonstrating high efficacy against insects. Currently, these compounds are effectively used to eliminate household pests like ants, termites, and cockroaches [9].

In 2022, the Sa Kaeo Area Excise Office seized a large quantity of illegal tobacco products, including 165,959 packs of smuggled or counterfeit cigarettes. On May 10, 2023, 57,743 packs from finalized legal cases were officially transferred to Valaya Alongkorn Rajabhat University under the Royal Patronage, Sa Kaeo, for use in agricultural research. These seized cigarettes, previously designated for destruction, were repurposed to study their potential as botanical insecticides in line with the Zero Waste concept and efforts to reduce chemical pesticide use, minimize production costs, and avoid harm to humans, animals, and the environment. Therefore, this study aimed to (1) determine the nicotine concentration in tobacco extracts after different fermentation durations, (2) evaluate their insecticidal efficacy against stable flies under laboratory conditions, and (3) assess their effectiveness in controlling stable flies in beef cattle under field conditions in Khok Sung District, Sa Kaeo Province.

2. Materials and Methods

In this experiment, tobacco was provided by the Sa Kaeo Area Excise Office. This tobacco came from illegal contraband that had completed legal proceedings and was authorized for destruction by the Sa Kaeo Area Excise Office, according to official memorandum no. 0605/1162 dated April 24, 2023, regarding auction authorization and minimum pricing determination for confiscated items under the authority of the Excise Department of Thailand. The study on the efficacy of tobacco extract for controlling stable flies in beef cattle was divided into three experiments: 1) determination of nicotine concentration in tobacco extract using different fermentation times, 2) laboratory assessment of tobacco extract efficacy against stable flies in beef cattle, and 3) field evaluation of tobacco extract efficacy against stable flies in beef cattle (Animal use license number U1-03142-2559). The details are as follows:

2.1 Study of nicotine concentration in tobacco extracts using different fermentation times

The tobacco used in this study was obtained from confiscated cigarettes provided by the Sa Kaeo Area Excise Office. Although the exact plant parts used in the cigarettes were not specified, commercial cigarettes mainly contain tobacco leaves. Tobacco was unwrapped from its paper covering, weighed to 500 grams, and fermented with 500 milliliters of 95% ethanol [10] for periods of 48, 72, 96, and 120 hours at 27±1°C and 60-70% relative humidity under a 16:8 h light: dark cycle. The experiment followed a completely randomized design (CRD) with three replications. After completing the fermentation period, the mixture was filtered through a 10-micron filter cloth. The filtered solution was then evaporated to separate the solvent using a rotary evaporator (BUCHI R-114, BUCHI Corp., USA) at 65°C. The tobacco extract obtained was weighed to determine the yield in comparison to the initial tobacco weight. The prepared tobacco extracts were stored in amber glass bottles at 4°C in darkness to maintain stability and prevent degradation. Storage stability testing was conducted by monitoring the physical characteristics (color, pH, viscosity) and nicotine content of tobacco extracts at various concentrations stored under these conditions for up to 240 days, with analysis performed at intervals of 0, 15, 30, 60, 120, and 240 days. Results demonstrated good shelf-life stability with minimal degradation when stored under proper conditions.

Tobacco extract samples from fermentation periods of 48, 72, 96, and 120 hours were analyzed for nicotine content using High Performance Liquid Chromatography (HPLC) (Waters, Co., Ltd., USA). Nicotine analysis followed a method modified from Mihranyan [11], using a Symmetry C-18 column, 150 mm×3.90 mm, 5 μm particle size (Waters, Co, Ltd.). The mobile phase consisted of 0.1% (v/v) triethylamine in water: acetonitrile (70:30 v/v) with a flow rate of 1.0 milliliter per minute, detected by a UV Detector (Waters 486 Tunable Absorbance Detector) at a wavelength of 260 nanometers. This experiment used (-)-Nicotine hemisulfate salt ≥95% (TLC) 40% (w/v) as a standard, preparing standard solutions in methanol at concentrations of 10, 20, 40, 60, 90, and 100 μg/mL. HPLC analyzed the standard solutions to create a standard

curve between concentration and peak area. Nicotine content in each treatment's tobacco extract was calculated using the standard curve. Data from each treatment were analyzed according to the experimental design, and means were compared using Duncan's New Multiple Range Test at a 95% confidence level ($P<0.05$).

2.2 Efficacy study of tobacco extracts in controlling stable flies in beef cattle in laboratory conditions

Stable flies *(Stomoxys calcitrans* L.) were collected using sweep nets from a beef cattle farm (GPS coordinates: 13°46'20.2"N 102°10'59.6" E) at Valaya Alongkorn Rajabhat University under the Royal Patronage, Sa Kaeo Province. The stable fly was identified based on morphological characteristics under a high-magnification stereomicroscope. Diagnostic features included the presence of a forward-projecting proboscis with piercing-sucking mouthparts, clear wings with distinct venation, and a checkered black pattern on the abdomen. The body length was approximately 5-7 mm. The flies were raised in a laboratory in cages measuring 20×30×20 centimeters, made from wire frames covered with white nylon fabric with a 30-centimeter flap serving as an entrance-exit. The environment inside the breeding cage was arranged to simulate natural conditions by placing grass in plastic bags with water in plastic containers. Fresh cattle blood on cotton was provided as food daily. Fermented grass that had undergone a 7-day fermentation process was placed in a circular plastic container (5.5×1 centimeters in diameter) to serve as an egg-laying site for stable flies.

When the eggs hatched into larvae, they were raised in plastic containers. The larval diet, modified from Bailey et al. [12], consisted of wheat bran, bagasse, and water in a ratio of 3:1:5, placed in circular plastic containers (3.1×1.9 centimeters in diameter). Cotton circles with a diameter of 3 centimeters were moistened and placed on the food surface to prevent drying. The larval rearing containers were kept in a temperature-controlled cabinet at 25 ± 1°C with a relative humidity of 76-84%. Upon pupation, the pupae were transferred to circular plastic containers of the same size as the larval containers, covered with nylon fabric. When the pupae developed into adults, they were used in experiments.

Laboratory bioassays were conducted using 3-5 day old adult stable flies after emergence from pupae. The sex ratio of flies used in testing was not predetermined, maintaining natural proportions from the colony. No starvation period was applied before bioassay testing. During the observation period, treated flies were maintained in cages measuring 20×30×20 centimeters under controlled environmental conditions. Fresh cattle blood soaked in cotton and water were provided as food sources in circular plastic containers (4 cm diameter × 3 cm height) placed inside each cage to ensure fly survival during the observation period. All bioassay experiments were conducted under controlled laboratory conditions at 27±1°C and 60-70% relative humidity under a 16:8 h light:dark cycle.

The experiments involved spraying tobacco extract from the previous experiment that yielded the highest nicotine content. The extract was adjusted to concentrations of 1%, 3%, 5%, 10%, and 20% (w/v). Emulsifiers, including 10 grams of Tween 80 followed by 10 grams of Span 80, were added to increase product stability, and the mixture was homogenized. Then, 100 grams of water was added to the mixture and homogenized with a homogenizer [13]. The treatments were compared with distilled water (control) and a commercial stable fly insecticide (35% w/v cypermethrin, used at a rate of 10 milliliters per 20 liters of water).

The direct spray method was used with a high-pressure water sprayer equipped with a hollow cone nozzle (Disc and Core). The spray nozzle was positioned approximately 15 centimeters from the insects, and 0.5 milliliters of extract solution was evenly distributed. The experiment followed a completely randomized design (CRD) with three replications, using 20 stable flies per concentration. The experimental treatments were as follows:

Treatment 1: Distilled water (control)
Treatment 2: 35% cypermethrin (w/v) (used at a rate of 10 milliliters per 20 liters of water)
Treatment 3: 1% tobacco extract (w/v)
Treatment 4: 3% tobacco extract (w/v)
Treatment 5: 5% tobacco extract (w/v)
Treatment 6: 10% tobacco extract (w/v)
Treatment 7: 20% tobacco extract (w/v)

Data on stable fly mortality was recorded at specific time intervals of 1, 3, 6, 12, 24, 48, and 72 hours post-treatment. Flies were considered dead when they showed no movement after gentle prodding with a fine brush. Mortality rates were calculated and the mortality rate data was statistically analyzed at a 95% confidence level, with differences compared using Duncan's New Multiple Range Test (DMRT), and LC_{50} values determined by Probit analysis.

2.3 Efficacy Study of Tobacco Extracts in Controlling Stable Flies in Beef Cattle in Field Conditions

The study was conducted at a small-scale farm located in Moo 2, Non Mak Mun Subdistrict, Khok Sung District, Sa Kaeo Province. Field trials were conducted under average meteorological conditions of 26°C temperature, 60-65% relative humidity, no rainfall, with southeast winds at 10-30 km/h. Twelve native-Brahman crossbred beef cattle were used, divided into three groups of four animals each. Cattle were randomly allocated to treatments using a random number table, with each animal assigned a number from 1 to 12 and randomly distributed to ensure equal representation across treatments. The animals were kept in individual pens. The experiment followed a completely randomized design (CRD) with three treatments as follows:

Treatment 1: Distilled water (control)

Treatment 2: 35% cypermethrin (w/v) (used at a rate of 10 milliliters per 20 liters of water)

Treatment 3: Tobacco extract that demonstrated the best mortality effect on stable flies in laboratory tests

All three treatments were applied by direct spraying on the pen floor and the cattle using a high-pressure water sprayer equipped with a hollow cone nozzle (Disc and Core).

The stable fly population on the front legs of the cattle was counted after spraying all three treatments at 24, 48, 72, 96, and 120 hours, following the method of Mullens & Peterson [14]. An expert counted the flies visually on the front legs from below the upper leg joint downward, with a survey time of 3 minutes per animal. Data on the stable fly population per individual cow were recorded.

Additionally, fly-repelling behaviors of the cattle were studied after spraying all three treatments at 24, 48, 72, 96, and 120 hours. The frequency of four repelling behaviors was recorded: Tail flicking, skin twitching, Foot stamping, and head swinging, for 2 minutes per animal, following the method of Mullens et al. [15]. The frequency of all four repelling behaviors was recorded.

The collected data were statistically analyzed using analysis of variance in a completely randomized experimental design, and the differences between means were analyzed using Duncan's New Multiple Range Test at a 95% confidence level ($P<0.05$).

3. Results and Discussion

3.1 Determination of nicotine concentration in tobacco extract using different fermentation times

The HPLC method for nicotine quantification was validated with appropriate analytical performance. The calibration curve showed strong linearity ($R^2 = 0.9991$) across the concentration range of 77.2-619.6 μg/ml. Method precision was assessed through replicate analyses, demonstrating excellent repeatability with relative standard deviation (RSD) values ranging from 0.21% to 0.63% (average 0.44%) for all fermentation treatments, which is well within acceptable limits (<2.0%). The extraction yield of tobacco extract varied significantly with fermentation time. The highest extraction yield was obtained after 48 hours of fermentation (12.4 ± 0.3%), followed by 72 hours (11.8±0.2%). More extended fermentation periods showed decreased yields, with 96 hours yielding 10.2 ± 0.4% and 120 hours yielding 9.6±0.3% (Table 1). The study found that the fermentation time significantly affected the nicotine content in tobacco extracts ($P<0.001$). Fermentation for 48 hours yielded the highest nicotine content at 46.71 ± 0.22 μg/mg, which was significantly different compared to other fermentation periods. This was followed by fermentation for 72 hours, which produced a nicotine content of 42.76 ± 0.09 μg/mg. More extended fermentation periods resulted in significantly decreased nicotine content, with fermentation for 96 and 120 hours yielding only 25.07 ± 0.16 and 21.44 ± 0.10 μg/mg, respectively (Table 1).

These results demonstrate that the nicotine content in tobacco leaf solution tends to decrease as fermentation time increases, especially after 72 hours, when the nicotine content decreases significantly. The decrease in both extraction yield and nicotine content with extended fermentation time may be attributed to

the degradation of nicotine and other extractable compounds during prolonged exposure to ethanol and potential oxidation processes. Li et al. [16] studied tobacco fermentation at 60, 90, 120, 150, and 180 hours using 20 cigarettes with 100 ml of hexane solution. They found that the highest nicotine extract content was 115 µg/mL at 60 hours, with a decreasing trend to 106.55 µg/mL at 180 hours. Similarly, Tassew & Chandravanshi [17] found a nicotine content of 4.2% when extracting tobacco leaves fermented with acid-base for 30 hours. Furthermore, fermentation of tobacco with methanol and ethanol yielded 17.91-19.55% content at fermentation periods of 48-60 hours [18]. Therefore, the 48-hour fermentation period was considered appropriate for further insect testing.

Table 1. Extraction yield and nicotine content from fermentation at 48, 72, 96, and 120 hours.

Fermentation time (hours)	Extraction yield (%)	Nicotine content in tobacco solution (µg/mg)
48	12.4 ± 0.3^{a}	46.71 ± 0.22^{a}
72	11.8 ± 0.2^{b}	42.76 ± 0.09^{b}
96	10.2 ± 0.4^{c}	25.07 ± 0.16^{c}
120	9.6 ± 0.3^{d}	21.44 ± 0.10^{d}
P-value	<0.001	<0.001

[a-d] Means in the same column with different superscripts are significantly different (P<0.001).

3.2 Efficacy study of tobacco extracts in controlling stable flies in beef cattle in laboratory conditions

The study of the efficacy of various concentrations of tobacco extracts in controlling stable flies in beef cattle, when tested in laboratory conditions, showed that the mortality rates of stable flies differed with high statistical significance (P<0.001) across all testing intervals. Treatment 2 (35% cypermethrin), a synthetic chemical, provided the highest fly control efficacy with a mortality rate of 53.33% at 1 hour, increasing to 100% after 24 hours. For tobacco extracts, the efficacy in eliminating flies increased with concentration and exposure time. The 20% tobacco extract (Treatment 7) provided the highest efficacy among natural extracts, with a mortality rate of 41.66% at 1 hour, increasing to 98.33% at 24 hours, and 100% at 48 hours. This was followed by 10% tobacco extract (Treatment 6) and 5% tobacco extract (Treatment 5), both achieving 100% mortality at 72 hours. Meanwhile, 3% tobacco extract (Treatment 4) showed 95% mortality at 72 hours, and 1% tobacco extract (Treatment 3) demonstrated the lowest efficacy with only 70% mortality even after 72 hours. Treatment 1 (water), which served as the control, showed very low mortality throughout the experiment, with only 6.67% mortality at 72 hours, which was significantly different from all other treatments (Table 2).

Generally, the amount of nicotine extracted from tobacco leaves ranges between 2%-6% [19], which aligns with Tayoub et al. [20], who measured nicotine content in the dry weight of five different tobacco leaves using HPLC and LS-MS techniques, yielding approximately 3.3% to 6.7%. Djapic et al. [21] extracted nicotine from two types of tobacco leaves using the SC-CO_2 extraction technique, with nicotine extraction ratios to dry weight of raw materials equaling 2.33% and 2.99%, respectively.

From the study of stable fly mortality rates, the results demonstrated that tobacco extracts at concentrations of 5-20% have potential for controlling stable flies in beef cattle, especially at 20% concentration, which provided efficacy comparable to the synthetic chemical cypermethrin 35% as contact time increased. Progressive increases in mortality rates over time were observed across all tobacco extract treatments, as demonstrated in Table 2, where mortality percentages consistently increased from 1-hour to 72-hour exposure periods. For example, a nicotine concentration of 25.2 mg/L showed LC_{50} mortality of stable flies at 24 hours after testing, with the mortality rate increasing after just 1 hour. Additionally, the results indicated that nicotine efficacy improves with increased quantity and contact time. Therefore, insect mortality rates are influenced by both concentration and time, consistent with the toxicity of essential oils extracted from various plants such as tea tree oil (*Melaleuca alternifolia*), catnip (*Nepeta cataria*), and Indian borage (*Plectranthus amboinicus*). When tested through contact and vapor methods against stable flies at a quantity of 20 milligrams, these essential oils achieved 100% mortality within 19 minutes [22-24]. This aligns with Kanmani et al. [25], where nicotine extract was the main active ingredient in eliminating adult *Sitophilus oryzae*. After 24 hours of spraying, 100% mortality of adults was observed with an extract concentration of 5.00 mg/L. Nicotine extract showed the highest percentage of adult mortality at the lowest concentration, with LD_{50} and LD_{90} values of

1.62 and 2.85 mg/L, respectively. This trend remained consistent after 48 and 72 hours of exposure. It has been reported that increased active ingredients can kill more insects at higher concentrations and longer exposure times.

According to reports on the active ingredients of tobacco leaves against pest insects, nicotine is one of the alkaloids extracted from plants that acts rapidly on the nervous system to eliminate insects [26], causing severe tremors, seizures, followed by paralysis. Additionally, nicotine inhibits the functioning of the nervous system, causing an imbalance in neural function. Stimulation of the nervous system is one of the most important mechanisms of traditional insecticides such as organophosphates and carbamates [27].

This research also noted that besides the action of nicotine in eliminating stable flies, factors affecting nicotine extract include the method used to apply substances to contact the insects, which affects the amount of insecticide received, causing differences in efficacy. Insect mortality rates depend on whether they receive a single dose or continuous exposure over a period. Additionally, the distribution and particle size of substances are important factors affecting the amount absorbed by insects and the permeation rate of pesticides into the insects. Moreover, the efficacy of extracts varies according to the sex of the flies. Langai, Muthomi & Mbega [28] reported that male houseflies (*Musca domestica*) and green bottle flies (*Chrysomya megacephala*) are more susceptible to eucalyptol than females because they are typically smaller. However, our study did not evaluate the influence of sex on insecticide susceptibility.

Table 2. Efficacy of Tobacco Extracts in Controlling Stable Flies in Beef Cattle in Laboratory Conditions.

Treatment	Mortality Rate (%)						
	1 hour	**3 hours**	**6 hours**	**12 hours**	**24 hours**	**48 hours**	**72 hours**
Treatment 1	0.00^{a}	0.00^{a}	0.00^{a}	0.00^{a}	1.67^{a}	3.33^{a}	6.67^{a}
Treatment 2	53.33^{f}	70.00^{e}	90.00^{f}	95.0^{e}	100.00^{f}	100.00^{e}	100.00^{c}
Treatment 3	11.67^{b}	21.67^{b}	31.67^{b}	41.67^{b}	50.00^{b}	58.33^{b}	70.00^{b}
Treatment 4	16.67^{bc}	31.67^{b}	43.33^{c}	56.67^{c}	71.67^{c}	81.67^{c}	95.00^{c}
Treatment 5	25.00^{cd}	43.33^{c}	60.00^{d}	71.67^{d}	81.67^{d}	91.67^{d}	100.00^{c}
Treatment 6	1.67^{d}	55.00^{d}	66.67^{d}	78.33^{d}	90.00^{de}	95.00^{de}	100.00^{c}
Treatment 7	41.66^{e}	66.67^{e}	78.33^{e}	90.00^{e}	98.33^{ef}	100.00^{e}	100.00^{c}
P-value	<0.001	<0.001	<0.001	<0.001	<0.001	<0.001	<0.001

$^{a-f}$ Means in the same column with different superscripts are statistically significantly different.
Treatment 1: Distilled water (Control), Treatment 2: 35% Cypermethrin, Treatment 3: Tobacco extract 1% concentration, Treatment 4: Tobacco extract 3% concentration, Treatment 5: Tobacco extract 5% concentration, Treatment 6: Tobacco extract 10% concentration, Treatment 7: Tobacco extract 20% concentration

Furthermore, the LC_{50} of tobacco extract that can cause 50% mortality of stable flies within 12 hours is a concentration of 3% or higher. Treatment 4 using 3% extract concentration showed a mortality rate of 56.67%, exceeding the specified 50% threshold. LC_{50} and LC_{90} values decreased significantly with increasing exposure time, from 40.56% (95% CI: 21.51-76.49%) at 1 hour to 0.40% (95% CI: 0.04-4.26%) at 72 hours. Similarly, LC_{90} values showed a dramatic reduction from 1850.27% (95% CI: 362.27-9450.02%) at 1 hour to 1.69% (95% CI: 0.46-6.16%) at 72 hours. The R^2 values ranged from 0.8166 to 0.9862, indicating strong dose-response relationships across all time intervals. At 12 hours, the LC_{50} was 1.73% (95% CI: 1.15-2.60%) and the LC_{90} was 23.17% (95% CI: 13.89-38.66%), confirming that the 3% concentration selected for field studies provides adequate control efficacy (Table 3). Although higher concentrations demonstrated better efficacy in eliminating stable flies, they may result in higher production costs or increased environmental risks. Therefore, the research team selected the 3% extract concentration (Treatment 4), which can control stable flies according to the specified criteria, for further study of nicotine efficacy in controlling stable flies in field conditions.

Table 3. Lethal Concentration (LC_{50} and LC_{90}) of Tobacco Extract (Treatment 4: 3% concentration) Against Stable Flies with 95% Confidence Intervals.

Time (hours)	LC_{50} (%)	LC_{50} 95% CI	LC_{90} (%)	LC_{90} 95% CI	R^2
1	40.56	21.51 - 76.49	1850.27	362.27 - 9450.02	0.9787
3	7.55	5.93 - 9.60	164.56	74.39 - 364.03	0.9862
6	3.37	2.45 - 4.66	67.48	29.56 - 154.02	0.9750
12	1.73	1.15 - 2.60	23.17	13.89 - 38.66	0.9779
24	1.18	0.63 - 2.22	7.75	5.20 - 11.54	0.9637
48	0.70	0.34 - 1.44	5.12	3.55 - 7.39	0.9833
72	0.40	0.04 - 4.26	1.69	0.46 - 6.16	0.8166

3.3 Efficacy Study of Tobacco Extracts in Controlling Stable Flies in Beef Cattle in Field Conditions

Field trials were conducted under average meteorological conditions of 26°C temperature, 60-65% relative humidity, no rainfall, with southeast winds at 10-30 km/h. No adverse effects were observed in any cattle during the entire experimental period, including skin irritation, behavioral changes, or alterations in feeding patterns following application of either cypermethrin or tobacco extract treatments. The results of the efficacy study of tobacco extracts in controlling stable flies in field conditions showed that the number of stable flies on the front legs of beef cattle differed with high statistical significance ($P<0.001$) between experimental treatments across all counting periods. Cypermethrin 35% (Treatment 2) showed the highest efficacy in controlling stable flies throughout the experimental period, with the lowest number of flies observed (5.75-8.00 flies/cattle). This was followed by 3% tobacco extract (Treatment 3), which showed 7.75-11.00 flies/cattle, while the control treatment (Treatment 1) had the highest number of flies (10.50-13.50 flies/cattle) (Table 3). It was observed that the efficacy of both substances tended to decrease over time, especially the tobacco extract, where the number of flies increased from 7.75 at 24 hours to 8.00 at 48 hours, 8.75 at 72 hours, 9.75 at 96 hours, and 11.00 at 120 hours, becoming increasingly similar to the control group (13.50 flies). This indicates that the residual effect of tobacco extract has a shorter duration than cypermethrin, likely because nicotine in tobacco is a natural substance that degrades faster than synthetic chemicals (Table 4). However, safety considerations must be addressed when using tobacco extracts containing nicotine. Neonicotinoids are a group of insecticides composed of seven types of insecticides, including acetamiprid, clothianidin, dinotefuran, imidacloprid, nitenpyram/nithiazine, thiacloprid, and thiamethoxam, which have been developed as safer alternatives compared to other insecticide groups such as carbamates, organochlorines, and pyrethroids commonly used worldwide. Studies by Leena et al. [29] reported that acetamiprid and imidacloprid cause reproductive toxicity, genotoxicity, neurotoxicity, and hepatotoxicity in newborn mice, but in adult mammals, toxicity levels are low. The effects of imidacloprid on the nervous system of adult mice require doses of 150 and 300 mg/kg body weight [30]. Regarding effects on humans, studies of impacts on farmers in Greece by extracting genomic DNA from blood samples of farmers and measuring levels of 8-hydroxydeoxy-guanosine (8-OHdG) found that farmers who used neonicotinoid compounds for extended periods showed increased levels of imidacloprid in their blood samples [31]. Furthermore, Loser et al. [32] studied certain metabolites of imidacloprid in nicotine-like forms, studying metabolites desnitro-imidacloprid and imidacloprid-olefin, and found low-level effects on human nervous systems. Farm workers should use appropriate personal protective equipment when handling tobacco extracts, including gloves, masks, and protective clothing to minimize skin contact and inhalation exposure. Regarding withdrawal periods for treated cattle, while nicotine is a naturally occurring compound that degrades relatively quickly in biological systems, further research is needed to establish appropriate withdrawal periods for meat and milk from cattle treated with tobacco extracts. The rapid degradation of nicotine compared to synthetic insecticides suggests that withdrawal periods may be shorter than those required for conventional chemical treatments. Still, comprehensive residue studies must be conducted to ensure food safety and comply with regulatory requirements. The establishment of maximum residue limits (MRLs) for nicotine in beef and dairy products would be essential for the commercial application of tobacco extract treatments. From an organic farming perspective, nicotine cannot be used in organic crop production because nicotine contains compounds that are classified as insecticides. Although nicotine is extracted from tobacco leaves, which are plants, organic farming certification has restrictions regarding

chemical residues in cultivated crops or in insect control applications. This limitation significantly restricts the use of tobacco extracts in certified organic livestock operations, despite their botanical origin [33]. Comparing the efficacy at 120 hours (5 days) after spraying, cypermethrin 35% could still reduce the number of flies by approximately 40.7% (compared to the control group), while 3% tobacco extract could reduce the number of flies by only 18.5%. This information is practically important for farmers in planning the frequency of spraying, especially when using tobacco extract, which may require more frequent application than cypermethrin. From an economic perspective, preliminary cost analysis reveals important considerations for practical implementation. Commercial cypermethrin 35% costs approximately 80 baht per 100 mL, while tobacco extract can be produced locally from waste tobacco products at significantly lower material costs. Although tobacco extract requires more frequent application due to its shorter residual effect, using agricultural waste tobacco materials offers substantial economic benefits, particularly for small-scale farmers who can produce extracts on-farm. The economic viability of tobacco extract becomes more attractive when considering the dual benefits of waste utilization and reduced dependency on imported synthetic chemicals, despite the increased labor costs associated with more frequent applications. However, a comprehensive economic analysis should include production costs, application frequency, labor requirements, and potential yield benefits from improved animal welfare to provide farmers with complete cost-benefit information for decision-making.

Furthermore, when comparing this study's results with research by Mullens et al. [15], the number of stable flies (*S. calcitrans* L.) in this study was considerably higher. The control group had an average of 10.50-13.50 flies per front leg, while Mullens et al. [15] reported a maximum of only 3.0-3.5 flies per leg (in late May). This difference may be due to geographical and climatic factors in Thailand, which have higher humidity and temperature (average 26°C), conditions conducive to fly development. This aligns with research by Mullens & Peterson [14], which indicated that March rainfall strongly correlates with stable fly density ($R^2 = 0.726$), as moisture promotes egg-laying and larval development. Additionally, the semi-confined farming system in the study area may have provided more breeding sites for flies compared to more strictly managed farms.

Table 4. Average number of stable flies on the front legs of cattle after spraying test substances.

Treatment	Hours after spraying				
	24	**48**	**72**	**96**	**120**
Treatment 1: Distilled water (control)	10.50[a]	11.00[a]	13.00[a]	13.00[a]	13.50[a]
Treatment 2: 35% Cypermethrin	6.00[c]	5.75[c]	6.50[c]	8.00[c]	8.00[c]
Treatment 3: 3% Tobacco extract	7.75[b]	8.00[b]	8.75[b]	9.75[b]	11.00[b]
P-value	<0.001	<0.001	<0.001	<0.001	<0.001

[a-c] Means in the same column with different superscripts are statistically significantly different.

Comparison with other botanical insecticides reveals the diversity of plant-based pest control options. Research has been conducted on the efficacy of various plant extracts in controlling Stomoxys calcitrans through contact methods, demonstrating the diversity of plant resources with potential for development as natural insect control agents. For tobacco leaf extract use, studies found that nicotine concentrations of 25.2 mg/L could achieve LC_{50} mortality in stable flies within 24 hours after testing. Comparative efficacy studies of various plant extracts found that rosalva (from rose flowers) had the highest efficacy with LD_{50} values of 13.10 μg/cm² and LC_{90} values of 18.54 μg/cm², followed by geranyl acetone (from cardamom, orange, and petitgrain essential oils) with LD_{50} values of 25.20 μg/cm² and LC_{90} values of 34.97 μg/cm². Citronellol (from eucalyptus) had LD_{50} values of 35.69 μg/cm² and LC_{90} values of 50.10 μg/cm². Black pepper (*Piper nigrum* L.) extract had the lowest efficacy in this group with LD_{50} values of 78.37 μg/cm² and LC_{90} values of 55.62 μg/cm² when tested with 24-hour exposure periods [34-36]. These efficacy differences reflect the diversity of active compounds in each plant species, which is valuable information for selecting and developing the most effective natural insect control agents for stable fly management in livestock systems.

Additionally, recent studies have demonstrated the effectiveness of botanical insecticides in livestock systems. Plant extracts have been used to control livestock insects such as flies, ticks, and mites. The use of bioactive compounds extracted from plants has been studied as insecticides in livestock systems to be effective against insect populations resistant to drugs and have relatively low environmental impacts [37]. The biodiversity of plant extracts shows toxicity to insects in livestock systems, particularly regarding modes of

action through contact or ingestion, with different mechanisms of action for insects in the order Diptera [38]. The efficacy of essential oils from lettuce (*Lactuca sativa*), chamomile (*Matricaria chamomilla*), anise (*Pimpinella anisum*), and rosemary (*Rosmarinus officinalis*) against Lucilia sericata has been evaluated, showing LD_{50} values of 0.57, 0.85, 2.74, and 6.77%, respectively [39].

The potential for resistance development in stable fly populations is an important consideration for long-term management strategies. While botanical insecticides like tobacco extract may have multiple modes of action due to their complex chemical composition, repeated use of any single control method can lead to selection pressure and potential resistance development. The diverse alkaloid profile in tobacco extracts, including nicotine, nornicotine, and anabasine, may provide some protection against rapid resistance development compared to synthetic insecticides with single active ingredients. However, monitoring programs should be established to detect early signs of reduced efficacy in treated fly populations. Rotation between different botanical extracts and integration with other control methods would help delay resistance development and maintain the effectiveness of these natural alternatives.

Regarding fly-repelling behaviors, tail flicking and skin twitching showed highly significant differences between treatments ($P<0.001$) across all time periods. Cattle in the cypermethrin 35% group exhibited these behaviors least frequently, followed by the tobacco extract group, while the control group showed these behaviors most frequently. For head swinging behavior, significant differences were found across all time periods, with cattle in the cypermethrin 35% group showing this behavior least often. No statistical differences were found between treatments in foot stamping behavior ($P>0.05$). However, at 96 and 120 hours after spraying, observational trends indicated declining efficacy of tobacco extract, with fly counts increasing from 8.75 flies/cattle at 72 hours to 9.75 flies/cattle at 96 hours and 11.00 flies/cattle at 120 hours (Table 4). Correspondingly, fly-repelling behaviors showed increasing trends, with tail flicking behavior rising from 11.00 times at 72 hours to 11.25 times at 96 hours and 11.75 times at 120 hours, though tobacco extract treatment remained significantly better than the control treatment at all time points ($P<0.001$) (Table 5).

Considering trends over time, the frequency of fly-repelling behaviors in both test substance groups showed a slight increasing trend, corresponding with the increasing number of flies observed on the front legs of cattle after spraying. This demonstrates that the efficacy of the test substances decreased over time. The results of fly-repelling behavior in this research align with Mullens et al. [15], who found that tail flicking and skin twitching occurred more frequently than foot stamping and head swinging, which is consistent with natural cattle behavior. However, Mullens et al. [15] found that foot stamping was most effective in repelling flies, with cattle that stamped more frequently tending to have fewer flies. An interesting observation in Mullens et al. [15] was the adaptation of cattle to pain from fly bites (habituation to pain), with the ratio of foot stamping and head swinging to fly numbers decreasing significantly over time. This may explain why this study found no statistical differences in foot-stamping behavior between experimental groups, possibly because cattle on the farm had already adapted to the disturbance of numerous flies. Additionally, Mullens et al. [15] found that older cattle tended to have more flies and stamped less frequently than younger cattle.

This temporal reduction in efficacy may be influenced not only by the degradation of active compounds but also by environmental factors, such as ambient temperature and relative humidity, which are known to affect stable fly activity and cattle response [40]. These behaviors are primary reflexive responses to biting flies and tend to increase with higher fly pressure. In support of this, Rencinova et al. [41] noted that fly activity increased in association with dry, hot conditions, resulting in more pronounced behavioral responses such as tail flicking and skin twitching in dairy cattle. Furthermore, ElAshmawy et al. [40] observed that environmental conditions and management factors, such as the presence of trees around cattle pens and specific feed components in the TMR, influenced stable fly activity, which in turn may alter the expression of fly-repelling behaviors like foot stamping. Taken together, the findings from this study and those of Gerry et al. [42] highlight the complexity of behavioral responses to stable flies, which are modulated not only by the efficacy of repellent substances but also by broader environmental and management contexts that shape cattle behavior over time.

Table 5. Average frequency of fly-repelling behaviors after spraying test substances.

Treatment	Hours after spraying				
	24	48	72	96	120
Tail flicking					
Treatment 1: Distilled water (control)	14.50[a]	14.50[a]	14.50[a]	14.50[a]	15.00[a]
Treatment 2: 35% Cypermethrin	8.00[c]	8.00[c]	7.75[c]	8.50[c]	9.25[c]
Treatment 3: 3% Tobacco extract	11.00[b]	10.50[b]	11.00[b]	11.25[b]	11.75[b]
P-value	<0.001	<0.001	<0.001	<0.001	<0.001
Skin twitching					
Treatment 1: Distilled water (control)	11.50[a]	11.50[a]	11.50[a]	11.50[a]	12.00[a]
Treatment 2: 35% Cypermethrin	7.50[b]	7.50[b]	8.00[b]	8.00[b]	8.50[c]
Treatment 3: 3% Tobacco extract	9.00[b]	8.75[b]	9.25[b]	9.25[b]	10.00[b]
P-value	<0.001	<0.001	0.003	0.001	<0.001
Foot stamping					
Treatment 1: Distilled water (control)	2.50	2.50	2.50	2.00	2.50
Treatment 2: 35% Cypermethrin	1.25	1.50	1.50	1.50	1.50
Treatment 3: 3% Tobacco extract	1.75	2.25	2.50	2.25	2.50
P-value	0.241	0.73	0.57	0.532	0.57
Head swinging					
Treatment 1: Distilled water (control)	5.00[b]	5.00[a]	4.75[a]	5.00[a]	5.50[a]
Treatment 2: 35% Cypermethrin	2.00[b]	2.50[b]	2.50[b]	2.50[b]	2.50[c]
Treatment 3: 3% Tobacco extract	3.50[ab]	2.75[b]	4.00[a]	4.00[a]	4.50[b]
P-value	0.007	0.035	0.009	0.003	<0.001

[a-c] Means in the same column with different superscripts are statistically significantly different.

The integration of tobacco extract with other IPM strategies represents the most sustainable approach to stable fly management. Integrated Pest Management (IPM) is a practical approach for controlling *S. calcitrans* by combining biological, physical, and chemical control methods. However, managing this insect species is challenging due to its behavioral characteristics of intermittent blood feeding rather than permanent host residence. When considering the effectiveness of individual control methods, no single method can provide complete control results. Therefore, using multiple methods in combination is essential.

Studies by Gonzalez et al. [43] during 2022-2023 on stable fly management in horses using natural enemies combined with herbal plant extracts found that insect populations tended to decrease and horse health improved. However, the study could not definitively conclude that the population decline was solely due to IPM implementation, as other factors might affect changes in this livestock fly population, particularly climatic factors including temperature, rainfall, and sunlight that differed between study periods. This data aligns with research by Taylor et al. [44], which found that climate change affects stable fly flight behavior, reproduction, and distribution, with population density varying seasonally due to temperature and rainfall changes. Therefore, evaluating IPM effectiveness must consider the influence of these environmental factors concurrently.

4. Conclusions

Tobacco leaf fermentation at 48 hours yielded the highest nicotine content, with a significant decline in nicotine content as fermentation time increased. Laboratory test results showed that the efficacy of tobacco extract in eliminating stable flies correlated with concentration and exposure time. At 20% concentration, the extract showed maximum effectiveness (100% mortality at 48 hours), while the 3% concentration extract caused 50% fly mortality within 12 hours (LC_{50}) and was therefore selected for field testing. Field experiment results confirmed that 3% tobacco extract significantly reduced stable fly numbers and decreased fly-repelling behaviors in cattle compared to the control group. Nicotine extract from tobacco thus represents a potential alternative for controlling stable flies, especially in environmentally friendly production systems.

5. Acknowledgements

Author Contributions: Conceptualization, J.N. and P.S.; methodology, J.N. and P.S.; formal analysis, P.S.; investigation, J.N.; writing—original draft preparation, J.N. and P.S.; writing—review and editing, J.N. and P.S.

Funding: This project is funded by Valaya Alongkorn Rajabhat University under the Royal Patronage Pathum Thani Province (Contract Number ๖๑001/2567)

Conflicts of Interest: The authors declare no conflict of interest.

References

[1] Rochon, K.; Hogsette, J.A.; Kaufman, P.E.; Olafson, P.U.; Swiger, S.L.; Taylor, D.B. Stable fly (Diptera: Muscidae)-biology, management, and research needs. *Journal of Integrated Pest Management.* **2021**, *12*(1), 38, 1-23. https://doi.org/10.1093/jipm/pmab029

[2] Baldacchino, F.; Muenworn, V.; Desquesnes, M.; Desoli, F.; Charoenviriyaphap, T.; Duvallet, G. Transmission of pathogens by Stomoxys flies (Diptera, Muscidae): A review. *Parasite.* **2013**, *20*(26),1-13. https://doi.org/10.1051/parasite/2013026

[3] Arjkumpa, O.; Suwannaboon, M.; Boonrod, M.; Punyawan, I.; Liangchaisiri, S.; Laobannue, P.; Lapchareonwong, C.; Sansri, C.; Kuatako, N.; Panyasomboonying, P. The first lumpy skin disease outbreak in Thailand (2021): Epidemiological features and spatio-temporal analysis. *Frontiers in Veterinary Science.* **2022**, *8*, 1-10. https://doi.org/10.3389/fvets.2021.799065

[4] Saetiew, N.; Stich, R.W.; Jittapalapong, S. Biodiversity of Blood Sucking Flies associated with the Prevalence of *Anaplasma marginale* infection in Dairy Farms in Ratchaburi Province. *Journal of Mahanakorn Veterinary Medicine.* **2018**, *13*(2), 171-184.

[5] Ahmad, M.F.; Ahmad, F.A.; Alsayegh, A.A.; Zeyaullah, M.; AlShahrani, A.M.; Muzammil, K.; Saati, A.A.; Wahab, S.; Elbendary, E.Y.; Kambal, N.; Abdelrahman, M.H.; Hussain, S. Pesticides impacts on human health and the environment with their mechanisms of action and possible countermeasures. *Heliyon*. **2024,** *10*, e29128. https://doi.org/10.1016/j.heliyon.2024.e29128

[6] Nascimento, V.F.; Auad, A.M.; Resende, T.T.; Visconde, A.J.M.; Dias, M.L. Insecticidal Activity of Aqueous Extracts of Plant Origin on *Mahanarva spectabilis* (Distant, 1909) (Hemiptera: Cercopidae). *Agronomy*. **2022,** *12*(947), 1-13. https://doi.org/10.3390/agronomy12040947

[7] Buszewski, B.; Bukowska, M.; Ligor, M.; Baranowska, I.S. A holistic study of neonicotinoids neuroactive Insecticides-properties, applications, occurrence, and analysis. *Environmental Science and Pollution Research.* **2019**, 26, 34723-34740. https://doi.org/10.1007/s11356-019-06114-w

[8] Phasuk, J.; Prabaripai, A; Chareonviriyaphap, T. A comparison of attractants for sampling *Stomoxys calcitrans* L. (Diptera: Muscidae) on dairy farms in Saraburi Province, Thailand. *Journal of Economic Entomology.* **2016**, *109*(2), 942-946. https://doi.org/10.1093/jee/tov334

[9] Jirapattharasate, C.; Changbunjong, T.; Sedwisai, P.; Weluwanarak, T. Molecular detection of piro-plasms in haematophagus flies in the Nakhon Pathom and Kanchanaburi Provinces, Thailand. *Veterinary Integrative Sciences.* **2018**, *16*(2), 123-133.

[10] Adnan, M.M.; Ahmad, A.G.; Omari, W.O. A single-step extraction method for the determination of nicotine and cotinine in Jordanian smokers' blood and urine samples by RP-HPLC and GC–MS. *Journal of Chromatographic Science*. **2009**, *47*, 170-177. https://doi.org/10.1093/chromsci/47.2.170

[11] Mihranyan, A.; Andersson, S.B.; Ek, R. Sorption of nicotine to cellulose powders. *European Journal of Pharmaceutical Sciences.* **2004**, *22*, 279-286. https://doi.org/10.1016/j.ejps.2004.03.012

[12] Bailey, D.L.; Whitfield, T.L.; Smittle, B.J. Flight and dispersal of the stable fly. *Journal of Economic Entomology.* **1975**, *66*(2), 410-411. https://doi.org/10.1093/jee/66.2.410

[13] Puripattanavong, J.; Songkram, C.; Lomlim, L.; Amnuaikit, T. Development of concentrated emul-sion containing Nicotiana tabacum extract for use as pesticide. *Journal of Applied Pharmaceutical Science.* **2013**, *3*(11), 16-21.

[14] Mullens, B.A.; Peterson, N.G. Relationship between rainfall and stable fly (Diptera: Muscidae) abundance on california dairies. *Journal of Medical Entomology*. **2005**, *42*(4), 705-708. https://doi.org/10.1603/0022-2585(2005)042[0705:RBRASF]2.0.CO;2

[15] Mullens, B.A.; Lii, K.S.; Mao, Y.; Meyer, J.A.; Peterson, N.G.; Szijj, C.E. Behavioural responses of dairy cattle to the stable fly, *Stomoxys calcitrans*, in an open field environment. *Medical and Veterinary Entomology*. **2006**, *20*(1), 122-137. https://doi.org/10.1111/j.1365-2915.2006.00608.x

[16] Li, L.; Jing, W.; Yuyang, D.; Juan, Y.; Yue, Y.; Yi, S.; Guoce, L.; Yonghong, T.; Dean, L. Direct extraction and determination of free nicotine in cigarette smoke. *Journal Analytical Methods in Chemistry*. **2024**, 1-13. https://doi.org/10.1155/2024/9273705

[17] Tassew, Z.; Chandravanshi, B.S. Levels of nicotine in Ethiopian tobacco leaves. *Springer Plus*. **2015**, 4, 649-654. https://doi.org/10.1186/s40064-015-1448-y

[18] Saengwan, W.; Muenkhwa, C.; Teweswarakul, J.; Khomkong, S.; Phonswai, A.; Khunlert, P.; Tongnak, N.; Klangboonkrong, A.; Punprakhon, A.; Bannakarn, I. Efficiency of Tobacco Solution on Controlling *Scirtothrips Dosalis* Hood. Department of Agriculture, Ministry of Agriculture and Cooperatives: Bangkok, Thailand, **2016.**

[19] Zheng, F.; Xie, Q.; Ren, Q.; Kong, J. Extraction and purification of nicotine from tobacco rhizomes by supercritical CO_2. *Molecules*. **2024**, *29*(5), 1147-1157. https://doi.org/10.3390/molecules29051147

[20] Tayoub, G.; Sulaiman, H.; Alorfi, M. Determination of nicotine levels in the leaves of some Nicotiana tabacum varieties cultivated in Syria. *Herba Polonica*. **2015**, 61, 23-30. https://doi.org/10.1515/hepo-2015-0028

[21] Djapic, N.; Supercritical carbon dioxide extraction of nicotiana tabacum leaves: Optimization of extraction yield and nicotine content. *Molecules*. **2022**, *27*(23), 8328-8329. https://doi.org/10.3390/molecules27238328

[22] Dillmann, J.B.; Cossetin, L.F.; de Giacometi, M.; Oliveira, D.; de Matos, A.F.I.M.; Avrella, P.D.; Garlet, Q.I.; Heinzmann, B.M.; Monteiro, S.G. Adulticidal activity of *Melaleuca alternifolia* (Myrtales: Myrtaceae) essential oil with high 1,8-Cineole content against stable flies (Diptera: Muscidae). *Journal of Economic Entomology*. **2020**, *113*, 1810-1815. https://doi.org/10.1093/jee/toaa117

[23] Leesombun, A.; Sungpradit, S.; Boonmasawai, S.; Weluwanarak, T.; Klinsrithong, S.; Ruangsittichai, J.; Ampawong, S.; Mas-meatathip, R.; Changbunjong, T. Insecticidal activity of *Plectranthus amboinicus* essential oil against the stable Fly *Stomoxys calcitrans* L. (Diptera: Muscidae) and the horse fly *Tabanus megalops* (Diptera: Tabanidae). *Insects*. **2022**, *13*(3), 255-269. https://doi.org/10.3390/insects13030255

[24] Zhu, J.J.; Li, A.Y.; Pritchard, S.; Tangtrakulwanich, K.; Baxendale, F.P.; Brewer, G. Contact and fumigant toxicity of a botanical-based feeding deterrent of the stable fly, *Stomoxys calcitrans* L. (Diptera: Muscidae). *Journal of Agricultural and Food Chemistry*. **2011**, *59*, 10394-10400. https://doi.org/10.1021/jf2016122

[25] Kanmani, S.; Kumar, L.; Raveen, R.; Tennyson, S.; Arivoli, S.; Jayakumar, M. Toxicity of tobacco Nicotiana *tabacum Linnaeus* (Solanaceae) leaf extracts to the rice weevil *Sitophilus oryzae* Linnaeus 1763 (Coleoptera: Curculionidae). *The Journal of Basic and Applied Zoology*. **2021**, *82*(10), 1-12. https://doi.org/10.1186/s41936-021-00207-0

[26] Onuminya, T.O.; Agboola, O.O., Ezeribe, S.R.; Insecticidal evaluation of some botanical powders as stored maize grain protectants against *Sitophilus zeamais* (Motschulsky) (Coleoptera: Curculionidae): A concern for postharvest loss. *Annals of West University of Timisoara, series of Biology*. **2018**, *21*(2), 157-164.

[27] Chowanski, S.; Adamski, Z.; Marciniak, P.; Rosinski, G.; Buyukguzel, E.; Buyukguzel, K.; Bufo, S. A review of bioinsecticidal activity of Solanaceae alkaloids. *Toxins.* **2016**, *8*(60), 1-28. https://doi.org/10.3390/toxins8030060

[28] Langai, G.M.W.; Muthomi, J.W.; Mbega, E.R. Phytochemical activity and role of botanical pesticides in pest management for sustainable agricultural crop production. *Scientific African*. **2020**, *7*(3), e00239. https://doi.org/10.1016/j.sciaf.2019.e00239

[29] Leena, K.; Payal, C.; Charu, S.; Pradeep, B.; Nidhi, G. Behavioral effects of adult male mice induced by low-level acetamiprid, imidacloprid, and nicotine exposure in early-life. *Frontiers in Neuroscience*. **2023,** 1-13.

[30] Lonare, M.K.; Kumar, M.; More, A.S.; Telang, A.G. Toxicological investigation of single oral dose adminis-tration of imidacloprid in male Wistar rats. *Toxicology International*. **2020,** 26, 8-14.

[31] Koureas, M.; Tsezou, A.; Tsakalof, A.; Orfanidou, T.; Hadjichristodoulou, C. Increased levels of oxidative DNA damage in pesticide sprayers in Thessaly Region (Greece). Implications of pesticide exposure. *Science of The Total Environment.* **2014,** *496*, 358-364. https://doi.org/10.1016/j.scitotenv.2014.07.062

[32] Loser, D.; Grillberger, K.; Hinojosa, M.G.; Blum, J.; Haufe, Y.; Danker, T.; Johansson, Y.; Moller, C.; Nicke, A.; Bennekou, S.H.; Gardner, I.; Bauch, C.; Walker, P.; Forsby, A.; Ecker, G.F.; Kraushaar, U.; Leist, M. Acute effects of the imidacloprid metabolite desnitro-imidacloprid on human nACh receptors relevant for neuronal signaling. *Archives of Toxicology*. **2021,** *95*(12), 3695-3716. https://doi.org /10.1007/s00204-021-03168-z

[33] Hirokatsu, S.; Yusuke, F.; Takahiro, S.; Satoshi, K.; Jun, K.; Kentaro, T. Toxic effects associated with neonicotinoid exposure on non-target organisms: A review. *Toxicology International*. **2023,** *30*(1), 41-50. https://doi.org/10.18311/ti/2023/v30i1/30246

[34] Weluwanarak, T.; Changbunjong, T.; Leesombun, A.; Boonmasawai, S.; Sungpradit, S. Effects of *Piper nigrum* L. fruit essential oil toxicity against stable fly (Diptera: Muscidae). *Plants.* **2023,** *12*(1043), 1-13. https://doi.org/10.3390/plants12051043

[35] Changbunjong, T.; Boonmasawai, S.; Sungpradit, S.; Weluwanarak, T.; Leesombun, A. Contact and fumigant activities of *Citrus aurantium* essential oil against the stable fly *Stomoxys calcitrans* (Diptera: Muscidae). *Plants.* **2022,** *11*, 1122. https://doi.org/10.3390/plants11091122

[36] Zhu, J.J.; Li, A.Y.; Pritchard, S.; Tangtrakulwanich, K.; Baxendale, F.P.; Brewer, G. Contact and fumigant toxicity of a botanical-based feeding deterrent of the stable fly, *Stomoxys calcitrans* (Diptera: Muscidae). *Journal of Agricultural and Food Chemistry*. **2011,** 59, 10394-10400. https://doi.org/10.1021/jf2016122

[37] Divekar, P. Botanical pesticides: An eco-friendly approach for management of insect pests. Acta Scientific *Agriculture.* **2023,** *7*(2), 75-81. https://doi.org/10.31080/ASAG.2023.07.1236

[38] Callander, J.T.; James, P.J. Insecticidal and repellent effects of tea tree (*Melaleuca alternifolia*) oil against *Lucilia cuprina*. *Vet Parasitol*. **2012,** *184*(2-4), 271-278. https://doi.org/10.1016/j.vetpar.2011.08.017

[39] Molento, M.; Chaaban, A.; Gomes, E.; Santos, V.; Maurer, J.B.B. Plant extracts used for the control of endo and ectoparasites of livestock: A review of the last 13 years of science. *Archives of Veterinary Science*. **2020,** *25*(4), 1-27. https://doi.org/10.5380/avs.v25i4.72145

[40] ElAshmawy, W.R.; Abdelfattah, E.M.; Williams, D.R.; Gerry, A.C.; Rossow, H.A.; Lehenbauer, T.W.; Aly, S.S. Stable fly activity is associated with dairy management practices and seasonal weather conditions. *PLoS ONE*. **2021,** 1-18. https://doi.org/10.1371/journal.pone.0253946

[41] Rencinova, V.; Voslarova, E.; Bedanova, I.; Vecerek, V. Pest flies on dairy farms affect behaviour and welfare of dairy cows during summer season. *Acta Veterinaria Brno*. **2021,** 90, 255-262. https://doi.org /10.2754/avb202190030255

[42] Gerry, A.C.; Higginbotham, G.E.; Periera, L.N.; Lam, A.; Shelton, C.R. Evaluation of surveillance methods for monitoring house fly abundance and activity on large commercial dairy operations. *Journal of Economic Entomology*. **2011,** *104*, 1093-1102. https://doi.org/10.1603/EC10393

[43] Gonzalez, M.A.; Gérard, D.; Damien, M.; Ignacio, B.; Elena, B.; Ignacio, R.A. An integrated pest management strategy approach for the management of the stable fly *Stomoxys calcitrans* (Diptera: Muscidae). *Insect.* **2024,** *15*(222), 1-19. https://doi.org/10.3390/insects15040222

[44] Taylor, D.B.; Friesen, K.; Zhu, J. Precipitation and temperature effects on stable fly (Diptera: Muscidae) population dynamics. *Environmental Entomology.* **2017,** *46*, 434-439. https://doi.org/10.1093/ee/nvx032

ASEAN
Journal of Scientific and Technological Reports
Online ISSN:2773-8752

Research article

Green Synthesis of ZnO–TiO_2 Nanoparticles Using *Allium ampeloprasum* (Kurrat) Extract and Their Antibacterial Activity

Zahraa A. Abdul Muhsin[1], Ghaith H. Jihad[2*], and Liath. A. Yaaqoob[3]

[1] Department of Biology, College of Science, University of Baghdad, 10015, Iraq
[2] Department of Physics, College of Science, University of Baghdad, 10081, Iraq
[3] Department of Biotechnology, College of Science, University of Baghdad 10001, Iraq
* Correspondence: e-mail: ghaith.jihad1104@sc.uobaghdad.edu.iq

Citation:
Muhsin, Z.A.A.; Jihad, H.G.; Yaaqoob, A.L. Green synthesis of ZnO-TiO_2 nanoparticles using *Allium ampeloprasum* (Kurrat) extract and their antibacterial activity. *ASEAN J. Sci. Tech. Report.* **2025**, *28*(4), e256572. https://doi.org/10.55164/ajstr.v28i4.256572.

Article history:
Received: November 3, 2024
Revised: May 1, 2025
Accepted: May 26, 2025
Available online: August 25, 2025

Abstract: The potential of nanotechnology in medical applications, particularly for infection treatment, is increasingly recognized. This study synthesized zinc oxide nanoparticles (ZnO NPs) using a green method, using *Allium ampeloprasum* (kurrat) plant extract as a reducing agent. These ZnO NPs were subsequently used to fabricate ZnO–TiO_2 core–shell nanoparticles. The antibacterial activity of the synthesized nanoparticles was evaluated using the agar well diffusion method. Results revealed notable antibacterial effects: *Staphylococcus aureus* (Gram-positive) exhibited a 25 mm inhibition zone, and *Pseudomonas aeruginosa* (Gram-negative) showed a 20 mm inhibition zone at 100 µg/mL concentration. The nanoparticles were characterized using FTIR, UV–Vis spectroscopy, EDX, and AFM. FTIR spectra confirmed core–shell formation at 813.90–613.32 cm^{-1}. UV–Vis analysis indicated absorption peaks at 260 nm for ZnO NPs and 300 nm for ZnO–TiO_2 NPs. EDX analysis confirmed the presence of zinc, titanium, and oxygen with no detectable impurities. AFM revealed an average diameter of 46.74 nm for ZnO NPs and 148.9 nm for ZnO–TiO_2 core–shell NPs. These green-synthesized nanoparticles exhibit promising antibacterial properties, supporting their potential in biomedical applications.

Keywords: Green synthesis; ZnO-TiO_2 (core-shell); ZnO nanoparticles; TiO_2nanoparticles; Antimicrobial activity

1. Introduction

The management of pathogenic microorganisms remains a critical challenge in modern life. While many microbes coexist harmlessly with humans, the uncontrolled growth of certain pathogenic strains can lead to serious health threats [1]. As antibiotic resistance continues to rise, there is growing interest in nanotechnology as a novel strategy to combat microbial infections [2–4]. Unlike conventional antibiotics, nanoparticles (NPs) interact with multiple bacterial components, making it difficult for pathogens to develop resistance [5]. Nanoparticles possess a high surface-area-to-volume ratio and exhibit unique physicochemical properties compared to their bulk counterparts, enabling them to interact with biological systems [6–8] effectively. Among various nanomaterials, zinc oxide (ZnO) and titanium dioxide (TiO_2) have been extensively studied for their antibacterial activity and biocompatibility [9–11]. These nanoparticles operate at the atomic or molecular scale (1–100 nm), and their reduced size enhances properties such as surface reactivity, optical absorption, and bioavailability [12].

Recent advances in green synthesis offer eco-friendly alternatives to conventional chemical and physical nanoparticle fabrication methods. Plant extracts, rich in natural reducing and stabilizing agents such as flavonoids, phenols, and sulfur-containing compounds, can replace toxic solvents and high-energy processes traditionally used in nanoparticle synthesis [13–15]. This sustainable approach minimizes environmental impact and may enhance the resulting nanoparticles' biological activity. Developing core–shell nanostructures, such as ZnO–TiO_2, has emerged as a further strategy to enhance nanoparticle stability, functionality, and safety. The core–shell architecture can protect the inner core from oxidation or degradation, reduce toxicity, and improve properties such as antibacterial activity, drug delivery efficiency, and catalytic performance [16–18]. Using Allium ampeloprasum (commonly known as kurrat, wild leek, or great-headed garlic) for this green synthesis is particularly advantageous due to its rich content of phytochemicals, including flavonoids, sulfur compounds, and antioxidants [19-20]. *Allium ampeloprasum* serves as a natural reducing agent and imparts bioactivity to the nanoparticles, potentially enhancing their antibacterial, antioxidant, and anticancer properties. Additionally, this plant-based synthesis eliminates the need for hazardous chemicals, making it a promising candidate for biomedical applications.

In this study, we first synthesized ZnO nanoparticles using *Allium ampeloprasum* extract, then fabricating ZnO–TiO_2 core–shell nanoparticles by depositing a TiO_2 layer. The synthesized nanoparticles were then evaluated for their antibacterial activity against Gram-positive (Staphylococcus aureus) and Gram-negative (Pseudomonas aeruginosa) bacteria using agar well diffusion. This work explores the potential of green-synthesized ZnO–TiO_2 nanoparticles in antimicrobial applications.

2. Materials and Methods

This experimental study was conducted in two stages. In the first stage, zinc oxide (ZnO) nanoparticles were synthesized. In the second stage, ZnO–TiO_2 core–shell nanoparticles were prepared by coating ZnO with titanium dioxide (TiO_2). The antibacterial activity of the synthesized nanoparticles was then evaluated.

2.1 Materials and chemicals

Zinc acetate dihydrate ($Zn(CH_3COO)_2{\cdot}2H_2O$) was obtained from Sigma-Aldrich (Germany), and titanium tetrachloride ($TiCl_4$) was purchased from ACROS Organics (France). Other materials used include Mueller-Hinton Agar (MHA) from HI-Media (India) and deionized and distilled water supplied by local Iraqi manufacturers.

2.2 Bacterial Strains and Culture Conditions

Two clinical bacterial strains were used *Staphylococcus aureus* (Gram-positive, standard strain) and *Pseudomonas aeruginosa* (Gram-negative), obtained from the Department of Biotechnology, College of Science, University of Baghdad. Each strain was cultured on Mueller-Hinton Agar using a sterile bacterial spreader. Plates were incubated at 37°C for 24 hours to assess bacterial growth and activity. Confluent bacterial lawns were observed after incubation.

2.3 Preparing *Allium ampeloprasum* (kurrat) extract plant

Fresh leaves of *Allium ampeloprasum* (kurrat) were collected from farms in Iraq. The leaves were washed thoroughly with double-distilled water and blended using an electric blender until a juice-like consistency was achieved. The resulting mixture was filtered through Whatman filter paper (0.2 mm pore size) to remove plant residues. The filtrate was then centrifuged at 8000 rpm for 30 minutes, and the supernatant was filtered again to obtain a clear extract. The extract was stored at 4°C and used for nanoparticle synthesis [21]. The procedure must be done many times to gather sufficient nanoparticles. This exploratory research began on January 3, 2024, and ended on January 6, 2024. (100) g were used, a liter of water (tap water) was added and mixed in the electric blender and continue mixing until become like juice, Afterward, filtered via a piece of cloth to get rid of plant residues, then filtered it anther time with filter papers with diameter (0.2) mm, and filtered again until we have clear solution without of any impurities, subsequently transferred the solution into tubes holding ten milliliters and centrifuged it for thirty minutes at a speed of at speed 60 cycle/ second.

Then, it was filtered with filter papers to have a clear solution, and it was saved for use in the manufacture of nanoparticles [22].

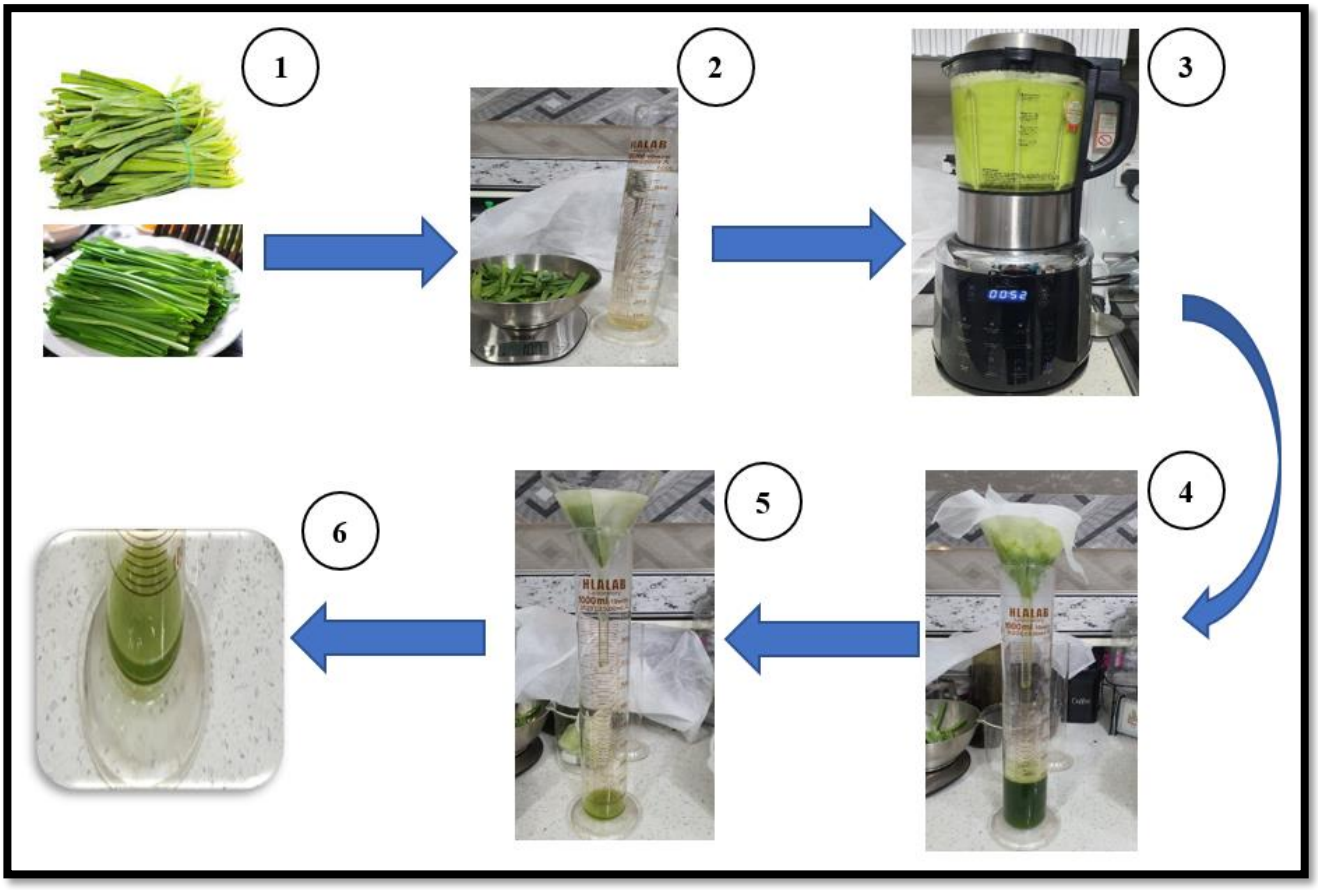

Figure 1. Kurrat leaves collection, 2. Kurrat leaves washing (100gm) with 1000 ml Distilled water, 3. Mixing in a blender, 4. Kurrat extract papers, 5. Filtration with a piece of paper, 6. Filtration with a piece of cloth.

2.4 Green Synthesis of ZnO Nanoparticles Using *Allium ampeloprasum* Extract

To synthesize zinc oxide (ZnO) nanoparticles, 200 mL of the prepared *Allium ampeloprasum* (kurrat) extract was mixed with 20 g of zinc acetate dihydrate ($Zn(CH_3COO)_2{\cdot}2H_2O$) in a flask. The mixture was stirred continuously on a magnetic stirrer at room temperature for 24 hours in the dark to prevent photochemical reactions and ensure complete dissolution. After incubation, the solution was centrifuged at 60 cycles/second for 30 minutes to collect the nanoparticle precipitate. The resulting pellet was washed twice with 5 mL of deionized distilled water to remove residual impurities. The cleaned precipitate was then transferred to sterile Petri dishes and incubated at 37 °C for 2–3 days to allow complete drying. Once dried, the solid product was gently scraped off using a spatula and stored in a dark, moisture-free incubator until further use [22].

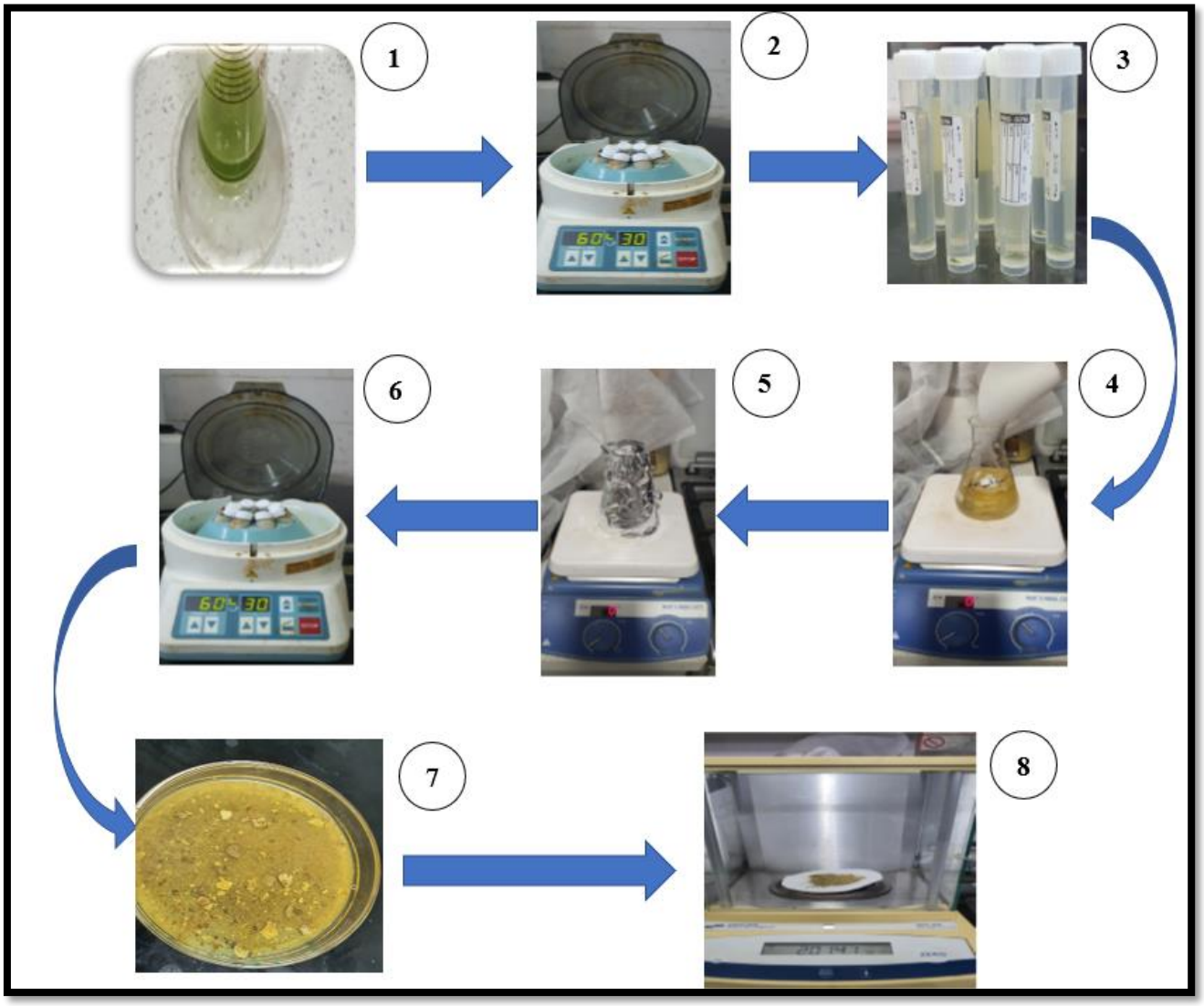

Figure 2. Kurrat extract papers, 2. A centrifuge is used to remove plant extract after centrifugation, as well as residue papers. 3. Extract after centrifugation papers, 4. Add zinc acetate salts, 5. stirring for 24 hours, 6. use the centrifuge twice, 7. Green Synthesis of ZnO Nanoparticles, 8. Net weight of ZnO Nanoparticles.

2.5 Green Synthesis of ZnO–TiO_2 Core–Shell Nanoparticles Using *Allium ampeloprasum* Extract

In the second stage, 150 mL of *Allium ampeloprasum* (kurrat) extract was mixed with 4.5 g of previously synthesized ZnO nanoparticles. Under continuous stirring, 3 mL of titanium tetrachloride ($TiCl_4$) was gradually added to the mixture, as illustrated in Figure 3. The resulting solution was kept under magnetic stirring at room temperature in the dark for 24 hours to ensure proper reaction and shell formation. The mixture was then centrifuged at 60 cycles/second for 30 minutes to collect the precipitate. The precipitate containing ZnO–TiO_2 core–shell nanoparticles was washed twice with deionized distilled water to eliminate residual plant material or unreacted components. The purified nanoparticles were dried overnight in a hot-air oven at 40 °C, then carefully collected and stored in a light-protected, airtight container to avoid degradation or moisture exposure [23].

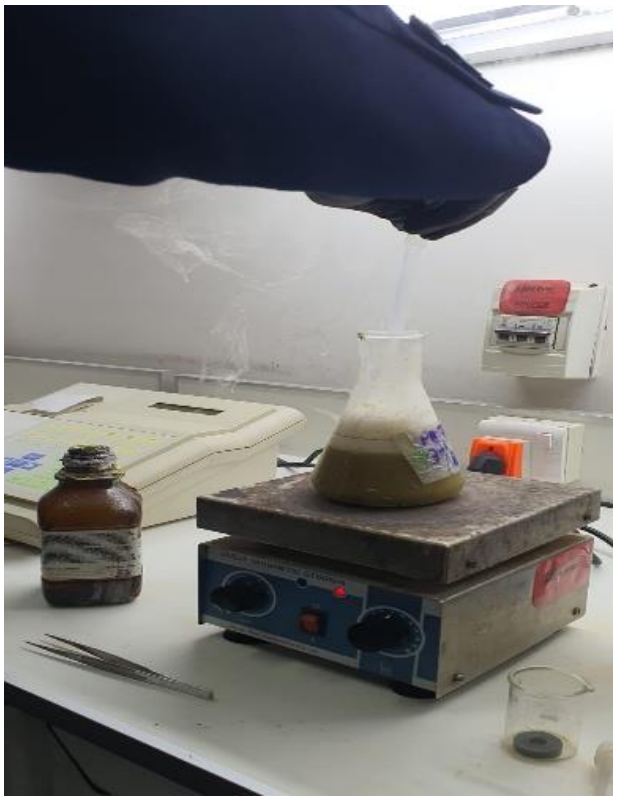

Figure 3. Synthesis of ZnO–TiO_2 Core–Shell Nanoparticles

2.6 Evaluation of Antibacterial Activity of ZnO–TiO_2 Core–Shell Nanoparticles

The agar well diffusion method assessed the antibacterial activity of green-synthesized ZnO–TiO_2 core–shell nanoparticles. The assay targeted two bacterial strains: *Staphylococcus aureus* (Gram-positive) and *Pseudomonas aeruginosa* (Gram-negative). Bacterial suspensions were uniformly spread on **Mueller-Hinton Agar (MHA)** plates using a sterile cotton swab. Wells (6 mm diameter) were then created in the agar, and **various concentrations of ZnO–TiO_2 nanoparticles (25, 50, 75, and 100 µg/mL)** were introduced into the wells. The plates were incubated at **37 °C for 24 hours**, after which **inhibition zones** were measured around each well to determine antibacterial effectiveness [23].

2.7 Statistical Analysis of Inhibition Zones

For precision, the diameters of the inhibition zones were measured using Vernier calipers. All measurements were performed in **triplicate** to ensure reproducibility and accuracy. Data were interpreted following standardized protocols like those provided by the **EUCAST (European Committee on Antimicrobial Susceptibility Testing)** guidelines.

3. Results and Discussion

3.1 Characterization of ZnO–TiO_2 Core–Shell Nanoparticles

3.1.1 UV–Visible Spectroscopy (UV–Vis)

The UV–Vis spectrum of *Allium ampeloprasum* (kurrat) extract reveals the presence of various phytochemicals, particularly **polyphenols**, **flavonoids**, and other organic chromophores. As shown in **Figure 4**, prominent absorption peaks are observed in the **200–300 nm** region, which is typical of *Allium* species and confirms the presence of bioactive compounds that likely act as **natural reducing and stabilizing agents** in nanoparticle synthesis.

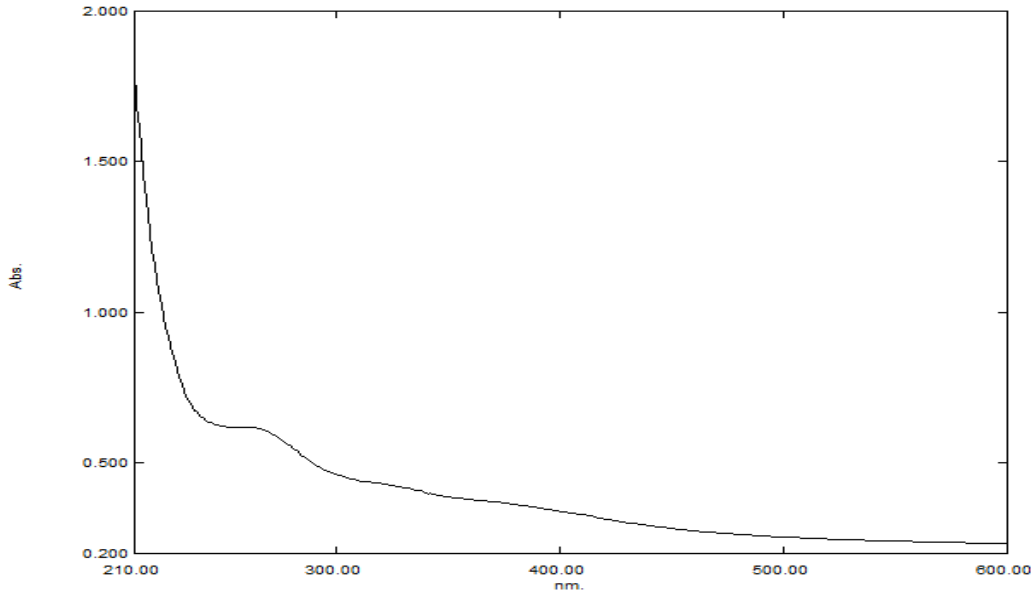

Figure 4. UV–Visible absorption spectrum of *Allium ampeloprasum* (kurrat) plant extract.

The synthesized ZnO nanoparticles' UV–Vis absorption spectrum (Figure 5) exhibits a characteristic peak in the **260–300 nm** range. This absorption band corresponds to the **intrinsic band-gap energy** of ZnO and serves as evidence of nanoparticle formation. The shift from the plant extract's profile confirms the successful synthesis of ZnO nanostructures.

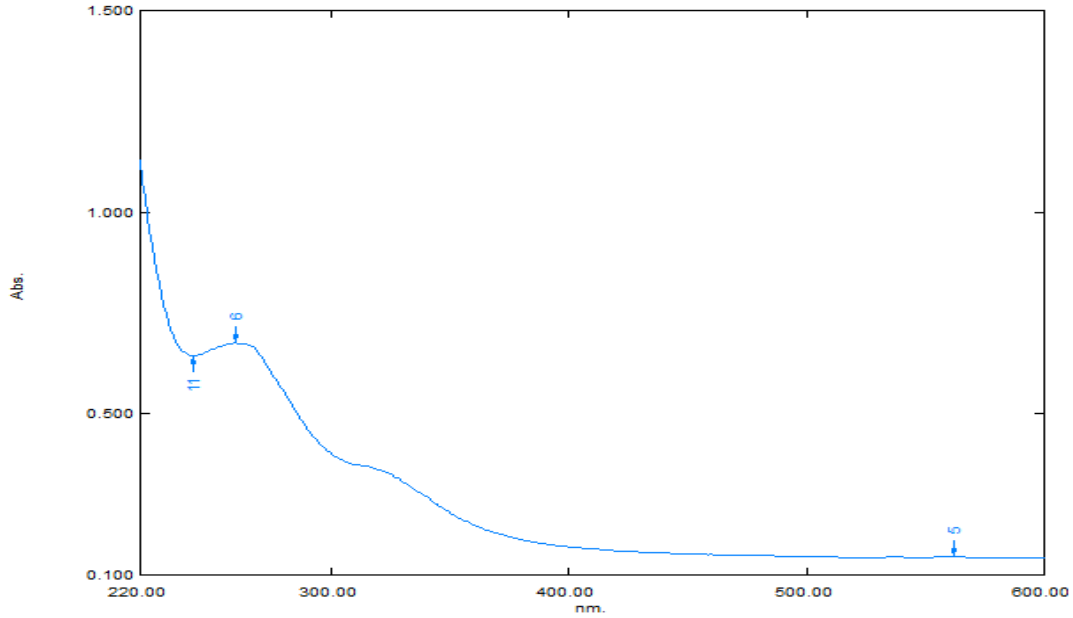

Figure 5. UV–visible absorption spectrum of green-synthesized ZnO nanoparticles.

Further, the **ZnO–TiO_2 core–shell nanoparticles** showed an absorption peak around **300 nm**, as illustrated in **Figure 6**. This slight shift in peak position compared to pure ZnO suggests the formation of the **TiO_2 outer shell**, which modifies the optical properties of the nanoparticles. These findings are consistent with previous literature reports on ZnO–TiO_2 hybrid structures [24].

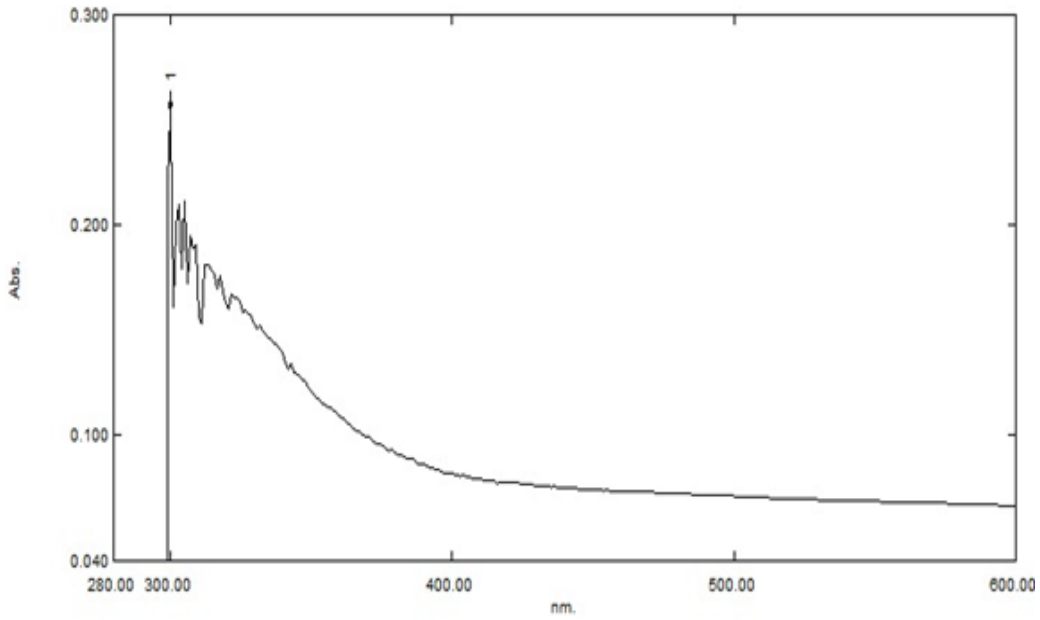

Figure 6. UV–visible absorption spectrum of ZnO–TiO_2 core–shell nanoparticles.

3.1.2 Fourier transform infrared (FTIR) ZnO-TiO_2 (core-shell) NPs

Functional groups, aliphatic primary amine at frequency 3423.41 cm^{-1} and primary alcohol at frequency 1064.63-1049.20 cm^{-1} in an extract of the plant indicate the groups found in the plant [25] as shown in Figure 7. The FT-IR spectrum of ZnO NPs (Figure 8) shows the wavenumbers at 3375, 2349, 1375, 915, and 481 cm-1, respectively. This was detected at 617.18-559.32 cm-1 frequency, which pointed to the zinc oxide nanoparticles' fingerprint location [26]. The metal oxide of the ZnO-TiO_2 functional group could be detected around 813.90-613.32 cm^{-1} in Table 1, which indicates the formation of the core-shell structure, as shown in Figure 9.

Table 1. FTIR of the extract and nanoparticle

Samples	Frequency of Absorption (cm^{-1})	Bonds	Compound class of Functional Groups
Plant Extract	3423.41	N-H stretching	of aliphatic primary amine
	1645.17	C=C stretching	monosubstituted
	1384.79	C-H bending	gem dimethyl
	1064.63-1049.20	C-O stretching	Primary Alcohol
ZnO NPs	3421.48-3404.13	N-H stretch	Primary Amine
	1645.17-1566.09	C=C stretching	cyclic alkene
	1448.44-1402.15	C-H	Alkane
	1043.42	CO-O-CO stretching	anhydride
	617.18-559.32	Metal oxide	ZnO
ZnO-TiO_2 (Core-shell)	3440.77-3296.12	N-H stretch	aliphatic primary amine
	1670.24-1645.17	C=C stretching	alkene
	1539.09-1517.87	N-O stretching	nitro compound
	1039.56	O-H bending	phenol
	813.90-613.32	Metal oxide	ZnO – TiO_2

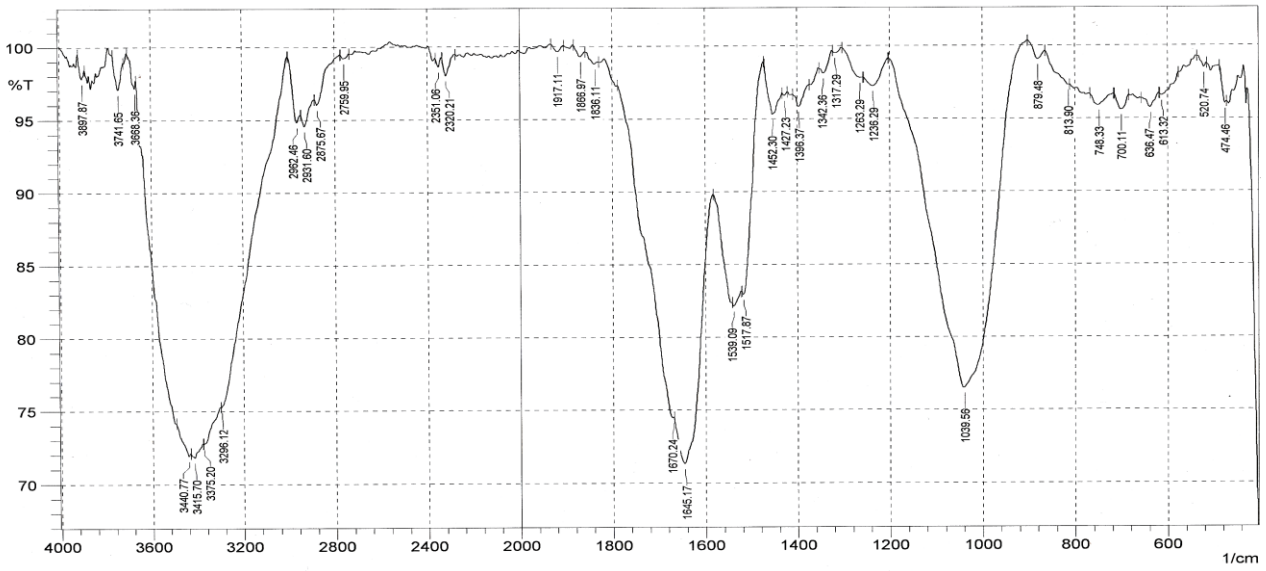

Figure 7. FTIR spectrum of *Allium ampeloprasum* (kurrat) plant extract.

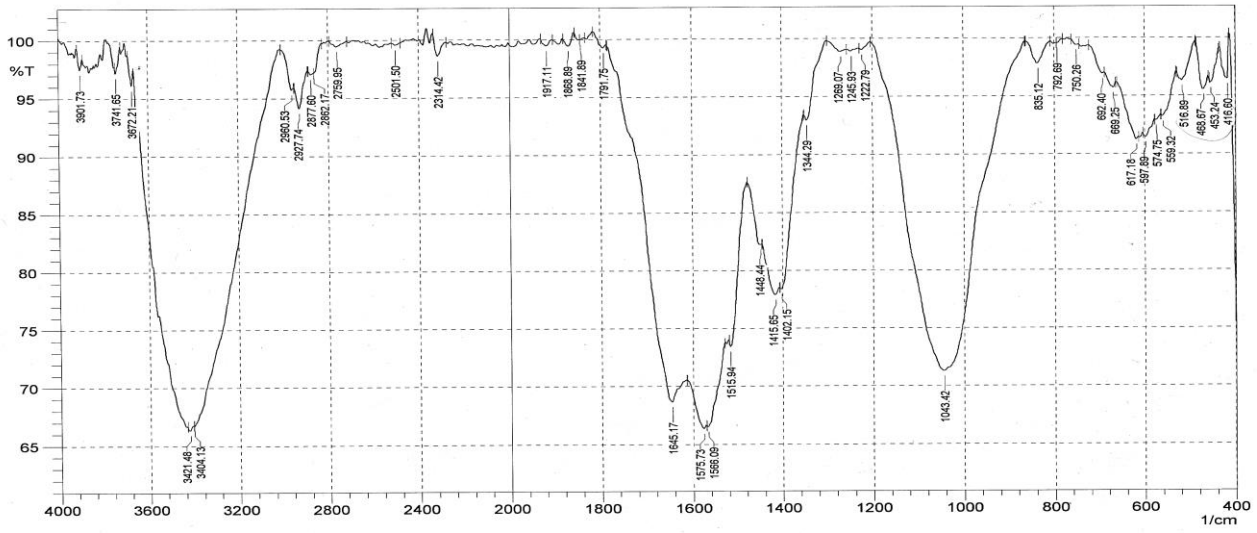

Figure 8. FTIR spectrum of green-synthesized ZnO nanoparticles.

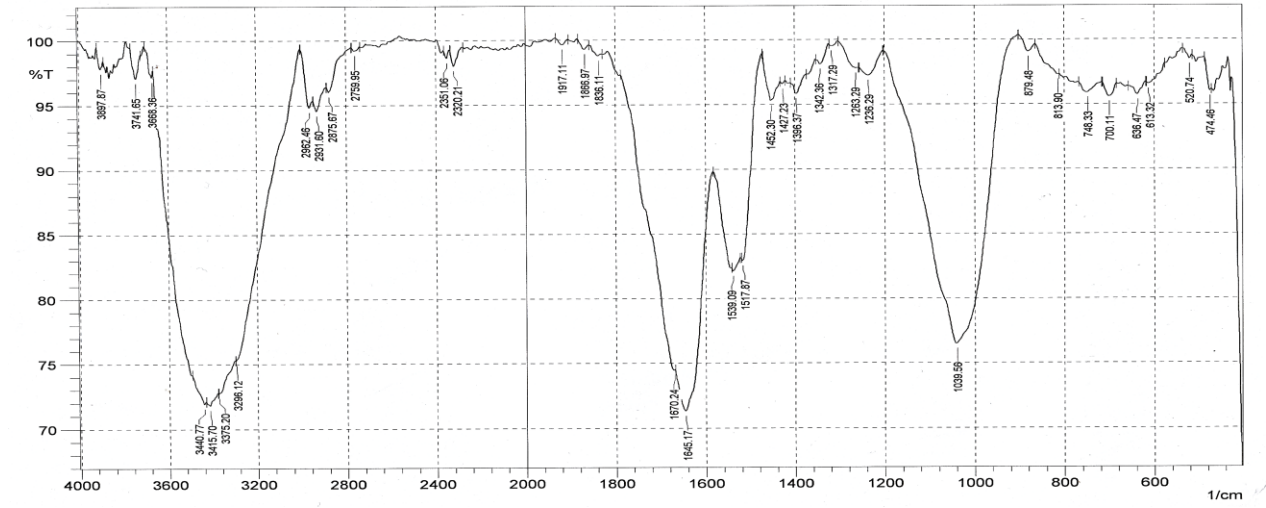

Figure 9. FTIR spectrum of ZnO–TiO_2 core–shell nanoparticles.

3.1.3 Energy-dispersive X-ray (EDX) analysis

EDX analysis was performed to determine the elemental composition of the synthesized nanoparticles. The EDX spectrum of ZnO nanoparticles (Figure 10 and Table 2) confirms the presence of zinc (Zn) as the dominant element, with a minor contribution from oxygen (O). The absence of other elements indicates the high purity of the green-synthesized ZnO nanoparticles [27].

Table 2. EDX elemental composition of ZnO nanoparticles.

Element	Atomic %	Atomic % Error	Weight %	Weight % Error
Zn	96.9	1.0	88.6	0.9
O	3.1	0.3	11.4	1.2

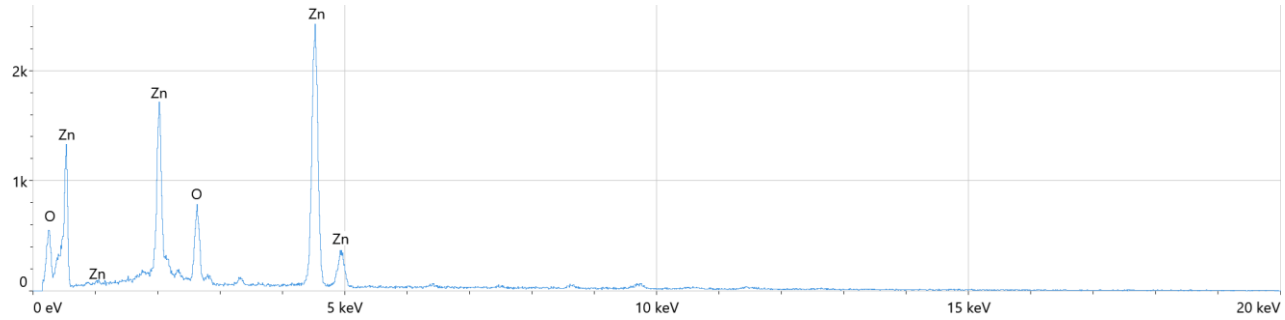

Figure 10. EDX spectrum of green-synthesized ZnO nanoparticles.

The EDX spectrum of ZnO–TiO_2 core–shell nanoparticles (Figure 11 and Table 3) reveals the presence of **oxygen (O)**, **titanium (Ti)**, and **zinc (Zn)** as the primary elements. This confirms the **successful coating of ZnO with TiO_2**, and the absence of any foreign elements suggests **no significant contamination** during synthesis [24].

Table 3. EDX elemental composition of ZnO–TiO_2 core–shell nanoparticles.

Element	Atomic %	Atomic % Error	Weight %	Weight % Error
O	90.5	1.0	74.7	0.8
Ti	7.5	0.1	18.7	0.2
Zn	2.0	0.1	6.7	0.4

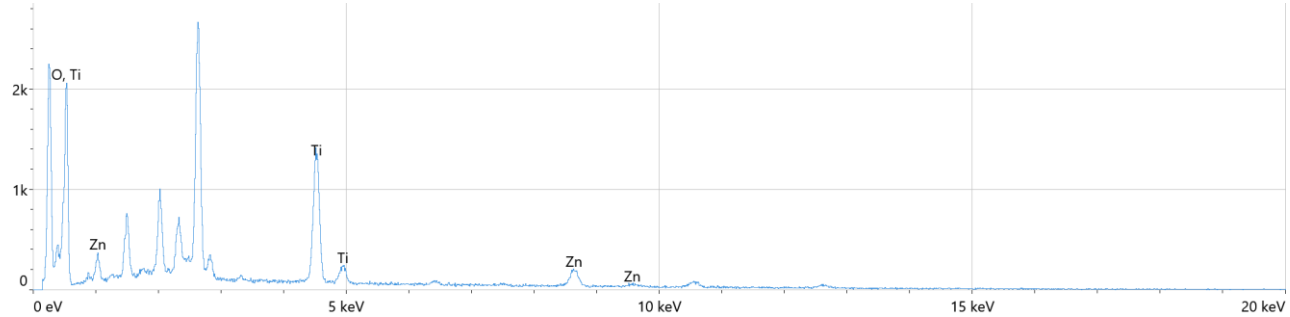

Figure 11. EDX spectrum of ZnO–TiO_2 core–shell nanoparticles.

3.1.4 Atomic Force Microscopy (AFM) Analysis

AFM was used to examine the surface morphology and grain size of ZnO and ZnO–TiO_2 core–shell nanoparticles. The AFM images (Figures 12 and 13) show the 2D and 3D surface topographies. The average grain size of ZnO nanoparticles was 46.76 nm, while the ZnO–TiO_2 core–shell nanoparticles exhibited an increased average size of 76.32 nm, consistent with shell layer formation. Furthermore, surface roughness (Ra) and root mean square (RMS) values indicate slightly increased surface irregularity for the core–shell structure compared to pure ZnO nanoparticles.

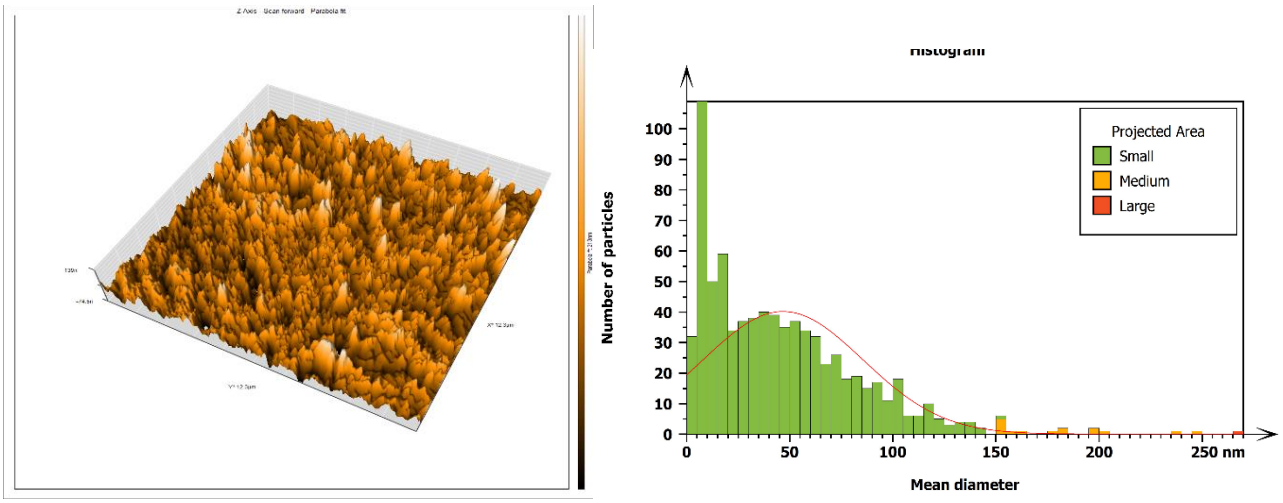

Figure 12. AFM image of ZnO nanoparticles (2D and 3D views).

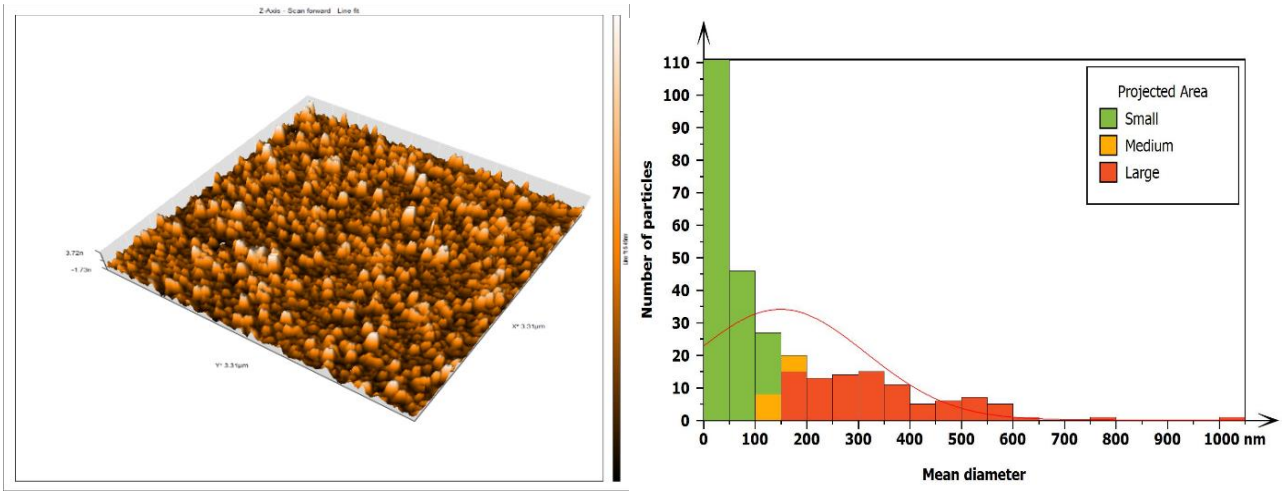

Figure 13. AFM image of ZnO–TiO_2 core–shell nanoparticles (2D and 3D views).

Table 4. AFM analysis: Average grain size, roughness, and RMS values..

Sample	Average grain size (nm)	Roughness (nm)	(RMS) (nm)
ZnO	46.76	0.84	50.79
ZnO-TiO_2	76.32	0.92	56.99

Based on the results, it appears that the laser energy has a direct impact on the average particle size. As the laser energy increases, the nanoparticle size increases as well. As the laser energy increases, it provides higher thermal and kinetic energy to the nanoparticles. This high energy increases the speed at which the ablated nanoparticles hit the quartz substrate, causing nanoparticles to obtain high surface mobility at the surface. Large clusters are formed to reduce the system's high surface energy. Hence, aggregations occur with an overall increase in the nanoparticle's grain size.

The etched surface consists of pores distributed over the whole surface. These ores lead to increased surface roughness, which is attributed to the etching parameters affecting the surface characterization.

3.2 Antibacterial Evaluation and Discussion:

Table 5 shows the outcomes of ZnO-TiO_2 nanoparticles' antibacterial activity against *Pseudomonas aeruginosa* at various doses. Demonstrate that the diameter of the growth inhibition zone has shrunk as ZnO-

TiO_2 nanoparticle concentration has reduced and that the antibacterial efficacy of ZnO-TiO_2 nanoparticles has significantly diminished at a concentration of 25 μg/ml, as shown in Figure 14.

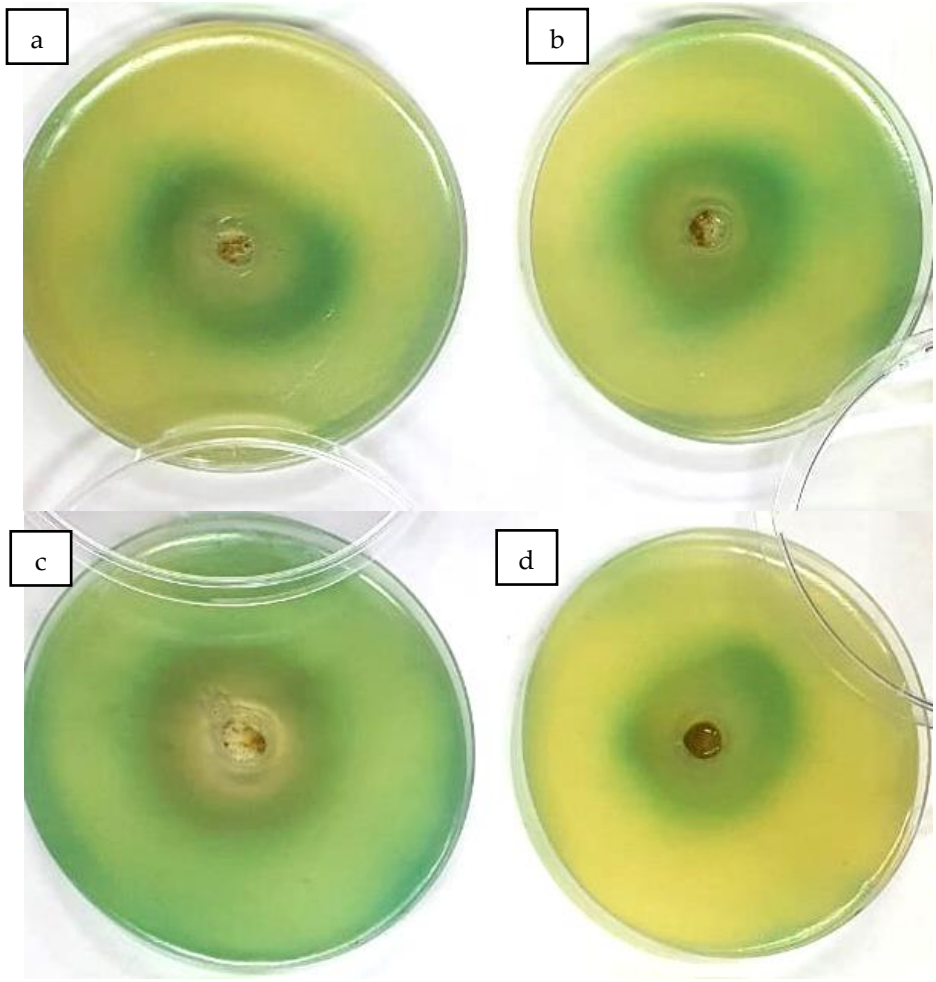

Figure 14. Inhibition zone of *Pseudomonas aeruginosa* bacteria at a)25 (μg/ml), b) 50 (μg/ml), c) 75 (μg/ml), and d) 100 (μg/ml) concentrations.

Table 5. Zones where ZnO-TiO_2 nanoparticles inhibit *Pseudomonas aeruginosa.*

ZnO-TiO_2 NPs concentration (μg/ml)	**Diameter of the inhibitory zone (mm)**
25	8
50	12
75	18
100	20

Whereas the *Staphylococcus aureus* showed more antibacterial activity against ZnO-TiO_2 with increasing the concentration of NPs, as shown in Figure 15, reaching (25 mm) at 100 μg/ml concentration, are listed in Table 6.

Table 6. Zones where ZnO-TiO_2 nanoparticles inhibit *Staphylococcus aureus*.

ZnO-TiO_2 NPs concentration (μg/ml)	**Diameter of the inhibitory zone (mm)**
25	10
50	15
75	20
100	25

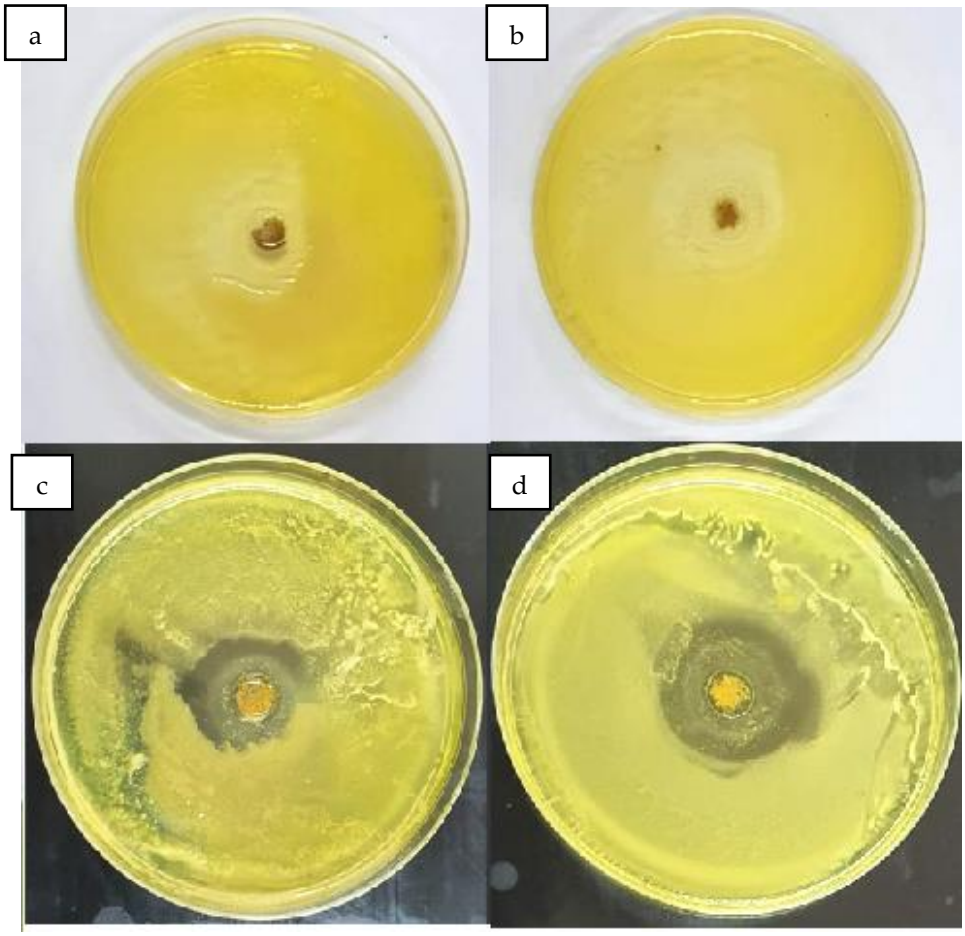

Figure 15. Inhibition zone of ***Staphylococcus aureus*** bacteria at a)25 (μg/ml), b) 50 (μg/ml), c) 75 (μg/ml), and d) 100 (μg/ml) concentrations.

Effect of Laser Energy on Nanoparticle Morphology

The results indicate a clear relationship between laser energy and nanoparticle size. As laser energy increases, it imparts greater thermal and kinetic energy to the particles, enhancing their surface mobility upon impact with the quartz substrate. This increased mobility leads to the formation of larger clusters, as nanoparticles aggregate to minimize the system's high surface energy. Consequently, a direct increase in average particle size is observed with higher laser energy. In addition, surface etching produced a porous texture uniformly distributed across the substrate. These pores contribute to increased surface roughness, which is directly influenced by the etching conditions and parameters.

Antibacterial Susceptibility of ZnO–TiO_2 Nanoparticles

The agar well diffusion method assessed the antimicrobial activity of ZnO–TiO_2 core–shell nanoparticles against Pseudomonas aeruginosa (Gram-negative) and Staphylococcus aureus (Gram-positive).

The results showed that the diameter of the inhibition zones increased proportionally with nanoparticle concentration.

For *P. aeruginosa*, inhibition zones ranged from 8 mm at 25 μg/mL to 20 mm at 100 μg/mL, indicating moderate sensitivity. *S. aureus*, on the other hand, displayed higher susceptibility, with inhibition zones increasing from 10 mm to 25 mm over the same concentration range [28]. This differential activity can be attributed to structural differences in the bacterial cell walls. The thicker peptidoglycan layer of Gram-positive bacteria like *S. aureus* may enhance interactions with ZnO–TiO_2 nanoparticles, leading to more effective antibacterial action. In contrast, the outer membrane in Gram-negative bacteria can act as a barrier, reducing nanoparticle penetration [28].

Nanoparticle Characterization Summary

The ZnO and ZnO–TiO_2 nanoparticles were thoroughly characterized using UV–Vis, FTIR, EDX, and AFM techniques. UV-Vis spectroscopy revealed a characteristic absorption peak for ZnO nanoparticles at 260 nm, consistent with previously reported values. For ZnO–TiO_2 core–shell particles, a red-shifted peak appeared at 300 nm, supporting the formation of the TiO_2 shell[30]. FTIR analysis confirmed Zn–O stretching vibrations at 617.18–559.32 cm^{-1} and Ti–O–Zn bonds at 813.90–613.32 cm^{-1}, clearly indicating the formation of a core–shell structure [29]. EDX spectra demonstrated the presence of zinc, titanium, and oxygen in the core–shell nanoparticles, with no detectable impurities, confirming successful and clean synthesis [29]. AFM measurements indicated an increase in average grain size from 46.76 nm (ZnO) to 76.32 nm (ZnO–TiO_2), consistent with surface coating and shell development. A moderate increase in roughness and RMS values also reflected morphological changes [30].

4. Conclusions

This study demonstrates that ZnO–TiO_2 core–shell nanoparticles, synthesized via a green method using *Allium ampeloprasum* (kurrat) extract, possess significant antibacterial potential, particularly against Gram-positive *Staphylococcus aureus*. Characterization confirmed the successful synthesis and shell formation through multiple techniques, including UV–Vis, FTIR, EDX, and AFM. The ZnO–TiO_2 nanoparticles showed concentration-dependent antibacterial effects, with greater efficacy at higher concentrations. Their activity is attributed to mechanisms such as membrane disruption, oxidative stress, and interference with DNA and protein synthesis. These findings suggest that ZnO–TiO_2 core–shell nanoparticles may serve as promising antimicrobial agents, especially in the context of antibiotic-resistant bacteria, offering an effective alternative to conventional antibiotics. Plant-based synthesis also presents a sustainable, non-toxic, and scalable approach for nanoparticle production.

5. Acknowledgements

Perspectives for Future Research: The relationship between preparing nanomaterials in different ways and their effectiveness in killing bacterial groups, which can be used for sterilization in the future or preservation of food materials.

Author Contributions: Authors substantially contributed to the drafting of the initial and revised versions of these papers

Conflict of Interest Disclosure: The authors declare no conflict of interest.

Funding: None

References

[1] Maleki, M. D. M. Antimicrobial Performance of Zinc Oxide Nanoparticles with Green Synthesis Against Gram-Positive and Gram-Negative Bacteria. *Pakistan Journal of Medical & Health Sciences* **2020**, *14* (3), 1577-1583.

[2] Noor H. Faiq and Mais E Ahmed. Effect of Biosynthesized Zinc Oxide Nanoparticles on Phenotypic and Genotypic Biofilm Formation of Proteus Mirabilis. *Baghdad Science Journal* **2024**, *21*(3), 894-908. https://doi.org/10.21123/bsj.2023.8067

[3] Halah Majeed Balasim, F. K. E. A. L. A. Y. Biosynthesis of Iron Oxide Nanoparticles and Combination with Glyphosate Herbicide and Effect Against Cogon Grass Control. *Diyala Agricultural Sciences Journal* **2024**, *16*(1), 145-158. https://doi.org/10.52951/dasj.24160113

[4] Ishita Matai , Abhay Sachdev , Poornima Dubey , S. Uday Kumar, Bharat Bhushan and P. Gopinath. Antibacterial Activity and Mechanism of Ag–ZnO Nanocomposite on S. Aureus and GFP-Expressing Antibiotic Resistant *E. Coli*. *Colloids and Surfaces B: Biointerfaces* **2014**, *115*(1), 359-367. https://doi.org/10.1016/j.colsurfb.2013.12.005

[5] Singaravelu, G.; Arockiamary, J.; Kumar, V. G.; Govindaraju, K. J. C.; Biointerfaces, s. B. novel extracellular synthesis of monodisperse gold nanoparticles using marine alga, Sargassum wightii Greville. *Colloids and Surfaces B: Biointerfaces* **2007**, *57*(1), 97-101. https://doi.org/10.1016/j.colsurfb.2007.01.010

[6] Ashe, B. A Detail Investigation to Observe the Effect of Zinc Oxide and Silver Nanoparticles in Biological System, Department of Biotechnology & Medical Engineering National Institute of Technology, Rourkela-769008, Orissa, India, **2011**.

[7] Chen, Y.; Liang, W.; Li, Y.; Wu, Y.; Chen, Y.; Xiao, W.; Zha, L.; Zhang, J.; Li. H. Modification, Application and Reaction Mechanisms of Nano-Sized Iron Sulfide Particles for Pollutant Removal from Soil and Water: A Review. *Chemical Engineering Journal* **2019**, *362*(15), 144-159. https://doi.org/10.1016/j.cej.2018.12.175

[8] Suleiman, H.M.; El-sheikh, M.S.; Mohamed, T.E.; El Raey, A.M.; El sherbiny, S.; Morsy, A.F.; El-hout, I.S.; Sheta, M.S. Green Synthesis of ZnO-NPs Using Sugarcane Bagasse Waste: Phytochemical Assessment of Extract and Biological Study of Nanoparticles. *Dalton Transactions* **2024**, *53*(46), 18494-18505. https://doi.org/10.1039/D4DT02449D

[9] Huh, J.A.; Kwon, J.Y. "Nanoantibiotics": A New Paradigm for Treating Infectious Diseases Using Nanomaterials in the Antibiotics Resistant Era. *Journal of Controlled Release* **2011**, *156*(2), 128-145. https://doi.org/10.1016/j.jconrel.2011.07.002

[10] Hamza, M. R.; Yaaqoob, L. A. EVALUATION THE EFFECT OF GREEN SYNTHESIS TITANIUM DIOXIDE NANOPARTICLES ON ACINETOBACTER BAUMANNII ISOLATES. *Iraqi Journal of Agricultural Sciences* **2020**, *51*(6), 1486-1495. https://doi.org/10.36103/ijas.v51i6.1176

[11] Kamel, R. M.; Yaaqoob, L. A. EVALUATION OF THE BIOLOGICAL EFFECT SYNTHESIZED IRON OXIDE NANOPARTICLES ON ENTEROCOCCUS FAECALIS. *IRAQI JOURNAL OF AGRICULTURAL SCIENCES* **2022**, *53*(2), 440-452. https://doi.org/10.36103/ijas.v53i2.1552

[12] Kim, I.-S.; Baek, M.; Soo-Jin, C. A. Comparative Cytotoxicity of Al_2O_3, CeO_2, TiO_2 and ZnO Nanoparticles to Human Lung Cells. *Journal of Nanoscience and Nanotechnology* **2010**, *10*(5), 3453-3458(6). https://doi.org/10.1166/jnn.2010.2340

[13] Sopchenski, L.; Cogo, S.; Dias-Ntipany, M.F.; Elifio-Espósito, S.; Popat, K.C. Soares, P. Bioactive and Antibacterial Boron Doped TiO_2 Coating Obtained by PEO. *Applied Surface Science* **2018**, *458*(1), 49-58. https://doi.org/10.1016/j.apsusc.2018.07.049

[14] Rasmussen, W.J.; Martinez, E.; Louka, P.; Wingett, G.D. Zinc Oxide Nanoparticles for Selective Destruction of Tumor Cells and Potential for Drug Delivery Applications. *Expert Opinion on Drug Delivery* **2010**, *7*(9), 1063-1077. https://doi.org/10.1517/17425247.2010.502560

[15] Perumal, P.; Sathakkathulla, A.N.; Kumaran, K.; Ravikumar, R.; Selvaraj, J.J. Nagendran, V. Gurusamy, M.; Shaik, N.; Prabhakaran, G.S.; Palanichamy, S.V.; Ganesan, V.; Thiraviam, P.P.; Gunalan, S.; Rathinasamy, S. Green Synthesis of Zinc Oxide Nanoparticles Using Aqueous Extract of Shilajit and Their Anticancer Activity against HeLa Cells. *Scientific Reports* **2024**, *14*(2204), 1-11. https://doi.org/10.1038/s41598-024-52217-x

[16] Kulkarni, D.; Sherkar, R.; Shirsathe, C.; Sonwane, R.; Varpe, N.; Shelke, S.; More, P.M.; Pardeshi, R.S.; Dhaneshwar, G.; Junnuthula, V.; Dyawanapelly, S. Biofabrication of Nanoparticles: Sources, Synthesis, and Biomedical Applications. *Frontiers in Bioengineering and Biotechnology* **2023**, *11*(1), 1-26. https://doi.org/10.3389/fbioe.2023.1159193

[17] Gawande, B.M.; Goswami, A.; Asefa, T.; Guo, H.; Biradar, V.A.; Peng, D.L.; Zboril, R.; Varma, S.R. Core–Shell Nanoparticles: Synthesis and Applications in Catalysis and Electrocatalysis. *Chemical Society Reviews* **2015**, *44*(1), 7540-7590. https://doi.org/10.1039/C5CS00343A

[18] Saaed, N. A. A. A. The Biosynthesis, Characterization, Antibacterial Activities, and Photocatalysis of Zinc Oxide Nanoparticles Using Allium Ambelloprasum (Leeks) Leaves Extract. *Journal of Chemistry and Environment* **2024**, *3*(2), 1-15. https://doi.org/10.56946/jce.v3i2.449

[19] Fereshteh Jalilian , Azam Chahardoli , Komail Sadrjavadi , Ali Fattahi and Yalda Shokoohinia. Green Synthesized Silver Nanoparticle from Allium Ampeloprasum Aqueous Extract: Characterization, Antioxidant Activities, Antibacterial and Cytotoxicity Effects. *Advanced Powder Technology* **2020**, *31*(3), 1323-1332. https://doi.org/10.1016/j.apt.2020.01.011

[20] Jones, F.C.; Resina, L.; Ferreira, C.F. Paola Sanjuan-Alberte and Teresa Esteves. Conductive Core–Shell Nanoparticles: Synthesis and Applications. *The Journal of Physical Chemistry C* **2024**, *128*(27), 11083-11100. https://doi.org/10.1021/acs.jpcc.4c02012

[21] Ghadban, Y.A.; Ali, H.L. Efficacy Of Green Synthesis Of Silver Nanoparticles Using Allium Ampeloprasum Against Isoproterenol Induced Myocardial Infarction In Adult Albino Rats. *Review of International Geographical Education Online* **2021**, *11*(9), 859-871.

[22] Alden, A.A.M.; Yaaqoob, A.L. EVALUATION OF THE BIOLOGICAL EFFECT SYNTHESIZED ZINC OXIDE NANOPARTICLES ON PSEUDOMONAS AERUGINOSA. *IRAQI JOURNAL OF AGRICULTURAL SCIENCES* **2022**, *53*(1), 27-37. https://doi.org/10.36103/ijas.v53i1.1502

[23] Hameed, R.U.; Yaaqoob, A.L. Antibacterial Activity of Cobalt and Titanium (Co: Tio2) Core-Shell Nanoparticles against E. Coli Isolated From Urinary Tract Infections. *Institution of Genetic Engineering and Biotechnology* **2023**, *21*(2), 341-357.

[24] Zhang, M.; An, T.; Liu, X.; Hu, X.; Sheng, G.; Fu, J. Preparation of a High-Activity ZnO/TiO_2 Photocatalyst via Homogeneous Hydrolysis Method with Low Temperature Crystallization. *Materials Letters* **2010**, *64*(17), 1883–1886. https://doi.org/10.1016/j.matlet.2010.05.054

[25] Rajendran, P.S.; Sengodan, K. Synthesis and Characterization of Zinc Oxide and Iron Oxide Nanoparticles Using Sesbania Grandiflora Leaf Extract as Reducing Agent. *Journal of Nanoscience* **2017**, 1-7. https://doi.org/10.1155/2017/8348507

[26] Vlazan, P.; Ursu, D.H.; Irina-Moisescu, C.; Miron, I.; Sfirloaga, P.; Rusu, E. Structural and Electrical Properties of TiO_2/ZnO Core–Shell Nanoparticles Synthesized by Hydrothermal Method. *Materials Characterization* **2015**, *101*(1), 153-158. https://doi.org/10.1016/j.matchar.2015.01.017

[27] Reinosa, J.J.; Leret, P.; Alvarez-Docio, M.C.; Campo, del.A.; Fernandez, F.J. Enhancement of UV Absorption Behavior in ZnO–TiO_2 compositesMejora Del Comportamiento de Absorción de UV En Materiales Compuestos ZnO–TiO_2. *Boletín de la Sociedad Española de Cerámica y Vidrio* **2016**, *55*(2), 55-62. https://doi.org/10.1016/j.bsecv.2016.01.004

[28] Saleem, S.; Ahmed, B.; Khan, S.M.; Al-Shaeri, M.; Musarrat, J. Inhibition of Growth and Biofilm Formation of Clinical Bacterial Isolates by NiO Nanoparticles Synthesized from Eucalyptus Globulus Plants. *Microbial Pathogenesis* **2017**, *111*(1), 375-387. https://doi.org/10.1016/j.micpath.2017.09.019

[29] Hammadi, H.A.; Habeeb, S.A.; Al-Jibouri, F.L.; Hussien, H.F. Synthesis, Characterization and Biological Activity of Zinc Oxide Nanoparticles (ZnO NPs). *Sys Rev Pharm* **2020**, *11*(5), 431-439.

[30] Ali Ehsani, Azizi-Lalabadi M.; Divband, B.; Alizadeh-Sani, M. Antimicrobial Activity of Titanium Dioxide and Zinc Oxide Nanoparticles Supported in 4A Zeolite and Evaluation the Morphological Characteristic. *Scientific Reports* **2019**, *9*, 1-10. https://doi.org/10.1038/s41598-019-54025-0

ASEAN
Journal of Scientific and Technological Reports
Online ISSN:2773-8752

Research article

Formulation of a Ketogenic Diet for Starter-Finisher and its Effect on the Growth Performance and Carcass Quality of Broiler Chicken (*Gallus gallus domesticus*)

Roy C. Limpangog[1*], Manuel D. Gacutan, Jr.[2], and Warren D. Come[3]

[1] Department of Animal Science, Faculty of Agriculture and Food Science, Visayas State University, Baybay City, Leyte, Philippines
[2] Department of Animal Science, Faculty of Agriculture and Food Science, Visayas State University, Baybay City, Leyte, Philippines
[3] Department of Animal Science, Faculty of Agriculture and Food Science, Visayas State University, Baybay City, Leyte, Philippines
* Correspondence: roy.limpangog@vsu.edu.ph

Citation:
Limpangog, R.; Gacutan, Jr., M.; Come, W. Formulation of a Ketogenic Diet for Starter-Finisher and its Effect on the Growth Performance and Carcass Quality of Broiler Chicken (*Gallus gallus domesticus*). *ASEAN J. Sci. Tech. Report.* **2025**, *28*(4), e257750. https://doi.org/10.55164/ajstr.v28i4.257750.

Article history:
Received: February 14, 2025
Revised: July 27, 2025
Accepted: August 6, 2025
Available online: August 21, 2025

Abstract: A study was conducted to evaluate the effects of ketogenic diets on the growth performance and carcass quality of broiler chickens. The ketogenic approach aims to shift caloric intake towards protein and fat, with reduced carbohydrate content. A total of 128 three-week-old, straight-run broiler chicks were randomly assigned to four dietary treatments: Diet A (control/commercial feed), Diet B (lipid-based ketogenic diet), Diet C (protein-based ketogenic diet), and Diet D (fiber-based ketogenic diet). The study followed a Randomized Complete Block Design (RCBD) with cage location as the blocking factor. Data were analyzed using ANOVA in SAS v.9, and treatment means were compared using Tukey's HSD at α = 0.05. Results revealed that Diet A outperformed all other treatments in terms of Voluntary Feed Intake (VFI), Body Weight (BW), Average Daily Gain (ADG), Weight Gain (WG), and Feed Conversion Ratio (FCR). It also yielded the highest carcass weight (CW) and dressing percentage (DP). In contrast, Diet D showed the poorest growth performance and the highest cost to produce (CTP), along with the lowest Broiler Production Efficiency Factor (BPEF). However, Diet D recorded the lowest abdominal fat (AF), comparable with Diet C, while both Diet C and D had the lowest visceral fat (VF) yield. The reduced performance of ketogenic diets may be due to the lower quality of raw materials used in home-mixed rations. Nonetheless, the notable reduction in AF and VF suggests that ketogenic feeding may offer a viable strategy for producing leaner broiler meat.

Keywords: Broiler chicken; carcass quality; growth performance; ketogenic diet

1. Introduction

Increased demand for poultry meat has led to the selection of rapid-growing broiler chickens with better feed conversion efficiency. These economic qualities, including breast output, have seen substantial advances as a result of active selection to fulfill market demand. However, today's broilers tend to have over-accumulation of fat in their abdominal region [1]. The quality of the carcass and feed efficiency is negatively impacted by excessive abdominal fat buildup [2]. There is a coincidental rise in the deposition of abdominal fat in genetically modified chickens with enhanced development and early maturity [3]. This results in lower-quality meat that may be deemed unhealthy, as well as an increase in feed costs [4]. One potential method for reducing fat deposition in

broiler chickens is the application of a ketogenic diet. The ketogenic diet has become one of the most popular diet trends in human nutrition today. The objective is to get the majority of one's caloric intake from protein and fat, with fewer calories coming from carbohydrates. In this type of diet, high production of ketone bodies, which are derived from the breakdown of fat into energy, is induced [5]. A diet high in lipids, proteins, or fiber can promote ketogenesis, the process by which ketone bodies are created. Fatty acids and glycerol are the building blocks of lipids. Excess levels of these components are transformed into fatty acids (FA) and stored as fats when this nutrient is consumed in large amounts. When blood glucose levels are low, the body will use its fat reserves, go through beta-oxidation, and produce acetyl-CoA. However, the utilized acetyl CoA will be used gradually because of low amounts of oxaloacetate, a glucose-dependent molecule. Excess acetyl-CoA will encourage the ketogenesis process, which is the process of producing ketone bodies. Amino acids (AA) make up proteins, and an excess of them encourages the synthesis of high concentrations of acetyl CoA, which, if not used, can lead to FA synthesis and fat deposition. These lipids will undergo beta-oxidation and create acetyl-CoA when blood glucose levels are low. Similar to this, when oxaloacetate levels are low, the body uses less acetyl CoA, which can lead to ketogenesis when there is an oversupply. Some of these AAs have a ketogenic nature and produce acetyl-CoA, which cannot be converted to glucose. Ketone bodies will be created by synthesizing these acetyl-CoAs. A low-carbohydrate diet lowers the amount of oxaloacetate produced, which is needed for the conversion of acetyl-CoA to citrate. Animals will turn to their body's fat reserves when glucose is in limited supply. Acetyl CoA is produced through the beta-oxidation of these. Oxaloacetate production will decrease due to the low glucose level, which will affect acetyl-CoA utilization. Acetyl CoA in excess will then be converted into ketone bodies.

Numerous studies have demonstrated that nutritional interventions could alter the accretion of fat deposits in the body, and the broiler industry is actively employing this strategy. Adjustments to the caloric, protein, amino acid, and mineral levels in the diet, as well as the addition of feed additives, triggered a decrease in abdominal fat deposition and carcass fatness[1]. However, it is not well understood and shown which of these methods for lowering fat deposition in broilers will have the best performance in terms of growth and carcass quality; hence, this study.

2. Materials and Methods

2.1 Procurement of Birds

A total of 128 day-old straight-run Cobb 500 strain of broiler chicks were acquired from a reliable source. These birds were presumed to have been vaccinated as prescribed by the local supplier.

2.2 Preparation of the Study Area

Thirty-two (32) cages with an area of 4.80 sq. ft. per cage were constructed to accommodate 4 birds each. The floor height of the cages was at least 1.80 meters from the ground to minimize the build-up of ammonia. For optimum ventilation, the ceiling height was at least 2.40 meters from the cage flooring [6]. A general light was also installed above the cages to stimulate feed and water intake and meet the birds' light requirements. To sanitize and prevent the entry of disease-causing microorganisms brought by people arriving from outside the study area, a foot bath and a hand washing station were positioned at the building's entrance. At least three days before the chicks' arrival, the building, cages, and equipment were thoroughly cleaned and disinfected.

2.3 Management of Birds

The brooder lamps were turned on at least 3-4 hours before the arrival of chicks. An electrolyte solution was prepared ahead of time and provided to the chicks upon arrival. The temperature in the first week was kept at 35°C. It was reduced by 2°C in the following week and continued until the 5th week. On the 1st day of brooding, a 24-hour lighting program was implemented and was reduced to 23 hours on the following day until the 5th day. By the time the birds reached the age of 6 – 11 days, the lighting program was reduced to 18 hours and was increased to 20 hours on days 12 - 35 [7]. Clean water was made available at all times. A medication and vaccination program designed for broilers was administered to the birds. For the first 2 weeks, all broiler chicks were provided with the same brand of commercial booster feeds. All animals

ASEAN J. Sci. Tech. Report. **2025**, *28*(4), e257750. 3 of 10

without ketogenic diet were provided with a commercial brand of broiler feeds (Table 1) upon entering the age of 15 days, which was also the start of data collection, while the remaining animals were provided with a ketogenic diet formulation for broiler starter (week 3) to broiler finisher (weeks 4 - 5) on *ad libitum* basis.

Table 1. Ingredient and Nutrient Composition of the Control Feed

Feed type	Ingredients	Guaranteed Analysis (%)					
		Moisture	CP	EE	CF	Ca	P
Broiler Starter	YC, SBM, RB, FM, WP, CM, Mol, CCO, MDCP, Lime, VMP, AA	12 max	19 min	5 min	4 max	0.9-1	0.70 min
Broiler Finisher	YC, SBM, RB, FM, WP, CM, Mol, CCO, MDCP, Lime, VMP, AA	12 max	18 min	6 min	6 max	0.8-0.9	0.70 min

YC – Yellow corn, SBM – Soybean meal, RB – Rice bran, WP – Wheat pollard, CM – Copra meal, Mol – Molasses, CCO – Crude Coconut Oil, MDCP – Monocalcium Phosphate, Lime – Limestone, VMP – Vitamin-mineral premix, AA – Amino acid, Min - Minimum, Max - Maximum

2.4 Design and Treatments

The study was conducted in a Randomized Complete Block Design (RCBD) using the location of cages as a blocking factor. Blocking was done because the temperature, humidity, and other environmental factors inside the broiler house are not automatically controlled. There were four treatments with eight blocks and four birds per block. The following were the diets given during the starter and finisher stages of broilers: Diet A – Commercial feed, Diet B – Lipid-based ketogenic diet, Diet C – Protein-based ketogenic diet, Diet D – Fiber-based ketogenic diet.

2.5 Preparation of Dietary Treatments

All birds were provided with the same brand of commercial feeds at the booster stage. The birds were given a broiler starter or finisher ration formulated using the Brill Feed Formulation Software (Tables 2 and 3). The broiler nutrient requirement as reflected in the 4th edition of PHILSAN Feed Reference Standards was used as a reference in feed formulation [8].

Table 2. Ingredient Composition of Different Dietary Treatments

Ingredient	Inclusion, %							
	Starter				Finisher			
	A Control	B Lipid-based	C Protein-based	D Fiber-based	A Control	B Lipid-based	C Protein-based	D Fiber-based
YC	Table 1	30.00	30.00	30.01	Table 1	20.97	29.99	30.00
SBM		30.46	31.04	17.35		23.58	26.73	11.58
RBD1		10.00	10.00	-		15.00	5.00	-
FM		1.00	1.00	1.00		1.00	1.00	7.91
WP		5.00	5.00	6.60		10.00	5.00	4.60
RBD2		-	-	15.00		-	-	20.00
CM		5.00	10.00	10.00		10.00	15.00	10.00
Mol		3.00	3.00	3.00		4.70	5.00	5.00
CCO		8.50	5.00	5.50		10.00	6.00	6.10
MDCP		2.69	1.16	1.26		0.99	1.08	-
Lime		1.58	1.05	1.02		1.03	2.48	0.96

Table 2. Ingredient Composition of Different Dietary Treatments (Continuation)

Ingredient	Inclusion, %							
	Starter				Finisher			
	A Control	B Lipid-based	C Protein-based	D Fiber-based	A Control	B Lipid-based	C Protein-based	D Fiber-based
VMP	Table 1	0.20	0.20	0.20	Table 1	0.20	0.20	0.20
AA		1.65	1.65	1.65		1.65	1.65	1.65
Salt		0.50	0.50	0.50		0.50	0.50	0.50
CC		0.01	0.01	0.01		0.01	0.01	0.01
Met		0.06	0.04	0.16		0.02	0.01	1.13
Lys		-	-	6.33		-	-	-
Enz		0.10	0.10	0.10		0.10	0.10	0.10
Zinc		0.05	0.05	0.05		0.05	0.05	0.50
Threo		-	-	0.06		-	-	-
Tryp		-	-	0.01		-	-	-
TB		0.20	0.20	0.20		0.20	0.20	0.20
TOTAL		100	100	100		100	100	100

YC – Yellow corn, SBM – Soybean meal, RBD1 – Rice bran D1, FM – Fishmeal, WP – Wheat pollard, RBD2 – Rice bran D2, CM – Copra meal, Mol – Molasses, CCO – Crude coconut oil, MDCP – Monodicalcium phosphate, Lime – Limestone, VMP – Vitamin-mineral premix, AA – Acetic acid, CC – Choline chloride, Met – Methionine, Lys – Lysine, Enz – Enzyme, Threo – Threonine, Tryp – Tryptophan, TB – Toxin binder

Table 3. Nutrient Composition of Different Dietary Treatments

Nutrient	Starter				Finisher			
	A Control	B Lipid-based	C Protein-based	D Fiber-based	A Control	B Lipid-based	C Protein-based	D Fiber-based
ME (kcal)	Table 1	2901.00	2702.00	2700.00	Table 1	2900.00	2700.00	2700.00
CP (%)		19.29	20.58	20.00		18.01	19.20	18.00
EE (%)		12.25	9.32	9.71		14.59	10.07	11.25
CF (%)		3.92	4.38	4.84		4.63	4.52	5.11
Ash (%)		3.75	4.10	3.68		4.04	3.78	4.77
Ca (%)		1.30	0.87	0.81		0.81	1.40	0.76
P (%)		0.72	0.41	0.41		0.38	0.38	0.38

ME - Metabolizable Energy, CP - Crude Protein, EE - Ether Extract, CF - Crude Fiber, Ca - Calcium, P - Phosphorus (Available)

2.6 Statistical Analysis

Data were analyzed using one-way Analysis of Variance (ANOVA) in RCBD in Proc GLM of SAS v.9. Differences among treatments were determined using Tukey's Honestly Significant Difference Test (HSD) and declared significant when $p<0.05$. The results were presented as mean values and standard error of the means.

3. Results and Discussion

3.1 Growth Performance

Table 4 shows the growth performance of broiler chickens fed with different ketogenic diet formulations at 3-5 weeks old based on voluntary feed intake (VFI), body weight (BW), average daily gain (ADG), weight gain (WG), and feed conversion ratio (FCR). Based on the result, significant differences can be observed in all growth performance parameters ($p<.0001$).

The VFI for the whole duration of the study revealed that Diets A (control), B (lipid-based), and C (fiber-based), with 2398.07 grams, 2335.39 grams, and 2290.73 grams, respectively, are comparable with each other. Diet D (fiber-based) with 1,723.09 grams had the lowest overall VFI. Diet B (lipid formulation) was formulated by reducing the corn inclusion in the diet and increasing the use of oil to provide the energy requirement of broiler chickens. In the study of Benitez et al. [9], when conventional corn was substituted with a high oil corn in the diet of broilers, comparable results in the VFI were observed. Diet C (protein-based), which also had comparable VFI with Diet A (control), was formulated by reducing the inclusion of corn and replacing it with materials that are high in protein. In the study of Ferguson et al. [10], no significant difference in VFI was observed in broilers fed with low CP (21.9% in starter and 16.53% in grower) and medium diet (24.13% in starter and 19.58% in grower). The combination of good quality raw materials in both Diet B (lipid-based) and Diet C (protein-based) may have contributed to comparable VFI with Diet A (control) and better VFI than Diet D (fiber-based). The VFI of Diet D (fiber-based) was consistent with the study of Khempaka et al. [11], who found that fiber-based diets, such as 12% and 16% dried cassava pulp, reduced feed intake in broilers between 14 and 35 days. According to the researchers, this could be attributed to the increased bulkiness of the feed and reduced digestive capacity in broilers. Furthermore, an increase in mass has been shown to diminish palatability, which may limit broiler feed intake. Moreover, Jha and Mishra [12] explained that soluble fibers such as β-glucans, arabinoxylans, and pectins increased intestinal viscosity and reduced the rate of passage of feed, thereby reducing feed intake (FI) and the rate at which nutrients are absorbed, which may influence the growth performance of poultry. Rice bran and wheat bran are rich sources of these dietary fibers. Additionally, Cui et al. [13] mentioned that wheat bran has 46% non-starch polysaccharides, comprising 70% arabinoxylan, 24% cellulose, and 6% beta-glucan, with small amounts of glucoglucomannan and arabinogalactan. Rice bran, on the other hand, contains about 12% dietary fiber, 90% of which is insoluble dietary fiber such as cellulose, hemicellulose, and arabinoxylans. Soluble dietary fibers, such as pectin and β-glucan, are present in trace amounts [14].

Table 4. Growth performance of broiler chickens fed with different types of ketogenic diet at 3-5 weeks old

Parameters	A (Control)	B (Lipid-based)	C (Protein-based)	D (Fiber-based)	SEM	p-value
VF (g)	2398.07[a]	2335.39[a]	2290.73[a]	1723.09[b]	47.03	<.0001
BW (g)	1819.29[a]	1367.42[b]	1337.78[b]	1161.64[b]	27.94	<.0001
ADG (g)	62.52[a]	42.11[b]	41.05[b]	33.48[c]	1.21	<.0001
WG (g)	1312.85[a]	884.32[b]	862.00[b]	703.14[c]	25.27	<.0001
FCR	1.83[a]	2.67[b]	2.68[b]	2.46[b]	0.10	<.0001

*Means with the same superscript are not statistically significant

In terms of BW, significant differences can be observed ($p<0.0001$) with Diet A (control) weighing the heaviest (1819.29 grams) upon completion of the study. It was followed by Diet B (lipid-based), Diet C (protein-based), and Diet D (fiber-based), which had comparable BW of 1367.42 grams, 1334.78 grams, and 1161.64 grams, respectively. The higher VFI in Diet B (lipid-based) and Diet C (protein-based), as well as the combination of highly digestible components of these dietary treatments may have contributed to the greater BW of broiler chickens relative to Diet D (fiber-based). In a study by Tabook et al. [15], when the amount of dietary fiber in the diet was increased from 10% to 15%, body weight gain was reduced by 8% and 12%, respectively. The inclusion of more than 5% dietary fiber reduced daily gain, feed intake, and feed conversion

ratio. Significant differences can also be observed in the ADG of broiler chickens ($p<0.0001$). Throughout the study, ADG was highest in Diet A (control) with 62.52 grams, whereas Diet B (lipid-based) and Diet C (protein-based) had no significant difference at 42.11 grams and 41.05 grams, respectively. The least was Diet D (fiber-based) with 33.48 grams. The aim of providing ketogenic-based diets was to limit the intake of calories from carbohydrates and increase intake from protein or fat. With this, inclusion of carbohydrate-rich raw materials such as corn was minimized, allowing usage of other ingredients, mostly milling by-products, to be maximized. Corn is a highly digestible feed material, and limiting the use of this ingredient may have affected the digestibility of the feed. This is one reason why ketogenic-based diets have lower ADG compared to Diet A (control). At increasing percentages of high fiber dietary ingredients, Loar et al. [16] also observed a decrease in broiler BW gain. Diet B (lipid-based) and Diet C (protein-based), although they had lower ADG than Diet A (control), performed better than Diet D (fiber-based) because of their higher nutrient level. Diet B (lipid-based) had the highest ME (kcal) content while Diet C (protein-based) had the highest CP. In the study of Maiorka et al. [17], broilers fed the diet containing 3200 kcal ME/kg had higher weight gain compared to those fed the diet containing 2900 kcal ME/kg. Moreover, Gheisari et al. [18] observed higher total feed consumption and WG of birds in the high protein group compared to the low and medium protein groups. The lower ADG of ketogenic-based dietary treatments compared to the control (commercial) can also be attributed to the form of the feeds. The control diet was in the form of crumble, while the ketogenic-based feeds were in mash form. In the study by Massuquetto et al. [19], broiler chickens given pelleted/crumbled feed had higher ADG than those provided with mash. The outcome was associated with the higher FI of pelleted diets as a result of the pellets' greater durability and physical quality.

For the WG of broiler chickens, a significant difference can be observed among treatments ($p<0.0001$), and with 1312.85 grams WG, Diet A (control) had the best performance out of the four diets. Diet B (lipid-based) and Diet C (protein-based) are comparable at 884.32 grams and 862.00 grams, respectively, while Diet D (fiber-based) had the least WG (703.14 grams). Commercial feeds in the Philippines are usually formulated on a corn-soya-based approach. They are much digestible compared to ketogenic diets that were formulated low in digestible carbohydrate and high in either protein or lipid. The reason that the two ketogenic-based diets, Diet B (lipid-based) and Diet C (protein-based), performed better in WG compared to Diet D (fiber-based) was because of the combination of better-quality raw materials (more digestible) and higher digestible nutrient levels, particularly energy and protein. A study by Gallinger et al. [20] in broiler chicks showed that the addition of rice bran significantly reduced WG. At certain periods in the study, diets with rice bran performed poorly on growth assessments compared to the control diet, and increasing its percentage in the diet from 30% to 40% had a significant negative impact on WG.

FCR is a measure of how efficient an animal converts feed into live weight. It measures how many kilograms of feed are needed to produce a kilogram of weight gain. Producers, therefore, are aiming to attain a lower FCR in their production. Significant differences can be observed ($p<0.0001$) in the FCR of the experimental animals. Diet A (control) had the best FCR (1.83), followed by Diet B (lipid-based), Diet C (protein-based), and Diet D (fiber-based), which were statistically comparable at 2.67, 2.68, and 2.46, respectively. Given the underwhelming results in VFI, BW, ADG, and WG of broilers fed ketogenic diets, it's not surprising that these also led to poor FCR performance.

3.2 Carcass Quality

Table 5 shows the carcass weight (CW), dressing percentage (DP), abdominal fat (AF), and visceral fat (VF) yield of broiler chickens fed with different ketogenic feed formulations at 5 weeks old. Significant difference in CW ($p<0.0001$), DP ($p<0.0001$), and AF ($p=0.0034$) can be observed in the study, while visceral fat results are comparable ($p=0.3599$) among treatments. Diet A (control) had the highest CW at 1241.50 grams. Both Diet B (lipid-based) and Diet C (protein-based) had comparable CW at 871.13 grams and 895.50 grams, respectively, while the lowest CW was in Diet D (fiber-based) at 738.75 grams. The DP of Diet A (control) was the highest of all four diets, with 76.16% followed by Diet B (lipid-based), Diet C (protein-based), and Diet D (fiber-based) with 71.69%, 72.10%, and 70.53%, respectively. The AF yield was highest in Diet B (lipid-based) with 1.42%, comparable to Diet A (control) with 1.31%. It was followed by Diet C (protein-based) with 0.91% and lastly by Diet D (fiber-based) with 0.83%. When it comes to the VF yield, despite having no significant

result, Diet A (control) relatively had the highest yield at 1.86%, followed by Diet B (lipid-based) with 1.70% and lastly by Diet C (protein-based) and Diet D (fiber-based) with both 1.37%.

A variety of factors, including breed, age, sex, environment, diet, and processing, can influence DP. Diets high in energy and protein will result in a higher dressing percentage [21]. The increased DP of the control animals can also be a result of commercial feeds that are high in digestible energy and protein, which promote better growth and muscular development. Finishing diets high in fiber can minimize DP. Diets high in fiber are thought to increase intestinal mass, reducing DP because intestinal mass accounts for a bigger share of live weight. This assumption agrees with the result of the study showing lower DP of broilers fed ketogenic-based diets. The abdominal fat also affected the DP of the carcass. Since this is included during the actual weighing of the broiler carcass, overestimation of the actual DP may occur. Moreover, visceral fat and DP had an indirect relationship. Since visceral fat is not included during carcass weighing but is included during live weighing, a higher percentage may result in lower DP.

The reduced abdominal fat yield in a protein-based diet was consistent with the study of Jlali et al. [22]. Their study revealed that chickens fed a high CP diet had a lower ($p<0.001$) accumulation of abdominal fat than chickens fed a low CP diet. It was also in agreement with the study of Sterling et al. [23] showing that dietary CP level significantly affected abdominal fat pad for both genotypes (Arbor Acre and Ross 508) of broiler chicks. Abdominal fat pad weights were higher for chicks fed the lower CP diets. Diet C (protein-based) had the highest DP among ketogenic-based diets and one of the lowest abdominal fat levels in the study. This is a positive outcome since abdominal fat, while included in the carcass weighing, is usually removed during fabrication. Diet B (lipid-based) had reduced DP but more abdominal fat. Because of the increased abdominal fat, the actual DP of broilers fed with this diet may be reduced even further. According to a study by Bhuiyan et al. [24], dietary fiber had a substantial ($p=0.0001$) impact on abdominal fat. Compared to birds with low fiber diets, those with medium (and high) fiber diets deposited less abdominal fat. Meanwhile, Nassar et al. [25] found that chickens fed a diet high in lignocellulose had less visceral fat deposition and less intramuscular fat than those fed a diet low in fiber. In general, crude fibers have three impacts on fat metabolism. First, they accelerate the flow of chyme through the intestinal tract, hence decreasing the possibility that intestinal cells would absorb fat [26]. Second, through interacting with bile acid in the digestive tract, crude fibers decrease lipid absorption and accelerate bile acid excretion [27]. Third, restricting poultry's dietary energy absorption can reduce cholesterol and fat synthesis [28].

Table 5. Carcass quality of broiler chickens fed with different types of ketogenic diet at 5 weeks old

Parameters	A (Control)	B (Lipid-based)	C (Protein-based)	D (Fiber-based)	SEM	p-value
CW (g)	1241.50^{a}	871.13^{b}	895.50^{b}	738.75^{c}	27.51	<.0001
DP (%)	76.16^{a}	71.69^{b}	72.10^{b}	70.53^{b}	0.54	<.0001
AF (%)	1.31^{ab}	1.42^{a}	0.91^{bc}	0.83^{c}	1.12	0.0034
VF (%)	1.86^{a}	1.70^{a}	1.37^{a}	1.37^{a}	0.23	0.3599

*Means with the same superscript are not statistically significant

3.3 Cost to Produce (CTP) and Broiler Production Efficiency Factor (BPEF)

The CTP and BPEF of broiler chickens fed with different ketogenic feeds are shown in Table 6. CTP was computed by dividing the total expenses of consumables (chick cost, feed cost, and medication) by the BW of the broiler chicken. On the other hand, BPEF is a comprehensive indicator of broiler performance. It is derived by dividing the BW of the broiler chicken by the FCR and multiplying the quotient by 100. Significant differences can be observed in both CTP ($p=0.0004$) and BPEF ($p<0.0001$). Based on the result, Diet A (control) had the lowest CTP at Php 89.43, whereas Diet B (lipid-based) with Php 101.68, Diet C (protein-based) with Php 101.32, and Diet D (fiber-based) with Php 102.32 were statistically comparable. These three ketogenic-based diets had higher CTP than the control, in terms of BPEF, Diet A (control) had the highest value with 99.72%. On the other hand, the three formulated ketogenic diets had comparable BPEF at 52.27%, 50.51%, and 48.27% for Diet B (lipid-based), Diet C (protein-based), and Diet D (fiber-based), respectively. ADG and FCR play a major role in determining animal performance. Commercial feeds use low-fiber ingredients like corn,

making them more digestible than ketogenic-based formulations. These ingredients can easily be broken down and utilized by the animal's body. Due to the reduction in the sources of digestible carbohydrates, ketogenic-based diets were typically high in dietary fiber. It was anticipated that poor growth performance would also affect production efficiency. Diet D (fiber-based) was mainly affected by this intervention.

Table 6. CTP and BPEF of broiler chickens fed with different types of ketogenic diet

Parameter	A	B	C	D	SEM	p-value
	(Control)	(Lipid-based)	(Protein-based)	Fiber-based)		
CTP	88.08[a]	100.21[b]	98.89[b]	100.93[b]	1.97	0.0004
BPEF	99.72[a]	52.27[b]	50.51[b]	48.27[b]	2.72	<.0001

*Means with the same superscript are not statistically significant

4. Conclusions

This study found that Diet A (control) has the best growth results, notably in terms of BW, ADG, and FCR. Additionally, it has the greatest BPEF and the lowest CTP. However, when solely comparing the three ketogenic diets, Diet C (protein-based) outperforms the others across all growth performance metrics. Moreover, Diet A (control) had the highest carcass yield and dressing percentage, but also the most abdominal and visceral fat. In contrast, ketogenic diets, especially Diets C (protein-based) and D (fiber-based), significantly reduced fat accumulation.

Author Contributions: Conceptualization, R.L. and M.G.; methodology, R.L. and M.G.; validation, R.L. and M.G.; formal analysis, R.L. and M.G.; investigation, R.L. and M.G.; resources, R.L.; data curation, R.L. and M.G.; writing—original draft preparation, R.L.; writing—review and editing, R.L., M.G., and W.C.; visualization, R.L. and M.G.; supervision, R.L. and M.G.; project administration, R.L. and M.G.; funding acquisition, R.L.. All authors have read and agreed to the published version of the manuscript.

Funding: This research was funded by the Department of Science and Technology - Accelerated Science and Technology Human Resource Development Program - National Science Consortium (DOST-ASTHRDP).

Conflicts of Interest: The authors declare no conflict of interest.

References

[1] Fouad, A. M.; El-Senousey, H. K. Nutritional Factors Affecting Abdominal Fat Deposition in Poultry: A Review. *Asian-Australasian Journal of Animal Science* **2014**, *27*(7), 1057-1068. https://doi.org/10.5713/ajas.2013.13702

[2] Dong, J. Q.; Zhang, H.; Jiang, X. F.; Wang, S. Z.; Du, Z. Q.; Wang, Z. P.; Leng, L.; Cao, Z. P.; Li, Y. M.; Luan, P.; Li, H. Comparison of Serum Biochemical Parameters between Two Broiler Chicken Lines Divergently Selected for Abdominal Fat Content. *Journal of Animal Science* **2015**, *93*(7), 3278-3286. https://doi.org/10.2527/jas.2015-8871

[3] Abdalla, B. A.; Chen, J.; Nie, Q.; Zhang, X. Genomic Insights into the Multiple Factors Controlling Abdominal Fat Deposition in a Chicken Model. *Frontiers in Genetics* **2018**, *9*, 262. https://doi.org/10.3389/fgene.2018.00262

[4] Jiang, M.; Fan, W. L.; Xing, S. Y.; Wang, J.; Li, P.; Liu, R. R.; Li, Q. H.; Zheng, M. Q.; Cui, H. X.; Wen, J.; Zhao, G. P. Effects of Balanced Selection for Intramuscular Fat and Abdominal Fat Percentage and Estimates of Genetic Parameters. *Poultry Science* **2017**, *96*(2), 282-287. https://doi.org/10.3382/ps/pew334

[5] Kosinski, C.; Jornayvaz, F. R. Effects of Ketogenic Diets on Cardiovascular Risk Factors: Evidence from Animal and Human Studies. *Nutrients* **2017**, *9*(5), 517. https://doi.org/10.3390/nu9050517

[6] Philippine Agricultural Engineering Standard. Agricultural Structures - Housing for Broiler Production. Retrieved July 25, 2022, from https://amtec.ceat.uplb.edu.ph/wp-content/uploads/2019/07/402.pdf.

[7] Atapattu, S.; Baker, A. Solid Broiler Management Training Manual. Supporting Opportunities in Livelihoods Development. United States Agency for International Development. Retrieved December 10, 2021, from https://pdf.usaid.gov/pdf_docs/PA00MGPT.pdf.
[8] PHILSAN. Feed Reference Standards (Fourth Edition); pp 127--37. Philippine Society of Animal Nutritionists, **2010**.
[9] Benitez, J. A.; Gernat, A. G.; Murillo, J. G.; Araba, M. The Use of High Oil Corn in Broiler Diets. *Poultry Science* **1999**, *78*(6), 861-865. https://doi.org/10.1093/ps/78.6.861
[10] Ferguson, N. S.; Gates, R. S.; Taraba, J. L.; Cantor, A. H.; Pescatore, A. J.; Ford, M. J.; Burnham, D. J. The Effect of Dietary Crude Protein on Growth, Ammonia Concentration, and Litter Composition in Broilers. *Poultry Science* **1998**, *77*(10), 1481-1487. https://doi.org/10.1093/ps/77.10.1481
[11] Khempaka, S.; Molee, W.; Guillaume, M. Dried Cassava Pulp as an Alternative Feedstuff for Broilers: Effect on Growth Performance, Carcass Traits, Digestive Organs, and Nutrient Digestibility. *Journal of Applied Poultry Research* **2009**, *18*(3), 487-493. https://doi.org/10.3382/japr.2008-00124
[12] Jha, R.; Mishra, P. Dietary Fiber in Poultry Nutrition and Their Effects on Nutrient Utilization, Performance, Gut Health, and on the Environment: A Review. *Journal of Animal Science and Biotechnology* **2021**, *12*(1), 1-16. https://doi.org/10.1186/s40104-021-00576-0
[13] Cui, S. W.; Wu, Y.; Ding, H. The Range of Dietary Fibre Ingredients and a Comparison of Their Technical Functionality. In Fibre-Rich and Wholegrain Foods: Improving Quality; **2013**; pp 96–119. https://doi.org/10.1533/9780857095787.1.96
[14] Sapwarobol, S.; Saphyakhajorn, W.; Astina, J. Biological Functions and Activities of Rice Bran as a Functional Ingredient: A Review. *Nutrition and Metabolic Insights* **2021**, *14*, 11786388211058559. https://doi.org/10.1177/11786388211058559
[15] Tabook, N. M.; Kadim, I. T.; Mahgoub, O.; Al-Marzooqi, W. The Effect of Date Fibre Supplemented with an Exogenous Enzyme on the Performance and Meat Quality of Broiler Chickens. *British Poultry Science* **2006**, *47*(1), 73-82. https://doi.org/10.1080/00071660500475160
[16] Loar II, R. E.; Moritz, J. S.; Donaldson, J. R.; Corzo, A. Effects of Feeding Distillers Dried Grains with Solubles to Broilers from 0 to 28 Days Posthatch on Broiler Performance, Feed Manufacturing Efficiency, and Selected Intestinal Characteristics. *Poultry Science* **2010**, *89*(10), 2242-2250. https://doi.org/10.3382/ps.2010-00894
[17] Maiorka, A.; Dahlke, F.; Santin, E.; Kessler, A. D. M.; Penz Jr, A. M. Effect of Energy Levels of Diets Formulated on Total or Digestible Amino Acid Basis on Broiler Performance. *Brazilian Journal of Poultry Science* **2004**, *6*, 87-91. https://doi.org/10.1590/S1516-635X2004000200003
[18] Gheisari, H. R.; Asasi, K.; Mostafa, I.; Mohsenifard, E. Effect of Different Levels of Dietary Crude Protein on Growth Performance, Body Composition of Broiler Chicken and Low Protein Diet in Broiler Chicken. *International Journal of Poultry Science* **2015**, *14*(5), 285-292. https://doi.org/10.3923/ijps.2015.285.292
[19] Massuquetto, A.; Durau, J. F.; Schramm, V. G.; Netto, M. T.; Krabbe, E. L.; Maiorka, A. Influence of Feed Form and Conditioning Time on Pellet Quality, Performance and Ileal Nutrient Digestibility in Broilers. *Journal of Applied Poultry Research* **2018**, *27*(1), 51-58. https://doi.org/10.3382/japr/pfx039
[20] Gallinger, C. I.; Suárez, D. M.; Irazusta, A. Effects of Rice Bran Inclusion on Performance and Bone Mineralization in Broiler Chicks. *Journal of Applied Poultry Research* **2004**, *13*(2), 183-190. https://doi.org /10.1093/japr/13.2.183
[21] Knight C. W. Bulletin #2223, understanding poultry yields - cooperative extension publications - University of Maine Cooperative Extension. Cooperative Extension Publications. Retrieved January 25, 2023, from https://extension.umaine.edu/publications/2223e/
[22] Jlali M.; Gigaud V.; Metayer-Coustard S.; Sellier N.; Tesseraud.; Le Bihan-Duval E.; Berri C. Modulation of glycogen and breast meat processing ability by nutrition in chickens: Effect of crude protein level in 2 chicken genotypes. *Journal of Animal Science* **2012**, *90*(2), 447-455. https://doi.org/10.2527/jas.2011-4405
[23] Sterling K. G.; Pesti G. M.; Bakalli R. I. Performance of different broiler genotypes fed diets with varying levels of dietary crude protein and lysine. *Poultry Science* **2006**, *85*(6), 1045-1054. https://doi.org/10.1093/ps/85.6.1045

[24] Bhuiyan M.; Cheng Z.; Bari M. S.; Iji P.A. High fibre diet reduced the energy cost of production and abdominal fat of broiler chickens. *Adv. Anim. Vet. Sci.* **2021**, *9*(10), 1585-1593. http://dx.doi.org/10.17582/journal.aavs/2021/9.10.1585.1593

[25] Nassar M. K.; Lyu S.; Zentek J.; Brockmann G. A. Dietary fiber content affects growth, body composition, and feed intake and their associations with a major growth locus in growing male chickens of an advanced intercross population. *Livestock Science* **2019**, *227*, 135-142. https://doi.org/10.1016/j.livsci.2019.07.015

[26] Yost T. J.; Jensen D. R.; Haugen B. R.; Eckel R. H. Effect of dietary macronutrient composition on tissue-specific lipoprotein lipase activity and insulin action in normal-weight subjects. *The American journal of clinical nutrition* **1998**, *68*(2), 296-302. https://doi.org/10.1093/ajcn/68.2.296

[27] Vicente J. G.; Isabel B.; Cordero G.; Lopez-Bote C. J. Fatty acid profile of the sow diet alters fat metabolism and fatty acid composition in weanling pigs. *Animal Feed Science and Technology* **2013**, *181*(1-4), 45-53. https://doi.org/10.1016/j.anifeedsci.2013.02.002

[28] Hermier D. Lipoprotein metabolism and fattening in poultry. *The Journal of nutrition* **1997**, *127*(5), 805S-808S. https://doi.org/10.1093/jn/127.5.805S

ASEAN
Journal of Scientific and Technological Reports
Online ISSN:2773-8752

Academic article

Innovative Use of Fly Ash as a Free Fatty Acid Reducer in Used Cooking Oil for Enhanced Biodiesel Production

Heni Anggorowati[1*], Perwitasari[2], Muhammad Syukron[3], and Yusmardhany Yusuf[4]

[1] Faculty of Industrial Engineering, Universitas Pembangunan Nasional Veteran Yogyakarta, 55283, Indonesia
[2] Faculty of Industrial Engineering, Universitas Pembangunan Nasional Veteran Yogyakarta, 55283, Indonesia
[3] Faculty of Mineral and Energy Technology, Universitas Pembangunan Nasional Veteran Yogyakarta, 55283, Indonesia
[4] Faculty of Industrial Engineering, Universitas Pembangunan Nasional Veteran Yogyakarta, 55283, Indonesia
* Correspondence: heni.anggorowati@upnyk.ac.id

Citation:
Anggorowati, H.; Perwitasari, Perwitasari.; Syukron, M.; Yusuf, Y; Innovative use of fly ash as a free fatty acid reducer in used cooking oil for enhanced biodiesel production. *ASEAN J. Sci. Tech. Report.* **2025**, *28*(4), e256662. https://doi.org/10.55164/ajstr.v28i4.256662.

Article history:
Received: November 12, 2024
Revised: June 21, 2025
Accepted: June 23, 2025
Available online: September 27, 2025

Abstract: High free fatty acid (FFA) levels in used cooking oil (UCO) hinder biodiesel production by reducing yield and complicating purification due to soap formation during transesterification. Traditional FFA reduction methods, such as acid-catalyzed esterification, have environmental and cost drawbacks. This study explores the use of activated fly ash, a coal combustion byproduct, as an eco-friendly, low-cost adsorbent for FFA reduction. Fly ash was treated with NaOH to enhance adsorption capacity, with effects of reaction time (1–4 hours) and adsorbent mass (1–5 grams) evaluated. Results showed that longer reaction times and higher fly ash masses significantly reduced FFA content, reaching equilibrium at extended times and higher masses. A power-law kinetic model (R^2 = 0.9895) confirmed the accuracy of FFA degradation data. The study concludes that activated fly ash offers a viable solution for improving biodiesel efficiency by repurposing industrial waste, supporting both renewable energy production and waste management.

Keywords: Fly ash; free fatty; used cooking oil; biodiesel; adsorption kinetics

1. Introduction

The quest for sustainable and renewable energy sources has intensified, with biodiesel emerging as a promising alternative to fossil fuels due to its biodegradability, lower greenhouse gas emissions, and potential production from waste materials, such as used cooking oil (UCO) [1, 2]. Among various feedstocks, UCO is particularly advantageous due to its cost-effectiveness and contribution to waste reduction, making it an ideal candidate for biodiesel production [3, 4]. However, a major challenge with UCO is its high free fatty acid (FFA) content, which reacts with alkaline catalysts to form soap during the transesterification process, thus reducing biodiesel yield and complicating purification [5, 6]

Traditional methods for FFA reduction in UCO, such as acid-catalyzed esterification using sulfuric acid, are widely used but present high operational costs, corrosion issues, and environmental concerns due to hazardous waste [3, 7]. Alternatively, adsorbents like activated carbon can be used, but high costs and limited reusability challenge large scale applications [1, 8]. Consequently, the search for sustainable and cost-effective alternatives has driven research into the use of industrial byproducts, such as fly ash [6, 9]. Fly ash, a waste product from coal combustion, is abundantly available and has gained attention due to

its potential in various applications, including as a catalyst or adsorbent in environmental and industrial processes [6, 8]. Its composition, including oxides like silica, alumina, and iron oxides, and its porous structure make it suitable for reducing FFAs in biodiesel feedstocks [2]. Recent studies suggest that fly ash can effectively remove pollutants and contaminants, thus improving the quality of processed materials. However, its specific application for FFA reduction in UCO is still underexplored, indicating a promising research area[1, 3].

Current research into fly ash utilization in biodiesel production shows mixed results. Some studies report that untreated fly ash can significantly reduce FFAs in UCO, enhancing biodiesel yield, while others suggest that untreated fly ash may lack sufficient catalytic sites and may require modifications like acid or base treatments to optimize its performance [5, 9]. This variation highlights the need for further investigation into the catalytic properties of fly ash, particularly to determine effective treatment methods for biodiesel applications. This study aims to explore the application of activated fly ash as a free fatty acid (FFA) reducer in used cooking oil (UCO) to improve biodiesel production. Specifically, it evaluates the effectiveness of modified fly ash in reducing FFAs by examining the influence of contact time and adsorbent mass on FFA adsorption. By identifying optimal conditions for fly ash application such as reaction time and fly ash quantity this research provides a comprehensive understanding of its potential as a sustainable solution in biodiesel feedstock processing.

The significance of this study lies in its potential to contribute to more sustainable biodiesel production practices by incorporating industrial byproducts like fly ash. This approach not only addresses technical challenges associated with high FFA content in UCO but also supports broader environmental goals of waste management and resource efficiency, ultimately advancing the field of renewable energy.

2. Materials and Methods

2.1 Material

This study employed various equipment, including an analytical balance, oven, magnetic stirrer, heating stove, beaker, measuring cylinder, stirring rod, watch glass, stopwatch, filter paper, Erlenmeyer flask, and burette. The materials utilized were fly ash from the steam power plant (PLTU) Cirebon, used cooking oil, distilled water, ethanol, and phenolphthalein indicator. Interventional studies involving animals or humans, and other studies that require ethical approval, must list the authority that provided approval and the corresponding ethical approval code.

2.2 Methods

Fly ash was washed with hot distilled water to remove impurities. The fly ash was then dried in an oven at 100°C until its mass was constant to remove moisture content. Subsequently, the fly ash was activated using a NaOH solution with a mass-to-volume ratio of 1:5 for 6 hours. The fly ash was then separated from the NaOH solution using filter paper and washed with distilled water until its pH was neutral. The fly ash was dried in an oven at 100°C until its mass was constant to remove moisture content. The next step involved adding 30 ml of used cooking oil into a glass beaker. 1-5 grams of fly ash were then added to the beaker. The mixture was stirred using a magnetic stirrer for 0 - 240 min. The used cooking oil was separated from the fly ash using a centrifuge at 3000 rpm for 20 minutes, and the FFA content was analyzed.

3. Results and Discussion

3.1 Effect of Reaction Time on %FFA Reduction

Figure 1 indicates that %FFA reduction improves significantly with increased reaction time across all tested adsorbent masses. As the reaction time extends from 1 to 4 hours, each adsorbent mass shows a consistent increase in %FFA reduction, highlighting the importance of adequate contact time for effective FFA adsorption. This trend is well-aligned with adsorption kinetics principles, which state that longer contact times enhance the interaction between FFA molecules and the adsorbent surface, leading to improved adsorption efficiency[10]

For lower adsorbent masses, such as 1 gram, %FFA reduction begins at approximately 20% after 1 hour and gradually reaches around 35% at the 4-hour mark. In contrast, for higher adsorbent masses like 5 grams, the %FFA reduction exceeds 60% after 4 hours, demonstrating that both reaction time and adsorbent mass play crucial roles in maximizing FFA removal. Manuale et al. (2013) observed similar results, noting that

increased adsorbent mass provides more active sites for FFA adsorption, which amplifies FFA reduction rates as reaction time increases[11].

Interestingly, the rate of increase in %FFA reduction begins to stabilize at longer reaction times, particularly for higher adsorbent masses. This behavior suggests that the adsorption process is nearing equilibrium, where most active sites on the adsorbent become occupied, leading to a plateau in FFA reduction. Such equilibrium phenomena are typical in adsorption processes, as additional reaction time contributes little to further reduction once the active sites are saturated [12].

The stabilization of %FFA reduction at extended reaction times implies that optimal adsorption time is crucial for efficient biodiesel production. Rezayan & Taghizadeh (2018) emphasize that optimizing reaction time not only enhances FFA reduction but also conserves resources, making the process more viable for industrial applications[13].

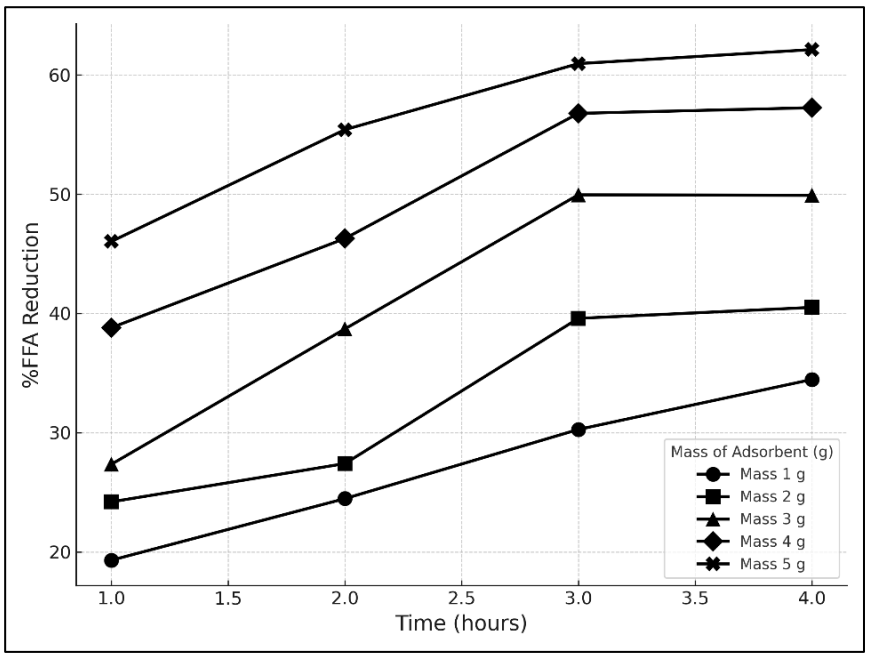

Figure 1. Effect of Reaction Time on % FFA Reduction

3.2 Effect of Adsorbent Mass on %FFA Reduction

The influence of adsorbent mass on the percentage reduction of free fatty acids (FFA) over a range of reaction times is illustrated in **Figure 2**. The data in this figure show a positive relationship between adsorbent mass and %FFA reduction, with higher masses resulting in greater FFA removal across various time intervals. This trend suggests that as the adsorbent mass increases, the availability of active sites also rises, enhancing the adsorption capacity and overall efficiency of FFA reduction. This observation aligns with findings by Hasan et al. (2019), who noted that using larger amounts of activated coal ash improved FFA reduction due to increased adsorption surface area [14].

In longer reaction times, the effect of adsorbent mass on %FFA reduction becomes more substantial. For example, at a reaction time of 4 hours, %FFA reduction reaches its peak with the highest adsorbent mass, indicating a synergistic effect of time and adsorbent quantity. This finding is consistent with Díaz et al. who reported similar improvements in FFA reduction when using energy crop shells as adsorbents, as increased mass provides a greater number of active sites for adsorption [10].

However, the trend toward equilibrium is evident at the highest adsorbent masses and longest reaction times, where %FFA reduction begins to plateau. This plateau effect indicates that additional adsorbent mass yields diminishing returns as the adsorption sites become saturated. Shafizah et al. observed this saturation effect in their optimization study, noting that beyond a certain adsorbent mass, the efficiency of FFA removal levels off [15].

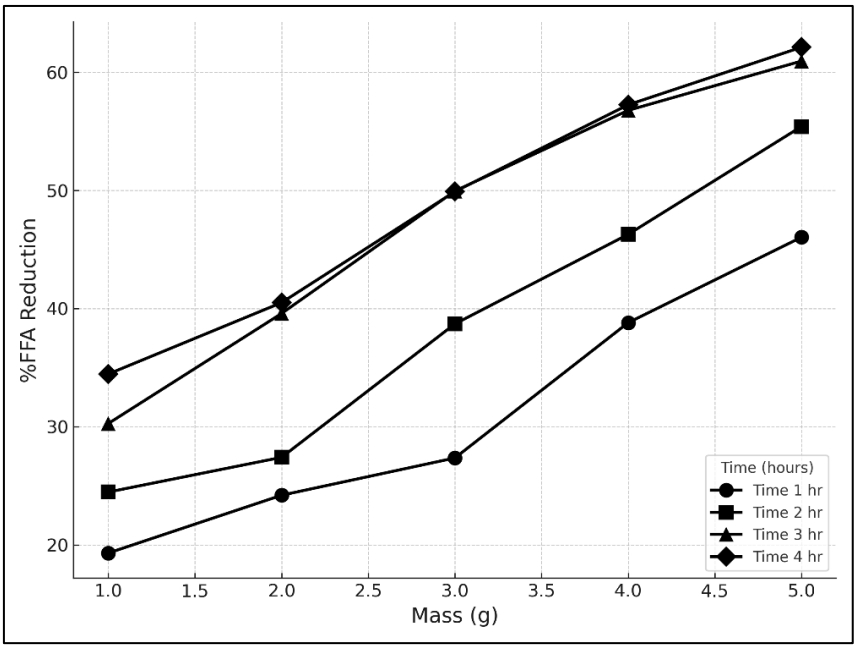

Figure 2. Effect of Adsorbent Mass on %FFA Reduction

4. Kinetic Model of Adsorption

The degradation kinetics of free fatty acids (FFA) were analyzed in this study using the kinetic model. $\frac{dC}{dt} = -kC^n$, where C is the FFA concentration, $k = 0{,}1027$ is the rate constant, and $n = 4.7834$ is the reaction order. These values were derived by fitting the experimental data to this kinetic model, capturing the behavior of FFA degradation over time.

Figure 3 illustrates the %FFA concentration over time, showing an initial rapid decline in FFA concentration that gradually slows as the reaction proceeds. This pattern is typical of reactions that follow power-law kinetics, particularly those with higher reaction orders, such as $n = 4.7834$. A high reaction order indicates that the reaction rate is initially susceptible to the concentration of FFA, decreasing significantly as the concentration diminishes. This trend is consistent with other studies where degradation reactions were modeled with power-law kinetics and high reaction orders, such as in the degradation of pollutants in water, where the rate constant k and reaction order n were found to have significant impacts on the reaction rate.

Figure 4, labeled "Data vs Estimated," further confirms the model's accuracy by comparing experimental %FFA data to estimated %FFA values, yielding a high coefficient of determination $R^2 = 0.9895$. This strong correlation between experimental and estimated values indicates that the kinetic model with k = 0.1027 and n = 4.7834 provides a good fit to the observed data. The high R^2 value aligns with findings from previous studies that used similar kinetic models, such as those investigating the degradation of organic compounds with rate constants in the range of k = 0.1 - 0.15 and reaction orders between 4 and 5, which yielded high correlation coefficients as well.

In conclusion, the kinetic model with parameters k = 0.1027 and n = 4.7834 accurately describes the degradation of FFA, as evidenced by the high correlation between experimental and model-predicted values. The high reaction order reflects a strong concentration dependency, particularly at higher initial concentrations, and the model's accuracy, supported by the high R^2 value, demonstrates its potential applicability for predicting degradation kinetics in similar systems.

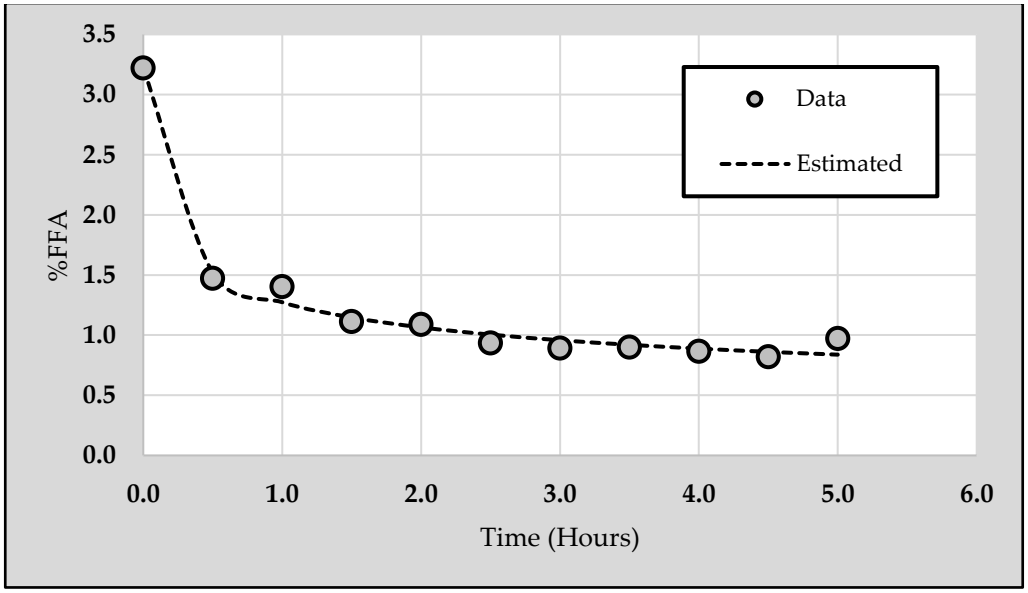

Figure 3. Plotting Time vs Concentration (%FFA)

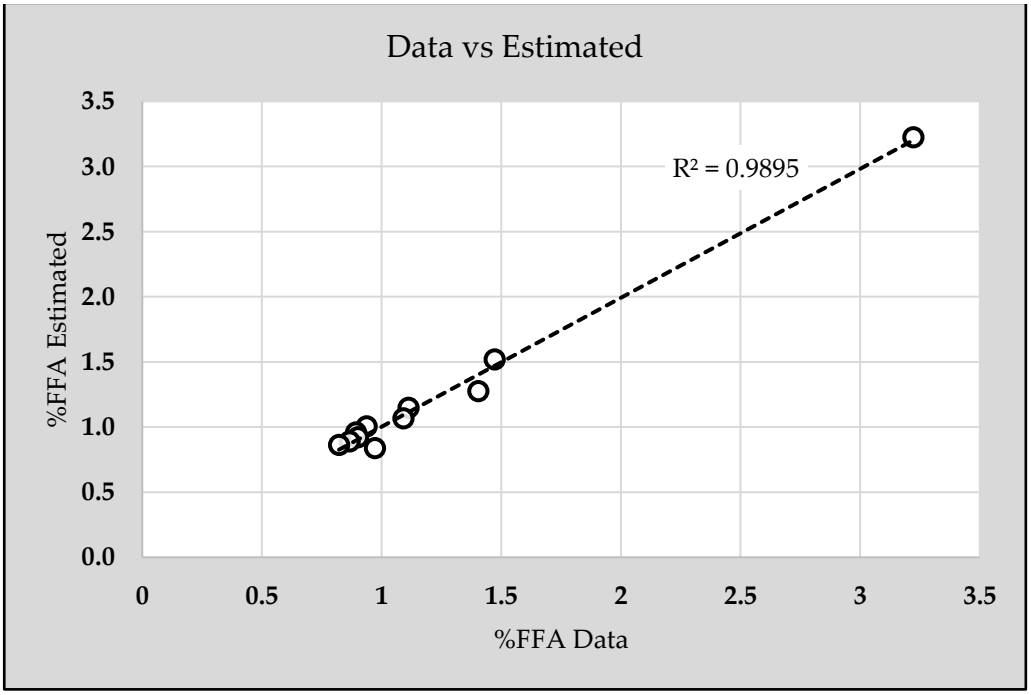

Figure 4. Plotting Data vs Estimated

4. Conclusions

Increasing reaction time and fly ash mass significantly enhances the reduction of free fatty acids (FFA) through adsorption. Extending the reaction time from 1 to 4 hours and using more fly ash improves FFA removal, but a saturation point is reached where additional time or fly ash yields minimal benefits due to occupied active sites. The kinetic model accurately described FFA degradation, confirming strong dependence on FFA concentration. Optimizing these parameters is crucial for efficient FFA reduction in biodiesel production..

5. Acknowledgements

The authors would like to thank to Lembaga Penelitian dan Pengabdian Masyarakat (LPPM) Universitas Pembangunan Nasional Veteran Yogyakarta for providing financial support for the implementation of this research.

Author Contributions: Heni Anggorowati: Conceptualization, Methodology, Formal analysis, Investigation, Data curation, Writing original draft preparation. Perwitasari: Validation, Resources, Visualization, Writing review & editing. Muhammad Syukron: Software, Data analysis, Model fitting, Writing review & editing. Yusmardhany Yusuf: Supervision, Project administration, Funding acquisition, Writing review & editing.

Funding: This research was funded by a grantfrom Lembaga Penelitian dan Pengabdian Masyarakat (LPPM) Universitas Pembangunan Nasional Veteran Yogyakarta, under a basic research scheme with contract number 121/UN62.21/DT.07.00/2024

Conflicts of Interest: The authors declare no conflict of interest

References

[1] Moazeni, F.; Chen, Y. C.; Zhang, G. Enzymatic Transesterification for Biodiesel Production from Used Cooking Oil, a Review. *J Clean Prod*, **2019**, *216*, 117–128. https://doi.org/10.1016/j.jclepro.2019.01.181.

[2] Miranda, A. C.; da Silva Filho, S. C.; Tambourgi, E. B.; CurveloSantana, J. C.; Vanalle, R. M.; Guerhardt, F. Analysis of the Costs and Logistics of Biodiesel Production from Used Cooking Oil in the Metropolitan Region of Campinas (Brazil). *Renewable and Sustainable Energy Reviews*, **2018**, *88* (August 2017), 373–379. https://doi.org/10.1016/j.rser.2018.02.028.

[3] Sahar; Sadaf, S.; Iqbal, J.; Ullah, I.; Bhatti, H. N.; Nouren, S.; Habib-ur-Rehman; Nisar, J.; Iqbal, M. Biodiesel Production from Waste Cooking Oil: An Efficient Technique to Convert Waste into Biodiesel. *Sustain Cities Soc*, **2018**, *41* (December 2017), 220–226. https://doi.org/10.1016/j.scs.2018.05.037.

[4] Abubakar, H. G.; Abdulkareem, A. S.; Jimoh, A.; Agbajelola, O. D.; Okafor, J. O.; Afolabi, E. A. Optimization of Biodiesel Production from Waste Cooking Oil. *Energy Sources, Part A: Recovery, Utilization and Environmental Effects*, **2016**, *38* (16), 2355–2361. https://doi.org/10.1080/15567036.2015.1040899.

[5] Singh, D.; Sharma, D.; Soni, S. L.; Singh, C.; Sharma, S.; Kumar, P.; Jhalani, A. A Comprehensive Review of Biodiesel Production from Waste Cooking Oil and Its Use as Fuel in Compression Ignition Engines : 3rd Generation Cleaner Feedstock FAME SIT PM IN AC ME. *J Clean Prod*, **2021**, *307* (April), 127299. https://doi.org/10.1016/j.jclepro.2021.127299.

[6] Gardy, J.; Hassanpour, A.; Lai, X.; Ahmed, M. H.; Rehan, M. Applied Catalysis B : Environmental Biodiesel Production from Used Cooking Oil Using a Novel Surface Functionalised TiO 2 Nano-Catalyst. *Appl Catal B*, **2017**, *207*, 297–310. https://doi.org/10.1016/j.apcatb.2017.01.080.

[7] Mohammadshirazi, A.; Akram, A.; Rafiee, S.; Bagheri Kalhor, E. Energy and Cost Analyses of Biodiesel Production from Waste Cooking Oil. *Renewable and Sustainable Energy Reviews*, **2014**, *33*, 44–49. https://doi.org/10.1016/j.rser.2014.01.067.

[8] Talebian-Kiakalaieh, A.; Amin, N. A. S.; Mazaheri, H. A Review on Novel Processes of Biodiesel Production from Waste Cooking Oil. *Appl Energy*, **2013**, *104*, 683–710. https://doi.org/10.1016/j.apenergy.2012.11.061.

[9] Sarno, M.; Iuliano, M. Self-Dual Leonard Pairs Biodiesel Production from Waste Cooking Oil. *Green process synth*, **2019**, *8* (1), 828–836.

[10] Díaz, L.; Mertes, L.; Brito, A.; Rodríguez, K. E. Valorization of Energy Crop Shells as Potential Green Adsorbents for Free Fatty Acid Removal from Oils for Biodiesel Production. *Biomass Convers Biorefin*, **2022**, *12* (3), 655–668. https://doi.org/10.1007/s13399-020-01089-y.

[11] Manuale, D. L.; Torres, G. C.; Badano, J. M.; Vera, C. R.; Yori, J. C. Adjustment of the Biodiesel Free Fatty Acids Content by Means of Adsorption. *Energy and Fuels*, **2013**, *27* (11), 6763–6772. https://doi.org/10.1021/ef401410v.

[12] Ifa, L.; Syarif, T.; Sartia, S.; Juliani, J.; Nurdjannah, N.; Kusuma, H. S. Techno-Economics of Coconut Coir Bioadsorbent Utilization on Free Fatty Acid Level Reduction in Crude Palm Oil. *Heliyon*, **2022**, *8* (3), e09146. https://doi.org/10.1016/j.heliyon.2022.e09146.

[13] Rezayan, A.; Taghizadeh, M. Synthesis of Magnetic Mesoporous Nanocrystalline KOH/ZSM-5-Fe3O4 for Biodiesel Production: Process Optimization and Kinetics Study. *Process Safety and Environmental Protection*, **2018**, *117*, 711–721. https://doi.org/10.1016/j.psep.2018.06.020.

[14] Susilowati, E.; Hasan, A.; Syarif, A. Free Fatty Acid Reduction in a Waste Cooking Oil as a Raw Material for Biodiesel with Activated Coal Ash Adsorbent. *J Phys Conf Ser*, **2019**, *1167* (1). https://doi.org/10.1088/1742-6596/1167/1/012035.

[15] Nor Shafizah, I.; Irmawati, R.; Omar, H.; Yahaya, M.; Alia Aina, A. Removal of Free Fatty Acid (FFA) in Crude Palm Oil (CPO) Using Potassium Oxide/Dolomite as an Adsorbent: Optimization by Taguchi Method. *Food Chem*, **2022**, *373*, 131668. https://doi.org/https://doi.org/10.1016/j.foodchem.2021.131668.

ASEAN
Journal of Scientific and Technological Reports
Online ISSN:2773-8752

ASEAN
Journal of Scientific and Technological Reports
Online ISSN: 2773-8752

Article type

Type of the Paper (Article, Review, Communication, etc.) *about 8,000 words maximum*

Title (Palatino Linotype 18 pt, bold)

Firstname Lastname[1], Firstname Lastname[2] and Firstname Lastname[2*]

[1] Affiliation 1; e-mail@e-mail.com
[2] Affiliation 2; e-mail@e-mail.com
* Correspondence: e-mail@e-mail.com; (one corresponding authors, add author initials)

Citation:
Lastname, F.; Lastname, F.; Lastname, F. Title. *ASEAN J. Sci. Tech. Report.* **2023**, *26*(X), xx-xx. https://doi.org/10.55164/ajstr.vxxix.xxxxxx

Article history:
Received: date
Revised: date
Accepted: date
Available online: date

Abstract: A single paragraph of about 400 words maximum. Self-contained and concisely describe the reason for the work, methodology, results, and conclusions. Uncommon abbreviations should be spelled out at first use. We strongly encourage authors to use the following style of structured abstracts, but without headings: (1) Background: Place the question addressed in a broad context and highlight the purpose of the study; (2) Methods: briefly describe the main methods or treatments applied; (3) Results: summarize the article's main findings; (4) Conclusions: indicate the main conclusions or interpretations.

Keywords: keyword 1; keyword 2; keyword 3 (List three to ten pertinent keywords specific to the article yet reasonably common within the subject discipline.)

1. Introduction

The introduction should briefly place the study in a broad context and highlight why it is crucial. It should define the purpose of the work and its significance. The current state of the research field should be carefully reviewed and critical publications cited. Please highlight controversial and diverging hypotheses when necessary. Finally, briefly mention the main aim of the work. References should be numbered in order of appearance and indicated by a numeral or numerals in square brackets—e.g., [1] or [2, 3], or [4–6]. See the end of the document for further details on references.

2. Materials and Methods

The materials and methods should be described with sufficient details to allow others to replicate and build on the published results. Please note that your manuscript's publication implicates that you must make all materials, data, computer code, and protocols associated with the publication available to readers. Please disclose at the submission stage any restrictions on the availability of materials or information. New methods and protocols should be described in detail, while well-established methods can be briefly described and appropriately cited.

Interventional studies involving animals or humans, and other studies that require ethical approval, must list the authority that provided approval and the corresponding ethical approval code.

2.1 Subsection

2.1.1. Subsubsection

3. Results and Discussion

This section may be divided by subheadings. It should provide a concise and precise description of the experimental results, their interpretation, as well as the experimental conclusions that can be drawn.Authors should discuss the results and how they can be interpreted from previous studies and the working hypotheses. The findings and their implications should be discussed in the broadest context possible. Future research directions may also be highlighted.

3.1. Subsection

3.1.1. Subsubsection

3.2. Figures, Tables, and Schemes

All figures and tables should be cited in the main text as Figure 1, Table 1, etc.

Figure 1. This is a figure. Schemes follow the same formatting.

Table 1. This is a table. Tables should be placed in the main text near the first time they are cited.

Title 1	Title 2	Title 3
entry 1	data	data
entry 2	data	data [1]

[1] Table may have a footer.

3.3. Formatting of Mathematical Components

This is example 1 of an equation:

$$a = 1, \tag{1}$$

The text following an equation need not be a new paragraph. Please punctuate equations as regular text. This is example 2 of an equation:

$$a = b + c + d + e + f + g + h + i + j + k + l + m + n + o + p + q + r + s + t + u \tag{2}$$

The text following an equation need not be a new paragraph. Please punctuate equations as regular text. The text continues here.

4. Conclusions

Concisely restate the hypothesis and most important findings. Summarize the significant findings, contributions to existing knowledge, and limitations. What are the future directions? Conclusions MUST be well stated, linked to original research question & limited to supporting results.

5. Acknowledgements

Should not be used to acknowledge funders – funding will be entered as a separate. As a matter of courtesy, we suggest you inform anyone whom you acknowledge.

Author Contributions: For research articles with several authors, a short paragraph specifying their individual contributions must be provided. The following statements should be used "Conceptualization, X.X. and Y.Y.; methodology, X.X.; software, X.X.; validation, X.X., Y.Y. and Z.Z.; formal analysis, X.X.; investigation, X.X.; resources, X.X.; data curation, X.X.; writing—original draft preparation, X.X.; writing—review and editing, X.X.; visualization, X.X.; supervision, X.X.; project administration, X.X.; funding acquisition, Y.Y. All authors have read and agreed to the published version of the manuscript." Please turn to the CRediT taxonomy for the term explanation. Authorship must be limited to those who have contributed substantially to the work reported.

Funding: Please add: "This research received no external funding" or "This research was funded by NAME OF FUNDER, grant number XXX" and "The APC was funded by XXX". Check carefully that the details given are accurate and use the standard spelling of funding agency names at https://search.crossref.org/funding. Any errors may affect your future funding.

Conflicts of Interest: Declare conflicts of interest or state "The authors declare no conflict of interest." Authors must identify and declare any personal circumstances or interest that may be perceived as inappropriately influencing the representation or interpretation of reported research results. Any role of the funders in the design of the study; in the collection, analyses or interpretation of data; in the writing of the manuscript, or in the decision to publish the results must be declared in this section. If there is no role, please state "The funders had no role in the design of the study; in the collection, analyses, or interpretation of data; in the writing of the manuscript, or in the decision to publish the results".

References

References must be numbered in order of appearance in the text (including citations in tables and legends) and listed individually at the end of the manuscript. We recommend preparing the references with a bibliography software package, such as EndNote, ReferenceManager to avoid typing mistakes and duplicated references. Include the digital object identifier (DOI) for all references where available.

Citations and references in the Supplementary Materials are permitted provided that they also appear in the reference list here.

In the text, reference numbers should be placed in square brackets [ ] and placed before the punctuation; for example [1], [1–3] or [1, 3]. For embedded citations in the text with pagination, use both parentheses and brackets to indicate the reference number and page numbers; for example [5] (p. 100), or [6] (pp. 101–105).

Using the American Chemical Society (ACS) referencing style

[1] Author 1, A.B.; Author 2, C.D. Title of the article. *Abbreviated Journal Name* Year, *Volume*, page range.

[2] Author 1, A.; Author 2, B. Title of the chapter. In *Book Title*, 2nd ed.; Editor 1, A., Editor 2, B., Eds.; Publisher: Publisher Location, Country. **2007**, Volume 3, pp. 154–196.

[3] Author 1, A.; Author 2, B. *Book Title*, 3rd ed.; Publisher: Publisher Location, Country, **2008**, pp. 154–196.
[4] Author 1, A.B.; Author 2, C. Title of Unpublished Work. *Abbreviated Journal Name* stage of publication (under review; accepted; in press).
[5] Author 1, A.B. (University, City, State, Country); Author 2, C. (Institute, City, State, Country). Personal communication, 2012.
[6] Author 1, A.B.; Author 2, C.D.; Author 3, E.F. Title of Presentation. In Title of the Collected Work (if available), Proceedings of the Name of the Conference, Location of Conference, Country, Date of Conference; Editor 1, Editor 2, Eds. (if available); Publisher: City, Country, Year (if available); Abstract Number (optional), Pagination (optional).
[7] Author 1, A.B. Title of Thesis. Level of Thesis, Degree-Granting University, Location of University, Date of Completion.
[8] Title of Site. Available online: URL (accessed on Day Month Year).

Reviewers sugestion

1. Name, Address, e-mail
2. Name, Address, e-mail
3. Name, Address, e-mail
4. Name, Address, e-mail

URL link:

Notes for Authors >>
https://drive.google.com/file/d/1r0zegnIVeQqe4iLQyT1xDEIinNggINPD/view?usp=sharing
https://drive.google.com/file/d/1r0zegnIVeQqe4iLQyT1xDEIinNggINPD/view?usp=sharing

Online Submissions >> https://ph02.tci-thaijo.org/index.php/tsujournal/user/register

Current Issue >> https://ph02.tci-thaijo.org/index.php/tsujournal/issue/view/16516

AJSTR Publication Ethics and Malpractice >> https://ph02.tci-thaijo.org/index.php/tsujournal/ethics

Journal Title Abbreviations >> http://library.caltech.edu/reference/abbreviations

ASEAN
Journal of Scientific and Technological Reports
Online ISSN:2773-8752

ASEAN
Journal of Scientific and Technological Reports
Online ISSN:2773-8752

ASEAN Journal of Scientific and Technological Reports (AJSTR)
Institute of Research and Innovation, Thaksin University, Phatthalung Campus
222 Moo. 2, Baan Prao Sub-District, Papayom District, Phatthalung, 93210, Thailand
Tel. +668 1540 7304